Syntheses of Bioactive Organoselenium Compounds and Evaluation of their Anti-cancer and Antioxidant Activities

A Thesis

Submitted in Partial Fulfilment of the

Requirements for the Degree of

Doctor of Philosophy

by

Kaustav Banerjee

Department of Chemistry

Indian Institute of Technology Guwahati

Assam – 781039, India

April 2021

Syntheses of Bioactive Organoselenium Compounds and Evaluation of their Anti-cancer and Antioxidant Activities

A Thesis

Submitted in Partial Fulfilment of the

Requirements for the Degree of

Doctor of Philosophy

in Chemistry

by

Kaustav Banerjee

Roll no. - 166122042

Department of Chemistry

Indian Institute of Technology Guwahati

Assam – 781039, India

April 2021

Dedicated To

All the souls deceased of cancer

Indian Institute of Technology Guwahati

Department of Chemistry

Guwahati

Assam – 781039

STATEMENT

I hereby declare that the research work described in the thesis entitled "***Syntheses of Bioactive Organoselenium Compounds and Evaluation of their Anti-cancer and Antioxidant Activities***" is the outcome of investigations carried out by me under the supervision of **Dr. Krishna P. Bhabak** at the Department of Chemistry, Indian Institute of Technology Guwahati, India, for the award of degree of Doctor of Philosophy.

In keeping with the general practice of reporting scientific observations, due acknowledgements have been made wherever the work described in this thesis is based on the findings of other investigators. Any omission that might have occurred by oversight or mistake is unintentional and gravely regretted.

Kaustav Banerjee
29.11.2021

Kaustav Banerjee

Roll No: 166122042

Dr. Krishna P. Bhabak
Assistant Professor
Department of Chemistry
Indian Institute of Technology Guwahati
Assam – 781039
Email: kbhabak@iitg.ac.in
Tel: 0361-258-3476

CERTIFICATE

This is to certify that the research work presented in the thesis entitled "**Syntheses of Bioactive Organoselenium Compounds and Evaluation of their Anti-cancer and Antioxidant Activities**" that is being submitted to Indian Institute of Technology Guwahati for the award of the degree of Doctor of Philosophy in Chemistry has been carried out by ***Mr. Kaustav Banerjee*** (Roll No: 166122042) under my supervision at this Institute. The research work reported in his thesis is original and the same has not been submitted elsewhere for a degree.

29.11.2021

Dr. Krishna P. Bhabak

Thesis Supervisor

Acknowledgements

I would like to take this opportunity to appreciate the kind help and support of all the people around me to make the journey, a very memorable one. Without their help, it would not have been possible to achieve this goal.

First and foremost, I would like to express my deepest gratitude towards my thesis supervisor **Dr. Krishna P. Bhabak** for his constant and persistent support, motivation and guidance throughout the entire tenure of my research work. His perseverant support, unparalleled efforts and never-ending patience, even in the midst of COVID-19 pandemic, proved to be extremely important for fulfilling this goal. Moreover, his mindful scrutiny and scrupulous suggestions of manuscripts were invaluable assets in this journey. Under his close supervision, the ideals of a true researcher have been inculcated within me. It has been, indeed, a very nice and pleasant experience in working with him.

I would like to extend my acknowledgement to my doctoral committee members **Prof. Anil K. Saikia** (Chairman), **Prof. Chandan K. Jana** (Member) and **Prof. Achalkumar A.S.** (member) for taking their time out of their busy schedule to review my progress and also to share their knowledge, provide invaluable suggestions to overall improve my research.

I am thankful to **Indian Institute of Technology Guwahati** for providing me fellowship, and to the **Department of Chemistry**, **Central Instruments Facility** (**CIF**) and **North East Centre for Biological Sciences and Healthcare Engineering** (**NECBH**) for providing me with instrumental facilities for nuclear magnetic resonance (NMR) and single crystal X-ray diffraction (SC-XRD) experiments. Additionally, I would like to acknowledge all the instrument operators and non-teaching staffs of Department of Chemistry and Administrative building, IIT Guwahati for extending their kind help in whichever ways, as applicable.

I would like to specially acknowledge my lab member **Mr. Debojit Bhattacherjee**, for performing the cellular works of my synthesized compounds. Additionally, his homely care, other professional help and moral support in every academic and personal pespectives, during the ups and downs of my PhD journey, provided me intense motivation throughout my journey. I am forever grateful and thankful towards other lab

members **Mr. Sulendar K. Mahato**, **Mr. Abu Sufian** and **Ms. Shivani Marandi** for bearing with me throughout the entirety of my research journey. Truly, all of them created an ambience and feeling of a "home, far from home" and no words are enough to thank them for what they did throughout my entire tenure.

Next I would like to thank all the project students **Mr. Arvind K. Gupta**, **Mr. Niladri Sekhar Mondal**, **Ms. Bishwanesha Panda**, **Mr. Paramesh Das**, **Mr. Dhiman Roy**, and **Mr. Ketan Gangadhar Mundkar** for their contributions towards my research work.

I would like to specially acknowledge my collaborators **Mrs. Padmavathi G**. and **Prof. Ajaikumar B. Kunnumakkara**, Dept. of Biosciences and Bioengineering, Indian Institute of Technology Guwahati, for their active collaborative effort. Additionally, I would also like to extend my sincere acknowledgements towards **Ms**. **Khyati Raina** and **Dr**. **Rajkumar B**. **Thummer**, Dept. of Biosciences and Bioengineering, Indian Institute of Technology Guwahati, for their significant collaborative contribution

I would like to extend my thanks to all of my batchmates, friends and juniors specially **Mr. Basab Kanti Das**, **Mr. Dipanjan Bhattacharyya**, **Mr. Sandip Mondal**, **Ms. Swapna Debnath**, **Mr. Nasim Akhtar** and **Ms. Archana Kumari Sahu** for providing me professional assistance out of their busy schedule.

Next, most importantly I would like to thank my family. I would like to mention my father **Mr. Anup Kumar Banerjee** and my mother **Mrs Snigdha Banerjee** for raising me into who I am. Last but not the least, I would like to specially mention my fiancé **Ms. Ritvika Goswami**, whose unparalleled motivation and constant encouragement during my tough times in every perspective, proved to be extremely useful. Her daily support and well wishes rejuvenated me, at the end of a busy and tiring day. I cannot thank her enough for her contribution in making me a better individual.

Finally, I would like to thank the Almighty God for making this possible and giving me the strength, perseverance and determination to work.

Kaustav Banerjee

Sd/- 29.11.2021

Kaustav Banerjee

Table of Contents

Abbreviations

Alb	Albumin
Anhyd.	Anhydrous
Arg	Arginine
BSA	Bovine Serum Albumin
Calcd	Calculated
CAT	Catalase
CCDC	Cambridge crystallographic data centre
$CDCl_3$	Chloroform-*d*
Cum-OOH	Cumene hydroperoxide
Cys	Cysteine
DCM	Dichloromethane
δ	Chemical shift (ppm)
DFT	Density Functional Theory
DHR	Dihydrorhodamine-123
DMEM	Dulbecco's modifeied Eagle medium
DMF	N,N-dimethylformamide
DPBS	Dulbecco's phosphate buffered saline
DTPA	Diethylene triamine penta acetic acid
ER+	Oestrogen receptor +
ESI-MS	Electrospray ionization mass spectroscopy
FBS	Fetal bovine serum
FT-IR	Fourier Transform Infra-Red
g	gram
GAPDH	Glyceraldehyde-3-phosphate dehydrogenase
Gln	Glutamine
Gly	Glycine
GPx	Glutathione peroxidase
GR	Glutathione reductase
GSSG	Glutathuione disulfide
GSH	Glutathione
h	Hour(s)
His	Histidine
HPLC	High performance liquid chromatography
Hz	Hertz
IC_{50}	Inhibitory concentration 50%
ID	Iodothyronine deiodinase
K_b	Binding Constant
K_m	Michaelis Constant
Met	Methionine
μM	micromolar
mM	milimolar
mmol	milimoles
MPO	Myeloperoxidase
NAC	N-acetyl cysteine
$NADP^+$	Nicotinamide adenine dinucleotide phosphate oxidized

NADPH	Nicotinamide adenine dinucleotide phosphate reduced
NMR	Nuclear Magnetic Resonance
Obs.	Observed
ORTEP	Oak Ridge thermal ellipsoid plot
PBS	Phosphate Buffer Saline
Pet. Ether	Petroleum Ether (60 – 80)
Ph	Phenyl
PI	Propidium iodide
PN	Peroxynitrite
Q-TOF	Quadrupole time-of-flight
RA	Relative activity
RNS	Reactive nitrogen species
ROS	Reactive oxygen species
rt	Room temperature
Sec	Selenocysteine
SeMet	Selenomethionine
Ser	Serine
SOD	Superoxide dismutase
^{t}BuOOH	Tert-butyl hydroperoxide
TLC	Thin layer chromatography
Trp	Tryptophan
TrxR	Thioredoxin reductase
DMBA	dimethylbenzanthracene
AOM	Azoxymethane
TNBC	Triple-negative breast cancer
UV-Vis	Ultra-violet visible

NMR	Nuclear Magnetic Resonance
Obs.	Observed
ORTEP	Oak Ridge thermal ellipsoid plot
PBS	Phosphate Buffer Saline
Pet. Ether	Petroleum Ether (60 – 80)
Ph	Phenyl
PI	Propidium iodide
PN	Peroxynitrite
Q-TOF	Quadrupole time-of-flight
RA	Relative activity
RNS	Reactive nitrogen species
ROS	Reactive oxygen species
rt	Room temperature
Sec	Selenocysteine
SeMet	Selenomethionine
Ser	Serine
SOD	Superoxide dismutase
^{t}BuOOH	Tert-butyl hydroperoxide
TLC	Thin layer chromatography
Trp	Tryptophan
TrxR	Thioredoxin reductase
DMBA	dimethylbenzanthracene
AOM	Azoxymethane
TNBC	Triple-negative breast cancer
UV-Vis	Ultra-violet visible

Synopsis

In the year of 1957, Schwarz reported selenium as an essential micronutrient for several bacteria, mammals and birds.[1] Approximately, 15 years later, selenocysteine was discovered as the 21st naturally occurring amino acid, at the active site of antioxidant enzyme glutathione peroxidase (GPx).[2] Since then, a wide array of selenium–containing enzyme has been identified. As mentioned, GPx has been extensively studied owing to its function particularly as an antioxidant. Apart from naturally occurring enzymes, over the last decade, synthesis of several small-molecule organoselenium compounds has gained significant scientific attention. Particularly, a vast repertoire of organoselenium compounds displaying GPx mimetic activities have been synthesized and widely studied.[3] Most notably among them, ebselen (**1**) is a small-molecule organoselenium compound, that displays very promising GPx-mimetic antioxidant activity (Figure 1). Application of selenium compounds as important chemotherapeutic and chemopreventive agents has been established since long ago. However, detailed studies of natural and synthetic organoselenium compounds as promising and versatile chemotherapeutic and/or chemopreventive agents, started after 1980s. Organoselenium compounds with promising anti-cancer activities are grossly classified into following categories such as inorganic selenium salts, selenides, diselenides, selenoureas, selenenic acids, selenoesters, selenium nanoparticles and selenocyanates. Apart from chemotherapeutic and/or chemopreventive activities, organoselenium compounds such as ebselen also show prominent anti-inflammatory activities. Studies reveal that ebselen affects intracellular calcium homeostasis by inhibiting inositol-3-phosphate (IP3)-induced calcium release.[4] Additionally, ebselen has also been found to be an effective inhibitor of galactosamine/endotoxin-induced hepatitis, that prevents liver and mucosal damage.[5] Selenazofurin analogues such as compound **2** are selenium-containing antivirals that display significant inhibitory activities against nucleoside synthetase.[6] Diselenides such as **3** have been shown to act as interferon-γ (IFNγ) and tumor necrosis factor (TNF) inducer in human peripheral blood leukocytes, therefore acting as cytokine inducers and immunomodulators.[7] Monoselenide **4** has been reported to be an anti-hypertensive agent by acting as an inhibitor of dopamine-β-monooxygenase (DBM) through turnover-dependent cofactor depletion mechanism.[8] Notable bio-active compounds are depicted in Figure 1.

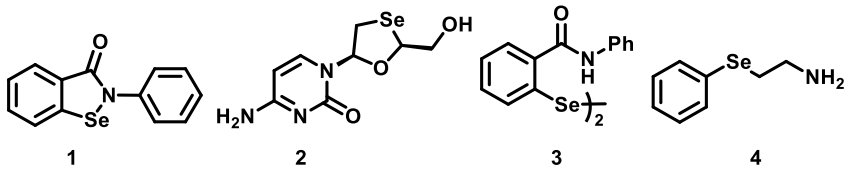

Figure 1. Organoselenium compounds displaying prominent biological activities.

The treatment scope of breast cancer in an advanced stage is limited owing to the high resistance to conventional treatments such as chemotherapy. Additionally, triple-negative breast cancer cells (MDA-MB-231) lacks estrogen and progesterone receptors, therefore further reducing the treatment scopes, unlike other ER(+) cancer cells such as MCF-7 and T-47D. Inspired from literature reports of prominent biological activities of organoselenium compounds, we developed interest in designing small molecule organoselenocyanates and evaluated their activities, primarily in triple-negative breast cancer cells such as MDA-MB-231.

The present thesis, entitled "**Syntheses of Bio-active Organoselenium Compounds and Evaluation of their Anti-cancer and Antioxidant Activities**" consists of total **five Chapters**, based on the results of experimental works performed during the complete course of Ph.D. research tenure.

Chapter 1: Introduction

The **first Chapter** contains general introduction relevant to cancer. Different causes and characteristics of cancer, along with the mechanism underlying the development and progression of cancer are discussed here. Additionally, a brief and concise review has been made regarding the available treatment strategies and limitations of each of the known strategies followed by a detailed elaboration regarding the importance of selenium in cancer treatments. As one of the most important functionalities in chemotherapeutic and chemopreventive compounds are selenocyanate, design and activity of several selenocyanate-containing compounds containing aliphatic or aromatic scaffolds are discussed herewith. Finally, possible metabolic pathways of the chemotherapeutic compounds having selenocyanate functionality is discussed in order to gain an insight in the pharmacodynamics profile of the chemotherapeutic selenocyanate compounds.

The chemopreventive and chemotherapeutic potential of benzyl-based selenocyanates were first reported in 1985, revealing that benzyl selenocyanate **5** prevents cancer

occurrence in different carcinogen-induced organ-specific cancer cell lines (Figure 2). However, higher toxicity of compound **5** restricted its use as a therapeutic agent. It was observed that compound **6**, bearing a 4-methoxy functionality, was significantly lesser toxic than compound **5**.[9] Additionally, it was observed that compound **8**, bearing two selenocyanate functionalities in a single molecule displayed much enhanced activity against experimentally induced colon, mammary, lung and oral carcinogenesis. Very recently, it has been observed that compound **7** displays promising nematicidal activity against *S. feltiae* with an LD_{50} of 4.90 µM.[10] Elaborate works of Bhattacharya and co-workers (2004) introduced diphenyl methyl selenocyanate (**9**) as a promising chemopreventive agent against DMBA/croton oil-induced two stage mouse skin carcinogenesis.[11] The same group demonstrated the activity of naphthalimide-based selenocyanate **10** as an efficient antioxidant against oxidative stress induced by DMBA-PMA two-stage mammary carcinogenesis.[12] Furthermore, it was observed that flavonyl-thiazolidinedione-based selenocyanate **11** attenuates the oxidative stress and DNA damage induced by cyclophosphamide in Ehrlich Ascites Carcinoma (EAC) in Swiss Albino mice.[13] Very recently, Arsenyan and co-workers (2020) developed mitochondria-targeting cationic selenazole compound **12** that was found to enhance ROS level in breast cancer cells thereby exhibiting cytotoxicity by pro-oxidant activity.[14] However, despite significant amount of studies being performed in the last decade, no comprehensive study has been put forward regarding the correlation between number of selenocyanate functionalities in a single molecule and its anti-cancer activity. Additionally, effect of pharmacophore on benzyl-based selenocyanates on the anti-cancer activities against triple-negative breast cancer (TNBC) cells is not widely understood till date. Furthermore, antioxidant activities of organoselenocyanates and analogues in general and cationic organoselenium compounds not much explored till date.

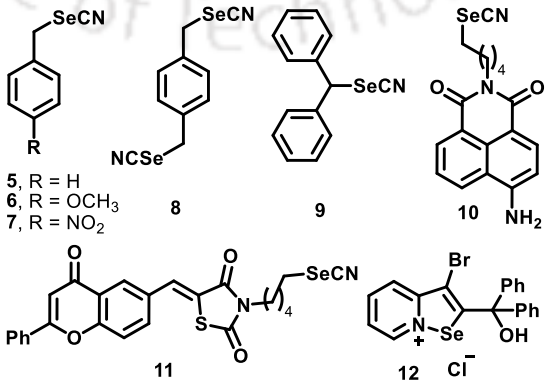

Figure 2. Selected organoselenium compounds **5-12** displaying promising anti-cancer and chemopreventive activities against different organ-specific cancer cells.

Chapter 2: Syntheses and Anti-proliferative Activities of Benzylic Selenocyanates: Structure-Activity Correlations with Multiple Selenocyanate Functionalities within a Molecule

Second Chapter of the thesis describes the synthesis and biological activity of a series of benzylic selenocyanates. In this Chapter, a series of benzyl- and mesitylene-based selenocyanates bearing one or more selenocyanate functionalities were developed (Figure 3) Our objective was to correlate the anti-proliferative activities of the compounds with the number of selenocyanate functionalities. The anti-cancer activities of all the synthesized selenocyanates were evaluated in triple-negative breast cancer cells such as MDA-MB-231, and other ER(+) breast cancer cell lines such as MCF-7 and T-47D. Additionally, the cytotoxicity of each of these compounds was tested in normal cell lines such as HaCaT cells. It was found that, compound **18** bearing three selenocyanate functionalities, was most active against both triple-negative and ER(+) cell lines having IC_{50} around 10.0 μM. However, compound **19**, containing six selenocyanate functionalities failed to exhibit expected anti-cancer activities, which could be due to the increased hydrophobicity and lesser solubility of the compound in biological media. All the experiments were compared against standard anti-cancer drug 5-fluorouracil (5-FU), and it was observed that two of the most active selenocyanates were better active than 5-FU.

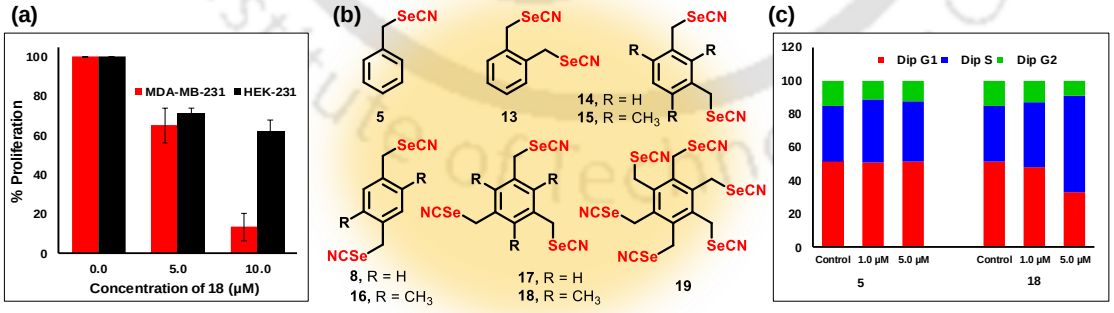

Ref: K. Banerjee, G. Padmavathi, D. Bhattacherjee, S. Saha, A. B. Kunnumakkara, K. P. Bhabak, *Org Biomol Chem* **2018**, *16*, 8769.

Figure 3. Brief highlights of Chapter 2 (a) Comparative anti-proliferative activity of compound **18** in MDA-MB-231 cells and HEK-231 cells in concentrations of 5.0 μM and 10.0 μM, compared against control (b) Chemical structures of synthesized compounds

(c) Cell cycle analysis of MDA-MB-231 cells of compounds **5** and **18** in three different concentrations 1.0 μM and 5.0 μM, compared against control

Chapter 3: Benzylic and Heterocycle-containing Organoselenocyanates: Impact of 4-Nitrobenzyl Group towards the Anti-proliferative Activities

It has been discussed earlier that both benzyl selenocyanate (**5**) and 4-methoxybenzyl selenocyanate (**6**) displays prominent chemopreventive activity against different carcinogen-induced organ-specific cancer. Moreover, it was also discussed previously that 4-nitrobenzyl selenocyanate (**7**) displays anti-nematicidal activity against *S. feltiae*. Taking inspiration from the activity of the benzyl- and mesitylene-based selenocyanates in the previous Chapter, we turned our attention to study the anti-proliferative and anti-cancer activity of compounds **5**, **6** and **7** in MDA-MB-231 cells. Furthermore, we intended to introduce pharmacophoric heterocycles with an intention to enhance the non-bonding interaction with certain key proteins. With that objective in mind we introduced 1,2,3-triazole and 2,4-thiazolidine-1,3-dione (TZD) within the aromatic scaffold which is described in **third Chapter**. A series of selenocyanates (**5**, **20**-**27**) containing 1,2,3-triazole and 2,4-thiazolidine-1,3-dione as pharmacophores were prepared (Figure 4). Following synthesis of the compounds, we evaluated the compounds for their anti-cancer activity in triple-negative breast cancer cell lines along with other ER(+) cell lines such as MCF-7. We also evaluated the antioxidant potential of the synthesized compounds using *in vitro* assay.

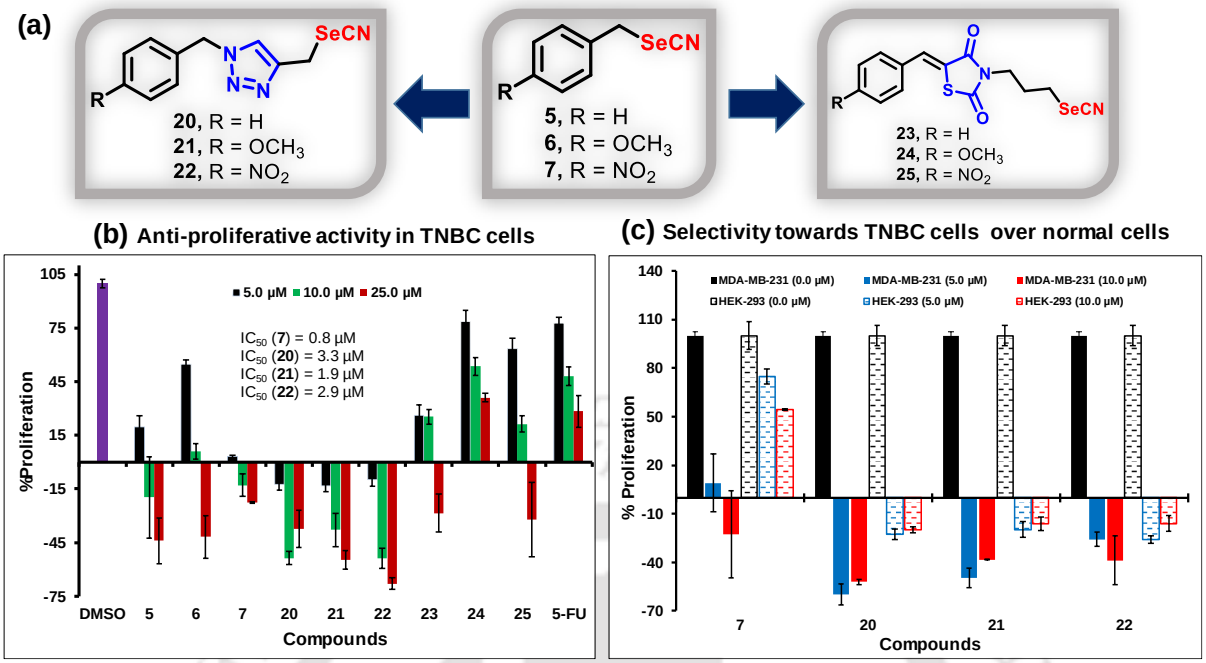

Figure 4. Brief Highlights of Chapter 3 (a) Synthetic strategies of benzylic and heterocycle-containing selenocyanates. (b) Anti-proliferative activities of the compounds in TNBC cells (MDA-MB-231). (c) Selective anti-proliferative activities towards TNBC cells over normal cells (HEK-293).

Chapter 4: Syntheses and Efficient Antioxidant Activities of Benzimidazole- and Imidazole-based Ionic Selenocyanates and the Corresponding Selenazolium and Selenazinium Selenocyanates

Chapter 4 reports for the first time the synthesis of N-substituted imidazole and benzimidazole-based ionic selenazolium and selenazinium selenocyanate from corresponding imidazole and benzimidazole-based acyclic bromides. However, we have observed in some cases where the cyclization is unfavorable due to internal ring strain, we obtained the corresponding open chain selenocyanate with a second selenocyanate moiety as counter-ion. Structures of the novel selenacycles and acyclic selenocyanates were further confirmed by NMR and single crystal X-ray diffraction studies. Following synthesis and characterization of ionic selenocyanates, we evaluated all the synthesized compounds for the antioxidant activities by *in vitro* studies such as GSH-GSSG coupled enzymatic assay and PhSH-PhSSPh coupled HPLC assay. Furthermore, activity of selected selenocyanate in scavenging endogenous ROS in RAW 264.7 macrophage cells as also evaluated, using already reported fluorescein-based fluorogenic probe in a turn-on mechanism, and compared against standard ROS quencher N-acetyl cysteine (NAC).

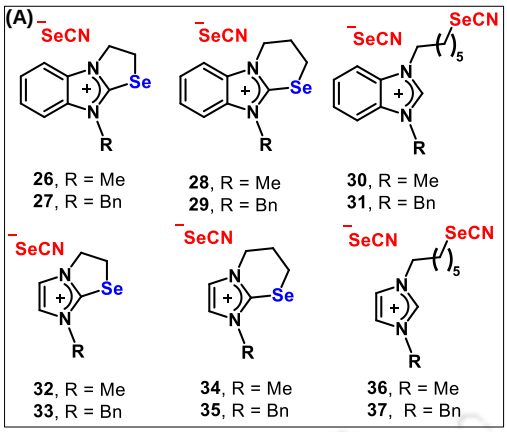

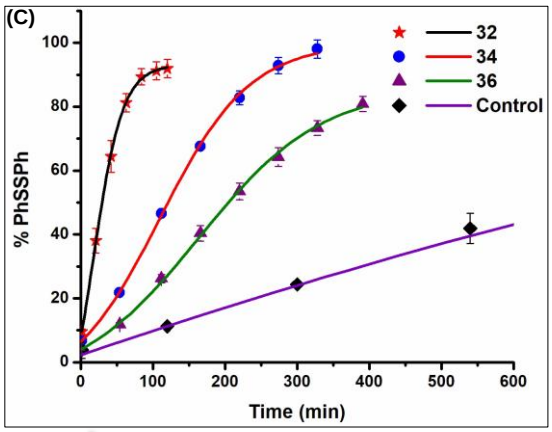

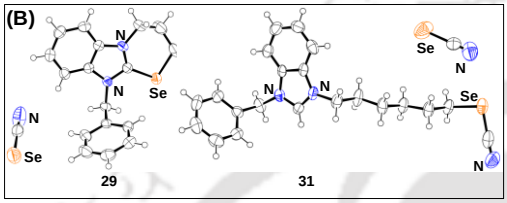

(D)

Compound	Initial Rate (μM min^{-1})		
	H_2O_2	Cum-OOH	*t*Bu-OOH
27	74.3 ± 2.9	41.0 ± 2.5	20.9 ± 3.7
30	72.6 ± 8.7	6.8 ± 0.2	2.4 ± 0.5
35	76.8 ± 6.0	12.4 ± 4.0	1.4 ± 0.5

Figure 5. Brief Highlights of Chapter 4. (A) Chemical structures of benzimidazole-based selenazolium, selenazinium and open chain acyclic selenocyanates. (B) Single crystal X-ray structures of compounds **29** and **31**. (C) Catalytic antioxidant activity of best three compounds in PhSH-PhSSPh coupled assay for the reduction of H_2O_2. (D) Catalytic antioxidant activities of best three compounds in GSH-GSSG coupled assay for the reduction of peroxides.

Chapter 5: Syntheses of Benzimidazole-based Ionic and non-ionic Selenocyanates: Impact of 4-Nitrophenyl Group towards their Anti-proliferative Activities

In **Chapter 5**, we turned our attention to understand the anti-cancer activities of benzimidazole-based ionic and non-ionic organoselenium compounds. Inspired by the reasonable antioxidant activities of benzimidazole and imidazole-based ionic compounds **26-37** in Chapter 4 and the literature reports on the anti-cancer activities of various benzimidazole-based organoselenium compounds, the anti-cancer potentials of the synthesized ionic compounds **26-37** were studied. Interestingly, benzimidazole-based acyclic selenocyanate **31** was found to be the most potent compound exhibiting anti-proliferative activity towards MDA-MB-231 cells. However, the activity of the corresponding cyclic compounds such as **27** and **29** were significantly lower. Therefore, considering the importance of selenocyanate moiety in the acyclic compound towards the anti-proliferative activity, the benzimidazole-backbone of compounds **27** and **29** was chosen to synthesize different series of related analogues **38-47** with the incorporation of

-OMe and -NO_2 groups and subsequently studied for their anti-proliferative activities. As the ionic benzimidazole-based acyclic selenocyanate could not be prepared in last Chapter due to cyclization process, a newer series of ionic selenocyanate analogues (**42-44**) were prepared upon C2-functionalization in benzimidazole ring. Additionally, a series of the corresponding neutral selenocyanates (**45-47**) were also developed. Interestingly, unlike ionic selenocyanates **42-44**, the neutral selenocyanates **45-47** exhibited significantly higher anti-proliferative activities. Particularly, as compound **47** containing 4-NO_2 group exhibited significantly higher selectivity towards triple-negative breast cancer cells (MDA-MB-231) over normal cells (HEK-293), this compound was chosen for further studies. The compound exhibits anti-migratory activity and exerts anti-proliferative activity by arresting cells in G_1 phase of the cell cycle (MDA-MB-231).

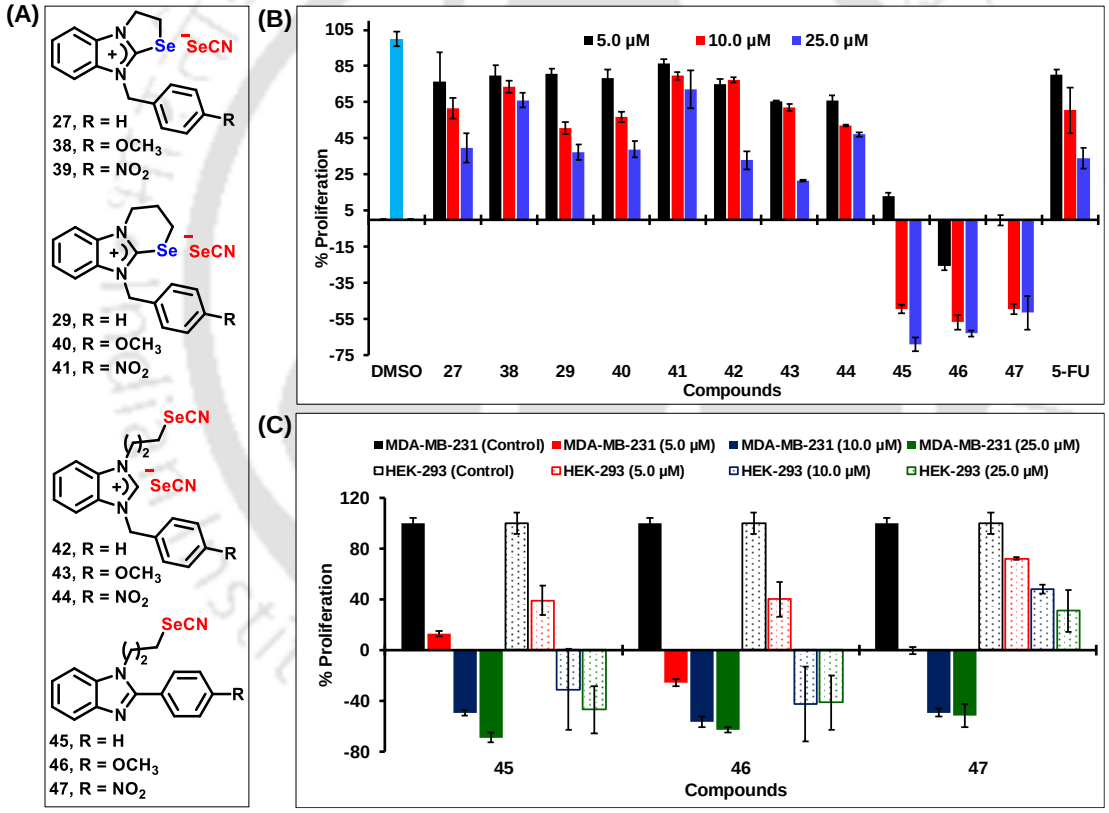

Figure 6. Schematic Overview of Chapter 5. (A) Chemical structures of the compounds synthesized and studied in this Chapter. (B) Anti-proliferative activities of the compounds in TNBC cells (MDA-MB-231). (C) Selective anti-proliferative activities of the most active compounds **45-47** towards TNBC cells over normal cells (HEK-293).

References

1. Schwarz, K.; Foltz, C. M., *J Am Chem Soc* **1957**, *79*, 3292.
2. Flohe, L.; Günzler, W. A.; Schock, H. H., *FEBS Lett* **1973**, *32*, 132.
3. Mugesh, G.; Singh, H. B., *Chem Soc Rev* **2000**, *29*, 347.
4. Cotgreave, I. A.; Duddy, S. K.; Kass, G. E. N.; Thompson, D.; Moldéus, P., *Biochem Pharmacol* **1989**, *38*, 649.
5. Wendel, A.; Tiegs, G., *Biochem Pharmacol* **1986**, *35*, 2115.
6. Chu, C. K.; Ma, L.; Olgen, S.; Pierra, C.; Du, J.; Gumina, G.; Gullen, E.; Cheng, Y.-C.; Schinazi, R. F., *J Med Chem* **2000**, *43*, 3906.
7. Inglot, A. D.; Zielińska-Jenczylik, J.; Piasecki, E.; Syper, L.; Młochowski, J., *Experientia* **1990**, *46*, 308.
8. May, S. W.; Wimalasena, K.; Herman, H. H.; Fowler, L. C.; Ciccarello, M. C.; Pollock, S. H., *J Med Chem* **1988**, *31*, 1066.
9. Reddy, B. S.; Rivenson, A.; El-Bayoumy, K.; Upadhyaya, P.; Pittman, B.; Rao, C. V., *J Natl Cancer Inst* **1997**, *89*, 506.
10. Nasim, M. J.; Witek, K.; Kincses, A.; Abdin, A. Y.; Żesławska, E.; Marć, M. A.; Gajdács, M.; Spengler, G.; Nitek, W.; Latacz, G.; Karczewska, E.; Kieć-Kononowicz, K.; Handzlik, J.; Jacob, C., *New J Chem* **2019**, *43*, 6021.
11. Das, R. K.; Ghosh, S.; Sengupta, A.; Das, S.; Bhattacharya, S., *Eur J Cancer Prev* **2004**, *13*.
12. Singha Roy, S.; Ghosh, P.; Hossain Sk, U.; Chakraborty, P.; Biswas, J.; Mandal, S.; Bhattacharjee, A.; Bhattacharya, S., *Bioorg Med Chem Lett* **2010**, *20*, 6951.
13. Roy, S. S.; Chakraborty, P.; Bhattacharya, S., *Eur J Med Chem* **2014**, *73*, 195.
14. Makrecka-Kuka, M.; Dimitrijevs, P.; Domracheva, I.; Jaudzems, K.; Dambrova, M.; Arsenyan, P., *Sci Rep* **2020**, *10*, 21595.

Chapter 1

Introduction

1.1. Cancer and its background

The word 'Cancer' was first coined by Hippocrates, a physician, who is considered as the 'father of medicine'. He actually used the term '*Carcinos*' to describe tumors, from which the term carcinoma was derived and he called cancer as '*Karkinos'*, which is a Greek word used to describe a crab. Cancer is one of the most dreaded diseases, which is actually characterized by rapid and uncontrolled cellular proliferation in certain organs. According to cancer facts and figures 2021, ACS researchers have estimated that in 2021, almost 1.9 million new cancer cases will be diagnosed and more than 6,00,000 people will die from cancer only in US.[1] Hannahan and Weinberg in their famous review "Hallmarks of cancer" (2000), described certain characteristics of cancerous cells that distinguish them from normal cells.[2] Proliferation of a normal cell is a series of interconnected mechanisms that require several signaling processes to control the lifetime of a cell. According to Hannahan *et al*, every cancerous cell has the ability to proliferate abnormally even in the absence of growth signals. As a natural defense, rapidly growing cells are generally destroyed by enzymatic pathway known as apoptosis. The cancer cells have the ability to ignore termination signals thereby evading apoptosis. Moreover, the cancer cells acquire the ability to develop blood vessels by the process of angiogenesis for the supply of nutrients. Additionally, the cancer cells develop the ability to travel to remotely located unaffected organs, thereby infecting them as well. In addition to cancer cells, tumors are closely related to cancer and pose a great deal of complexity. Tumors are conglomerate of tissues containing multiple cell types possessing the six traits such as i) sustaining proliferative signaling, ii) evading growth suppressors, iii) resisting cell death, iv) induction of angiogenesis, v) activating metastasis and vi) enabling replicative immortality. Some of the causative agents of cancer are represented in Figure 1.1, which include one or several factors such as environmental toxins, carcinogens, aging, DNA damage, non-coding genes and so on.[3] Due to the ever increasing hazards it poses towards human living system, accurate and proper treatment of the same demands early diagnosis and immediate attention in the modern society.

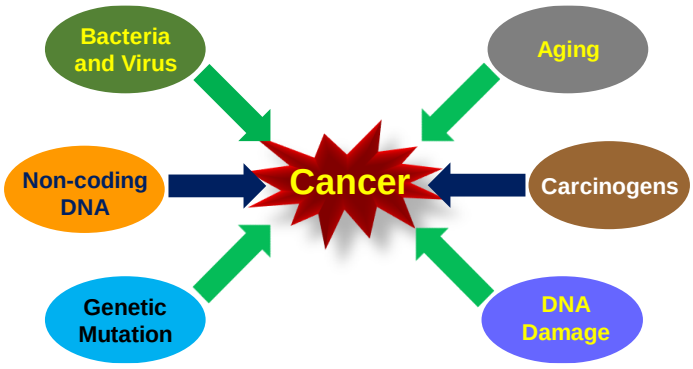

Figure 1.1. Some of the key factors that induce cancer.

1.2. Different stages of cancer development

The first stage of cancer development is initiation, mediated by initiators. Many initiators may either interact directly with DNA or they may undergo metabolism/modification by drug-metabolizing enzymes to generate active initiators for their interactions with DNA. Impacts of initiators are mostly irreversible in nature and are generally carried over to the daughter cells. Once the DNA of a cell is modified by initiators, it becomes vulnerable to promoters and they have no effect if the cells are not previously damaged by initiators. Proliferation of the infected cells, give rise to abundant quantities of daughter cells containing the mutation caused by initiators. In contrast to initiator, promoters do not covalently bind with macromolecules or DNA within the cells. Rather, promoters sequester with the cell surface to affect the physiological pathways that lead to increased cellular proliferation. The term 'progression' refers to the transformation of the benign tumor to neoplasm and finally to malignant cells. Progression is associated with karyotypic change since virtually all tumors that advance is aneuploid *i.e.* having the wrong number of chromosomes. This karyotypic change is coupled with an increased growth rate, invasiveness, metastasis and an alteration in biochemistry and morphology.[4,5,6]

It is important to classify the progression of the cancer cells in order to segregate patients according to the extent of progression of cancer and aid in treatment planning.[7] In the year of 1993, The Union for International Cancer Control (UICC) introduced the TNM convention to classify different stages of cancer progression. Broadly speaking, TNM classification describes the extent of cancer in patients. The presence of tumors at the primary site is characterized by T, the presence or absence of tumors in the lymph nodes is denoted by N, and the presence or absence of metastasis beyond the lymph node is denoted by M. Additionally, tumors are classified into clinical staging (cTNM), and

post-surgical intervention (pTNM). Furthermore, there are subdivisions of the above notations. T phase is classified into 4 major parts (T1 to T4) that depends upon the increasing size and spread of the tumors, N and M are subdivided into two categories (0 and 1) indicating presence or absence of tumor.[8]

The tumor growth from a genetically modified cell is a step-wise process. Similar to solid tumors such as carcinoma or sarcoma, blood cell tumors follow a similar developmental progress. However, since the cells float freely, they are not limited to only one location. Various phases of tumor development are described as follows.

Hyperplasia. This is a condition where the altered cells undergo uncontrolled proliferation leading to high accumulation of cells at a particular region possessing normal cellular appearances.

Dysplasia. This is a condition in which, additional genetic modifications accompany the hyperplasic cells. Unlike in hyperplasia, the appearance of the cells changes significantly in this stage with cells and tissues disorganized completely.

Carcinoma. This condition is characterized by further genetic modifications accompanying infected cells and the cellular appearance changes more significantly. Infected cells spread over to a larger area and they often "regress" therefore becoming more primitive in their capabilities. Cells of this type are termed as anaplastic or de-differentiated. An important feature of carcinoma is that infected cells often remain within the initial location without crossing the basal lamina to invade other tissues. Cancers in this stage is often completely curable by surgery. However, cells of these types have the capability to become invasive and develop malignant growth.

***Cancer* (*malignant tumors*)**. These tumors have the ability to spread to other organs and tissues/organs and metastasize outside the region of local tissue. These metastatic tumors possess the most invasive form and account for major number of cancer death. However, there are some tumors, termed as benign tumors that are cancerous but do not spread beyond their initial locations to invade distantly located tissues. Strictly, they are not cancerous, but they can pose severe health issues. Very matured benign tumors can put pressure on the nearby organ and can cause serious problem. For example, in brain, the limited space within the skull poses fatality threat for the overly matured brain tumors. It has been observed that, multiple genes are differentially expressed between metastatic and benign tumor models and several genes have the capability to suppress or induce metastasis. For instance, nm23 and Elm1 genes have been shown to suppress the

metastatic activity of the cancer cells by forced expression, while p9Ka/mta1 gene functions as inducers of metastasis.[9,10,11] part from these, several other genes such as KAI1, KiSS1 and Tiam1, obtained by molecular methods, were also observed to suppress or induce metastasis.[12,13,14]

1.3. Natural defense against the progression of cancer

During the progression of cancer in human system, infected cells undergo programmed cellular death or apoptosis by complex signaling mechanism. Apoptosis has been established as one of the most important mechanism of anti-cancer defense. The proliferation of cells is closely monitored by controlling the rate of destruction of infected cells apart from controlling the cellular division. According to the definition in "Hallmarks of Cancer", cancer is characterized by uncontrolled proliferation of cells in a living system. Under this condition, a complex network of signaling mechanism is triggered and the cells "commit suicide" by activating an intracellular death program, called programmed cell death. Programmed cell death is also called "apoptosis" (from a Greek word meaning "falling off"). However, according to the currently accepted biological models, there are grossly two main types of cell death namely apoptosis and necrosis. Apoptosis is the mechanism of cell death that is brought about by activation of certain protease enzyme of caspase family, such as caspase 3.[15] It may be classified into two broad categories such as extrinsic and intrinsic apoptosis. While extrinsic apoptosis is initiated by extracellular stimulation acting on plasma membrane receptors, intrinsic apoptosis follows the permeabilization of mitochondrial membrane driven by intracellular stimulus.[16]

1.4. Conventional treatments of cancer

Cancer treatment has observed several modifications and improvements throughout the course of time not only due to the ineffectiveness of treatments and side-effects, but also due to the failure in complete remission or cure in several cases. Modern treatment of cancer includes a vast array of techniques which are discussed below.

1.4.1. Surgical treatment. One of the most popular technique in treatment of cancer is the surgical procedure, in which the entire benign or malignant tumor is removed either by open surgical or by minimally non-invasive means. In open surgery, one large hole is made, through which the tumor along with some healthy tissues associated with the closely occurring lymph nodes is removed. In minimally non-invasive procedure, one or

multiple small holes are made, through which tumors are removed by specialized surgical tools. However, surgical treatment suffers from severe limitation of less precision in removing the complete tumor, therefore giving rise to a chance of recurrence.[3]

1.4.2. Radiation therapy. Radiation based treatment is a very popular method in cancer treatment, where a very high dose of radiation (γ-ray, high energy X-ray, or proton beam) is bombarded to accurately destroy the malignant tumor within an organ. It is primarily used in cases of brain tumor where normal surgical procedure is rendered impossible. Unfortunately, this technique is limited due to the harshness on the cells in vicinity of the cancer cells.[3]

1.4.3. Chemotherapy: Among the various available strategies to defend cancer, the most widely used one is chemotherapy. In this particular treatment, certain drugs or combination of drugs are administered to patients by means of oral, intravenous or intraperitoneal. However, the limitation of this treatment is that, rapidly growing normal cells such as hair cells, bone marrow cells are also targeted and destroyed by these treatments. Additionally, such drugs are non-specific towards dormant cells, which can lead to post-treatment recurrence. Furthermore, several chemotherapeutic drugs suffer from the limitation of poor bioavailability in biological media and uptake in cancer cells. With detailed understanding of the molecular mechanism of cellular proliferation and cancer progression, it is now possible to design highly specific compounds that may be administered single or in combination to minimize the overall toxicity.[3]

1.4.4. Nanomedicines in cancer therapy: Nanoparticles are small systems, typically having the size from 1 – 1000 nm.[17] Due to their high surface-to-volume ratio, they give rise to several interesting surface properties. Biocompatible nanoparticles are utilized in cancer treatments to address some of the drawbacks of conventional therapy such as low specificity and poor bioavailability of drugs.[18] Hence, encapsulation of active anti-cancer agents within appropriate nanoparticles and specific release at the target site serves as one of the most important strategies in cancer treatment.

Organic nanoparticles such as liposomes and micelles are excellent delivery agents for anti-cancer drugs. Liposomes are spherical particles having lipid bilayers, that are used to encapsulate hydrophilic drugs in their aqueous core.[19] On the other hand, micelles have a hydrophobic core that are mainly used to encapsulate hydrophobic drugs.[20] The

first nanoparticle, approved by FDA for AIDS-associated Kaposi's sarcoma is Doxil, which is doxorubicin-loaded PEGylated liposomes.[21] Several modifications such as DaunoXome and Myocet had been approved by FDA following the success of Doxil.[22,23,24]

Polymeric nanoparticles are made up of biocompatible or natural polymers such as poly(lactide-co-glycolide), poly(ε-caprolactone), albumin etc. Abraxane which is albumin-paclitaxel conjugate, is a widely successful FDA-approved formulation, for the treatment of pancreatic ductal adenocarcinoma and metastatic breast cancer. This process of enhancing the specificity of the active anti-cancer drug by conjugating it with nanoparticles is an example of passive targeting.[25] However, passive targeting is sometimes difficult to control and can lead to multidrug resistance (MDR).[26]

1.4.5. Targeted therapy: In order to avoid the drawback of passive targeting by nanoparticles, strategies are developed to enhance the uptake of the therapeutic agents by active targeting certain specific receptors overexpressed by tumor cells. Of special mention, folic acid and biotin are small molecules whose receptors are over-expressed by tumor cells.[27] Therefore, several nanoparticles are functionalized with biotin or folic acid, in order to active targeting cancer cells. Moreover, several peptides are also important agents in targeted cancer therapy. For example, angiopep-2 binds to low-density lipoprotein receptor-related protein-1 (LRP-1) of endothelial cells in the blood-brain barrier. Owing to this property, this peptide has attracted special attraction in the treatment of brain cancer.[28]

Antibodies are one of the most widely exploited ligands for active targeting. Antibodies are proteins which have Y-shaped arms, that are responsible for the selective interaction with the antibodies.[29] Exploiting this property, certain antibodies can be used to target antigens such as HER2, EGFR, TfR-specific antigens, that are over-expressed on cancer cells.[30] Rapamycin-PLGA nanoparticle conjugated to EGFR antibody exhibited significant cellular uptake by MCF-7 cells.[31]

1.5. Different types of chemotherapeutic drugs and common side effects

Different chemotherapeutic drugs may be classified under broad categories depending upon the mechanism of their action. Some drug may be classified under more than one category as they have multiple mode of action. The general categories of classification

of chemotherapeutic drugs are as follows. Few representative compounds of specific categories are depicted in Figure 1.2.

1.5.1. Alkylating agents. Drugs like *cis*-platin (**1.1**), carboplatin (**1.2**), oxaliplatin (**1.3**) perform direct DNA damage by breaking DNA double strands and arresting the rapid proliferation of cancer cells. These types of drugs are useful in all stages of cancer and are particularly useful in lymphoma, leukemia, Hodgkin's disease etc. Apart from platinum metal-based drugs, several nitrogen mustard derivatives such as cyclophosphamide (**1.4**), chlorambucil (**1.5**) are also used as an alkylating agents against cancer. However, applications of alkylating agents do suffer from the limitation of damaging bone marrow cells. Additionally, such drugs may cause leukemia upon prolonged dosage that may start 5 to 10 years' post-treatment.

1.5.2. Antimetabolites. Drugs like 5-fluorouracil (**1.6**), gemcitabine (**1.7**), 6-thioguanine (**1.8**) are analogues of specific fragments of DNA and RNA and upon treatment, they arrest the synthesis of RNA and DNA. Specifically, they arrest the growth of the cell in S-phase and are particularly useful for the treatment of leukemia, ovarian cancer, intestinal cancer etc.

1.5.3. Anthracyclines. Certain kind of antibiotics such as daunorubicin (**1.9**), doxorubicin (**1.10**) that target the enzyme for the replication of DNA and hence influence the growth of cancer cells in all phases of cell cycle. These types of drugs have a major limitation of damaging the heart if the dosage increases a certain critical limit.

1.5.4. Topoisomerase inhibitors. Drugs like topotecan (**1.11**), irinotecan (**1.12**), etoposide (**1.13**) are topoisomerase inhibitors inhibit the unwinding of DNA and hence stop DNA replication. These types of drugs are used to treat leukemia, ovarian, gastrointestinal and some forms of lung cancer.

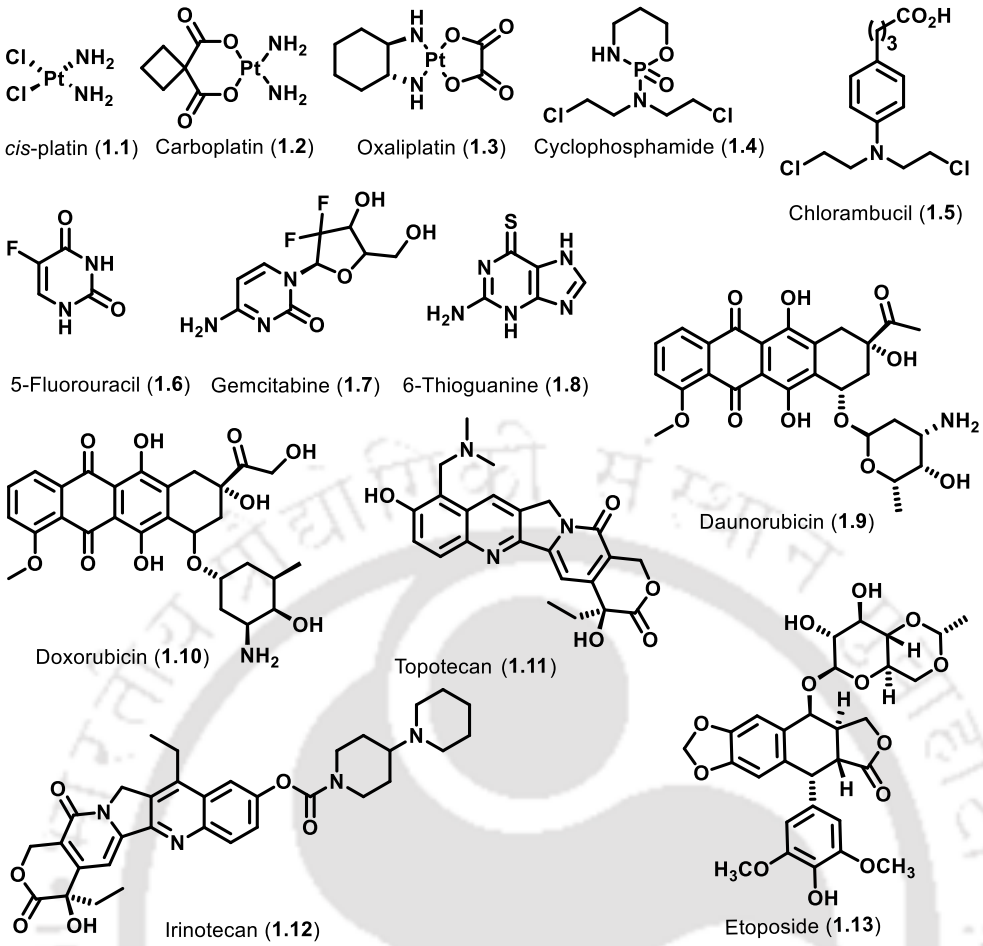

Figure 1.2. Chemical structures of some of the commonly used chemotherapeutic drugs.

1.6. Biological generation of reactive oxidants and its natural detoxification

Reactive oxidants are highly reactive intermediates or free radicals that can lead to rapid chemical modifications. In case of aerobic organism, due to essential cellular metabolism, highly reactive oxidants such as superoxide radical anion, hydroxyl radical and hydrogen peroxide is produced as a by-product.[32] These three species mentioned above, in conjunction with some other unstable intermediates formed from the peroxidation of lipids, are collectively known as reactive oxygen species (ROS). In addition to ROS, certain highly reactive nitrogen species (RNS) such as peroxynitrite, generated from diffusion-controlled reaction of superoxide and nitric oxide are also considered as strong biological oxidants. The production of ROS and RNS from oxygen in mitochondria, as a result of aerobic metabolism is outlined in Scheme 1.1.

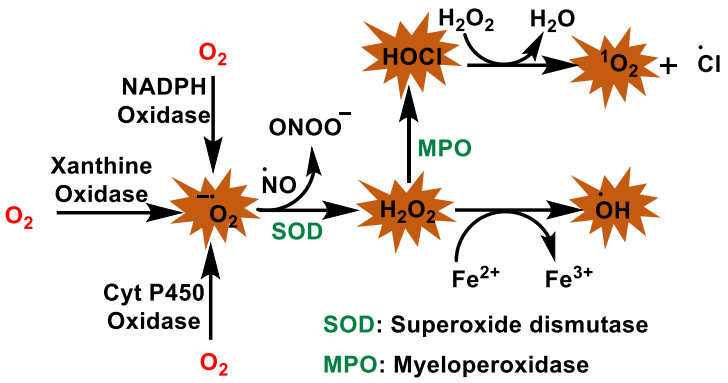

Scheme 1.1. Mechanism for generation of reactive oxygen and reactive nitrogen species.

In the mitochondria, the oxygen is metabolized into superoxide species ($O_2^{\cdot-}$) by the action of oxidative enzymes. The produced superoxide is rapidly dismuted into hydrogen peroxide (H_2O_2) by the action of superoxide dismutase (SOD). The generated H_2O_2 is catalytically reduced to water by the action of antioxidant enzymes such as catalase (Cat) and glutathione peroxidase (GPx). The antioxidant enzymes thus maintain the redox balance and cellular homeostasis in normal cells. However, over-expression of oxidative enzymes or down-regulation of antioxidant enzymes may produce and accumulate higher level of ROS inside the cells, leading to the condition known as 'oxidative stress'. Essentially, oxidative stress is a condition caused due to upset of the balance between generation of ROS and their detoxification mechanism.

1.7. Reactive biological oxidants and their role in progression of cancer

It is well established that oxidative stress is intricately related to the proliferation of cell. At lower concentration, ROS can promote cell survival by Akt-mTOR and nuclear factor kB (NF-kB) mediated pathways. Additionally, ROS at lower concentration upregulates different cyclins, hence promoting cellular passage in through G_1/S and G_2/M phase. However, at higher concentration, ROS induces apoptosis by the release of cytochrome C that triggers apoptosis by caspase cascade. Additionally, higher level of ROS also has damaging effect on lipid layer and DNA.[33,34] Hence, any means to detoxify the ROS either by restoring the enzyme balance or by administering antioxidants, may serve as an important strategy to defend cancer.

1.7.1. Cancer metastasis and ROS

Metastasis involves progression of cancer from primary tumors to surrounding tissues and to remote organs, which is considered as the primary cause of morbidity and mortality.[35] Epithelial to mesenchymal transition (EMT) is a significant cause of cancer metastasis and ROS plays a significant role in the induction of EMT. Several studies reveal that ROS enhances tumor migration by inducing hypoxia mediated matrix metalloproteinase (MMP) and cathepsin expression, that leads to the induction of cancer metastasis.[36,37]

1.7.2. Angiogenesis and ROS

During the early stages of tumorigenesis, the formation of new blood vessels from pre-existing vacuoles is known as angiogenesis, and this process leads to tumor proliferation and survival. ROS-dependent angiogenesis is initiated through cancer proliferation and increases the metabolic rate leading to generation of higher ROS levels.[38] It is established through several studies that both exogenous and endogenous ROS induces stimulation of growth factors, cytokines and transcription factors such as vascular endothelial growth factor (VEGF), hypoxia-inducible factor 1-alpha (HiF-1α) leading to promotion of tumor migration and proliferation through ROS-dependent cellular signaling.[39,40,41]

1.7.3. Cellular apoptosis and ROS

Reactive oxidant species has proved to be highly potent in inducing apoptotic cell death, which provides an excellent strategy in cancer treatment. Mechanistically, ROS ruptures the mitochondrial membrane and opens the mitochondrial permeability transition pore, resulting in the release of cytochrome-c in the cytosol. Once released, together with Apaf-1 and pro-caspase-9, cytochrome-c forms apoptosomes leading to the activation of caspase-9. Caspase-9 in turn activates caspase-3 that results in the cleavage of cellular proteins and induces apoptotic cell death.[42,43,44]

1.8. Selenoenzymes and organoselenium compounds as potential antioxidants

As described earlier, oxidative stress is caused by the imbalance between generation of ROS and the ability of the biological species to detoxify those reactive intermediates. However, several selenium-containing enzymes such as glutathione peroxidase (GPx), thioredoxin reductase (TrxR), Type-I iodothyronine deiodinase (ID-I) provide an internal mechanism of defense against oxidative stress by catalyzing the reduction of harmful peroxides into water, with the help of thiol cofactors. Structures of above-

mentioned selenium-containing enzymes are described in Figure 1.3. The selenocysteine (sec) residue at the active site of GPx forms a catalytic triad with tryptophan and glutamine that activates the selenium center for efficient reduction of the peroxide. It has now been well-established that 2-phenyl-1,2-benzoselenazole-3-one (ebselen) functions as glutathione peroxidase mimic both *in vivo* and *in vitro*.[45] This further inspired extensive research by various research groups to develop different series of synthetic mimics of GPx including ebselen analogues and related organoselenium compounds either by modifying the basic structure of the ebselen or by introducing some of the structural features present at the active site of the native enzymes. The catalytic cycle of GPx involves glutathione (GSH) as co-factor. The selenium center of the selenocysteine residue undergoes redox reactions in the presence of GSH and H_2O_2 forming intermediates of selenol (GPx-SeH), selenenyl sulphide (GPx-SeSG), selenenic acid (GPx-SeOH), and selenonic acid (GPx-SeO_2H)

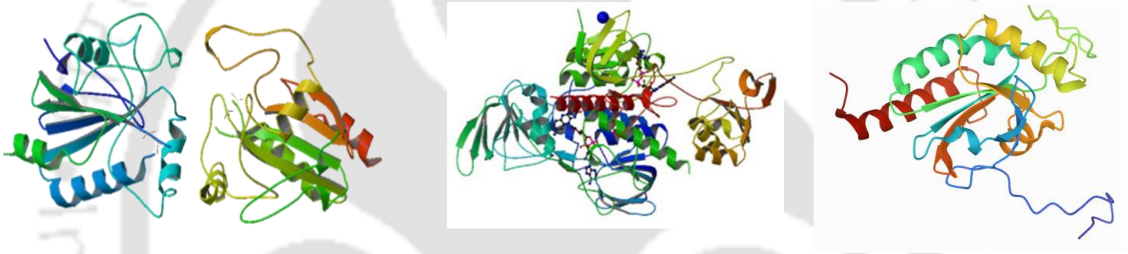

(a) GPx **(b) TrxR** **(c) ID-I**

Figure 1.3. X-ray crystal structures of antioxidant enzymes such as (a) GPx (PDB ID: 1GP1), (b) TrxR (PDB ID: 5M5J) and (c) ID-I (PDB ID: 4TR4).

Similarly, ebselen also exhibit significant catalytic activity in reducing peroxides in the presence of GSH as cofactors. Presence of similar intermediates are also observed for the redox process. However, the catalytic activity of ebselen is highly controversial and ebselen has been shown to be a poor catalyst for reducing peroxides in the presence of aromatic or benzylic thiols as co-factors. The catalytic cycle of ebselen is explained in Scheme 1.2, which involves the facile ring opening of the ebselen leading to intermediates such as selenenyl sulfide, selenol and selenenic acid.

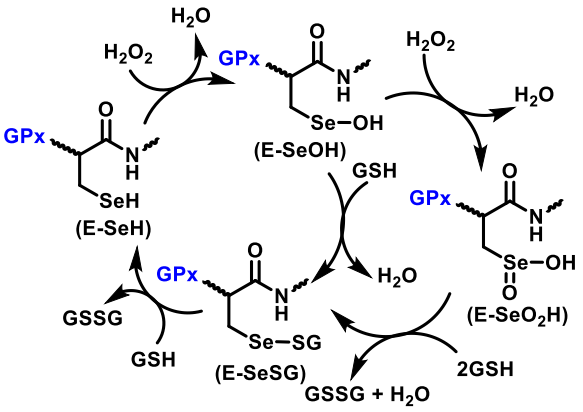

Scheme 1.2. Catalytic cycle of GPx for the reduction of H_2O_2 in the presence of GSH.

Although successful mimics of thioredoxin reductase and iodothyronine are not successful, several GPx mimics are synthesized in order to have a better insight at the chemistry of GPx at the active site. Different category of organoselenium compounds are being developed by various research groups over last few decades as synthetic GPx mimics that are capable of catalytically reducing peroxides via similar or different catalytic cycles. Strategically, novel GPx mimics are designed by modifying the basic skeleton of ebselen or by incorporating certain structural features of GPx within small molecules. Based on the literature reports, the synthetic mimics can be classified into three major categories (i) cyclic selenenyl amides containing Se-N bonds (ii) aromatic or aliphatic monoselenides (iii) diaryl diselenides. Representative synthetic mimics from each class is discussed in Figure 1.4.

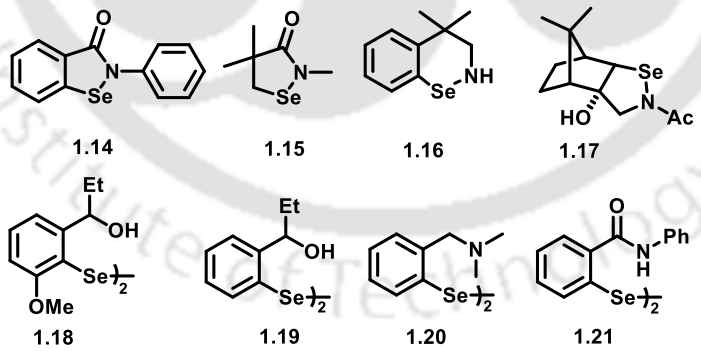

Figure 1.4. Chemical structures of some literature reported small-molecule GPx mimics.

Ebselen (**1.14**, 2-phenyl-1,2-benzoisoselenazol-3-(2H)-one) is one of the most widely studied organoselenium compounds that underwent clinical trial and exhibits antioxidant and other biological activities both *in vitro* and *in vivo* systems. Ebselen is shown to be highly potent in scavenging several biological reactive oxidants such as ROS and/or

RNS, and the rate of the peroxynitrite scavenging is about three times faster than that of naturally occurring small molecules such as ascorbate, cysteine, and methionine.[46] Following the excellent antioxidant, anti-inflammatory and cytoprotective properties of ebselen (**1.14**) several novel synthetic organoselenium antioxidants were introduced bearing structural resemblance with ebselen. Compounds **1.15** – **1.17** feature Se-N linkage similar to ebselen, that gets converted to selenol species upon reaction with excess thiophenol.[47,48,49] On the other hand, **1.18** – **1.21** contains diselenide bond that gets reduced to selenol by the action of thiol present in the biological system.[50, 51, 52] The presence of proximal amine functionality aids in weak non-bonding interaction in compounds **1.18** – **1.21** that leads to enhancement of the reactivity of the selenium center towards thiol, by weakening the diselenide bond.

1.9. Importance of selenium compounds in cancer treatment

In the year of 2000, Conklin reported for cancer patients under the administration of chemotherapy, several dietary supplements such as Vitamin E, Vitamin C, carotenoids, polyphenols can act as potential antioxidants and attenuate the harmful toxicity of the chemotherapeutic drugs.[53] However, controversies exist, where it is reported that, chemotherapeutic drugs that induce oxidative stress to destroy cancer cells by inducing caspase-mediated apoptosis, gets attenuated by the antioxidant supplements.

It must be noted that, a clinical trial, named SELECT, was carried out by South-west oncology group (SWOG), which was designed to evaluate the role of Vitamin E and Selenium in the prevention of prostate cancer when taken as dietary supplements, alone or in combination.[54] The result indicated greater occurrence of prostate cancer in test group, administered with only Vitamin E alone. It is interesting to note that, there was no increase in prostate cancer occurrence in test group under the administration of Vitamin E and Selenium in combination, indicating the protective effect of selenium by attenuating the increased risk associated with the administration of Vitamin E alone.

1.9.1. Pharmacodynamics of selenium in normal and malignant cells

Various cellular processes and molecular pathways that may be involved in cancer development and progression are affected by selenium containing compounds.[55] These include, but not limited to the following points.

(i) Antioxidant selenoenzymes help in minimizing the DNA damage, oxidative stress and inflammation.

(ii) Selenoamino acids induce over-expression of phase II detoxifying enzymes that leads to detoxification of carcinogens more efficiently and reduce genetic mutation by DNA alteration and adduct formation.

(iii) Organoselenium compounds enhance immune response including cytotoxic lymphocyte and natural killer cell activity.

(iv) Selenoenzymes induce overexpression of tumor suppressor protein p53 that inhibits the proliferation of malignant cells, repairs DNA and promotes apoptotic activity by acting as transcription factor of several genes such as GADD genes. Additionally, selenoenzymes lead to the inactivation of protein kinase C, a signaling receptor that plays crucial roles in tumor promotion by antioxidants.

(v) Organoselenium compounds interfere in the cell cycle process, leading to DNA repair to take place. Furthermore, they are shown to induce apoptosis by sequential activation of several caspases and inhibition of angiogenesis, resulting in cellular homeostasis.

Despite several beneficial effects of organoselenium compounds and selenoenzymes in controlling cancer, there are challenges involved while using organoselenium compound sin combination with chemotherapeutic drugs in cancer patients. It is still grossly unknown, which form and dosage of selenium is most effective and has the highest differential impact towards malignant and non-malignant cells. Although, clinical dose of selenium is mainly guided by pharmacokinetic profile, the pharmacokinetic and pharmacodynamic relationship is not well-established in human model.

1.9.2. Efficiency of selenium compounds as antitumor agents

Although, selenium is selectively cytotoxic towards cancer cells at higher doses, they have greater ability to augment the anti-cancer efficiency of chemotherapeutic drugs in cells and tumor xenograft models. However, their efficiency depends on the nature of the chemotherapeutic drugs and the xenograft models being used in the study.[29] For example, both methyl selenocysteine and selenomethionine were superior to sodium selenite in combination with irinotecan while administering orally against head and neck squamous cell carcinoma xenograft at a dose of 200 µg/day. On the other hand, sodium selenite and selenomethionine were dosimetrically equipotent and effective when administered in combination with *cis*-platin in ovarian cancer xenograft model.[56,57] In a study by Asfour *et al* in 2007, the impact of high doses of sodium selenite on the

expression of Bcl-2 was studies in fifty patients with non-Hodgkin lymphoma (NHL). The patients were given 0.2 mg/Kg/day of sodium selenite along with standard chemotherapeutic drug for 30 days and compared to the control group treated with only the standard chemotherapeutic drugs. Interestingly, it was observed that sodium selenite administration significantly declined the Bcl-2 level in patients after the therapy with improve clinical outcomes.[58]

1.10. Small molecule selenium compounds as anti-cancer agents

Selenium serves as an essential micronutrient in the human body due to its essential biological functions. Selenium is present in human body in several forms of selenoproteins or selenoenzymes, as a part of selenoamino acids. These selenoenzymes regulate many biological processes such as thyroid hormone regulation, redox homoeostasis, carbohydrate metabolism, inflammatory and immunological response and so on.[59]

1.10.1. Inorganic selenium compounds

Among the inorganic selenium compounds, the most studied one is sodium selenite (**1.22**). As reported by Rudolf *et al* in 2008 sodium selenite exhibit anti-cancer activities by several pathways that include induction of apoptosis via p53 mediated caspase pathway, arresting cell cycle by inhibiting p21 and induction of ROS inside cells.[60] Moreover, it overexpresses Bax protein, which is the downstream regulator of apoptosis. Additionally, in 2011, Freitas and co-workers have shown that the combination therapy comprised of sodium selenite and docetaxel work synergistically and exhibited much higher efficiency for the inhibition of cellular growth (74 % growth inhibition) than the individual efficacy of docetaxel or sodium selenite.[61] However, it suffers from the limitation of having relatively higher toxicity, with a lethal dose of 0.5 mg/Kg, which is just 2.5 times higher than the essential dietary supplemental requirement.

1.10.2. Selenoamino acids

Among the organic selenium compounds one important class of naturally occurring compounds are selenoamino acids such as selenocysteine, selenomethionine and methyl selenocysteine. Fan and co-workers (2017) showed that selenocysteine (**1.23**) expresses both Caspase 8 and Caspase 9, thus inducing both intrinsic and extrinsic pathways, respectively.[62] Moreover, their results also revealed the induction of S-phase arrest of human glioma cells by selenocysteine. Furthermore, it has also been confirmed that

inhibition of MAPK and AKT/PI3K pathways form a central mechanism of inhibition of cell survival pathway. As reported by Redman and co-workers, in the year of 1998, selenomethionine (**1.24**) exhibited promising cytotoxic activity against a panel of cancer cell lines such as MCF-7 (IC_{50} = 45.0 µM), UACC-375 (IC_{50} = 50.0 µM), DU-145 (IC_{50} = 40.0 µM) with considerable selectivity towards normal diploid fibroblast cells (IC_{50} = 1.0 mM).[63] Additionally, in another report in 2017, Marshall and co-workers (2017), reported that methyl selenocysteine **(1.25**) gets converted *in vivo* to methyl selenol exhibiting profound anti-cancer activity.[64]

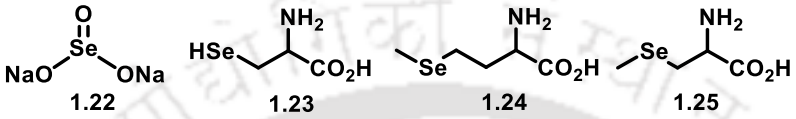

Figure 1.5. Chemical structures of sodium selenite (**1.22**), selenocysteine (**1.23**), selenomethionine (**1.24**) and methyl selenocysteine (**1.25**).

1.10.3. Selenoproteins

Additionally, in human living system, genes are encoded for around 25 selenoproteins such as glutathione peroxidase (GPx), Thioredoxin Reductase (TrxR), which are important in cancer defense. However, the role of TrxR in cancer defense is controversial. Summarily, the thiol moiety in TrxR detects an increasing oxidative stress, and triggers a signaling cascade that encodes for antioxidant proteins.[65,66] However, it has also been found that TrxR has a favorable tumorigenic role in case of well advanced tumors. On the other hand, GPx is a well-established antioxidant protein, which serves as a natural defense against oxidative stress build-up. Mechanistically, the selenol moiety of selenocysteine residue of GPx reduces hydrogen peroxide to water and itself gets oxidized to selenenic acid, which further regenerates the selenol form by two equivalents of reduced glutathione. Hence it is evident that, thiol moiety in both the proteins contribute significantly to the antioxidant nature of the proteins.

1.11. Small-molecule organoselenium compounds as anti-cancer agents

1.11.1. Ebselen and related selenazole analogues as anti-cancer agents

As mentioned earlier, ebselen (**1.17**) is an excellent mimic of GPx and therefore serves as a strong antioxidant. Apart from the antioxidant properties of **1.17**, elaborate works by Zhang *et.al*. (2014) has proved the anti-cancer and anti-proliferative effects of ebselen on multiple myeloma (MM) cells with an IC_{50} of 40.0 µM. In ebselen-treated multiple myeloma cells at a concentration of 40.0 µM, it was shown that the rate of apoptosis

gradually increases as a function of time.[67] Following the promising activity of **1.17**, wide number of synthetic ebselen analogues have been made to further enhance the anticancer activity and improve the selectivity of the synthesized compounds. Some of the representative compounds are listed in Figure 1.6. A closely related analogue known as ethaselen or 1,2-[bis(1,2-benzisoselenazolone-3(2H)-ketone)]ethane (**1.26**), has been extensively studied for its anti-cancer activity by several research groups. In the year of 2006, Zhao documented the anti-cancer activity of ethaselen (**1.26**) on A-549, HeLa, Bel-7402, BGC823 and KB cells in terms of TrxR inactivation and cellular proliferation inhibition. It has been found that, **1.26** reduced the activity of TrxR at doses of 5.0 μM and 10.0 μM with respect to untreated control.[68]

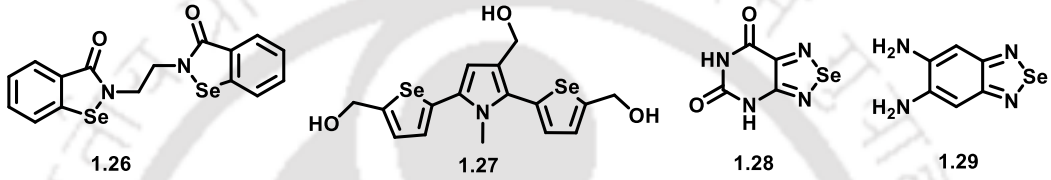

Figure 1.6. Chemical structures of ebselen and some related selenazole analogues.

Certain selenium containing 5-membered rings have been prepared and evaluated for their anti-cancer activities. Notably, selenophene class of compound **1.27** or 2,5-bis(5-hydroxymethyl-2-selenienyl)-3-hydroxymethyl-N-methylpyrrole, displays highly promising activity as neoplastic agent in a wide variety of cancer cell lines, having very high selectivity towards cancer cells over normal cells and having high effectivity against multi-drug resistant cancer cells. Mechanistically, it was found to induce cell death through p53 and mitochondria-mediated apoptotic pathway. Additionally, this compound exhibited strong anti-tumor activity in mouse xenograft model of human renal carcinoma.[69,70]

Certain selenadiazoles attracted special attraction, in the past decade owing to their significant potential as anti-cancer agents. Arsenyan and co-workers in the year of 2008, designed and synthesized an array of 20 selenadiazole compounds and evaluated their activity against murine cancer models with the most active compound being compound **1.28** or 1,2,5-selenadiazolo-[3,4-d]-pyrimidine-5,7-(4H,6H)-dione. This compound was found to be toxic towards a number of human cancer cells such as melanoma, hepatoma and breast cancer cells, by inducing both intrinsic and extrinsic apoptosis.[71]

In the year of 2014, Zhang and co-workers developed a novel selenodiazole compound **1.29** or 4-(benzo[c][1,2,5]-selenadiazol-6-yl) benzene-1,2-diamine and tested it against

different human cancer cell lines. Interestingly, all the compounds were effective at micromolar doses against all tested cell lines with high selectivity over normal cells. Detailed mechanistic insights confirmed the activation of caspase-dependent mitochondrial mediated apoptotic cell death as a consequence of Akt-dephosphorylation and p53 activation.[72]

1.11.2. Diselenides and monoselenides as promising anti-cancer agents

A wide array of diselenides comprising of a series of dipyridazinyl diselenides, substituted diaralkyl diselenides, substituted dipyridinyl diselenides, have been evaluated for anti-proliferative ability against human breast cancer cells (MCF-7). Few selected compounds are described in Figure 1.7. Chloro-substituted pyridazine derivative **1.30** showed highest activity against MCF-7 cells with an IC_{50} of 10.3 µM in a dose-dependent manner. Additionally, other compounds (**1.31** – **1.36**) in the series exhibited higher potency than 5-FU against MCF-7, suggesting higher anti-proliferative activity of the organoselenium compound.[73]

Nedel in the year of 2012, determined the anti-proliferative activity of diselenide **1.37** in HT-29 cells. It was proposed by them that such action was produced through the activation of caspase-dependent and independent pathways, apart from cell-cycle arrest.[74] In a study by Rizvi and co-workers in the year 2014, cytotoxic and apoptotic potential of diselenide (**1.38**) has been confirmed through DNA cell cycle analysis and through microscopic monitoring of the formation of apoptotic bodies.[75] Among the other compounds in the series, diselenide **1.38** exhibited highest inhibition of cellular proliferation, having an IC_{50} of 8.0 µM in HL-60 cells. Furthermore, the cytotoxic effect of compound **1.38** on other organ-specific cancer cells such as PC-3 (prostate), MCF-7 (breast), MIA-PA-Ca-2 (pancreas), and HCT-116 (Colon) cancer cells had also been evaluated with an IC_{50} of 13.0, 18.0, 25.0 and 27.0 µM, respectively. Following further investigation, the authors reported cell cycle arrest at S-phase and induction of apoptosis of HL-60 cells through the mitochondrial-dependent pathway, following treatment of the cells with compound **1.38**.

Additionally, elaborate works by Plano and co-authors (2010), screened several symmetrical diselenides in different organ-specific cell lines such as MCF-7, PC-3, CCRF-CEM, and HT-29 cells.[76] It was found that, compound **1.39** displayed the best therapeutic profile regarding superoxide generation and cytotoxicity, with an IC_{50} of 1.7

µM in PC-3 cells which is 8-fold more potent than etoposide (IC_{50} = 13.6 µM). Additionally, this compound was found to exhibit significant anti-proliferative activity in MCF-7 (IC_{50} = 4.3 µM), CCRF-CEM (IC_{50} = 9.0 µM), and HT-29 cells (IC_{50} = 9.8 µM).

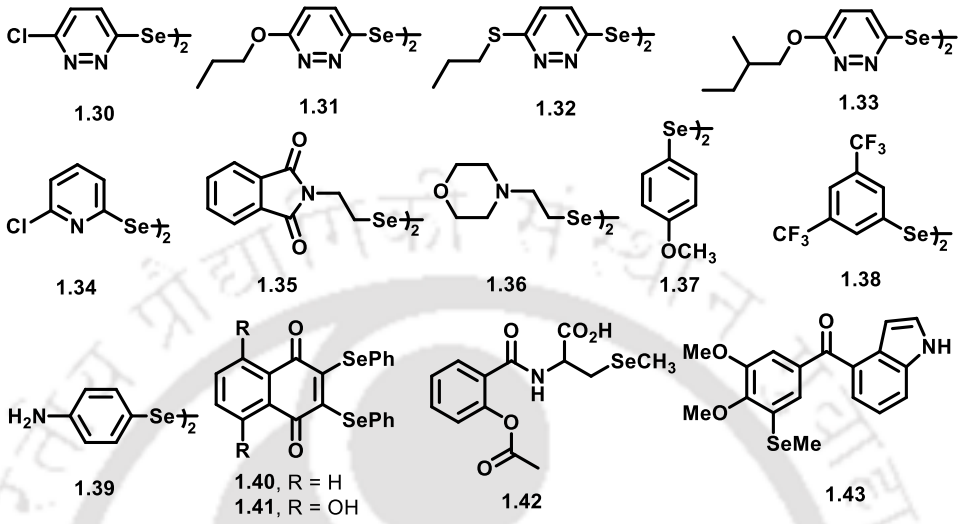

Figure 1.7. Small-molecule organoselenium compounds as potential anti-cancer agents.

Apart from diselenides, synthetic monoselenides are also widely studied for their anti-proliferative activity against cancer cells. When tested in chronic lymphocytic leukemia (CLL) B-cells isolated from peripheral blood of leukemia patients, compounds **1.40** and **1.41**, showed promising activity in reducing CLL B-cell viability at very low concentrations.[77] Interestingly, viability of healthy peripheral blood cells was unaffected by compound **1.40**, giving rise to excellent selectivity of compound **1.40** towards CLL cells. However high toxicity of compound **1.41** was observed in case of healthy control cells. Interesting work by Plano and co-workers (2016) revealed the synthesis of several synthetic hybrids containing anti-inflammatory drugs and organoselenium compounds and evaluation of their anti-cancer activities against four cancer cell lines. compound **1.42**, which is an aspirin-methyl selenocysteine hybrid was found to be moderately toxic towards PANC-1 cells.[78]

Recent report by Zhang and co-workers (2017) described the evaluation of anti-proliferative activity of several synthetic indole-chalcone and phenylindolyl ketone derivatives.[79] Most of these compounds exhibited good to excellent activities in six different organ-specific cancer cell lines such as A549 (lung), MDA-MB-231 (triple negative breast cancer cells), Hep-G2 (liver), HeLa (cervix), HCT-116 and RKO

(colon). Among the evaluated indole-chalcone derivatives, compound **1.43** exhibited highest activity in the selected cell lines. Compound **1.43**, which is a phenylindolyl ketone, displayed strongest anti-proliferative activity in the selected cell lines in sub-micromolar concentrations. Detailed mechanistic investigations confirmed that compound **1.43** inhibited tubulin polymerization in HeLa cells with an IC_{50} of 2.1 μM and induces G_2/M phase arrest.

1.12. Selenium-Drug hybrids as anti-cancer agents

In recent times, several hybrid compounds were reported by combining different drugs with organoselenium compounds in order to improve their therapeutic activities against cancer. Notable selenium-drug hybrid compounds are documented in Figure 1.8. In 2013, Gowda and co-workers have reported the synthesis of selenium-containing celecoxib hybrid (**1.44**) and evaluated for its anti-proliferative activity. It was found that the compound had excellent ability to arrest cell growth in case of human melanoma cells by inducing cell cycle arrest in the G_0/G_1 phase of the cell cycle.[80] In addition to the NSAID-methyl selenocysteine derivative **1.42** as shown above, Plano and co-workers have also developed Se-Aspirin hybrid **1.45** by combining aspirin with selenocyanate functionality. This hybrid was found to display promising activity against human colon carcinoma (HT-29), human malignant carcinoma (UACC-903), human pancreatic carcinoma (PANC-1) and triple-negative breast cancer (MDA-MB-231) cells. In all the cancer cells, the IC_{50} was found to be lower than 10.0 μM following 48 h incubation. Mechanistically, it was found out that the novel compound inhibited the expression of cyclin B_1 and cyclin E_1 thus arresting the proliferation of cells in G_1/S and G_2/M phases, respectively. Additionally, the compounds overexpressed p21 level, which is a cyclin dependent kinase inhibitor and also prolonged treatment of the compound produced ROS that triggered apoptosis and cellular death.[78]

Histone deacetylase (HDAC) are responsible for the regulation of the gene expression by the remodeling of chromatin through their deacetylase activity. Inhibition of HDAC is an useful strategy for specific epigenetic changes related to cancer or other diseases.[81] FDA-approved HDAC inhibitor suberoylanilide hydroxamic acid (SAHA) has been chemically modified to develop compound **1.46**, which is a selenocyanate variant of SAHA. This hybrid compound was found to be much more active than native SAHA in several lung cancer cells and has also been found to have MAPK and PI3K/Akt pathway inhibitory property.

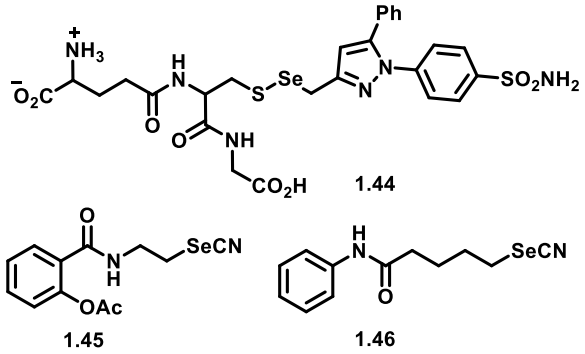

Figure 1.8. Chemical structures of selenium-drug hybrid compounds.

1.13. Organoselenium compounds as chemopreventive agents

Functionalization of several small-molecules with selenocyanate moiety serves as a very promising perspective in cancer treatment. Apart from selenium-drug hybrids, as described in the previous section, several novel small-molecules functionalized with selenocyanate moiety were synthesized and evaluated for their anti-cancer activities by several research groups.

Benzylic selenocyanates were first reported and evaluated for their chemopreventive activities by El-Bayoumy and co-workers during 1980s. In 1985, El-Bayoumy and co-workers have compared the potential of benzyl selenocyanate (**1.48**) with 4-methoxybenzyl selenol (**1.47**), against benzo-[a]-pyrene induced fore-stomach cancer in female CD-1 mice (Figure 1.9).[82] The results indicated slightly improved efficiency of benzyl selenocyanate (**1.48**) over 4-methoxybenzyl selenol (**1.47**) in terms of reduction in tumor incidence in mice. Interestingly, the benzyl thiocyanate, the sulfur analogue of the selenocyanate **1.48** failed to exhibit any chemopreventive activity under the identical condition.[83] Furthermore, they have also used 4-methoxybenzyl selenol **1.47** for the azoxymethane-induced colon carcinogenesis in female F-344 rats.[84] However, the drug had the limitation of the absence of any activity against tumors in small intestine. Moreover, the drug also induced ear duct tumor in some of the test subjects. Detailed works attributed the detoxification of carcinogen azoxymethane to be the underlying mechanism for the chemoprevention of the above compound.[85] However, benzyl selenocyanate (**1.48**) suffered from the limitation of more toxicity than the 4-methoxybenzyl selenol (**1.47**) as reported by their LD_{50} values. It was also found that subjects treated with benzyl selenocyanate suffered from gradual loss in weight. In 1997, Reddy *et al*, have reported a new selenocyanate derivative, 4-methoxybenzyl selenocyanate (**1.49**) and tested for its abilities to inhibit colon carcinogenesis in F344

rats induced by azoxymethane and fed low or high-fat diet. Compound **1.49** at a dose of 20.0 ppm with a high-fat diet, inhibits azoxymethane-induced colon carcinogenesis during the initiation and post-initiation phases without any significant toxicity at 10.0 ppm or 20.0 ppm doses.[86]

The next breakthrough came with the synthesis of 1,4-phenylenebis(methylene) selenocyanate (*p*–xylenyl selenocyanate, *p*-XSC) (**1.52**) in an attempt to reduce the toxicity and volatility of benzyl selenocyanate, by introducing another methylselenocyanato group at the para-position of benzyl selenocyanate (**1.48**).[87] As expected, the novel compound reduced the tumor incidence in 7,12-dimethyl-[a]-benzanthracene (DMBA)-induced mammary carcinoma in female Sprague Dawley Rats by 68%. Additionally, it showed a major inhibition in binding of the carcinogen with mammary DNA, in the presence of *p*-XSC supplemented diet. With these observations, Reddy *et al*, have studied three positional isomers of xylene-based selenocyanates namely *p*-xylyl selenocyanate (**1.52**), *m*-xylyl selenocyanate (**1.51**), *o*-xylyl selenocyanate (**1.50**). It was observed that, **1.52** was slightly more potent than the other two analogues in terms of inhibition of tumor.[88] In a more detailed analysis by El-Bayoumy and co-workers (2004), **1.52** was shown to induce cell cycle arrest at G_1/S phase and induced apoptosis by upregulating p21 and Bad protein expression in DMBA-induced mammary carcinogenesis.[83]

In 1995, Ip and co-workers have reported the chemopreventive activities of a series of aliphatic selenocyanates. They have shown that methyl selenocyanate **1.53** is a promising candidate for tumor inhibition in DMBA-induced mammary carcinoma in female Sprague-Dawley rats.[89] Their results clearly indicated the increasing order of chemopreventive efficacy of alkyl selenocyanates **1.54** – **1.56** with increase in chain length from methyl to heptyl *via* propyl and pentyl analogues (Figure 1.9). For example, the percentage of tumor incidence in mice treated with methyl, propyl, pentyl and heptyl selenocyanates were nearly 63%, 43%, 37% and 37%, respectively. Additionally, *in vivo* experiments also showed that carcinogen-DNA binding interaction was reduced significantly for heptyl selenocyanate **1.56** (26.0 pmol/mg) in comparison with methyl selenocyanate **1.53** (16.0 pmol/mg) indicating the effect of chain length on the chemopreventive nature against the carcinogen DMBA.

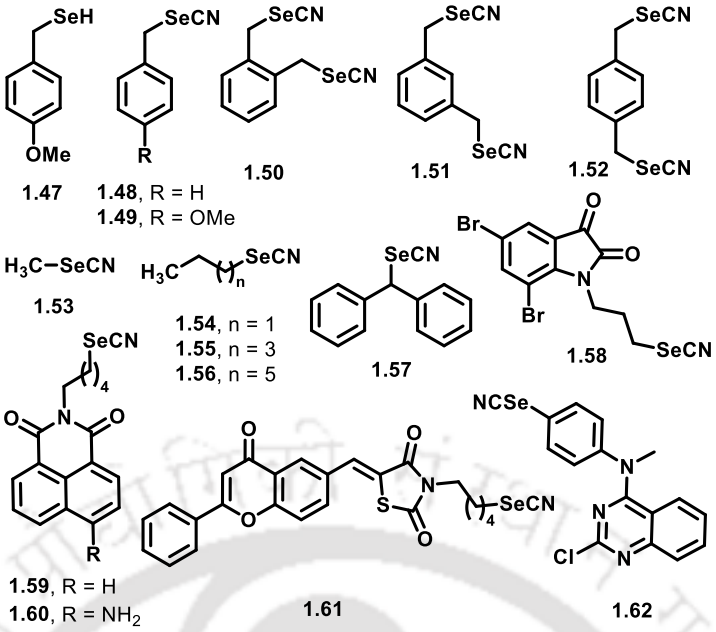

Figure 1.9. Chemical structures of different organoselenium small-molecules having promising anti-cancer and/or chemopreventive properties.

In 2011, Chakraborty *et al* have demonstrated the application of diphenylmethyl selenocyanate **1.57** with a dose of 3.0 mg/Kg body weight of Swiss albino mice in attenuating the toxic effect of *cis*-platin administered at 5.0 mg/Kg body weight.[90] Treatment with compound **1.57**, notably reduced the *cis*-platin-induced lipid peroxidation, serum creatinine and blood urea nitrogen (BUN) level. Additionally, several renal antioxidant enzymes such as GST, GPx, SOD, CAT activities, which get depleted by the administration of *cis*-platin, were restored upon the treatment of compound **1.57**. In the same year (2011), Krishnegowda *et al*, developed dibromoisatin hybrid of benzyl selenocyanate and observed that the resulting compound **1.58** is highly cytotoxic against three cancer cell lines such as HT-29, MCF-7, A-549 with IC_{50} of 3.18, 1.65, 3.46 µM, respectively. Compound **1.58** also induced apoptosis at a concentration of 5.0 µM on HT-29 cells after 24 h treatment.[91] Subsequently, In 2012, Roy and co-workers have reported a series of naphthalimide-based selenocyanates and assessed their cytoprotective roles in different biological model systems. It has been observed that the 4-aminonaphthalimide-based compound **1.60**, upon the introduction of 4-amino functionality in compound **1.59** exhibited enhanced antioxidant activity. However, the authors failed to rationalize the effect of electron-releasing functionality on antioxidant activity of the compound **1.60**.[92] Compound **1.60** displayed excellent cytoprotective activity in Swiss albino female mice models against genotoxicity and oxidative stress

induced by standard drug cyclophosphamide (CP). It has been observed that, increase of ROS level by the administration of CP was greatly attenuated by the concomitant treatment of compound **1.60** and CP. Additionally, treatment with compound **1.60** on CP-treated mice models resulted in the drastic increase in GPx activity.[93]

Roy and co-workers in the year of 2014 developed a novel flavonyl-thiazolidinedione-based organoselenocyanate **1.61**, which was found to be non-toxic at the doses upto 5.0 mg/Kg body weight in mice. Concomitant treatment of the compound with cyclophosphamide resulted in significant improvement of the therapeutic activity of the latter that was mostly observed in terms of tumor burden and protection of normal cells.[94] In another study, An and co-workers (2018) have synthesized and evaluated compound **1.62** that is a 4-anilinoquinazoline derivative as novel anti-mitotic agent having potent anti-proliferative activities in six different organ-specific cancer cells such as A549, HCT-116, Hep-G2, MDA-MB-231, LOVO and RKO cells to be in the sub-micromolar range. It has also been observed that compound **1.62** induces cell cycle arrest at G_2 / M phase at a concentration of 4.0 nM, with a concomitant decrease of cells at G_1 and S phase. Detailed mechanistic studies revealed that compound **1.62** has significant activity in inhibiting tubulin polymerization, in a dose-dependent manner with IC_{50} of 3.1 µM.[95]

1.14. Natural sources of selenocyanate species

In 2011, the first biosynthesis of selenocyanate as a result of biotransformation of selenate (SeO_4^{2-}) species in *Chlorella vulgaris* is reported by Wallschläger and co-workers.[96] The group treated green fresh water algae *Chlorella vulgaris* with selenate (SeO_4^{2-}), selenite (SeO_3^{2-}) or selenocyanate ($SeCN^-$) containing 10.0 µg/L selenium for 10 days. It was observed that, upon uptake of selenate, significant quantities of selenite and selenocyanate were produced by algae and released back into growth medium. However, the authors were unable to characterize the formed selenocyanate species by spectroscopic technique owing to much lower concentration of selenocyanate species formed (< 5.0 µg/L). Mechanistically, it was proposed that formation of selenocyanate species occurs by the reaction between Se^0 and cyanide ion. *Chlorella vulgaris* can convert the N-terminal amine groups in amino acids into free cyanide ion. Additionally, the formation of reduced selenium, Se^0 from selenates has been reported previously in higher plants. Se^0 and free cyanide ions promote the formation of selenocyanate species.

In a follow-up study by the same group in 2012, the selenocyanate formation was also observed in other green algae and blue-green algae such as *Chlorella kesslerii*, *Scenedesmus obliquus* and *Synechococcus leopoliensis*.[97] Additionally, in this study the presence of selenocyanate species was conclusively proved by ESI-MS technique.

1.15. Metabolism and biodegradation of organoselenium compounds

As selenocyanates exhibited potential chemopreventive activities against the carcinogenesis in different mice models, it is important to understand their possible metabolic pathways upon their administration. Additionally, it is also necessary to understand whether the parent organoselenium compounds or any of their metabolites are responsible for the anti-carcinogenesis activities of the compounds. In 1987, Vadhanavikit and co-workers have administered inorganic [^{75}Se] selenocyanate with a dose of 2 mg/Kg of body weight of male Sprague-Dawley rats and observed the metabolized products. They have observed the excretion of dimethyl selenide (DMSe) through breath and trimethyl selenonium compound (TMSe) through urine. Additionally, they observed thiocyanate species as a major metabolite excreted through urine. They postulated that selenocyanates are actively metabolized and excreted in methylated form by the cleavage of C-Se bond.[98]

In 1998, El-Bayoumy and co-workers administered the ^{14}C-labeled *p*-XSC (p-[^{14}C]XSC, **1.52**) in female CD rats with a dose of 15.8 mg/Kg, and analyzed the excreted metabolized products using radioactivity and selenium content. They observed that 24% of the dose was recovered from urine and 75% of the dose was excreted through feces over 7 days. However, contrastingly with the previous report, it was observed that the exhaled air consists of less than 1% of the administered dose. The excreted fecal portions upon extraction with ethyl acetate recovered only 15% of the administered dose, which was observed to contain tetraselenocyclophane (**1.65**) upon HPLC analysis. Reduction of the unextracted materials from the feces by sodium borohydride ($NaBH_4$) in THF and 0.5 (N) NaOH mixture (4:1) resulted in tetraselenocyclophane **1.65** in 10% yield. The formation of tetraselenocyclophane (**1.65**) under reducing conditions might take place via the formation of the corresponding selenol species **1.64** followed by the oxidative dimerization. The results indicated that urine is a minor mode of excretion of compound **1.52** and from the urine sample, only 1.8% of the dose was recovered by ethyl acetate. HPLC analysis of the urine sample collected after 24 h from administration of compound **1.52**, led to the formation of glucuronic acid and sulfate conjugates of the

drug along with terephthalic acid. Unfortunately, the structures of the glucuronic acid and sulfate conjugates were not elucidated.[99] The metabolism of compound **1.52** is elaborately discussed in Scheme 1.3.

In another report, El-Bayoumy and Sinha have proposed the detailed metabolic pathways of selenocyanate **1.52**.[83] It can react with glutathione (GSH) and produce the corresponding selenenyl sulfide **1.63**, which may further react with GSH leading to the generation of selenol **1.64**. The selenol could undergo oxidation to the corresponding diselenide **1.65** or the polyselenide **1.66**. Evidence of such species was found in the feces samples (75%). Additionally, oxidation of the selenocyanate **1.52** can generate the corresponding seleninic acid **1.67**, which might undergo deselenation to yield **1.68** as evidenced in urine samples (24%). Another minor pathway involves the benzylic hydroxylation of selenocyanate **1.52** to generate the intermediate **1.69**, which undergoes deselenation to form terephthaldehyde **1.70** and highly unstable selenocyanic acid (HSeCN). While **1.70** gets oxidized further to form terephthalic acid **1.71**, HSeCN decomposes further to generate hydrogen selenide (H_2Se) gas, which gets functionalized in proteins. Very recently in the year of 2020, Takahashi and co-workers, administered sodium selenite, selenomethionine and potassium selenocyanate to specific pathogen-free male Wistar rats, and confirmed the existence of a common metabolites from the bile of the rats, 10 minutes after administration.[100] However the amount of the selenometabolite obtained was dependent on selenium source. Eventually, sodium selenite was found to be the most effectively metabolized than that of selenomethionine. Further investigations by ICP-MS, ESI-Q/TOF and specific isotope pattern analysis confirmed the metabolite to be the selenotrisulfide derivative of glutathione (GS-Se-SG). The group hypothesized that selenium compounds used in the study such as sodium selenite, potassium selenocyanate and selenomethionine were rapidly transformed into a common intermediate selenide species *in vivo*.

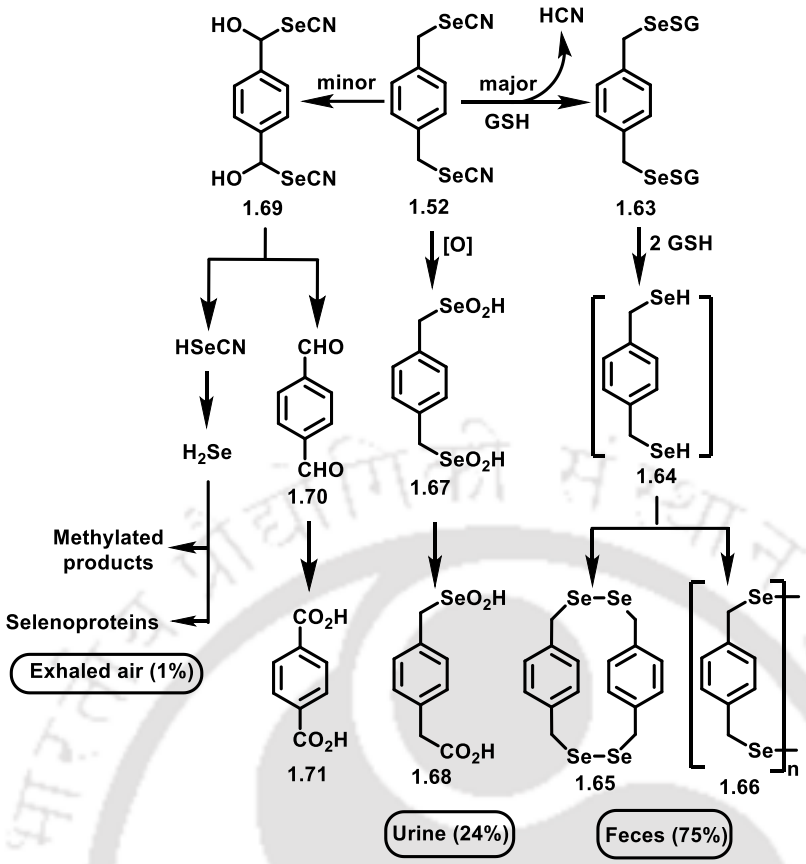

Scheme 1.3. Metabolic pathway of selenocyanate **1.52** into different excretory metabolites.

Notable to mention that as described in Scheme 1.3, biotransformation of **1.52** into **1.63** leads to the formation of HCN which may impart considerable amount of toxicity towards biological system. The toxicity imposed by cyanide is significantly attenuated by the action of an enzyme known as rhodanese which is present in all living organism from bacteria to human.[101] Biologically ubiquitous enzyme rhodanese or thiosulphate:cyanide sulfur transferase catalyzes cyanide-dependent cleavage of thiosulphate to form thiocyanate and sulphate, therefore minimizing the toxic effect of cyanide released from **1.52**. Since rhodanese is a mitochondrial enzyme and inorganic thiosulphate has poor cellular penetration property, serum albumin-sulfane complex serves a major role in transporting sulfur donors to rhodanese.[102] Apart from rhodanese metabolism, another important metabolic pathway for cyanide detoxification is the formation of cyanocobalamine from hydroxocobalamine in presence of cyanide. However, one of the most important pathway for cyanide detoxification is the cystin-mediated formation of 2-aminothiazoline-4-carboxylic acid (**1.73)** via the intermediacy of β-thiocyanato-alanine (**1.72**) as described in Scheme 1.4.[103] However, cyanide

detoxification by rhodanese remains controversial as Craston in the year 1991, proposed the production of selenocyanate by the action of purified beef liver rhodanese from selenosulphate.[104]

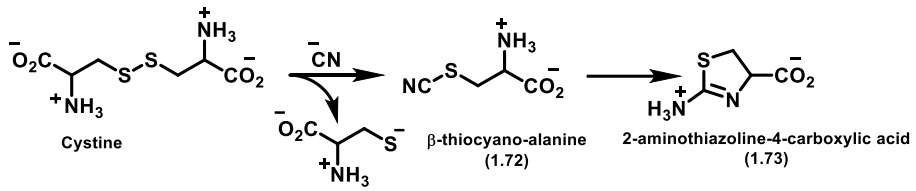

Scheme 1.4. Cyanide detoxification mechanism by cystine to form non-toxic metabolite **1.73**.

1.16. Thesis objectives

Based on the previous literature reports on the versatility of organoselenium compounds against various organ-specific cancer cells, the current thesis intends to explore the chemistry and biology of organoselenocyanates involving design, synthesis, characterization and pharmaceutical application as small-molecule antioxidants as well as anti-proliferative agents. It is worth mentioning that the sustained administration of most of the chemotherapeutic drugs result in unwanted side-effects mainly by generation of ROS and inflammation. Additionally, it has been documented that the efficiency of the chemotherapeutic drugs for the treatment of cancer could be significantly improved upon the dietary supplement of antioxidants. Therefore, evaluation of the synthesized organoselenocyanates and related derivatives as potent antioxidants warrants further attention. Although there exist several reports on in vivo chemopreventive activities of various selenocyanates towards carcinogenesis and tumorigenesis, detailed molecular level understanding on the antioxidant and anti-cancer activities of organoselenocyanates is not yet well-established. Therefore, the present thesis orients towards unravelling the synthesis and pharmaceutical applications of different series of charged and neutral organoselenocyanates and related derivatives.

1.17. Thesis overview

The thesis comprises of five chapters. **Chapter 1** highlights the basic information and introduction about cancer and detailed literature reports on the utilization of organoselenium compounds for the treatment of cancer. In **Chapter 2**, a series of benzylic selenocyanates were developed and the impact of multiple selenocyanate functionalities in a single compound towards their anti-cancer activities has been

explored. In **Chapter 3**, unsubstituted, 4-methoxy and 4-nitrobenzyl selenocyanates are identified as standard model compounds having significant anti-cancer activities, and heterocyclic pharmacophores such as 1,2,3-triazole and 2,4-thiazolidine-1,3-dione are introduced in each of the model compounds and are evaluated for their anti-cancer activities. In **Chapter 4**, we took interest on the effect of cationic charge over heterocyclic scaffold of the selenocyanate molecule. We therefore developed the synthetic methodology for a series of imidazole and benzimidazole-based ionic selenazolium, selenazinium or acyclic selenocyanate analogues, and evaluated the compounds for their antioxidant activities. Bearing resemblance with benzyl, 4-methoxybenzyl and 4-nitrobenzyl selenocyanates, **Chapter 5** deals with the synthesis of 4-substituted benzimidazole-based selenazolium and selenazinium selenocyanates. Additionally, a newer class of C2-phenyl substituted benzimidazole-based open chain selenocyanates have also been synthesized. Furthermore, a series of benzimidazole-based neutral selenocyanates have also been synthesized and each of the compounds have been studied for their anticancer activities.

1.18. References

1. Siegel, R. L.; Miller, K. D.; Fuchs, H. E.; Jemal, A., *CA Cancer J Clin* **2021**, *71*, 7.
2. Hanahan, D.; Weinberg, R. A., *Cell* **2000**, *100*, 57.
3. Zaigham Abbas, S. R., *An Overview of Cancer Treatment Modalities*. 2018.
4. Troll, W.; Wiesner, R., *Annu Rev Pharmacol Toxicol* **1985**, *25*, 509.
5. Pitot, H. C.; Goldsworthy, T.; Moran, S., *J supramol struct cell biochem* **1981**, *17*, 133.
6. Yamagiwa, K.; Ichikawa, K., *J Cancer Res* **1918**, *3*, 1.
7. Brierley, J.; Gospodarowicz, M.; O'Sullivan, B., *Ecancermedicalscience* **2016**, *10*, ed61.
8. Greene, F. L.; Sobin, L. H., *CA: Cancer J Clin* **2008**, *58*, 180.
9. Leone, A.; Flatow, U.; King, C. R.; Sandeen, M. A.; Margulies, I. M. K.; Liotta, L. A.; Steeg, P. S., *Cell* **1991**, *65*, 25.
10. Hashimoto, Y.; Shindo-Okada, N.; Tani, M.; Nagamachi, Y.; Takeuchi, K.; Shiroishi, T.; Toma, H.; Yokota, J., *J Exp Med* **1998**, *187*, 289.
11. Davies, B. R.; Davies, M. P.; Gibbs, F. E.; Barraclough, R.; Rudland, P. S., *Oncogene* **1993**, *8*, 999.
12. Dong, J. T.; Lamb, P. W.; Rinker-Schaeffer, C. W.; Vukanovic, J.; Ichikawa, T.; Isaacs, J. T.; Barrett, J. C., *Science* **1995**, *268*, 884.
13. Lee, J.-H.; Welch, D. R., *Cancer Res* **1997**, *57*, 2384.
14. Habets, G. G. M.; Scholtes, E. H. M.; Zuydgeest, D.; van der Kammen, R. A.; Stam, J. C.; Berns, A.; Collard, J. G., *Cell* **1994**, *77*, 537.
15. Galluzzi, L.; Bravo-San Pedro, J. M.; Vitale, I.; Aaronson, S. A.; Abrams, J. M.; Adam, D.; Alnemri, E. S.; Altucci, L.; Andrews, D.; Annicchiarico-Petruzzelli, M., *et al.*, *Cell Death Differ* **2015**, *22*, 58.
16. Galluzzi, L.; Vitale, I.; Abrams, J. M.; Alnemri, E. S.; Baehrecke, E. H.; Blagosklonny, M. V.; Dawson, T. M.; Dawson, V. L.; El-Deiry, W. S.; Fulda, S., *et al.*, *Cell Death Differ* **2012**, *19*, 107.
17. Tinkle, S.; McNeil, S. E.; Mühlebach, S.; Bawa, R.; Borchard, G.; Barenholz, Y.; Tamarkin, L.; Desai, N., *Ann N Y Acad Sci* **2014**, *1313*, 35.
18. Martinelli, C.; Pucci, C.; Ciofani, G., *APL Bioeng* **2019**, *3*, 011502.
19. Gubernator, J., *Expert Opin Drug Deliv* **2011**, *8*, 565.

20. Narang, A. S.; Delmarre, D.; Gao, D., *Int J Pharm* **2007**, *345*, 9.
21. Barenholz, Y., *J Control Release* **2012**, *160*, 117.
22. Markman, M., *Expert Opin Pharmacother* **2006**, *7*, 1469.
23. Hofheinz, R.-D.; Gnad-Vogt, S. U.; Beyer, U.; Hochhaus, A., *Anti-Cancer Drugs* **2005**, *16*.
24. Malam, Y.; Loizidou, M.; Seifalian, A. M., *Trends Pharmacol Sci* **2009**, *30*, 592.
25. Nasir, A.; Kausar, A.; Younus, A., *Polym Plast Technol Eng* **2015**, *54*, 325.
26. Barua, S.; Mitragotri, S., *Nano Today* **2014**, *9*, 223.
27. Senol, S.; Ceyran, A. B.; Aydin, A.; Zemheri, E.; Ozkanli, S.; Kösemetin, D.; Sehitoglu, I.; Akalin, I., *Int J Clin Exp* **2015**, *8*, 5633.
28. Huang, S.; Li, J.; Han, L.; Liu, S.; Ma, H.; Huang, R.; Jiang, C., *Biomaterials* **2011**, *32*, 6832.
29. Sharkey, R. M.; Goldenberg, D. M., *CA Cancer J Clin* **2006**, *56*, 226.
30. Bazak, R.; Houri, M.; El Achy, S.; Kamel, S.; Refaat, T., *J Cancer Res Clin Oncol* **2015**, *141*, 769.
31. Acharya, S.; Dilnawaz, F.; Sahoo, S. K., *Biomaterials* **2009**, *30*, 5737.
32. Murphy, M. P., *Biochem* **2009**, *417*, 1.
33. Liou, G.-Y.; Storz, P., *Free Radic Res* **2010**, *44*, 479.
34. Basu, A. K., *Int J Mol Sci* **2018**, *19*.
35. Seyfried, T. N.; Huysentruyt, L. C., *Crit Rev Oncog* **2013**, *18*, 43.
36. Kamiya, T.; Goto, A.; Kurokawa, E.; Hara, H.; Adachi, T., *Oxid Med Cell Longev* **2016**, *2016*, 1284372.
37. Shin, D. H.; Dier, U.; Melendez, J. A.; Hempel, N., *Biochim Biophys Acta Mol Basis Dis* **2015**, *1852*, 2593.
38. de Sá Junior, P. L.; Câmara, D. A. D.; Porcacchia, A. S.; Fonseca, P. M. M.; Jorge, S. D.; Araldi, R. P.; Ferreira, A. K., *Oxid Med Cell Longev* **2017**, *2017*, 2467940.
39. Ushio-Fukai, M.; Nakamura, Y., *Cancer Lett* **2008**, *266*, 37.
40. Dewhirst, M. W.; Cao, Y.; Moeller, B., *Nat Rev Cancer* **2008**, *8*, 425.
41. Ushio-Fukai, M.; Alexander, R. W., *Mol Cell Biochem* **2004**, *264*, 85.
42. Giorgio, M.; Migliaccio, E.; Orsini, F.; Paolucci, D.; Moroni, M.; Contursi, C.; Pelliccia, G.; Luzi, L.; Minucci, S.; Marcaccio, M., *et al.*, *Cell* **2005**, *122*, 221.
43. Danial, N. N.; Korsmeyer, S. J., *Cell* **2004**, *116*, 205.

44. Simon, H. U.; Haj-Yehia, A.; Levi-Schaffer, F., *Apoptosis* **2000**, *5*, 415.
45. Chen, Z.; Lai, H.; Hou, L.; Chen, T., *Chem Commun* **2020**, *56*, 179.
46. Hiroshi, M.; Kissner, R.; Koppenol, W. H.; Sies, H., *FEBS Lett* **1996**, *398*, 179.
47. Reich, H. J.; Jasperse, C. P., *J Am Chem Soc* **1987**, *109*, 5549.
48. Chaudiere, J.; Erdelmeier, I.; Moutet, M.; Yadan, J.-C., *Phosphorus Sulfur Silicon Relat Elem* **1998**, *136*, 467.
49. Back, T. G.; Dyck, B. P., *J Am Chem Soc* **1997**, *119*, 2079.
50. Wilson, S. R.; Zucker, P. A.; Huang, R. R. C.; Spector, A., *J Am Chem Soc* **1989**, *111*, 5936.
51. Engman, L.; Hallberg, A., *J Org Chem* **1989**, *54*, 2964.
52. Wirth, T., *Molecules* **1998**, *3*.
53. Conklin, K. A., *Nutr Cancer* **2000**, *37*, 1.
54. Klein, E. A.; Thompson, I. M.; Tangen, C. M.; Crowley, J. J.; Lucia, M. S.; Goodman, P. J.; Minasian, L. M.; Ford, L. G.; Parnes, H. L.; Gaziano, J. M., *et al.*, *J Am Med Assoc* **2011**, *306*, 1549.
55. Rayman, M. P., *Proc Nutr Soc* **2007**, *64*, 527.
56. Fakih, M.; Cao, S.; Durrani, F. A.; Rustum, Y. M., *Clin Colorectal Cancer* **2005**, *5*, 132.
57. Frenkel, G. D.; Caffrey, P. B., *Curr Pharm Des* **2001**, *7*, 1595.
58. Asfour, I. A.; Fayek, M.; Raouf, S.; Soliman, M.; Hegab, H. M.; El-Desoky, H.; Saleh, R.; Moussa, M. A. R., *Biol Trace Elem Res* **2007**, *120*, 1.
59. Tan, H. W.; Mo, H.-Y.; Lau, A. T. Y.; Xu, Y.-M., *Int J Mol Sci* **2019**, *20*.
60. Rudolf, E.; Rudolf, K.; Červinka, M., *Cell Biol Toxicol* **2008**, *24*, 123.
61. Freitas, M.; Alves, V.; Sarmento-Ribeiro, A. B.; Mota-Pinto, A., *Biochem Biophys Res Commun* **2011**, *408*, 713.
62. Fan, C.-D.; Fu, X.-Y.; Zhang, Z.-Y.; Cao, M.-Z.; Sun, J.-Y.; Yang, M.-F.; Fu, X.-T.; Zhao, S.-J.; Shao, L.-R.; Zhang, H.-F., *et al.*, *Sci Rep* **2017**, *7*, 6465.
63. Redman, C.; Scott, J. A.; Baines, A. T.; Basye, J. L.; Clark, L. C.; Calley, C.; Roe, D.; Payne, C. M.; Nelson, M. A., *Cancer Lett* **1998**, *125*, 103.
64. Marshall, J. R.; Burk, R. F.; Payne Ondracek, R.; Hill, K. E.; Perloff, M.; Davis, W.; Pili, R.; George, S.; Bergan, R., *Oncotarget* **2017**.
65. Lu, J.; Holmgren, A., *J Biol Chem* **2009**, *284*, 723.
66. Moghadaszadeh, B.; Beggs, A. H., *Physiology* **2006**, *21*, 307.

67. Zhang, L.; Zhou, L.; Du, J.; Li, M.; Qian, C.; Cheng, Y.; Peng, Y.; Xie, J.; Wang, D., *Biomed Res Int* **2014**, *2014*, 696107.
68. Zhao, F.; Yan, J.; Deng, S.; Lan, L.; He, F.; Kuang, B.; Zeng, H., *Cancer Lett* **2006**, *236*, 46.
69. Juang, S. H.; Lung, C. C.; Hsu, P. C.; Hsu, K. S.; Li, Y. C.; Hong, P. C.; Shiah, H. S.; Kuo, C. C.; Huang, C. W.; Wang, Y. C., *et al.*, *Mol Cancer Ther* **2007**, *6*, 193.
70. Shiah, H.-S.; Lee, W.-S.; Juang, S.-H.; Hong, P.-C.; Lung, C.-C.; Chang, C.-J.; Chou, K.-M.; Chang, J.-Y., *Biochem Pharmacol* **2007**, *73*, 610.
71. Chen, T.; Zheng, W.; Wong, Y.-S.; Yang, F., *Biomed Pharmacother* **2008**, *62*, 77.
72. Zhang, Y.; Zheng, S.; Ngai, S.-M.; Zheng, W.; Li, J.; Chen, T.; Zhong, X., *Chem Pharm Bull* **2014**, *62*, 994.
73. Kim, C.; Lee, J.; Park, M.-S., *Arch Pharm Res* **2015**, *38*, 659.
74. Nedel, F.; Campos, V. F.; Alves, D.; McBride, A. J. A.; Dellagostin, O. A.; Collares, T.; Savegnago, L.; Seixas, F. K., *Life Sci* **2012**, *91*, 345.
75. Rizvi, M. A.; Guru, S.; Naqvi, T.; Kumar, M.; Kumbhar, N.; Akhoon, S.; Banday, S.; Singh, S. K.; Bhushan, S.; Mustafa Peerzada, G., *et al.*, *Bioorg Med Chem Lett* **2014**, *24*, 3440.
76. Plano, D.; Baquedano, Y.; Ibáñez, E.; Jiménez, I.; Palop, J. A.; Spallholz, J. E.; Sanmartín, C., *Molecules* **2010**, *15*.
77. Doering, M.; Ba, L. A.; Lilienthal, N.; Nicco, C.; Scherer, C.; Abbas, M.; Zada, A. A. P.; Coriat, R.; Burkholz, T.; Wessjohann, L., *et al.*, *J Med Chem* **2010**, *53*, 6954.
78. Plano, D.; Karelia, D. N.; Pandey, M. K.; Spallholz, J. E.; Amin, S.; Sharma, A. K., *J Med Chem* **2016**, *59*, 1946.
79. Zhang, S.; An, B.; Li, J.; Hu, J.; Huang, L.; Li, X.; Chan, A. S. C., *Org Biomol Chem* **2017**, *15*, 7404.
80. Gowda, R.; Madhunapantula, S. V.; Desai, D.; Amin, S.; Robertson, G. P., *Mol Cancer Ther* **2013**, *12*, 3.
81. Karelia, N.; Desai, D.; Hengst, J. A.; Amin, S.; Rudrabhatla, S. V.; Yun, J., *Bioorg Med Chem Lett* **2010**, *20*, 6816.
82. El-Bayoumy, K., *Cancer Res* **1985**, *45*, 3631.

83. El-Bayoumy, K.; Sinha, R., *Mut Res Fund Mol M* **2004**, *551*, 181.
84. Reddy, B. S.; Tanaka, T.; El-Bayoumy, K., *J Natl Cancer Inst* **1985**, *74*, 1325.
85. Tanaka, T.; Reddy, B. S.; el-Bayoumy, K., *Jpn J Cancer Res* **1985**, *76*, 462.
86. Reddy, B. S.; Rivenson, A.; El-Bayoumy, K.; Upadhyaya, P.; Pittman, B.; Rao, C. V., *J Natl Cancer Inst* **1997**, *89*, 506.
87. El-Bayoumy, K.; Chae, Y.-H.; Upadhyaya, P.; Meschter, C.; Cohen, L. A.; Reddy, B. S., *Cancer Res* **1992**, *52*, 2402.
88. Reddy, B. S.; Upadhyaya, P.; Simi, B.; Rao, C. V., *Anticancer Res* **1994**, *14*, 2509.
89. Clement, I.; Vadhanavikit, S.; Ganther, H., *Carcinogenesis* **1995**, *16*, 35.
90. Chakraborty, P.; Roy, S. S.; Sk, U. H.; Bhattacharya, S., *Free Rad Res* **2011**, *45*, 177.
91. Krishnegowda, G.; Prakasha Gowda, A. S.; Tagaram, H. R. S.; Carroll, K. F. S.-O.; Irby, R. B.; Sharma, A. K.; Amin, S., *Bioorg Med Chem* **2011**, *19*, 6006.
92. Singha Roy, S.; Ghosh, P.; Hossain Sk, U.; Chakraborty, P.; Biswas, J.; Mandal, S.; Bhattacharjee, A.; Bhattacharya, S., *Bioorg Med Chem Lett* **2010**, *20*, 6951.
93. Roy, S. S.; Chakraborty, P.; Ghosh, P.; Ghosh, S.; Biswas, J.; Bhattacharya, S., *Redox Rep* **2012**, *17*, 157.
94. Roy, S. S.; Chakraborty, P.; Bhattacharya, S., *Eur J Med Chem* **2014**, *73*, 195.
95. An, B.; Zhang, S.; Hu, J.; Pan, T.; Huang, L.; Tang, J. C.-o.; Li, X.; Chan, A. S. C., *Org Biomol Chem* **2018**, *16*, 4701.
96. Simmons, D. B. D.; Wallschläger, D., *Environ Sci Technol* **2011**, *45*, 2165.
97. LeBlanc, K. L.; Smith, M. S.; Wallschläger, D., *Environ Sci Technol* **2012**, *46*, 5867.
98. Vadhanavikit, S.; Kraus, R. J.; Ganther, H. E., *Arch Biochem Biophys* **1987**, *258*, 1.
99. El-Bayoumy, K.; Upadhyaya, P.; Sohn, O. S.; Rosa, J. G.; Fiala, E. S., *Carcinogenesis* **1998**, *19*, 1603.
100. Takahashi, K.; Ogra, Y., *Metallomics* **2020**, *12*, 241.
101. Aminlari, M.; Malekhusseini, A.; Akrami, F.; Ebrahimnejad, H., *Comp Clin Path* **2007**, *16*, 47.
102. Sylvester, D. M.; Hayton, W. L.; Morgan, R. L.; Way, J. L., *Toxicol Appl Pharmacol* **1983**, *69*, 265.

103. Baskin, S. I.; Petrikovics, I.; Platoff, G. E.; Rockwood, G. A.; Logue, B. A., *Toxicol Mech Methods* **2006**, *16*, 339.

104. Craston, J. S. Biochemical Effects Of Chronic Cyanide Exposure In The Chicken And Their Relevance To The Mechanism By Which Cyanide Alleviates Selenium Toxicity. Wye College, University of London, 1991.

Chapter 2

Syntheses and Anti-proliferative Activities of Benzylic Selenocyanates: Structure-Activity Correlations with Multiple Selenocyanate Functionalities within a Molecule

2.1. Introduction

As described in chapter 1, the pronounced anti-cancer and chemopreventive activity of organoselenium compounds have attracted much research attention over last two decades. In addition to diselenides, monoselenides and ebselen analogues, organoselenocyanates serve as an important class of organoselenium compounds that exhibit potent chemopreventive and anti-cancer activities. For example, In 1985, El-Bayoumy and co-workers showed that a simple benzyl selenocyanate (**1.48**), effectively inhibits benzo[a]pyrene-induced forestomach tumors in rats during the initiation phase of carcinogenesis and the corresponding sulfur analogue benzyl thiocyanate were inactive under the identical condition.[1] Subsequently, in 1997, Reddy *et al* reported the chemopreventive ability of two synthetic organoselenocyanates, namely *p*-methoxybenzyl selenocyanate (**1.49**) and 1,4-phenylenebis(methylene) selenocyanate (**1.52**) towards azoxymethane-induced colon carcinogenesis in rats maintained on low- or high-fat diets.[2] The chemopreventive activity of compound **1.52** was found to be more pronounced when it was administered along with a low-fat diet. The metabolic pathway of compound **1.52** was studied further and it was found that the selenocyanate moiety reacted with the cellular abundant glutathione (GSH) with the replacement of the cyano group leading to the formation of the corresponding selenenyl sulfide compound. In another study, Bhattacharya and co-workers have shown that diphenylmethyl selenocyanate (**1.57**) has the ability to counter the xenobiotic-induced oxidative stress *in vivo*.[3] They have further developed a series of naphthalimide-based selenocyanates such as **1.59** and **1.60** that were found to be very effective towards the cyclophosphamide (CP)-induced genotoxicity and oxidative stress.[4] These compounds protect against chemotherapeutic drug-induced toxicity *in vivo* and chemoprevention can be initiated without blocking the antitumor effects of chemotherapeutic drugs. In addition to the chemopreventive activities, the anti-cancer activities of different organoselenocyanates are also reported recently. For example, in 2011, Krishnegowda and co-workers have reported the cytotoxicity of a series of 5,7-dibromoisatin-based organoselenium compounds against human cancer cells.[5] Among the reported compounds N-propyl-substituted isatin-based selenocyanate **1.58** exhibited selective cytotoxicity towards breast cancer cells (MCF-7) over other organ-specific cells. Further mechanistic studies indicated that the compound exhibited anti-cancer activity by inhibiting tubulin polymerization process. In 2016, Sanmartín and co-workers have reported pyrrole-linked

benzylic selenocyanate **2.1** that exhibited selective anti-proliferative activity towards malignant breast cancer cells (MCF-7) with very low GI_{50} value (2.4 µM).[6] It was shown to induce cellular death via Caspase-mediated pathway and arrested cells in G_2/M phase. In 2018, An et.al. have reported a series of 4-anilinoquinazoline-based organoselenium compounds including compounds **2.2** and **2.3** evaluated them for their anti-proliferative activities in different organ-specific cell lines (A549, HCT-116, Hep-G2, MDA-MB-231, LOVO and RKO).[7] Similar to several other compounds in the series, both compounds **2.2** – **2.3** exhibited highly potent anti-cancer activities in different organ-specific cell lines. However, the activity of benzylic selenocyanate **2.3** was relatively lower than the corresponding aryl selenocyanate **2.2** under identical condition. Structures of reported organoselenocyanates are documented in Figure 2.1.

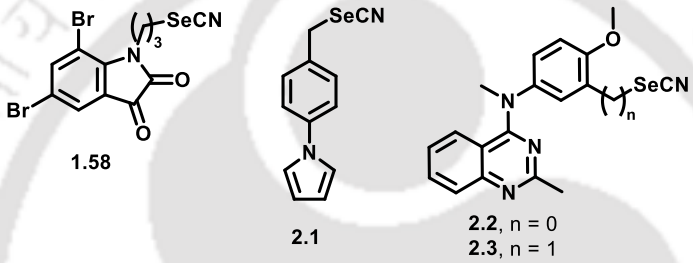

Figure 2.1. Chemical structures of benzyl or aryl-based selenocyanates containing heteronuclear substitutions.

Although compound **1.48** proved to be effective in inhibiting induced tumors in animal model as discussed in previous sections, its instability and toxicity warranted the requirement for exploration of further research, that eventually led to xylene-based selenocyanates, containing two selenocyanate groups in a single compound having three isomers **1.50**, **1.51**, **1.52**. Compound **1.52** was one of the first poly-selenocyanates discovered and attracted the attention of researchers for quite a long time. It was observed that, compound **1.52** displayed promising chemopreventive activities towards the development of carcinogen-induced tumors such as colon, lung, mammary and oral carcinogenesis. Moreover, it was also observed that, compound **1.52** was more active and was better tolerated by the host than simple benzyl selenocyanate.

2.2. Outline of the chapter

In this chapter, we describe the design and synthesis of a series of benzylic and mesitylenic selenocyanates having one or more selenocyanate units in a single molecule. Chemical structures of molecules targeted for synthesis are described in Figure 2.2.

Anti-proliferative activity of these organoselenocyanates in different breast cancer cells show that the activity of benzyl selenocyanate (**1.48**) could be significantly enhanced by the incorporation of two more selenocyanate units in a single molecule such as mesitylenic selenocyanate (**2.7**). The new selenocyanate **2.7** was found to be more active towards triple-negative breast cancer cells (MDA-MB-231) and other ER+ breast cancer cells (MCF-7 and T-47D). Our studies further indicate that the apoptotic activities of selenocyanates are associated with modulation of cellular morphology and cell cycle arrest at S-phase. They also inhibited cellular migration and exerted weak antioxidant activities. An effective binding interaction of compound **2.7** with serum albumin indicates its feasible transport in blood stream for its enhanced anti-cancer properties. Mechanistic studies by western blot analyses demonstrate that benzylic selenocyanates exhibit anti-proliferative activities by modulating key cellular proteins such as survivin, bcl-2 and COX-2, which was further supported by molecular docking studies.

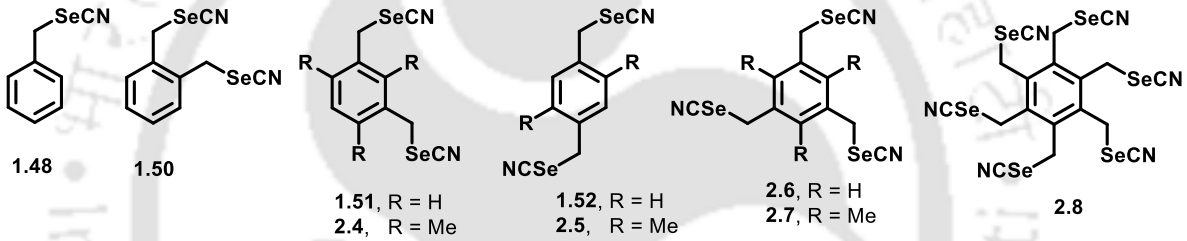

Figure 2.2. Chemical structures of the synthesized benzylic and mesitylenic selenocyanates.

2.3. Results and Discussion

2.3.1 Synthesis of organoselenocyanates

The selenocyanate compounds are conventionally prepared following literature methods with appropriate modifications, in good yields by nucleophilic substitution from the corresponding benzylic or mesitylenic halides in the presence of potassium selenocyanate in acetonitrile at room temperature.[8] Some of the halide precursors that are not available commercially, were synthesized and used in the next step after purification as applicable. The final selenocyanates and thiocyanates were purified by active neutral alumina column chromatography using petroleum ether and ethyl acetate as eluents. The purified final compounds were characterized by NMR, FT-IR, and ESI-MS spectral techniques.

2.3.2 Anti-proliferative activities of the synthesized organoselenocyanates

As the treatment scopes of triple negative breast cancer cells are limited and some of the reported organoselenocyanates exhibited good potencies towards different organ-specific cell lines including breast cancer cells, we have evaluated synthesized organoselenocyanates **1.48** – **2.8** (Figure 2.1) towards MDA-MB-231 cells, which is a representative triple negative breast cancer cells (TNBC). The anti-proliferative activities of the compounds were evaluated using conventional MTT assay in MDA-MB-231 cells and the results are described in Figure 2.3. All the experiments were independently carried out at least three times and the results were summarized after 72 h of incubation at 37 °C. To understand the dose-dependency of these compounds for growth inhibition of MDA-MB-231 cells over 72 h, the percentage of cell proliferation was estimated at four different concentrations (1.0 μM, 5.0 μM, 10.0 μM and 25.0 μM) and compared to that in the absence of compounds (controls) as well as with a well-known anti-cancer drug, 5-fluorouracil (5-FU). As shown in Figure 2.3, most of the organoselenocyanates were found to be active in the growth inhibition of MDA-MB-231 cells. Interestingly, all of the compounds exhibited greater anti-proliferative activity than commercially available drug 5-FU, in MDA-MB-231 under identical experimental conditions.

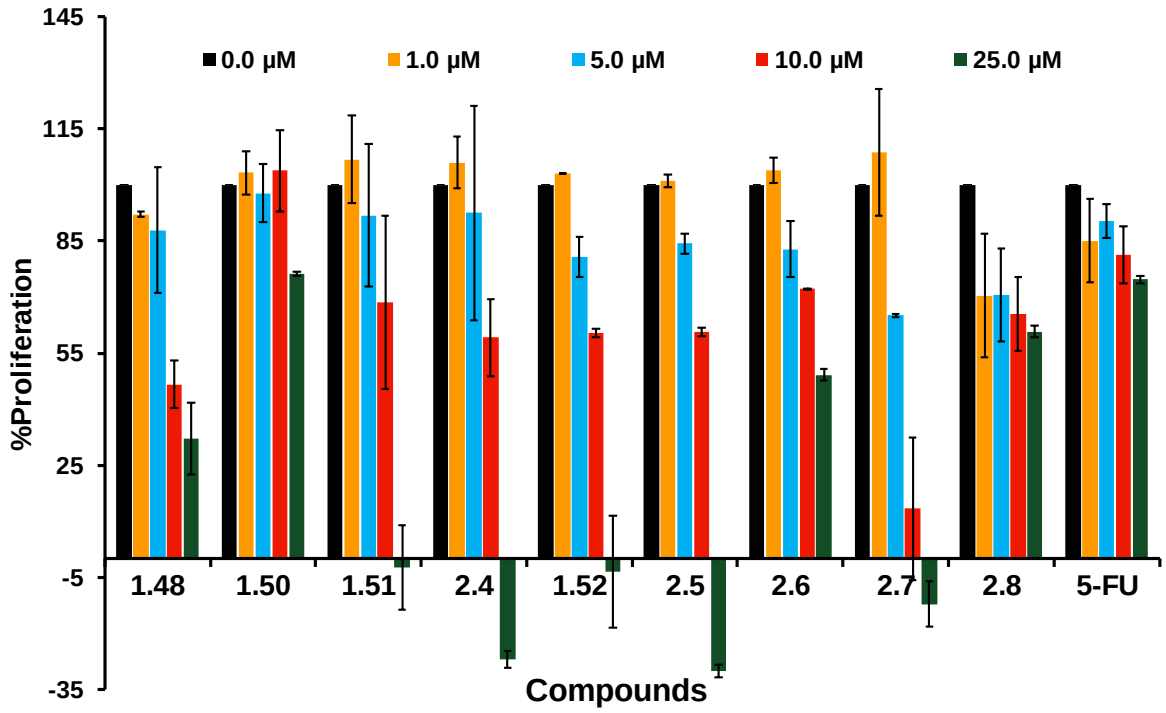

Figure 2.3. Percentage proliferation of MDA-MB-231 cells treated with the test compounds in a dose-dependent manner. Apart from control condition (*i.e.* in the

absence of the compounds), percentage proliferation was studied in four different concentrations (1.0, 5.0, 10.0, 25.0 μM). The % proliferation after 72 h as shown above was calculated from the resultant OD values at 72 h after subtracting the OD values of an identical set of cells at 0 h.

Upon the determination of dose-dependency of the test compounds towards growth inhibition of MDA-MB-231 cells, inhibitory concentrations towards cell proliferation were determined for the potent compounds to understand their relative anti-proliferative activities. As shown in Table 2.1, previously reported chemopreventive selenocyanates such as benzyl selenocyanate (**1.48**) and *p*-XSC (**1.52**) exhibited good anti-proliferative activities with an IC_{50} of 11.15 and 12.13 μM, respectively. Similar to **1.52** other *bis*-selenocyanates such as **1.50**, **1.51**, **2.5** exhibited comparable IC_{50} values in the range of 11.0 – 14.0 μM as shown in Table 2.1. However, the corresponding *ortho*-derivative **1.50** was found to have weaker anti-proliferative activity and IC_{50} could not be determined for it under the similar concentration range. A significant difference in anti-proliferative activity was observed between compounds **2.6** and **2.7** having three selenocyanate units. While IC_{50} could not be determined for compound **2.6** up to a concentration of 25.0 μM, the corresponding mesitylenic derivative **2.7** exhibited a significantly improved anti-proliferative activity (IC_{50} = 6.4 μM). These results indicate that the presence of methyl group in benzylic selenocyanates might play important roles for their anti-proliferative activities, which is clearly reflected in the activities of compounds having two (**1.51**, **2.4**, **1.52**, **2.5**) and three (**2.6** and **2.7**) selenocyanate units. However, to our surprise, IC_{50} value could not be determined in the MTT assay for compound **2.8** with six selenocyanate units. A decrease in cell proliferation was observed in the beginning with increasing concentration of compound **2.8**, however, a negligible change was observed after 40% inhibition. This is also reflected in the dose-response data as shown in Figure 2.3. In order to explain this anomaly, we postulated that, due to the presence of six selenocyanate units in a single molecule, compound **2.8** became very lipophilic in nature and was sparingly soluble in the buffered medium during cellular assays. Therefore, the accurate inhibitory activity could not be determined at higher concentrations. It should be noted here that the thiocyanates corresponding to some of the selenocyanates were also evaluated for their anti-proliferative activities, however, all of them were found to be almost inactive under the identical condition. As observed from Figure 2.3 and Table 2.1, it is evident that the

anti-proliferative activity of benzyl selenocyanate **1.48** can be significantly enhanced by a proper balance of methyl and multiple selenocyanato groups in a single molecule (compound **2.7**).

Table 2.1. Anti-proliferative activities of chalcogenocyanates in MDA-MB-231 cells as determined by MTT assay.[a]

Compound	IC_{50} (μM)	Compound	IC_{50} (μM)
1.48	11.15 ± 2.75	**2.5**	11.73 ± 0.23
1.51	13.90 ± 0.12	**2.7**	6.43 ± 0.10
2.4	11.66 ± 2.61	**5-FU**	>25
1.52	12.13 ± 2.19		

[a]Data represents the mean IC_{50} values (±SD) of % cell proliferation determined by the MTT assay from the dose-response curves in triplicates after 72 h of incubation at 37 °C. About 4000 cells/100μl/well were seeded in 96-well culture plates and treated with various concentrations of test compounds for 72 h. The % proliferation after 72 h as shown above are calculated from the resultant OD values at 72 h after subtracting the OD values of an identical sets of cells at 0 h.

Upon the evaluation of all the selenocyanates in triple-negative breast cancer cells (MDA-MB-231), we have further screened some of the active compounds (**1.48** and **2.7**) along with the standard drug 5-FU in two additional ER+ breast cancer cells (MCF-7 and T-47D) to understand the impact of these compounds towards breast cancer cells in general. As shown in Figure 2.4, the mesitylenic selenocyanate **2.7** was found to be almost equally potent in both the ER+ breast cancer cell lines [IC_{50} (MCF-7) = 4.64 ± 0.13 μM; IC_{50} (T-47D) = 3.53 ± 0.74 μM]. These results indicate that compound **2.7** is significantly more active than the standard benzyl selenocyanate **1.48** in all three breast cancer cells studied herein.

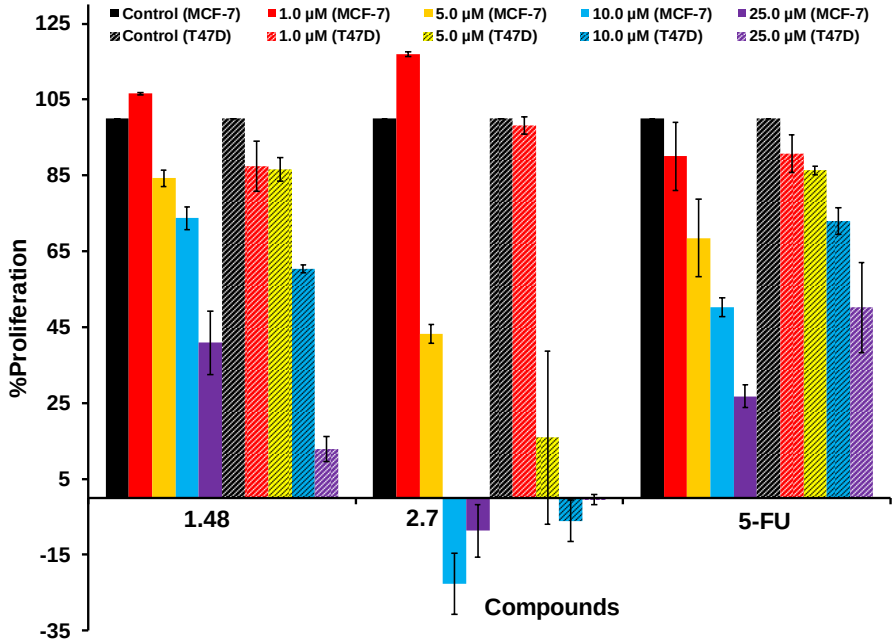

Figure 2.4. Percentage proliferation of MCF-7 and T-47D cells treated with selected test compounds (**1.48** and **2.7**) at a dose-dependent manner. Apart from control condition (*i.e*. in the absence of the compounds), percentage proliferation was studied in four different concentrations (1.0, 5.0, 10.0, 25.0 µM). The % proliferation after 72 h as shown above was calculated from the resultant OD values at 72 h after subtracting the OD values of an identical set of cells at 0 h.

To understand the toxicity and selectivity of the most active compound **2.7**, towards normal cell over cancer cell, compound **2.7** was further tested in a representative normal cell HEK-293 (Human Embryonic Kidney) and the results were compared with MDA-MB-231 cells, in concentrations of 5.0 µM and 10.0 µM. As expected, compound **2.7** was found to be significantly lesser active in HEK-293 cells than in MDA-MB-231 cells (Figure 2.5).

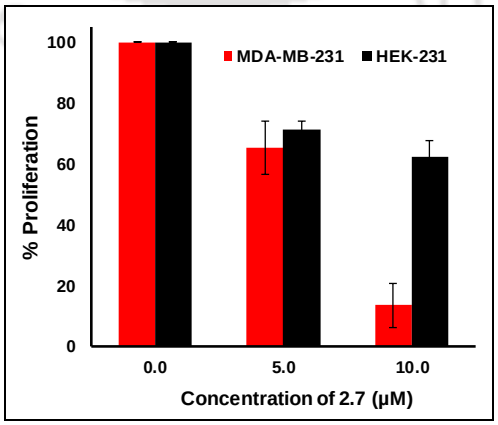

Figure 2.5. Cellular proliferation of triple negative breast cancer (MDA-MB-231) cells and normal cells (HEK-293) in presence of varying concentrations of compound **2.7**.

2.4. Dose-dependent cellular death by flow cytometry

As some of the selenocyanates in the present study exhibited cytotoxic behavior at higher concentrations, this was further confirmed using propidium iodide (PI)-flow cytometric assay. PI is a fluorescent compound that can bind to nucleic acids with little or no sequence preferences. An increased red fluorescence is indicative of damaged cell membrane, which in turn represents cell death. Among the selenocyanates in the present study, five selected selenocyanates such as **1.48**, **1.51**, **1.52**, **2.4**, **2.7** that exhibitied cytotoxic behavior were chosen in PI-flow cytometric assay. Treatment of MDA-MB-231 cells with different concentrations of these compounds for a duration of 72 h resulted in profound cell death which was found to be dose-dependent as shown in Figure 2.6. At concentrations of 10.0 and 25.0 µM of selenocyanates, a significant cell death was observed, which is in agreement with the observation on anti-proliferative activity data as obtained from MTT assay method. This study along with anti-proliferative activity data confirms the inhibition of cell growth and induction of cell death by organoselenocyanates used in the present study.

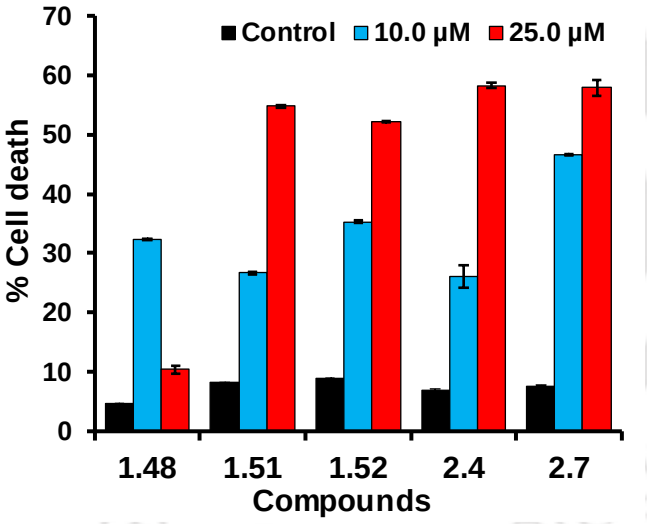

Figure 2.6. Cytotoxicity profiles of the test compounds (**1.48**, **1.51**, **1.52**, **2.4**, **2.7**) on MDA-MB-231 cells in propidium iodide (PI)-flow cytometric studies. About 5×10^4 cells per 2 mL were seeded in 6-well culture plates and treated with two different concentrations (10.0 µM and 25.0 µM) of test compounds for 72 h. The cells were stained with 5.0 µl of 1.0 mg mL^{-1} of PI and analyzed by the flow-cytometric method.

2.5. Cell cycle analysis of MDA-MB-231 cells treated with selected selenocyanates

As described earlier, abnormal proliferation of cells is an important requirement for the progression of cancer and the cellular proliferation is controlled by cell cycle. Hence, an

inhibition of cell cycle progression, thereby arresting cell growth and inducing apoptosis, may serve as a promising strategy in cancer defense. In order to understand the mechanism of inhibition of cellular proliferation by cell cycle arrest, we investigated the effects of most active compound **2.7** and compared with **1.48** on the cell cycle distribution of MDA-MB-231 cells using PI-based flow cytometric assay in two concentrations of 1.0 μM and 5.0 μM. Cell cycle distribution was observed after incubation of the compounds to the cells for 24 h. As described in Figure 2.7, it has been observed that upon treatment of the cells with the compounds at the above-mentioned concentrations, there has been a significant arrest of cells at S phase with a simultaneous decrease in the G_1 and G_2 phase. Specifically, in presence of compound **2.7**, S phase population of MDA-MB-231 cells was increased to 39.3 % and 43.1 % at 1.0 μM and 5.0 μM respectively from a control value of 33.3%. However, there was no significant changes in the cell cycle distribution for **1.48** under the identical experimental condition. This indicates that, the induction of apoptosis and anti-proliferative activity of the compounds was due to S phase arrest of the cells.

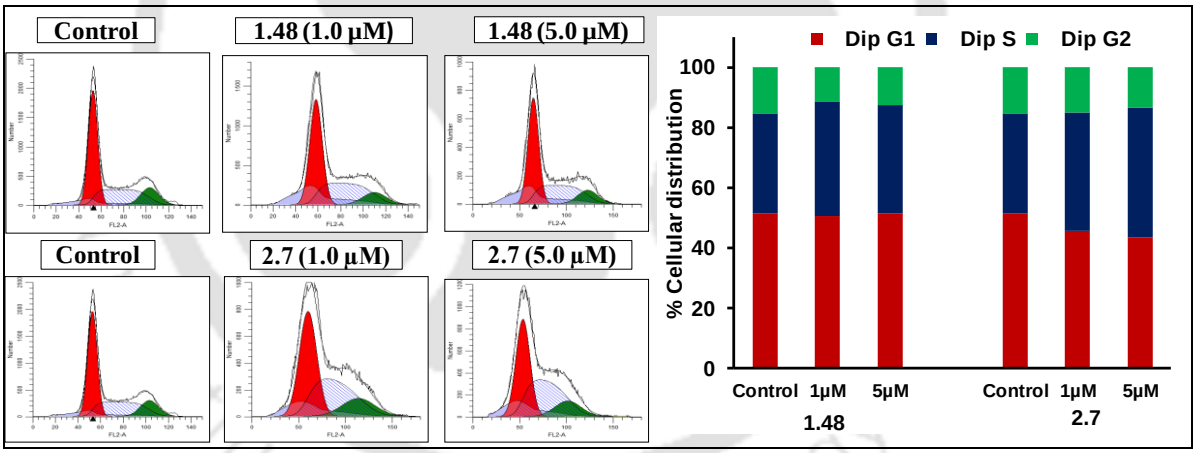

Figure. 2.7. Graphical representation of distribution patterns of MDA-MB-231 cells in different phases of cell cycle in the presence of selenocyanates 1.48 and 2.7. About 1 × 10^5 cells per 2.0 mL were seeded in 6-well plates and treated with two different concentrations (1.0 and 5.0 μM) of test compounds for 24 h and the cell cycle distribution was analyzed by flow-cytometric assay after staining with PI/RNase.

2.6. Selenocyanate-induced inhibition of cellular migration

As mentioned earlier, metastatic cells have the property to migrate to other uninfected organs to spread itself throughout the body. Hence, inhibition of cellular migration is a very promising aspect in cancer defense strategy. It is noteworthy that TNBC has a high

rate of cellular mobility and very few drugs are known to arrest the cellular mobility. We have therefore evaluated our test selenocyanates towards the inhibition of migration of MDA-MB-231 cells using wound healing scratch assay. As shown in Figure 2.8, while the untreated cells migrated to the scratched region over 72 h, a significant dose-dependent anti-migratory activity towards triple-negative cells (MDA-MB-231) was observed upon the treatment with most-active compound **2.7** at concentrations of 1.0 µM and 2.5 µM, therefore indicating the anti-migratory activity of the selenocyanates.

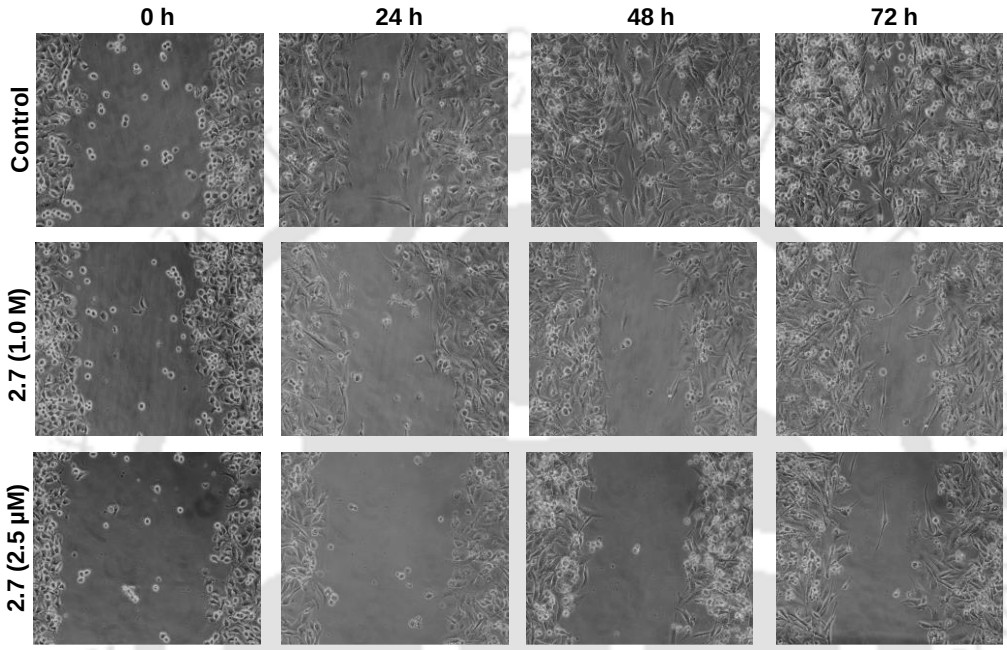

Figure 2.8. Wound healing studies on MDA-MB-231 cells in the presence of compounds **2.7** at concentrations of 1.0 µM and 2.5 µM after incubation for 0 h, 24 h, 48 h and 72 h.

2.7. Selenocyanate-induced cellular morphological changes

The initiation of apoptosis and cell death is accompanied by significant change in cellular morphology of cancer cells. Cell shrinkage accompanied by a significant reduction in volume is associated with apoptotic cellular death. Several visualization techniques are employed to confirm the mode of cellular death by investigating the cellular debris. Among those various techniques, microscopy is a very commonly used method to visualize the cellular debris. In the present study, triple negative breast cancer cells (MDA-MB-231) were treated with compounds **2.7** for 24 h and 48 h and the cells were visualized under microscope post-incubation. As shown in Figure 2.7, significant cell death was observed for cells treated with compounds **2.4** and **2.16,** which enhanced with the increase in incubation time as compared to the control experiments. Visual

changes in the morphology of the cells are due to formation of dead cell debris, which loses its adherent property and are suspended randomly in the culture media. In addition to visualization by microscope, the cells were stained with fluorescent dye propidium iodide (PI) after incubation with the compounds for 72 h. Since PI is non-permeable to cell-membrane of living cell, it can stain the nuclei of dead cell with high selectivity, hence furnishing a very convenient way to visualize dead cells. As shown in Figure 2.9, a significant number of cellular death was observed by PI which further supports the fact of occurrence of cellular death.

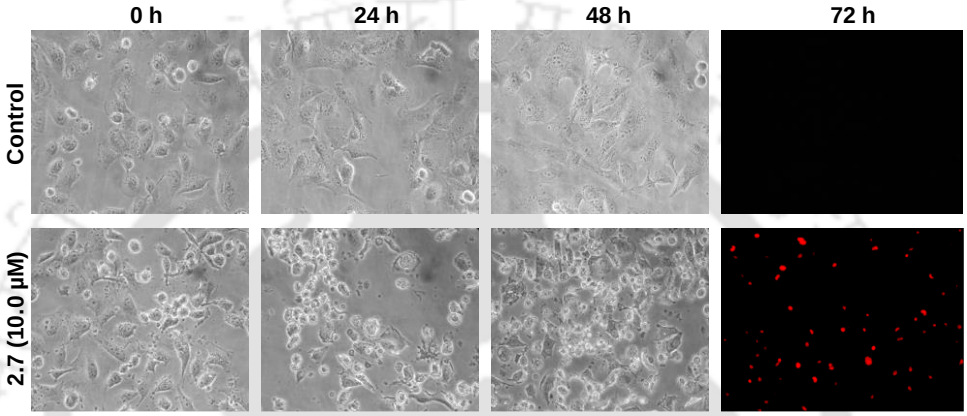

Figure 2.9. Change in cellular morphology of MDA-MB-231 cells in the absence and presence of **2.7** at a concentration of 10.0 μM after incubation for 0 h, 24 h, and 48 h. PI-stained images after incubation of cells for 72 h in the presence of test compounds represent dead cells.

2.8. Antioxidant activities of organoselenocyanates

A number of synthesized organoselenium compounds are known to exhibit promising antioxidant activities and catalytically scavenges biologically relevant reactive oxygen and nitrogen species (ROS and RNS) such as hydrogen peroxide, hydroxyl radical, peroxynitrite and so on.[9] However, the antioxidant activities of organoselenocyanates are not explored in great details. Herein, we took the initiative to evaluate the synthesized organoselenocyanates for *in vitro* antioxidant activities.

2.8.1. Hydrogen peroxide scavenging activity

To understand the capability of the test compounds to catalytically reduce hydrogen peroxide, initial rate of reduction of the same was evaluated spectrophotometrically using a GSH/GSSG coupled system in presence of synthesized selenocyanates.[10] The relative rates were compared against standard anti-oxidant organoselenium compound 2-

phenyl-1,2-benzoselenazol-3-one, commonly known as ebselen (**1.14**). The activity of most of the selenocyanates were found to be much lower than that of ebselen under the identical experimental condition as shown in Figure 2.10. This indicates that selenocyanates in the present study are relatively weaker antioxidants for the reduction of oxidants such as H_2O_2 in the presence of GSH as co-substrate.

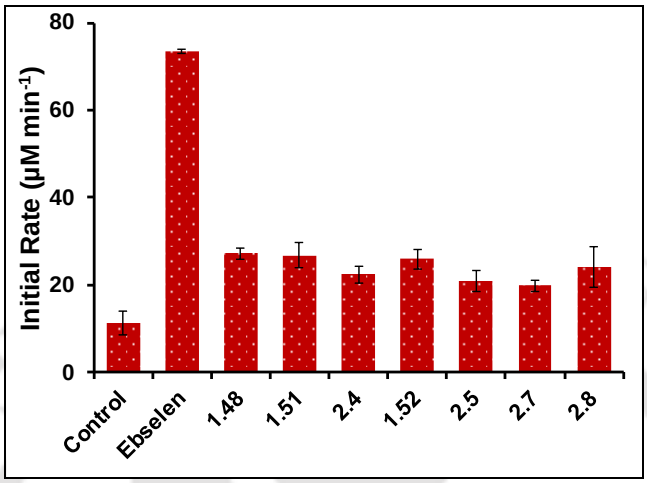

Figure 2.10. Initial rates (v_o) for the reduction of H_2O_2 using GSH as co-substrate in the presence and absence of some selected test compounds. The assay mixture contains GSH (2.0 mM), EDTA (1.0 mM), Glutathione disulfide reductase (1.0 units/ml), NADPH (0.4 mM) in phosphate buffer (100 mM, pH = 7.5). The sample concentrations were maintained at 50 μM and the reaction was started by the addition of 0.16 mM H_2O_2.

2.8.2. Peroxynitrite scavenging activity

Peroxynitrite (PN, $ONOO^-$) is a reactive nitrogen species, which is formed by the metabolism of nitric oxide that is formed from L-arginine by nitric oxide synthase (NOS) and NADPH in presence of oxygen through a five electron process, can lead to chemical modification of biomolecules such as amino acid, enzymes by oxidation or nitration.[10] A number of small-molecules especially organochalcogen compounds have been developed as catalytic or stoichiometric scavengers of PN as monitored by the oxidation of dihydrorhodamine-123 (DHR-123) to highly fluorescent rhodamine-123.[11] The scavenging potentials of selenocyanates were compared to that of ebselen, which has been shown to be a catalytic scavenger of PN.[11c] Unfortunately, it was observed that the activities of selenocyanates in scavenging peroxynitrite in a dose-dependent manner were poor (Figure 2.11). Although few selenocyanates such as **2.6** and **2.7** exhibited good scavenging activity under identical condition, the IC_{50} values could not be calculated for some of the selenocyanates such as **1.48**, **1.50**, **1.52** These compounds exhibited some scavenging properties in the beginning however, the inhibition remained

less than 50% even up to 150.0 – 200.0 µM concentrations. In general, the selenocyanates used in the present study were found to be weaker scavengers of PN as compared to other organoselenium compounds studied previously.[11,12]

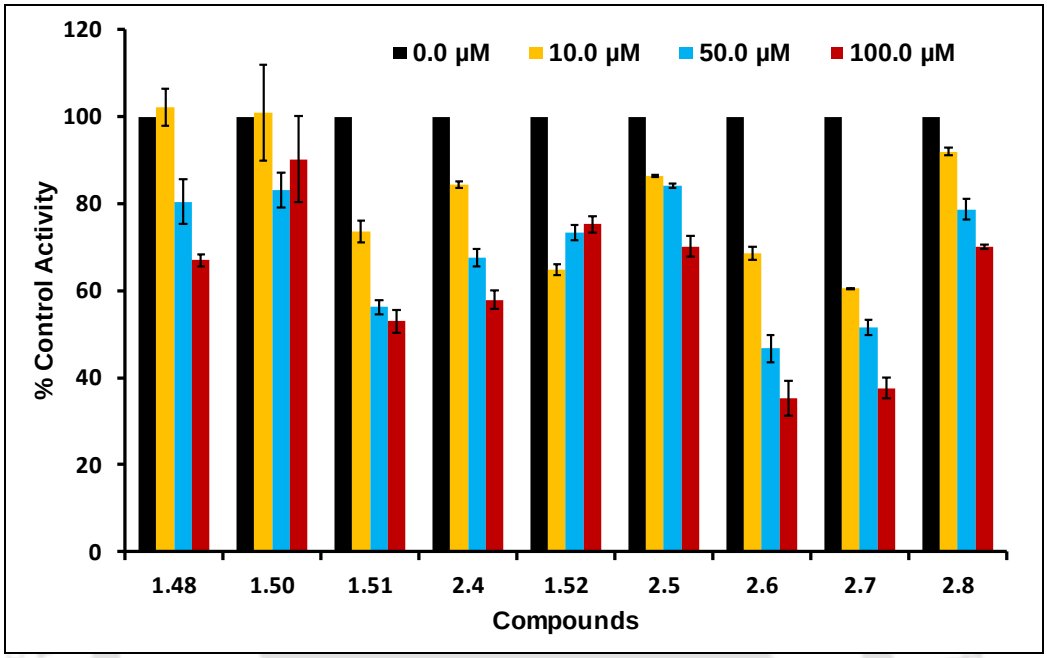

Figure 2.11. Peroxynitrite scavenging activity of some selected selenocyanates at different concentrations (0.0 µM, 10.0 µM, 50.0 µM and 100.0 µM). The assay mixture contained DHR-123 (1.0 µM), with variable concentration of test compounds in phosphate buffer (0.1 M, pH = 7.4) with appropriate concentration of PN to have fluorescence emission of rhodamine-123 in the range of 7.0×10^6 - 9.0×10^6.

2.9. Binding interaction with bovine serum albumin

Serum albumin is a highly abundant protein in blood plasma and plays a very crucial role in the transportation of several essential nutrients, small molecules, drugs etc. by binding the guest molecule at one site and selectively releasing it at the other. Hence, study of the interaction of the most active selenocyanate **2.7** with bovine serum albumin was studied and the binding affinity was compared to that of benzyl selenocyanate **1.48**. Bovine serum albumin (BSA) is a fluorescent protein and is used as a homology model for human serum albumin for its economic and ready availability. The fluorescence of the protein mainly arises due to one tyrosine and two tryptophan residues, namely Trp-134 and Trp-212, located on the surface of the sub-domain IB and in the hydrophobic pockets of sub-domain IIA. Interaction of small molecule or drugs with BSA leads to quenching of the fluorescence and the monitoring of the quenching of the fluorescence

with increasing concentration of the drug may serve as an important tool for understanding the protein-ligand binding interaction.

The binding interaction of selenocyanates with BSA was studied following the reported procedure.[13] The BSA solution exhibits strong fluorescence emission at 344 nm upon an excitation at 280 nm. The fluorescence intensity gradually decreases with an increasing concentration of the test compounds without any shift in the emission λ_{max}, indicating that the compound quenches the intrinsic fluorescence of BSA in a static manner. The fluorescence quenching was performed by titration method and the binding parameters such as quenching constant (K_q) and Stern-Volmer constant (K_{SV}) were determined using Stern–Volmer equation as shown in Table 2.2.

Table 2.2. The binding parameters such as K_{SV} (Stern–Volmer constant) and Kq (quenching constant) of different test compounds with BSA as obtained from the Stern–Volmer equation[a].

Compound	K_{SV} ($\times 10^4$) M^{-1}	K_q ($\times 10^{12}$) $M^{-1}S^{-1}$	R^2
1.48	1.94	1.94	0.9907
2.7	4.81	4.81	0.9905

[a]The quenching experiment was performed using a fluorescence spectrophotometer with excitation and emission wavelengths of 280 nm and 344 nm, respectively. BSA (10.0 μM) in Tris-HCl buffered saline (100 mM, pH 7.2) was titrated with increasing concentrations of test compounds (0.0–50.0 μM).

The binding constant (K_b) and number of binding sites (n) have been determined by Scatchard plot as reflected in Table 2.3. These results represent that both selenocyanates exhibited significantly good binding affinity towards BSA with high K_{SV} and K_q values. The value of n for all the compounds are nearly 1.0, indicating a single molecular binding with BSA. Particularly, the most active selenocyanate **2.7** exhibits much higher binding affinities as reflected with its higher K_{SV} and K_q values as compared to **1.48**, indicating the higher feasibility of **2.7** for its transport in blood stream. A similar static interaction of selenadiazole derivatives with BSA with good binding affinity has recently been reported by Chen and co-workers.[14] They showed that the binding of selenadiazole derivatives with serum albumin facilitated the drug transport through plasma and significantly enhanced their anti-tumor activities and cellular uptakes.

Table 2.3. The binding parameters such as K_b (binding constant) and n (number of molecules per unit protein) of different test compounds with BSA as determined by using a Scatchard plot[a]

Compound	K_b ($\times 10^4$) M^{-1}	N	R^2
1.48	0.89	0.93	0.9913
2.7	4.84	1.00	0.9879

[a]The quenching experiment was performed using a fluorescence spectrophotometer with excitation and emission wavelengths of 280 nm and 344 nm, respectively. BSA (10.0 μM) in Tris-HCl buffered saline (100 mM, pH 7.2) was titrated with increasing concentrations of test compounds (0.0–50.0 μM).

2.10. Conclusions

In summary, we reported the synthesis, purification and characterization of benzylic and mesitylenic selenocyanates bearing one or multiple selenocyanate functionalities in a single molecule and evaluated their anti-cancer activity towards triple-negative breast cancer cells (MDA-MB-231) and other ER+ breast cancer cell lines (MCF-7 and T-47D). Activity of all the selenocyanates studied herein exhibited significantly higher activity than the commercial chemotherapeutic drug 5-FU. Interestingly, the anti-proliferative activity of mesitylenic selenocyanate **2.7** was significantly higher than simple benzyl selenocyanate **1.48**, indicating the importance of multiple selenocyanate and methyl groups in a single molecule. Detailed investigations reveal that, the selenocyanate **2.7** arrested the cancer cells at S-phase of the cell cycle and exhibited anti-invasive property by inhibiting the cellular migration. Significant binding affinity towards BSA might help in transporting the compound in blood stream. Although, we were unable to confirm the exact mechanism of anti-proliferative activity of the selenocyanate, our results would be a platform for initiating further detailed research to explore the *in vivo* anti-proliferative potential of the selenocyanates.

2.11. Experimental section

2.11.1 Materials and method

All chemical reagents were used as delivered without further purification. Solvents used for purification (n-hexane, ethyl acetate, petroleum ether) were distilled before use. Dry solvents were used for reactions wherever applicable. Melting point of the compounds reported here, were recorded on Buchi B-540 melting point apparatus and the values were uncorrected. Thin-layer chromatography analyses were done on pre-coated silica

gel K_{254} on aluminium sheets. NMR spectroscopy was done on a Bruker Ascend^{TM} 600 spectrometer (^{1}H NMR at 600 MHz, ^{13}C at 150 MHz and ^{77}Se at 114 MHz) or a Varian Mercury Plus 400 MHz spectrometer. Chemical shifts were reported with respect to tetramethylsilane (^{1}H and ^{13}C as an internal standard) and dimethyl selenide for ^{77}Se as an external standard. High resolution mass spectra (HRMS) and liquid chromatography mass spectra (LCMS) were recorded on Agilent 6520 Accurate-Mass Quadrupole Time-of-Flight (Q-TOF) LC/MS spectrometer. IR spectra was recorded on Perkin-Elmer Spectrum Two FT-IR spectrometer.

General procedure (GP1) for synthesis of selenocyanates

Selenocyanates were prepared according to reported literature with minor modifications.[8] To a stirred solution of benzylic or mesitylenic halides in acetonitrile, a solution of potassium selenocyanate in acetonitrile was added and was stirred at room temperature. Appearance of white precipitate indicated the progress of reaction. The progress was monitored by TLC analysis.

Work-up method 1

The reaction mixture was added to cold and distilled water and was stirred for 30 minutes. The residue was filtered off and was washed with water to remove any residual inorganic salts. The residue was dried and was purified using column chromatography to afford the pure product

Work-up method 2

The solvent was evaporated under reduced pressure and the residue was extracted using ethyl acetate (3 × 10 ml) and was washed with water (2 × 10 ml) and brine (1 × 10 ml). Combined organic layer was dried over anhydrous sodium sulphate and was evaporated under reduced pressure to yield the crude product. It was further purified by column chromatography using petroleum ether and ethyl acetate as eluting solvent, to afford the purified product.

Compound **1.48**: Prepared according to **GP1**, using benzyl bromide (0.40 mL, 3.40 mmol) and potassium selenocyanate (0.50 g, 3.16 mmol) in acetonitrile (15.0 mL). The reaction mixture was stirred for 1 h at room temp. Work-up method 1 was utilized to afford the crude compound as white solid. The crude product was purified by column chromatography using petroleum ether and ethyl acetate as

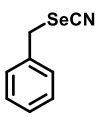

eluting solvent to afford the title compound as purified product. R_f = 0.5 (4% ethyl acetate in petroleum ether 60–80). Yield: 0.39 g (59%). M.P. = 73–75 °C. ^{1}H NMR ($CDCl_3$, 600 MHz): δ (ppm) = 7.39 – 7.33 (m, 5H), 4.31 (s, 2H); ^{13}C NMR ($CDCl_3$, 150 MHz): δ (ppm) = 35.7, 129.4, 129.2, 128.9, 102.2, 33.0; ^{77}Se NMR ($CDCl_3$, 114 MHz): δ (ppm) = 283. IR ($\bar{\nu}$, cm^{-1}): 2146 (s), 1491 (m), 1454 (m), 1217 (m), 1191 (m), 1069 (m). ESI-MS *m/z* calcd. for C_8H_7NSe $[M + Na]^+$: 219.9641; obs: 220.0526.

Compound **1.50**: Prepared according to **GP1**, using 1,2-phenylenebismethylene bromide

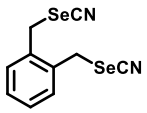

(0.40 g, 1.52 mmol) and potassium selenocyanate (0.50 g, 3.47 mmol) in acetonitrile (15 mL). The reaction mixture was stirred at room temperature for 2 h. Work-up method 1 was utilized to afford the crude compound as white crystalline solid. The crude product was purified by silica gel column chromatography using 25% ethyl acetate in petroleum ether as eluting solvent to afford the title compound as purified product. R_f = 0.5 (50% ethyl acetate in hexane). Yield: 0.41 g (88%). M.P. = 105–107 °C. ^{1}H NMR (DMSO-d_6, 600 MHz): δ (ppm) = 7.34 – 7.31 (m, 4H), 4.43 (s, 4H); ^{13}C NMR (DMSO-d_6, 150 MHz): δ (ppm) = 136.9, 131.8, 129.1, 105.2, 30.3; ^{77}Se NMR (DMSO-d_6, 114 MHz): δ (ppm) = 314; IR ($\bar{\nu}$, cm^{-1}): 2923 (m), 2148 (s), 1451 (m), 1194 (m). ESI-MS *m/z* calcd for $C_{10}H_8N_2Se_2$ $[M + Na]^+$: 337.8916; obs: 337.4143.

Compound **1.51**: Prepared according to **GP1**, using 1,3-phenylenebis(methylene)

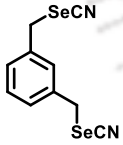

bromide (0.40 g, 1.52 mmol) and potassium selenocyanate (0.50 g, 3.47 mmol) in acetonitrile (20 mL). The reaction mixture was stirred at room temperature for 2 h. Work-up method 2 was utilized to afford the crude compound as a pale yellow solid. The crude product was purified by silica gel column chromatography using 35% ethyl acetate in petroleum ether as eluting solvent to afford the title compound as purified product. R_f = 0.4 (32% ethyl acetate in 60 – 80 petroleum ether). Yield: 0.46 g (97%). M.P. = 108–110 °C. ^{1}H NMR ($CDCl_3$, 600 MHz): δ (ppm) = 7.39 – 7.33 (m, 4H), 4.27 (s, 4H); ^{13}C NMR ($CDCl_3$, 150 MHz): δ (ppm) = 136.9, 130.2, 129.6, 129.5, 101.9, 32.3; ^{77}Se NMR ($CDCl_3$, 114 MHz): δ (ppm) = 295; IR ($\bar{\nu}$, cm^{-1}): 2923 (m), 2150 (s), 1200 (m). ESI-MS *m/z* calcd for $C_{10}H_8N_2Se_2$ $[M + Na]^+$: 337.0937; obs: 337.1142.

Compound **1.52**: Prepared according to **GP1**, using 1,4-phenylenebismethylene bromide

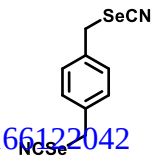

(0.40 g, 1.52 mmol) and potassium selenocyanate (0.50 g, 3.47 mmol) in

acetonitrile (20 mL). The reaction mixture was stirred for 2h at room temp. Work-up method 2 was utilized to afford the crude compound as white amorphous solid. The crude product was purified by silica gel column chromatography using 40% ethyl acetate and petroleum ether as eluting solvent to afford the title compound as purified product. R_f = 0.5 (36% ethyl acetate in petroleum ether). Yield: 0.46 g (95%). M.P. = 152–155 °C. ^{1}H NMR ($CDCl_3$, 600 MHz): δ (ppm) = 7.38 (s, 4H), 4.28 (s, 4H); ^{13}C NMR ($CDCl_3$, 150 MHz): δ (ppm) = 136.4, 130.0, 101.8, 32.3; ^{77}Se NMR ($CDCl_3$, 114 MHz): δ (ppm) = 293. IR ($\bar{\nu}$, cm^{-1}): 2924 (s), 2853 (m), 2147 (s), 1426 (m), 1190 (m), 1092 (s). ESI-MS *m*/*z* calcd for $C_{10}H_8N_2Se_2$ $[M + H]^+$: 316.9096; obs: 316.9086.

Compound **2.4**: Prepared according to **GP1**, using 1,3-bis(bromomethyl)mesitylene

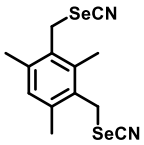

(0.50 g, 1.63 mmol) and potassium selenocyanate (0.50 g, 3.47 mmol) in acetonitrile (15 mL). The reaction mixture was stirred at room temperature for 2 h. Work-up method 2 was utilized to afford the crude compound as a pale yellow solid. The crude product was purified by silica gel column chromatography using 30% ethyl acetate in petroleum ether as eluting solvent to afford the title compound as white solid. R_f = 0.5 (26% ethyl acetate in 60 – 80 petroleum ether). Yield: 0.52 g (89%). M.P. = 154 – 157 °C; ^{1}H NMR ($CDCl_3$, 600 MHz): δ (ppm) = 6.95 (s, 1H), 4.48 (s, 4H), 2.47 (s, 3H), 2.40 (s, 6H); ^{13}C NMR ($CDCl_3$, 150 MHz): δ (ppm) = 138.6, 137.2, 131.6, 129.9, 101.7, 29.0, 20.3, 16.1; ^{77}Se NMR (DMSO-d_6, 114 MHz): δ (ppm) = 252; IR ($\bar{\nu}$, cm^{-1}): 2916 (w), 2148 (s), 1458 (m), 1190 (s); ESI-MS *m*/*z* calcd for $C_{13}H_{14}N_2Se_2$ $[M + NH_4]^+$: 375.9831; obs: 375.9830.

Compound **2.5**: Prepared according to **GP1**, using 1,4-bis(bromomethyl)-2,5-

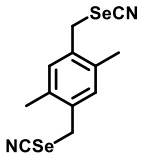

dimethylbenzene (0.30 g, 1.03 mmol) and potassium selenocyanate (0.32 g, 2.26 mmol) in acetonitrile (5 mL). The reaction mixture was stirred at room temperature for 2 h. Work-up method 1 was utilized to afford the crude compound as yellow amorphous solid. The crude product was purified by silica gel column chromatography using 25% ethyl acetate in petroleum ether as eluting solvent to afford the title compound as purified product. R_f = 0.5 (25% ethyl acetate in hexane). Yield: 0.23 g (65%). M.P. = 207–209 °C. ^{1}H NMR (DMSO-d_6, 600 MHz): δ (ppm) = 7.13 (s, 2H), 4.32 (s, 4H), 2.29 (s, 6H); ^{13}C NMR (DMSO-d_6, 150 MHz): δ (ppm) = 136.1, 134.6, 133.0, 105.2, 31.1, 19.1; ^{77}Se NMR (DMSO-d_6, 114 MHz): δ (ppm) = 292; IR ($\bar{\nu}$, cm^{-1}): 2953 (m), 2922 (s), 2854 (m), 2147 (s), 1447 (m). ESI-MS *m*/*z* calcd for $C_{12}H_{12}N_2Se_2$ $[M + NH_4]^+$: 361.9675; obs: 361.9665.

Compound **2.6**: Prepared according to **GP1**, using 1,3,5-tris(bromomethyl)benzene (0.20 g, 0.56 mmol) and potassium selenocyanate (0.26 g, 1.8 mmol) in acetonitrile (7 mL). The reaction mixture was stirred at room temperature for 2 h. Work-up method 2 was utilized to afford the crude compound as an off-white crystalline solid. The crude product was purified by silica gel column chromatography using 30% ethyl acetate in petroleum ether as eluting solvent to afford the title compound as purified product. R_f = 0.6 (50% ethyl acetate in hexane). Yield: 0.13 g (53%). M.P. = 158–160 °C. ^{1}H NMR (DMSO-d_6, 600 MHz): δ (ppm) = 7.30 (s, 3H), 4.29 (s, 6H); ^{13}C NMR (DMSO-d_6, 150 MHz): δ (ppm) = 139.7, 129.4, 105.5, 32.9; ^{77}Se NMR (DMSO-d_6, 114 MHz): δ (ppm) = 315; IR ($\bar{\nu}$, cm^{-1}): 2925 (m), 2151 (s), 1455 (m), 1430 (m), 1196 (m). ESI-MS *m*/*z* calcd for $C_{12}H_9N_3Se_3$ $[M + Na]^+$: 455.0897; obs: 455.2540.

Compound **2.7**: Prepared according to **GP1**, using 1,3,5-tris(bromomethyl)mesitylene (0.40 g, 1.00 mmol) and potassium selenocyanate (0.58 g, 4.03 mmol) in acetonitrile (15 mL). The reaction mixture was stirred at room temperature for 2 h. Work-up method 2 was utilized to afford the crude compound as a white crystalline solid. The crude product was purified by silica gel column chromatography using 40% ethyl acetate in petroleum ether as eluting solvent to afford the title compound as white solid. R_f = 0.5 (40% ethyl acetate in 60 – 80 petroleum ether). Yield: 0.42 g (88%). M.P. = 160–163 °C. ^{1}H NMR (DMSO-d_6, 600 MHz): δ (ppm) = 4.52 (s, 6H), 2.41 (s, 9H); ^{13}C NMR (DMSO-d_6, 150 MHz): δ (ppm) = 138.0, 132.6, 104.3, 29.9, 17.4; ^{77}Se NMR (DMSO-d_6, 114 MHz): δ (ppm) = 251; IR ($\bar{\nu}$, cm^{-1}): 2923 (s), 2853 (m), 2148 (m), 1730 (m), 1461 (m), 1191 (m); ESI-MS *m*/*z* calcd for $C_{15}H_{15}N_3Se_3$ $[M+Na]^+$: 497.1695; obs: 497.8654.

Compound **2.8**: To a stirred solution of 1,2,3,4,5,6-hexakis(bromomethyl)benzene (0.10 g, 0.16 mmol) in dry acetonitrile was added a solution of KSeCN (0.15 g, 0.97 mmol) in dry acetonitrile (10 mL) and the solution was stirred at room temperature for 7 h. The progress of the reaction was monitored by the thin layer chromatographic (TLC) method. Work-up method 1 was utilized to afford the crude compound as white solid. R_f = 0.6 (65% ethyl acetate in 60 – 80 petroleum ether). Yield: 0.070 g (59%). M.P. = 190–192 °C. ^{1}H NMR (DMSO-d_6, 600 MHz): δ (ppm) = 4.81 (s, 12H); ^{13}C NMR (DMSO-d_6, 150 MHz): δ (ppm) = 137.1, 112.4, 31.7; ^{77}Se NMR (DMSO-d_6, 114 MHz): δ (ppm) = 305. IR (KBr

pellet, cm^{-1}): 2924 (w), 2161 (s), 2147 (s), 1190 (m); ESI-MS *m/z* calcd for $C_{18}H_{12}N_6S_6$ $[M + NH_4]^+$: 521.9791; obs: 521.9907.

2.11.2. Cell Culture

Triple negative cell line (MDA-MB-231) was a generous gift from Dr. Anil Mukund Limaye, Associate Professor, Department of Bioscience and Bioengineering, Indian Institute of Technology, Guwahati, Assam, India. RPMI 1640 medium supplemented with 10% fetal bovine serum (Gibco) and 1% penicillin-streptomycin cocktail (Gibco) was used as a nutrient for MDA-MB-231 cells. T-47D cells were procured from Dr VGM Naidu, Associate Professor, Department of Pharmacology & Toxicology, National Institute of Pharmaceutical Education and Research, Guwahati. MCF-7 and L-132 cells were purchased from National Center for Cell Science, Pune, India. T-47D, MCF-7 and L-132 cells were cultured in Dulbecco's modified Eagle Medium (Gibco) supplemented with 10% fetal bovine serum and 1% penicillin-streptomycin solution in a CO_2 regulated and humidified incubator, maintained at 37 ˚C.

2.11.3. Anti-proliferative assay (MTT assay)

The cells were seeded on a 96-well culture plate at a density of 2×10^3 cells per 100 µL per wall for L-132 cells and 4×10^3 cells per 100 µl per well for other cancer cells followed by treatment with 0.0, 1.0, 5.0 10.0, 25.0 µM of test compounds for 0 h (Set 1) and 72 h (Set 2). Post-treatment, 10.0 µl of 5.0 mg ml^{-1} of MTT was added to the plate of set 1 and incubated for 2 h in dark. Following the treatment, the culture media was removed and the purple formazan crystals were dissolved in 100 µl of DMSO (Merck Life Science Pvt. Ltd.) and the absorbance at 570 nm was measured using a microplate reader (TECAN Infinite 200 PRO multimode reader). In Set 2, a similar MTT treatment protocol was followed only after 72 h. The mean OD values of a 0 h plate (Set 1) were subtracted from the mean OD values of identical wells at a 72 h plate (Set 2) ΔOD and the inhibition of proliferation was calculated keeping the ΔOD of the untreated control as 100%.

2.11.4. Propidium iodide-mediated flow cytometric assay

5×10^4 cells per 2 mL were seeded in 6-well plate and treated with selected selenocyanates as mentioned above and was incubated for 72 h. Post-incubation, the cells were harvested and washed with PBS (1X), stained with 5.0 µl of 1.0 mg mL^{-1} propidium iodide and analyzed using BD FACSCalibur™ instrument.

2.11.5. Cell Cycle analysis

1×10^5 cells per 2 mL per well were seeded in 6-well plates and treated with 0.0, 1.0 and 5.0 μM of compounds 12 and 24 and incubated for 24 h. Following the 24 h drug treatment, the cells were collected; washed with PBS (1X); fixed with ice-cold 70% ethanol at −20 °C for 30 min; again washed with PBS (1X) and stained with PI/RNase staining buffer (BD Biosciences) for 10 min at room temperature. The prepared samples were then analyzed using a BD FACSCalibur™ instrument.

2.11.6. Study of inhibition of cellular migration (Wound healing assay)

MDA-MB-231 cells were seeded in a 24-well plate at a concentration of 1.5×10^5 cells per 2 mL per well and incubated in a CO_2 incubator at 37 °C to form a monolayer of cells. After the monolayer formation, the cells were pre-incubated in serum free medium for 6 h. Using a 100 μL tip, a scratch was made on the monolayer and the debris was removed by washing with PBS (1X). Then, the cells were re-incubated with serum free medium and treated with 0.0, 1.0 and 2.5 μM of active selenocyanates **12** and **24**. Images of the scratch were captured at regular time intervals (0, 24, 48 and 72 h) using a Nikon inverted microscope and a camera. The extent of wound healing denotes the anti-migratory effect of the compounds tested.

2.12. References

1. El-Bayoumy, K., *Cancer Research* **1985**, *45*, 3631.
2. Reddy, B. S.; Rivenson, A.; El-Bayoumy, K.; Upadhyaya, P.; Pittman, B.; Rao, C. V., *J Natl Cancer Inst* **1997**, *89*, 506.
3. Das, J. K.; Sarkar, S.; Hossain, S. U.; Chakraborty, P.; Das, R. K.; Bhattacharya, S., *Ind J Med Res* **2013**, *137*, 1163.
4. Roy, S. S.; Chakraborty, P.; Ghosh, P.; Ghosh, S.; Biswas, J.; Bhattacharya, S., *Redox Rep* **2012**, *17*, 157.
5. Krishnegowda, G.; Prakasha Gowda, A. S.; Tagaram, H. R. S.; Carroll, K. F. S.-O.; Irby, R. B.; Sharma, A. K.; Amin, S., *Bioorg Med Chem* **2011**, *19*, 6006.
6. Alcolea, V.; Plano, D.; Encío, I.; Palop, J. A.; Sharma, A. K.; Sanmartín, C., *Eur J Med Chem* **2016**, *123*, 407.
7. An, B.; Zhang, S.; Hu, J.; Pan, T.; Huang, L.; Tang, J. C.-o.; Li, X.; Chan, A. S. C., *Org Biomol Chem* **2018**, *16*, 4701.
8. Jacob, L. A.; Matos, B.; Mostafa, C.; Rodriguez, J.; Tillotson, J. K., *Molecules* **2004**, *9*.

9. Mugesh, G.; Singh, H. B., *Chem Soc Rev* **2000**, *29*, 347.
10. Bhabak, K. P.; Mugesh, G., *Chem Eur J* **2008**, *14*, 8640.
11. (a) Bhabak, K. P.; Mugesh, G., *Chem-Eur J* **2010**, *16*, 1175; (b) Bhabak, K. P.; Satheeshkumar, K.; Jayavelu, S.; Mugesh, G., *Org Biomol Chem* **2011**, *9*, 7343; (c) Bhabak, K. P.; Vernekar, A. A.; Jakka, S. R.; Roy, G.; Mugesh, G., *Org Biomol Chem* **2011**, *9*, 5193.
12. Bhabak, K. P.; Mugesh, G., *Chem Eur J* **2010**, *16*, 1175.
13. Anjomshoa, M.; Fatemi, S. J.; Torkzadeh-Mahani, M.; Hadadzadeh, H., *Spectrochim Acta A* **2014**, *127*, 511.
14. Deng, S. L.; Zeng, D. L.; Luo, Y.; Zhao, J. F.; Li, X. L.; Zhao, Z. N.; Chen, T. F., *Rsc Adv* **2017**, *7*, 16721.

Chapter 3

Benzylic and Heterocycle-containing Organoselenocyanates: Impact of 4- Nitrobenzyl Group towards the Anti-proliferative Activities

3.1. Introduction

It has been discussed in the first chapter that compound **1.48**, bearing a selenocyanate functionality is found to be highly effective against benzo-[a]-pyrene induced fore-stomach cancer in female CD-1 mice.[1] However, therapeutic use of compound **1.48** is greatly limited owing to its toxicity. It was also discussed earlier that, compound **1.49** bearing a 4-methoxy functionality in compound **1.48** is much less toxic than compound **1.48** and highly active in inhibiting azoxymethane-induced colon carcinogenesis in F-344 rats.[2] Among many heterocyclic pharmacophores, triazole has drawn immense scientific attraction through several decades owing to its versatile applications as anti-microbial, anti-inflammatory, anti-hypertensive, anti-diabetic, anti-cancer agents and so on.[3] Although the anti-cancer activity with respect to tumoricidal or cytostatic properties of the organoselenium compounds containing triazole moiety are not well explored till date, the triazole moiety stands as one of the most important and well-known heterocycle, which is an integral part of many naturally occurring bioactive as well as environmentally active molecules. In 2011, Nishina and co-workers reported the synthesis and anti-cancer activities of selenoxo-thiazolidinedione-based compounds. It was observed that compound **3.1** displayed superoxide anion scavenging activities with an IC_{50} of 25.9 µM. Similar to ebselen (**1.14**), compound **3.1** activates ERK1/2 pathway, and suppresses hydrogen peroxide-induced cytotoxicity in rat PC-12 cells.[4] In 2016, Savegnago and co-workers described the synthesis and antioxidant properties of a series of triazole-based monoselenides. In a series of compounds synthesized therein, compound **3.2** exhibited the highest antioxidant activity as observed spectrofluorimetrically from the formation of reactive species induced by dichlorofluorescein in rat hippocampus and cortex.[5] Additionally, compound **3.2** also inhibited sodium nitroprusside-induced lipid peroxidation in rat cortex. In 2016, da Cruz and co-workers used the strategy of coupling two redox centers, such as quinoid moiety and selenium atom and evaluated the activities of novel and diverse selenium-containing quinone-based 1,2,3-triazole compounds against cancer and normal cell lines.[6] Their findings revealed compound **3.3** as a very potent anti-proliferative compound against a wide panel of cancer cells such as HL-60 (IC_{50} = 0.07 µM), HCT-116 (IC_{50} = 0.14 µM), MDA-MB-435 (IC_{50} = 0.23 µM) and OVCAR-8 (IC_{50} = 0.20 µM). Moreover, compound **3.3** was more potent than *β*-lapachone or doxorubicin (Dox). Additionally, it was found that the cytotoxic mechanism of compound **3.3** was intrinsically related with ROS contribution on the cytotoxicity, suggesting that the apoptosis induced by

compound **3.3** is associated with ROS production. In 2016, Panaka and co-workers reported the synthesis and characterization of a series of chalcogenyl triazole-bridged ferrocene-carbohydrate conjugates and evaluated their cytotoxicity in five different cell lines.[7] They have shown that, compound **3.4** exhibited highest anti-proliferative activity with IC_{50} ranging from 2.9 µM to 11.6 µM in A-549, MCF-7, MDA-MB-231 cells and was found to be non-toxic against HEK-293 cells. Another work of the same group in 2018, described the synthesis of another series of *β*-lapachone-1,2,3-triazole-selenium derivatives and their subsequent evaluation of cytotoxic activity against different cancer cell lines. It was found that compound **3.5** displayed promising anti-proliferative activity against HL-60 (IC_{50} = 0.53 µM), SF-295 (IC_{50} = 2.13 µM), NCIH-460 (IC_{50} = 2.75 µM) and PC-3 (IC_{50} = 2.47 µM).[8] Apart from triazole-containing selenium compounds, thiazolidinedione-containing selenium compounds are also widely studied for their anti-cancer activities. It has already been discussed in Chapter 1 that the activity of flavonyl-based thiazolidinedione selenocyanate **1.61** displayed promising chemopreventive activity, when treated in combination with cyclophosphamide.[9] Corigliano and co-workers (2018) reported a series of thiazolidinedione–indole conjugate, and evaluated each of the compounds for anti-cancer activity against breast and prostate cancer. Among all the synthesized compounds it was found out that compounds **3.6** and **3.7** inhibited the proliferation of MCF-7 and PC-3 cells at a concentration of 5.0 µM.[10] Very recently, the pronounced anti-bacterial activity of compound **3.8** bearing a 4-nitro functionality in compound **1.48**, against *Candida albicans* was reported by Jacob and co-workers (2019). **3.8** displayed an MIC_{50} of 7.53 µg mL^{-1} against pathogenic yeast. Additionally, compound **3.8** displayed promising nematicidal activity against *S. feltiae* with an LD_{50} of 4.90 µM.[11] Chemical structures of representative compounds from each category is listed in Figure 3.1.

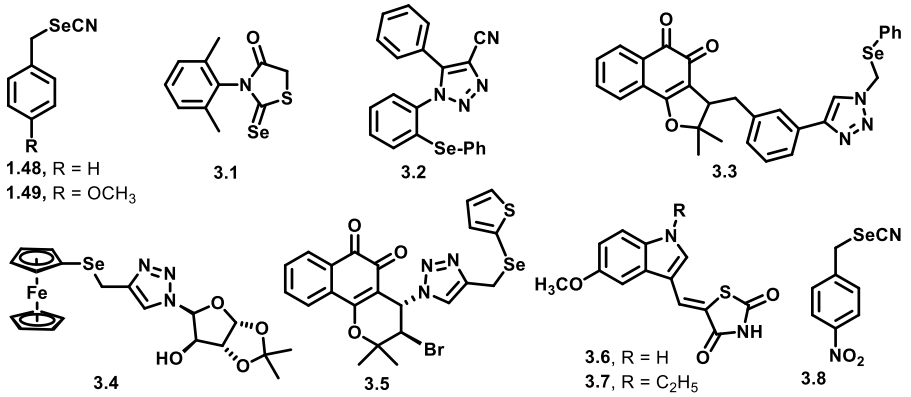

Figure 3.1. Chemical structures of some of the literature known 1,2,3-triazole and 1,3-thiazolidine-2,4-dione-based organoselenium compounds.

In last chapter (Chapter 2), we have seen that the anti-proliferative activity of benzyl selenocyanate (**1.48**) towards breast cancer cells can be enhanced further upon the introduction of multiple selenocyanate units (**2.7**).[12] However the activity could not be enhanced further with the incorporation of more selenocyanate units (e.g., compound **2.8**) probably due to more hydrophobic nature of the compound lacking the solubility in polar organic solvents and biological media. Therefore, we have taken the initiative to introduce heterocyclic pharmacophores such as triazole or 2,4-thiazolidine-1,3-dione in benzylic selenocyanates.

3.2. Outline of the chapter

In Chapter 1, we observed the chemopreventive activity of compound **1.48** and **1.49**, where we observed better chemopreventive activity of **1.49** than **1.48** towards azoxymethane-induced colon carcinogenesis in F344 rats fed with low and high-fat diets, during the initiation and post-initiation phases, therefore indicating the importance of methoxy group in benzyl selenocyanate, towards chemoprevention. Furthermore, investigation of compound **3.8** for anti-nematicidal activity was done by Jacob and co-workers, that confirmed compound **3.8** to have significant anti-nematicidal activity against *S. feltiae* with an LD_{50} of 4.9 µM. Above report indicates the presence of 4-nitro functionality in benzyl selenocyanate to be important for nematicidal activity. Additionally, in Chapter 2 we observed significant enhancement of anti-proliferative activity upon the introduction of multiple selenocyanate moieties in benzylic selenocyanates towards triple-negative breast cancer cells (MDA-MB-231) as well as in other ER+ cell lines such as MCF-7 and T-47D. For example, compound **2.7** having three selenocyanate units exhibited better anti-proliferative activity than simple benzyl

selenocyanate **1.48**. However, the activity was not enhanced further for compound **2.8** containing six selenocyanate units. It was rather hydrophobic and had limited solubility in polar organic solvents. We hypothesized the lack of any non-bonding interaction with key proteins, that resulted in attenuation of the anti-proliferative activity. In this Chapter, we selected **1.48**, **1.49** and **3.8** as standard selenocyanate model and evaluated the anti-cancer activity of each compounds against triple-negative and other ER(+) breast cancer cells. Additionally, we introduced polar heterocyclic pharmacophores (1,2,3-triazole and 2,4-thiazolidine-1,3-dione) in each of the three benzylic selenocyanates, with an intention to enhance the anti-proliferative activity further. Considering these two initiatives, three sets of selenocyanates were prepared as shown in Figure 3.2, and all of the synthesized compounds were evaluated for their anti-proliferative and anti-cancer activity against triple-negative and other ER(+) breast cancer cells.

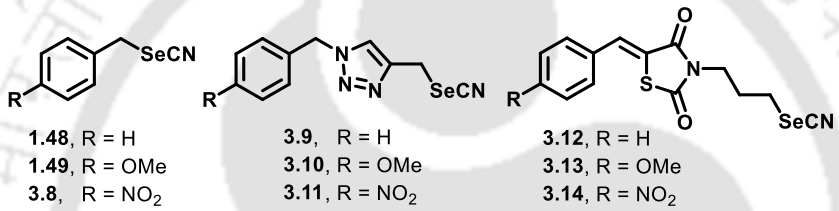

Figure 3.2. Chemical structures of targeted 1,2,3-triazole and 2,4-thiazolidine-1,3-dione-containing selenocyanates along with substituted benzyl selenocyanates.

3.3. Results and discussion

3.3.1. Synthesis of selenocyanates

The synthesis of benzylic selenocyanates was accomplished following the method used in Chapter 2. The treatment of benzylic bromides **3.15** – **3.17** with potassium selenocyanate in acetonitrile afforded the benzylic selenocyanates **1.48**, **1.49** and **3.8** in good yields (Scheme 3.1). The 1,2,3-triazole-based selenocyanates **3.9** – **3.11** were synthesized from the benzylic bromides **3.15** – **3.17** in four steps as shown in Scheme 3.1A. The bromides were converted to the corresponding azides **3.18** – **3.20** upon the reaction with sodium azide in DMF at room temperature. The azides were coupled with propargyl alcohol using click reaction to form the 1,2,3-triazole-based alcohols **3.21** – **3.23** with good to excellent yields. Treatment of triazole-based alcohols **3.21** – **3.23** were converted to the corresponding bromides **3.24** – **3.26** using phosphorus tribromide (PBr_3) as a brominating reagent. While PBr_3 afforded the bromides in good yields, our initial attempts with other common brominating agents such as hydrobromic acid or carbon tetrabromide were unsuccessful. The purified triazole-based bromides **3.24** –

3.26 were used in the final selenocyanation reaction to afford the triazole-based selenocyanates **3.9** – **3.11** in good yields (Scheme 3.1 A).

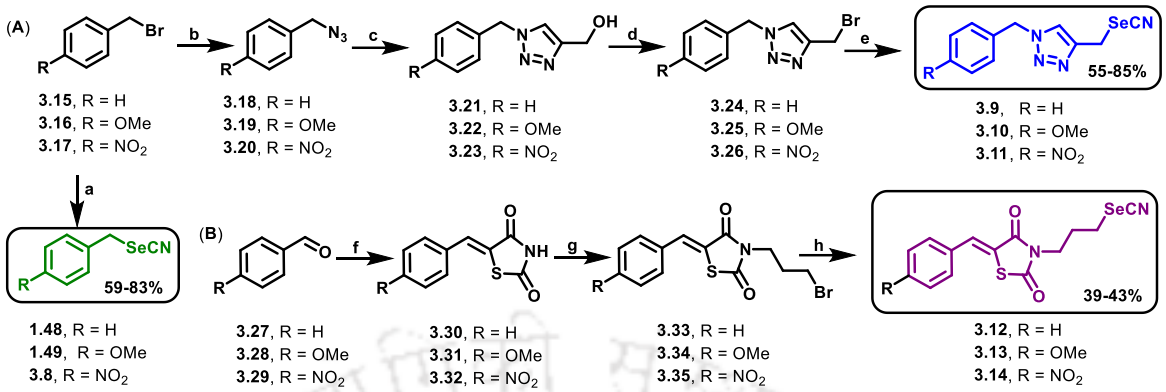

Scheme 3.1. Synthetic schemes to benzylic selenocyanates (**1.48, 1.49**, **3.8**), triazole-based selenocyanates (**3.9 - 3.11**) and 2,4-thiazolidine-1,3-dione-based selenocyanates (**3.12 - 3.14**). Reagents and conditions: (a) KSeCN, CH_3CN, r.t., 4 h (b) NaN_3/DMF, r.t,. 6 h (c) propargyl alcohol, $Cu(OAc)_2.5H_2O$, ^tBuOH, 16 h, (d) PBr_3/DCM, r.t., 4h (e) KSeCN, CH_3CN, r.t., 4 h, (f) 2,4-Thiazolidine-1,3-dione, piperidine, EtOH, 80 ºC, overnight (g) 1,3-dibromopropane, Et_3N, acetonitrile, 70 ºC. (h) KSeCN, CH_3CN, r.t., 6 h

The 2,4-thiazolidine-1,3-dione-based selenocyanates **3.12** – **3.14** were prepared starting from the aldehyde precursors **3.27** – **3.29**, as discussed in Scheme 3.1B. The aldehydes were coupled with 2,4-thiazolidine-1,3-dione utilizing Knoevenagel condensation to afford the 2,4-thiazolidine-1,3-dione-coupled products **3.30** – **3.32** in good yields. The imide-functionalization in compounds **3.30** – **3.32** with 1,3-dibromopropane in the presence of sodium hydroxide and a catalytic amount of sodium iodide resulted in the corresponding bromides **3.33** – **3.35** in moderate to good yields. Final selenocyanation with potassium selenocyanate in acetonitrile afforded the desired 2,4-thiazolidine-1,3-dione-based selenocyanates **3.12** – **3.14** in good yields. All the important intermediates and final compounds were purified and characterized by analytical and spectroscopic methods.

3.3.2. Anti-proliferative activities of the selenocyanates

In Chapter 2, we have described that benzylic and mesitylenic organoselenocyanates having one or multiple selenocyanate units exhibited significant anti-proliferative activities in different breast cancer cell lines and the efficiency of mesitylenic selenocyanate **2.7** was studied in details in triple-negative breast cancer cells (MDA-MB-231). In search of even better anti-proliferative agents for TNBC cells, we have

evaluated the anti-proliferative activities of synthesized benzylic, triazole- and 2,4-thiazolidine-1,3-dione-based selenocyanates towards MDA-MB-231 cells. The anti-proliferative activities were evaluated using conventional MTT assay in MDA-MB-231 cells and the results are described in Figure 3.3. To understand the dose-dependency of these compounds for growth inhibition of MDA-MB-231 cells over 48 h, the percentage of cell proliferation was estimated at three different concentrations (5.0 μM, 10.0 μM and 25.0 μM) and compared to that in the absence of compounds (control) as well as with a well-known anti-cancer drug, 5-fluorouracil (5-FU). As shown in Figure 3.3, all the organoselenocyanates were found to be active in inhibiting the proliferation of MDA-MB-231 cells. Interestingly, all of the compounds exhibited higher anti-proliferative activity than commercially available drug 5-FU, in MDA-MB-231 cells under identical experimental conditions.

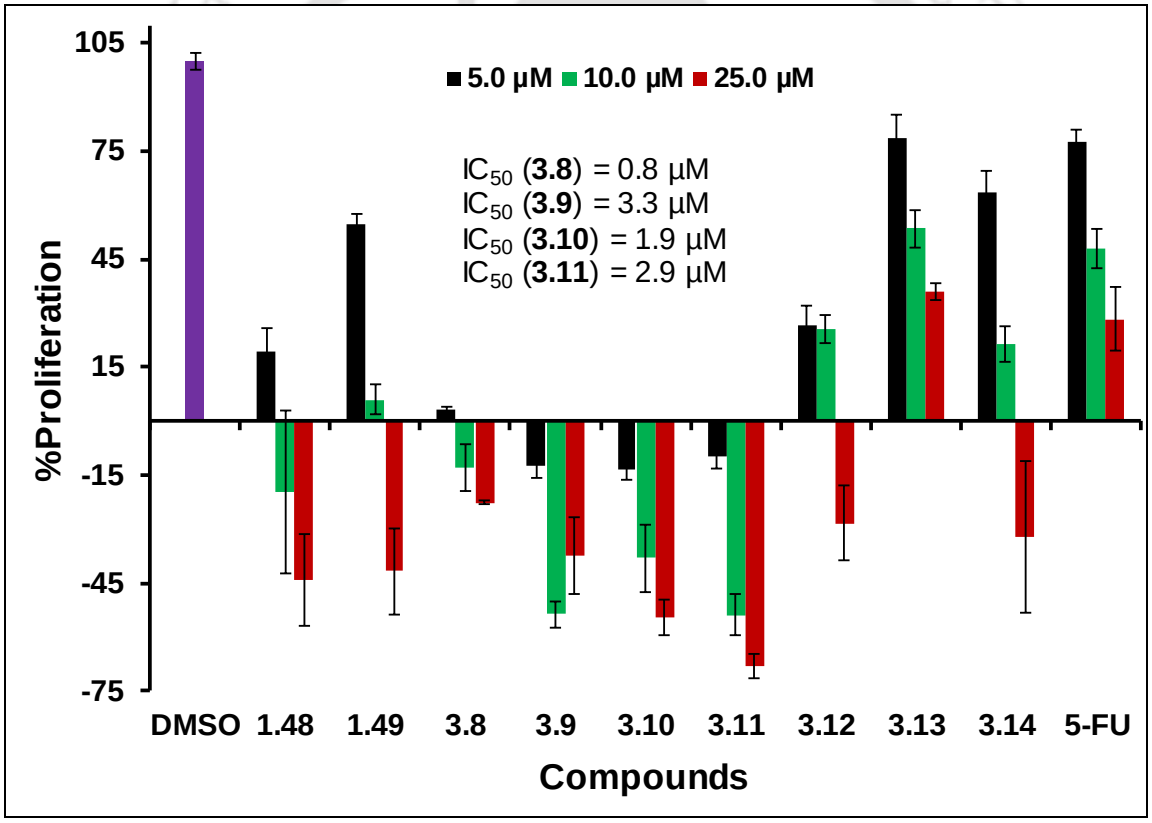

Figure 3.3. Dose-response of the compounds towards inhibition of proliferation of MDA-MB-231 cells.

In general, all the triazole-based selenocyanates **3.9-3.11** exhibited higher anti-proliferative activities than benzyl selenocyanate **1.48**, However, all the 2,4-thiazolidine-1,3-dione-based compounds **3.12-3.14** were found to be relatively less potent. It was observed that 4-nitrobenzyl selenocyanate **3.8** displayed best anti-cancer activity among

the compounds studied herein, with an IC_{50} of 0.8 µM. To further understand the selectivity of these compounds towards cancer cells over normal cells, MTT-based anti-proliferative assay of compounds **3.8**-**3.11** was performed in HEK-293 cells. Since compounds **3.12**-**3.14** displayed lesser anti-proliferative activities on MDA-MB-231 cells, we eliminated the series from further studies. The results of anti-proliferative activity of compounds **3.8**-**3.11** towards normal cells (HEK-293), confirms significant cytotoxicity of **3.9**-**3.11** towards normal cell (Figure 3.4). However, compound **3.8** exhibited very weak anti-proliferative activity towards HEK-293 cells, indicating its significant selectivity towards cancer cells.

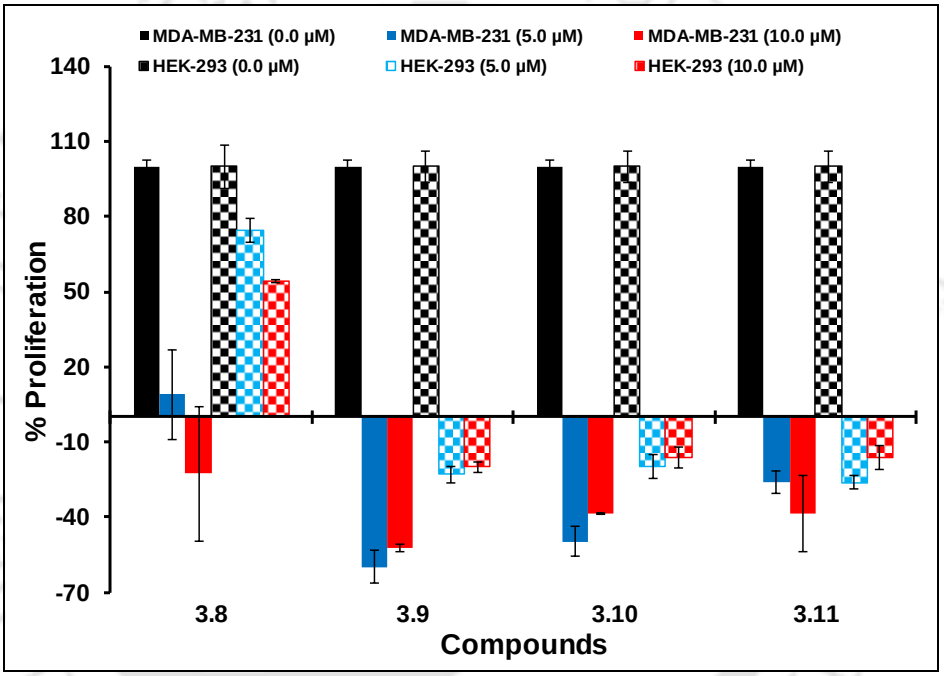

Figure 3.4. Comparative anti-proliferative activity data of **3.8** – **3.11** on MDA-MB-231 and HEK-293 cells.

Therefore, considering higher cytotoxicity and poor selectivity of triazole-based compounds **3.9**-**3.11** and higher selectivity of compound **3.8**, it was selected for further detailed studies to understand the mechanism of anti-cancer activity.

3.3.3. Dose dependant cellular death study by PI-Flow cytometric assay

As shown in Figure 3.3, compound **3.8** displayed highest anti-proliferative activity upto a concentration of 5.0 µM. However, most of the selenocyanates exhibited cytotoxic behavior at higher concentrations, and this was further confirmed using propidium iodide (PI)-flow cytometric assay. PI is a fluorescent compound that can bind to nucleic acids with little or no sequence preferences. An increased red fluorescence is indicative

of damaged cell membrane which in turn represents cell death. Among the test compounds used in this study, compound **3.8** that exhibited anti-proliferative activity at lower concentration and cytotoxic behavior at higher concentration, were chosen in PI-mediated flow cytometric assay. Treatment of MDA-MB-231 cells with different concentrations of compound **3.8** for a duration of 72h resulted in profound cell death which was found to be dose-dependent (around 40% cell death was observed at 10.0 µM concentration) as shown in Figure 3.5. At concentrations of 10.0 and 25.0 µM of selenocyanates, significant cell death was observed, which is in agreement with the observation on anti-proliferative activity data as obtained from MTT method. This study along with anti-proliferative activity data confirms the inhibition of cell growth by organoselenocyantes used in the present study.

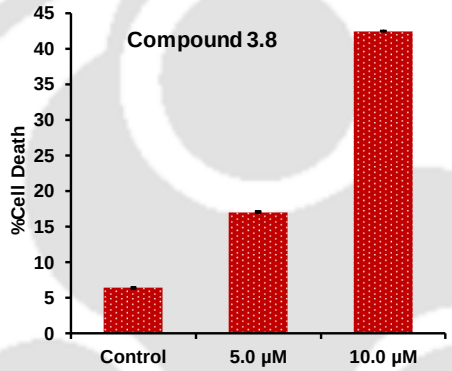

Figure 3.5. Cytotoxicity profile of the compound **3.8** on MDA-MB-231 cells in Propidium Iodide (PI)-mediated flow cytometric studies. About $5x10^4$ cells/2 mL were seeded in 6-well culture plates and treated with two different concentrations (5.0 µM and 10.0 µM) of test compound for 72 h. The cells were stained with 5.0 µl of 1.0 mg/mL of PI and analyzed by flow-cytometric method.

3.3.4. Cell cycle progression analysis of MDA-MB-231 cells in the presence of selenocyanates

A proper regulation of cell cycle is an essential process for the normal cell development and cellular functions. A de-regulation of which may induce aberrant cell proliferation leading to cancer. Therefore, an inhibition of abnormal cell cycle progression, which would result in reduced cell proliferation and increased apoptosis is one of the main strategies of cancer therapy. In the present study, in order to understand the mechanism of inhibition of cellular proliferation by the test compounds, we have investigated the effects of most potent selenocyanate **3.8** along with standard and simple benzyl selenocyanate **1.48** on cell cycle distribution of MDA-MB-231 cells using PI-mediated

flow-cytometric experiments. Cell cycle distribution was observed upon the incubation of cells with test compounds for 24 h at two different concentrations such as 1.0 µM and 5.0 µM. As shown in Figure 3.6, a noticeable difference in the cellular population at different phases of cell cycle was observed in the presence of compound **3.8**. This was in contrast to the compound **1.48** that did not change the cellular distribution of the untreated cells (control). Interestingly, a dose-dependent increase in cellular population has been observed at S-phase in the presence of compound **3.8** with the concomitant decrease in populations in G1 and G2 phases. For example, S-phase population is increased to 38.8% (1.0 µM) and 57.9% (5.0 µM) from 33.3% (control) in the presence of compound **3.8**. On the other hand, neither of dip G1, dip S, dip G2 displayed increase in cell population with increase in concentration of **1.48** with respect to control. These results indicate that the pronounced anti-proliferative activity of compound **3.8** is probably through the induction of cell cycle arrest in S-phase.

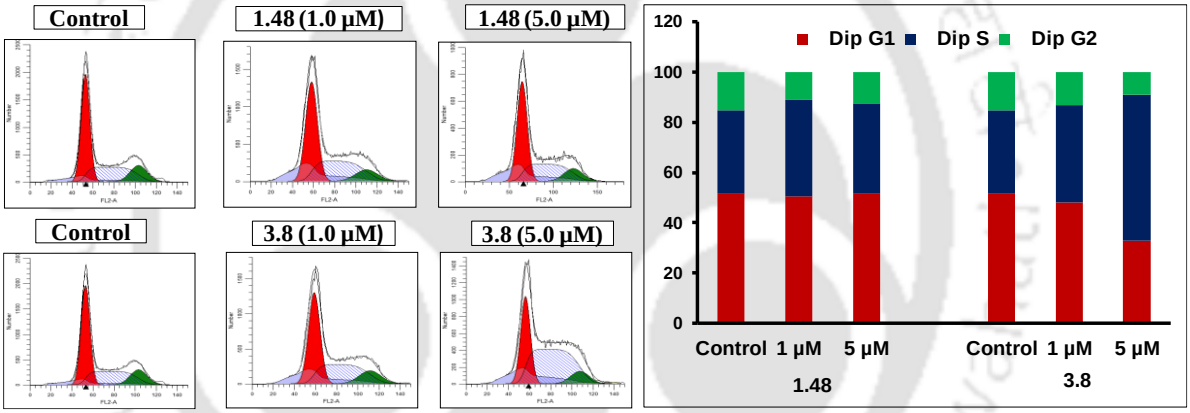

Figure 3.6. Graphical visualization of cellular distribution pattern of MDA-MB-231 cells in different phases of cell cycle in the presence of selenocyanates **1.48** and **3.8**. About $1x10^5$ cells/1 mL were seeded in 6-well plates and treated with two different concentrations (1.0 and 5.0 µM) of test compounds for 24 h and cell cycle distribution was analyzed by flow-cytometric assay after staining with PI.

3.3.5. Inhibition of migration of cancer cells (scratch assay)

In addition to primary cancer cells, the metastatic cells mainly spread the cancer to other parts of body. As the metastasis takes place due to cell migration, the inhibition of cancer cell migration is very important for therapeutic process. Furthermore, a high rate of metastasis is observed for the TNBC cells and there are limited drugs known to have significant anti-migratory property towards TNBC cells. We have therefore evaluated compound **3.8** for their anti-migratory properties in MDA-MB-231 cells using Scratch assay.[13] A scratch was made on the monolayer of cells and incubated in presence or

absence of test compounds for 72 h. Regular monitoring of the cells revealed that **3.8** inhibited migration of the cells to the wounded area indicating the anti-invasive nature of test compounds (Figure 3.7). For example, as observed clearly, a significant dose-dependent anti-migratory activity of compound **3.8** are reflected as compared to the control experiment under identical condition up to a duration of 72 h. These results indicate that **3.8** in present study have the capability to suppress the movement and re-population of scratched wound region even up to 72 h.

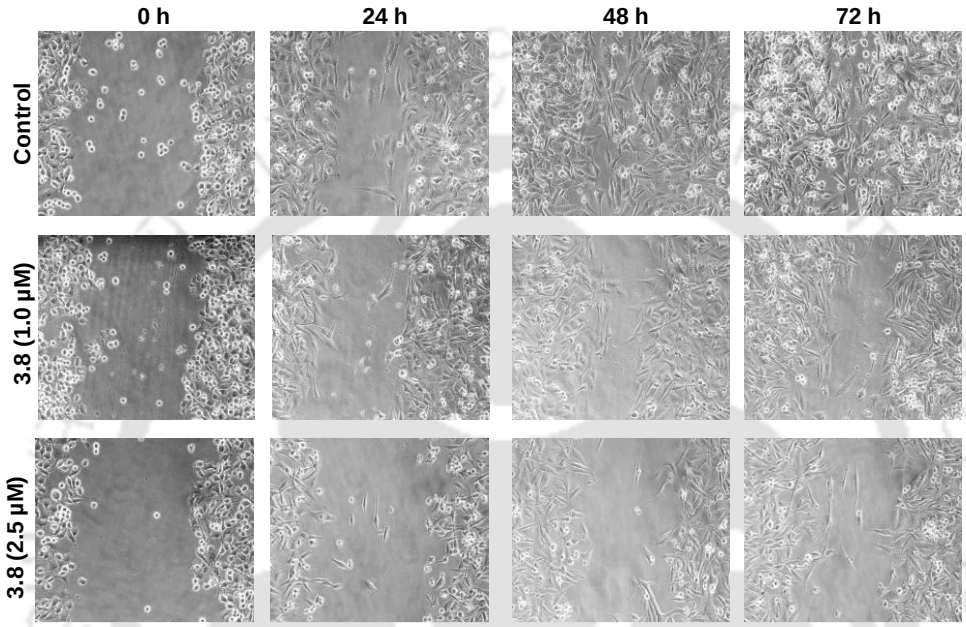

Figure 3.7. Wound healing studies on MDA-MB-231 cells in the presence of **3.8** at a concentration of 1.0 µM and 2.5 µM with respect to control following incubation of 0 h, 24 h, 48 h and 72 h.

3.3.6. Study of cellular morphology upon the treatment of selenocyanates

Occurrence of apoptosis is accompanied by notable changes in the cellular morphology of cancerous cells. There are several techniques to understand or detect these changes confirming the mode of cell death. Cell shrinkage by the reduction of volume of cellular nucleus and cytoplasm is commonly associated with apoptotic cell death. The morphological changes upon cell death can be easily visualized under microscope. In the present study, MDA-MB-231 cells were incubated with active compound **3.8** (10.0 µM) and the cellular morphology was visualized under microscope after 24 h and 48 h. As shown in Figure 3.6, significant visual changes were observed after 24 h and 48 h in the presence of compounds **3.8**. Visual changes in morphology during cell death takes place by the formation of dead cell debris, which lose their adherent properties and get detached from the surface and float randomly in the culture media. A significant cell

death was found for the test compounds and it was also enhanced with incubation time as compared to the control experiments. In addition to the visualization by microscope, the incubated cells after 72 h were further stained with the nuclear staining fluorescent dye PI to detect the dead cell nuclei under inverted microscope. As PI cannot permeate through the cell membrane of live cells, it can selectively stain the nuclei of dead cells, indicating the extent of cell death. A significant numbers of dead cells were visualized upon PI-staining as shown in Figure 3.8, supporting the occurrence of cell death.

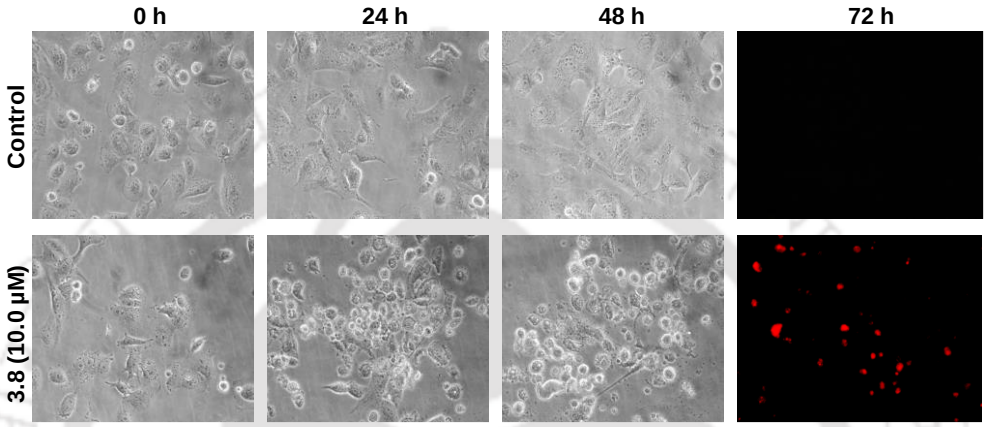

Figure 3.8. Change in cellular morphology of MDA-MB-231 cells in the absence and presence of selenocyanates **3.8** at a concentration of 10.0 µM with an incubation of 0 h, 24 h, 48 h. PI-stained images after incubation of cells for 72 h in the presence of test compounds represent dead cells.

3.3.7. Expression of some cancer-marker proteins in MDA-MB-231 cells

To understand the mode or pathway of anti-proliferative activities of active selenocyanates such as compound **3.8**, western blot analyses were performed on MDA-MB-231 cells. Some important cancer-marker protein expression levels were estimated in the presence of active selenocyanate **3.8** at different concentrations (0.0, 0.25, 0.5, 1.0, 2.0 and 2.5 µM) and incubated for 24 h. Glyceraldehyde 3-phosphate dehydrogenase (GAPDH) was used as a housekeeping gene loading control for this experiment. As shown in Figure 3.9, the expression level of important proteins involved in cell survival, proliferation and angiogenesis such as COX-2, Survivin, Bcl-2 and VEGF-A, AKT, p-AKT etc were studied in the presence of compound **3.8**. It is well-known that while COX-2 expression is crucial for invasive breast cancer and resistant to apoptosis, Survivin and Bcl-2 act as an anti-apoptotic protein markers, responsible for the progression of carcinogenesis.[14] It is reflected in Figure 3.9 that compound **3.8** reduces the levels of COX-2, Bcl-2 and survivin in a dose-dependent manner and a significant

down-regulation was observed at higher concentrations such as 2.0 and 2.5 µM. These results indicate that the active selenocyanate **3.8** probably have high impact on the expression level of important cancer marker proteins. In contrast to these observations, the levels of proteins such as AKT, *p*-AKT (S476) and VEGF-A were almost unaltered in the presence of compound **3.8** up to a concentration of 2.5 µM. These observations indicate that compound **3.8** exhibits anti-proliferative activity *via* AKT-independent pathway.[15] Although our results from western blot analysis on the levels of some key cancer marker proteins cannot be considered for a conclusive remarks on the mode of action of compound **3.8**, these observations could be a platform for further studies on the molecular mechanisms of selenocyanates towards TNBC cells such as MDA-MB-231.

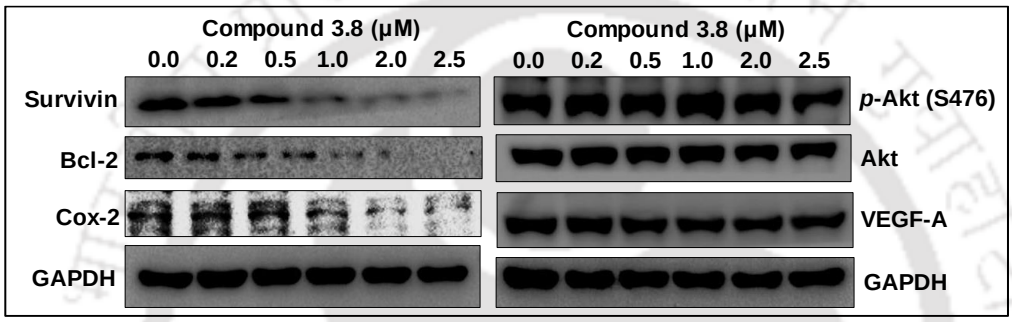

Figure 3.9. Western blot for the estimation of key protein expression level in MDA-MB-231 cells in the presence of compound **3.8** at different concentrations (0.0, 0.2, 0.5, 1.0, 2.0 and 2.5 µM) with an incubation of 24 h. Equal protein loading was confirmed by the analysis of GAPDH expression.

3.3.8. Hydrogen peroxide scavenging activity of heterocyclic selenocyanates

To understand the antioxidant activity of the compound **3.8** that exhibited most potent anti-cancer activity, the hydrogen peroxide scavenging activity was studied using two different thiols such as glutathione (GSH) and thiophenol (PhSH). A standard benzyl selenocyanate **1.48** was chosen as a reference for these studies. The GPx-like antioxidant activity in reducing hydrogen peroxide in the presence of GSH was carried out using UV-Vis spectrophotometric method and the activity in the presence of PhSH was studied using reverse-phase HPLC method.[16]

The initial rates for the reduction of H_2O_2 by GSH in the presence and absence of the test compounds were calculated from a linear fit covering the first 5-10% of the reactions. As shown in Table 3.1, compound **1.48** exhibits slightly higher rate for the reduction of H_2O and compound **3.8** shows reasonably higher initial rate for the reduction of H_2O_2 in the presence of biothiol GSH. However, these compounds could be considered as weak

antioxidants as the small-molecule GPx-mimics are known to exhibit significantly higher rates than these compounds.[17] With this result in hand, the antioxidant activity of these two compounds were further evaluated in the presence of aromatic thiol (PhSH) and the half-life ($t_{1/2}$) for the reduction of 50% of H_2O_2 was calculated by monitoring the formation of PhSSPh with time using HPLC method. A lower $t_{1/2}$ value is indicative of higher antioxidant activity of the compound. As shown in Table 3.1, both the selenocyanates exhibited significantly higher $t_{1/2}$ values than that of the control reaction without any selenium compound under identical condition. These results indicate that benzylic selenocyanates used herein are not good antioxidants for the reduction of H_2O_2 in the *in vitro* assay conditions and the observed anti-cancer activity of compound **3.8** may not be associated with their antioxidant activities.

Table 3.1. Initial rate for the catalytic reduction of H_2O_2 by GSH in the presence of organoselenocyanates.

Compound	Initial rate ($\mu M\ min^{-1}$)[a]	Compound	Half-life ($t_{1/2}$, min)[b]
Control	11.2 ± 2.7	**Control**	232
1.48	27.2 ± 1.2	**1.48**	370
3.8	69.3 ± 15.1	**3.8**	267

[a]The experiment was carried out in phosphate buffer (100 mM) of pH 7.5 at room temperature (22 °C). Assay mixture contained selenium compound (100.0 µM), GSH (2.0 mM), NADPH (0.4 mM), EDTA (1.0 mM) glutathione disulfide reductase (1.0 unit/mL) and H_2O_2 (1.6 mM). The rates of control reactions were measured under the identical experimental conditions in the absence of any selenium compound.

[b]The experiment was carried out in methanol at room temperature (22 °C) using analytical HPLC instrument. Assay mixture contained selenium compound (20.0 µM), PhSH (1.0 mM), H_2O_2 (2.0 mM). Amount of disulphide formed with time was determined using standardized calibration plot of known solutions of DPDS. The rates of control reactions were measured under the identical experimental conditions in the absence of any selenium compound.

3.3.9. Binding interaction with bovine serum albumin

Serum albumin is one of the highly abundant proteins in blood plasma of living system and serves important role in the transportation by complexing with several essential biomolecules, drugs, and releasing them specifically at some other site. Therefore, proper insight in the interaction of selenocyanates with bovine serum albumin in this

context, gives a better understanding of pharmacodynamics of selenocyanates. Bovine serum albumin is used as a homology model for human serum albumin owing to its abundant and easy availability. BSA inherently displays fluorescence due to the presence of tryptophan (W) units namely Trp-134 and Trp-212 located on the surface of sub-domain IB and in the hydrophobic pocket of subdomain IIA, respectively. Therefore, fluorescence quenching of BSA upon its interaction with small molecules serves as a very important tool for understanding the affinity for protein-ligand binding interaction. In the present method, the binding interaction of selenocyanate **1.48** and **3.8** was studied following an earlier reported procedure.[18] BSA solution exhibits strong fluorescence emission at λ = 344 nm upon excitation at λ = 280 nm. In the present study, the fluorescence intensity was found to decrease gradually upon increasing the concentration of test compounds without any significant shift in the emission λ_{max}, indicating the static quenching of BSA by compounds **1.48** and **3.8**. Experimentally, binding constant (K_b) and number of compounds per protein (n) were determined and shown in Table 3.2. Furthermore, using the Stern-Volmer equation, the binding parameters such as the quenching constant (K_q) and Stern-Volmer constant (K_{SV}) were calculated and shown in Table 3.3.

Table 3.2. Interaction parameters such as binding constant (K_b), number of compounds per protein (n) of **1.48** and **3.8** with BSA as obtained from spectrofluorimetric titration[c].

Compound	$K_b \times 10^4$ (M^{-1})	n	R^2
1.48	0.89	0.93	0.9913
3.8	1.04	0.81	0.9924

[c]The quenching experiment was performed using a fluorescence spectrophotometer with excitation and emission wavelengths of 280 nm and 344 nm, respectively. BSA (10.0 µM) in Tris-HCl buffered saline (100 mM, pH 7.2) was titrated with increasing concentrations of test compounds (0.0–50.0 µM).

Table 3.3. Interaction parameters Stern-Volmer constant (K_{SV}) and quenching constant (K_q) of **1.48** and **3.8** with BSA as obtained from spectrofluorimetric titration[d].

Compound	$K_{SV} \times 10^4$ M^{-1}	$K_q \times 10^{12}$ $M^{-1}S^{-1}$	R^2
1.48	1.94	1.94	0.9907
3.8	8.74	8.74	0.9910

[d]The quenching experiment was performed using a fluorescence spectrophotometer with excitation and emission wavelengths of 280 nm and 344 nm, respectively. BSA (10.0 µM) in Tris-HCl buffered saline (100 mM, pH 7.2) was titrated with increasing concentrations of test compounds (0.0–50.0 µM)

3.3.10. Molecular interaction of selenocyanates with proteins

As compound **3.8** exhibited significant potency for the down-regulation of some key cancer-marker proteins such as Survivin, Bcl-2 and COX-2, we have carried out docking studies to understand the possible molecular interaction of **3.8** with these proteins. Additionally the molecular interaction was also studied with BSA as these compounds exhibited good BSA-binding interactions. Compound **1.48** was used as a representative selenocyanate to have a comparative interaction profiles. As shown in Table 3.4, compound **3.8** has much higher binding affinity than **1.48** towards BSA. This is represented by a higher binding energy and lower inhibitory constant of **3.8** as compared to **1.48**. Similar to BSA, the binding affinity of **3.8** was found to be significantly higher than that of **1.48** towards all the marker proteins such as Survivin, Bcl-2 and COX-2, which are used in the present study.

Table 3.4. The binding parameters such as binding energy (E_B), inhibitory constant (K_i) and the proximal amino acid residues of proteins involved in non-bonding interactions with ligands.

Compound	Protein[a]	E_B (kcal mol^{-1})	K_i (µM)	Interactions
1.48	BSA	-4.2	829.4	-
	Survivin	-3.8	1750.0	L6.B, W10.A
	Bcl-2	-3.9	1310.0	Y67.B
	COX-2	-4.7	331.8	R376.B
3.8	BSA	-7.1	5.9	K114.A
	Survivin	-5.2	154.6	W10.A, L6.B
	Bcl-2	-6.0	39.5	K22.A, R26.A, R68.A
	COX-2	-6.3	24.6	R376.B, V538.B

[a]The docking study was performed with four proteins such as BSA (PDB: 4F5S), Survivin (PDB: 1F3H), Bcl-2 (PDB: 2W3L) and COX-2 (PDB: 5KIR). The crystal structures of these proteins were collected from RCSB database.

The value of inhibitory constant of compound **1.48** towards all four proteins was enormously decreased by an introduction of simple nitro group at the 4-position of phenyl ring of compound **1.48**. This increased affinity is probably due to an additional non-bonding interactions with the proximal amino acid residues of proteins involving nitro group in compound **3.8**. The higher non-bonding interactions of compound **3.8** as compared to compound **1.48** with the proximal amino acids of proteins is reflected in Figure 3.10. These results support our experimental results that serum albumin may help in transporting these selenocyanates in the blood stream and significant binding affinities reflect an effective interaction of compound **3.8** with marker proteins that contributes in altering their expression levels in MDA-MB-231 cells.

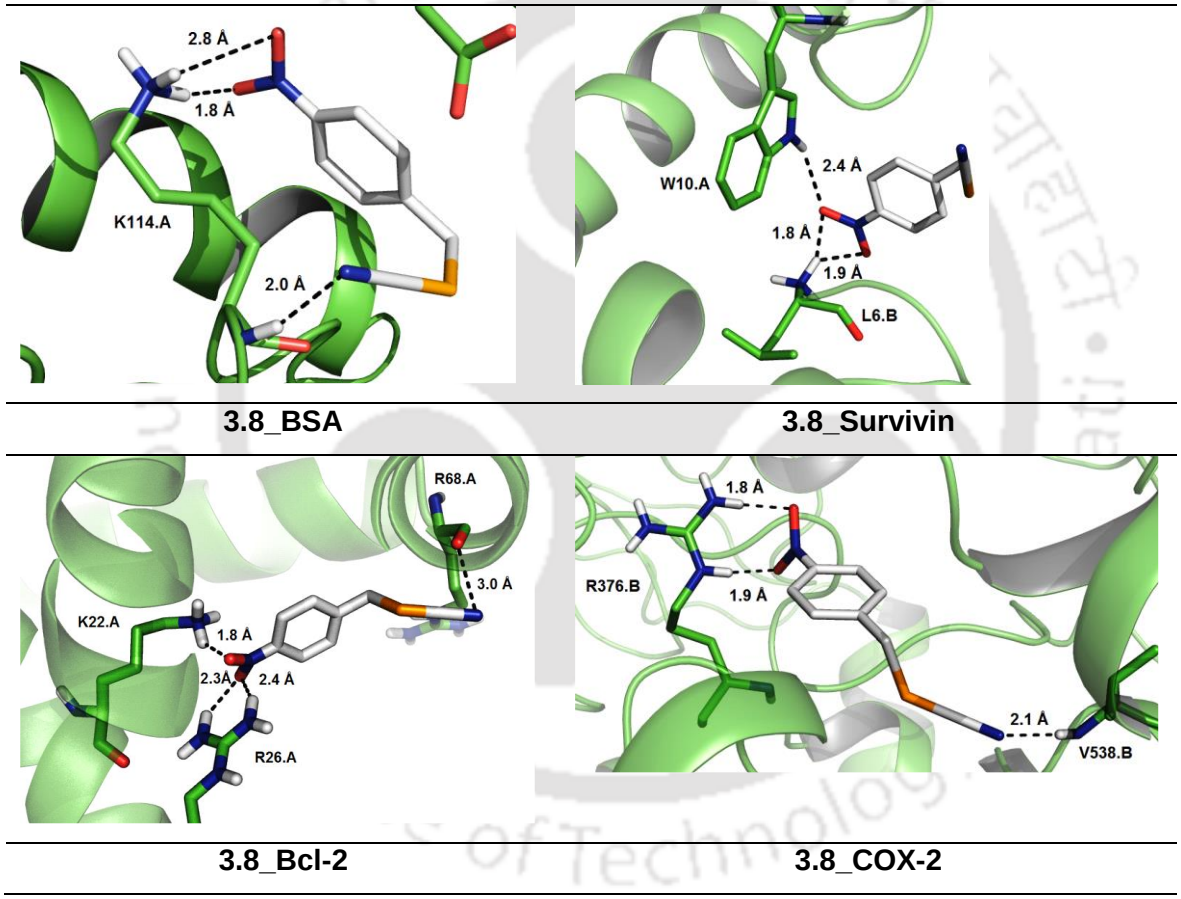

Figure 3.10. Docking interaction of compound **3.8** in docked pose with key proteins such as BSA, surviving, Bcl-2, and COX-2.

3.4. Conclusions

In summary, investigations of anti-cancer activities of 4-substituted benzylic selenocyanates with methoxy and nitro groups and two additional series with the incorporation of heterocyclic pharmacophores were carried out in triple-negative breast cancer cells (MDA-MB-231) upon their successful synthesis, purification and

characterization. While the triazole-based selenocyanates exhibited potent antiproliferative activities than 2,4-thiazolidine-1,4-dione substituted compounds, they were found to be cytotoxic towards the normal cells (HEK-293), losing the selectivity towards cancer cells. Interestingly, 4-nitrobenzyl selenocyanate **3.8** exhibited potent antiproliferative activity as well as enhanced selectivity towards MDA-MB-231 cells over normal cells. Detailed mechanistic investigation with compound **3.8** revealed that the compound exhibited anti-cancer activity by arresting cells at S phase of the cell cycle and probably by down-regulating the expression of key anti-apoptotic and inflammatory proteins such as Bcl-2, survivin and Cox-2. Protein-ligand docking studies further supported the interaction of compound **3.8** with key proteins as described above. Although, the chosen heterocyclic selenocyanates failed to display selective and potent anti-cancer activities than benzylic selenocyanates, our study would promote further exploration to select other pharmacophores for optimized anti-cancer activities with enhanced selectivity.

3.5. Experimental procedure

3.5.1. Materials and method

All chemical reagents were used as delivered without further purification. Solvents used for purification (n-hexane, ethyl acetate, petroleum ether) were distilled before use. Dry solvents were used for reactions wherever applicable. Melting point of the compounds reported here, were recorded on Buchi B-540 melting point apparatus and the values were uncorrected. Thin-layer chromatography analyses were done on pre-coated silica gel K_{254} on aluminium sheets. NMR spectroscopy was done on a Bruker Ascend^{TM} 600 spectrometer (^{1}H NMR at 600 MHz, ^{13}C at 150 MHz and ^{77}Se at 114 MHz) or a Varian Mercury Plus 400 MHz spectrometer. Chemical shifts were reported with respect to tetramethylsilane (^{1}H and ^{13}C as an internal standard) and diphenyl diselenide for ^{77}Se as an external standard. High resolution mass spectra (HRMS) and liquid chromatography mass spectra (LCMS) were recorded on Agilent 6520 Accurate-Mass Quadrupole Time-of-Flight (Q-TOF) LC/MS spectrometer. FT-IR spectra were recorded on Perkin-Elmer Spectrum Two FT-IR spectrometer.

General Procedure (GP1) for synthesis of 4-functionalized benzyl selenocyanate compounds (1.48, 1.49, 3.8)

4-functionalized benzyl selenocyanates were synthesized following reported literature method, with minor modifications wherever applicable.[19] Briefly, to a stirred solution of appropriately substituted benzylic halides in acetonitrile, a solution of potassium selenocyanate in acetonitrile was added and was stirred at room temperature. Appearance of white precipitate indicated the progress of reaction. The progress was monitored by TLC analysis. After completion, the solvent was evaporated under reduced pressure and the residue was extracted using ethyl acetate (3 × 10 mL) and was washed with water (2 × 10 mL) and brine (1 × 10 mL). Combined organic layer was dried over anhydrous sodium sulphate and was evaporated under reduced pressure to yield the crude product.

Compound **1.48**: Prepared according to **GP1** using benzyl bromide (0.57 g, 3.47 mmol), potassium selenocyanate (0.50 g, 3.16 mmol), in acetonitrile (15 mL) for 4 h. Crude product was further purified by column chromatography using petroleum ether and ethyl acetate as eluting solvent, to afford the purified product as slightly reddish solid. R_f = 0.5 (4% ethyl acetate in petroleum ether 60–80). Yield: 0.39 g (59%). M.P.: 73 – 75 °C. ^{1}H NMR ($CDCl_3$, 600 MHz): δ (ppm) = 7.39 – 7.33 (m, 5H), 4.31 (s, 2H); ^{13}C NMR ($CDCl_3$, 150 MHz): δ (ppm) = 35.7, 129.4, 129.2, 128.9, 102.2, 33.0; ^{77}Se NMR ($CDCl_3$, 114 MHz): δ (ppm) = 283. IR ($\bar{\nu}$, cm^{-1}): 2146 (s), 1491 (m), 1454 (m), 1217 (m), 1191 (m), 1069 (m). ESI-MS *m/z* calcd. for C_8H_7NSe $[M + Na]^+$: 219.9641; obs: 220.0526.

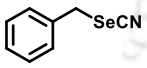

Compound **1.49**: Prepared according to **GP1** using 4-methoxybenzyl chloride (0.34 g, 2.20 mmol), potassium selenocyanate (0.40 g, 2.78 mmol) in acetonitrile (20 mL) for 4 h. Crude product was further purified by column chromatography using petroleum ether and ethyl acetate as eluting solvent, to afford the purified product as white solid. R_f = 0.5 (4% ethyl acetate in petroleum ether 60–80). Yield: 0.39 g (59%). ^{1}H NMR ($CDCl_3$, 400 MHz): δ (ppm) = 7.19 (d, 2H, *J* = 8.6 Hz), 6.79 (d, 2H, *J* = 8.6 Hz), 4.30 (s, 2H), 3.81 (s, 3H); ^{13}C NMR ($CDCl_3$, 150 MHz): δ (ppm) = 160.0, 130.6, 127.6, 114.7, 102.7, 55.6, 33.1; ^{77}Se NMR ($CDCl_3$, 114 MHz): δ (ppm) = 283. IR ($\bar{\nu}$, cm^{-1}): 2146 (s), 1491 (m), 1454 (m), 1217 (m), 1191 (m), 1069 (m). ESI-MS *m/z* calcd. for C_8H_7NSe $[M + Na]^+$: 219.9641; obs: 220.0526

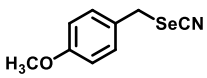

Compound **3.8**: Prepared according to **GP1** from 4-nitrobenzyl bromide (0.42 g, 1.85 mmol), potassium selenocyanate (0.40 g, 2.78 mmol) in acetonitrile (20 mL). Crude product was further purified using column chromatography using ethyl acetate in petroleum ether as eluent, to afford the purified product as white solid. R_f = 0.7 (25% ethyl acetate in petroleum ether 60-80). Yield: 0.39 g (83%). M.P. = 120-123 ºC. ^{1}H NMR ($CDCl_3$, 600 MHz): δ (ppm) = 8.18 (d, *J* = 8.4 Hz, 2H), 7.48 (d, *J* = 8.4 Hz, 2H), 4.30 (s, 2H); ^{13}C NMR ($CDCl_3$, 150 MHz): δ (ppm) = 148.1, 143.3, 130.1, 124.6, 100.8, 31.1; ^{77}Se NMR ($CDCl_3$, 114 MHz): δ (ppm) =312; IR ($\bar{\nu}$, cm^{-1}): 2924 (s), 2146 (m), 1597 (m), 1519 (s), 1342 (s). ESI-MS *m/z* calcd for $C_8H_6N_2O_2Se$ $[M+H]^+$: 242.9673; obs: 242.2854.

General procedure (GP2) for synthesis of 4-(selenocyanatomethyl)-1-aryl-1H-1,2,3-triazole (**3.9**, **3.10**, **3.11**): Triazole-based selenocyanates were synthesized following reported literature method.[19] Precursor triazole-based bromides (**3.24**, **3.25**, or **3.26**) (1.0 equiv) was stirred with potassium selenocyanate (1.2 equiv) in dry acetonitrile for 4 – 6 h at room temperature under inert. Progress of the reaction was monitored by TLC analysis. After completion, the solution was evaporated to dryness under reduced pressure. The residue was extracted with ethyl acetate (3 × 10 mL) and was washed with water (2 × 10 mL) and brine (1 × 10 mL). Combined organic layer was dried in over anhyd. sodium sulfate and was concentrated *in vacuo* to yield the crude compound.

Compound **3.9**: Prepared according to **GP2** from precursor **3.24** (0.07 g, 0.03 mmol), potassium selenocyanate (0.05 g, 0.32 mmol) in acetonitrile (3 mL). The crude compound was further purified by neutral alumina column chromatography using 50% ethyl acetate in petroleum ether as eluent, to afford the purified compound as white solid. R_f = 0.5 (50% ethyl acetate in petroleum ether). Yield: 0.070 g (85%). M.P.: 126 – 128 °C; ^{1}H NMR ($CDCl_3$, 400 MHz): δ (ppm) = 7.55 (s, 1H), 7.39 (d, 3H, *J* = 8 Hz), 7.29 – 7.27 (m, 2H), 5.54 (s, 2H), 4.34 (s, 2H). ^{13}C NMR ($CDCl_3$, 100 MHz): δ (ppm) = 142.8, 134.1, 129.3, 129.0, 128.1, 122.2, 101.8, 54.4, 21.9. ^{77}Se NMR ($CDCl_3$, 76 MHz): δ (ppm) = 288, ESI-MS *m/z* calcd for $C_{11}H_{10}N_4Se$ $[M + H]^+$: 279.0149; obs: 279.0119. FT-IR ($\bar{\nu}$, cm^{-1}): 3137 (m), 2140 (s), 1500 (m), 1455 (s), 1192 (s), 748 (s).

Compound **3.10**: Prepared according to **GP2** from precursor **3.25** (0.12 g, 0.39 mmol),

potassium selenocyanate (0.07 g, 0.47 mmol) in acetonitrile (5 mL). The crude compound was further purified by neutral alumina column chromatography using 75% ethyl acetate in petroleum ether as eluent to afford the purified compound as white solid R_f = 0.6 (75% ethyl acetate in petroleum ether). Yield: 0.10 g (76%). M.P.: 134 – 136 °C; ^{1}H NMR ($CDCl_3$, 600 MHz): δ (ppm) = 7.52 (s, 1H), 7.24 (d, 2H, *J* = 8.6 Hz), 6.91 (d, 2H, *J* = 8.6 Hz), 5.47 (s, 2H), 4.33 (s, 2H), 3.81 (s. 3H) ^{13}C NMR ($CDCl_3$, 150 MHz): δ (ppm) = 160.0, 142.7, 129.7, 126.0, 121.9, 114.6, 101.9, 55.3, 54.0, 21.9; ^{77}Se NMR ($CDCl_3$, 76 MHz): δ (ppm) = 287. ESI-MS *m/z* calcd for $C_{12}H_{12}N_4OSe$ $[M + H]^+$: 309.0255, $[M+Na]^+$: 331.074, obs: 309.0270, 331.0093. FT-IR ($\bar{\nu}$, cm^{-1}): 3443 (br), 2926 (m), 2144 (m), 1612 (m), 1516 (s), 1254 (s), 1052 (w), 778 (s)

Compound **3.11**: Prepared according to **GP2** from precursor **3.26** (0.01 g, 0.34 mmol), 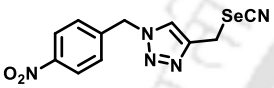

potassium selenocyanate (0.05 g, 0.37 mmol) in acetonitrile (4 mL). The crude compound was further purified by neutral alumina column chromatography using 75% ethyl acetate in petroleum ether as eluent, to afford the purified compound as yellow solid. R_f = 0.5 (75% ethyl acetate in petroleum ether). Yield: 0.06 g (55%). M.P.: 139 – 141 °C; ^{1}H NMR ($CDCl_3$, 600 MHz): δ (ppm) = 8.26 (d, 2H, *J* = 8.7 Hz), 7.67 (s, 1H), 7.42 (d, 2H, *J* = 8.7 Hz), 5.67 (s, 2H), 4.35 (s, 2H); ^{13}C NMR ($CDCl_3$, 150 MHz): δ (ppm) = 143.5, 141.1, 128.6, 124.4, 122.5, 101.8, 53.3, 21.6; ESI-MS *m/z* calcd for $C_{11}H_9N_5O_2Se$ $[M + H]^+$: 324.0000, obs: 324.0024. FT-IR ($\bar{\nu}$, cm^{-1}): 3135 (w), 2963 (w), 2156 (w), 1610 (w), 1516 (s), 1345 (s), 1042 (w), 805 (s).

General procedure (GP3) for synthesis of 5-arylidene-3-(3-selenocyanatopropyl)thiazolidine-2,4-dione (**3.12**, **3.13**, **3.14**): Title compounds were synthesized according to previously reported literature.[19] Precursor thiazolidinedione-based bromides (**3.33**, **3.34**, or **3.35**) (1.0 equiv) was stirred with potassium selenocyanate (1.5 equiv) in dry acetonitrile for 4 – 6 h at room temperature under inert. Progress of the reaction was monitored by TLC analysis. After completion, the solution was evaporated to dryness under reduced pressure. The residue was extracted with ethyl acetate (3 × 10 mL) and was washed with water (2 × 10 mL) and brine (1 × 10 mL). Combined organic layer was dried over anhyd. sodium sulfate and was concentrated *in vacuo* to yield the crude compound.

Compound **3.12**: Prepared according to **GP3** from precursor **3.33** (0.15 g, 0.46 mmol), potassium selenocyanate (0.10 g, 0.69 mmol) in acetonitrile (4 mL). The crude compound was further purified by neutral alumina column chromatography using 40% dichloromethane in petroleum ether to afford the purified compound as white solid. R_f = 0.2 (30% ethyl acetate in petroleum ether). Yield: 0.07 g (43%). M.P.: 119 – 121 °C; ^{1}H NMR ($CDCl_3$, 400 MHz): δ (ppm) = 7.92 (s, 1H), 7.53 – 7.45 (m, 5H), 3.96 (t, 2H, *J* = 6.3 Hz), 3.05 (t, 2H, *J* = 7.0 Hz), 2.30 (q, 2H, *J* = 6.7 Hz); ^{13}C NMR ($CDCl_3$, 150 MHz): δ (ppm) = 168.2, 166.5, 134.7, 133.0, 130.3, 129.3, 120.9, 101.4, 40.5, 29.4, 26.7; ^{77}Se NMR ($CDCl_3$, 76 MHz): δ (ppm) = 211. ESI-MS *m/z* calcd for $C_{14}H_{12}N_2O_2SSe$ $[M + H]^+$: 352.9863, obs: 352.9916. FT-IR ($\bar{\nu}$, cm^{-1}): 3746 (w), 2147 (m), 1746 (m), 1681 (s), 1605 (m), 1442 (m), 1231 (m), 765 (m),

Compound **3.13**: Prepared according to **GP3** from precursor **3.34** (0.11 g, 0.31 mmol), potassium selenocyanate (0.08 g, 0.55 mmol) in acetonitrile (4 mL) as yellow solid. The crude compound was further purified by neutral alumina column chromatography using 20% ethyl acetate in petroleum ether to afford the purified compound as yellow solid. R_f = 0.4 (50% ethyl acetate in petroleum ether). Yield: 0.09 g (39%); M. P.: 106 – 108 °C; ^{1}H NMR ($CDCl_3$, 400 MHz): δ (ppm) = 7.87 (s, 1H), 7.47 (d, 2H, *J* = 8.8 Hz), 7.00 (d, 2H, *J* = 8.8 Hz), 3.96 (t, 2H, *J* = 6.3 Hz), 3.88 (s, 3H), 3.05 (t, 2H, *J* = 7.0 Hz), 2.30 (p, 2H, *J* = 6.8 Hz); ^{13}C NMR ($CDCl_3$, 100 MHz): δ (ppm) = 168.3, 163.7, 161.7, 134.6, 132.4, 125.6, 117.7, 114.9, 101.6, 55.5, 40.4, 29.4, 26.8; ^{77}Se NMR ($CDCl_3$, 76 MHz): δ (ppm) = 211. ESI-MS *m/z* calcd for $C_{15}H_{14}N_2O_3SSe$ $[M+H]^+$: 382.9969, $[M+K]^+$:420.9527 obs: 382.9994, 420.9552, FT-IR ($\bar{\nu}$, cm^{-1}): 2924 (m), 2853 (m), 2149 (w), 1737 (m), 1680 (s), 1599 (s), 1514 (m), 1264 (m), 1184 (m), 828 (m).

Compound **3.14**: Prepared according to **GP3** from precursor **3.35** (0.12 g, 0.32 mmol), potassium selenocyanate (0.07 g, 0.48 mmol) in acetonitrile (3 mL). The crude compound was further purified by neutral alumina column chromatography using 40% ethyl acetate and petroleum ether to afford the purified compound as white solid. R_f = 0.5 (40% ethyl acetate in petroleum ether). Yield: 0.05 g (39%); M. P.: 155 – 157 °C; ^{1}H NMR ($CDCl_3$, 400 MHz): δ (ppm) = 8.34 (d, 2H, *J* = 8.6 Hz), 7.94 (s, 1H), 7.67 (d, 2H, *J* = 8.6 Hz), 3.99 (t, 2H, *J* = 6.4 Hz), 3.05 (t, 2H, *J* = 7.1 Hz), 2.37 – 2.28 (m, 2H); ^{13}C NMR ($CDCl_3$,

100 MHz): δ (ppm) = 167.0, 165.8, 148.2, 139.0, 131.3, 130.7, 125.5, 124.4, 101.1, 40.9, 29.3, 26.4; ^{77}Se NMR ($CDCl_3$, 76 MHz): δ (ppm) = 213. ESI-MS *m/z* calcd for $C_{14}H_{11}N_3O_4SSe$ $[M + H]^+$: 419.9533, obs: 419.9446. FT-IR ($\bar{\nu}$, cm^{-1}): 3111 (w), 2150 (m), 1732 (s), 1674 (m), 1513 (m), 1343 (s), 1137 (m), 854 (w).

General procedure (GP4) for Synthesis of 4-substituted benzyl azides (**3.18**, **3.19**, **3.20**)**:** 4-substituted benzyl azides were synthesized following literature method.[20] Appropriately substituted precursor 4-substituted benzyl halide was stirred with sodium azide in N,N-dimethylformamide for 4 - 6 h at room temperature under inert. Progress was monitored by TLC analysis. After completion, the solution was quenched by water and was extracted with ethyl acetate (3 × 20 mL) and was washed with brine (3 × 20 mL). Combined organic layer was dried over anhyd. sodium sulfate and was evaporated *in vacuo* to afford the crude compound. The crude compound was purified by column chromatography using petroleum ether and ethyl acetate as eluting solvent, to afford the purified compound in moderate to good yield.

Compound **3.18**: Prepared according to **GP4** from benzyl bromide (1.00 g, 5.84 mmol), 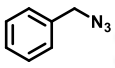 sodium azide (0.76 g, 11.69 mmol) in N,N-dimethylformamide (25 mL).[20] The crude compound was purified by 60-120 silica gel column chromatography using 100% petroleum ether as eluting solvent, to afford the purified compound as yellow oil. R_f = 0.6 (100% petroleum ether). Yield: 1.08 g (70%).^{1}H NMR ($CDCl_3$, 400 MHz): δ (ppm) = 7.41 – 7.31 (m, 5H). 4.33 (s, 2H).

Compound **3.19**:[21] Prepared according to **GP4** from 4-methoxybenzyl chloride (0.50 g, 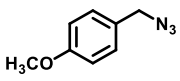 3.19 mmol), sodium azide (0.41 g, 6.38 mmol) in N,N-dimethyl formamide (10 mL). The crude compound was further purified by silica gel column chromatography using 5% ethyl acetate in petroleum ether as eluting solvent, to afford the purified title compound as yellow oil. R_f = 0.5 (10% ethyl acetate in petroleum ether). Yield: 0.41 g (78%). ^{1}H NMR ($CDCl_3$, 600 MHz): δ (ppm) = 7.24 (d, 2H, *J* = 8.6 Hz), 6.91 (d, 2H, *J* = 8.6 Hz), 4.26 (s, 2H), 3.81 (s, 3H).

Compound **3.20**:[21] Prepared according to **GP4** from 4-nitrobenzyl bromide (0.50 g, 2.31 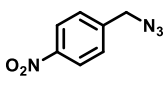 mmol), sodium azide (0.30 g, 4.63 mmol) in N,N-dimethylformamide (10 mL). The crude compound was further purified by 60-120 silica gel column chromatography using 10% ethyl acetate in petroleum ether as eluting solvent, to afford the purified title compound as yellow oil. R_f = 0.5 (10% ethyl acetate in

petroleum ether). Yield: 0.28 g (68%). ^{1}H NMR ($CDCl_3$, 400 MHz): δ (ppm) = 8.25 (d, 2H, *J* = 8.1 Hz), 7.51 (d, 2H, *J* = 8.2 Hz), 4.52 (s, 2H).

General procedure (GP5) for synthesis of Aryl-1H-1,2,3-triazol-4-yl)methanol (**3.21**, **3.22**, **3.23**): Prepared according to literature method with appropriate modifications.[22,23] Precursor azides (**3.18**, **3.19** or **3.20**) (1.0 equiv) was stirred with propargyl alcohol (1.1 equiv), 5 mol% copper(I) acetate, in *tert*-butanol under inert for 16 h. Progress of the reaction was monitored by TLC analysis. After completion, the solution was concentrated as much as possible under reduced pressure to yield a green pasty mass as the crude product.

Compound **3.21**:[24] Prepared according to **GP5** from precursor **3.18** (0.20 g, 1.5 mmol), 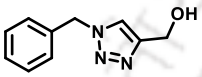

propargyl alcohol (0.09 g, 1.65 mmol), copper (II) acetate (0.01 g, 5 mol%) in *tert*-butanol (2 mL) for 16 h. The crude product was further purified by 60-120 silica gel column chromatography using ethyl acetate as eluting solvent to afford the purified title compound as white solid.[22] R_f = 0.5 (100% ethyl acetate). Yield: 0.95 g (84%). ^{1}H NMR ($CDCl_3$, 400 MHz): δ (ppm) =7.46 (s, 1H), 7.38 – 7.36 (m, 3H), 7.28 – 7.26 (m, 2H), 5.52 (s, 2H), 4.76 (s, 2H). ^{13}C NMR ($CDCl_3$, 150 MHz) = 148.2, 134.5, 129.1, 128.8, 128.1, 121.7, 56.2, 54.2.

Compound **3.22**:[25] Prepared according to **GP5** from precursor **3.19** (0.40 g, 2.45 mmol), 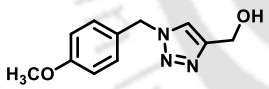

propargyl alcohol (0.15 g, 2.69 mmol), copper (II) acetate (0.02 g, 5 mol%) in *tert*-butanol (3 mL) for 16 h. The crude product was further purified by 60-120 silica gel column chromatography neutralized with triethylamine using 5% methanol in ethyl acetate as eluting solvent to afford the purified title compound as white solid.[25] R_f = 0.5 (5% methanol in ethyl acetate). Yield: 0.5 g (93%). ^{1}H NMR ($CDCl_3$, 600 MHz): δ (ppm) = 7.41 (s, 1H), 7.23 (d, 2H, *J* = 8.7 Hz), 6.90 (d, 2H, *J* = 8.7 Hz), 5.45 (s, 2H), 4.75 (s, 2H), 3.81 (s, 3H). ^{13}C NMR ($CDCl_3$, 150 MHz): δ (ppm) = 159.9, 147.9, 129.7, 126.4, 121.3, 114.5, 56.6, 55.3, 53.8.

Compound **3.23**:[26] Prepared according to **GP5** from precursor **3.20** (0.25 g, 1.40 mmol), 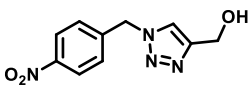

propargyl alcohol (0.09 g, 1.54 mmol), copper (II) acetate (0.02 g, 5 mol%) in *tert*-butanol (2 mL) for 16 h. The crude product was further purified by 230-400 silica gel column chromatography neutralized with triethylamine using 10% methanol in ethyl acetate as eluting solvent to

afford the purified title compound as white solid. R_f = 0.5 (5% methanol in ethyl acetate). Yield: 0.29 g (72%). ^{1}H NMR ($CDCl_3$, 600 MHz): δ (ppm) = 8.24 (d, 2H, *J* = 8.2 Hz), 7.53 (s, 1H), 7.41 (d, 2H, *J* = 8.7 Hz), 5.65 (s, 2H), 4.82 (s, 2H). ^{13}C NMR ($CDCl_3$, 150 MHz): δ (ppm) = 148.5, 148.1, 141.5, 128.6, 124.4, 121.8, 56.7, 53.1.

General procedure (GP6) for synthesis of 4-(bromomethyl)-1-aryl-1H-1,2,3-triazole (3.24, 3.25, 3.26): Title compounds were synthesized following previously reported literature method.[22] Precursor triazole-based alcohols (**3.21, 3.22**, **3.23**) (1.0 equiv) was stirred with phosphorus tribromide (2.0 equiv) in dry dichloromethane for 4 - 6 h at room temperature under inert. The progress was monitored by TLC analysis. After completion the solution was quenched by equal volume of water and was stirred for 10 min. The solution was then extracted with dichloromethane (2 × 10 mL) and was washed with water (2 × 10 mL) and brine (1 × 10 mL). Combined organic layer was dried over anhyd. sodium sulfate and was concentrated *in vacuo* to yield the crude product. This was directly used for the next step without further purification.

Compound **3.24**:[27] Prepared according to **GP6** using precursor **3.21** (0.15 g, 0.79 mmol), phosphorus tribromide (0.43 g, 1.58 mmol) in dry dichloromethane (3 mL) as white solid.[22] Crude product was directly used for next step without further purification. R_f = 0.7 (50% ethyl acetate in petroleum ether). Yield: 0.3 g (75%). ^{1}H NMR ($CDCl_3$, 400 MHz): δ (ppm) = 7.48 (s, 1H), 7.38 (s, 3H), 7.28 (s, 3H), 5.51 (s, 2H), 4.54 (s, 2H). ^{13}C NMR ($CDCl_3$, 150 MHz): δ (ppm) = 145.0, 134.2, 129.2, 128.9, 128.2, 122.7, 54.3, 21.6.

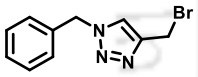

Compound **3.25**:[28] Prepared according to **GP6** using precursor **3.22** (0.2 g, 0.91 mmol), phosphorus tribromide (0.49 g, 1.8 mmol) in dry dichloromethane (3 mL) as white solid. Crude product was directly used for next step without further purification. R_f = 0.5 (50% ethyl acetate in petroleum ether). Yield: 0.17 g (66%). ^{1}H NMR ($CDCl_3$, 600 MHz): δ (ppm) = 7.45 (s, 1H), 7.24 (d, 2H, *J* = 8.6 Hz), 6.91 (d, 2H, *J* = 8.6 Hz), 5.45 (s, 2H), 4.54 (s, 2H), 3.81 (s, 3H). ^{13}C NMR ($CDCl_3$, 150 MHz): δ (ppm) = 160.1, 144.9, 129.8, 126.1, 122.5, 114.6, 55.4, 53.9, 21.7.

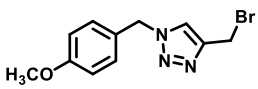

Compound **3.26**:[23] Prepared according to **GP6** using precursor **3.23** (0.12 g, 0.51 mmol), phosphorus tribromide (0.28 g, 1.02 mmol) in dry

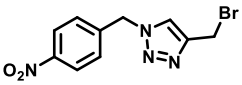

dichloromethane (2.5 mL) as white solid. The crude product was directly used for next step without further purification. R_f = 0.8 (75% ethyl acetate in petroleum ether). Yield: 0.11 g (75%). ^{1}H NMR ($CDCl_3$, 600 MHz): δ (ppm) = 8.25 (d, 2H, *J* = 8.7 Hz), 7.59 (s, 1H), 7.42 (d, 2H, *J* = 8.7 Hz), 5.65 (s, 2H), 4.57 (s, 2H). ^{13}C NMR ($CDCl_3$, 150 MHz): δ (ppm) = 148.2, 145.7, 141.2, 128.6, 124.4, 123.0, 53.2, 21.2.

General procedure (GP7) for synthesis of 5-arylidenethiazolidine-2,4-dione (**3.30**, **3.31**, **3.32**): Title compounds were accessed using reported literature method.[29] Briefly, appropriately substituted aldehyde (1.0 equiv) was refluxed at 80 ˚C with 2,4-thiazolidine-1,3-dione (2.0 eq.) and piperidine (1.3 equiv) in ethanol solvent for 12 h. Solid precipitate was formed with the course of the reaction. Progress of the reaction was monitored by TLC analysis. After completion, the solution was cooled to room temp. and the solid precipitate was filtered. The residue was washed with ethanol (3 × 10 mL) and diethyl ether (1 × 10 mL) and was dried in air to afford the crude product. The crude product was directly used for the next step without further purification.

Compound **3.30**:[30] Prepared according to **GP7** using 2,4-thiazolidine-1,3-dione (0.16 g, 1.41 mmol), benzaldehyde (0.30 g, 2.80 mmol), piperidine (0.07 g, 0.85 mmol) in ethanol (5 mL) as yellow solid. Crude product was directly used for the next step without further purification. R_f = 0.5 (30% ethyl acetate in petroleum ether). Yield: 0.15 g (51%). ^{1}H NMR ($CDCl_3$, 400 MHz): δ (ppm) = 7.86 (s, 1H), 7.51 – 7.46 (m, 5H).

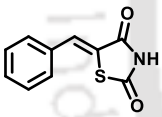

Compound **3.31**: Prepared according to **GP7** using 2,4-thiazolidine-1,3-dione (0.21 g, 1.83 mmol), 4-methoxybenzaldehyde (0.50 g, 3.67 mmol), piperidine (0.09 g, 1.10 mmol) in ethanol (4 mL) as yellow solid. Crude product was directly used for the next step without further purification. R_f = 0.5 (50% ethyl acetate in petroleum ether). Yield: 0.23 g (26%). ^{1}H NMR ($CDCl_3$, 600 MHz): δ (ppm) =7.81 (s, 1H), 7.46 (d, 2H, *J* = 8.8 Hz), 7.00 (d, 2H, *J* = 8.8 Hz), 3.87 (s, 3H).

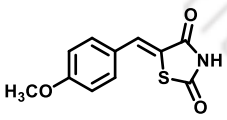

Compound **3.32**: Prepared according to **GP7** using 2,4-thiazolidine-1,3-dione (0.15 g, 1.32 mmol), benzaldehyde (0.40 g, 2.6 mmol), piperidine (0.07 g, 0.79 mmol) in ethanol (4 mL) as yellow solid. Crude product was directly used for next step without purification. R_f =. Yield: 0.18 g

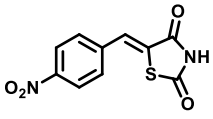

(27%); ^{1}H NMR (DMSO-d_6, 500 MHz): δ (ppm) = 8.34 (d, 2H, *J* = 8.5 Hz), 7.89 (s, 1H), 7.86 (d, 2H, *J* = 8.7 Hz).

General procedure (GP8) for synthesis of compounds 5-arylidene-3-(3-bromopropyl)-thiazolidine-2,4-dione (**3.33**, **3.34**, **3.35**): Title compounds were synthesized using literature procedure with minor modifications as required.[31] Precursor compound (**3.30**, **3.31**, or **3.32**) (1.0 equiv) was refluxed with 1,3-dibromopropane (3.0 equiv) and triethylamine (1.0 equiv) at 85 ˚C for 4 h under inert. The progress was monitored by TLC analysis. After completion, the solution was evaporated to dryness under reduced pressure. The residue was extracted with ethyl acetate (3 × 10 mL) and was washed with water (2 × 10 mL) and brine (1 × 10 mL). Combined organic layer was dried over anhyd. sodium sulfate and was concentrated *in vacuo* to yield the crude product.

Compound **3.33**: Prepared according to **GP8** using precursor **3.30** (0.18 g, 0.88 mmol), 1,3-dibromopropane (0.44 g, 2.19 mmol), trimethylamine (0.10 g, 0.96 mmol) in acetonitrile (2 mL). Crude product was further purified by neutral alumina column chromatography using 10% dichloromethane in petroleum ether to afford purified compound as yellow solid. R_f = 0.7 (30% ethyl acetate in petroleum ether). Yield: 0.17 g (76%). ^{1}H NMR ($CDCl_3$, 600 MHz): δ (ppm) = 7.92 (s, 1H), 7.53 – 7.44 (m, 5H), 3.92 (t, 2H, *J* = 6.9 Hz), 3.42 (t, 2H, *J* = 6.6 Hz), 2.27 (p, 2H, *J* = 6.8 Hz). ^{13}C NMR ($CDCl_3$, 600 MHz): δ (ppm) = 167.9, 166.3, 134.2, 133.2, 130.7, 130.3, 129.3, 121.2, 40.7, 30.8, 29.4.

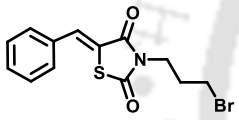

Compound **3.34**: Prepared according to **GP8** using precursor **3.31** (0.15 g, 0.64 mmol), 1,3-dibromopropane (0.39 g, 1.91 mmol), trimethylamine (0.07 g, 0.70 mmol) in acetonitrile (2 mL). Crude product was further purified using neutral alumina column chromatography using 50% dichloromethane in petroleum ether to afford purified compound as yellow solid. R_f = 0.7 (50% ethyl acetate in petroleum ether). Yield: 0.3 g (25%) ^{1}H NMR ($CDCl_3$, 600 MHz): δ (ppm) = 7.89 (s, 1H), 7.48 (d, 2H, *J* = 8.7 Hz), 7.00 (d, 2H, *J* = 8.7 Hz), 3.91 (t, 2H, *J* = 6.9 Hz), 3.90 (s, 3H), 3.44 (t, 2H, *J* = 6.6 Hz), 2.26 (p, 2H, *J* = 6.8 Hz).

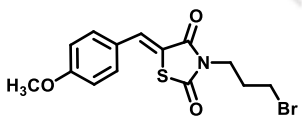

Compound **3.35**: Prepared according to **GP8** using precursor **3.32** (0.15 g, 0.60 mmol), 1,3-dibromopropane (0.36 g, 1.80 mmol), trimethylamine (0.07

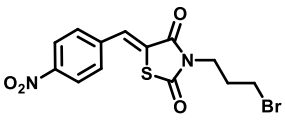

g, 0.66 mmol) in acetonitrile (2 mL) as yellow solid. Crude product was not purified further and was directly used for next step without purification. R_f = 0.8 (30% ethyl acetate in petroleum ether). Yield: 0.16 g (71%) ^{1}H NMR ($CDCl_3$, 400 MHz): δ (ppm) = 8.33 (d, 2H, *J* = 8.8 Hz), 7.92 (br s, 2H), 7.67 (d, 2H, *J* = 8.7 Hz), 3.95 (t, 2H, *J* = 6.9 Hz), 3.42 (t, 2H, *J* = 6.6 Hz), 2.28 (p, 2H, J = 6.7 Hz). ^{13}C NMR ($CDCl_3$, 150 MHz): δ (ppm) = 166.7, 165.6, 148.1, 139.2, 130.8, 130.6, 125.9, 124.4, 41.1, 30.6, 29.3.

3.5.2. Cell culture

TNBC cell lines were obtained from NCCS Pune. Dulbecco's modified Eagle's medium (DMEM) added with 10 % fetal bovine serum and 1% penicillin-streptomycin (Gibco) was used as a nutrient supplement for the MDA-MB-231 and HEK-293 cells. All the cells were maintained in CO_2-regulated humidified (95% air/5% CO_2 atmosphere) incubator at 37 °C.

3.5.3. MTT assay

The cells were plated in 96-well culture plates at a density of 2×10^3 cells per 100 µl per well for L-132 cells and 4×10^3 cells per 100 µl per well for all other cells and treated with 0.0, 1.0, 5.0, 10.0 and 25.0 µM of test compounds for 0 h (Set 1) and 72 h (Set 2). At the end of the treatment period, 10.0 µL of 5.0 mg mL^{-1} of MTT was added to the plate (Set 1) and incubated for 2 h. Following the 2 h incubation, the culture medium from the plate was removed and the purple formazan crystals were dissolved using 100 µl of DMSO (Merck Life Science Pvt Ltd) and the absorbance at 570 nm was measured using a microplate reader (TECAN Infinite 200 PRO multimode reader). In Set 2, a similar MTT treatment protocol was followed only after 72 h. The mean OD values of a 0 h plate (Set 1) were subtracted from the mean OD values of identical wells at a 72 h plate (Set 2) ΔOD and the inhibition of proliferation was calculated keeping the ΔOD of the untreated control as 100%.

3.5.4. Cell cycle analysis

1×10^5 cells per 2 mL per well were seeded in 6-well plates and treated with 0.0, 1.0 and 5.0 µM of compounds **1.48** and **3.8** and incubated for 24 h. Following the 24 h drug treatment, the cells were collected; washed with PBS (1X); fixed with ice-cold 70% ethanol at −20 °C for 30 min; again washed with PBS (1X) and stained with PI/RNase

staining buffer (BD Biosciences) for 10 min at room temperature. The prepared samples were then analysed using a BD FACSCalibur™ instrument (BD Biosciences).

3.5.5. Wound healing (scratch) assay

MDA-MB-231 cells were seeded in a 24-well plate at a concentration of 1.5×10^5 cells per 2 mL per well and incubated in a CO_2 incubator at 37 °C to form a monolayer of cells. After the monolayer formation, the cells were pre-incubated in serum free medium for 6 h. Using a 100 µl tip, a scratch was made on the monolayer and the debris was removed by washing with PBS (1X). Then, the cells were re-incubated with serum free medium and treated with 0.0, 1.0 and 2.5 µM of active selenocyanates **3.8**. Images of the scratch were captured at regular time intervals (0, 24, 48 and 72 h) using a Nikon inverted microscope and a camera. The extent of wound healing denotes the anti-migratory effect of the compounds tested.

3.5.6. Assessment of cellular morphology and apoptotic bodies

5×10^4 cells per 1 mL per well were plated in 24-well plates and treated with 0.0 and 10.0 µM of compounds **3.8**. The cells were observed for any morphological changes and the change in morphology was captured at regular time intervals (0, 24 and 48 h) using a Nikon inverted microscope and a camera. After 72 h, the formation of apoptotic nuclei was analysed by staining the cells with 5 µl of 1 mg mL^{-1} PI and images were taken using an Eclipse Ti-S inverted fluorescence microscope.

3.5.7. Western Blot analysis

MDA-MB-231 cells were treated with 0.0, 0.2, 0.5, 1.0, 2.0 and 2.5 µM of compound **3.8** for 24 h and the whole cell protein lysate was made using lysis buffer (20 µM HEPES buffer, 1 M NaCl, 0.5 M EDTA, 1 mg mL^{-1} leupeptin, 100 mM PMSF, 5 mg mL^{-1} aprotinin, 1 M DTT and 0.1% (v/v) Triton-X100). Total protein concentration was estimated with the Bradford protein assay; 20 µg of protein lysate was loaded and separated on a 12% sodium dodecyl sulfate (SDS)–polyacrylamide gel by electrophoresis and transferred to a nitrocellulose membrane. Protein transfer was confirmed by Ponceau-S (HiMedia) staining. The blots were blocked with 5% non-fat dry milk or BSA in 1X TBST buffer for 2 h at room temperature and incubated with an appropriate dilution of the primary antibodies specific for COX-2, Survivin, Bcl-2, VEGF-A, Akt, p-Akt and GAPDH (Cell Signaling Technology) overnight at 4 °C. Following the primary antibody incubation, the blots were washed and incubated with

HRP-conjugated secondary antibodies (Abcam) for 2 h and developed with an Optiblot ECL Detect Kit (Abcam) and ChemiDoc™ XRS System (Bio-Rad). The housekeeping gene GAPDH was used as a loading control.

3.5.8. Antioxidant activity using GSH-GSSG coupled assay

GPx-like activity was carried out UV-VIS spectroscopically using enzymatic method. The assay mixture consisted of reduced glutathione (2.0 mM), glutathione disulfide reductase enzyme (1.0 units mL^{-1}), NADPH (0.4 mM) in 0.1 M potassium phosphate (pH = 7.5). GPx-like samples (100.0 µM) were added at room temperature, and the reaction was initiated by the addition of peroxides (1.6 mM). The initial reduction rates were calculated from the rate of NADPH oxidation at λ = 340 nm. Initial rates were calculated from three replicates of the reaction for 5.0 to 20.0 seconds, using 6.22 $mM^{-1}cm^{-1}$ as the molar extinction co-efficient for the NADPH.

3.5.9. Antioxidant activity using PhSH-PhSSPh assay

HPLC mediated thiophenol assay: The GPx-like activity was measured using high-performance liquid chromatography apparatus in a 1.5 ml sample vials and in-built autosampler was used for sample injection in a pre-programmed sequence. In this assay, a solution of 1.0 mM thiophenol and 2.0 mM peroxide in HPLC-grade methanol at ambient temperature were used as a model system. Runs in presence (20.0 µM) and absence of test compounds were carried out under identical conditions. Periodically, reaction aliquots were injected into reversed-phase column (Phenomenex Luna™ 5 µm, C-18(2) 100 Å, diameter: 250 × 4.6 mm) and eluted with 95:5 methanol-water solvent system for a runtime of 7.0 min. The amount of PhSSPh formed as a product was determined by comparison with standardized calibration plot obtained from known concentrations of PhSSPh. The chromatograms were recorded at λ = 250 nm and half-life of formation of PhSSPh was calculated from kinetic graph. Each experiment was replicated thrice under identical conditions. However, two concordant datasets were used to calculate the half-life of formation of PhSSPh

3.6. References

1. El-Bayoumy, K., *Cancer Res* **1985**, *45*, 3631.
2. Reddy, B. S.; Rivenson, A.; El-Bayoumy, K.; Upadhyaya, P.; Pittman, B.; Rao, C. V., *J Natl Cancer Inst* **1997**, *89*, 506.
3. Alves, D.; Goldani, B.; Lenardão, E. J.; Perin, G.; Schumacher, R. F.; Paixão, M. W., *Chem Rec* **2018**, *18*, 527.
4. Nishina, A.; Kimura, H.; Kozawa, K.; Sommen, G.; Favero, F.; Heimgartner, H.; Koketsu, M.; Furukawa, S., *Int J Toxicol* **2011**, *30*, 690.
5. Savegnago, L.; Sacramento, M. d.; Brod, L. M. P.; Fronza, M. G.; Seus, N.; Lenardão, E. J.; Paixão, M. W.; Alves, D., *RSC Adv* **2016**, *6*, 8021.
6. da Cruz, E. H. G.; Silvers, M. A.; Jardim, G. A. M.; Resende, J. M.; Cavalcanti, B. C.; Bomfim, I. S.; Pessoa, C.; de Simone, C. A.; Botteselle, G. V.; Braga, A. L., *et al.*, *Eur J Med Chem* **2016**, *122*, 1.
7. Panaka, S.; Trivedi, R.; Jaipal, K.; Giribabu, L.; Sujitha, P.; Kumar, C. G.; Sridhar, B., *J Organomet Chem* **2016**, *813*, 125.
8. Jardim, G. A. M.; Lima, D. J. B.; Valença, W. O.; Lima, D. J. B.; Cavalcanti, B. C.; Pessoa, C.; Rafique, J.; Braga, A. L.; Jacob, C.; Da Silva Júnior, E. N., *et al.*, *Molecules* **2018**, *23*.
9. Roy, S. S.; Chakraborty, P.; Bhattacharya, S., *Eur J Med Chem* **2014**, *73*, 195.
10. Corigliano, D. M.; Syed, R.; Messineo, S.; Lupia, A.; Patel, R.; Reddy, C. V. R.; Dubey, P. K.; Colica, C.; Amato, R.; De Sarro, G., *et al.*, *PeerJ* **2018**, *6*, e5386.
11. Nasim, M. J.; Witek, K.; Kincses, A.; Abdin, A. Y.; Żesławska, E.; Marć, M. A.; Gajdács, M.; Spengler, G.; Nitek, W.; Latacz, G., *et al.*, *New J Chem* **2019**, *43*, 6021.
12. Banerjee, K.; Padmavathi, G.; Bhattacherjee, D.; Saha, S.; Kunnumakkara, A. B.; Bhabak, K. P., *Org Biomol Chem* **2018**, *16*, 8769.
13. Yarrow, J. C.; Perlman, Z. E.; Westwood, N. J.; Mitchison, T. J., *Bmc Biotechnol* **2004**, *4*.
14. (a) Bocca, C.; Bozzo, F.; Miglietta, A., *Anticancer Res* **2014**, *34*, 1793; (b) Bocca, C.; Ievolella, M.; Autelli, R.; Motta, M.; Mosso, L.; Torchio, B.; Bozzo, F.; Cannito, S.; Paternostro, C.; Colombatto, S., *et al.*, *Expert Opin Ther Tar* **2014**, *18*, 121; (c) Rahman, K. M. W.; Li, Y. W.; Wang, Z. W.; Sarkar, S. H.; Sarkar, F. H., *Cancer Res* **2006**, *66*, 4952.

15. Boopalan, T.; Arumugam, A.; Damodaran, C.; Rajkumar, L., *Anticancer Res* **2012**, *32*, 2801.
16. Bhabak, K. P.; Mugesh, G., *Chem Eur J* **2009**, *15*, 9846.
17. Bhabak, K. P.; Mugesh, G., *Chem Eur J* **2008**, *14*, 8640.
18. Anjomshoa, M.; Fatemi, S. J.; Torkzadeh-Mahani, M.; Hadadzadeh, H., *Spectrochim Acta A Mol Biomol Spectrosc* **2014**, *127*, 511.
19. Jacob, L. A.; Matos, B.; Mostafa, C.; Rodriguez, J.; Tillotson, J. K., *Molecules* **2004**, *9*.
20. Park, J. Y.; Kim, Y.; Bae, D. Y.; Rhee, Y. H.; Park, J., *Organometallics* **2017**, *36*, 3471.
21. Nunes, P. S. G.; da Silva, G.; Nascimento, S.; Mantoani, S. P.; de Andrade, P.; Bernardes, E. S.; Kawano, D. F.; Leopoldino, A. M.; Carvalho, I., *Bioorg Chem* **2021**, *113*, 104982.
22. Barsoum, D. N.; Brassard, C. J.; Deeb, J. H. A.; Okashah, N.; Sreenath, K.; Simmons, J. T.; Zhu, L., *Synthesis* **2013**, *45*, 2372.
23. Reddyrajula, R.; Dalimba, U., *ChemistrySelect* **2019**, *4*, 2685.
24. Rafi, A. A.; Ibrahem, I.; Córdova, A., *Sci Rep* **2020**, *10*, 20547.
25. Song, H.; Rogers, N. J.; Brabec, V.; Clarkson, G. J.; Coverdale, J. P. C.; Kostrhunova, H.; Phillips, R. M.; Postings, M.; Shepherd, S. L.; Scott, P., *Chem Commun* **2020**, *56*, 6392.
26. Bonyasi, R.; Gholinejad, M.; Saadati, F.; Nájera, C., *New J Chem* **2018**, *42*, 3078.
27. Counsell, A. J.; Yu, M.; Shi, M.; Jones, A. T.; Batten, J. M.; Turner, P.; Todd, M. H.; Rutledge, P. J., *Dalton Trans* **2021**, *50*, 3931.
28. Takizawa, K.; Nulwala, H.; Thibault, R. J.; Lowenhielm, P.; Yoshinaga, K.; Wooley, K. L.; Hawker, C. J., *J Polym Sci A Polym Chem* **2008**, *46*, 2897.
29. Ha, Y. M.; Park, Y. J.; Kim, J.-A.; Park, D.; Park, J. Y.; Lee, H. J.; Lee, J. Y.; Moon, H. R.; Chung, H. Y., *Eur J Med Chem* **2012**, *49*, 245.
30. Tilekar, K.; Upadhyay, N.; Schweipert, M.; Hess, J. D.; Macias, L. H.; Mrowka, P.; Meyer-Almes, F.-J.; Aguilera, R. J.; Iancu, C. V.; Choe, J.-y., *et al.*, *Eur J Pharm Sci* **2020**, *154*, 105512.
31. Mohan, R.; Sharma, A. K.; Gupta, S.; Ramaa, C. S., *Med Chem Res* **2012**, *21*, 1156.

Chapter 4

Syntheses and Efficient Antioxidant Activities of Benzimidazole- and Imidazole-based Ionic Selenocyanates and the Corresponding Selenazolium and Selenazinium Selenocyanates

4.1. Introduction

Reactive oxygen species (ROS) are strong oxidants that are generated in the mammalian system upon the metabolism of molecular oxygen in the presence of several key enzymes.[1] Importantly, a regulated generation of endogenous ROS is essential for maintaining the cellular homeostasis and important biological processes such as signal transduction, neurotransmission, platelet aggregation, blood pressure regulation and the metabolism of xenobiotics.[1] However, an overproduction of ROS hampers the cellular redox equilibrium and leads to severe oxidative damages with the depletion of antioxidant level.[2,3] An elevated level of ROS is considered as a hallmark of oxidative stress in several pathological conditions as well as disease states such as cancer, inflammation, atherosclerosis, cardiovascular disease, neurodegenerative disease, ageing etc.[4] In mammalian system, a cascade of antioxidant enzymes catalytically scavenge the excess ROS and regulate the cellular redox level. Among these, glutathione peroxidase (GPx), a selenocysteine-containing enzyme catalytically reduce hydrogen peroxide (H_2O_2) using glutathione (GSH) as a cofactor.[5] Considering the redox chemistry at the selenium center of selenocysteine residue at the active site of GPx, a number of synthetic organoselenium compounds have been developed over last few decades as functional mimics of GPx.[6] After the discovery of the anti-inflammatory drug ebselen (**1.14**) containing selenenyl amide group, many different categories of organoselenium compounds are reported by various research groups that include *ortho*-coordinated diselenides, selenenyl amides, azaselenonium chloride, cyclic selenenate ester and alkyl/allyl selenides etc.[7] Among those small-molecule synthetic mimics, monoselenides are reported as highly efficient functional mimics of GPx. Chemical structures of some of the small molecular organoselenium compound that function as efficient antioxidant agents are summarized in Figure 4.1. In 2004, Back and co-workers have reported di-(3-hydroxypropyl) selenide **4.1** as a novel GPx mimic that exhibits catalytic activity *via* the formation of spirodioxaselenanonane species.[8] In 2015, Iwaoka and co-workers studied the effect of ring size on the GPx-like antioxidant activity of a series of cyclic monoselenides. It was observed that compound **4.2** bearing two hydroxyl functionalities with five membered ring is the optimum size for exhibiting highest antioxidant activity.[9] In 2007, Back and co-workers reported the ionic unsymmetrical azaselenonium chloride **4.3** that exhibited better GPx-like activity than the standard compound ebselen **1.14**.[10]

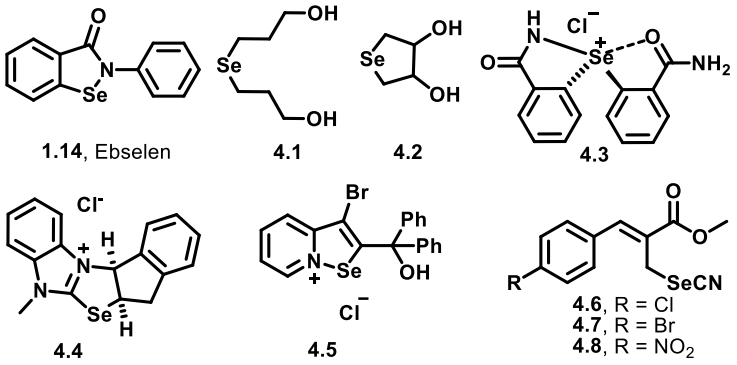

Figure 4.1. Chemical structures of some literature reported antioxidant synthetic organoselenium compounds.

In 2012, Borisov *et al* reported the synthesis of benzimidazole-based cationic selenazolium compound **4.4** by the ring closure method utilizing selenocyclization process.[11] However, the compounds were not studied for any other *in vitro* study. Recently, in 2020, Arsenyan and co-workers have reported another ionic mitochondria-targeting fused isoselenazolium chloride **4.5** that rather enhanced the intracellular level of ROS in breast cancer cells and thus exhibited potent anti-cancer activity rather antioxidant activity.[12] In the same year, Frizon *et al* have reported a series of allylic selenocyanates such as compounds **4.6-4.8** and evaluated for their antioxidant activities in cultured mouse neurons under oxidative stress induced by H_2O_2.[13] Interestingly, compounds **4.6-4.8** exhibited significant antioxidant activities comparable to that of diphenyl diselenide (Ph_2Se_2).

4.2. Outline of the chapter

In the present chapter, we describe three new classes of ionic organoselenium compounds containing cationic benzimidazolium and imidazolium ring systems with selenocyanates as counterions. The cyclization of *N,N´*-disubstituted benzimidazolium and imidazolium bromides having *N*-$(CH_2)_2$-Br and *N*-$(CH_2)_3$-Br in the presence of potassium selenocyanate led to the formation of the corresponding selenazolium selenocyanates (**4.11a-b**, **4.12a-b**) and selenazinium selenocyanates (**4.11c-d**, **4.12c-d**). In contrast, open chain selenocyanates (**4.11e-f, 4.12e-f)** with additional selenocyanate counterion was formed from the *N,N´*-disubstituted benzimidazolium and imidazolium bromides having *N*-$(CH_2)_6$-Br group. Mechanistic studies were carried out to understand the feasibility of such cyclization process in the presence of KSeCN. The compounds were studied further for their potencies to catalytically reduce H_2O_2 in the presence of thiols such as glutathione and thiophenol (antioxidant activities). Interestingly, most of

the compounds exhibited significant *in vitro* antioxidant activities in both of GSH-GSSG coupled assay as well as in PhSH-PhSSPh assay. Furthermore, the compounds were also evaluated for their potencies in modulating the intracellular level of ROS in a representative macrophage cell lines (RAW 264.7).

4.3. Results and Discussion

4.3.1. Synthesis of selenazolium, selenazinium and open-chain ionic selenocyanates

A series of ionic organoselenium compounds **4.11a-f** and **4.12a-f** were synthesized using benzimidazole and imidazole as readily available and cheap precursors (Scheme 4.1). The *N*-substituted derivatives (**4.9a-b**, **4.10a-b**) were synthesized upon the *N*-functionalization of benzimidazole and imidazole with methyl iodide or benzyl bromide using powdered potassium hydroxide in acetonitrile at room temperature. The *N*-substituted compounds were then treated with 10.0–12.0 equiv of the appropriate dibromoalkanes to afford the *N*,*N*´-disubstituted ionic bromides (**4.9a-n**, **4.9b-n**, **4.10a-n** and **4.10b-n**; with n = 1, 2 and 5). The final compounds **4.11a-f** and **4.12a-f** having selenocyanate as counterion were afforded from the bromides in the presence of three equivalents of potassium selenocyanate (KSeCN) (Scheme 4.1A). While cyclic selenazolium and selenazinium compounds (**4.11b** and **4.11d**) were obtained from the *N*-$(CH_2)_2$-Br and *N*-$(CH_2)_3$-Br substituted benzimidazolium and imidazolium derivatives, the corresponding *N*-$(CH_2)_6$-Br substituted derivatives did not cyclize under the identical condition and afforded open chain benzimidazolium and imidazolium selenocyanates (**4.11e-f** and **4.12e-f**) with an additional selenocyanate moiety as counterion. This is not surprizing as the cyclization of *N*-$(CH_2)_6$-Br derivatives would produce nine-membered rings that might have much higher ring strains. To further generalize the feasibility of cyclization with variable alkyl bromide chain length in ionic bromides, we have explored the product distribution from *N*-$(CH_2)_4$- and *N*-$(CH_2)_5$- bromides corresponding to *N*-benzyl-benzimidazole under identical conditions. Both the bromides reacted with potassium selenocyanate and afforded open chain benzimidazolium selenocyanates as evidenced by NMR spectroscopic studies of crude mixtures. However, both the products decomposed during the column chromatographic purification process using neutral alumina as stationary phase. The final ionic compounds (**4.11a-f** and **4.12a-f**) were purified by neutral alumina column chromatography and characterized by analytical methods (experimental section).

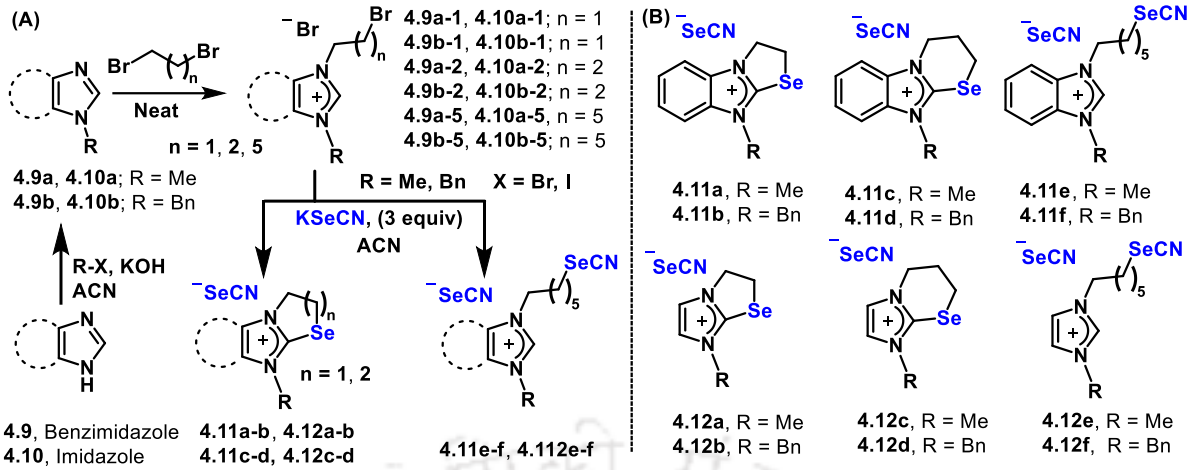

Scheme 4.1. (A) General synthetic scheme to benzimidazole- and imidazole-based ionic selenocyanates **4.11a-f** and **4.12a-f** (B) Chemical structures of selenazolium selenocyanates (**4.11a-b, 4.12a-b**), selenazinium selenocyanates (**4.11c-d**, **4.12c-d**) and benzimidazolium/imidazolium selenocyanates (**4.11e-f**, **4.12e-f**).

The structural difference of cyclic compounds **4.11a-d** and the open chain compounds **4.11e-f** were detected from NMR and IR spectroscopic studies. For example, the chemical shift values of Se-CH_2 protons in ^{1}H NMR indicated the structural differences particularly with the connectivity of Se atoms in compounds **4.11d** and **4.11f**. The cyclization in compound **4.11d** unlike in **4.11f** was indicated mainly by the disappearance of ^{1}H NMR signal for the heterocyclic ring C2-H atom (Figure 4.2A). Furthermore, a clear difference in the chemical shift of Se-center was reflected between these two compounds in ^{77}Se NMR spectra. For example, while two signals were observed for compound **4.11d** in ^{77}Se NMR at 278 ppm and -277 ppm, the values were at 215 ppm and -276 ppm, respectively for compound **4.11f** (Figure 4.2B). The signal at around -277 ppm was indicative of the presence of selenocyanate counterion in all the ionic compounds (**4.11a-f** and **4.12a-f**) reported herein. The structural difference was further evidenced by the characteristic stretching frequency of cyanide group in FT-IR spectral data at around 2050-2060 cm^{-1}. For example, while a single characteristic cyanide signal was observed for all the cyclic selenazolium and selenazinium selenocyanates (**4.11a-d** and **4.12a-d**), two adjacent signals characteristic of cyanide group were observed for the benzimidazolium and imidazolium selenocyanates (**4.11e–f** and **4.12e-f**). Two cyanide signals were indicative of the presence of two types of selenocyanate groups. The cationic components of the molecules were also characterized by ESI-MS analysis. Finally, the structure of the representative cyclic and open chain

selenocyanates were unambiguously confirmed from single crystal X-ray studies (Figure 4.2C).

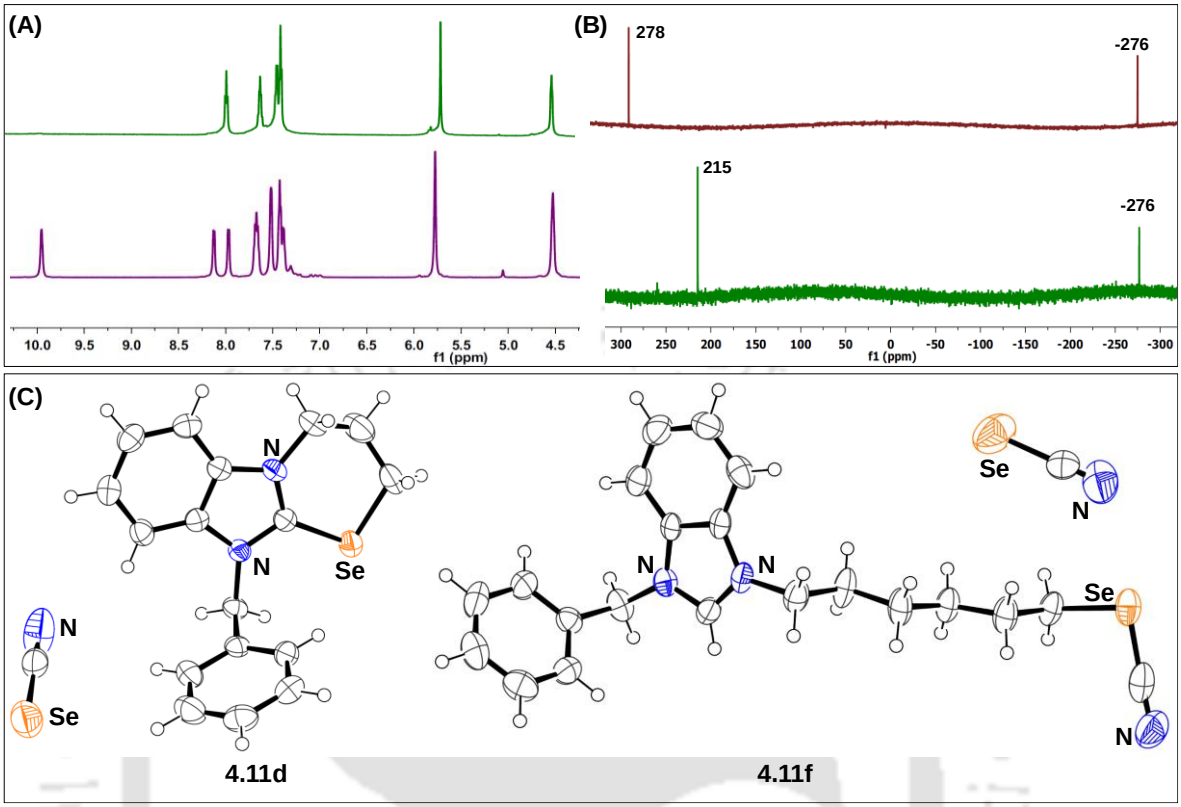

Figure 4.2. (A) ^{1}H NMR spectra (DMSO-d_6, 600 MHz) of **4.11d** and **4.11f**; (B) ^{77}Se spectra (DMSO-d_6, 114 MHz) of **4.11d** and **4.11f**; (C) Single crystal X-ray structures of compounds **4.11d** and **4.11f**. The ORTEP diagrams were drawn with the ellipsoids representing 50% probability level.

With the confirmation of structures of final products **4.11a-f** and **4.12a-f** in the present study, we have further investigated the necessity of three equivalents (equiv) of KSeCN for the product formation. Reaction of ionic bromide **4.9b-2** was carried out with variable equiv (1.0 - 3.0) of KSeCN in acetonitrile-d_3 (CD_3CN) at room temperature and the product distribution was analyzed using ^{1}H, ^{13}C and ^{77}Se NMR studies in a mixture of solvents involving CD_3CN: DMSO-d_6: D_2O (7:2:1). As shown in Scheme 4.2, reaction of **4.9b-2** with one equiv of KSeCN afforded the cyclic compound **4.17b-2** having bromide or cyanide as counterion along with a trace amount of unreacted starting material **4.9b-2**. However, in the presence of two equiv of KSeCN, the cyclization reaction was found to be completed as observed from the complete disappearance of signals in the precursor bromide **4.9b-2** in ^{1}H NMR spectra. Cationic component of the

cyclic product **4.19b-2** was observed by ^{1}H NMR as well as ^{77}Se NMR (δ = 276 ppm) spectra. However, the counterion was not confirmed at this stage which might comprise either of $^{-}$SeCN, $^{-}$CN or $^{-}$Br ions. A relatively weaker ^{77}Se signal at δ = -308 ppm (Figure 4.3C-b) represents partial formation of cyclic product **4.11d** and the remaining cyclic compound could be **4.19b-2** having X^{-} counterion (X = Br, CN). The product distribution was unchanged in the presence of three equiv of KSeCN. The complete formation of compound **4.11d** with third equivalent $SeCN^{-}$ was observed from ^{77}Se NMR spectral data with the replacement of X^{-} (X = Br, CN) counterion from **4.19b-2** by the third equivalent of $^{-}$SeCN. This observation indicates the necessity of at least two equiv of KSeCN for the final product formation (compound **4.11d**).

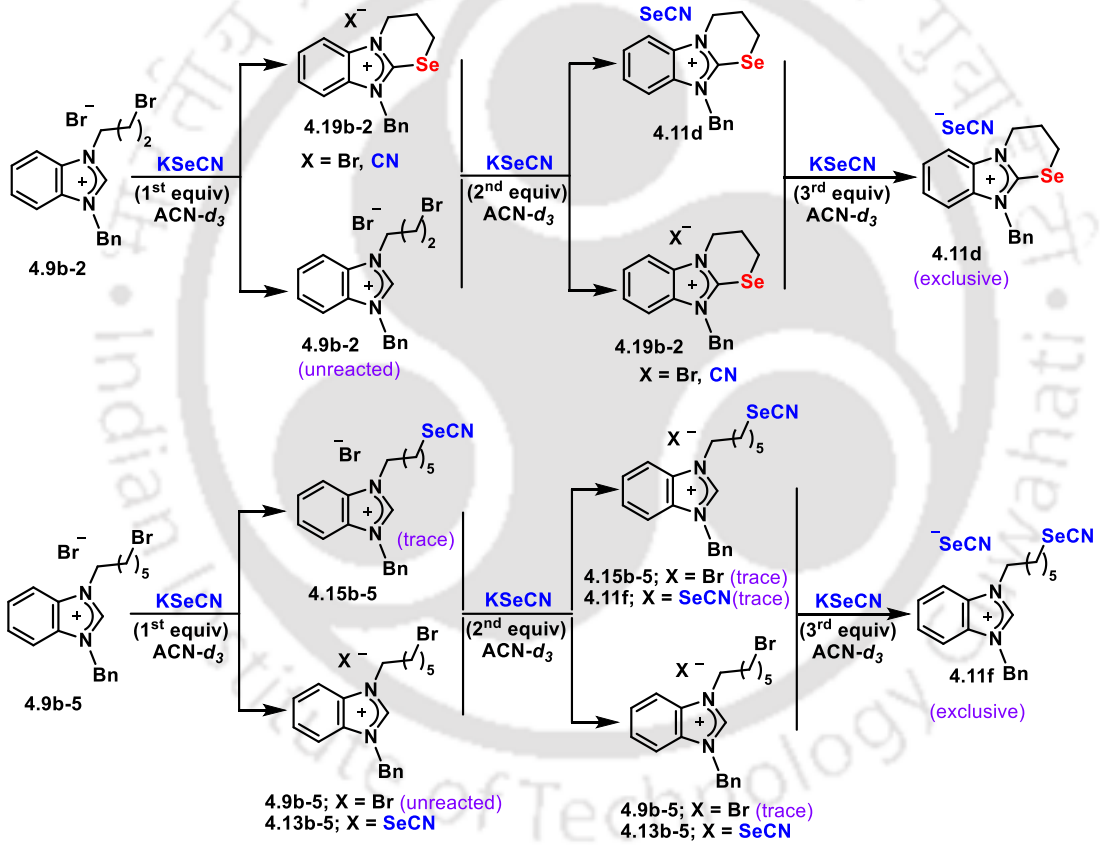

Scheme 4.2. Schematic representation of the product distribution in the reaction of ionic bromides **4.11b-2** and **4.11b-5** with 1.0-3.0 equiv of KSeCN in ACN-d_3.

However, the scenario was different for the reaction of relatively longer chain bromide **4.9b-5** with 1.0-3.0 equiv of KSeCN under identical condition. Unlike **4.9b-2**, the reaction of **4.9b-5** with one equiv of KSeCN led to the formation of compound **4.13b-5** by the exchange of Br^{-} counterion with $SeCN^{-}$ and the precipitation of potassium

bromide (KBr), along with trace amount of substitution product **4.15b-5** with Br^- as counterion and unreacted bromide as observed from ^1H spectroscopy. Although **4.9b-5** and **4.13b-5** has identical chemical shifts in ^1H spectra, the difference was observed from ^{77}Se spectra of the two compounds (Figure 4.3F). The product distribution was not much changed upon the treatment of an additional equiv (two equiv) of KSeCN to **4.9b-5** as evidenced by NMR studies. Interestingly, the intramolecular process was not feasible due to longer alkyl chain length. The acyclic final product **4.11f** was obtained in the presence of three equiv of KSeCN. It should be noted here that, while two equiv of KSeCN was sufficient for the effective formation of selenazinium selenocyanate **4.11d**, three equiv of KSeCN was necessary for the synthesis of benzimidazolium selenocyanate **4.11f** with selenocyanate as a counterion. This could probably be due to the slower reactivity of the relatively distant *N*-$(CH_2)_6$-Br center in the ionic bromide **4.9b-5** than that in the bromide **4.9b-2**. However, for the synthetic generalization of all the products **4.11a-f** and **4.12a-f** in the present study, three equiv of KSeCN was used in the selenocyanation step.

Variation of the equivalence of KSeCN in the final selenocyanation reaction provided us some useful information in elucidating the mechanistic insights for the final product distribution. Considering the evidences from ^1H, ^{13}C and ^{77}Se NMR spectroscopic and ESI-MS spectrometric analyses, the mechanistic pathways for the formation of cyclic selenocyanates (**4.11a-d** and **4.12a-d**) and the acyclic selenocyanates (**4.11e-f** and **4.12e-f**) has been proposed as shown in Scheme 4.2.

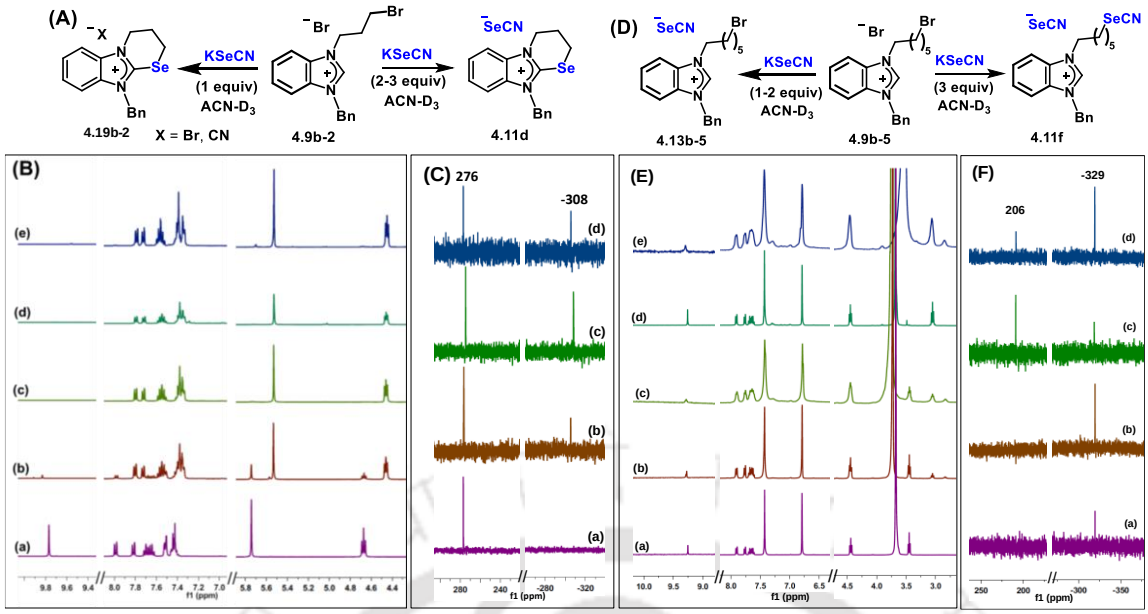

Figure 4.3. (A) Schematic representation of the product distribution in the reaction of ionic bromides **4.9b-2** and **4.9b-5** with 1.0 - 3.0 equivalents of KSeCN in CD_3CN. (B) ^1H NMR spectra of the reaction mixture of **4.9b-2** with 1.0 - 3.0 equivalents of KSeCN in a mixture of solvents CD_3CN: DMSO-d_6: D_2O (7:2:1); (a) pure bromide **4.9b-2**; (b) **4.9b-2** + KSeCN (1 equiv); (c) **4.9b-2** + KSeCN (2 equiv); (d) **4.9b-2** + KSeCN (3 equiv); (e) pure **4.11d**. (C) ^{77}Se NMR of the reaction mixture of **4.9b-2** with 1.0 - 3.0 equivalents of KSeCN in a mixture of solvents CD_3CN: DMSO-d_6: D_2O (7:2:1); (a) **4.9b-2** + KSeCN (1 equiv); (b) **4.9b-2** + KSeCN (2 equiv); (c) **4.9b-2** + KSeCN (3 equiv); (d) pure **4.11d**. (E) ^1H NMR spectra of the reaction mixture of **4.9b-5** with 1.0 - 3.0 equivalents of KSeCN in a mixture of solvents CD_3CN: DMSO-d_6: D_2O (7:2:1); (a) pure bromide **4.9b-5**; (b) **4.9b-5** + KSeCN (1 equiv); (c) **4.9b-5** + KSeCN (2 equiv); (d) **4.9b-5** + KSeCN (3 equiv); (e) pure **4.11f**. (F) ^{77}Se NMR of the reaction mixture of **4.9b-5** with 1.0 - 3.0 equivalents of KSeCN in a mixture of solvents CD_3CN: DMSO-d_6: D_2O (7:2:1); (a) **4.9b-5** + KSeCN (1 equiv); (b) **4.9b-5** + KSeCN (2 equiv); (c) **4.9b-5** + KSeCN (3 equiv); (d) pure **4.11f**.

For the cyclic product formation (n = 1 and 2), the reaction of bromides **4.9a-n**, **4.9b-n**, **4.10a-n** or **4.10b-n** with KSeCN may proceed in stepwise manner. Reaction with one equiv of KSeCN would readily replace the bromide counterion with the precipitate of KBr from the solution leading to the formation of open chain bromides **4.13a-m**, **4.13b-m**, **4.14a-m** or **4.14b-m** with selenocyanate as the counterion. The selenocyanate counterion may undertake intramolecular nucleophilic attack with the formation of the corresponding selenocyanates **4.15a-m**, **4.15b-m**, **4.16a-m**, or **4.16b-m** having bromide as the counterion. Remaining amount of KSeCN of the first equivalent can act as a base to deprotonate the C2-hydrogen of the heterocyclic ring in **4.15a-m**, **4.15b-m**, **4.16a-m**,

or **4.16b-m** with the generation of N-heterocyclic carbene **4.17a-m**, **4.17b-m**, **4.18a-m** and **4.18b-m**, which upon intramolecular cyclization reaction would produce the cyclic compounds **4.19a-m**, **4.19b-m**, **4.20a-m** or **4.20b-m** with X^- counterion (X = CN, Br). Compounds **4.19a-m**, **4.19b-m**, **4.20a-m** or **4.20b-m** were detected along with unreacted starting bromides **4.9a-n**, **4.9b-n**, **4.10a-n** or **4.10b-n** in ^1H and ^{77}Se NMR spectroscopy (Figure 4.3). Subsequent addition of 2nd equivalent of KSeCN was probably consumed to facilitate all the above-mentioned processes with the unreacted bromides and the remaining amount was consumed to replace the X^- counterion (X = CN, Br) with ^-SeCN leading to the formation of final products **4.11a-d**, **4.12a-d** along with **4.19a-m**, **4.19b-m**, **4.20a-m** or **4.20b-m**. Final third equivalent of KSeCN led to the complete conversion of **4.19a-m**, **4.19b-m**, **4.20a-m** or **4.20b-m** to the final cyclic products **4.11a-d** and **4.12a-d** upon the replacement of X^- (Br^- or CN^-) with $SeCN^-$.

On the other hand, the proposed pathways for the formation of acyclic products (n = 5) **4.11e-f** and **4.12e-f** is rather relatively simpler. The treatment of one equiv of KSeCN with the bromides **4.9a-5**, **4.9b-5**, **4.10a-5** or **4.10b-5** leads to the partial exchange of Br^- counterion with $SeCN^-$ with the formation of compounds **4.13a-5**, **4.13b-5**, **4.14a-5** or **4.14b-5** along with some amount of unreacted starting bromide. Trace amount of open-chain selenocyanate (**4.15a-5**, **4.15b-5**, **4.16a-5**, **4.16b-5**) was also formed by the nucleophilic substitution reaction at the remote Br-center of the starting bromide. Subsequent reaction of these intermediates with second equiv of KSeCN only exchanged the counterion from remaining **4.9a-5**, **4.9b-5**, **4.10a-5** or **4.10b-5**. A subsequent reaction of all these intermediates with third equivalent of KSeCN led to the formation of the final products **4.11e-f** and **4.12e-f** as outlined in Scheme 4.2.

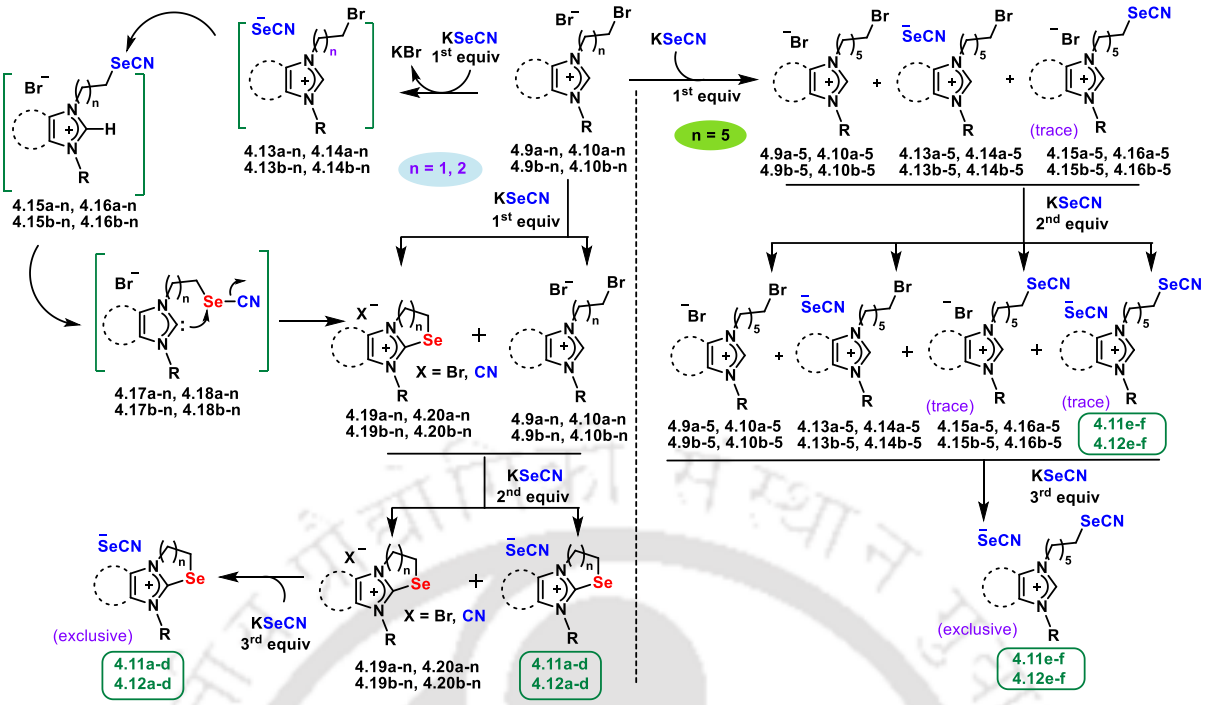

Scheme 4.2. Proposed mechanistic pathways for the formation of cyclic (**4.11a-d** and **4.12a-d**) and acyclic compounds (**4.11e-f** and **4.12e-f**) from the corresponding bromides in the presence of 1-3 equiv of KSeCN.

4.3.2. GPx-like antioxidant activity

Upon the synthesis of different series of organoselenium compounds as shown above, they were evaluated for their antioxidant activities for the reduction of peroxides such as hydrogen peroxide (H_2O_2), cumene hydroperoxide (Cum-OOH) and *tert*-butyl hydroperoxide (^{t}Bu-OOH) using the conventional enzymatic assay. In the assay, reduced glutathione (GSH) was used as the co-substrate and the antioxidant activity of these three sets of ionic organoselenium compounds were compared to that of standard antioxidant organoselenium compound ebselen (**1.14**).[14] As shown in Table 4.1, all the compounds exhibited significant antioxidant activities for the reduction of H_2O_2. Moreover, several compounds exhibited reasonably higher initial rates for the reduction of H_2O_2 than the standard antioxidant compound ebselen (Table 4.1). In general, the antioxidant activities of all the compounds studied herein were found to be much higher for the reduction of H_2O_2 than Cum-OOH and ^{t}Bu-OOH except compound **4.11a** that exhibited highest activity for reducing Cum-OOH. All the compounds exhibited relatively lower rates for the reduction of ^{t}Bu-OOH. This is in line with the observation made for the ebselen analogues and *sec*-amine-based GPx mimics reported earlier.[15] For the reduction of H_2O_2, some structure-activity correlations were observed for both

benzimidazole- and imidazole-based ionic compounds with respect to the *N*-methyl and *N*-benzyl substitutions. In general, the antioxidant activities of *N*-benzyl substituted compounds were found to be higher than the corresponding *N*-methyl analogues in both of benzimidazole- and imidazole-based compounds. Only exceptions were observed for the pairs of **4.11c** *vs* **4.11d** and **4.11e** *vs* **4.11f**. Furthermore, unlike *N*-methyl-substituted compounds, most of the *N*-benzylated analogues exhibited higher activity than ebselen.

Table 4.1. Initial rates for the catalytic reduction of peroxides by GSH in the presence of compounds **4.11a**-**f** and **4.12a**-**f**.

Compound	Initial rates (μM min^{-1})[a]		
	H_2O_2	Cum-OOH	^{t}Bu-OOH
Control	10.8 ± 2.6	6.9 ± 1.5	3.1 ± 1.5
4.11a	51.4 ± 5.5	60.2 ± 8.6	15.5 ± 1.1
4.11b	74.3 ± 2.9	41.0 ± 2.5	20.9 ± 3.7
4.12a	56.4 ± 2.6	38.7 ± 5.1	16.3 ± 1.9
4.12b	71.1 ± 3.2	34.9 ± 7.2	22.4 ± 6.2
4.11c	46.7 ± 9.5	9.8 ± 3.4	4.8 ± 3.3
4.11d	45.0 ± 3.7	6.5 ± 1.8	5.8 ± 1.4
4.12c	49.2 ± 7.3	4.5 ± 0.3	1.0 ± 0.2
4.12d	76.8 ± 6.0	12.4 ± 4.0	1.4 ± 0.5
4.11f	64.7 ± 2.9	6.6 ± 2.3	5.9 ± 3.1
4.12e	39.5 ± 6.2	9.7 ± 0.4	1.1 ± 0.3
4.12f	68.4 ± 3.4	8.1 ± 3.1	1.4 ± 0.5
Ebselen	64.4 ± 4.6	33.2 ± 7.9	4.6 ± 4.8

[a]The experiments were carried out in phosphate buffer (100 mM) of pH 7.5 at room temperature (22 °C). Assay mixture contained selenium compound (100.0 μM), GSH (2.0 mM), NADPH (0.4 mM), EDTA (1.0 mM) glutathione disulfide reductase (1.0 unit/ml) and peroxide (1.6 mM). The rates of control reactions were measured under the identical experimental conditions in the absence of any selenium compound.

As the activities were found to be highest for the reduction of H_2O_2 than other two peroxides in the GSH-GSSG coupled assay (Table 4.1), H_2O_2 was chosen further to understand the antioxidant activities of the synthesized compounds in the presence of an aromatic thiol such as thiophenol (PhSH) as a co-substrate. In this method, the conversion of PhSH to the corresponding disulfide (PhSSPh) in the presence of

organoselenium compounds and H_2O_2 was monitored over time using reverse phase HPLC method. The time required for 50% conversion of PhSH to PhSSPh was defined as $t_{1/2}$ and it was determined by measuring the peak area of PhSSPh formed at different time intervals and that was compared with the standard calibration curve of PhSSPh.[16] Therefore, a lower $t_{1/2}$ value is associated with the higher antioxidant activity. Relative activity (RA) was determined from the ratio of $t_{1/2}$ values of the control reactions and in the presence of different compounds. RA values therefore, directly implies the relative potencies of different antioxidants under the identical condition. Interestingly, as shown in Table 4.2, all the synthesized ionic organoselenium compounds in the present study exhibited significantly higher antioxidant activity than the control reaction. The relative activities of test compounds were in the range of 3.6- to 24.2-fold higher than the control reaction (in the absence of any test compound). Furthermore, unlike in GSH-GSSG assay, all the compounds **4.11a-f** and **4.12a-f** exhibited much higher activity than the standard anti-inflammatory compound ebselen under the identical experimental condition. The imidazole-based selenazolium selenocyanate **4.12a** was found to be most active antioxidant ($t_{1/2}$ = 30.7 min) among all the synthesized compounds screened herein. The activity was reduced significantly for the corresponding six-membered cyclic selenazinium selenocyanate **4.12c** ($t_{1/2}$ = 122.8 min) and a further drop was observed for the acyclic counterpart **4.12e** ($t_{1/2}$ = 205.8 min) as represented in Table 4.2 and Figure 4.4. Moreover, a reasonable structure-activity correlation was observed among three different sub-types of compounds studied herein. For example, both the benzimidazole- and imidazole-based cyclic selenazolium selenocyanates **4.11a-b** and **4.12a-b** exhibited remarkably higher activities for the reduction of H_2O_2. However, the corresponding six-membered cyclic selenazinium selenocyanates **4.11c-d** and **4.12c** were relatively less active except compound **4.12d** that exhibited almost comparable activity to the five-membered analogues although the possible reason for such discrepancy is not very clear. In contrast, all the acyclic selenocyanates **4.11e-f** and **4.12e-f** were found to be much weaker catalysts for the reduction of H_2O_2 in the presence of PhSH as a co-substrate under the identical condition (Table 4.2). This could be due to varied reactivity of cyclic selenazonium/selenazinium compounds and acyclic selenocyanate analogues towards PhSH and H_2O_2 in general. Unlike in GSH-GSSG coupled assay, the structure-activity correlation with respect to the *N*-methyl *vs N*-benzyl substitution has not been observed for the antioxidant activities in PhSH assay.

Table 4.2. Catalytic reduction of hydrogen peroxide by PhSH in the presence of compounds **4.11a-f** and **4.12a-f**.

Compound	$t_{1/2}$ (min)[a]	RA[b]	Compound	$t_{1/2}$ (min)[a]	RA[b]
Control	742.3 ± 70.0	1.0	**4.12c**	122.8 ± 3.1	6.0
4.11a	33.2 ± 1.0	22.3	**4.12d**	41.1 ± 3.5	18.0
4.11b	39.7 ± 5.5	18.7	**4.11f**	133.3 ± 19.3	5.6
4.12a	30.7 ± 3.4	24.2	**4.12e**	205.8 ± 10.8	3.6
4.12b	31.5 ± 4.2	23.6	**4.12f**	143.7 ± 6.3	5.2
4.11c	152.2±11.9	4.9	Ebselen	374.7 ± 22.1	2.0
4.11d	180.4 ± 17.0	4.1			

[a]The reactions were performed in MeOH at 22 °C. Assay mixture contained organoselenium compound (100.0 µM); PhSH (1.0 mM) and H_2O_2 (2.0 mM). The control reaction was carried out under the identical condition but in the absence of any selenium compound. [b]Relative activities (RA) of experimental compounds are calculated with reference to the control activities.

It should be mentioned here that the reactivities of selenium atom in selenazolium rings (**4.11a-b**, **4.12a-b**) selenazinium rings (**4.11c-d**, **4.12c-d**) and acyclic selenocyanates (**4.11e-f**, **4.12e-f**) are different due to the difference in the electron density on selenium atoms. Electron density at the selenium centers of selenacycles (**4.11a-d**, **4.12a-d**) is much higher than the electron density at the selenium center in acyclic selenocyanates (**4.11e-f**, **4.12e-f**). This is primarily due to the direct linkage of selenium atom with the electron withdrawing cyano group (CN) in the later set of the compounds. Therefore, the former series of the compounds are expected to be more susceptible to oxidation than the later set. Additionally, the higher reactivity of the selenazolium selenocyanates than selenazinium selenocyanates could be due to the higher reactivity of selenium center in 5-membered selenacycle than in 6-membered selenacycle. Furthermore, ebselen was found to be much weaker catalyst than all the ionic organoselenium compounds used herein. The lower catalytic activity of ebselen in the presence of aromatic and benzylic thiols is well-studied that involves the occurrence of thiol-exchange reactions in the catalytic cycle.[17]

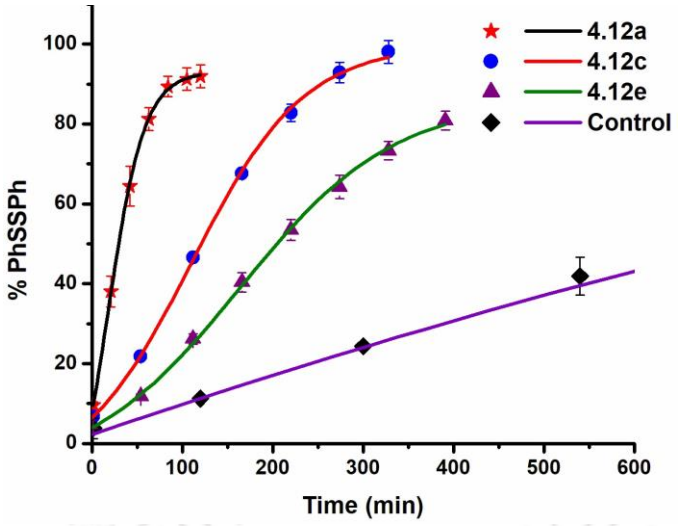

Figure 4.4. Catalytic reduction of H_2O_2 (2.0 mM) by PhSH (1.0 mM) in the absence and presence of organoselenium compounds **4.12a**, **4.12c**, **4.12e** (100.0 μM). The experiments were performed in methanol at room temperature (22 °C). The control reaction was carried out under identical condition in the absence of any selenium compound.

4.3.3. Intracellular H_2O_2 scavenging abilities of organoselenium compounds

With the observation that the synthesized ionic organoselenium compounds exhibit significant catalytic antioxidant activities for the reduction of H_2O_2 in the presence of two different thiols such as GSH and PhSH, we have extended the study further to understand their antioxidant efficacies for scavenging the intracellular level of H_2O_2. Considering GSH as the biologically abundant endogenous thiol present at high concentration, the compound that exhibited highest antioxidant activity in GSH-GSSG assay (**4.12d**) was chosen to study its potency in scavenging the endogenous level of H_2O_2. The murine macrophage RAW 264.7 cell line was chosen as a model to study the activity of the most active compound **4.12d**. The least active organoselenium compound **4.12e** was also evaluated under the identical condition to have a comparative data. Peroxide-responsive fluorescein-based turn-on fluorogenic probe **4.21** having boronate ester group was used as a model probe to understand the scavenging activity of the test compounds in the present study (Figure 4.5). In the control reaction, the cultured cells were incubated with the turn-on probe **4.21** (5.0 μM) for 1 h to understand the fluorescence turn-on process due to the reaction with endogenous H_2O_2 and the formation of the fluorogenic probe **4.22**. The identical experiments were then conducted RAW 264.7 cells pre-treated with the antioxidants **4.12d** and **4.12e** (incubation for 1 h)

followed by the treatment of **4.21**. The final fluorescence intensity of the released fluorophore **4.22** was imaged using fluorescence microscope after an incubation of 1 h. Interestingly, as shown in Figure 4.5, the emission intensity of **4.22** in the presence of the active antioxidant **4.12d** was significantly decreased in a dose-dependent manner as compared to that of the control reaction. Furthermore, the higher antioxidant potential of **4.12d** than **4.12e** was also evident from the relatively lower emission intensity of the cells treated with **4.12d** than **4.12e** at similar concentrations. The reactivity of these antioxidants as well as the boronate probe **4.21** with the endogenous H_2O_2 was validated further by the pre-treatment of cells with an excess amount of a well-known antioxidant *N*-acetyl cysteine (NAC) and subsequent treatment of the probe **4.21**. Almost negligible fluorescence turn-on from this experiment confirms endogenous H_2O_2 as the likely target of the observed fluorescence turn-on process. Furthermore, the above observation further indicates that the turn-on fluorogenic probe was quite stable under cellular environment and there was no background fluorescence from the intact probe. The observation clearly indicates the antioxidant potentials of these ionic organoselenium compounds in scavenging the endogenous level of H_2O_2.

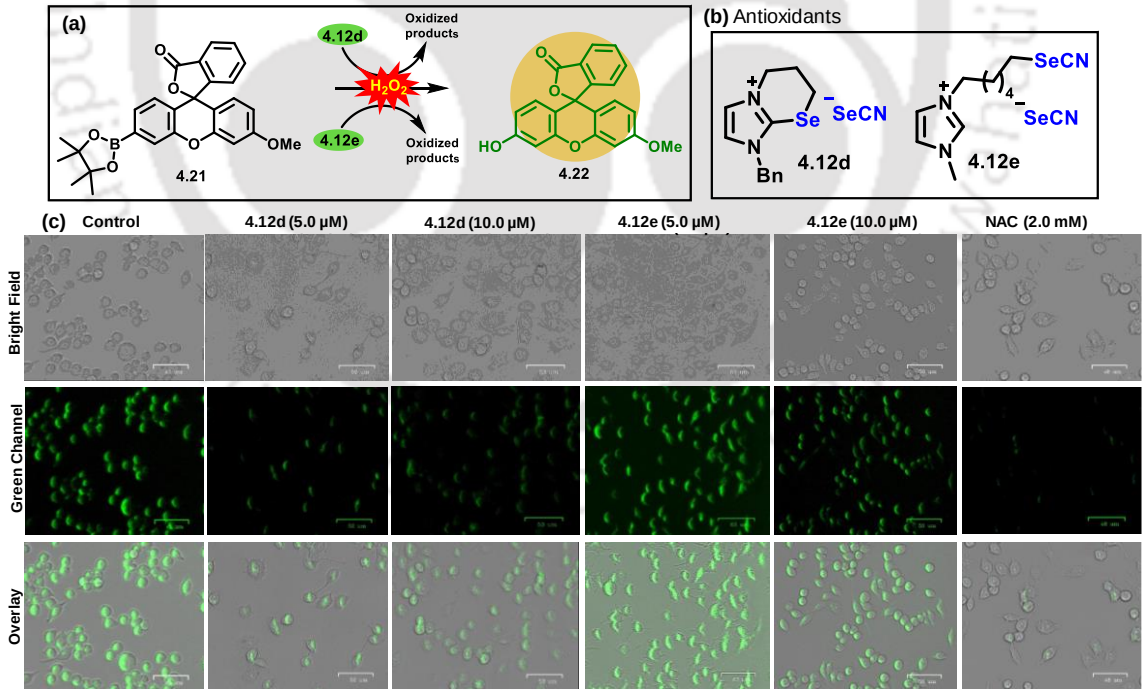

Figure 4.5. (a) Reaction scheme for the H_2O_2-triggered fluorescence turn-on process from the boronate ester containing fluorescein-based probe **4.21** and the inhibition of this process by the antioxidants **4.12d** and **4.12e**. (b) Chemical structures of the antioxidants **4.12d** and **4.12e**. (c) Fluorescence microscopic images (bright field, green

channel and merged) of RAW 264.7 cells (3.0 x 10^5 / 2 ml) pre-incubated with antioxidants **4.12d** and **4.12e** (5.0 μM and 10.0 μM) followed by the incubation with turn-on probe **4.21**. Pre-treatment of cells with standard antioxidant NAC (2.0 μM) was studied to understand the reactivity with endogenous H_2O_2.

4.4. Conclusions

In summary, herein we describe three new classes of ionic organoselenium compounds containing cationic benzimidazolium and imidazolium ring systems with selenocyanate as counterion. A facile cyclization process was observed for *N*,*N*´-disubstituted benzimidazolium and imidazolium bromides having *N*-$(CH_2)_2$-Br and *N*-$(CH_2)_3$-Br in the presence of potassium selenocyanate leading to the formation of the corresponding selenazolium selenocyanates (**4.11a-b**, **4.12a-b**) and selenazinium selenocyanates (**4.11c-d**, **4.12c-d**) having five-membered and six-membered selenacycle ring. In contrast, open chain selenocyanates (**4.11e-f**, **4.12e-f)** with additional selenocyanate counterion was the sole product from the *N*,*N*´-disubstituted benzimidazolium and imidazolium bromides having *N*-$(CH_2)_6$-Br group. Most plausible mechanistic pathways were proposed based on the above observations as well as several control experiments. Interestingly, most of the compounds exhibited significant *in vitro* antioxidant activities to catalytically reduce peroxides in the presence of thiols. However, cyclic selenazolium and selenazinium compounds exhibited significantly better antioxidant activities than the corresponding acyclic analogues in the presence of aromatic thiol assay. Furthermore, the compounds were also evaluated for their potencies in modulating the intracellular level of ROS in a representative macrophage cell lines (RAW 264.7).

4.5. Experimental section:

4.5.1. Materials and Method

Potassium selenocyanate (KSeCN) was purchased from Sigma-Aldrich and was used as supplied without further purification. Solvents (petroleum ether 60 – 80, ethyl acetate) were distilled freshly before using. Due to unpleasant odor of most of the reaction mixture involved, the reactions were carried out in a well-ventilated fume hood. Thin-layer chromatography was carried out on pre-coated silica gel plates (F_{254}), purchased from Merck, and spots were visualized by UV irradiation at λ = 254 nm and/or iodine staining. Column chromatography were performed either with glass column loaded with neutral alumina or with an automated flash chromatography system (CombiFlash

NextGen100, Teledyne^{TM}) using manually packed cartridges. ^{1}H, ^{13}C and ^{77}Se NMR spectra were recorded Bruker (400, 500 or 600 MHz) NMR spectrometers and the chemical shifts are cited with respect to TMS (Me_4Si) as an internal standard (^{1}H and ^{13}C nuclei) and Ph_2Se_2 as external standard (^{77}Se nuclei). Perkin-Elmer Lambda 25 UV-Vis spectrophotometer was used to perform GPx-like activity. Mass spectrometric analysis were performed using Agilent Q-TOF 6520 High Resolution Mass Spectrometer in ESI-positive mode analysis. Melting points were recorded in a Büchi B-540 melting point apparatus and the readings were uncorrected. Fourier Transform Infra-red sprctroscopy (FT-IR) was performed either in a Perkin Elmer Spectrum Two instrument using KBr pellet or in a Perkin Elmer UATR Two instrument, following appropriate background correction.

General Procedure 1 (**GP1**) for synthesis of *N*-substituted imidazole and benzimidazole derivatives (**4.9a-b**, **4.10a-b**):

The compounds were synthesized following the previously reported literature with minor modifications wherever necessary.[18] Briefly, benzimidazole or imidazole and KOH was dissolved in acetonitrile and to it methyl iodide was added dropwise slowly. The solution was stirred at room temperature for appropriate time. Progress of the reaction was monitored by thin layer chromatographic analysis. After completion of the reaction, the solid was filtered and washed with acetonitrile. The filtrate was concentrated *in vacuo*. The residue was extracted with ethyl acetate and washed with water and brine. Combined organic layer was dried over anhyd. Na_2SO_4 and was concentrated *in vacuo* to yield the crude compound. Unless mentioned specifically, the crude product was purified using neutral alumina column chromatography using petroleum ether and ethyl acetate as eluents.

General Procedure 2 (**GP2**) for synthesis of (*N*-substituted, *N'*-bromoalkyl)-benzimidazole or imidazole precursors (**4.9a-n**, **4.9b-n**, **4.10a-n**, **4.10b-n**; n = 1, 2, 5):

The compounds were synthesized according to literature method with minor modifications, whenever applicable.[19] Briefly, to a high excess of 1,n-dibromoalkane (n = 2-6), *N*-substituted benzimidazole or imidazole derivative was added and the solution was heated at 85 ºC for appropriate time without any additional solvent. The progress of the reaction was monitored by thin layer chromatographic analysis. After completion,

the excess of dibromoalkane was evaporated under vacuum to afford the crude compound. The crude product was purified using neutral alumina column chromatography using appropriate mixtures of ethyl acetate and methanol.

General Procedure 3 for synthesis of benzimidazolium- or imidazolium-based cyclic and acyclic compounds (**4.11a-f**, **4.12a-f**):

Title compounds were synthesized using reported literature methods with minor modifications.[20] Precursor bromide was stirred with potassium selenocyanate in dry acetonitrile for appropriate time at room temperature under inert atmosphere. Progress of the reaction was monitored by thin layer chromatographic analysis. After completion, the solution was evaporated to dryness under reduced pressure to afford the crude product. The product was purified using neutral alumina column chromatography using appropriate mixtures of ethyl acetate and methanol as eluents.

Compound 4.9a: Prepared according to **GP1** using benzimidazole **4.9** (2.00 g, 16.94 mmol), KOH (1.42 g, 25.40 mmol), methyl iodide (2.38 g, 16.94 mmol) in acetonitrile (50.0 mL) and reaction time of 3 h. Crude compound was further purified using silica gel (60-120 mesh) column chromatography using 80% ethyl acetate in petroleum ether to afford the pure compound **4.9a** as yellow oil. R_f = 0.3 (40% ethyl acetate in petroleum ether). Yield: 1.80 g (37%). ^{1}H NMR ($CDCl_3$, 400 MHz): δ (ppm) = 7.81 – 7.79 (m, 2H), 7.35 – 7.27 (m, 3H), 3.74 (s, 3H), ^{13}C NMR ($CDCl_3$, 100 MHz): δ (ppm) = 143.7, 143.5, 134.5, 122.9, 122.0, 120.2, 109.4, 30.9.

Compound 4.9a-1: Prepared using **GP2** using 1,2-dibromoethane (7.11 g, 37.87 mmol), *N*-methylbenzimidazole **4.9a** (0.50 g, 3.79 mmol) and reaction time of 12 h. Crude product was further purified by neutral alumina column chromatography using 20% methanol in ethyl acetate to afford the pure compound **4.9a-1** as yellow solid. R_f = 0.3 (20% methanol in ethyl acetate). Yield: 0.25 g (20%). ^{1}H NMR (DMSO-d_6, 400 MHz): δ (ppm) = 9.94 (s, 1H), 8.18 (dd, 1H, J_1 = 6.5 Hz, J_2 = 2.6 Hz), 8.06 (dd, 1H, J_1 = 6.7 Hz, J_2 = 2.7 Hz), 7.76 – 7.71 (m, 2H), 5.01 (t, 2H, J = 5.8 Hz), 4.15 (s, 3H), 4.06 (t, 2H, J = 5.8 Hz). ^{13}C NMR (DMSO-d_6, 150 MHz): δ (ppm) = 143.6, 132.1, 131.2, 127.2, 127.1, 114.2, 48.3, 33.9, 31.5.

Compound 4.9a-2: Prepared using **GP2** using 1,3-dibromopropane (7.38 g, 36.00 mmol), *N*-methylbenzimidazole **4.9a** (0.40 g, 3.00 mmol) and reaction time

of 12 h. Crude product was further purified by neutral alumina column chromatography using 20% methanol in ethyl acetate to afford the pure compound **4.9a-2** as white solid. R_f = 0.6 (20% methanol in ethyl acetate using alumina TLC plate). Yield: 0.25 g (24%). ^{1}H NMR ($CDCl_3$, 600 MHz): δ (ppm) = 11.14 (s, 1H), 7.87 – 7.86 (m, 1H), 7.77 – 7.75 (m, 1H), 7.69 (dt, J_1 = 3.7 Hz, J_2 = 3.1 Hz, 2H), 4.88 (t, 2H, J = 7.2 Hz), 4.31 (s, 3H), 3.59 (t, 2H, J = 6.0 Hz), 2.72 (dt, 2H, J_1 = 12.7 Hz, J_2 = 6.5 Hz). ^{13}C NMR ($CDCl_3$, 150 MHz): δ (ppm) = 143.4, 131.9, 131.3, 127.4, 127.3, 113.0, 112.9, 112.9, 45.7, 34.0, 32.3, 29.9.

Compound 4.9a-5: Prepared using **GP2** using 1,6-dibromohexane (9.20 g, 37.87 mmol), *N*-methylbenzimidazole **4.9a** (0.50 g, 3.79 mmol) and reaction time of 12 h. Crude product was further purified by neutral alumina column chromatography using 20% methanol in ethyl acetate to afford the pure compound **4.9a-5** as colorless sticky solid. R_f = 0.2 (20% methanol in ethyl acetate). Yield: 0.40 g (28%), ^{1}H NMR ($CDCl_3$, 500 MHz): δ (ppm) = 11.49 (d, 1H, J = 2.9 Hz), 7.70 (dq, 4H, J_1 = 13.3 Hz, J_2 = 4.5 Hz, 4H), 4.63 (q, 2H, J_1 = 6.3, J_2 = 5.4 Hz), 4.31 (s, 3H), 3.41 (q, 2H, J_1 = 5.8 Hz, J_2 = 5.4 Hz), 2.11 (t, 2H, J = 8.0 Hz), 1.87 (q, 2H, J = 7.6 Hz), 1.55 – 1.49 (m, 2H), 1.59 - 1.46 (m, 5H). ^{13}C NMR ($CDCl_3$, 125 MHz): δ (ppm) = 143.4, 132.1, 131.2, 127.3, 112.9, 112.8, 47.5, 33.8, 33.7, 32.3, 29.3, 27.5, 25.7.

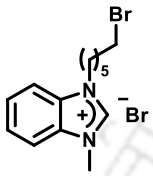

Compound 4.9b: Prepared using **GP1** using benzimidazole **4.9** (5.00 g, 4.23 mmol), KOH (3.56 g, 6.35 mmol), benzyl bromide (7.24 g, 4.23 mmol) and acetonitrile (100 mL) and reaction time of 2 h. Crude product was further purified by silica gel (60 – 120 mesh) column chromatography using 50% ethyl acetate in petroleum ether as eluting solvent to afford the purified compound **4.9b** as a white solid. R_f = 0.5 (80% ethyl acetate in petroleum ether). Yield: 2.00 g (22%). ^{1}H NMR ($CDCl_3$, 400 MHz): δ (ppm) = 7.95 (s, 1H), 7.83 (d, 1H, J = 6.8 Hz), 7.35 – 7.18 (m, 8H), 5.37 (s, 2H). ^{13}C NMR ($CDCl_3$, 150 MHz): δ (ppm) = 143.9, 143.2, 135.4, 133.9, 129.0, 128.3, 127.1, 123.1, 122.3, 120.4, 110.0, 48.8.

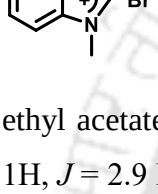

Compound 4.9b-1: Prepared using **GP2** using 1,2-dibromoethane (3.25 g, 17.33 mmol) and *N*-benzylbenzimidazole **4.9b** (0.16 g, 0.62 mmol) and reaction time of 24 h. Crude product was further purified by neutral alumina column chromatography using methanol in dichloromethane to afford the pure

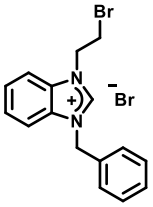

compound **4.9b-1** as off-white solid. R_f = 0.2 (10% methanol in ethyl acetate), Yield: 0.17 g (55%). ^{1}H NMR (DMSO-d_6, 400 MHz): δ (ppm) = 10.10 (d, 1H, J = 9.9 Hz), 8.19 (d, 2H, J = 7.6 Hz), 8.01 (d, 2H, J = 8.0 Hz), 7.73 – 7.65 (m, 2H), 7.51 (d, 2H, J = 7.0 Hz), 7.40 (dt, 3H, J_1 = 19.1 Hz, J_2 = 7.0 Hz), 5.85 (s, 2H), 5.03 (t, 2H, J = 5.5 Hz), 4.09 (t, 2H, J = 5.6 Hz). ^{13}C NMR (DMSO-d_6, 150 MHz): δ (ppm) = 143.4, 134.4, 131.5, 131.1, 129.5, 129.2, 128.6, 127.4, 114.6, 114.5, 50.4, 48.6, 31.7.

Compound 4.9b-2: Prepared using **GP2** using 1,3-dibromopropane (4.87 g, 24.00 mmol) and *N*-benzylbenzimidazole **4.9b** (0.50 g, 2.40 mmol) and reaction time of 12 h. Crude product was further purified by neutral alumina column chromatography using 5% methanol in dichloromethane to afford the pure compound **4.9b-2** as white solid. R_f = 0.2 (10% methanol in ethyl acetate). Yield: 0.50 g (52%). ^{1}H NMR (DMSO-d_6, 400 MHz): δ (ppm) = 10.04 (s, 1H), 8.13 (d, 1H, J = 7.9 Hz), 7.96 (d, 1H, J = 7.9 Hz), 7.71 – 7.64 (m, 2H), 7.55 (d, 2H, J = 7.0 Hz), 7.44 – 7.38 (m, 3H), 5.79 (s, 2H), 4.66 (t, 2H, J = 6.9 Hz), 3.66 (t, 2H, J = 6.5 Hz), ^{13}C NMR (DMSO-d_6, 100 MHz): δ (ppm) = 143.3, 134.4, 131.8, 131.4, 129.4, 129.2, 128.8, 127.2, 114.4, 114.2, 50.4, 46.0, 31.8, 31.3.

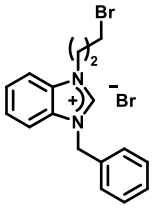

Compound 4.9b-5: Prepared using **GP2** using 1,6-dibromohexane (2.81 g, 11.50 mmol) and *N*-benzylbenzimidazole **4.9b** (0.20 g, 0.96 mmol) and reaction time of 12 h. Crude product was further purified by neutral alumina column chromatography using 15% methanol in ethyl acetate to afford the pure compound **4.9b-5** as floppy white solid. R_f = 0.4 (10% methanol in ethyl acetate). Yield: 0.18 g (42%). ^{1}H NMR (DMSO-d_6, 600 MHz): δ (ppm) = 9.95 (s, 1H), 8.12 (d, 1H, J = 8.0 Hz), 7.97 (d, 1H, J = 7.9 Hz), 7.67 (ddd, 2H, J_1 = 15.5 Hz, J_2 = 14.5 Hz, J_3 = 7.0 Hz), 7.51 (d, 2H, J = 7.3 Hz), 7.40 (dt, 3H, J_1 = 24.8 Hz, J_2 = 7.2 Hz), 5.77 (s, 2H), 4.52 (t, 2H, J = 7.3 Hz), 3.54 (t, 2H, J = 6.7 Hz), 1.94 (dt, 2H, J_1 = 14.9 Hz, J_2 = 7.5 Hz), 1.84 – 1.78 (m, 2H), 1.45 (dt, 2H, J_1 = 14.6 Hz, J_2 = 7.3 Hz), 1.36 (dt, 2H, J_1 = 14.7 Hz, J_2 = 7.3 Hz). ^{13}C NMR ($CDCl_3$, 150 MHz): δ (ppm) = 142.9, 132.7, 131.4, 131.2, 129.4, 129.3, 128.4, 127.3, 127.2, 113.9, 113.0, 51.4, 47.6, 33.8, 32.3, 29.2, 27.4, 25.7.

Compound 4.10a-1: Prepared using **GP2** us ing 1,2-dibromoethane (4.01 g, 21.30 mmol), *N*-methylimidazole **4.10a** (0.50 g, 6.09 mmol), and acetone (5 mL) and reaction time of 12 h. Crude product was further purified by neutral alumina

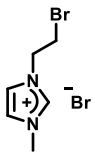

column chromatography using 30% methanol in ethyl acetate to afford the pure compound **4.10a-1** as yellow oil. R_f = 0.1 (30% methanol in ethyl acetate). Yield: 0.30 g (18%). ^{1}H NMR (DMSO-d_6, 400 MHz): δ (ppm) = 9.33 (s, 1H), 7.90 (br, 1H), 7.80 (br, 1H), 4.65 (t, 2H, J = 5.8 Hz), 3.97 (t, 2H, J = 5.8 Hz), 3.91 (s, 3H). ^{13}C NMR (DMSO-d_6, 100 MHz): δ (ppm) = 137.5, 124.2, 122.8, 50.5, 36.4, 32.1.

Compound 4.10a-2: Prepared using **GP2** using 1,3-dibromopropane (12.30 g, 60.9 mmol) *N*-methylimidazole **4.10a** (0.50 g, 6.09 mmol) in acetone (20 mL) and reaction time of 12 h. Crude product was further purified by neutral alumina column chromatography using 20% methanol in ethyl acetate to afford the pure compound **4.10a-2** as reddish yellow oil. R_f = 0.1 (10% methanol in ethyl acetate). Yield: 0.40 g (23%). ^{1}H NMR (DMSO-d_6, 400 MHz): δ (ppm) = 9.18 (s, 1H), 7.80 (s, 1H), 7.72 (s, 1H), 4.30 (t, 2H, J = 6.9 Hz), 3.87 (br, 3H), 2.35 (p, 2H, J = 6.8 Hz). ^{13}C NMR (DMSO-d_6, 100 MHz): δ (ppm) = 137.2, 124.2, 122.7, 47.9, 36.3, 32.6, 30.9.

Compound 4.10a-5: Prepared using **GP2** using 1,6-dibromohexane (20.8 g, 85.4 mmol) *N*-methylimidazole **4.10a** (1.0 g, 12.2 mmol) in acetone (12 mL) and reaction time of 7 h. Crude product was further purified by neutral alumina column chromatography using 20% methanol in ethyl acetate to afford the pure compound **4.10a-5** as yellow oil. R_f = 0.1 (20% methanol in ethyl acetate). Yield: 0.93 g (23%). ^{1}H NMR ($CDCl_3$, 600 MHz): δ (ppm) = 10.48 (s), 7.34 (s, 1H), 7.30 (s, 1H), 4.36 (t, 2H, J = 7.4 Hz), 4.11 (s, 3H), 3.41 (t, 2H, J = 6.6 Hz), 1.95 (dt, 2H, J_1 = 15.2 Hz, J_2 = 7.6 Hz), 1.88 – 1.84 (m, 2H), 1.50 (dt, 2H, J_1 = 15.1 Hz, J_2 = 7.5 Hz), 1.39 (dt, 2H, J_1 = 15.9 Hz, J_2 = 7.7 Hz). ^{13}C NMR ($CDCl_3$, 150 MHz): δ (ppm) = 138.0, 123.1, 121.6, 50.0, 36.8, 33.8, 32.2, 30.1, 27.4, 25.3.

Compound 4.10b: Prepared using **GP1** using imidazole **4.10** (2.00 g, 29.40 mmol), KOH (2.50 g, 44.10 mmol) and benzyl bromide (5.00 g, 29.40 mmol) in acetonitrile (50 mL) and reaction time of 4 h. The crude product was further purified by silica gel flash chromatography using 100% ethyl acetate as eluting solvent to afford the purified compound **4.10b** as a yellow oil. R_f = 0.3 (30% ethyl acetate in petroleum ether). Yield: 2.60 g (55%). ^{1}H NMR ($CDCl_3$, 400 MHz): δ (ppm) = 7.53 (s, 1H), 7.32 (m, 3H), 7.14 (d, 2H, J = 8.0 Hz), 7.07 (s, 1H), 6.89 (s, 1H), 5.09 (s, 2H). ^{13}C NMR ($CDCl_3$, 100 MHz): δ (ppm) = 137.4, 136.2, 129.7, 129.0, 128.3, 127.3, 119.3, 50.8.

Compound 4.10b-1: Prepared using **GP2** using 1,2-dibromoethane (5.80 g, 31.60 mmol) and *N*-benzylimidazole **4.10b** (0.50 g, 3.16 mmol) and reaction time of 12 h. Crude product was further purified by neutral alumina column chromatography using 25% methanol in ethyl acetate to afford the pure compound **4.10b-1** as pale yellow oil. R_f = 0.3 (10% methanol in ethyl acetate). Yield: 0.20 g (18%). ^{1}H NMR (DMSO-d_6, 600 MHz): δ (ppm) = 9.44 (s, 1H), 7.90 (d, 2H, J = 1.4 Hz), 7.44 – 7.40 (m, 5H), 5.50 (s, 2H), 4.65 (t, 2H, J = 5.8 Hz), 3.98 (t, 2H, J = 5.8 Hz). ^{13}C NMR (DMSO-d_6, 150 MHz): δ (ppm) = 136.2, 133.9, 129.6, 129.5, 128.5, 122.8, 122.7, 52.9, 50.7, 30.9.

Compound 4.10b-2: Prepared according to **GP2** using 1,3-dibromopropane (7.60 g, 37.92 mmol), *N*-benzylimidazole **4.10b** (0.50 g, 3.16 mmol) and reaction time of 12 h. Crude product was further purified by neutral alumina column chromatography using 15% methanol in ethyl acetate to afford the pure compound **4.10b-2** as yellow oil. R_f = 0.1 (10% methanol in ethyl acetate). Yield: 0.22 g (18%). ^{1}H NMR (DMSO-d_6, 400 MHz): δ (ppm) = 9.38 (s, 1H), 7.85 - 7.84 (m, 2H), 7.44 – 7.40 (m, 5H), 5.44 (s, 2H), 4.32 (t, 2H, J = 7.0 Hz), 3.54 (t, 2H, J = 6.5 Hz), 2.39 (p, 2H, J = 6.7 Hz). ^{13}C NMR (DMSO-d_6, 150 MHz): δ (ppm) = 137.0, 135.2, 129.5, 129.2, 128.8, 123.4, 123.1, 52.4, 48.2, 32.4, 31.1.

Compound 4.10b-5: Prepared according to **GP2** using 1,6-dibromohexane (5.39 g, 22.10 mmol), *N*-benzylimidazole **4.10b** (0.50 g, 3.20 mmol) in acetone (5 mL) and reaction time of 7 h. Crude product was further purified by neutral alumina column chromatography using 30% methanol in ethyl acetate to afford the pure compound **4.10b-5** as yellow oil. R_f = 0.3 (5% methanol in ethyl acetate). Yield: 0.69 g (54%). ^{1}H NMR (DMSO-d_6, 400 MHz): δ (ppm) = 9.40 (s, 1H), 7.85 - 7.84 (m, 2H), 7.44 – 7.39 (m, 5H), 5.45 (s, 2H), 4.19 (t, 2H, J = 7.2 Hz), 3.51 (t, 2H, J = 5.0 Hz), 1.80 (m, 4H), 1.40 (dt, 2H, J_1 = 14.8 Hz, J_2 = 7.3 Hz), 1.24 (m, 2H). ^{13}C NMR ($CDCl_3$, 150 MHz): δ (ppm) = 136.6, 133.2, 129.4, 129.3, 129.0, 122.4, 122.1, 53.2, 49.9, 33.9, 32.2, 30.0, 27.3, 25.3.

Compound 4.11a: Prepared according to **GP3** using bromide **4.9a-1** (0.18 g, 0.55 mmol) and potassium selenocyanate (0.24 g, 1.66 mmol) in dry acetonitrile (6 mL) and reaction time of 30 h. Crude product was further purified by flash chromatography using neutral alumina and

methanol in ethyl acetate as eluent to afford the pure compound **4.11a** as yellow solid. R_f = 0.3 (20% methanol in ethyl acetate). Yield: 0.10 g (47%), M.P. = 128–130 °C. ^{1}H NMR (DMSO-d_6, 600 MHz): δ (ppm) = 7.87 – 7.85 (m, 1H), 7.83 – 7.81 (m, 1H), 7.56 – 7.54 (m, 2H), 4.73 (t, 2H, J = 7.5 Hz), 4.25 (t, 2H, J = 7.4 Hz), 3.97 (s, 3H). ^{13}C NMR (DMSO-d_6, 150 MHz): δ (ppm) = 158.3, 137.0, 131.5, 126.0, 125.4, 113.0, 112.9, 48.2, 34.6, 33.6. ^{77}Se NMR (DMSO-d_6, 114 MHz): δ (ppm) = 302, -278. ESI-MS *m/z* calcd for $C_{10}H_{11}N_2Se^+$ [M^+]: 239.0082; obs: 239.0082. FT-IR ($\bar{\nu}$ cm^{-1}): 3390 (w), 2059 (s), 1568 (m), 1414 (m), 1025 (m), 752 (s).

Compound 4.11b: Prepared according to **GP3** using bromide **4.9b-1** (0.10 g, 0.25 mmol) and potassium selenocyanate (0.11 g, 0.76 mmol) in dry acetonitrile (4 mL) and reaction time of 24 h. Crude product was further purified by neutral alumina column chromatography using 5% methanol in dichloromethane to afford the pure compound **4.11b** as grey solid powder. R_f = 0.5 (5% methanol in dichloromethane). Yield: 0.06 g (67%). M.P. = 123–125 °C. ^{1}H NMR (methanol-d_4, 400 MHz): δ (ppm) = 7.83 (d, 1H, J = 7.3 Hz), 7.74 (d, 1H, J = 7.2 Hz), 7.60 – 7.44 (m, 7H), 5.59 (s, 2H), 4.74 (t, 2H, J = 7.6 Hz), 4.22 (t, 2H, J = 7.6 Hz). ^{13}C NMR (DMSO-d_6, 150 MHz): δ (ppm) = 136.6, 132.1, 131.6, 129.3, 129.1, 129.0, 125.9, 125.4, 118.3, 112.2, 112.1, 51.1, 31.7. ^{77}Se NMR (DMSO-d_6, 76 MHz): δ (ppm) = 317, -274; ESI-MS *m/z* calcd for $C_{16}H_{15}N_2Se^+$ [M^+]: 315.0395; obs: 315.0737. FT-IR ($\bar{\nu}$, cm^{-1}): 3022 (w), 2069 (s), 1515 (m), 1453 (s), 1026 (s), 754 (s).

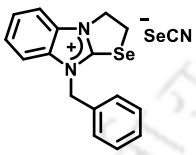

Compound 4.11c: Prepared according to **GP3** using bromide **4.9a-2** (0.15 g, 0.59 mmol) and potassium selenocyanate (0.25 g, 1.77 mmol) in dry acetonitrile (6 mL) and reaction time of 24 h. Crude product was further purified by neutral alumina column chromatography using 30% methanol in ethyl acetate to afford the pure compound **4.11c** as yellow solid. Yield: 0.12 g (70%), R_f = 0.2 (30% methanol in ethyl acetate). M.P. = 124–126 °C. ^{1}H NMR (DMSO-d_6, 600 MHz): δ (ppm) = 7.93 (dd, 1H, J_1 = 6.7 Hz, J_2 = 1.9 Hz), 7.89 (dd, 1H, J_1 = 6.7 Hz, J_2 = 2.0 Hz), 7.59 – 7.57 (m, 2H), 4.47 (t, 2H, J = 5.4 Hz), 3.57 (t, 2H, J = 5.6 Hz), 2.55 (dt, 2H, J_1 = 11.2 Hz, J_2 = 5.5 Hz). ^{13}C NMR (DMSO-d_6, 150 MHz): δ (ppm) = 148.0, 133.6, 132.8, 126.0, 125.4, 112.2, 112.0, 44.8, 32.5, 23.6, 23.1. ^{77}Se NMR (DMSO-d_6, 114 MHz): 266, -278. ESI-MS *m/z* calcd for $C_{11}H_{13}N_2Se^+$ [M^+]: 253.0238; obs: 253.0238. FT-IR ($\bar{\nu}$, cm^{-1}): 2057 (m), 1400 (m), 1262 (w), 1006 (m), 757 (s).

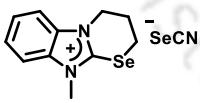

Compound 4.11d: Prepared according to **GP3** using bromide **4.9b-2** (0.20 g, 0.49 mmol) and potassium selenocyanate (0.21 g, 1.46 mmol) in dry acetonitrile (6 mL) and reaction time of 12 h. Crude product was further purified by neutral alumina column chromatography using methanol in dichloromethane to afford the pure compound **4.11d** as solid powder. R_f = 0.4 (10% methanol in dichloromethane). Yield: 0.11 g (52%). M.P. = 164–166 °C. ^{1}H NMR (DMSO-d_6, 600 MHz): δ (ppm) = 7.95 – 7.92 (m, 2H), 7.58 – 7.56 (m, 2H), 7.40 - 7.35 (m, 5Hz), 5.66 (s, 2H), 4.49 (t, 2H, *J* = 6.0 Hz), 3.54 (t, 2H, *J* = 6.0 Hz), 2.56 (br, 3H). ^{13}C NMR (DMSO-d_6, 100 MHz): δ (ppm) = 148.4, 134.2, 134.0, 132.4, 129.4, 129.0, 128.1, 126.3, 125.7, 116.7, 112.4, 49.2, 49.6, 23.9, 22.9; ^{77}Se NMR (DMSO-d_6, 76 MHz): δ (ppm) = 277, -276; ESI-MS *m/z* calcd for $C_{17}H_{17}N_2Se^+$ [M^+]: 329.0551; obs: 329.0668; FT-IR ($\bar{\nu}$, cm^{-1}): 2921 (w), 2065 (s), 1467 (s), 1422 (s), 1006 (m), 756 (s).

Compound 4.11e: Prepared according to **GP3** using bromide **4.9a-5** (0.20 g, 0.53 mmol) and potassium selenocyanate (0.23 g, 1.60 mmol) in dry acetonitrile (6 mL) and reaction time of 12 h. Crude product was further purified by neutral alumina column chromatography using 20% methanol in ethyl acetate to afford the pure compound **4.11e** as yellow oil. ^{1}H NMR ($CDCl_3$, 500 MHz): δ (ppm) = 10.17 (s, 1H), 7.80 – 7.66 (m, 5H), 4.66 (t, 2H, *J* = 7.5 Hz), 4.32 (s, 3H), 2.94 (t, 2H, *J* = 7.3 Hz), 2.17 – 2.07 (m, 3H), 1.85 – 1.68 (m, 4H), 1.63 – 1.50 (m, 4H); ^{77}Se NMR ($CDCl_3$, 95 MHz): δ (ppm) = 209, -299; ESI-MS *m/z* calcd for $C_{17}H_{17}N_2Se^+$ [M^+]: 322.0817; obs: 322.0817; FT-IR ($\bar{\nu}$, cm^{-1}): 3418 (w), 2932 (m), 2147 (w), 2060 (s), 1569 (s), 1458 (m), 1351 (w), 1209 (w), 1094 (w), 1012 (w), 749 (s).

Compound 4.11f: Prepared according to **GP3** using bromide **4.9b-5** (0.13 g, 0.30 mmol) and potassium selenocyanate (0.13 g, 0.90 mmol) in dry acetonitrile (4 mL) and reaction time of 12 h. Crude product was further purified by neutral alumina column chromatography using 100% ethyl acetate to afford the pure compound **4.11f** as white solid. R_f = 0.5 (100% ethyl acetate). Yield: 0.15 g, M.P. = 105–107 °C. ^{1}H NMR (DMSO-d_6, 600 MHz): δ (ppm) = 10.01 (s, 1H), 8.18 (d, 2H, *J* = 6.0 Hz), 8.03 (d, 2H, *J* = 6.0 Hz), 7.75 – 7.72 (m, 2H), 7.58 (br, 2H), 7.48 – 7.44 (m, 3H), 5.83 (s, 2H), 4.58 (br, 2H), 3.41 (br, 2H), 3.13 (br, 2H), 2.01 (br, 2H), 1.87 (br, 2H), 1.52 (br, 2H), 1.45 (br, 2H). ^{13}C NMR (DMSO-d_6, 150 MHz): δ (ppm) = 142.9, 134.5, 131.8, 131.3, 129.5, 129.2, 128.7, 127.2, 127.1, 114.4, 114.3, 105.2, 50.4, 47.2, 31.1, 30.2, 28.7, 28.3, 25.6. ^{77}Se NMR

(DMSO-d_6, 76 MHz): δ (ppm) = 215, -276. ESI-MS *m/z* calcd for $C_{21}H_{24}N_3Se^+$ [M^+]: 398.1130; obs: 398.1175. FT-IR ($\bar{\nu}$, cm^{-1}): 2936 (w), 2151 (w), 2042 (s), 1694 (m), 1556 (s), 1188 (m), 1013 (w), 750 (s)

Compound 4.12a: Prepared according to **GP3** using bromide **4.10a-1** (0.20 g, 0.74 mmol) and potassium selenocyanate (0.32 g, 2.22 mmol) in dry acetonitrile (6 mL) and reaction time of 48 h. Crude product was further purified by flash chromatography using neutral alumina and 20% methanol in ethyl acetate to afford the pure compound **4.12a** as reddish yellow solid powder. R_f = 0.5 (20% methanol in ethyl acetate using alumina TLC plate). Yield: 0.16 g (73%). M.P. = 96–98 °C. ^{1}H NMR (DMSO-d_6, 600 MHz): δ (ppm) = 7.73 (s, 1H), 7.60 (s, 1H), 4.48 (t, 2H, *J* = 7.4 Hz), 4.11 (t, 2H, *J* = 7.4 Hz), 3.74 (s, 3H). ^{13}C NMR (DMSO-d_6, 150 MHz): δ (ppm) = 146.6, 127.8, 121.5, 116.7, 50.3, 37.3, 33.6. ^{77}Se NMR (DMSO-d_6, 114 MHz): δ (ppm) = 299, -278. ESI-MS *m/z* calcd for $C_6H_9N_2Se^+$ [M^+]:188.9925; obs: 188.9925. FT-IR ($\bar{\nu}$, cm^{-1}): 3392 (m), 2056 (s), 1559 (m), 1412 (w), 1215 (m), 1172 (m), 1044 (w), 757 (s).

Compound 4.12b: Prepared according to **GP3** using bromide **4.10b-1** (0.20 g, 0.58 mmol) and potassium selenocyanate (0.25 g, 1.73 mmol) in dry acetonitrile (6 mL) and reaction time of 12 h. Crude product was further purified by flash chromatography using neutral alumina and 20% methanol in ethyl acetate to afford the pure compound **4.12b** as yellow liquid. R_f = 0.6 (100% ethyl acetate in alumina TLC plate). Yield: 0.18 g (70%). ^{1}H NMR (DMSO-d_6, 600 MHz): δ (ppm) = 7.78 (d, 2H, *J* = 2.1 Hz), 7.45 – 7.40 (m, 6H), 5.33 (s, 2H), 4.45 (t, 2H, *J* = 7.5 Hz), 4.04 (t, 2H, *J* = 7.5 Hz); ^{13}C NMR (DMSO-d_6, 150 MHz): δ (ppm) = 146.1, 134.1, 129.5, 129.5, 129.3, 127.1, 121.8, 53.4, 49.8, 33.3; ^{77}Se NMR (DMSO-d_6, 114 MHz): δ (ppm) = 307, -278. ESI-MS *m/z* calcd for $C_{12}H_{13}N_2Se^+$ [M^+]: 265.0238; obs: 265.0242. FT-IR ($\bar{\nu}$, cm^{-1}): 3400 (m), 2059 (s), 1557 (m), 1514 (m), 1439 (m), 1233 (m), 1171 (m), 730 (s), 702 (s).

Compound 4.12c: Prepared according to **GP3** using bromide **4.10a-2** (0.20 g, 0.70 mmol) and potassium selenocyanate (0.30 g, 2.11 mmol) in dry acetonitrile (6 mL) and reaction time of 48 h. Crude product was further purified by flash chromatography using neutral alumina and 20% methanol in ethyl acetate to afford the pure compound **4.12c** yellow oil. R_f = 0.1 (10%

methanol in ethyl acetate). Yield: 0.06 g (27%), ^{1}H NMR (DMSO-d_6, 600 MHz): δ (ppm) = 7.75 (dd, 2H, J_1 = 9.1 Hz, J_2 = 2.0 Hz), 4.22 (t, 2H, J = 6.0 Hz), 3.65 (s, 3H), 3.46 – 3.42 (m, 2H), 2.37 (dt, 2H, J_1 = 11.3 Hz, J_2 = 5.6 Hz). ^{13}C NMR (DMSO-d_6, 150 MHz): δ (ppm) = 136.2, 124.6, 123.8, 116.8, 47.8, 35.2, 23.5, 22.6. ^{77}Se NMR (DMSO-d_6, 95 MHz): δ (ppm) = 262, -274. ESI-MS *m/z* calcd for $C_7H_{11}N_2Se^+$ [M^+]: 203.0082; obs: 203.0105. FT-IR ($\bar{\nu}$, cm^{-1}): 3430 (w), 2061 (s), 1566 (m), 1508 (m), 1319 (w), 1213 (m), 1168 (m), 1094 (w), 745 (m).

Compound 4.12d: Prepared according to **GP3** using bromide **4.10b-2** (0.15 g, 0.40 mmol) and potassium selenocyanate (0.17 g, 1.20 mmol) in dry acetonitrile (5 mL) and reaction time of 12 h. Crude product was further purified by flash chromatography using neutral alumina and 30% methanol in ethyl acetate to afford the pure compound **4.12d** as yellow liquid. R_f = 0.2 (15% methanol in ethyl acetate). Yield: 0.08 g (50%). ^{1}H NMR ($CDCl_3$, 600 MHz): δ (ppm) = 7.68 (d, 1H, J = 2.1 Hz), 7.48 (d, 1H, J = 2.1 Hz), 7.40 – 7.36 (m, 3H), 7.33 – 7.31 (m, 2H), 5.18 (s, 2H), 4.46 (t, 2H, J = 5.6 Hz), 3.56 (t, 2H, J = 5.8 Hz), 2.60 (dt, 2H, J_1 = 11.4 Hz, J_2 = 5.6 Hz). ^{13}C NMR ($CDCl_3$, 150 MHz): δ (ppm) = 135.4, 132.1, 129.5, 129.5, 128.7, 125.1, 122.7, 52.9, 48.3, 23.5, 22.4; ^{77}Se NMR ($CDCl_3$, 95 MHz): δ (ppm) = 274, -298; ESI-MS *m/z* calcd for $C_{13}H_{15}N_2Se^+$ [M^+]: 279.0400; obs: 279.0425. FT-IR ($\bar{\nu}$, cm^{-1}): 3418 (w), 2059 (s), 1567 (m), 1498 (m), 1433 (m), 1356 (w), 1275 (w), 1234 (w), 1178 (w), 726 (s).

Compound 4.12e: Prepared according to **GP3** using bromide **4.10a-5** (0.30 g, 0.99 mmol) and potassium selenocyanate (0.40 g, 2.76 mmol) in dry acetonitrile (10 mL) and reaction time of 12 h. Crude product was further purified by neutral alumina column chromatography using 15% methanol in ethyl acetate to afford the pure compound **4.12e** as red liquid. R_f = 0.1 (10% methanol in ethyl acetate). Yield: 0.20 g (58%); ^{1}H NMR (DMSO-d_6, 600 MHz): δ (ppm) = 9.10 (s, 1H), 7.77 (s, 1H), 7.70 (s, 1H), 4.16 (t, 2H, J = 7.0 Hz), 3.85 (s, 3H), 3.07 (t, 2H, J = 7.0 Hz), 1.80 (dt, 4H, J_1 = 14.6 Hz, J_2 = 7.2 Hz), 1.42 (dt, 2H, J_1 = 15.1 Hz, J_2 = 7.5 Hz), 1.28 (dt, 2H, J_1 = 14.9 Hz, J_2 = 7.4 Hz). ^{13}C-NMR (DMSO-d_6, 150 MHz): δ (ppm) = 136.9, 124.1, 122.7, 116.8, 105.2, 49.2, 31.0, 30.1, 29.7, 28.2, 25.3. ^{77}Se NMR (DMSO-d_6, 114 MHz): 212, -278; ESI-MS *m/z* calcd for $C_{11}H_{18}N_3Se^+$ [M^+]: 272.0660; obs: 272.0661. FT-IR ($\bar{\nu}$, cm^{-1}): 3414 (w), 2931 (m), 2149 (w), 2060 (s), 1570 (m), 1458 (m), 1260 (w), 1164 (s), 821 (w), 620 (s).

Compound 4.12f: Prepared according to **GP3** using bromide **4.10b-5** (0.30 g, 0.75 mmol) and potassium selenocyanate (0.32 g, 2.24 mmol) in dry acetonitrile (6 mL) and reaction time of 12 h. Crude product was further purified using neutral alumina column chromatography using 15% methanol in ethyl acetate as eluent to afford purified **4.12f** as yellow oil. R_f = 0.7 (10% methanol in ethyl acetate). Yield: 0.18 g (53%). ^{1}H NMR (DMSO-d_6, 400 MHz): δ (ppm) = 9.30 (s, 1H), 7.82 (d, 2H, J = 1.5 Hz), 7.45 – 7.40 (m, 5H), 5.42 (s, 2H), 4.18 (t, 2H, J = 7.2 Hz), 3.06 (t, 2H, J = 7.03 Hz), 1.81 (m, 4H), 1.42 (m, 2H), 1.27 (dt, 2H, J_1 = 15.0 Hz, J_2 = 7.5 Hz). ^{13}C NMR (DMSO-d_6, 100 MHz): (ppm) = 136.6, 135.3, 129.5, 129.2, 128.7, 123.3, 123.1, 105.1, 52.5, 49.4, 31.0, 30.1, 29.5, 28.2, 25.3; ^{77}Se NMR (DMSO-d_6, 76 MHz): δ (ppm) = 214, -276; ESI-MS *m/z* calcd for $C_{17}H_{22}N_3Se^+$ [M^+]: 348.0973; obs: 348.1012. FT-IR ($\bar{\nu}$, cm^{-1}): 3426 (w), 2933 (s), 2151 (w), 2059 (s), 1559 (m), 1455 (m), 1153 (s), 711 (s).

4.5.2. Antioxidant activity using GSH-GSSG coupled assay

GPx-like activity was carried out UV-VIS spectroscopically using enzymatic method. The assay mixture consisted of reduced glutathione (2.0 mM), glutathione disulfide reductase enzyme (1.0 units mL^{-1}), NADPH (0.4 mM) in 0.1 M potassium phosphate (pH = 7.5). Gpx-like samples (100.0 µM) were added at room temperature, and the reaction was initiated by the addition of peroxides (1.6 mM). The initial reduction rates were calculated from the rate of NADPH oxidation at λ = 340 nm. Initial rates were calculated from three replicates of the reaction for 5.0 to 20.0 seconds, using 6.22 $mM^{-1}cm^{-1}$ as the molar extinction co-efficient for the NADPH.

4.5.3. Antioxidant activity using PhSH-PhSSPh assay

HPLC mediated thiophenol assay: The GPx-like activity was measured using high-performance liquid chromatography apparatus in a 1.5 ml sample vials and in-built autosampler was used for sample injection in a pre-programmed sequence. In this assay, a solution of 1.0 mM thiophenol and 2.0 peroxide in HPLC-grade methanol at ambient temperature were used as a model system. Runs in presence (100.0 µM) and absence of test compounds were carried out under identical conditions. Periodically, reaction aliquots were injected into reversed-phase column (Phenomenex LunaTM 5 µm, C-18(2) 100 Å, diameter: 250 × 4.6 mm) and eluted with 95:5 methanol-water solvent system for

a runtime of 7.0 min. The amount of PhSSPh formed as a product was determined by comparison with standardized calibration plot obtained from known concentrations of PhSSPh. The chromatograms were recorded at λ = 250 nm and half-life of formation of PhSSPh was calculated from kinetic graph. Each experiment was replicated thrice under identical conditions. However, two concordant datasets were used to calculate the half-life of formation of PhSSPh.

4.5.4. Fluoroscence microscopic experiment

RAW 264.1 macrophage cells were cultured in high glucose Dulbecco's modified Eagle's medium (DMEM), supplemented with 10 % fetal bovine serum (FBS) and 1% penicillin/streptomycin at 37 °C under 5 % CO_2 atmosphere. Cells were then plated (3×10^5 / plate) in 35 mm cell culture petri dishes containing 2.0 mL of DMEM medium and incubated at 37 °C under 5 % CO_2 for 24 h. The confluent cells were washed thrice with DPBS and finally incubated with antioxidant compounds **4.12a** and **4.12e** at concentrations of 2.5 μM and 5.0 μM at 37 °C under 5% CO_2 for 1 h. After washing with DPBS thrice, cells were incubated with fluorogenic probe **4.19** at a concentration of 5.0 μM for 1 h. Following incubation with fluorogenic probe, cells were finally washed with DPBS cellular morphology was carefully observed and imaged in a Bio-rad ZOE™ fluorescent cell imager under bright field and green fluorescent colored filters. Additionally, the control experiments were performed with the pre-treatment of N-acetyl cysteine (NAC) at a concentration of 2.0 mM, as a positive control to affirm the quenching of endogenous peroxide.

4.6. References

1. Ray, P. D.; Huang, B.-W.; Tsuji, Y., *Cell Signal* **2012**, *24*, 981.
2. Birben, E.; Sahiner, U. M.; Sackesen, C.; Erzurum, S.; Kalayci, O., *World Allergy Organ J* **2012**, *5*, 9.
3. Chovatiya, R.; Medzhitov, R., *Mol Cell* **2014**, *54*, 281.
4. (a) Ohshima, H.; Tatemichi, M.; Sawa, T., *Arch Biochem Biophys* **2003**, *417*, 3; (b) Shah, A. M.; Channon, K. M., *Heart* **2004**, *90*, 486; (c) Sies, H., *Am J Med* **1991**, *91*, S31; (d) Barnham, K. J.; Masters, C. L.; Bush, A. I., *Nat Rev Drug Discov* **2004**, *3*, 205; (e) Buonocore, G.; Perrone, S.; Tataranno, M. L., *Seminars in Fetal and Neonatal Medicine* **2010**, *15*, 186; (f) Förstermann, U., *Nature Clinical Practice Cardiovascular Medicine* **2008**, *5*, 338.
5. Lubos, E.; Loscalzo, J.; Handy, D. E., *Antioxid Redox Signal* **2011**, *15*, 1957.

6. Mugesh, G.; Singh, H. B., *Chem Soc Rev* **2000**, *29*, 347.
7. Barbosa, N. V.; Nogueira, C. W.; Nogara, P. A.; de Bem, A. F.; Aschner, M.; Rocha, J. B. T., *Metallomics* **2017**, *9*, 1703.
8. Back, T. G.; Moussa, Z.; Parvez, M., *Angew Chem Int Ed* **2004**, *43*, 1268.
9. Arai, K.; Kumakura, F.; Takahira, M.; Sekiyama, N.; Kuroda, N.; Suzuki, T.; Iwaoka, M., *J Org Chem* **2015**, *80*, 5633.
10. Kuzma, D.; Parvez, M.; Back, T. G., *Org Biomol Chem* **2007**, *5*, 3213.
11. Borisov, A. V.; Matsulevich, Z. V.; Osmanov, V. K.; Borisova, G. N., *Chem Heterocycl Compd* **2012**, *47*, 1321.
12. Makrecka-Kuka, M.; Dimitrijevs, P.; Domracheva, I.; Jaudzems, K.; Dambrova, M.; Arsenyan, P., *Sci Rep* **2020**, *10*, 21595.
13. Frizon, T. E. A.; Cararo, J. H.; Saba, S.; Dal-Pont, G. C.; Michels, M.; Braga, H. C.; Pimentel, T.; Dal-Pizzol, F.; Valvassori, S. S.; Rafique, J., *Oxid Med Cell Longev* **2020**, *2020*, 5417024.
14. Bhabak, K. P.; Mugesh, G., *Chem Eur J* **2007**, *13*, 4594.
15. (a) Bhabak, K. P.; Mugesh, G., *Chem-Eur J* **2007**, *13*, 4594; (b) Bhabak, K. P.; Mugesh, G., *Chem-Eur J* **2009**, *15*, 9846.
16. Bhabak, K. P.; Mugesh, G., *Chem Eur J* **2008**, *14*, 8640.
17. Sarma, B. K.; Mugesh, G., *J Am Chem Soc* **2005**, *127*, 11477.
18. Lin, Y.-R.; Chiu, C.-C.; Chiu, H.-T.; Lee, D.-S.; Lu, T.-J., *Appl Organometal Chem* **2018**, *32*, e3896.
19. Bernhammer, J. C.; Huynh, H. V., *Organometallics* **2014**, *33*, 172.
20. Jacob, L. A.; Matos, B.; Mostafa, C.; Rodriguez, J.; Tillotson, J. K., *Molecules* **2004**, *9*.

Chapter 5

Syntheses of Benzimidazole-based Ionic and non-ionic Selenocyanates: Impact of 4-Nitrophenyl Group towards their Anti-proliferative Activities

5.1. Introduction

In chapters 2 and 3, we have shown that organoselenocyanates exhibit significant anti-cancer activities towards different breast cancer cells and particularly towards triple-negative breast cancer cells (MDA-MB-231). Moreover, we have also represented that the anti-proliferative activities of benzylic organoselenocyanates could be enhanced either by the incorporation of more than one selenocyanate groups in a compound (Chapter 2) or by the suitable functionalization at 4-position of the phenyl ring (Chapter 3). Between 1,2,3-triazole and 2,4-thiazolidine-1,3-dione pharmacophores, the former enhanced the anti-cancer potentials but was not selective towards the cancer cells. Whereas, 2,4-thiazolidine-1,3-dione pharmacophore further decreased the anti-cancer potencies (Chapter 3). In search of other pharmacophores, we found that several benzimidazole-based organoselenium compounds are reported in the literature exhibiting promising anti-cancer activities in different organ-specific cancer cells. For example, in 2009, Talas and co-workers have reported 1,3-disubstituted benzimidazole-based selone **5.1**, which was shown to exhibit significant protective effects against DMBA-induced cancer in female Wistar mice model (Figure 5.1).[1] It was observed that compound **5.1** significantly enhanced the level of antioxidant markers such as catalase, SOD, GR and GSH as compared to the untreated controls. In another study, Braga and co-workers (2011) have reported a series of imidazolium-based ionic liquids containing monoselenide functionality.[2] Among the compounds studied therein, compound **5.2** displayed significant antimicrobial activity against *P. Zopfii*, with a minimum inhibitory concentration (MIC) of 0.01 µM. They have demonstrated enhanced antimicrobial activities of the ionic liquids against *P. Zopfii* upon the incorporation of selenium. In 2014, Guan *et al* reported an interesting work describing the anti-proliferative activities of diverse series of benzimidazole-based carbamates. Interestingly, compound **5.3** containing a monoselenide linkers connecting benzimidazole and indole ring was found to be the most potent anti-proliferative agent towards different cancer cells such as SGC-7901, A-549, HT-1080 with IC_{50} values in the nanomolar range of 98.0 nM, 150.0 nM and 130.0 nM, respectively.[3] Subsequently, in 2016, Chen and co-workers have reported benzimidazole-based selenadiazole compound **5.4** as highly cytotoxic towards triple-negative breast cancer cells MDA-MB-231 with an IC_{50} of 1.0 µM.[4] Notably, this compound exhibited good selectivity towards triple-negative breast-cancer cells over ER+ breast cancer cells (MCF-7) and normal cells (L-02). Detailed mechanistic insights

revealed cell cycle arrest at G2/M phase and induction of apoptosis by inducing DNA damage. Additionally, compound **5.4** exhibited anti-proliferative activities via inhibition of protein kinase B (Akt) and mitogen activated protein kinase (MAPK) pathways through the over-expression of ROS. In 2019, Kamal and co-workers have reported a series of benzimidazole-based selones and studied for their antimicrobial and anti-cancer potentials. For example, compound **5.5** was shown as a promising cytotoxic compound against cervical cancer cells (HeLa) and retinal ganglion cell (RGC-5) having IC_{50} values of 0.11 and 9.16 μM, respectively.[5] Interestingly, the activity of compound **5.5** was significantly higher than that of standard drug 5-FU. Computational studies revealed high binding energy of compound **5.5** with several angiogenetic proteins such as VEGF, EGF, HIF and COX-1, therefore suggesting that anti-cancer effect of the compound may be attributed due to strong anti-angiogenetic effect. Very recently, in 2020, Matsumura *et al* have reported a methodology to synthesize a wide range of diaryl diselenides and the corresponding monoselenides containing imidazo[1,2-a]pyridine rings and evaluated them for their anti-proliferative activities in HeLa cells. Interestingly, the diselenide **5.6** containing 4-methoxyphenyl moiety exhibited highly potent anti-proliferative activity in HeLa cells.[6] Interestingly, this compound was found to be even more active than standard chemotherapeutic drug doxorubicin.

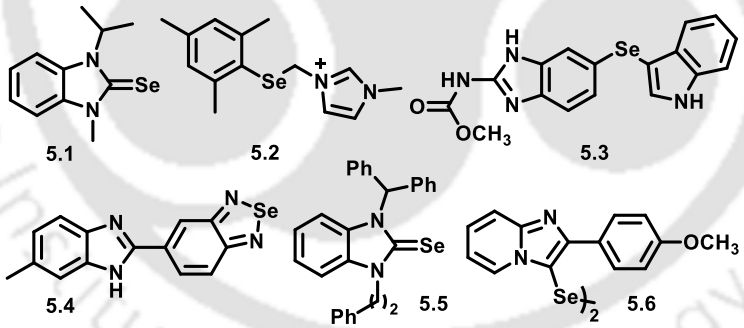

Figure 5.1. Chemical structures of some of the literature reported heterocyclic organoselenium compounds containing benzimidazole or imidazo[1,2-a]pyridine rings that exhibited promising anti-cancer activities against different cell lines.

5.2. Outline of the chapter

In this chapter, we turned our attention to understand the anti-cancer activities of benzimidazole-based ionic and non-ionic organoselenium compounds. Inspired by the reasonable antioxidant activities of benzimidazole and imidazole-based ionic compounds **4.11a-f** and **4.12a-f** in last chapter and the literature reports on the anti-cancer activities

of various benzimidazole-based organoselenium compounds, the anti-cancer potentials of the synthesized ionic compounds were studied. As benzimidazole-based acyclic selenocyanate **4.11f** exhibited potent anti-proliferative activities, the same backbone was chosen to synthesize different series of related analogues considering the impact of -methoxy and nitro groups and subsequently studied for their anti-cancer activities. As the ionic benzimidazole-based acyclic selenocyanate could not be prepared in last chapter due to cyclization process, a newer series of ionic selenocyanate analogues (**5.9-5.11**) are prepared upon C2-functionalization in benzimidazole ring. Additionally, a series of the corresponding neutral selenocyanates (**5.12-5.14**) were also developed. Interestingly, unlike ionic selenocyanates **5.9-5.11**, the neutral selenocyanates **5.12-5.14** exhibited significantly higher anti-proliferative activity. Particularly, as compound **5.14** containing 4-NO_2 group exhibited significantly higher selectivity towards triple-negative breast cancer cells (MDA-MB-231) over normal cells (HEK-293), this compound was chosen for further studies. The compound exhibits anti-migratory activity and exerts anti-proliferative activity by arresting cells in G1 phase of the cell cycle (MDA-MB-231).

5.3. Results and discussion

5.3.1. Evaluation of anti-proliferative activities of 4.11a-f and 4.12a-f

In last chapter, we have studied the antioxidant activities of the benzimidazole- and imidazole-based ionic organoselenium compounds **4.11a-f** and **4.12a-f** (Figure 5.2). Efficiency for the catalytic reduction of peroxides was monitored in the presence of two different thiols (GSH and PhSH). Interestingly, in general, cyclic selenazolium selenocyanates (**4.11a-b** and **4.12a-b**) and selenazinium selenocyanates (**4.11c-d** and **4.12c-d**) exhibited significantly higher antioxidant activities than the corresponding acyclic selenocyanates (**4.11e-f** and **4.12e-f**) as discussed in Chapter 4. With this information in hand and the literature reports on the anti-cancer activities of various classes of benzimidazole-based compounds (as discussed in previous section), we have focused our attention to evaluate the complete sets of compounds for their anti-proliferative activities in triple-negative breast cancer cells (MDA-MB-231).

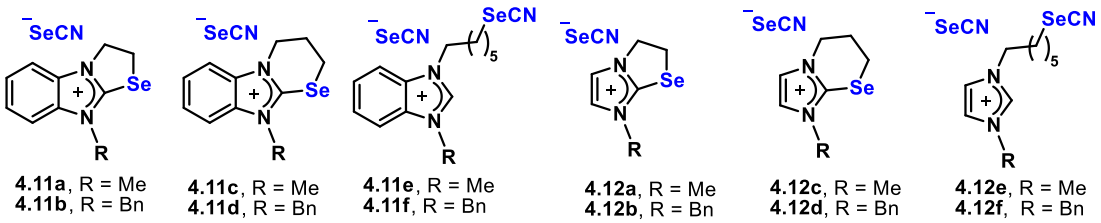

Figure 5.2. Chemical structures of the benzimidazole- and imidazole-based ionic organoselenium compounds **4.11a-f** and **4.12a-f** studied in Chapter 4.

As shown in Figure 5.3, in general, all the cyclic compounds **4.11a-d** and **4.12a-d** exhibited weaker anti-proliferative activities up to 10.0 μM concentration except compound **4.11a**. In contrast, among four acyclic compounds (**4.11e-f** and **4.12e-f**), benzimidazole-based acyclic compounds **4.11e-f** exhibited significantly higher anti-proliferative activities and compound **4.11f** has been found to be the most potent compound in the series.

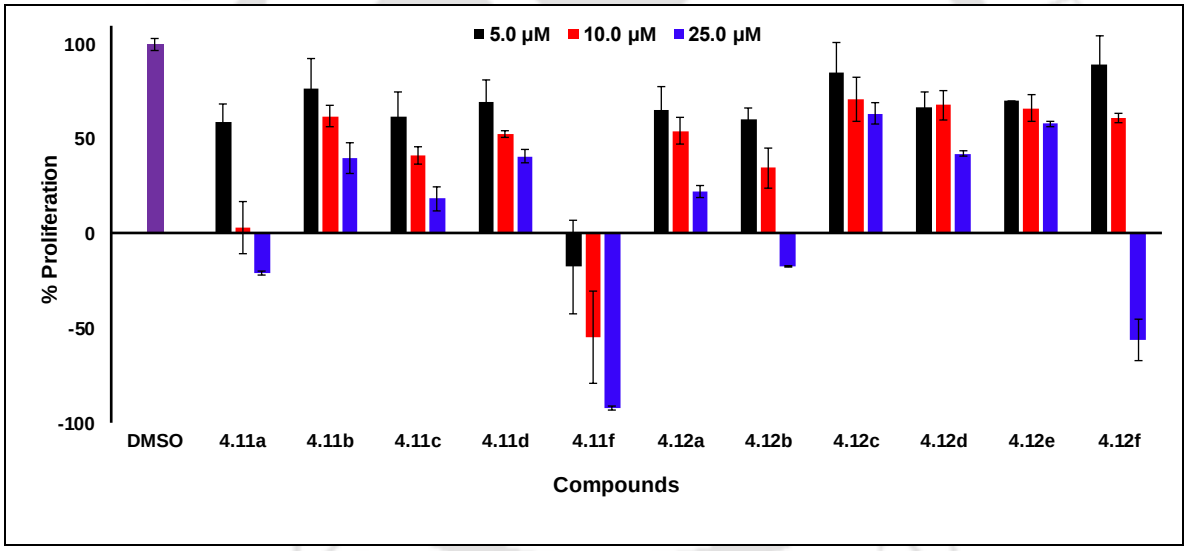

Figure 5.3. Dose-dependent anti-proliferative activities of compounds **4.11a-f** and **4.12a-f** towards triple-negative breast cancer cells (MDA-MB-231). The bar with DMSO indicates vehicle control without any selenium compound.

5.3.2. Synthesis of benzimidazole-based organoselenium compounds

The observation with highest anti-proliferative activity of benzimidazole-based acyclic selenocyanate having *N*-benzyl substitution (**4.11f**) and relative weaker activity of the corresponding selenazolium and selenazinium selenocyanates **4.11b** and **4.11d** inspired us further to explore the possibilities of developing newer categories of *N*-benzylbenzimidazole-based cyclic/acyclic ionic/non-ionic organoselenium compounds

considering the importance of 4–OMe and 4–NO_2 substitution on the phenyl ring. The introduction of 4–OMe and 4–NO_2 group may have impact on the anti-proliferative activities as observed in chapter 3. Considering these aspects, we have attempted to synthesize several categories of newer generation of compounds (**5.7** to **5.16**) in the present Chapter (Figure 5.4).

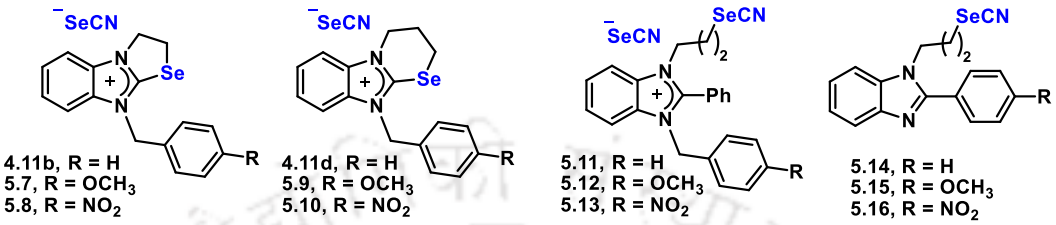

Figure 5.4. Chemical structures of benzimidazole-based compounds considered in the present chapter.

The synthesis of cyclic selenazolium and selenazinium selenocyanates (**5.7**-**5.10**) with 4–OMe and 4-NO_2 substitution were attempted using the strategy shown in chapter 4 (Scheme 4.1A). However, unlike other compounds, 4-NO_2 substituted selenazolium selenocyanate **5.8** could not be synthetically achieved in pure form as the compound decomposed during the purification process. Briefly, the synthesis is outlined in scheme 5.1.

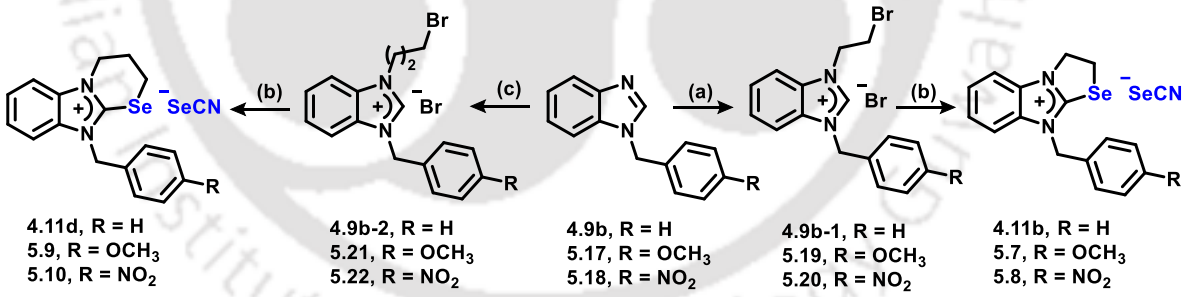

Scheme 5.1. Reagents and conditions (a) 1,3-dibromopropane (neat), 85 °C, 12 h (b) KSeCN (3.0 equiv), CH_3CN, 12 h (c) 1,2-dibromopropane (neat), 85 °C.

The acyclic ionic selenocyanates **5.11-5.13** were attempted starting with the C2-functionalized benzimidazole derivatives to prevent the selenocyclization process as observed in chapter 4. The synthetic precursor was *o*-phenylenediamine **5.23**, which was reacted with benzaldehyde to form the C2-phenyl functionalized benzimidazole derivative **5.24** (Scheme 5.2). This was subsequently reacted with benzylic bromides leading to the formation of *N*-benzylated benzimidazole derivatives **5.25-5.26** in good

yields. Treatment of **5.25-5.26** with 1,3-dibromopropane led to the formation of ionic compounds **5.28-5.30** having bromide counterion. The final ionic acyclic selenocyanates **5.11-5.13** were achieved upon the treatment of **5.28-5.30** with potassium selenocyanate (3.0 equiv). Similarly, the non-ionic selenocyanates **5.14-5.16** were synthesized starting from the same precursor **5.23** as shown in Scheme 5.2. Treatment of **5.23** with aryl aldehydes in the presence of aqueous sodium bisulfite led to the formation of C2-arylated benzimidazole derivatives **5.24**, **5.31-5.32**. Subsequent *N*-functionalization produced the corresponding bromides **5.33-5.35** in good yields. Final selenocyanation was carried out using potassium selenocyanate in acetonitrile leading to the formation of **5.14-5.16**. All the synthesized final compounds were purified and characterized using analytical methods.

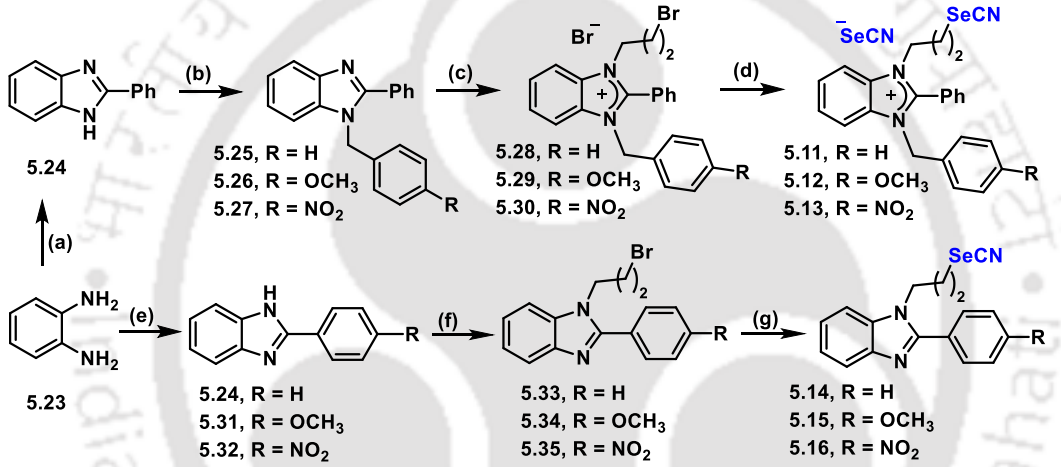

Scheme 5.2. Reagents and conditions: (a) PhCHO, $NaHSO_3$, H_2O, 100 °C, 2 h; (b) $ArCH_2Br$, KOH, rt, 4 h, (c) 1,3-dibromopropane (neat), 85 °C, 12 h; (d) KSeCN, CH_3CN, rt, 12 h; (e) ArCHO, $NaHSO_3$, H_2O, 100 °C, 2 h; (f) 1,3-dibromopropane, NaI (cat), NaOH, acetone, 50 °C, 4 h; (g) KSeCN, CH_3CN, rt, 4 h.

5.3.3. Anti-proliferative activities of benzimidazole-based organoselenium compounds

In Chapter 3, we have seen that the anti-proliferative activities of benzyl selenocyanate could be enhanced by the introduction of 4-NO_2 group at the phenyl ring. A similar trend was also observed for the corresponding heterocyclic pharmacophore containing compounds. Furthermore, the anti-proliferative activities of the compounds **4.11a-f** and **4.12a-f** represent that cyclic compounds are relatively less potent than the corresponding acyclic selenocyanates. Therefore, in the present chapter, the anti-proliferative activities of all the synthesized compounds are evaluated to discover more potent anti-proliferative compounds towards TNBC cells. The anti-proliferative activity was evaluated using

conventional MTT assay in MDA-MB-231 cells at three different doses (5.0, 10.0 and 25.0 µM) and compared to that of a standard anti-cancer drug such as 5-FU (Figure 5.5). In general, all the cyclic compounds were found to be moderately active towards MDA-MB-231 cells. Furthermore, the activity could not be enhanced by converting the selenazinium selenocyanates **4.11**, **5.9** and **5.10** to the corresponding acyclic ionic selenocyanates **5.11-5.13**. However, a remarkable enhancement of anti-proliferative activity was observed for the C2-functionalized neutral selenocyanates **5.14-5.16**. The activity of both 4-OMe and 4-NO_2 substituted analogues exhibited relatively better potency than the corresponding unsubstituted compound (**5.14**), showing the importance of these two functionalities towards their anti-proliferative activities.

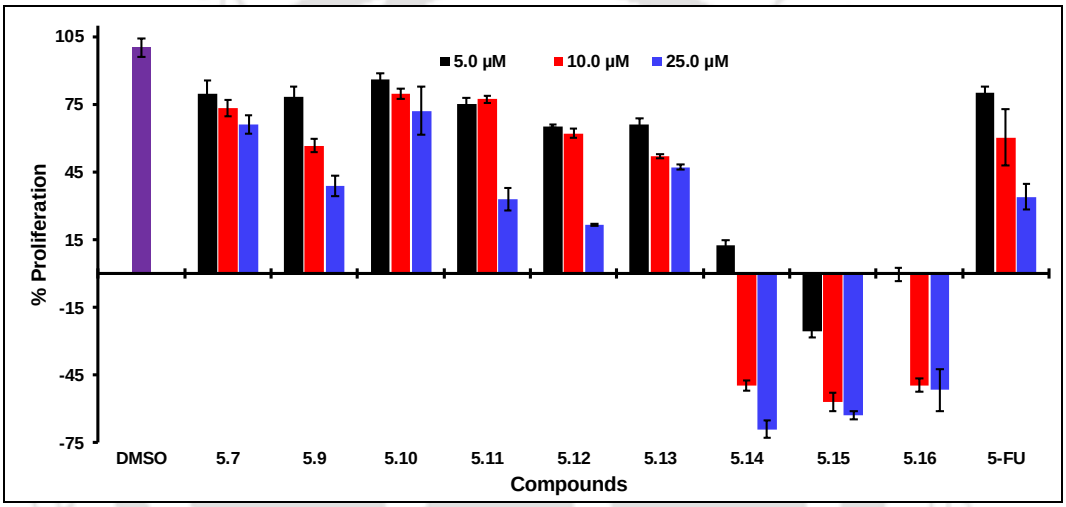

Figure 5.5. Dose-dependent anti-proliferative activities of compounds **5.7** and **5.9-5.16** towards MDA-MB-231 cells. The bar with DMSO indicates vehicle control without any selenium compound.

With the preliminary anti-proliferative activity results of the compounds in TNBC, we proceeded to evaluate the cytotoxicity profile of the most active neutral selenocyanates towards human embryonic kidney cells (HEK-293). As shown in Figure 5.6, comparative results indicate that both **5.14** and **5.15** exhibited significant toxicities towards HEK-293 cells at all three concentrations (5.0, 10.0 and 25.0 µM). Particularly, the cellular growth was completely prevented at 10.0 and 25.0 µM concentrations. Interestingly, compound **5.16**, containing 4-NO_2 substitution exhibited significantly weaker anti-proliferative activities towards HEK-293 cells, indicating higher selectivity towards the cancer cells over normal cells (Figure 5.6). Therefore, compound **5.16** was chosen for further detailed studies.

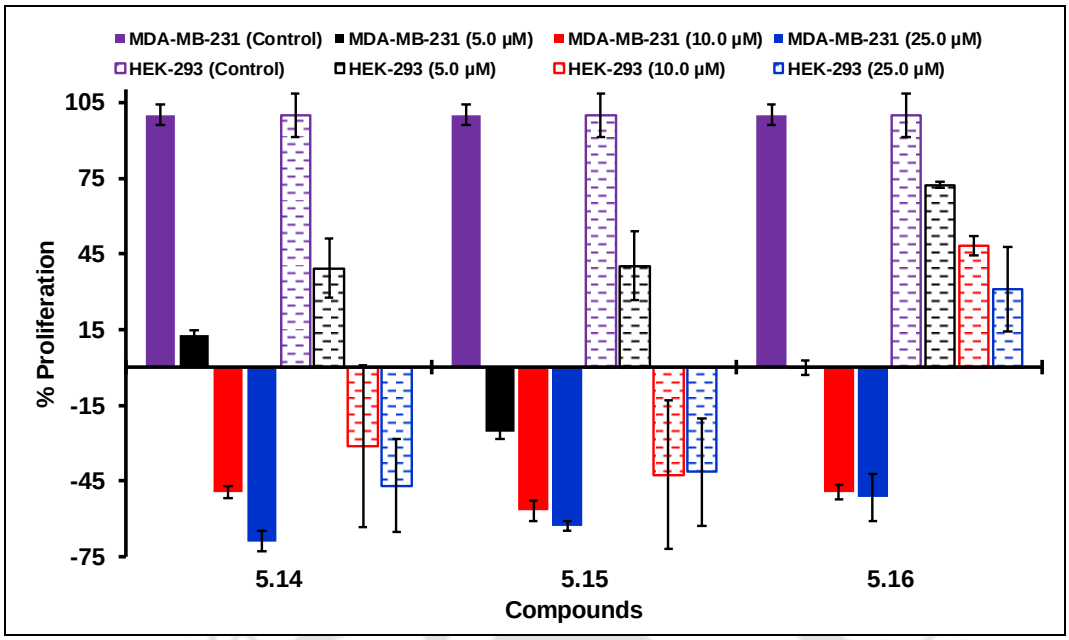

Figure 5.6. Comparative anti-proliferative activities of compounds **5.14**-**5.16** on MDA-MB-231 (filled bars) and HEK-293 (patterned bars) cells at concentrations of 5.0, 10.0 and 25.0 µM.

5.3.4. Inhibition of cellular migration by compound 5.16

As discussed in previous sections, metastatic cancer cells have the property to spread to other remote organs in different parts of the body. Since metastasis takes place due to migration of cancer cells, inhibition of migration of cancer cells is very crucial in the treatment of cancer. As mentioned earlier, a high rate of metastasis occurs in case of triple-negative breast cancer cells and very few drugs are reported to have inhibitory activities towards the migration of cancer cells. Therefore, we have evaluated compound **5.16** against MDA-MB-231 cells for its anti-migratory activity using scratch assay (Figure 5.7). A scratch was made on the cellular monolayer and was treated with compound **5.16** at two different doses (1.2 and 2.5 µM) and the cells were incubated for 48 h. Images were captured at 0, 24 and 48 h to understand the dose-dependent anti-migratory potential of compound **5.16** as compared to the control reaction (DMSO).

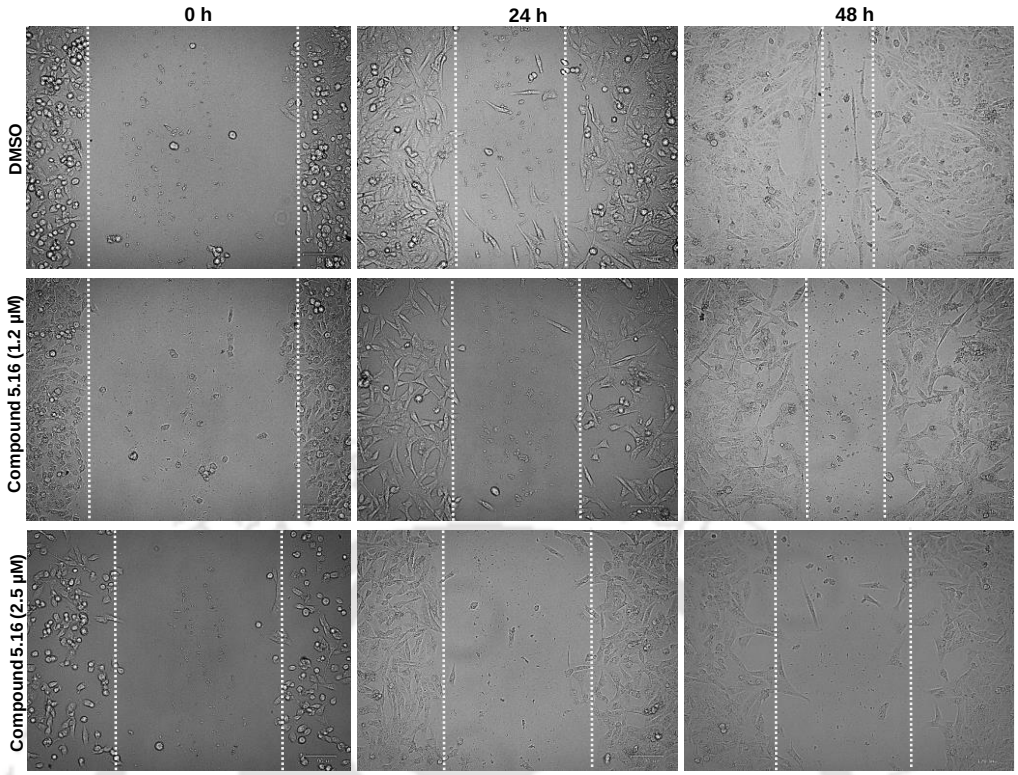

Figure 5.7. Anti-migratory activity of compound 5.16 towards MDA-MB-231 cells. The compound (1.2 and 2.5 µM) was incubated up to 48 h and images were captured at 0, 24 and 48h.

As shown in Figure 5.7, the cells migrated to the scratched area and almost compensated the vacant spaces (DMSO control) over 48 h. However, a prevention of such migration was observed in the presence of compound **5.16** in a dose-dependent manner over time as evidenced by the more vacant unpopulated spaces in the presence of compound over time. These results suggest that, compound **5.16** in the present study have the capability to suppress the movement and re-populate the wound region within 48 h.

5.3.5. Cellular morphological changes upon the treatment of selenocyanate 5.16

Process of cell death is accompanied by significant morphological changes in cancerous cells such as cell shrinkage by reduction in volume. Microscopic visualization technique is commonly utilized to understand the morphological changes over time. In the present study, MDA-MB-231 cells were incubated with the most active compound **5.16** and the cellular morphological changes were visualized under inverted microscope after 24 and 48 h (Figure 5.8).

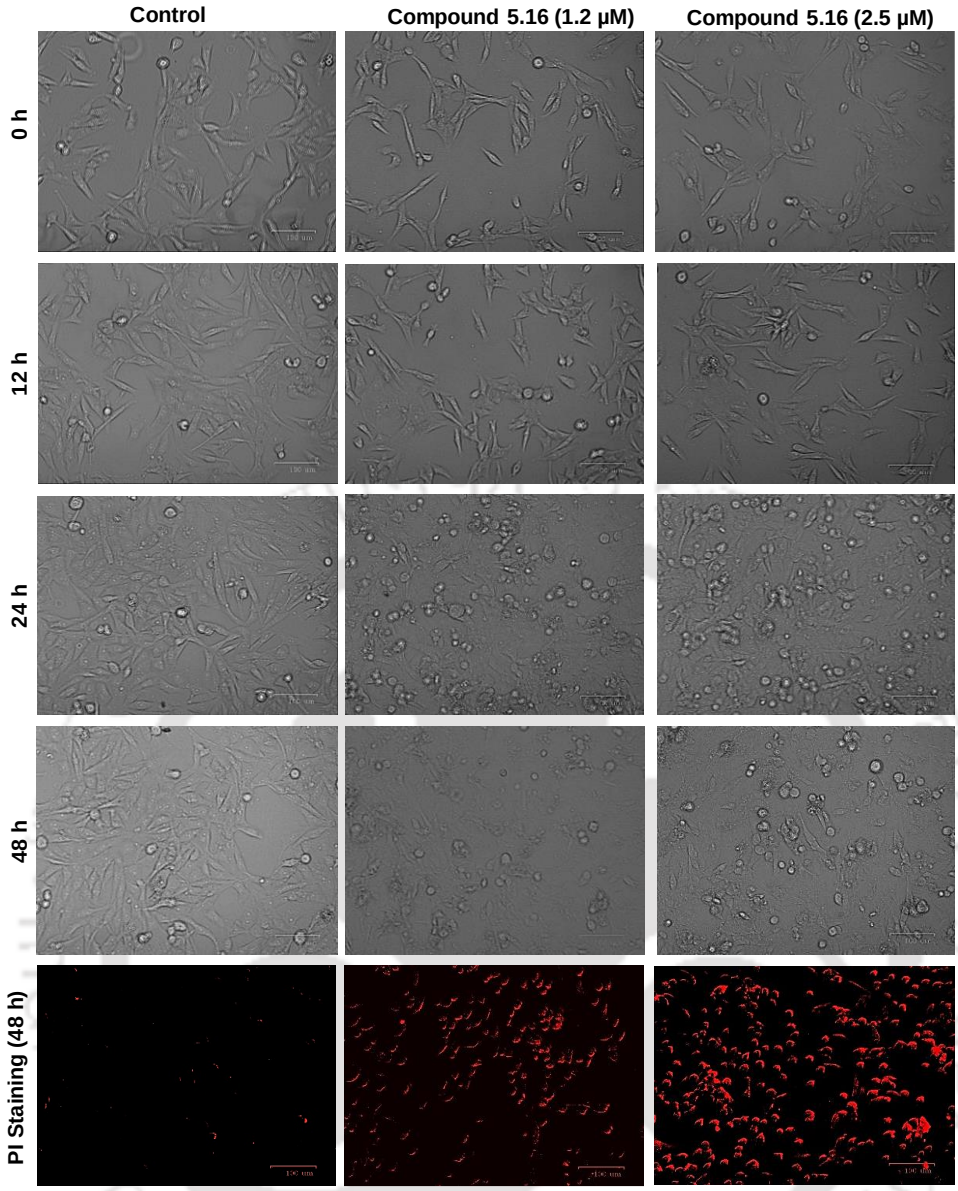

Figure 5.8. Changes in cellular morphology of MDA-MB-231 cells in the absence and presence of compound **5.16** at concentrations of 1.2 and 2.5 µM. PI-stained images (red channel) after incubation of cells for 48 h in the presence of test compounds represent dead cells.

After 48 h, the cells were stained with propidium iodide (PI) to identify apoptotic cells. PI is a fluorescent dye, which cannot pass through the cell membrane of living cells, therefore selectively staining only the dead cell nuclei, indicating the extent of cell death. The visualization can be done using fluorescent microscope under red channel. As observed in Figure 5.8, significant morphological changes are observed upon the treatment of cells with compound **5.16**. Visual changes in morphology takes place due to

the cellular death and the formation of cell debris, that get detached from surface and float randomly in the culture media. The results were compared against DMSO control.

5.3.6. Cell cycle analysis of MDA-MB-231 cells in the presence of compound 5.16

As described in the previous chapters, a proper regulation of cell cycle is an important process for cellular homeostasis and cellular functions. Therefore, in the present study, in order to understand the mechanism of inhibition of cellular proliferation by the most potent compound **5.16**, we investigated the effects of compound **5.16** on cell cycle distribution of MDA-MB-231 cells using PI-mediated flow-cytometric experiments. Cell cycle distribution was observed upon incubation of cells with the test compound for 24 h at two different concentrations such as 5.0 and 10.0 μM. As shown in Figure 5.9, a noticeable alteration of cellular distribution was observed in the presence of compound **5.16**. Interestingly, the cellular population at G1 was found to be significantly enhanced upon the incubation of cells with compound **5.16** and the population of cells in S-phase was decreased. For example, while the population of G1 and S phases were 57.98% and 26.25%, respectively in the absence of any selenium compound, the population was changed to 71.54% and 14.12%, respectively in the presence of 5.0 μM of compound **5.16**. However, no further change in distribution was observed at a relatively higher dose (10.0 μM). These results reveal that compound **5.16** effectively arrests MDA-MB-231 cells at G1 phase of the cell cycle with subsequent decrease in the population at S phase. These results indicate that the potent anti-proliferative activity of the selenocyanate **5.16** could be the result of hampering the cell cycle distribution and the arresting cells in G1 phase. This could be the result of inhibiting the marker proteins such as cyclin dependent kinases (CDKs) that facilitate the transition of cells from G1 phase to S phase.[7]

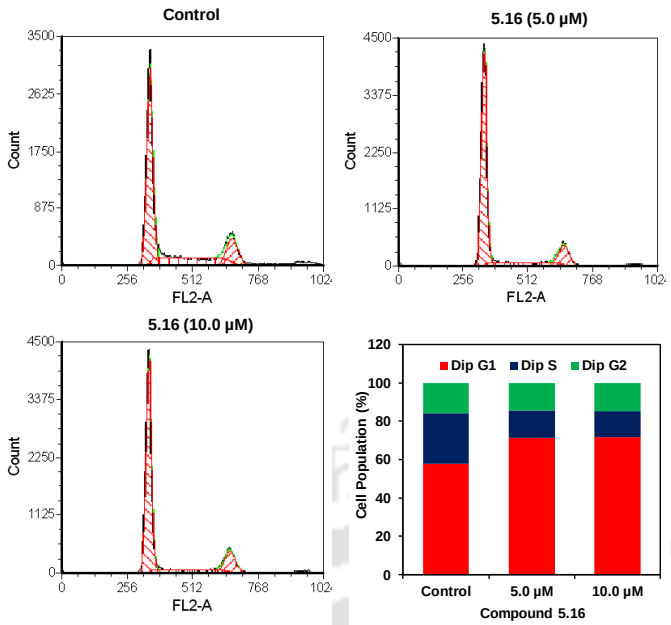

Figure 5.9. Graphical visualization of cellular distribution pattern of MDA-MB-231 cells in different phases of cell cycle in the presence of selenocyanates **5.16**. Cell cycle distribution was analyzed by flow-cytometric assay after treatment of cells with selenocyanate **5.16** for 24 h followed by the staining with PI.

5.4. Conclusions

In summary, we have shown that the longer chain ionic acyclic benzimidazole-based organoselenocyanates exhibit better anti-proliferative activities than the ionic selenazolium and selenazinium compounds. Therefore, a number of synthetically relevant C2-protected acyclic selenocyanates were developed. However, the anti-proliferative activity of benzimidazole-based selenazinium selenocyanates could not be enhanced by converting them to the corresponding acyclic ionic selenocyanates. Interestingly, a significant enhancement in activity was observed for the corresponding neutral selenocyanates having 4-OMe and 4-NO_2 substitutions on the C2-phenyl ring. Considering the selectivity towards triple-negative breast cancer cells over normal cells (HEK-293), 4-NO_2-substituted neutral selenocyanate **5.16** was found to be the best compound among the series exhibiting potent anti-proliferative activity towards MDA-MB-231 cells. The compound **5.16** exhibited reasonable anti-migratory activity in a dose-dependent manner destroyed the morphology of cells over time. Furthermore, cell cycle studies revealed that the anti-proliferative activity of compound **5.16** could be due to cell cycle arrest at G1 phase.

5.5. Experimental section

5.5.1. Materials and Method.

Potassium selenocyanate (KSeCN) was purchased from Sigma-Aldrich and was used as supplied without further purification. Solvents (petroleum ether 60 – 80, ethyl acetate) were distilled freshly before using. Due to unpleasant odor of most of the reaction mixture involved, the reactions were carried out in a well-ventilated fume hood. Thin-layer chromatography was carried out on pre-coated silica gel plates (F_{254}), purchased from Merck, and spots were visualized by UV irradiation at λ = 254 nm and/or iodine staining. Column chromatography were performed either with glass column loaded with neutral alumina or with an automated flash chromatography system (CombiFlash NextGen100, Teledyne^{TM}) using manually packed cartridges. ^{1}H, ^{13}C and ^{77}Se NMR spectra were recorded Bruker (400, 500 or 600 MHz) NMR spectrometers and the chemical shifts are cited with respect to TMS (Me_4Si) as an internal standard (^{1}H and ^{13}C nuclei) and Ph_2Se_2 as external standard (^{77}Se nuclei). Perkin-Elmer Lambda 25 UV-Vis spectrophotometer was used to perform GPx-like activity. Mass spectrometric analysis were performed using Agilent Q-TOF 6520 High Resolution Mass Spectrometer in ESI-positive mode analysis. Melting points were recorded in a Büchi B-540 melting point apparatus and the readings were uncorrected. Fourier Transform Infra-red sprctroscopy (FT-IR) was performed either in a Perkin Elmer Spectrum Two instrument using KBr pellet or in a Perkin Elmer UATR Two instrument, following appropriate background correction.

General procedure 1 (GP1) for synthesis of 1-aryl-3-(2-selenocyanatoethyl)-benzimidazole (**4.11b**, **5.7**, **5.8**):

Title compounds were synthesized using reported literature methods with minor modifications. Precursor bromide (1.0 equiv) was stirred with potassium selenocyanate (3.0 equiv) in dry acetonitrile for appropriate time at room temperature under inert atmosphere. Progress of the reaction was monitored by thin layer chromatographic analysis. After completion, the solution was evaporated to dryness under reduced pressure to afford the crude product. The product was purified using neutral alumina column chromatography using appropriate mixtures of ethyl acetate and methanol as eluents.

Compound **4.11b**: Prepared according to **GP1** using bromide **4.9b-1** (0.10 g, 0.25 mmol)

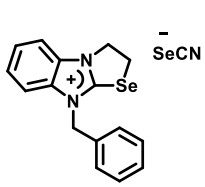

and potassium selenocyanate (0.11 g, 0.76 mmol) in dry acetonitrile (4 mL) and reaction time of 24 h. Crude product was further purified by neutral alumina column chromatography using methanol in dichloromethane to afford the pure compound **4.11b** as grey solid powder. R_f = 0.5 (5% methanol in dichloromethane). Yield: 0.06 g (67%). M.P. = 123 – 125 °C. ^{1}H NMR (Methanol-d_4, 400 MHz): δ (ppm) = 7.85 – 7.83 (m, 1H), 7.75 – 7.73 (m, 1H), 7.60 – 7.53 (m, 2H), 7.50 – 7.44 (m, 5H), 5.59 (s, 2H), 4.74 (t, 2H, *J* = 7.6 Hz), 4.22 (t, 2H, *J* = 7.6 Hz). ^{13}C NMR (DMSO-d_6, 100 MHz): δ (ppm) = 158.2, 138.0, 133.6, 133.0, 130.1, 130.6, 130.5, 127.4, 126.8, 119.8, 113.6, 113.5, 52.5, 33.1. ^{77}Se NMR (DMSO-d_6, 76 MHz): δ (ppm) = 317, -274; ESI-MS *m/z* calcd for $C_{16}H_{15}N_2Se^+$ [M^+]: 315.0395; obs: 315.0456. FT-IR ($\bar{\nu}$, cm^{-1}): 3022 (w), 2069 (s), 1515 (m), 1453 (s), 1026 (s), 754 (s).

Compound **5.7**: Prepared according to **GP1** from compound **5.19** (0.34 g, 0.80 mmol),

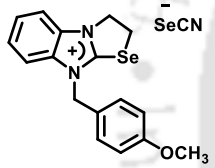

potassium selenocyanate (0.35 g, 2.40 mmol) and acetonitrile (8 ml). Crude product was further purified using neutral alumina column chromatography using methanol in dichloromethane as eluent to afford the purified title compound as yellowish white solid. R_f = 0.4 (5% methanol in ethyl acetate). Yield: 0.10 g (28%). M.P.: 145 – 146 °C. ^{1}H NMR (DMSO-d_6, 600 MHz): δ (ppm) = 7.95 (d, 1H, *J* = 7.7 Hz), 7.83 (d, 1H, *J* = 7.4 Hz), 7.58 – 7.53 (m, 2H), 7.45 (d, 2H, *J* = 8.3 Hz), 7.01 (d, 2H, *J* = 8.4 Hz), 5.58 (s, 2H), 4.69 (t, 2H, *J* = 7.6 Hz), 4.14 (t, 2H, *J* = 7.5 Hz), 3.77 (s, 3H). ^{13}C NMR (DMSO-d_6, 150 MHz): δ = 160.3, 157.3, 136.4, 131.7, 131.5, 126.1, 125.5, 125.0, 116.7, 114.9, 113.2, 113.1, 55.7, 50.6, 47.6, 33.4. ^{77}Se NMR (DMSO-d_6, 76 MHz): δ = 317, -276. ESI-MS *m/z* calcd for $C_{17}H_{18}N_2OSe^+$ [$M]^+$: 345.0501; obs: 345.0566. FT-IR ($\bar{\nu}$, cm^{-1}): 2062 (s), 1607 (w), 1509 (s), 1461 (s), 1438 (s), 1305 (w), 1177 (s), 1018 (s), 824 (s), 761 (s).

General procedure 2 (GP2) for synthesis of 1-aryl-3-(3-selenocyanatopropyl)-benzimidazole (**4.11d**, **5.9**, **5.10**):

Prepared according to literature procedure with minor modifications as required.[8] Precursor bromides (compound **4.9b-2**, **5.21**, **5.22**) (1.0 equiv) were stirred with potassium selenocyanate (3.0 equiv) in dry acetonitrile for 12 h at room temperature under inert. Progress of the reaction was monitored by TLC analysis. After completion,

the solution was evaporated to dryness under reduced pressure. The residue was directly purified by column chromatography using ethyl acetate and petroleum ether to afford the purified compound as solid powder in good to excellent yields.

Compound 4.11d: Prepared according to **GP2** from compound **4.9b-2** (0.20 g, 0.49 mmol), KSeCN (0.21 g, 1.46 mmol) and acetonitrile (6 mL). Crude product was further purified using neutral alumina column chromatography using dichloromethane in methanol in ethyl acetate as eluent to afford the purified title compound as orange solid. R_f = 0.4 (10% methanol in dichloromethane). Yield: 0.11 g (52%). M.P. = 164 – 166 °C. ^{1}H NMR (DMSO-d_6, 600 MHz): δ (ppm) = 7.95 – 7.92 (m, 2H), 7.60 – 7.55 (m, 2H), 7.42 – 7.35 (m, 5H), 5.67 (s, 2H), 4.49 (t, 2H, *J* = 5.6 Hz), 3.56 – 3.54 (m, 2H), 2.58 – 2.54 (m, 2H). ^{13}C NMR (DMSO-d_6, 150 MHz): δ (ppm) = 148.5, 134.2, 134.0, 132.4, 129.4, 129.0, 128.1, 126.3, 125.7, 116.7, 112.4, 49.2, 45.0, 23.9, 22.9; ^{77}Se NMR (DMSO-d_6, 76 MHz): δ (ppm) = 277, -276; ESI-MS *m/z* calcd for $C_{17}H_{17}N_2Se^+$ $[M]^+$: 329.0551; obs: 329.0668. FT-IR ($\bar{\nu}$, cm^{-1}): 2921 (w), 2065 (s), 1467 (s), 1422 (s), 1006 (m), 756 (s).

Compound 5.9: Prepared according to **GP2** from compound **5.17** (0.20 g, 0.56 mmol), KSeCN (0.24 g, 1.66 mmol) and acetonitrile (6 mL). Crude product was further purified using neutral alumina column chromatography using 5% methanol in ethyl acetate as eluent to afford the purified title compound as pale yellow solid. R_f = 0.4 (10% methanol in ethyl acetate). Yield: 0.10 g (40%). M.P.: 139 - 141 °C. ^{1}H NMR (DMSO-d_6, 600 MHz): δ (ppm) = 8.03 – 7.98 (m, 2H), 7.64 – 7.63 (m, 2H), 7.39 (d, 2H, *J* = 7.7 Hz), 7.01 (d, 2H, *J* = 8.2 Hz), 5.63 (s, 2H), 4.54 (t, 2H, *J* = 5.6 Hz), 3.80 (s, 3H), 3.60 (t, 2H, *J* = 5.9 Hz), 2.61 (t, 2H, *J* = 5.9 Hz). ^{13}C NMR (DMSO-d_6, 150 MHz): δ (ppm) = 159.8, 148.1, 134.0, 132.4, 129.9, 126.2, 125.6, 114.8, 112.5, 112.4, 55.7, 48.9, 44.9, 23.8, 22.9. ^{77}Se NMR (DMSO-d_6, 76 MHz): δ (ppm) = 278, -276. ESI-MS *m/z* calcd for $C_{18}H_{19}N_2OSe^+$ $[M^+]$: 329.0551; obs: 329.0668. FT-IR ($\bar{\nu}$, cm^{-1}): 2061 (m), 1466 (m), 1416 (m), 1246 (s), 1015 (s), 808 (m), 762 (s).

Compound 5.10: Prepared according to **GP2** from compound **5.22** (0.15 g, 0.33 mmol), KSeCN (0.14 g, 0.99 mmol), and acetonitrile (6 mL). Crude product was further purified using neutral alumina column chromatography using 10% methanol in ethyl acetate as eluent to afford the purified title

compound as reddish solid. R_f = 0.3 (10% methanol in ethyl acetate). Yield: 0.13 g (82%). M.P.: 144 - 146 °C. ^{1}H NMR (DMSO-d_6, 400 MHz): δ (ppm) = 8.25 (d, 2H, *J* = 8.4 Hz), 7.96 (d, 1H, *J* = 7.8 Hz), 7.87 (d, 1H, *J* = 7.7 Hz), 7.62 – 7.56 (m, 2H), 5.85 (s, 2H), 4.50 (t, 2H, *J* = 5.5 Hz), 3.55 (t, 2H, *J* = 5.8 Hz), 2.57 (br s, 2H). ^{13}C NMR (DMSO-d_6, 100 MHz): δ (ppm) = 148.9, 147.9, 141.6, 134.0, 132.4, 129.1, 126.4, 125.8, 124.4, 112.5, 112.2, 48.4, 45.0, 24.0, 22.9. ^{77}Se NMR (DMSO-d_6, 76 MHz): δ (ppm) = 278, -276. ESI-MS *m/z* calcd for $C_{17}H_{16}N_3O_2^+$ $[M]^+$: 374.0402, obs: 374.0409. FT-IR ($\bar{\nu}$, cm^{-1}): 3434 (m), 2926 (w), 2078 (s), 2053(m), 1522 (s), 1345 (s), 1011 (w), 763 (m).

General procedure 3 (GP3) for synthesis of 1-aryl-2-phenyl-3-(3-selenocynatopropyl)-benzimidazole (Compound **5.11**, **5.12**, **5.13**):

Title compounds were synthesized according to literature method with modifications as required.[8] Precursor compound (Compound **5.28**, **5.29, 5.30**) (1.0 equiv) was stirred with potassium selenocyanate (3.0 equiv) in dry acetonitrile for 12 h at room temperature under inert. Progress of the reaction was monitored by thin layer chromatographic analysis. After completion, the solution was evaporated to dryness under reduced pressure. The residue was directly purified by column chromatography using ethyl acetate and petroleum ether to afford the purified compound as sticky liquid.

Compound 5.11: Prepared according to **GP3** from compound **5.28** (0.15 g, 0.31 mmol), KSeCN (0.13 g, 0.90 mmol) and acetonitrile (2 mL). Crude product was further purified using neutral alumina column chromatography using 100% ethyl acetate as eluent to afford the purified title compound as colorless liquid. R_f = 0.5 (100% ethyl acetate). Yield: 0.09 g (68%). ^{1}H NMR ($CDCl_3$, 600 MHz): δ (ppm) = 8.28 (d, 1H, *J* = 8.4 Hz), 7.96 (d, 1H, *J* = 8.4 Hz), 7.91 (d, 2H, *J* = 7.6 Hz), 7.85 – 7.70 (m, 5H), 7.31 (d, 3H, *J* = 5.9 Hz), 7.19 (d, 2H, *J* = 6.8 Hz), 5.57 (s, 2H), 4.44 (t, 2H, *J* = 7.6 Hz), 3.05 (t, 2H, *J* = 7.3 Hz), 2.31 (t, 2H, *J* = 7.6 Hz). ^{13}C NMR ($CDCl_3$, 150 MHz): δ (ppm) = 151.2, 134.3, 133.6, 131.7, 131.6, 130.8, 130.2, 129.2, 128.8, 127.7, 127.4, 121.4, 114.4, 114.2, 104.8, 49.4, 45.8, 30.7, 26.5. ^{77}Se NMR ($CDCl_3$, 95 MHz): δ (ppm) = 218, -301. ESI-MS *m/z* calcd for $C_{24}H_{22}N_3Se^+$ $[M]^+$ 432.0973; Obs: 432.1207. FT-IR ($\bar{\nu}$, cm^{-1}): 3029 (w), 2145 (w), 2060 (s), 1505 (m), 1463 (s), 1026 (m), 748 (s).

Compound 5.12: Prepared according to **GP3** from compound **5.24** (0.06 g, 0.12 mmol),

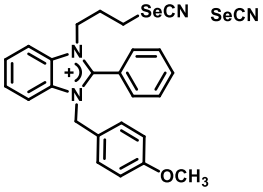

KSeCN (0.05 g, 0.36 mmol) and acetonitrile (2 mL). Crude product was further purified using neutral alumina column chromatography using 10% methanol in ethyl acetate as eluent to afford the purified title compound as colorless sticky liquid. R_f = 0.3 (100% ethyl acetate). Yield: 0.06 g (91%). ^{1}H NMR (DMSO-d_6, 600 MHz): δ (ppm) = 8.27 (d, 1H, *J* = 8.3 Hz), 7.99 (d, 1H, *J* = 8.3 Hz), 7.94 (d, 2H, *J* = 7.6 Hz), 7.85 (t, 1H, *J* = 7.6 Hz), 7.78 (t, 3H, *J* = 7.7 Hz), 7.72 (t, 1H, *J* = 7.9 Hz), 7.13 (d, 2H, *J* = 8.3 Hz), 6.86 (d, 2H, *J* = 8.4 Hz), 5.49 (s, 2H), 4.43 (t, 2H, *J* = 7.7 Hz), 3.71 (s, 3H), 3.06 (t, 2H, *J* = 7.3 Hz). 2.31 (m, 2H). ^{13}C NMR (DMSO-d_6, 150 MHz): δ (ppm) = 159.6, 151.0, 133.6, 131.7, 131.5, 130.9, 130.2, 129.4, 127.3, 126.0, 121.5, 116.8, 114.6, 114.5, 114.2, 104.8, 55.6, 49.1, 45.8, 30.7, 26.5. ^{77}Se NMR (DMSO-d_6, 95 MHz): δ (ppm) = 221, -274. ESI-MS *m/z* calcd for $C_{25}H_{24}N_3OSe^+$ $[M]^+$: 462.1079; Obs: 462.1325. FT-IR ($\bar{\nu}$, cm^{-1}): 3032 (w), 2150 (w), 2060 (s), 1603 (m), 1479 (s), 1342 (s).

Compound 5.13: Prepared according to **GP3** from compound **5.30** (0.10 g, 0.23 mmol),

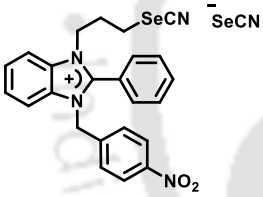

KSeCN (0.07 g, 0.05 mmol) and acetonitrile (2 mL). Crude product was further purified using neutral alumina column chromatography using 100% ethyl acetate as eluent to afford the purified title compound as red sticky solid. R_f = 0.3 (100% ethyl acetate). Yield: 0.04 g (52%). ^{1}H-NMR (DMSO-d_6, 600 MHz): δ (ppm) = 8.31 (d, 1H, *J* = 8.4 Hz), 8.16 (d, 2H, *J* = 8.8 Hz), 7.96 (d, 1H, *J* = 8.4 Hz), 7.87 – 7.86 (m, 2H), 7.83 – 7.80 (m, 2H), 7.75 – 7.71 (m, 3H), 7.47 (d, 2H, *J* = 8.0 Hz), 5.74 (s, 2H), 4.44 (t, 2H, *J* = 7.4 Hz), 3.07 (t, 2H, *J* = 6.6 Hz), 2.33 (p, 2H, *J* = 7.1 Hz). ^{13}C NMR (DMSO-d_6, 150 MHz): δ (ppm) = 151.5, 147.7, 141.9, 133.7, 131.8, 131.7, 130.7, 130.2, 128.8, 127.6, 127.5, 124.2, 121.2, 116.8, 114.3, 114.2, 104.8, 48.8, 45.9, 30.7, 26.4. ^{77}Se NMR (DMSO-d_6, 95 MHz): δ (ppm) = 221, -275. ESI-MS *m/z* calcd for $C_{24}H_{21}N_4O_2Se^+$: 477.0830; Obs: 477.1068. FT-IR ($\bar{\nu}$, cm^{-1}): 3419 (w), 2937 (w), 2150 (w), 2060 (s), 1603 (m), 1518 (s), 1479 (s), 1342 (s), 1027 (w), 846 (w), 751 (s).

General procedure 4 (GP4) for synthesis of 1-(3-selenocyanatopropyl)-2-aryl-1H-benz[d]imidazole (Compound **5.12**, **5.13**, **5.14):**

Title compounds were prepared according to reported literature method.[8] Briefly, precursor bromides **5.28**, **5.29** or **5.30** (1.0 equiv) were stirred with potassium

selenocyanate (1.5 equiv) in dry acetonitrile for 4 – 6 hours at room temperature under inert. Progress of the reaction was monitored by TLC analysis. After completion, the solution was evaporated to dryness under reduced pressure. The residue was extracted with ethyl acetate (3 × 10 mL) and was washed with water (2 × 10 mL) and brine (1 × 10 mL). Combined organic layer was dried over anhyd. sodium sulfate and was concentrated *in vacuo* to yield the crude compound. The crude compound was further purified by column chromatography using ethyl acetate and petroleum ether to afford the purified compound as solid powder in good to excellent yields.

Compound **5.14**: Prepared according to **GP4** from compound **5.33** (0.13 g, 0.41 mmol), KSeCN (0.09 g, 0.62 mmol) and acetonitrile (4 mL). Crude product was further purified using neutral alumina column chromatography using 20% ethyl acetate in petroleum ether as eluent to afford the purified title compound as sticky white solid. Yield: 0.06 g (44%). M.P.: 94 – 96 °C. ^{1}H NMR ($CDCl_3$, 400 MHz): δ (ppm) = 7.86 – 7.83 (m, 1H), 7.70 – 7.67 (m, 2H), 7.58 – 7.53 (m, 3H), 7.45 – 7.42 (m, 1H), 7.37 – 7.32 (m, 2H), 4.50 (t, 2H, *J* = 6.7 Hz), 2.75 (t, 2H, *J* = 6.8 Hz), 2.40 – 2.33 (m, 2H). ^{13}C NMR ($CDCl_3$, 100 MHz): δ (ppm) = 153.6, 143.2, 135.1, 130.2, 130.1, 129.3, 129.2, 123.3, 122.9, 120.4, 109.8, 100.7, 43.0, 30.4, 25.9. ^{77}Se NMR ($CDCl_3$, 76 MHz): δ (ppm) = 212. ESI-MS *m/z* calcd for $C_{17}H_{16}N_3Se$ $[M+H]^+$: 342.0509; Obs: 342.0594. FT-IR ($\bar{\nu}$, cm^{-1}): 2918 (w), 2145 (w), 1454 (s), 1253 (m), 1207 (w), 1019 (m), 748 (s), 697 (s).

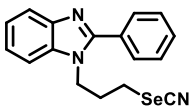

Compound **5.15:** Prepared according to **GP4** from compound **5.34** (0.08 g, 0.23 mmol), KSeCN (0.06 g, 0.39 mmol) and acetonitrile (3 mL). Crude product was further purified using neutral alumina column chromatography using ethyl acetate and petroleum ether as eluent to afford the purified title compound as white solid. R_f = 0.4 (50% ethyl acetate in petroleum ether). Yield: 0.03 g (40%). M.P.: 129 – 131 °C. ^{1}H NMR ($CDCl_3$, 100 MHz): δ (ppm) = 7.83 – 7.81 (m, 1H), 7.63 (d, 2H, *J* = 8.3 Hz), 7.42 – 7.40 (m, 1H), 7.35 – 7.31 (m, 2H), 7.07 (2H, d, *J* = 8.3 Hz), 4.48 (t, 2H, *J* = 6.7 Hz), 3.90 (s, 3H), 2.76 (t, 2H, *J* = 6.9 Hz), 2.37 (m, 2H). ^{13}C NMR ($CDCl_3$, 100 MHz): δ (ppm) = 160.0, 152.6, 142.2, 134.2, 129.8, 122.0, 121.7, 121.4, 119.1, 113.6, 108.6, 99.6, 54.4, 42.0, 29.4, 24.9. ^{77}Se NMR ($CDCl_3$, 76 MHz): δ (ppm) = 215. ESI-MS *m/z* calcd for $C_{18}H_{18}N_3OSe$ $[M+H]^+$: 372.0615; Obs:

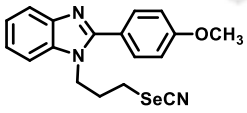

372.0645. FT-IR ($\bar{\nu}$, cm^{-1}): 2994 (w), 2925 (w), 2146 (w), 1610 (m), 1455 (s), 1248 (s), 1176 (m), 835 (m), 750 (m).

Compound **5.16**: Prepared according to **GP4** from compound **5.35** (0.05 g, 0.14 mmol), 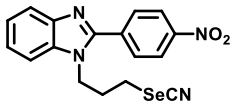

KSeCN (0.03 g, 0.24 mmol) and acetonitrile (3 mL). Crude product was further purified using neutral alumina column chromatography using 50% ethyl acetate in petroleum ether as eluent to afford the purified title compound as yellow solid. R_f = 0.4 (50% ethyl acetate in petroleum ether). Yield: 0.05 g (93%). M.P.: 148 – 150 °C. ^{1}H NMR ($CDCl_3$, 400 MHz): δ (ppm) = 8.43 (d, 2H, *J* = 8.8 Hz), 7.95 (d, 2H, *J* = 8.8 Hz), 7.88 – 7.86 (m, 1H), 7.49 – 7.47 (m, 1H), 7.41 – 7.38 (m, 2H), 4.51 (t, 2H, *J* = 7.2 Hz), 2.86 (t, 2H, *J* = 6.9 Hz), 2.43 (m, 2H). ^{13}C NMR ($CDCl_3$, 100 MHz): δ (ppm) = 150.9, 148.2, 143.2, 136.4, 135.5, 130.3, 124.3, 124.2, 123.5, 120.8, 110.0, 43.6, 30.6, 25.42. ^{77}Se NMR ($CDCl_3$, 76 MHz): δ (ppm) = 214. ESI-MS *m/z* calcd for $C_{17}H_{15}N_4O_2Se$ $[M+H]^+$: 387.0360; Obs: 387.0440. FT-IR ($\bar{\nu}$, cm^{-1}): 3069 (w), 2925 (w), 2153 (m), 1600 (s), 1511 (s), 1347 (s), 1107 (w), 854 (m), 742 (m).

General procedure 5 (GP5) for synthesis of 1-arylbenzimidazole (**4.9b**, **5.17**, **5.18**):

Prepared following previously reported literature with minor modification as required.[9] Benzimidazole **4.9** (2.0 equiv) and KOH (1.5 equiv) was dissolved in acetonitrile and to it, corresponding benzylic halides (1.5 equiv) was added dropwise slowly. The solution was stirred at room temperature for 5 h. Progress of the reaction was monitored by TLC analysis. After completion of the reaction, the solid was filtered and washed with acetonitrile. The filtrate was concentrated *in vacuo*. The residue was extracted with ethyl acetate and washed with water and brine. Combined organic layer was dried over anhyd. Na_2SO_4 and was concentrated *in vacuo* to yield the crude compound. It was further purified by column chromatography using ethyl acetate and petroleum ether as eluting solvent to afford the purified compound.

Compound 4.9b: Prepared according to **GP5** using benzimidazole (0.50 g, 4.23 mmol), 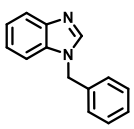

benzyl bromide (1.08 g, 6.35 mmol), KOH (0.47 g, 8.46 mmol) and acetonitrile (10 mL). Crude product was further purified using silica gel (60 – 120) column chromatography using 50% ethyl acetate in petroleum ether as eluent to afford the purified title compound as white solid. ^{1}H NMR ($CDCl_3$, 600 MHz): δ (ppm) = 7.95 (s, 1H), 7.83 (d, 1H, *J* = 7.9 Hz), 7.35 – 7.25 (m, 6H), 7.19 (d,

2H, *J* = 6.1 Hz), 5.37 (s, 2H), ^{13}C NMR ($CDCl_3$, 150 MHz): δ (ppm) = 143.9, 143.2, 135.4, 133.9, 129.0, 128.2, 127.0, 123.1, 122.3, 120.4, 110.0, 48.8.

Compound 5.17: Prepared according to **GP5** from benzimidazole (0.25 g, 2.12 mmol), 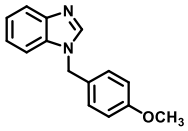 4-methoxybenzyl chloride (0.4 g, 2.54 mmol), KOH (0.24 g, 4.23 mmol) and acetonitrile (5 mL).[10] Crude product was further purified using silica gel (230 – 400) flash chromatography using to afford the purified title compound as beige solid. R_f = 0.6 (100% ethyl acetate). Yield: 0.5 g (99%). ^{1}H NMR ($CDCl_3$, 600 MHz): δ (ppm) = 7.92 (s, 1H), 7.82 (d, 1H, *J* = 7.2 Hz), 7.33 – 7.23 (m, 3H), 7.14 (d, 2H, *J* = 8.5 Hz), 6.87 (d, 2H, *J* = 8.7 Hz), 5.29 (s, 2H), 3.79 (s, 3H). ^{13}C NMR ($CDCl_3$, 125 MHz): δ (ppm) = 159.6, 144.0, 143.1, 133.9, 128.7, 127.4, 123.0, 122.3, 120.4, 114.5, 110.1, 55.3, 48.5. ESI-MS *m/z* calcd for $C_{15}H_{15}N_2O$ $[M+H]^+$: 239.1184; Obs: 239.1208.

Compound 5.18: Prepared according to **GP5** from benzimidazole (0.25 g, 2.12 mmol), 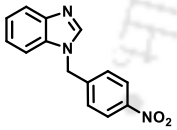 4-nitrobenzyl bromide (0.68 g, 3.17 mmol), KOH (0.24 g, 4.23 mmol) and acetonitrile (5 mL).[11] Crude product was further purified using silica gel (230 – 400) flash chromatography to afford the purified title compound as white solid. R_f = 0.6 (100% ethyl acetate). Yield: 0.35 g (83%). ^{1}H NMR ($CDCl_3$, 600 MHz): δ (ppm) = 8.21 – 8.17 (m, 1H), 8.01 (s, 1H), 7.85 (d, 1H, *J* = 8.0 Hz), 7.34 – 7.24 (m, 4H), 7.20 (d, 1H, *J* = 7.9 Hz), 5.49 (s, 2H). ^{13}C NMR ($CDCl_3$, 125 MHz): δ (ppm) = 147.9, 143.9, 143.1, 142.7, 133.6, 127.6, 124.4, 123.7, 122.9, 120.8, 109.7, 48.1. ESI-MS *m/z* calcd for $C_{14}H_{12}N_3O_2$ $[M+H]^+$: 254.0930; Obs: 254.0961.

General procedure 6 (GP6) for synthesis of 1-aryl-3-(2-bromoethyl)-benzimidazole (4.9b-1, 5.19, 5.20):

Title compounds were synthesized according to literature method with minor modifications as required. To a high excess of 1,2-dibromoethane (11.0 – 13.0 equiv), precursor **4.9b**, **5.17** or **5.18** (1.0 equiv) was added dropwise and the solution was heated at 85 ºC for 12 hours. The progress of the reaction was monitored by TLC analysis. After completion, the solvent was evaporated under vacuum and the residue was treated with dichloromethane and filtered. The filtrate was concentrated *in vacuo* to afford the crude compound. The crude compound was purified by column chromatography using petroleum ether and ethyl acetate to afford the purified product.

Compound **4.9b-1**: Prepared using **GP6** using 1,2-dibromoethane (3.25 g, 17.33 mmol) and *N*-benzylbenzimidazole **4.9b** (0.16 g, 0.62 mmol) and reaction time of 24 h. Crude product was further purified by neutral alumina column chromatography using methanol in dichloromethane to afford the pure compound **4.9b-1** as off-white solid. R_f = 0.2 (10% methanol in ethyl acetate), Yield: 0.17 g (55%). ^{1}H NMR (DMSO-d_6, 400 MHz): δ (ppm) = 10.10 (d, 1H, J = 9.9 Hz), 8.19 (d, 2H, J = 7.6 Hz), 8.01 (d, 2H, J = 8.0 Hz), 7.67 (m, 2H), 7.51 (d, 2H, J = 7.0 Hz), 7.40 (dt, 3H, J_1 = 19.1 Hz, J_2 = 7.0 Hz), 5.85 (s, 2H), 5.03 (t, 2H, J = 5.5 Hz), 4.09 (t, 2H, J = 5.6 Hz). ^{13}C NMR (DMSO-d_6, 150 MHz): δ (ppm) = 143.4, 134.4, 131.5, 131.1, 129.5, 129.2, 128.6, 127.4, 114.6, 114.5, 50.4, 48.6, 31.7.

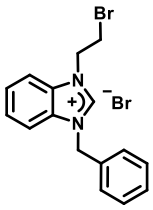

Compound **5.19**: Prepared according to **GP6** from compound **5.17** (0.35 g, 1.47 mmol), and 1,2-dibromoethane (3.31 g, 17.62 mmol). Crude product was further purified using neutral alumina column chromatography using dichloromethane in methanol as eluent to afford the purified title compound as white solid. Yield: 0.36 g (57%). ^{1}H NMR (DMSO-d_6, 400 MHz): δ (ppm) = 9.99 (s, 1H), 8.17 (dd, 1H, J_1 = 6.3 Hz, J_2 = 2.3 Hz), 8.04 (d, 1H, J = 7.0 Hz), 7.74 – 7.65 (m, 2H), 7.49 (d, 2H, J = 8.6 Hz), 6.98 (d, 2H, J = 8.7 Hz), 5.78 – 5.74 (m, 2H), 5.00 (t, 2H, J = 5.7 Hz), 4.06 (t, 2H, J = 5.8 Hz). ^{13}C NMR (DMSO-d_6, 150 MHz): 160.0, 143.1, 131.5, 131.1, 130.5, 127.3, 126.0, 114.8, 114.5, 55.7, 50.0, 48.5, 31.6. ESI-MS *m/z* calcd for $C_{17}H_{18}BrN_2O$ $[M]^+$: 345.0597; Obs: 345.0659.

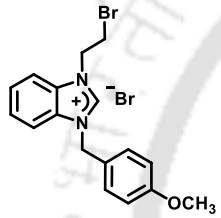

Compound **5.20**: Prepared according to **GP6** from compound **5.18** (0.30 g, 1.18 mmol), 1,2-dibromopropane (2.60 g, 14.16 mmol). Crude product was further purified using neutral alumina column chromatography using methanol in dichloromethane as eluent to afford the purified title compound as red sticky solid. Yield: 0.23 g (43%). ^{1}H NMR (DMSO-d_6, 600 MHz): δ (ppm) = 10.23 – 10.12 (m, 1H), 8.35 – 8.33 (m, 2H), 8.28 – 8.26 (m, 1H), 8.03 – 8.01 (m, 1H), 7.83 – 7.73 (m, 4H), 6.10 – 6.07 (m, 2H), 5.12 – 5.04 (m, 2H, J = 5.8 Hz), 4.16 – 4.14 (m, 2H). ^{13}C NMR (DMSO-d_6, 150 MHz): δ (ppm) = 148.11, 143.9, 141.7, 131.5, 131.2, 129.9, 127.6, 127.5, 124.5, 114.6, 114.3, 49.6, 48.7, 31.4. ESI-MS *m/z* calcd for $C_{16}H_{15}BrN_3O_2$ $[M+H]^+$: 360.0342; Obs: 360.0386.

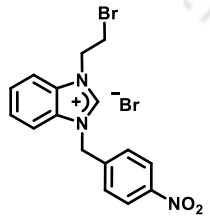

General procedure 7 (GP7) for synthesis of 1-aryl-3-(2-bromopropyl)-benzimidazole (**4.9b-2**, **5.21**, **5.22**):

Title compounds were synthesized according to literature method with minor modifications as required. To a high excess of 1,3-dibromoethane (11.0 – 13.0 equiv), precursor **4.9b**, **5.17** or **5.18** (1.0 equiv) was added dropwise and the solution was heated at 85 ºC for 12 hours. The progress of the reaction was monitored by TLC analysis. After completion, the solvent was evaporated under vacuum and the residue was treated with dichloromethane and filtered. The filtrate was concentrated *in vacuo* to afford the crude compound. The crude compound was purified by column chromatography using petroleum ether and ethyl acetate to afford the purified product.

Compound 4.9b-2: Prepared according to **GP7** from compound **4.9b** (0.19 g, 0.91 mmol), 1,3-dibromopropane (1.94 g, 9.60 mmol). Crude product was further purified using neutral alumina column chromatography using 10% methanol in dichloromethane as eluent to afford the purified title compound as white solid. Yield: 0.26 g (69%). ^{1}H NMR (DMSO-d_6, 600 MHz): δ (ppm) = 10.04 (s, 1H), 8.13 (d, 2H, *J* = 8.0 Hz), 7.96 (d, 1H, *J* = 7.9 Hz), 7.68 (p, 2H, *J* = 7.2 Hz), 7.56 – 7.54 (m, 2H), 7.44 – 7.36 (m, 3H), 5.79 (s, 2H), 4.66 (t, 2H, *J* = 7.0 Hz), 3.66 (t, 2H, *J* = 6.5 Hz), 2.54 – 2.48 (m, 2H). ^{13}C NMR (DMSO-d_6, 150 MHz): δ (ppm) = 143.3, 134.4, 131.8, 131.4, 129.4, 129.2, 128.8, 127.2, 114.4, 114.3, 50.4, 46.0, 31.8, 31.3.

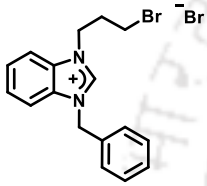

Compound 5.21: Prepared following **GP7** from compound **5.17** (0.25 g, 1.05 mmol), 1,3-dibromopropane (2.54 g, 12.6 mmol). Crude product was purified using neutral alumina column chromatography using 10% methanol in ethyl acetate as eluent to afford the purified title compound **5.21** as white solid. R_f = 0.2 (10% methanol in ethyl acetate). Yield: 0.24 g (45%). ^{1}H NMR ($CDCl_3$, 500 MHz): δ (ppm) = 11.42 (s, 1H), 7.79 (t, 1H, *J* = 8.7 Hz), 7.62 – 7.60 (m, 2H), 7.54 (t, 1H, *J* = 7.8 Hz), 7.48 (d, 2H, *J* = 8.2 Hz), 6.87 (d, 2H, *J* = 8.7 Hz), 5.77 (s, 2H), 4.85 (t, 2H, *J* = 7.2 Hz), 3.75 (s, 3H), 3.71 (t, 1H, *J* = 5.8 Hz), 3.55 (t, 1H, *J* = 5.9 Hz), 2.75 – 2.61 (m, 2H). ^{13}C NMR ($CDCl_3$, 125 MHz): δ (ppm) = 160.3, 143.1, 131.7, 131.1, 130.1, 127.3, 127.2, 124.6, 114.8, 113.9, 113.1, 113.0, 55.4, 51.3, 45.9, 44.8, 41.7, 32.2, 32.1, 29.8. ESI-MS *m/z* calcd for $C_{18}H_{20}BrN_2O$ $[M]^+$: 359.0754; Obs: 359.0799.

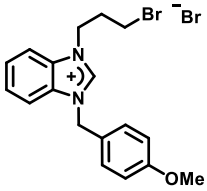

Compound 5.22: Prepared according to **GP7** from compound **5.18** (0.40 g, 1.58 mmol), 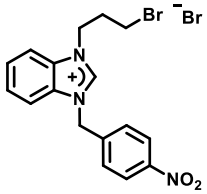 and 1,3-dibromopropane (3.83 g, 18.96 mmol). Crude product was further purified using neutral alumina column chromatography using 10% methanol in ethyl acetate as eluent to afford the purified title compound as pale yellow solid. Yield: 0.53 g (73%). ^{1}H NMR (DMSO-d_6, 500 MHz): δ (ppm) = 10.00 (s, 1H), 8.27 (d, 2H, *J* = 8.4 Hz), 8.14 (d, 1H, *J* = 8.3 Hz), 7.91 (d, 1H, *J* = 8.3 Hz), 7.78 (d, 2H, *J* = 8.4 Hz), 7.73 – 7.65 (m, 4H), 5.95 (s, 2H), 4.66 (t, 2H, *J* = 6.9 Hz), 3.66 (t, 2H, *J* = 6.5 Hz), 2.54 – 2.53 (m, 2H). ^{13}C NMR ($CDCl_3$, 125 MHz): δ (ppm) = 148.1, 143.7, 141.7, 131.9, 131.4, 130.0, 127.4, 127.3, 124.4, 114.3, 114.2, 49.6, 46.1, 45.1, 42.5, 31.8, 31.6, 31.2. ESI-MS *m/z* calcd for $C_{17}H_{17}BrN_3O_2$ $[M+H]^+$: 374.0499; Obs: 374.0502

Synthesis of Compound 5.24: Title compound was synthesized following literature 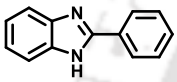 method.[12,13] *o*-phenylenediamine (0.20 g, 1.85 mmol.) was dissolved in water and sodium bisulphite (2.10 g, 20.35 mmol) was added to it and refluxed at 100 °C for 10 min. Then benzaldehyde (0.20 g, 1.85 mmol) was added to it and was refluxed for 30 min. Solid precipitate was formed in course of the reaction. Progress of the reaction was monitored by TLC analysis. After completion, the solid was filtered and the residue was washed with water (3 × 20 mL), and diethyl ether (1 × 10 mL) and was dried under reduced pressure to afford the crude compound. The crude compound was further purified by column chromatography using petroleum ether and ethyl acetate as eluting solvent to afford the purified title compound **5.24** as white solid. R_f = 0.5 (50% ethyl acetate in petroleum ether). Yield: 0.18 g (50%). ^{1}H NMR ($CDCl_3$, 400 MHz): δ (ppm) = 8.06 (d, 2H, *J* = 6.6 Hz), 7.65 (s, 2H), 7.52 – 7.45 (m, 1H), 7.28 (dd, 2H, J_1 = 6.1 Hz, J_2 = 3.1 Hz). ^{13}C NMR ($CDCl_3$, 125 MHz): δ (ppm) = 151.6, 130.3, 129.8, 129.1, 126.6, 123.0. ESI-MS *m/z* calcd for $C_{13}H_{11}N_2$ $[M+H]^+$: 195.0922; Obs: 195.1005.

General procedure 8 (GP8) for synthesis of 1-aryl-2-phenylbenzimidazole (compounds 5.25, 5.26, 5.27):

Title compounds were synthesized according to literature method with minor modifications.[9] To a solution of compound **5.24** (1.0 equiv), and KOH (1.0 equiv) in acetonitrile, appropriately substituted aryl halide (1.0 equiv) was added and was stirred at room temperature for 3 h. Progress of the reaction was monitored by TLC analysis.

After completion, the solvent was evaporated to dryness under reduced pressure. The residue was extracted with ethyl acetate (2 × 20 mL) and was washed with water (2 × 10 mL) and brine (1 × 10 mL). Combined organic layer was dried over anhyd. sodium sulfate and was concentrated *in vacuo* to afford the crude product. It was further purified by column chromatography using ethyl acetate and petroleum ether as eluting solvent to afford the purified product as title compound.

Compound 5.25: Prepared according to **GP8** from compound **5.24** (0.20 g, 1.03 mmol), benzyl bromide (0.18 g, 1.03 mmol), KOH (0.12 g, 2.06 mmol) and acetonitrile (5 mL). Crude product was further purified using neutral alumina column chromatography using ethyl acetate in petroleum ether as eluent to afford the purified title compound as white solid.[14] R_f = 0.7 (10% ethyl acetate in pet. ether), yield: 0.21 g (71%). ^{1}H NMR ($CDCl_3$, 400 MHz): δ (ppm) = 7.87 (d, 1H, *J* = 8.0 Hz), 7.70 – 7.68 (m, 2H), 7.48 – 7.44 (m, 3H, *J* = 5.8 Hz), 7.34 – 7.30 (m, 4H), 7.24 – 7.22 (m, 2H), 7.11 (d, 2H, *J* = 6.7 Hz), 5.46 (s, 2H). ^{13}C NMR ($CDCl_3$, 125 MHz): δ (ppm) = 154.2, 143.3, 136.5, 136.1, 130.2, 129.9, 129.3, 129.1, 128.8, 127.8, 126.0, 123.1, 122.7, 120.1, 110.5, 48.4. ESI-MS *m/z* calcd for $C_{20}H_{17}N_2$ $[M+H]^+$: 285.1392; Obs: 285.1473.

Compound 5.26: Prepared according to **GP8** from compound **5.24** (0.13 g, 0.67 mmol), 4-methoxybenzyl chloride (0.16 g, 1.00 mmol), KOH (0.07 g, 1.34 mmol) and acetonitrile (2 mL). Crude product was further purified using neutral alumina column chromatography using 50% ethyl acetate in petroleum ether as eluent to afford the purified title compound as yellow solid. R_f = 0.5 (50% ethyl acetate in pet. ether), yield: 0.14 g (66%). ^{1}H NMR ($CDCl_3$, 600 MHz): δ (ppm) = 7.86 (d, 1H, *J* = 8.0 Hz), 7.70 – 7.69 (m, 2H), 7.49 – 7.46 (m, 2H), 7.32 – 7.29 (m, 1H), 7.24 – 7.23 (m, 2H), 7.02 (d, 2H, *J* = 8.4 Hz), 6.85 (d, 2H, *J* = 8.7 Hz), 5.40 (s, 2H), 3.78 (s, 3H). ^{13}C NMR ($CDCl_3$, 150 MHz): δ (ppm) = 159.1, 154.1, 143.2, 136.0, 130.2, 129.9, 129.3, 128.7, 128.4, 127.3, 123.0, 122.6, 119.9, 114.4, 110.6, 55.3, 47.9, 29.7. ESI-MS *m/z* calcd for $C_{21}H_{19}N_2O$ $[M+H]^+$: 315.1497; Obs: 315.1551.

Compound 5.27: Prepared according to **GP8** from compound **5.24** (0.30 g, 1.50 mmol), 4-nitrobenzyl bromide (0.40 g, 1.85 mmol), KOH (0.17 g, 3.00 mmol)

as yellow solid.[15] R_f = 0.5 (50% ethyl acetate in pet. ether), yield: 0.20 g (39%). ^{1}H N MR ($CDCl_3$, 500 MHz): δ (ppm) = 8.19 (d, 2H, *J* = 8.7 Hz), 7.89 (d, 1H, *J* = 8.0 Hz), 7.63 – 7.61 (m, 1H), 7.51 – 7.44 (m, 3H), 7.35 (t, 1H, *J* = 7.8 Hz), 7.28 – 7.24 (m, 3H), 7.15 (d, 1H, *J* = 8.0 Hz), 5.54 (s, 2H). ^{13}C NMR ($CDCl_3$, 125 MHz): δ (ppm) = 154.1, 147.7, 143.6, 143.3, 135.7, 130.2, 129.8, 129.2, 129.0, 126.9, 124.4, 123.5, 123.2, 120.4, 110.0, 47.9. ESI-MS *m/z* calcd for $C_{20}H_{16}N_3O_2$ $[M+H]^+$: 330.1243; Obs: 330.1288.

General procedure 9 (GP9) for synthesis of 1-aryl-2-phenyl-3-(3-bromopropyl)-benzimidazole (Compound **5.28**, **5.29**, **5.30)**:

Synthesis was performed following reported literature with minor modifications.[16] To a high excess of 1,3-dibromoethane (12.0 - 14.0 equiv), precursor compound **5.25**, **5.26**, **5.27** (1.0 equiv) was added dropwise and the solution was heated at 100 ºC for 12 h. The progress of the reaction was monitored by TLC analysis. After completion, the solvent was evaporated under vacuum and the residue was treated with dichloromethane and filtered. The filtrate was concentrated *in vacuo* to afford the crude compound. The crude compound was purified by column chromatography using petroleum ether and ethyl acetate to afford the purified product.

Compound 5.28: Prepared according to **GP9** from compound **5.20** (0.20 g, 0.70 mmol) and 1,3-dibromopropane (1.70 g, 8.40 mmol). Crude product was further purified using neutral alumina column chromatography using 10% methanol in ethyl acetate as eluent to afford the purified title compound as white sticky solid. R_f = 0.5 (5% methanol in ethyl acetate), yield: 0.18 g (63%).^{1}H NMR ($CDCl_3$, 600 MHz): δ (ppm) = 8.09 (d, 1H, *J* = 8.5 Hz), 8.04 (d, 2H, *J* = 7.6 Hz), 7.75 (t, 1H, *J* = 7.5 Hz), 7.70 – 7.58 (m, 5H), 7.31 – 7.30 (m, 3H), 7.08 – 7.07 (m, 2H), 5.63 (s, 2H), 4.65 (t, 2H, *J* = 7.0 Hz), 3.62 (t, 2H, *J* = 5.6 Hz), 2.40 (m, 2H). ^{13}C NMR ($CDCl_3$, 125 MHz): δ (ppm) = 151.1, 133.4, 133.2, 131.8, 131.7, 130.8, 130.1, 129.4, 128.9, 127.6, 127.5, 127.0, 120.9, 114.2, 113.7, 50.9, 44.4, 42.0, 31.9. ESI-MS *m/z* calcd for $C_{23}H_{22}BrN_2$ $[M]^+$: 405.0961, 407.0941; Obs: 405.1023, 407.1019.

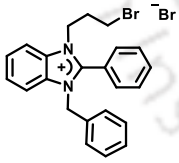

Compound 5.29: Prepared according to **GP9** from compound **5.21** (0.13 g, 0.41 mmol) and 1,3-dibromopropane (1.00 g, 4.96 mmol). Crude product was further purified using neutral alumina column chromatography using 20%

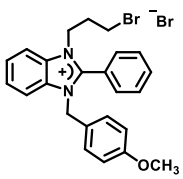

methanol in ethyl acetate as eluent to afford the purified title compound as gummy white solid. R_f = 0.5 (5% methanol in ethyl acetate), yield: 0.06 g (63%). ^{1}H NMR ($CDCl_3$, 500 MHz): δ (ppm) = 8.09 – 8.04 (m, 3H), 7.76 (t, 1H, *J* = 7.5 Hz), 7.71 – 7.64 (m, 4H), 7.59 – 7.56 (m, 1H), 7.02 (d, 2H, *J* = 8.3 Hz), 6.82 (d, 2H, *J* = 8.5 Hz), 5.55 (s, 2H), 4.64 (t, 2H, *J* = 7.1 Hz), 3.76 (s, 3H), 3.62 (t, 2H, *J* = 5.6 Hz), 2.39 (p, 2H, *J* = 6.6 Hz). ^{13}C NMR ($CDCl_3$, 125 MHz): δ (ppm) = 160.0, 150.9, 133.4, 131.7, 131.6, 130.9, 130.1, 130.0, 128.6, 127.5, 125.0, 121.0, 114.7, 114.3, 113.7, 55.4, 50.5, 44.4, 42.0, 31.9. ESI-MS *m/z* calcd for $C_{24}H_{24}BrN_2O$ $[M]^+$: 435.1067; Obs: 435.1148.

Compound 5.30: Prepared according to **GP9** from compound **5.22** (0.20 g, 0.60 mmol) and 1,3-dibromopropane (1.45 g, 7.20 mmol). Crude product was further purified using neutral alumina column chromatography using 15% methanol in ethyl acetate as eluent to afford the purified title compound as gummy red solid. R_f = 0.1 (100% ethyl acetate), yield: 0.22 g (67%). ^{1}H NMR (DMSO-d_6, 500 MHz): δ (ppm) = 8.27 – 8.25 (m, 1H), 8.15 (d, 2H, *J* = 8.4 Hz), 7.98 – 7.96 (m, 1H), 7.87 (t, 2H, *J* = 7.3 Hz), 7.80 (t, 2H, *J* = 7.8 Hz), 7.75 – 7.71 (m, 3H), 7.46 – 7.44 (m, 2H), 5.76 (s, 2H), 4.50 – 4.47 (m, 2H), 3.66 – 3.51 (m, 2H), 2.33 – 2.22 (m, 2H). ^{13}C NMR ($CDCl_3$, 125 MHz): δ (ppm) = 151.6, 147.8, 141.8, 133.7, 131.7, 130.7, 130.2, 130.1, 128.8, 127.6, 127.5, 124.2, 124.1, 121.2, 114.3, 114.2, 58.2, 48.8, 45.3, 44.2, 42.3, 31.9, 31.7, 31.3. ESI-MS *m/z* calcd for $C_{23}H_{21}BrN_3O_2$ $[M]^+$: 450.0812, 452.0792; Obs: 450.0876, 452.0857.

Synthesis of compound 5.31: Prepared following literature method with minor modification as required. Briefly, *o*-phenylenediamine (Compound **12**, 0.10 g, 0.92 mmol) was dissolved in water and excess sodium bisulfite (1.06 g, 10.16 mmol) was added to it and refluxed at 100 °C for 10 min. Then 4-methoxybenzaldehyde (0.15 g, 1.11 mmol) was added to it and was refluxed for 30 min. Solid precipitate was formed in course of the reaction. Progress of the reaction was monitored by TLC analysis. After completion, the solid was filtered off and the residue was washed with water (3 × 20 mL), and ether (1 × 10 mL) and was dried under reduced pressure to afford the crude compound. The crude compound was purified by column chromatography using petroleum ether and ethyl acetate as eluting solvent to afford the purified title compound **14** as white solid. R_f = 0.6 (50% ethyl acetate in petroleum ether). Yield: 0.11 g (53%). ^{1}H NMR ($CDCl_3$, 400 MHz): δ (ppm) = 7.99 (d, *J*

= 8.4 Hz, 2H), 7.62 (br s, 2H), 7.26 (s, 4H), 7.01 (d, *J* = 8.4 Hz, 2H), 3.87 (s, 3H). ^{13}C NMR ($CDCl_3$, 125 MHz): δ (ppm) = 161.3, 151.6, 128.0, 122.8, 122.4, 114.5, 55.4. ESI-MS *m/z* calcd for $C_{14}H_{13}N_2O$ $[M+H]^+$: 225.1028; Obs: 225.1109.

Synthesis of compound 5.32:

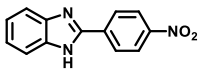

Prepared according to reported literature method with minor modifications.[17] Briefly, 4-nitrobenzaldehyde (0.26 g, 1.73 mmol) was dissolved in distilled water (20 mL) and boric acid (2.06 g, 33.3 mmol) was added to it and stirred at room temperature for 10 minutes. Next o-phenylenediamine (0.2 g, 1.85 mmol) was added to it and stirring was continued for 4 h at room temperature. Progress of the reaction was monitored by thin layer chromatography analysis. After completion, the solution was filtered under reduced pressure and the residue was washed with water (50 ml) and was dried under reduced pressure to afford the crude product. The crude product was purified using neutral alumina column chromatography using petroleum ether and ethyl acetate as eluent to afford pure title compound **5.32** as orange solid. R_f = 0.8 (10% ethyl acetate in petroleum ether). Yield: 0.30 g (72%). ^{1}H NMR ($CDCl_3$, 500 MHz): δ (ppm) = 8.63 (s, 1H), 8.31 (d, 2H, *J* = 8.7 Hz), 8.06 (d, 2H, *J* = 8.7 Hz), 7.13 – 7.11 (m, 2H), 6.81 – 6.76 (m, 2H). ^{13}C NMR ($CDCl_3$, 125 MHz): δ (ppm) = 153.8, 143.1, 142.0, 135.7, 129.3, 129.2, 129.1, 124.0, 118.5, 116.9, 115.8. ESI-MS *m/z* calcd for $C_{13}H_{10}N_3O_2$ $[M+H]^+$: 240.0773; Obs: 240.0844.

General procedure 10 (GP10) for synthesis of 1-(3-bromopropyl)-2-aryl-1H-benzo[d]imidazole (Compound **5.33**, **5.34**, **5.35)**:

Title compounds were prepared according to previously reported literature method with minor modifications.[18] Briefly, compounds **5.24**, **5.31**, or **5.32** (1.0 equiv) 1,3-dibromopropane (5.0 equiv), sodium hydroxide (5.0 equiv) and sodium iodide (*cat*.) was dissolved in acetone and was heated to 50 °C for 5 hours. Progress of the reaction was monitored by TLC analysis. After completion the solvent was evaporated to dryness under reduced pressure. The residue was extracted with ethyl acetate (2 × 10 ml) and was washed with water (2 × 10 mL) and brine (1 × 10 mL). Combined organic layer was dried over anhyd. sodium sulfate and was concentrated *in vacuo* to afford the crude product. It was further purified by column chromatography using ethyl acetate and petroleum ether to yield the purified title compound.

Compound **5.33**: Prepared according to **GP10** from compound **5.24** (0.17 g, 0.87 mmol), 1,3-dibromopropane (0.88 g, 4.37 mmol), NaOH (0.17 g, 4.37 mmol), sodium iodide (0.01 g, 10 mol%) in acetone (4 mL). Crude product was further purified using neutral alumina column chromatography using 20% ethyl acetate in petroleum ether as eluent to afford the purified title compound as yellow oil.[19] R_f = 0.7 (50% ethyl acetate in petroleum ether). Yield: 0.13 g (47%). ^{1}H NMR ($CDCl_3$, 600 MHz): δ (ppm) = 7.84 – 7.83 (m, 1H), 7.73 – 7.71 (m, 2H), 7.55 – 7.52 (m, 3H), 7.48 – 7.47 (m, 2H), 7.34 – 7.32 (m, 2H), 4.47 – 4.43 (m, 2H), 3.29 (t, 2H, J = 6.2 Hz), 2.35 – 2.30 (m, 2H). ^{13}C NMR ($CDCl_3$, 125 MHz): δ (ppm) = 153.6, 143.0, 135.5, 130.3, 130.0, 129.3, 129.0, 123.0, 122.6, 120.1, 109.9, 43.0, 32.4, 29.6. ESI-MS *m/z* calcd for $C_{16}H_{18}BrN_2$ $[M+H]^+$: 315.0497; Obs: 315.0514.

Compound **5.34**: Prepared according to **GP10** from compound **5.31** (0.11 g, 0.49 mmol), 1,3-dibromopropane (0.50 g, 2.45 mmol), NaOH (0.10 g, 2.45 mmol), NaI (0.01 g, 10 mol%) in acetone (3 mL). Crude product was further purified using neutral alumina column chromatography using 10% ethyl acetate in petroleum ether as eluent to afford the purified title compound as colorless liquid. R_f = 0.5 (25% ethyl acetate in petroleum ether). Yield: 0.08 g (36%). ^{1}H NMR ($CDCl_3$, 500 MHz): δ (ppm) = 7.82 – 7.80 (m, 1H), 7.66 (d, 2H, *J* = 8.7 Hz), 7.45 – 7.44 (m, 1H), 7.31 – 7.30 (m, 2H), 7.04 (d, 2H, *J* = 8.7 Hz), 4.45 – 4.42 (m, 2H), 3.89 (s, 3H), 3.30 (t, 2H, *J* = 6.2 Hz), 2.35 – 2.29 (m, 3H). ^{13}C NMR ($CDCl_3$, 125 MHz): δ (ppm) = 160.9, 153.6, 143.1, 135.6, 130.7, 122.8, 122.6, 122.5, 119.9, 114.4, 109.8, 55.4, 43.1, 32.5, 29.6. ESI-MS *m/z* calcd for $C_{17}H_{18}BrN_2O$ $[M+H]^+$: 345.0603; Obs: 345.0628.

Compound **5.35**: Briefly, compound **15** (0.2 g, 0.84 mmol), 1,3-dibromopropane (0.85 g, 4.2 mmol), potassium carbonate (0.58 g, 4.2 mmol) and sodium iodide (0.01 g, 10 mol%) was dissolved in acetone (3 mL) and was refluxed for 6 h. Progress of the reaction was monitored by TLC analysis. After completion, the solvent was evaporated to dryness under reduced pressure. The residue was extracted with ethyl acetate (2 × 10 mL) and was washed with water (2 × 10 mL) and brine (1 × 10 mL). Combined organic layer was dried over anhyd. sodium sulfate and was concentrated *in vacuo* to afford the crude product. The crude product was purified using neutral alumina column chromatography using 40% ethyl acetate in petroleum ether as eluent to afford the purified title compound **5.35** as orange solid. R_f =

0.7 (50% ethyl acetate in petroleum ether). Yield: 0.08 g (26%). ^{1}H NMR ($CDCl_3$, 600 MHz): 8.4 (d, 2H, *J* = 8.2 Hz), 7.96 (d, 2H, *J* = 8.3 Hz), 7.86 (d, 1H, *J* = 7.7 Hz), 7.50 (d, 1H, *J* = 7.7 Hz), 7.38 (p, 2H, *J* = 7.3 Hz), 4.51 (t, *J* = 7.3 Hz), 3.30 (t, 2H, *J* = 5.9 Hz), 2.36 (m, 2H). ^{13}C NMR ($CDCl_3$, 125 MHz): δ (ppm) = 151.0, 148.5, 143.1, 136.5, 135.7, 130.3, 124.1, 124.0, 123.3, 120.6, 110.2, 43.2, 32.3, 29.3. ESI-MS *m/z* calcd for $C_{16}H_{18}BrN_3O_2$ $[M+H]^+$: 360.0348; Obs: 360.0412.

5.5.2. Cell culture

TNBC cell lines were obtained from NCCS Pune. Dulbecco's modified Eagle's medium (DMEM) added with 10 % fetal bovine serum and 1% penicillin-streptomycin (Gibco) was used as a nutrient supplement for the MDA-MB-231 and HEK-293 cells. All the cells were maintained in CO_2-regulated humidified (95% air/5% CO_2 atmosphere) incubator at 37 °C.

5.5.3. MTT assay

The cells were plated in 96-well culture plates at a density of 2×10^3 cells per 100 µl per well for L-132 cells and 4×10^3 cells per 100 µl per well for all other cells and treated with 0.0, 5.0, 10.0 and 25.0 µM of test compounds for 0 h (Set 1) and 72 h (Set 2). At the end of the treatment period, 10.0 µL of 5.0 mg mL^{-1} of MTT was added to the plate (Set 1) and incubated for 2 h. Following the 2 h incubation, the culture medium from the plate was removed and the purple formazan crystals were dissolved using 100 µl of DMSO (Merck Life Science Pvt Ltd) and the absorbance at 570 nm was measured using a microplate reader (TECAN Infinite 200 PRO multimode reader). In Set 2, a similar MTT treatment protocol was followed only after 72 h. The mean OD values of a 0 h plate (Set 1) were subtracted from the mean OD values of identical wells at a 72 h plate (Set 2) ΔOD and the inhibition of proliferation was calculated keeping the ΔOD of the untreated control as 100%.

5.5.4. Cell cycle analysis

1×10^5 cells per 2 mL per well were seeded in 6-well plates and treated with 0.0, 5.0 and 10.0 µM of compounds **5.16** and incubated for 24 h. Following the 24 h drug treatment, the cells were collected; washed with PBS (1X); fixed with ice-cold 70% ethanol at −20 °C for 30 min; again washed with PBS (1X) and stained with PI/RNase staining buffer

(BD Biosciences) for 10 min at room temperature. The prepared samples were then analysed using a BD FACSCalibur™ instrument (BD Biosciences).

5.5.5. Wound healing (scratch) assay

MDA-MB-231 cells were seeded in a 24-well plate at a concentration of 1.5×10^5 cells per 2 mL per well and incubated in a CO_2 incubator at 37 °C to form a monolayer of cells. After the monolayer formation, the cells were pre-incubated in serum free medium for 6 h. Using a 100 µl tip, a scratch was made on the monolayer and the debris was removed by washing with PBS (1X). Then, the cells were re-incubated with serum free medium and treated with 0.0, 1.2 and 2.5 µM of active selenocyanates **5.16**. Images of the scratch were captured at regular time intervals (0, 24, 48 and 72 h) using a Nikon inverted microscope and a camera. The extent of wound healing denotes the anti-migratory effect of the compounds tested.

5.5.6. Assessment of cellular morphology and apoptotic bodies

5×10^4 cells per 1 mL per well were plated in 24-well plates and treated with 0.0, 1.2 and 2.5 µM of compounds **5.16**. The cells were observed for any morphological changes and the change in morphology was captured at regular time intervals (0, 24 and 48 h) using a Nikon inverted microscope and a camera. After 72 h, the formation of apoptotic nuclei was analysed by staining the cells with 5 µl of 1 mg mL^{-1} PI and images were taken using an Eclipse Ti-S inverted fluorescence microscope.

5.6. References

1. Talas, Z. S.; Ozdemir, I.; Yilmaz, I.; Gok, Y., *Ecotoxicol Environ Saf* **2009**, *72*, 916.
2. Alberto, E. E.; Rossato, L. L.; Alves, S. H.; Alves, D.; Braga, A. L., *Org Biomol Chem* **2011**, *9*, 1001.
3. Guan, Q.; Han, C.; Zuo, D.; Zhai, M. a.; Li, Z.; Zhang, Q.; Zhai, Y.; Jiang, X.; Bao, K.; Wu, Y., *et al.*, *Eur J Med Chem* **2014**, *87*, 306.
4. Liang, Y.; Zhou, Y.; Deng, S.; Chen, T., *ChemMedChem* **2016**, *11*, 2339.
5. Kamal, A.; Nazari V, M.; Yaseen, M.; Iqbal, M. A.; Ahamed, M. B. K.; Majid, A. S. A.; Bhatti, H. N., *Bioorg Chem* **2019**, *90*, 103042.

6. Matsumura, M.; Takahashi, T.; Yamauchi, H.; Sakuma, S.; Hayashi, Y.; Hyodo, T.; Obata, T.; Yamaguchi, K.; Fujiwara, Y.; Yasuike, S., *Beilstein J Org Chem* **2020**, *16*, 1075.
7. Murad, H.; Hawat, M.; Ekhtiar, A.; AlJapawe, A.; Abbas, A.; Darwish, H.; Sbenati, O.; Ghannam, A., *Cancer Cell Int* **2016**, *16*, 39.
8. Jacob, L. A.; Matos, B.; Mostafa, C.; Rodriguez, J.; Tillotson, J. K., *Molecules* **2004**, *9*.
9. Lin, Y.-R.; Chiu, C.-C.; Chiu, H.-T.; Lee, D.-S.; Lu, T.-J., *Appl Organometal Chem* **2018**, *32*, e3896.
10. Shao, X.; Zheng, Y.; Tian, L.; Martín-Torres, I.; Echavarren, A. M.; Wang, Y., *Org Lett* **2019**, *21*, 9262.
11. Kandathil, V.; Fahlman, B. D.; Sasidhar, B. S.; Patil, S. A.; Patil, S. A., *New J Chem* **2017**, *41*, 9531.
12. Jiang, Y.-q.; Jia, S.-h.; Li, X.-y.; Sun, Y.-m.; Li, W.; Zhang, W.-w.; Xu, G.-q., *Chem Pap* **2018**, *72*, 1265.
13. Wu, J.; Darcel, C., *J Org Chem* **2021**, *86*, 1023.
14. Kaliyan, P.; Selvaraj, L.; Muthu, S. P., *J Het Chem* **2021**, *58*, 340.
15. Senapak, W.; Saeeng, R.; Jaratjaroonphong, J.; Promarak, V.; Sirion, U., *Tetrahedron* **2019**, *75*, 3543.
16. Bernhammer, J. C.; Huynh, H. V., *Organometallics* **2014**, *33*, 172.
17. Bahrami, K.; Khodaei, M. M.; Kavianinia, I., *Synthesis* **2007**, *2007*, 547.
18. Chandrasekera, N. S.; Alling, T.; Bailey, M. A.; Files, M.; Early, J. V.; Ollinger, J.; Ovechkina, Y.; Masquelin, T.; Desai, P. V.; Cramer, J. W., *et al.*, *J Med Chem* **2015**, *58*, 7273.
19. Cai, J.-X.; Ye, T.-L.; Fan, X.-F.; Han, C.-M.; Xu, H.; Wang, L.-L.; Ma, D.-G.; Lin, Y.; Yan, P.-F., *J Mat Chem* **2011**, *21*, 15405.

भारतीय प्रौद्योगिकी संस्थान गुवाहाटी
Indian Institute of Technology Guwahati

Annexure I

Thesis Overview and Future Perspectives

Thesis Summary and Future Perspectives

The present thesis entitled "**Syntheses of Bio-active Organoselenium Compounds and Evaluation of their Anti-cancer and Antioxidant Activities**" brings forward the design and synthesis of different series of small-molecule organoselenium compounds with a particular emphasis on organoselenocyanates. All the synthesized compounds were purified, characterized and evaluated for *in vitro* anti-cancer activities towards triple-negative breast cancer cells (MDA-MB-231) as well as in a representative normal cells. The antioxidant activities of the compounds were also studied to understand the peroxide reducing capabilities of the synthesized organoselenium compounds under *in vitro* conditions.

During 1980s, benzyl selenocyanate, a simple organoselenocyanate was reported to exhibit chemopreventive activities in mice models and shown to attenuate the chemotherapeutics-induced toxicities. Inspired by this observation, we have taken the initiative to understand the anti-cancer and antioxidant activity of benzyl selenocyanate and developed several series of structural analogues to upgrade their anti-cancer activities towards triple-negative breast cancer cells (MDA-MB-231) that have limited treatment strategies. Interestingly, we have observed that the anti-proliferative activity of benzyl selenocyanate could be significantly enhanced either by increasing the number of selenocyanate functionalities in a single molecule (mesitylene-based selenocyanate **2.7**, Chapter 2) or by introducing 4-NO2 group in the phenyl ring of benzyl selenocyanate (compound **3.8**, Chapter 3). Although our strategies with the incorporation of heterocyclic pharmacophores (1,2,3-triazole and 2,4-thiazolidine-1,3-dione) significantly enhanced the anti-proliferative activities, the compounds exhibited some toxicities towards normal cells.

Our next strategies include development of benzimidazole- and imidazole-based organoselenocyanates and analogous compounds. Interestingly, our initial attempts for preparing benzimidazolium- or imidazolium-based acyclic ionic selenocyanates were not completely successful. While long chain selenocyanates could be prepared, shorter-chain selenocyanates led to cyclization with the formation of newer sets of ionic selenazolium and selenazinium selenocyanates. Interestingly, most of the cyclic compounds exhibited strong antioxidant activities for the reduction of hydrogen peroxide (Chapter 4).

Furthermore, the imidazole-based selenazolium selenocyanate **4.12d** exhibited potent antioxidant activity in scavenging the intracellular ROS level in a representative macrophage cell line (RAW 264.7).

Finally, anti-proliferative activities of the benzimidazole- and imidazole-based compounds were investigated and the results indicated better potencies of benzimidazole-based acyclic ionic selenocyanates over the cyclic compounds. Therefore, newer sets of ionic and non-ionic structural analogues were developed to improve anti-cancer potentials. Interestingly, unlike benzimidazole-based ionic selenocyanates, the corresponding non-ionic selenocyanates exhibited more potent anti-proliferative activities. Particularly, 4-NO2 substituted benzimidazole-based neutral selenocyanate (compound **5.16**, Chapter 5) exhibited highest anti-proliferative activity with enhanced selectively towards cancer cells (MDA-MB-231) over normal cells (HEK-293).

In summary, with the synthesis of diverse series of organoselenium compounds followed by the evaluation of their anti-cancer and antioxidant activities, we could identify several key compounds having pharmaceutical implications. With the available resources and facilities, we have undertaken all possible investigations with the synthesized organoselenium compounds towards their *in vitro* anti-proliferative and antioxidant activities to identify the potent compounds as described in this thesis. However, further investigations, as listed below, may be considered as important future perspectives of the present thesis to take the potent compounds forward up to their applications.

i. **Understanding the metabolism** of synthesized organoselenocyanates is important for assessing the pharmacodynamics of the compounds. This understanding might aid in designing a more potent and less toxic selenocyanates.

ii. **Exact mechanistic pathway** of the mode of anti-proliferative activity of selenocyanates is still not elucidated completely. This warrants further investigations on the levels of different cancer marker proteins using immunoblotting techniques.

iii. **Combination treatment** of synthesized compounds with commercial anti-cancer drugs such as doxorubicin, *cis*-platin, gemcitabine, 5-fluorouracil etc. is crucial

to understand the chemopreventive potentials of the synthesized compounds in attenuating the toxicities and side-effects exerted by the commonly used commercial chemotherapeutic drugs.

iv. **Synthesis of newer generation organoselenium compounds** could be planned based on the feedback of above studies for the development of potent organoselenium compounds for anti-cancer therapeutics in future.

Annexure II

List of Publications and Conferences

List of Publications and Presentations

Publications

1. **K. Banerjee**, D. Bhattacherjee, S. K. Mahato, A. Sufian, K. P. Bhabak* "Benzimidazole- and Imidazole-Fused Selenazolium and Selenazinium Selenocyanates: Ionic Organoselenium Compounds with Efficient Peroxide Scavenging Activities" *Inorg Chem* **2021**, *60*, 12984.

2. D. Bhattacherjee, A. Sufian, S. K. Mahato, S. Begum, **K. Banerjee**, S. De, H. K. Srivastava*, K. P. Bhabak*, "Trisulfides over disulfides: highly selective synthetic strategies, anti-proliferative activities and sustained H_2S release profiles" *Chem. Commun*., **2019**, *55*, 13534.

3. **K. Banerjee**, G. Padmavati, D. Bhattacherjee, S. Saha, A. B. Kunnumakkara, K. P. Bhabak* "Potent anti-proliferative activities of organochalcogenocyanates towards breast cancer" *Org*. *Biomol*. *Chem*., **2018**, *16*, 8769.

Patents

1. Bhabak, K. P. and **Banerjee, K**. "Heterocyclic Ionic Organoselenium Compounds and Method of Synthesis" **Patent Application No**: 202131030739; Date: June 08, 2021

Poster Presentations

1. Presented a poster in **Frontiers in Chemical Sciences** (**FICS**) held at Indian Institute of Technology Guwahati, India during **Dec 6 – 8**, **2018**.
2. Presented a poster in **Research Conclave**, held at Indian Institute of Technology Guwahati, India (*Received best poster award)* during **Mar 14 – 17**, **2019**.
3. Presented a poster in **National Organic Symposium Trust** (**XVI-J-NOST**), held at Indian Institute of Science, Bangalore during **Oct 31 – Nov 1**, **2020**.

Manuscripts under preparation

1. **K. Banerjee**, D. Bhattacherjee, K. P. Bhabak* "Organoselenocyanates containing 1,2,3-triazole and 1,3-thiazolidine-2,4-dione pharmacophores: Synthesis and highly selective anti-

proliferative activities against triple-negative breast cancer cells" (*manuscript under preparation*).

2. **K. Banerjee**, D. Bhattacherjee, K. P. Bhabak* "Ionic vs Non-ionic Heterocyclic Organoselenium Compounds: Rational Synthetic Strategies and Potent Anti-cancer Activities" (*manuscript under preparation*).

Annexure III

NMR spectral data of compounds discussed in Chapter 2

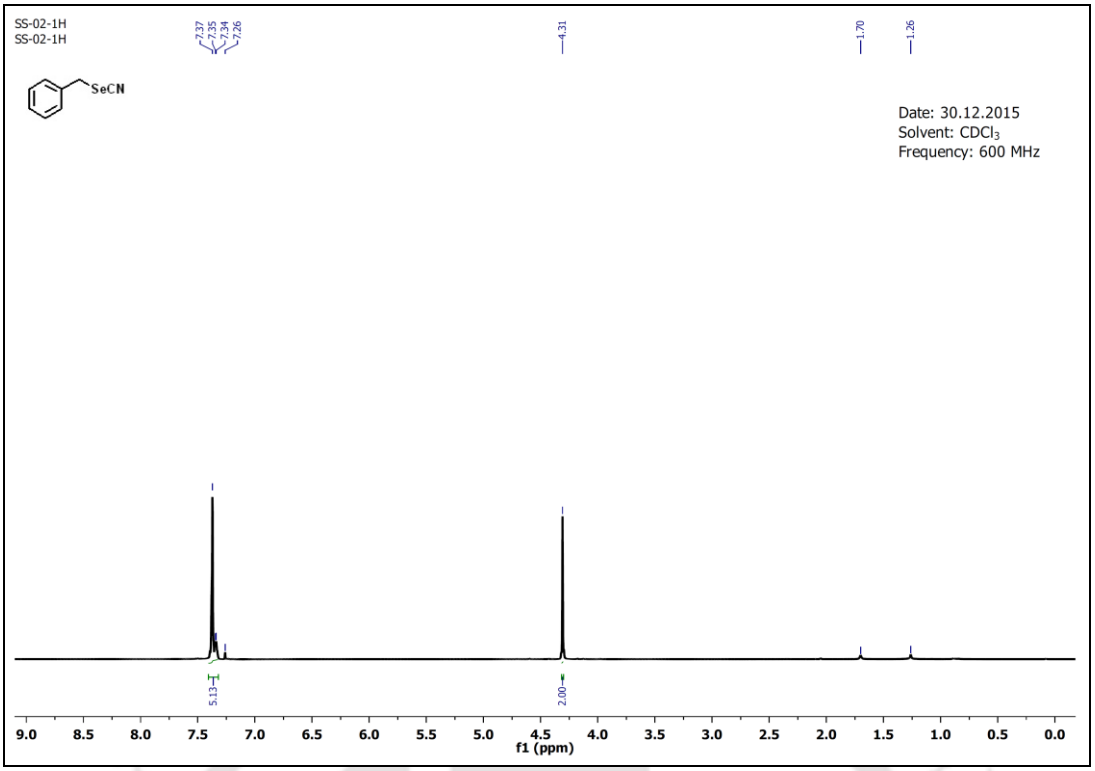

Figure A3.1. ^{1}H NMR spectrum (600 MHz, $CDCl_3$) of Compound **1.48**.

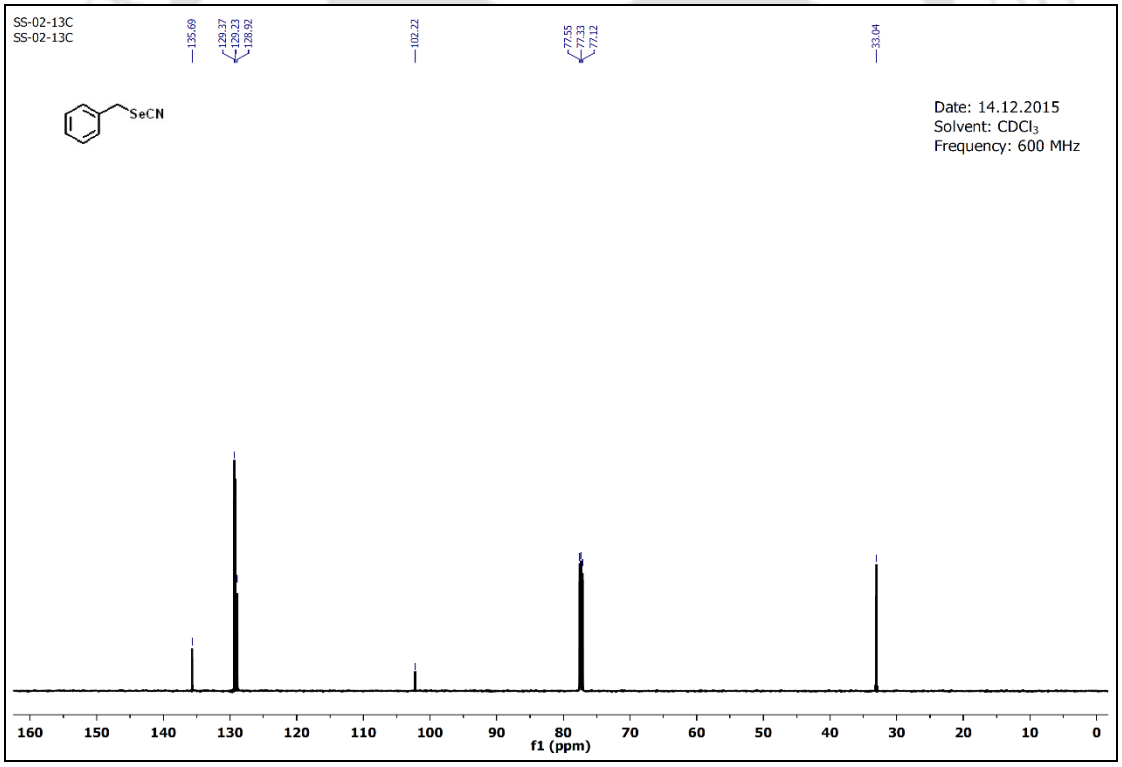

Figure A3.2. ^{13}C NMR spectrum (150 MHz, $CDCl_3$) of Compound **1.48**.

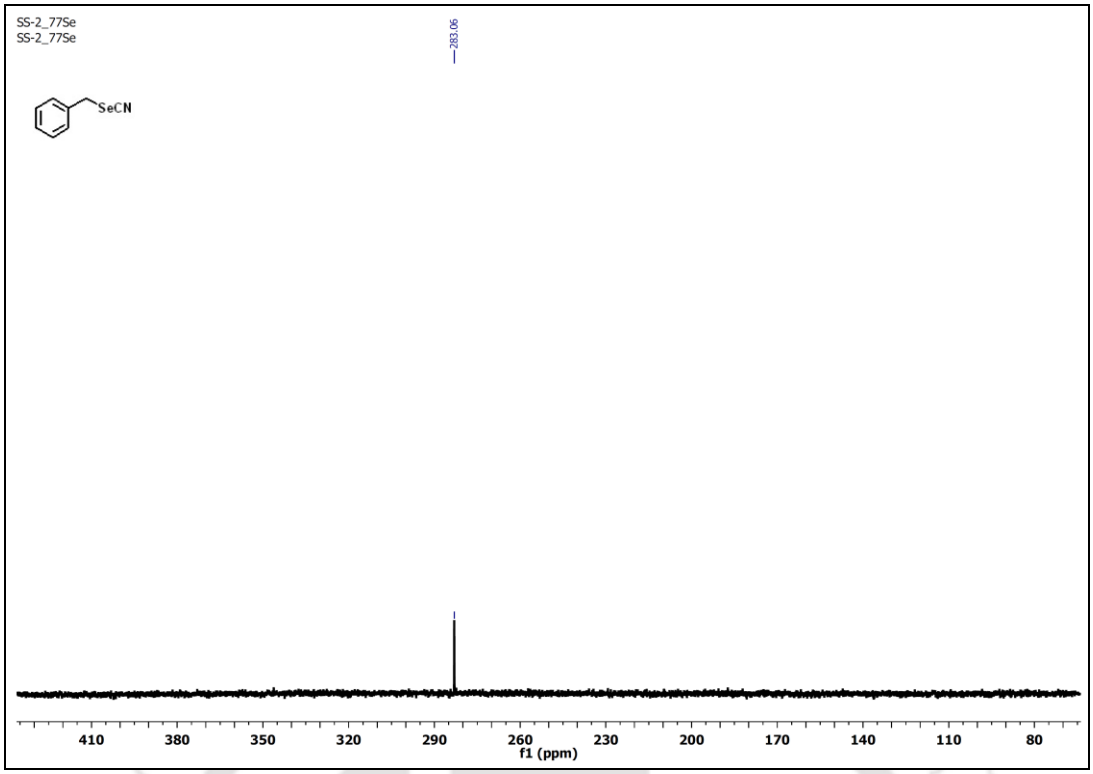

Figure A3.3. ^{77}Se NMR spectrum (76 MHz, $CDCl_3$) of Compound **1.48**.

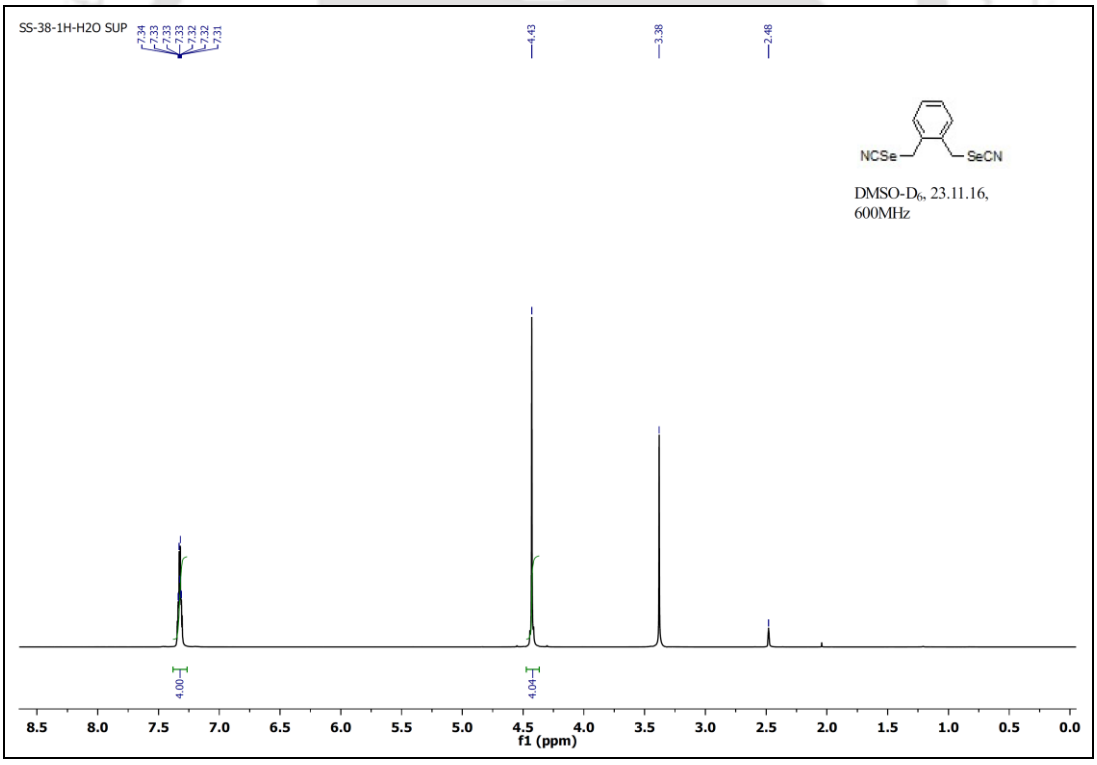

Figure A3.4. ^{1}H NMR spectrum (600 MHz, DMSO-d_6) of Compound **1.50**.

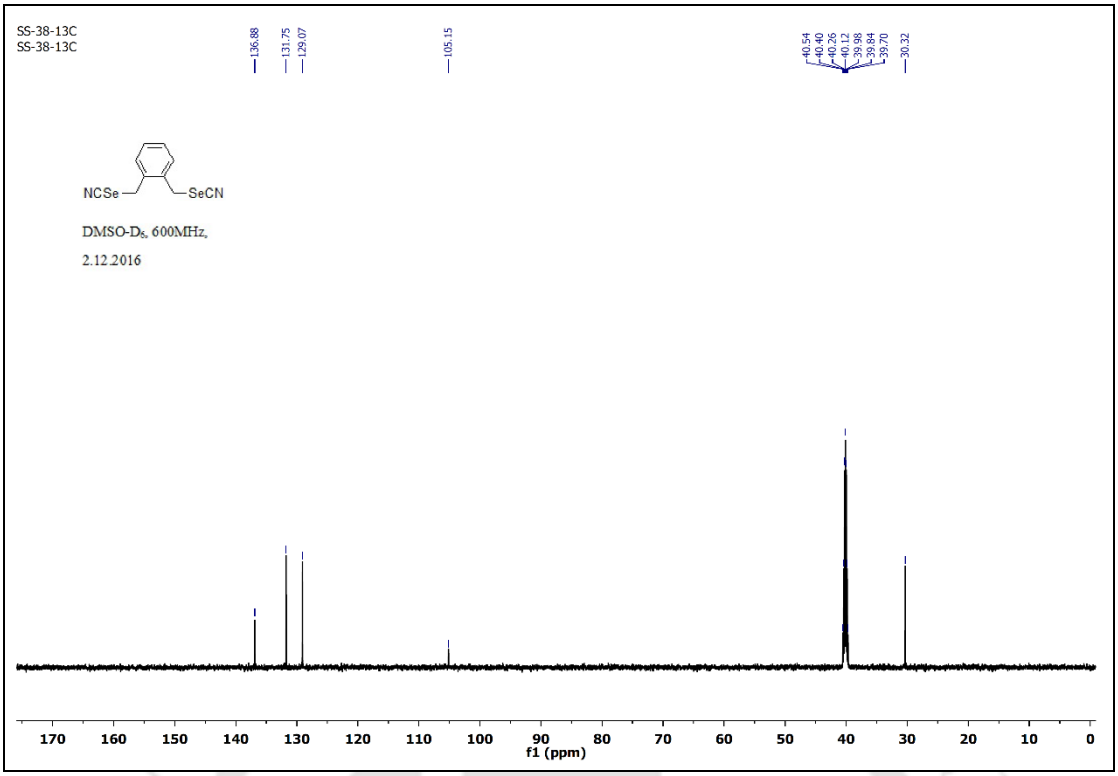

Figure A3.5. ^{13}C NMR spectrum (150 MHz, DMSO-d_6) of Compound **1.50**.

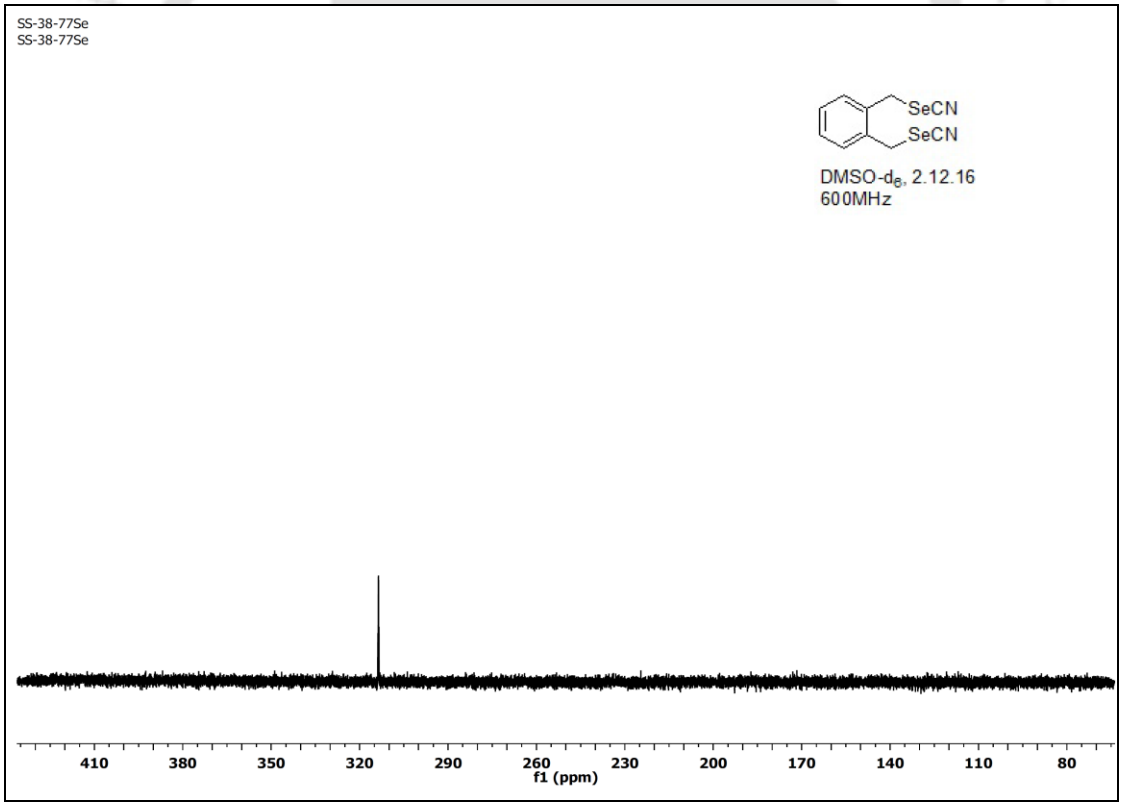

Figure A3.6. ^{77}Se NMR spectrum (114 MHz, DMSO-d_6) of Compound **1.50**.

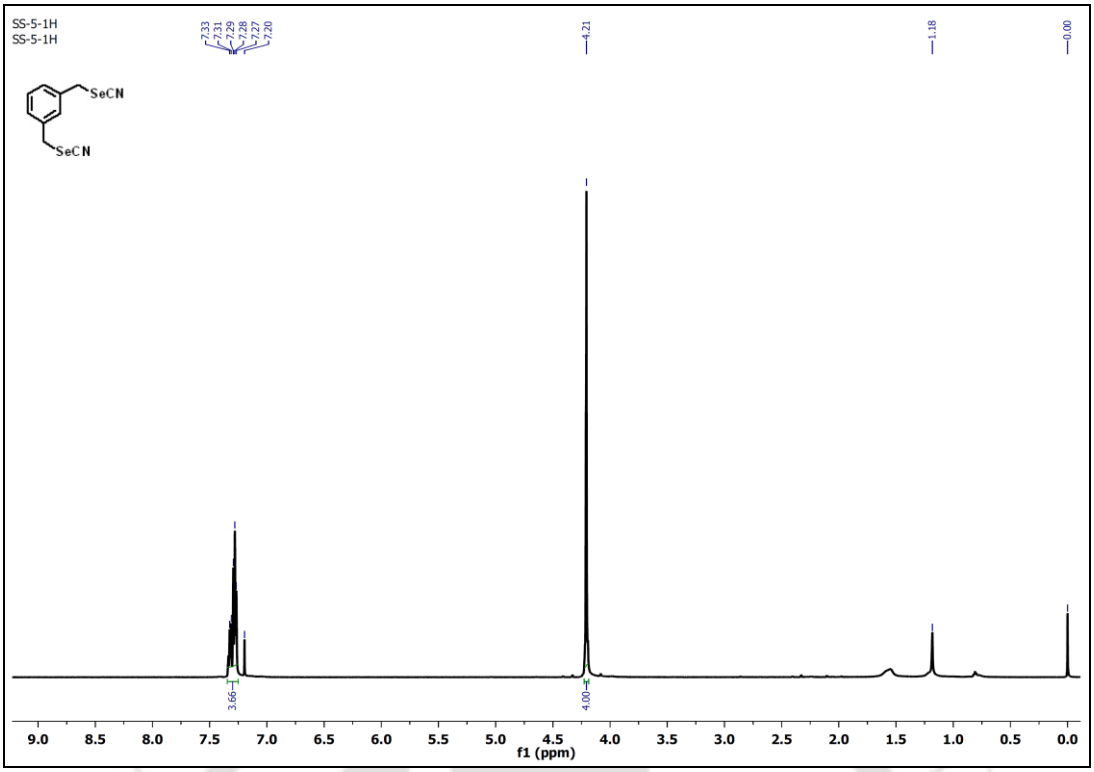

Figure A3.7. ^{1}H NMR spectrum (600 MHz, $CDCl_3$) of compound **1.51**.

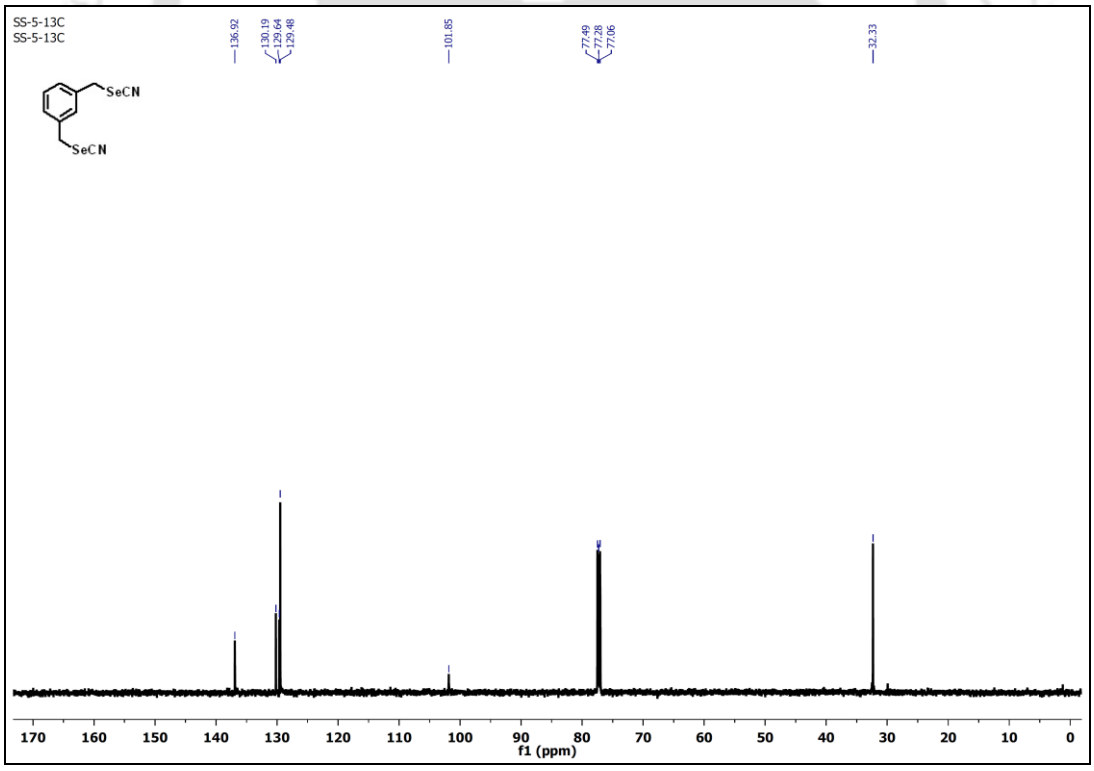

Figure A3.8. ^{13}C NMR spectrum (150 MHz, $CDCl_3$) of compound **1.51**.

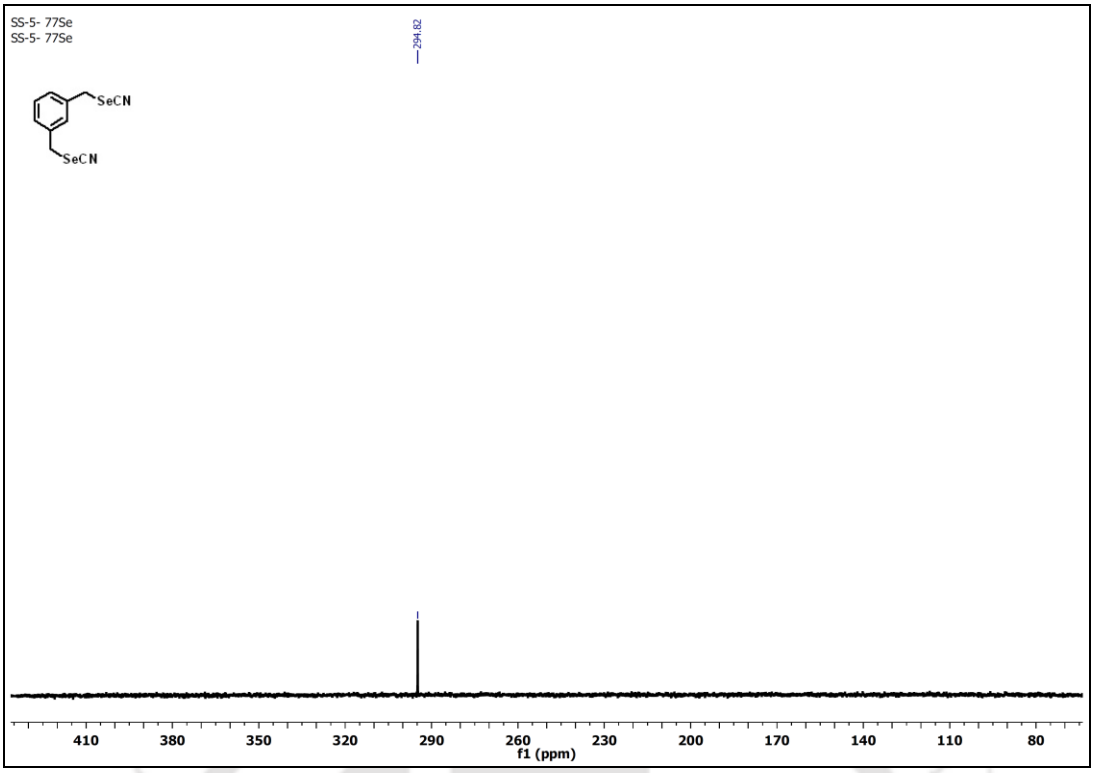

Figure A3.9. ^{77}Se NMR spectrum (76 MHz, $CDCl_3$) of compound **1.51**.

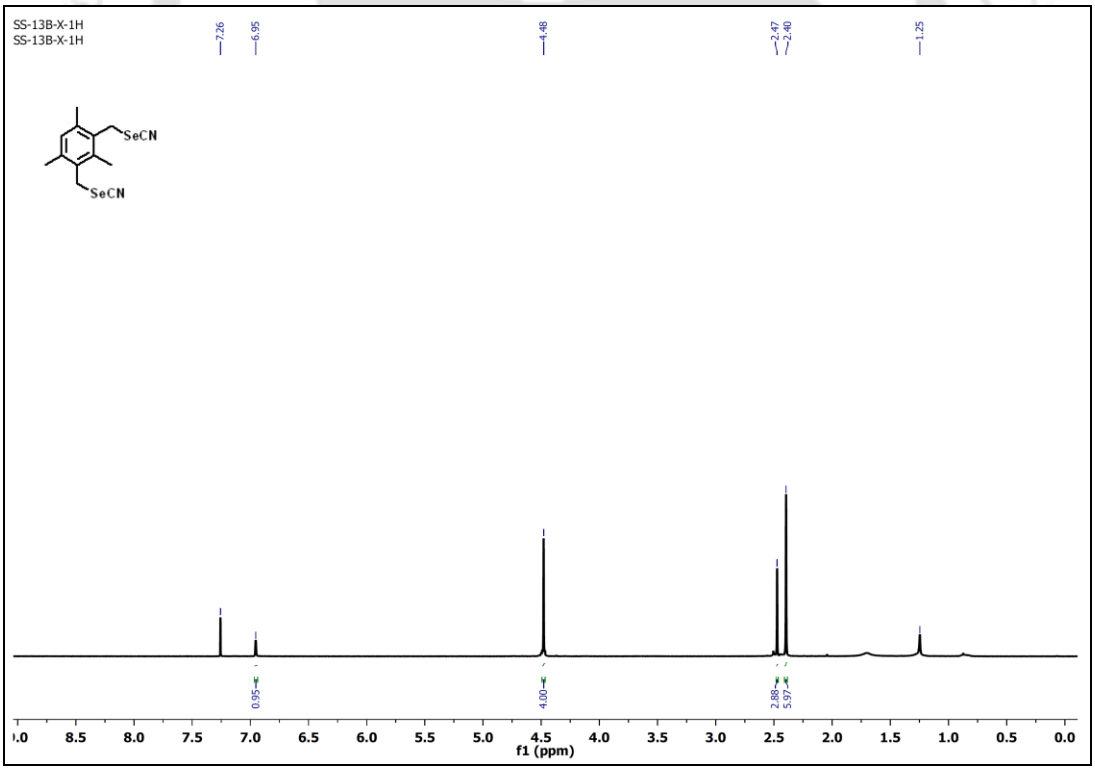

Figure A3.10. ^{77}Se NMR spectrum (76 MHz, $CDCl_3$) of compound **1.51**.

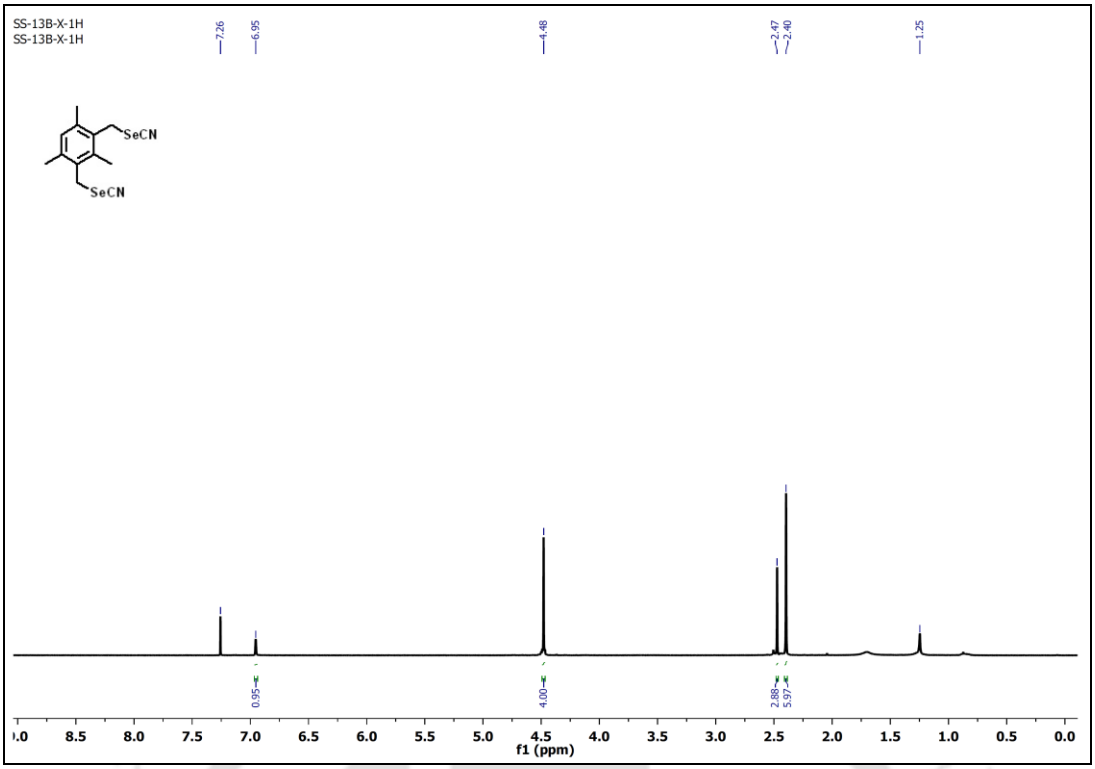

Figure A3.11. ^{1}H NMR spectrum (600 MHz, $CDCl_3$) of compound **2.4**.

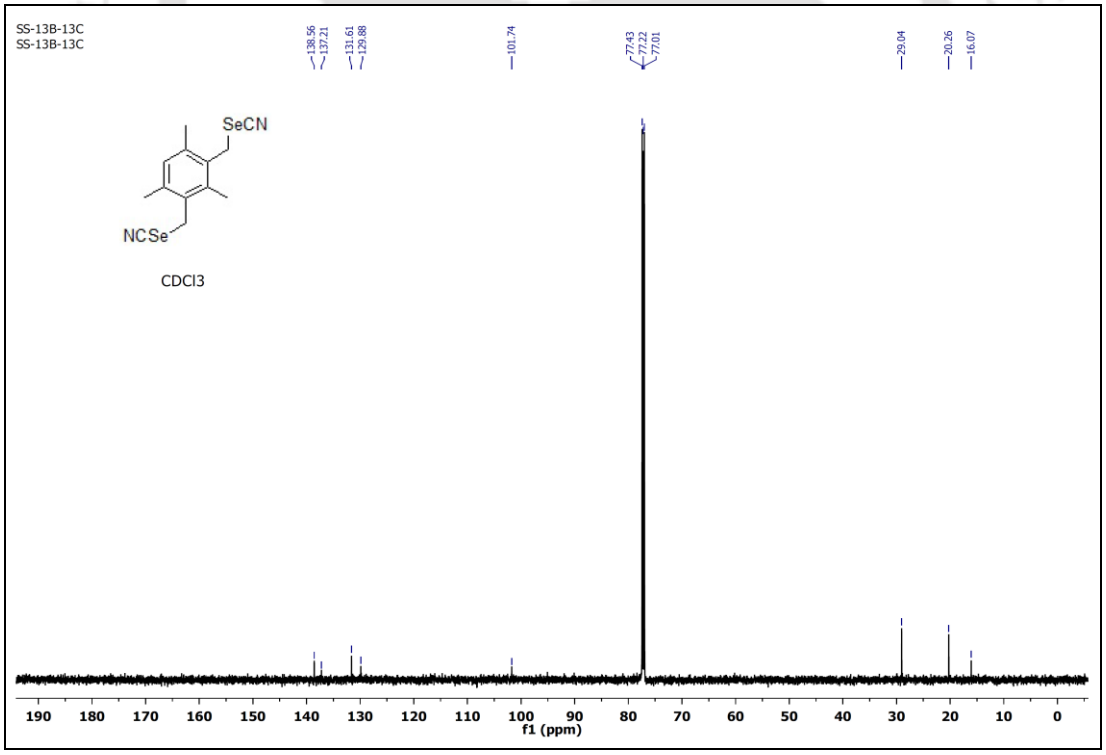

Figure A3.12. ^{13}C NMR spectrum (150 MHz, $CDCl_3$) of compound **2.4**.

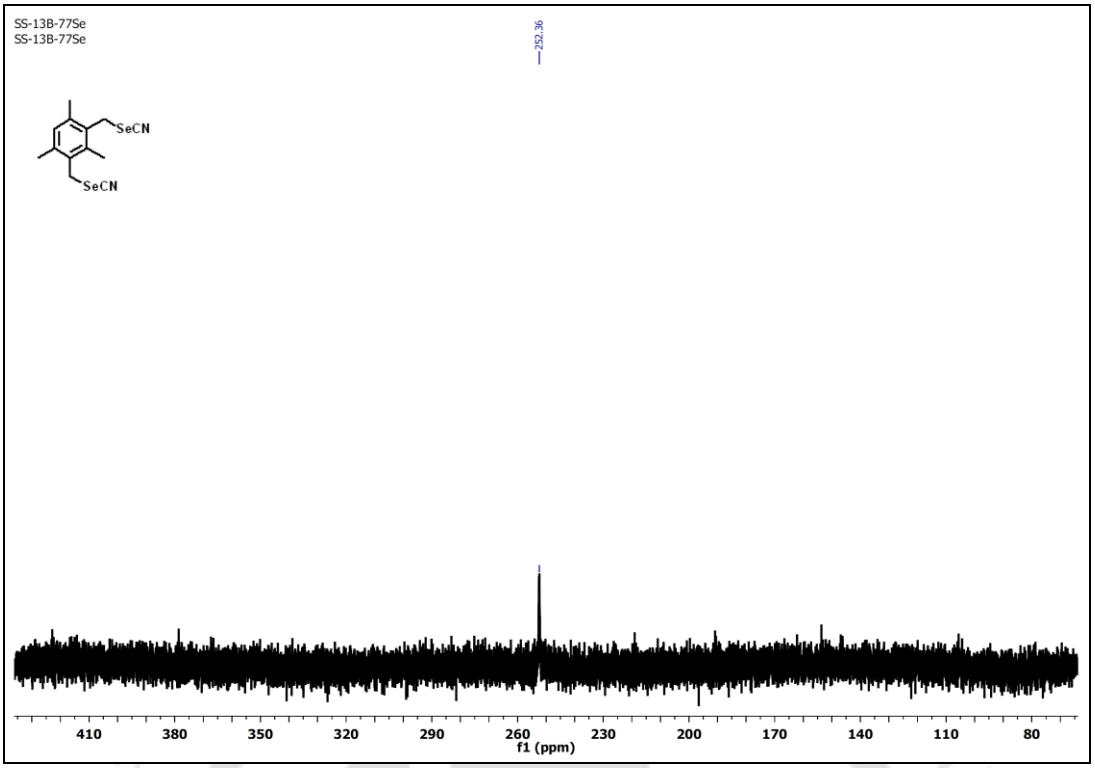

Figure A3.13. ^{77}Se NMR spectrum (114 MHz, $CDCl_3$) of compound **2.4**.

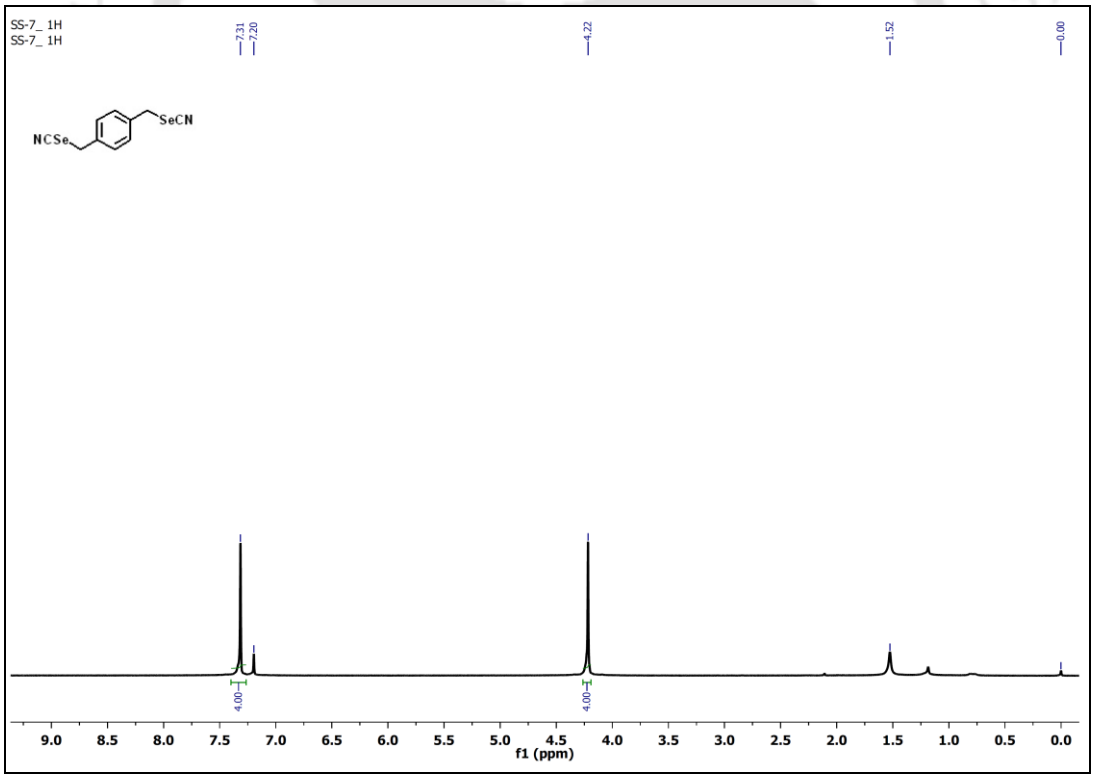

Figure A3.14. ^{1}H NMR spectrum (600 MHz, $CDCl_3$) of compound **1.52**.

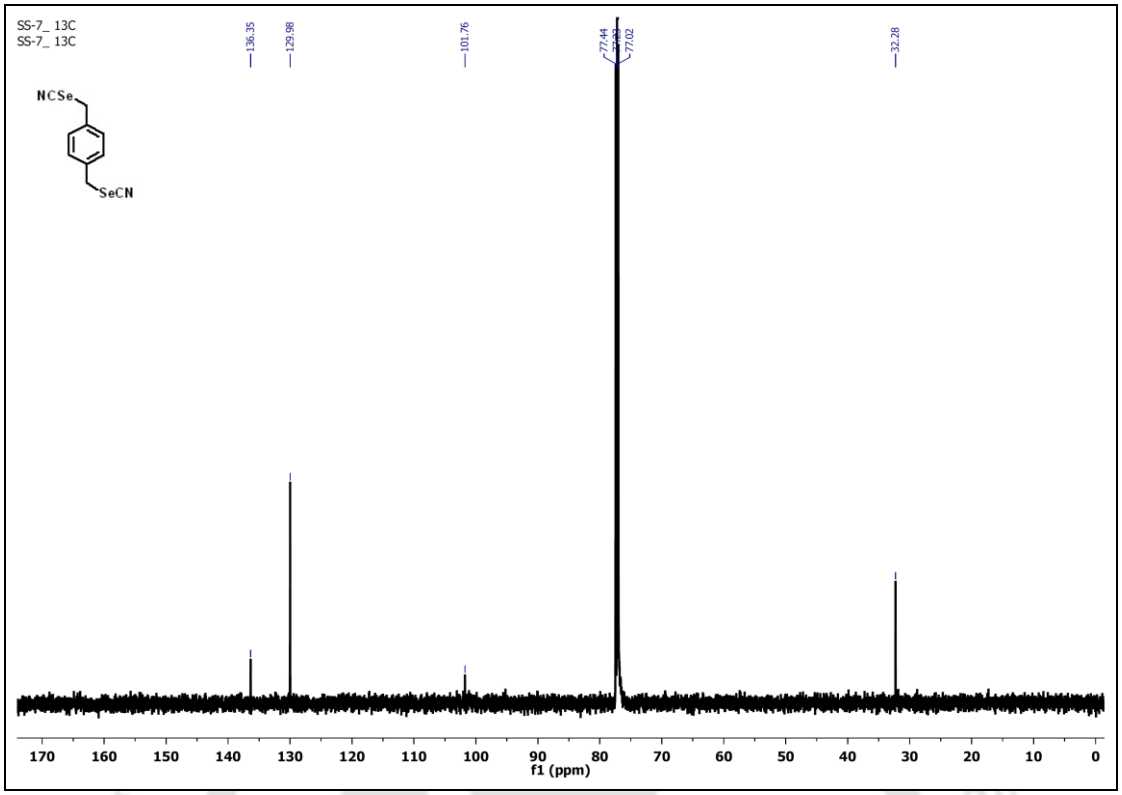

Figure A3.15. ^{13}C NMR spectrum (150 MHz, $CDCl_3$) of Compound **1.52**.

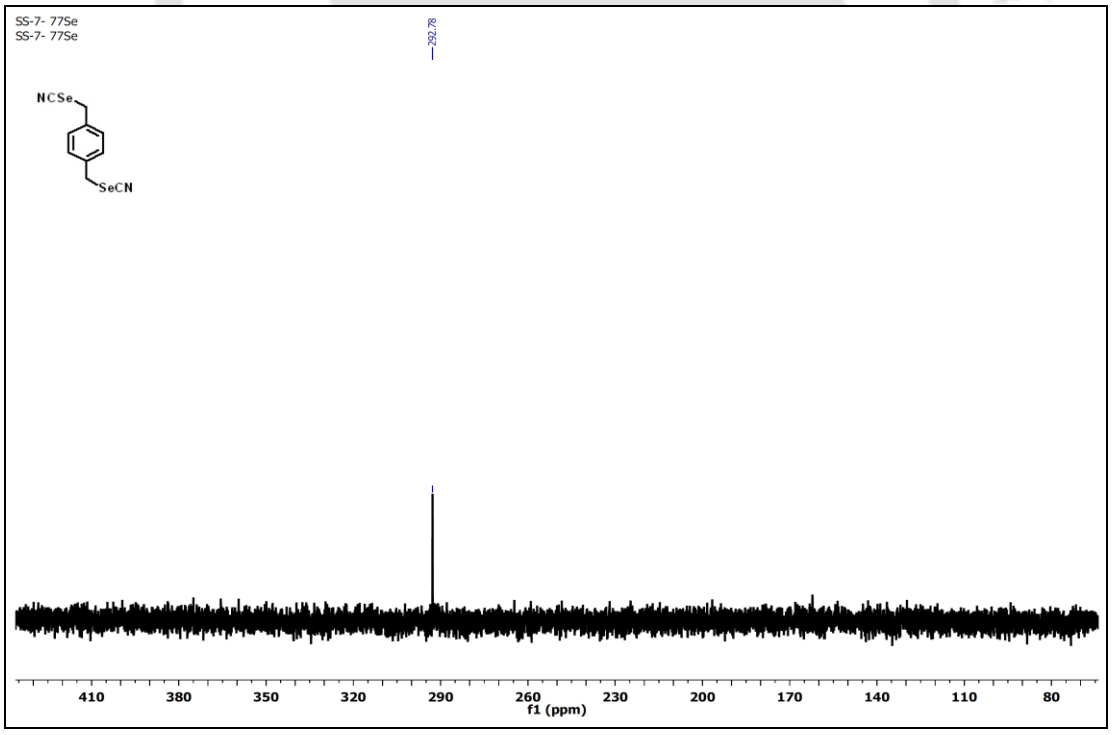

Figure A3.16. ^{77}Se NMR spectrum (114 MHz, $CDCl_3$) of Compound **1.52**.

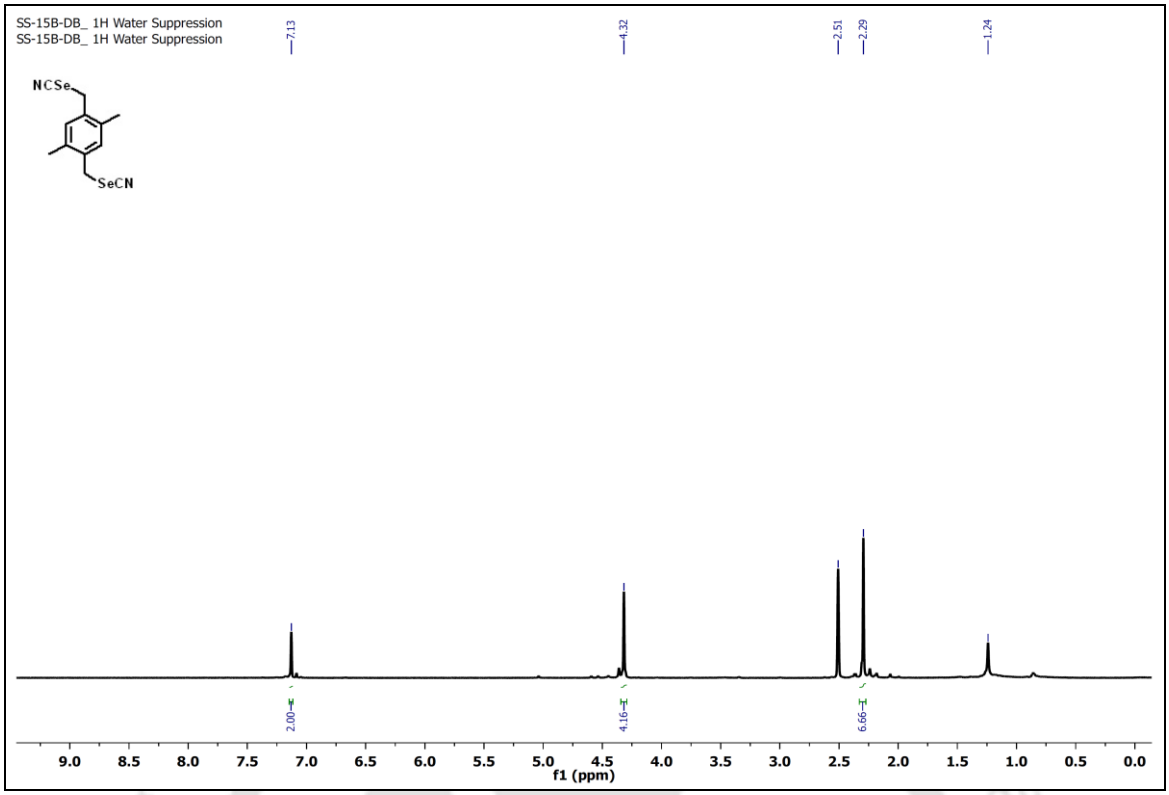

Figure A3.17. ^{1}H NMR spectrum (600 MHz, $CDCl_3$) of Compound **2.5**.

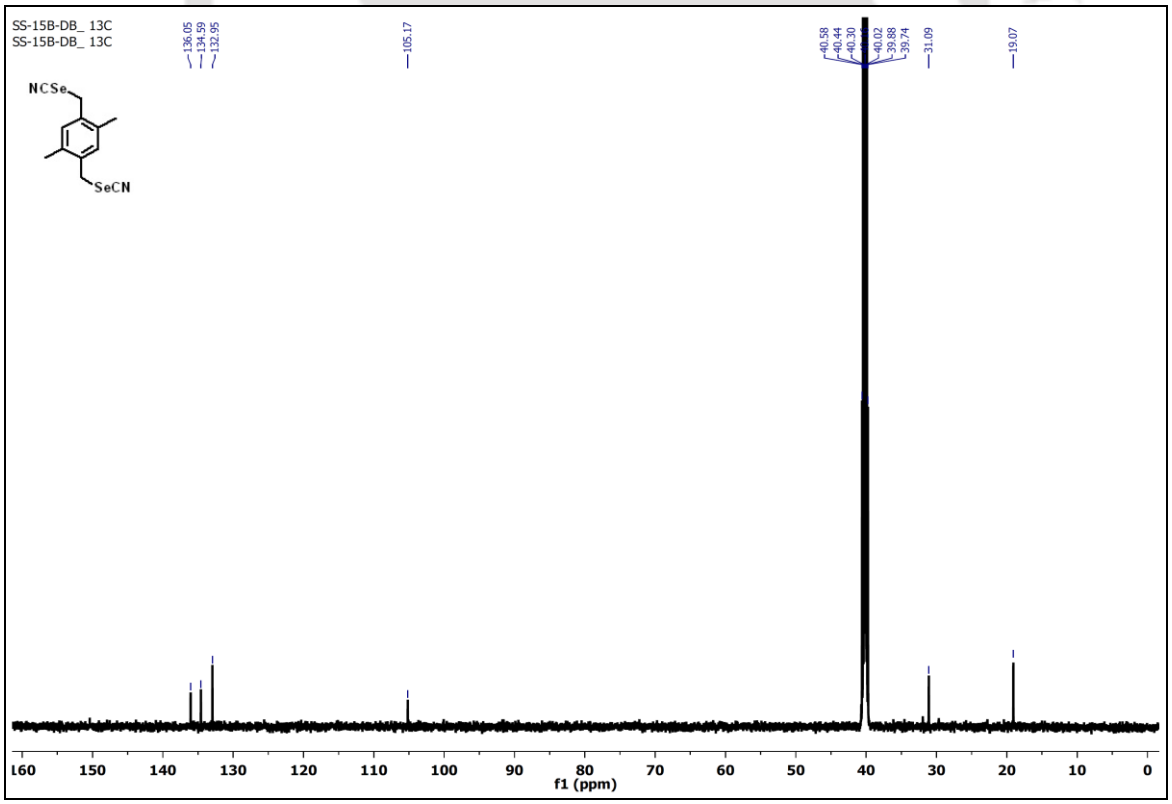

Figure A3.18. ^{13}C NMR spectrum (150 MHz, $CDCl_3$) of compound **2.5**.

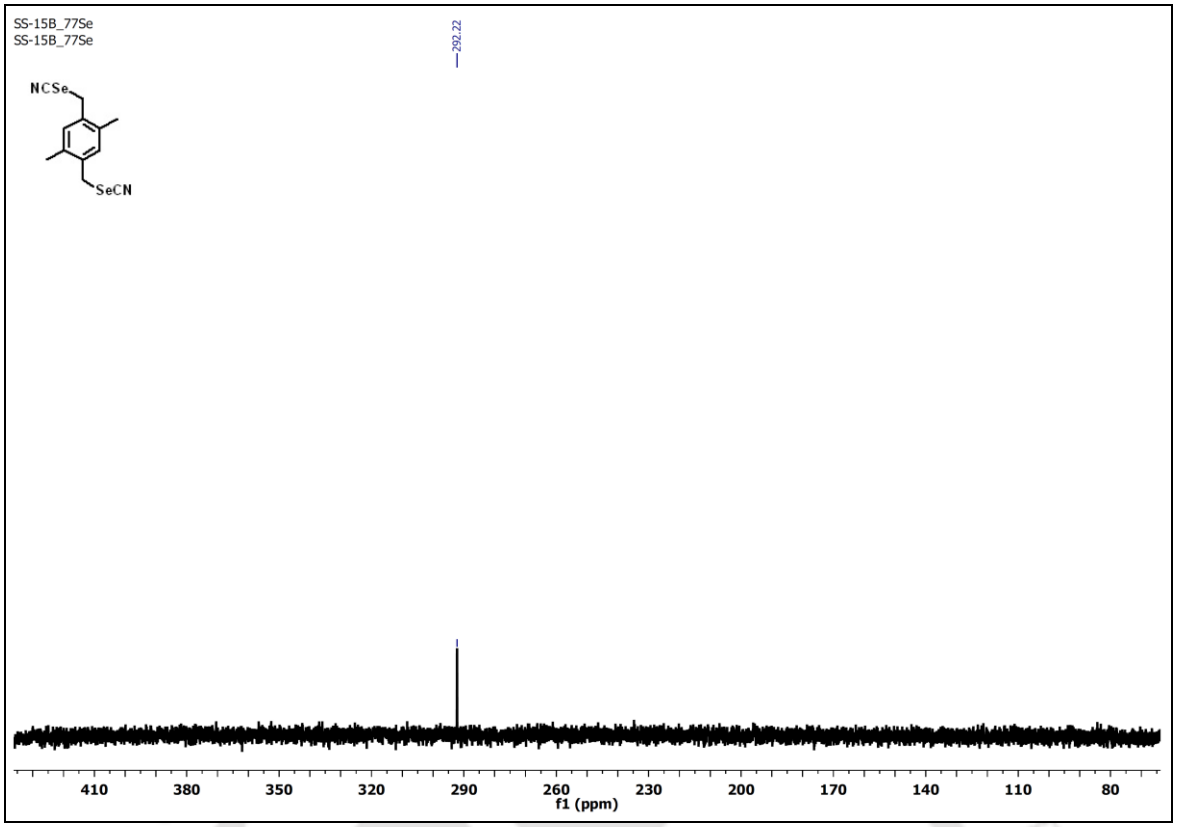

Figure A3.19. ^{77}Se NMR spectrum (114 MHz, DMSO-d_6) of Compound **2.5**.

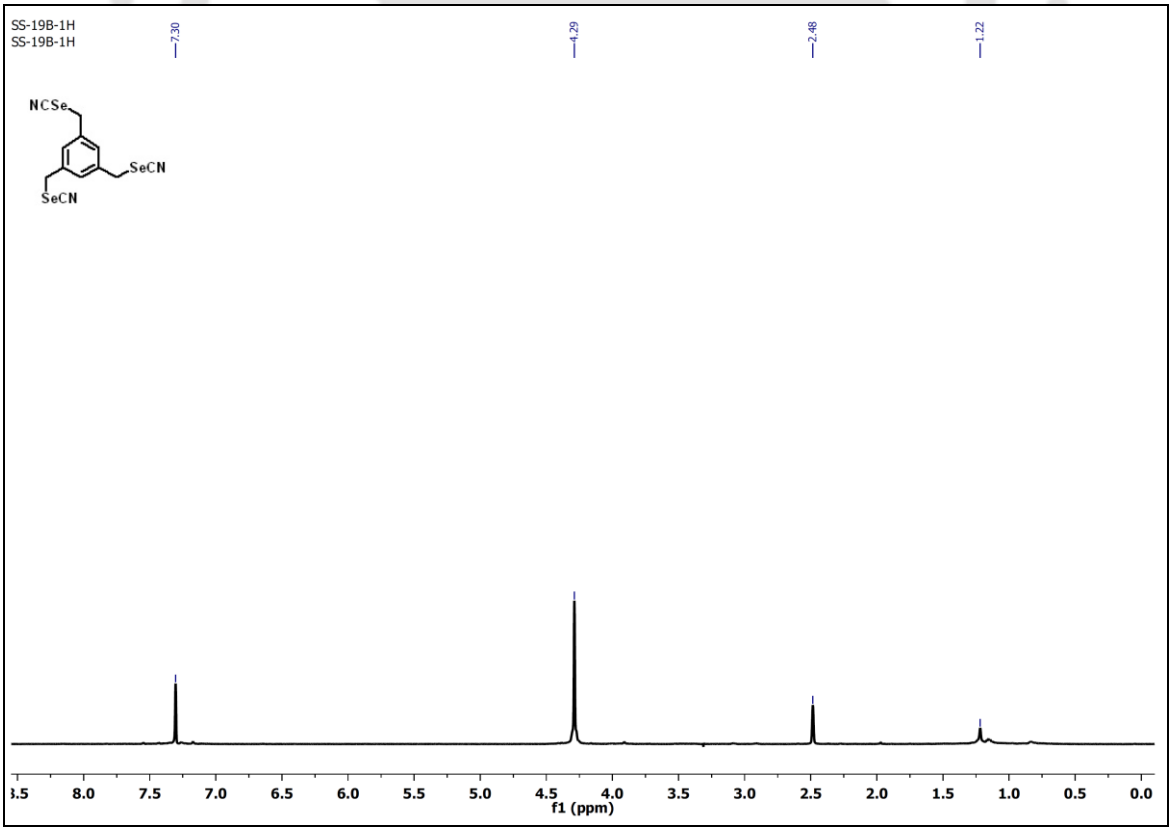

Figure A3.20. ^{1}H NMR spectrum (600 MHz, DMSO-d_6) of Compound **2.6**.

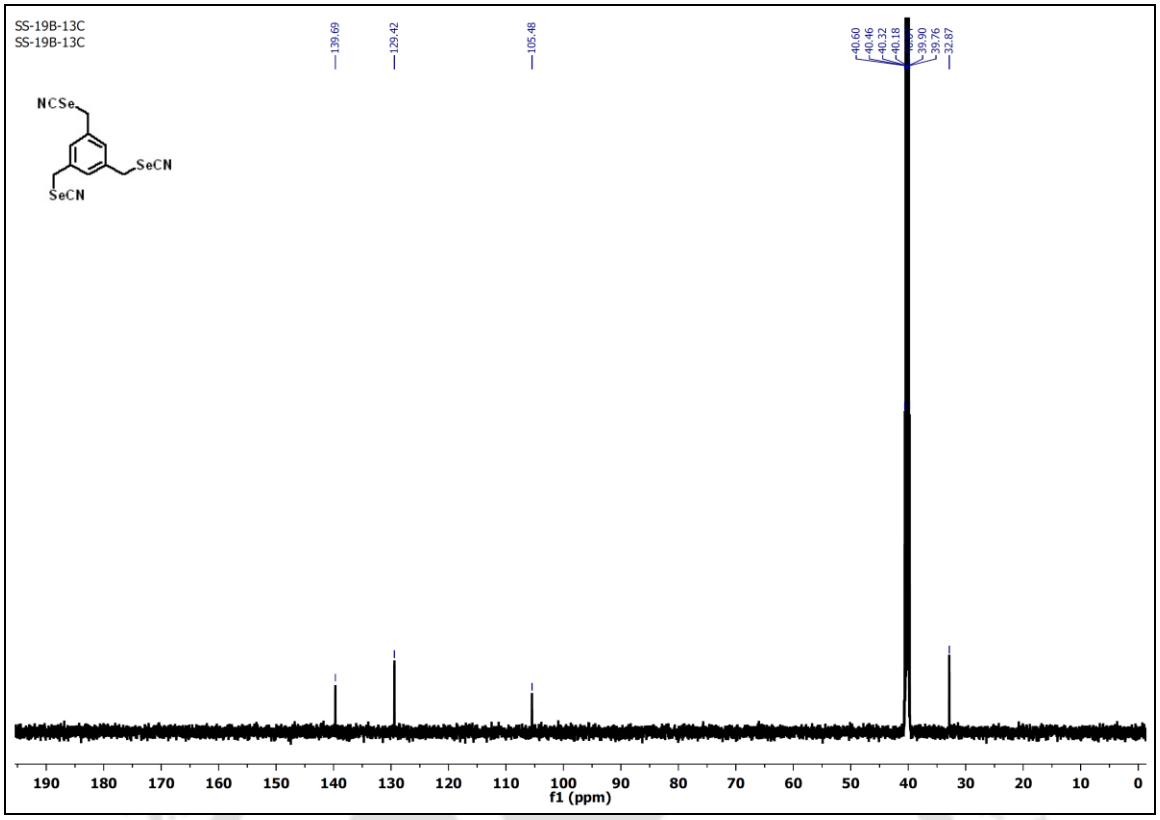

Figure A3.21. ^{13}C NMR spectrum (150 MHz, DMSO-d_6) of **Compound 2.6**.

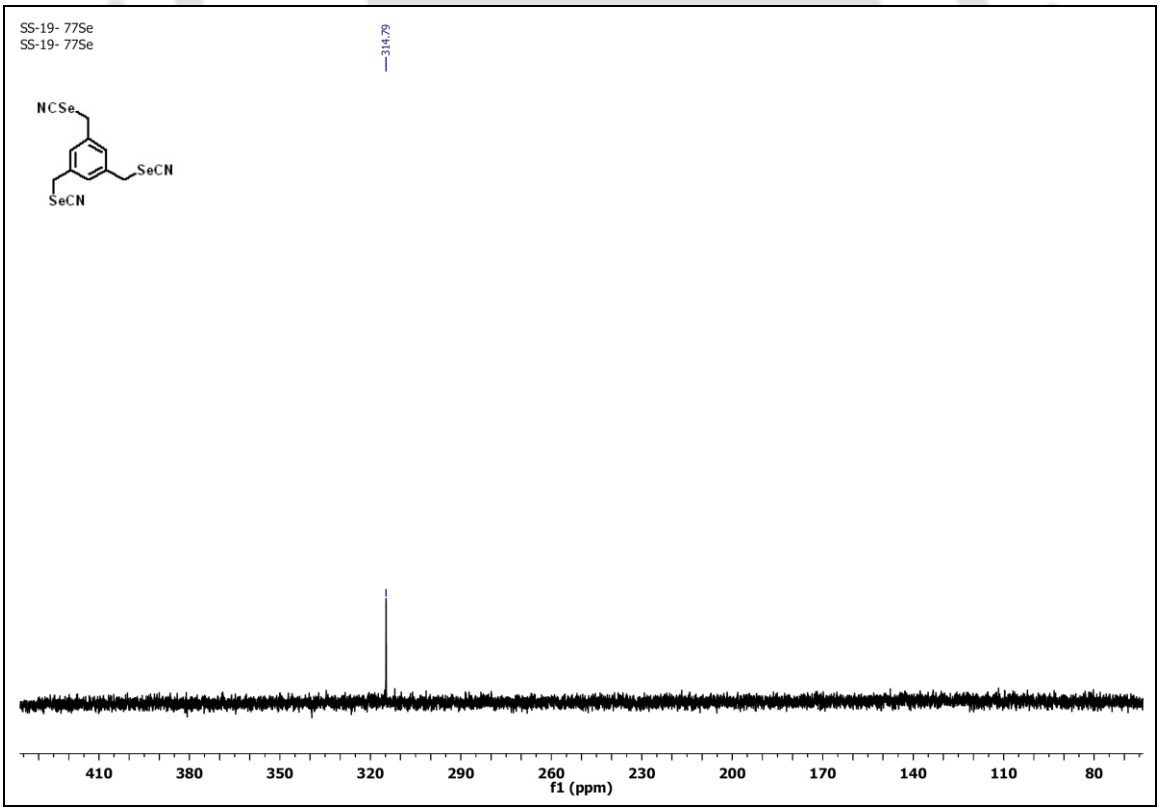

Figure A3.22. ^{77}Se NMR spectrum (114 MHz, DMSO-d_6) of Compound **2.6**.

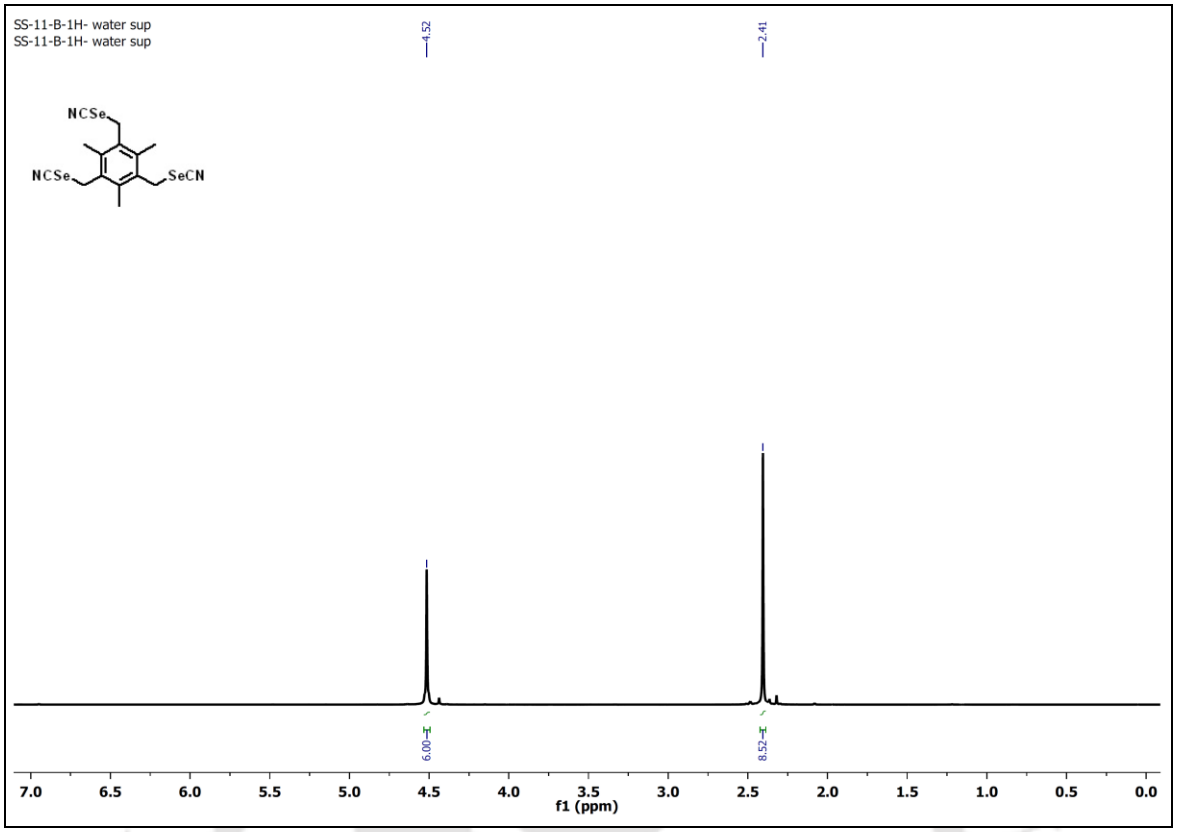

Figure A3.23. ^{1}H NMR spectrum (600 MHz, DMSO-d_6) of Compound **2.7**.

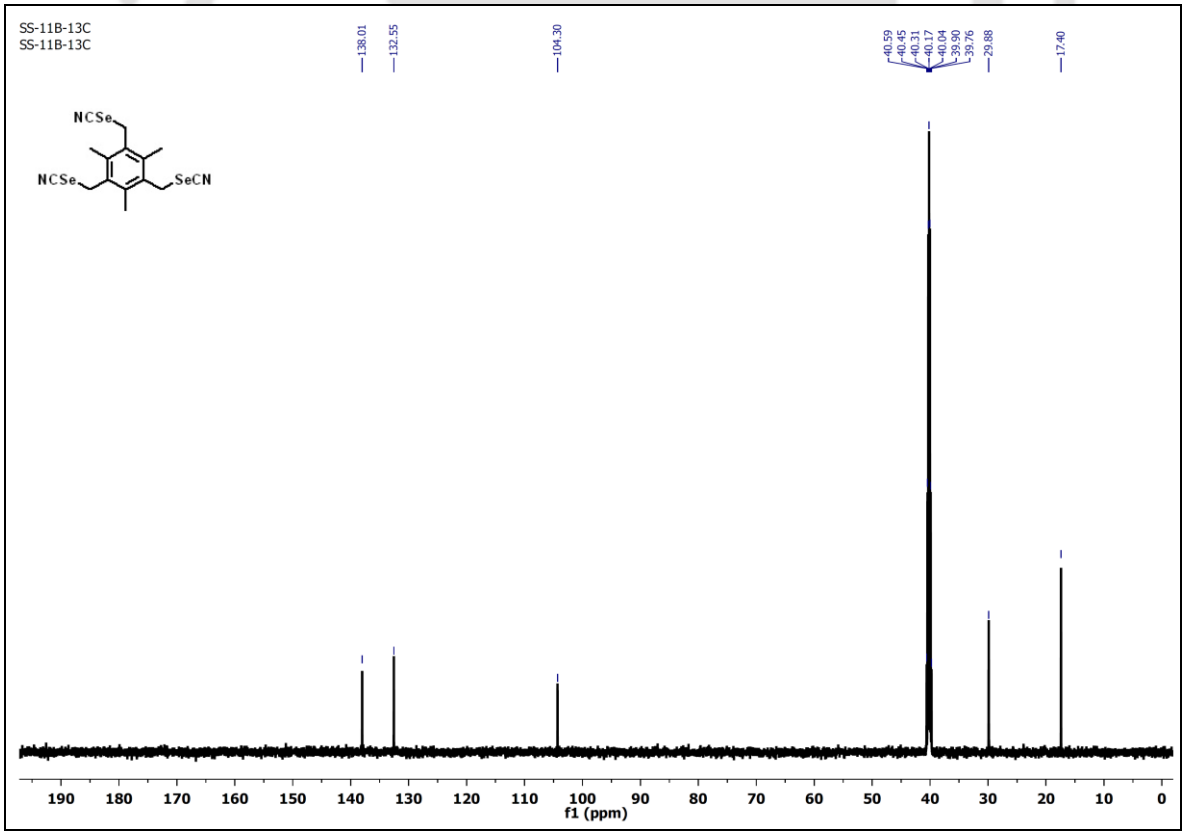

Figure A3.24. ^{13}C NMR spectrum (150 MHz, DMSO-d_6) of Compound **2.7**.

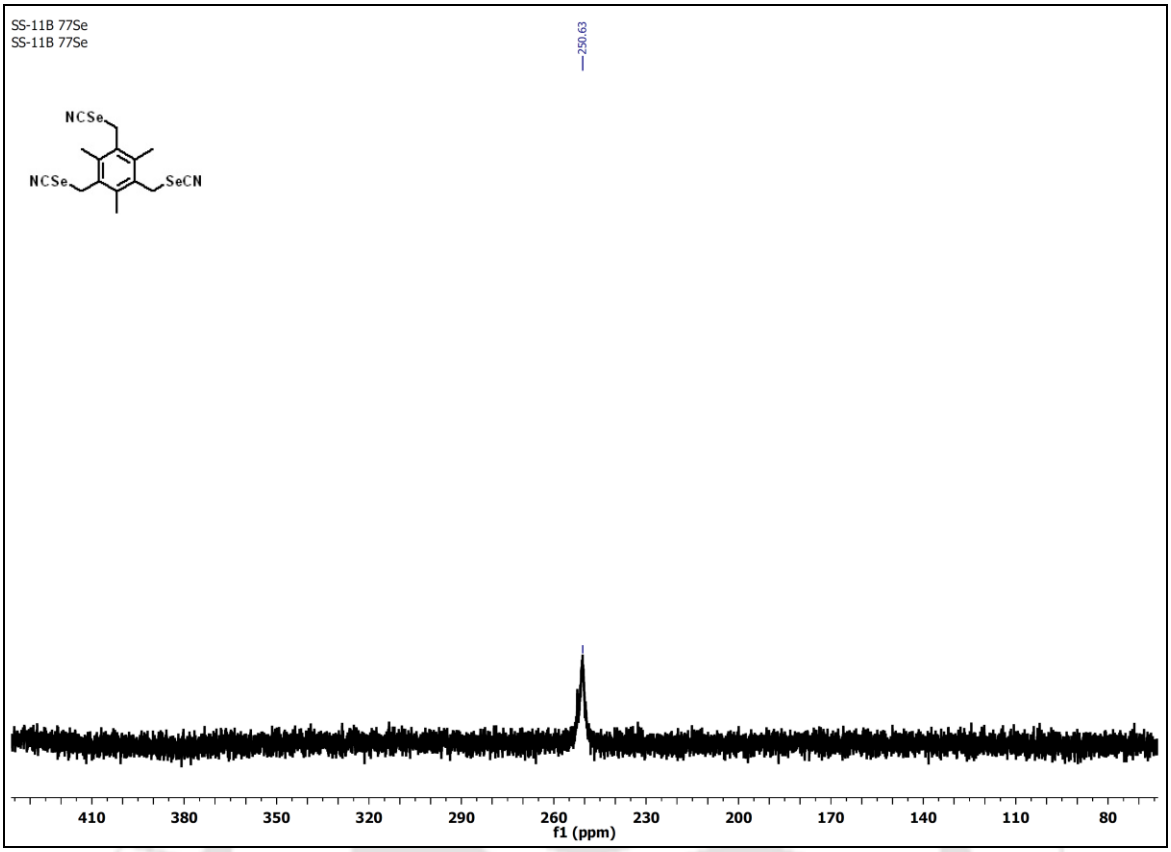

Figure A3.25. ^{77}Se NMR spectrum (114 MHz, DMSO-d_6) of Compound **2.7**.

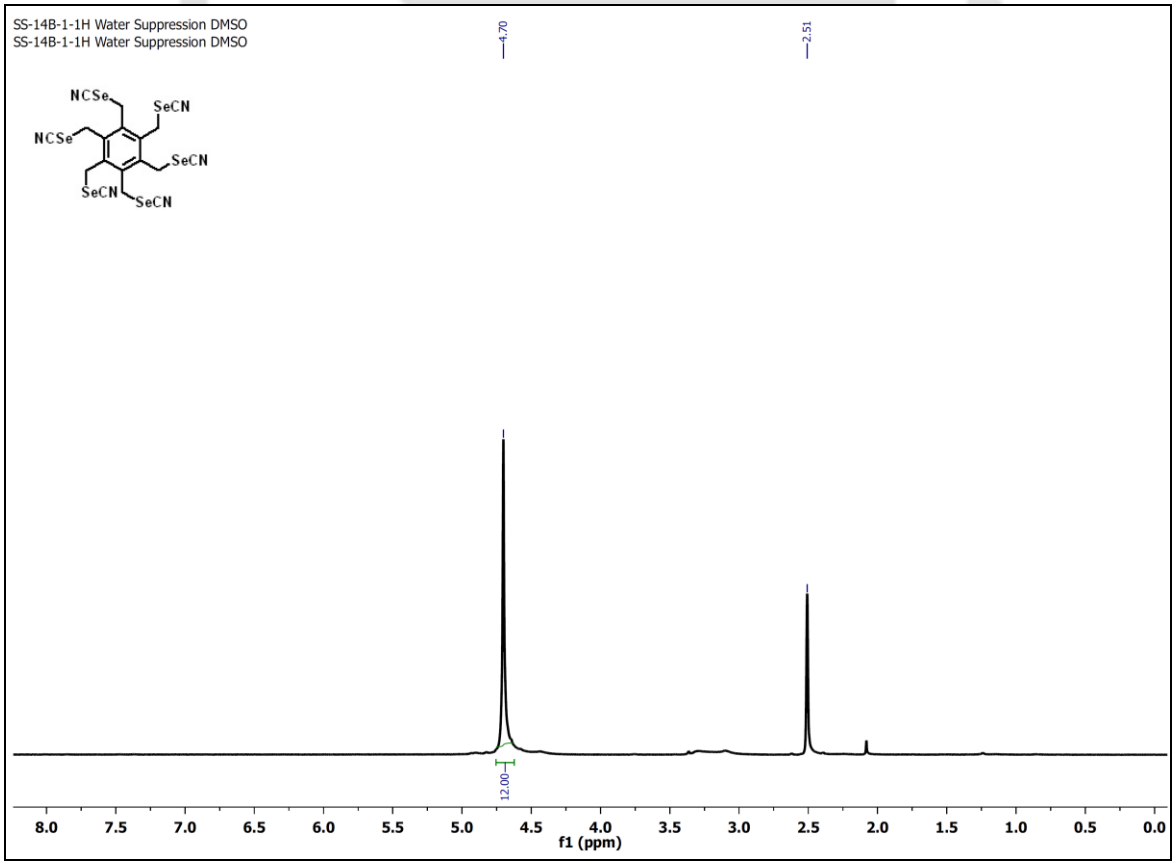

Figure A3.26. ^{1}H NMR spectrum (600 MHz, DMSO-d_6) of Compound **2.8**.

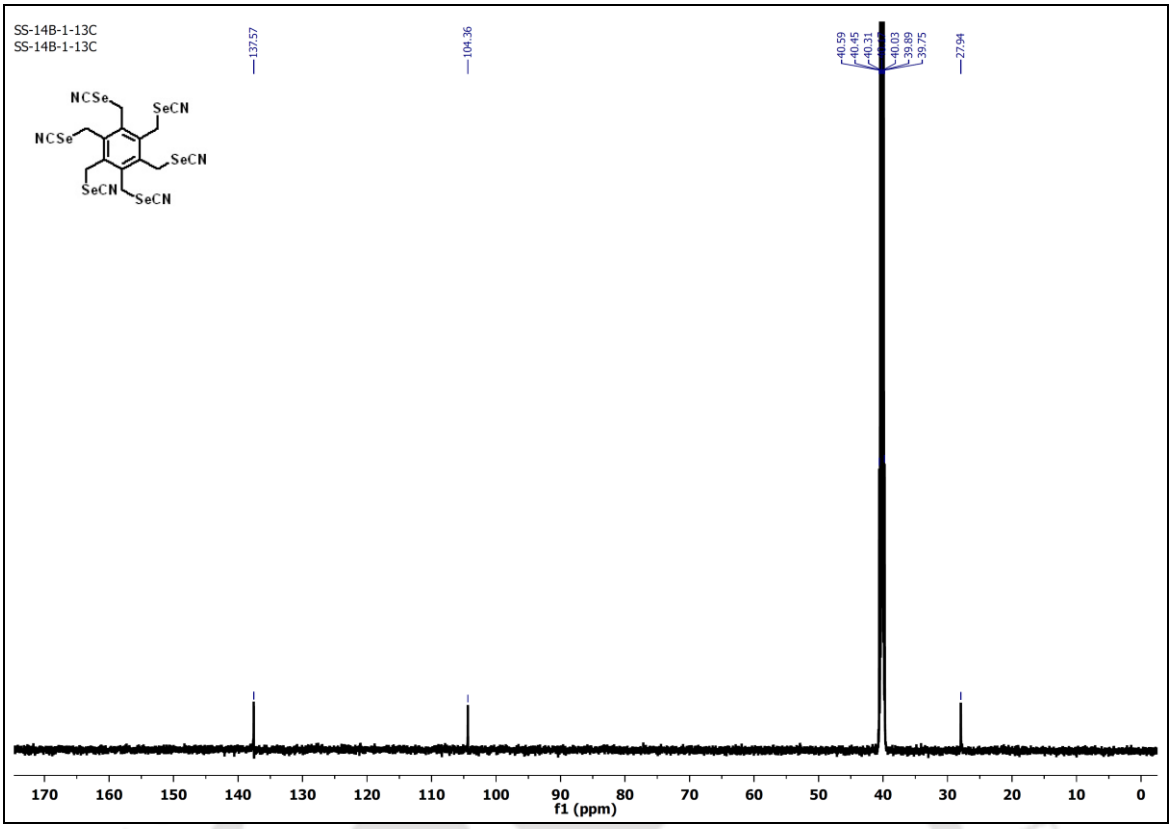

Figure A3.27. ^{13}C NMR spectrum (150 MHz, DMSO-d_6) of Compound **2.8**.

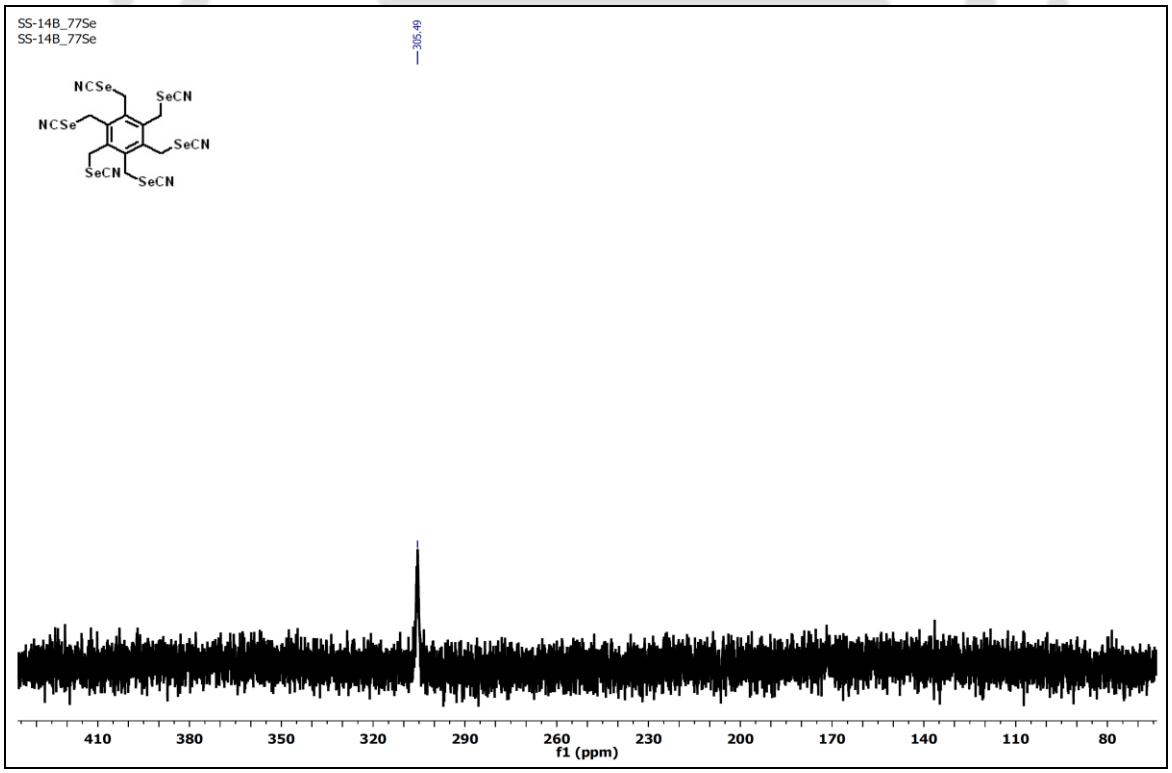

Figure A3.28. ^{77}Se NMR spectrum (114 MHz, DMSO-d_6) of Compound **2.8**.

Annexure IV

NMR spectral data of compounds discussed in Chapter 3

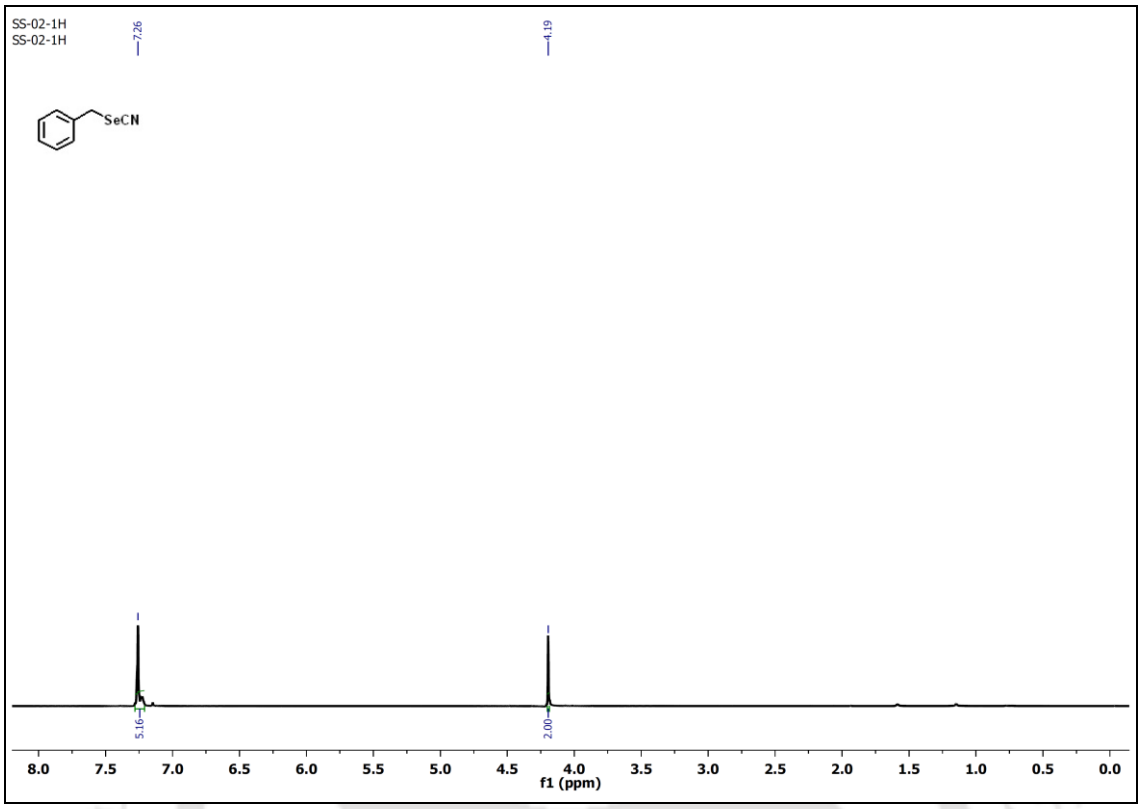

Figure A4.1. ^{1}H NMR spectrum ($CDCl_3$, 600 MHz) of compound **1.48**.

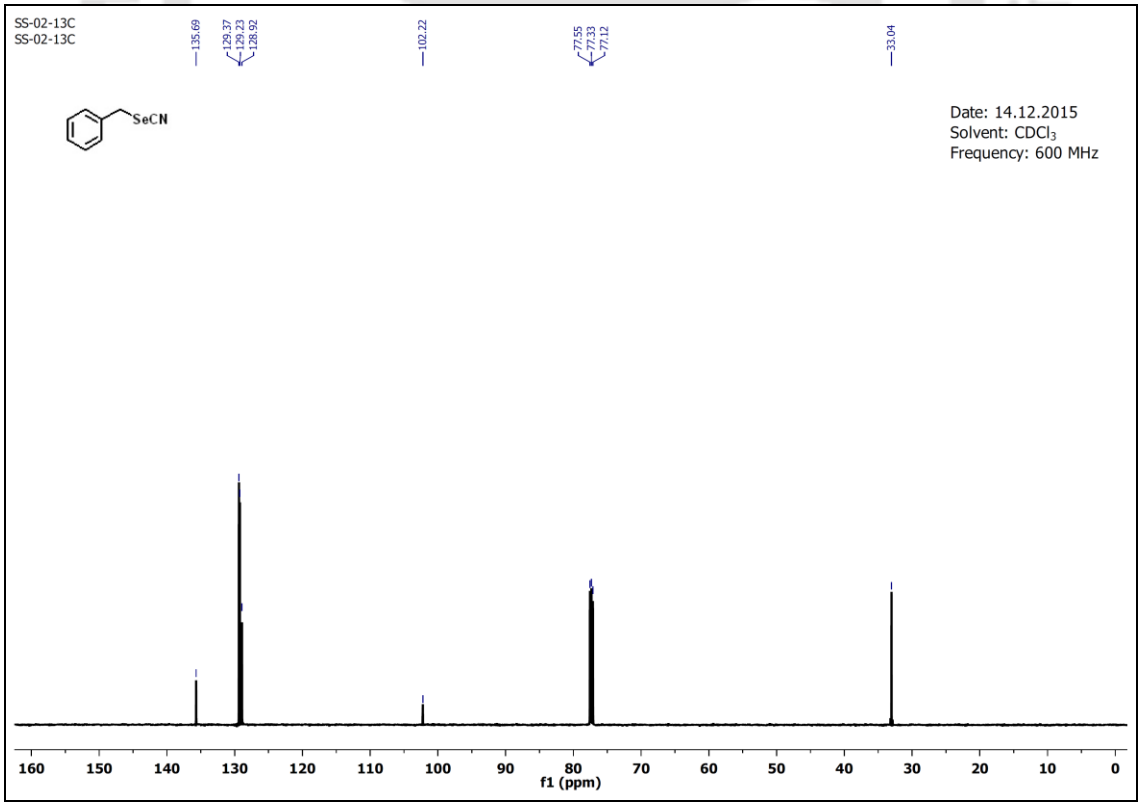

Figure A4.2. ^{13}C NMR spectrum ($CDCl_3$, 150 MHz) of compound **1.48**.

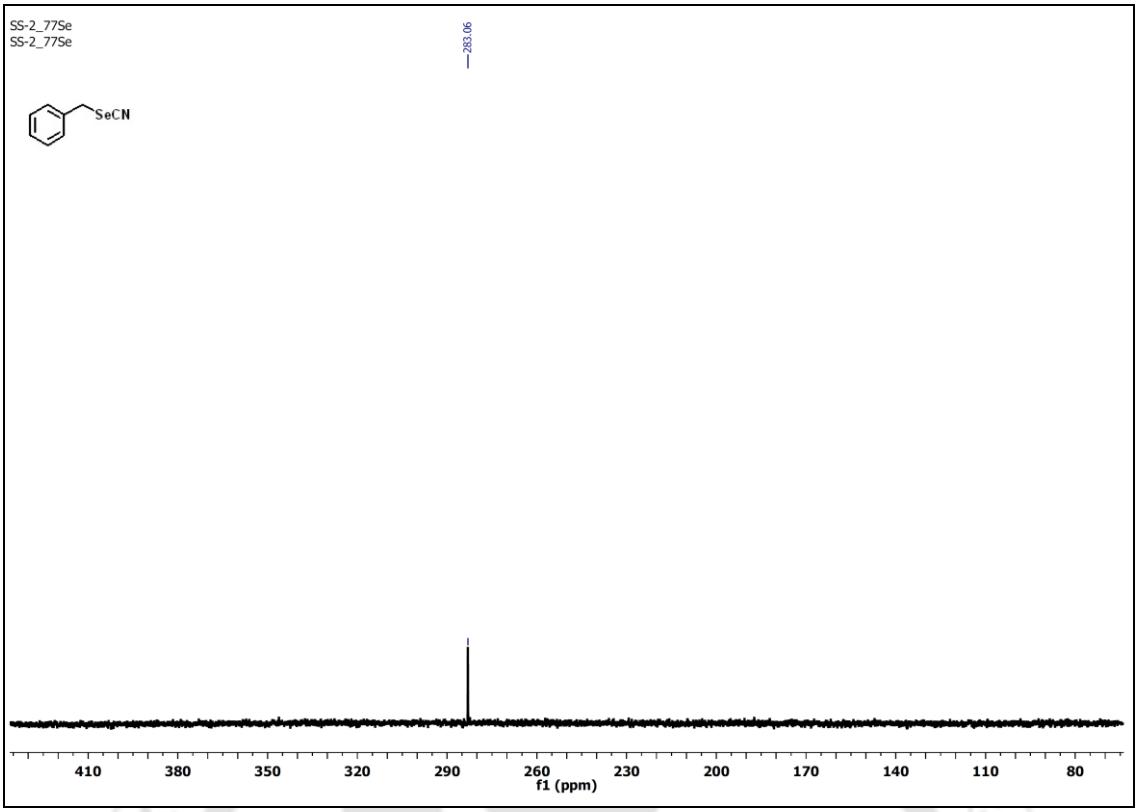

Figure A4.3. ^{77}Se NMR spectrum ($CDCl_3$, 114 MHz) of compound **1.48**.

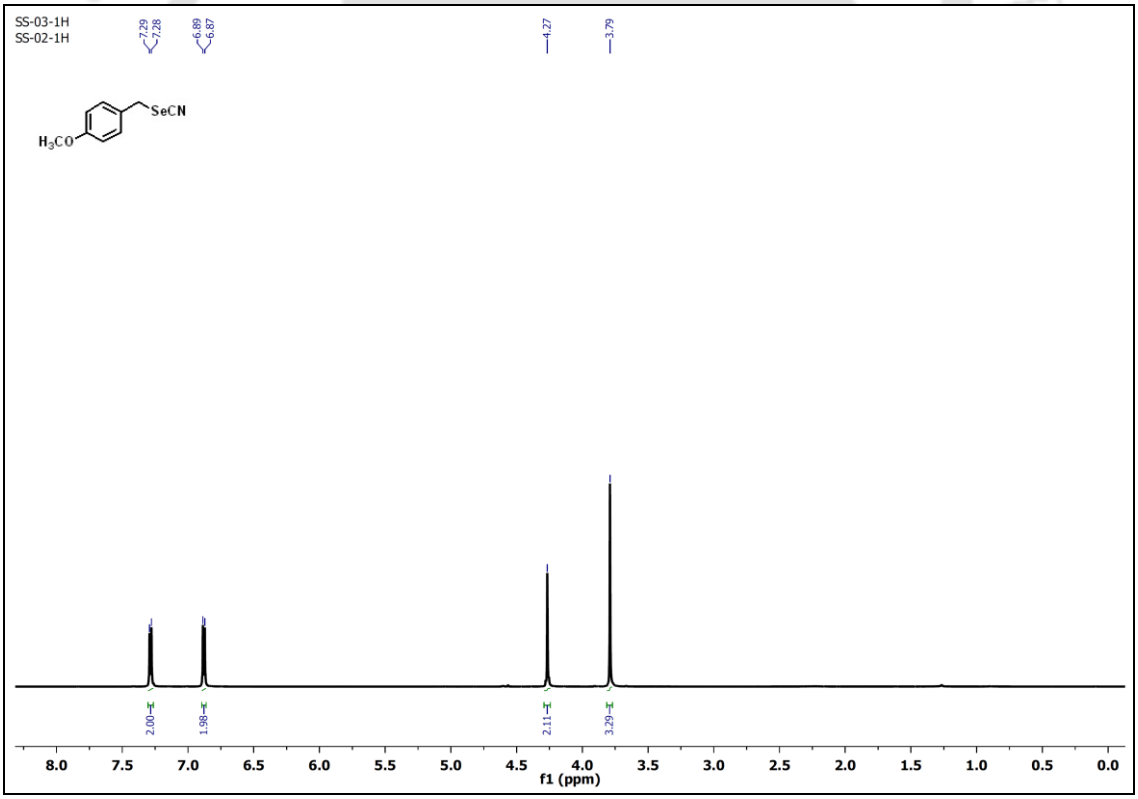

Figure A4.4. ^{1}H NMR spectrum ($CDCl_3$, 600 MHz) of compound **1.49**.

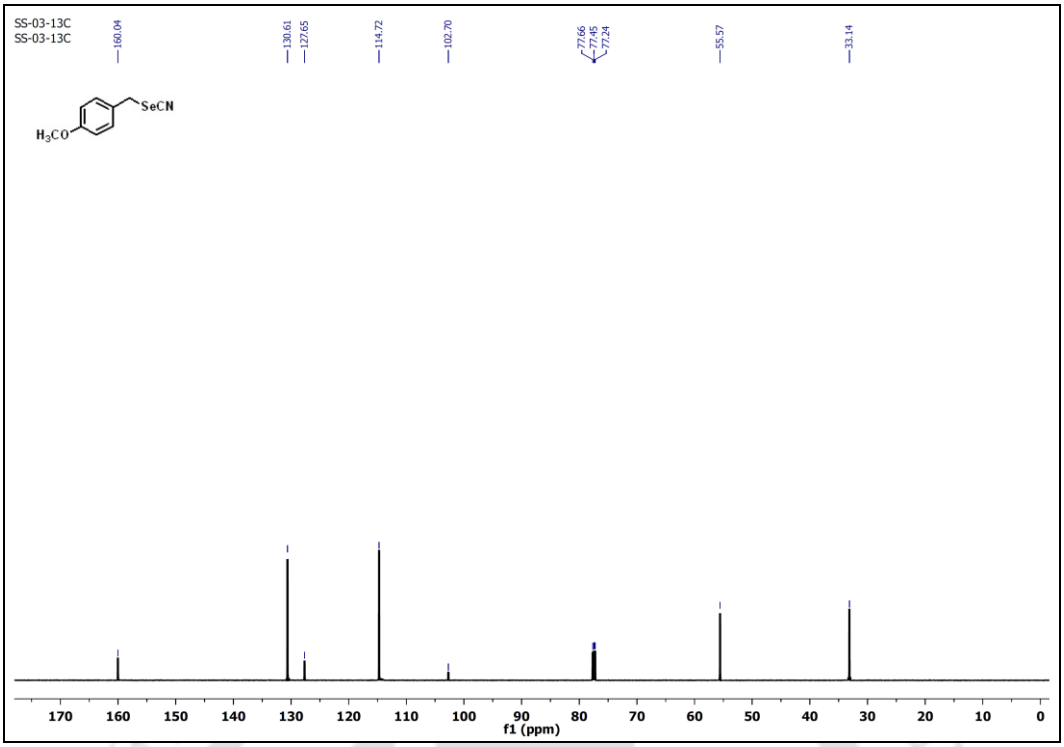

Figure A4.5. ^{13}C NMR spectrum ($CDCl_3$, 150 MHz) of compound **1.49**.

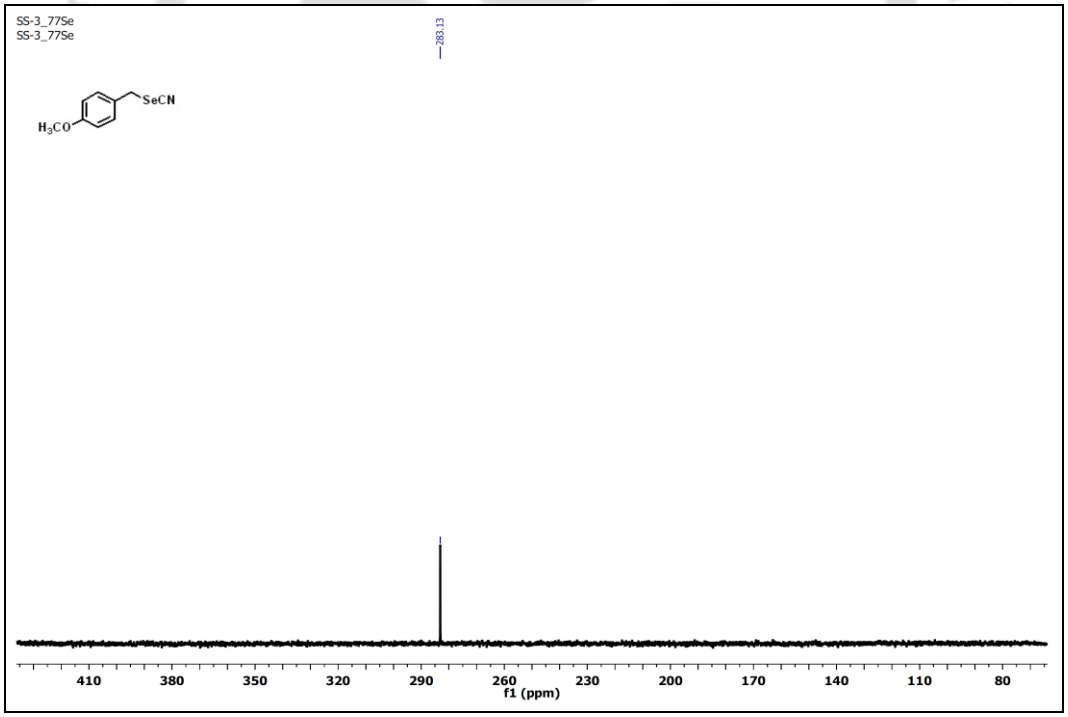

Figure A4.6. ^{77}Se NMR spectrum ($CDCl_3$, 114 MHz) of compound **1.49**.

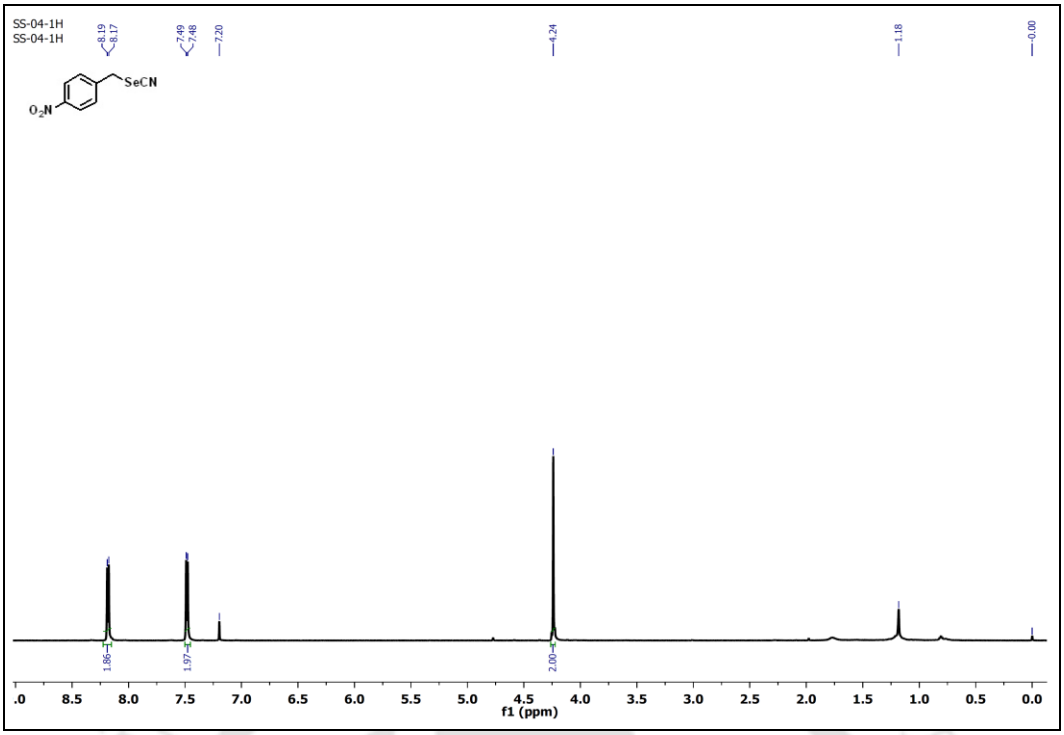

Figure A4.7. ^{1}H NMR spectrum ($CDCl_3$, 600 MHz) of compound **3.8**.

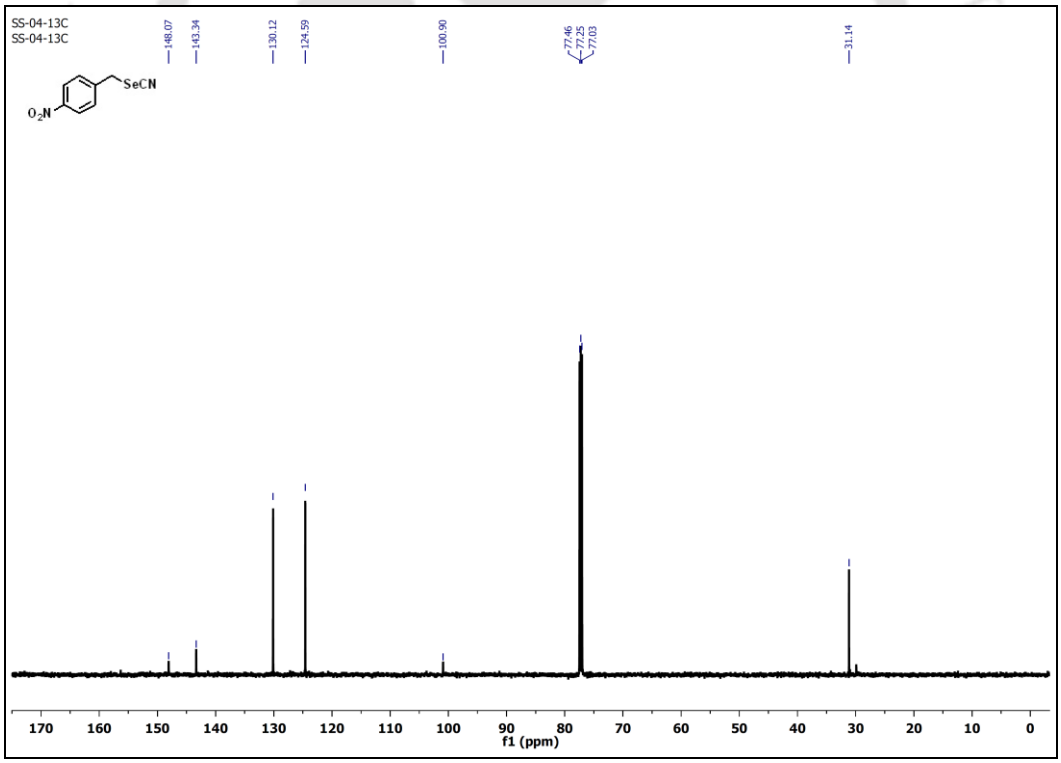

Figure A4.8. ^{13}C NMR spectrum ($CDCl_3$, 150 MHz) of compound **3.8**.

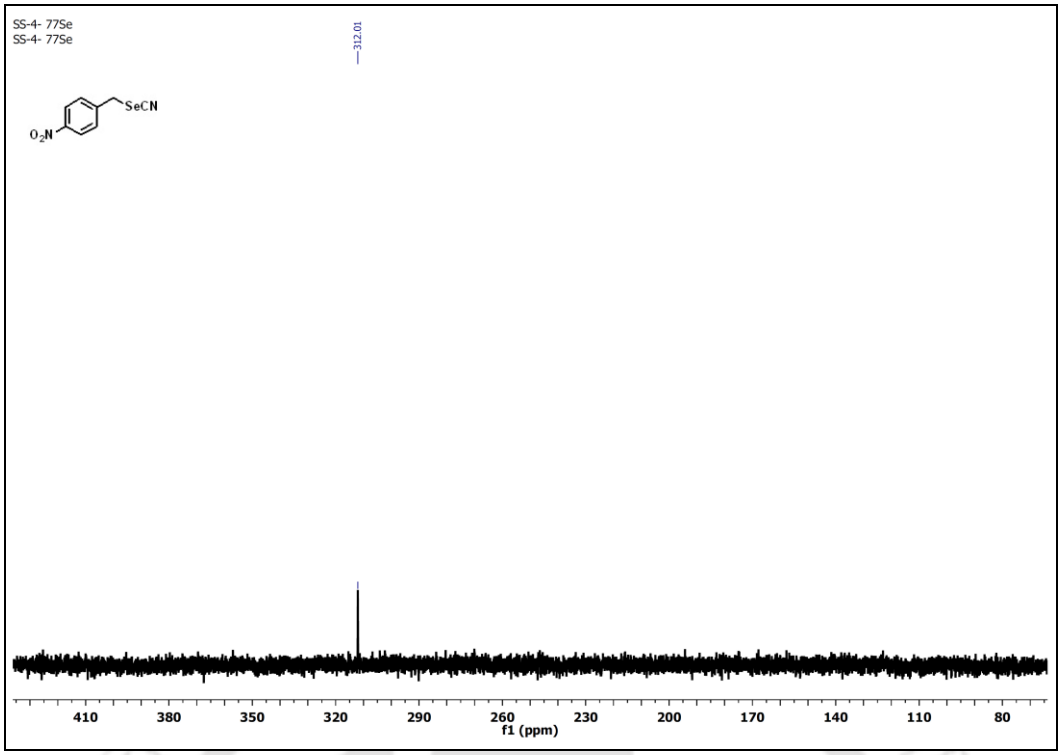

Figure A4.9. ^{77}Se NMR spectrum ($CDCl_3$, 114 MHz) of compound **3.8**.

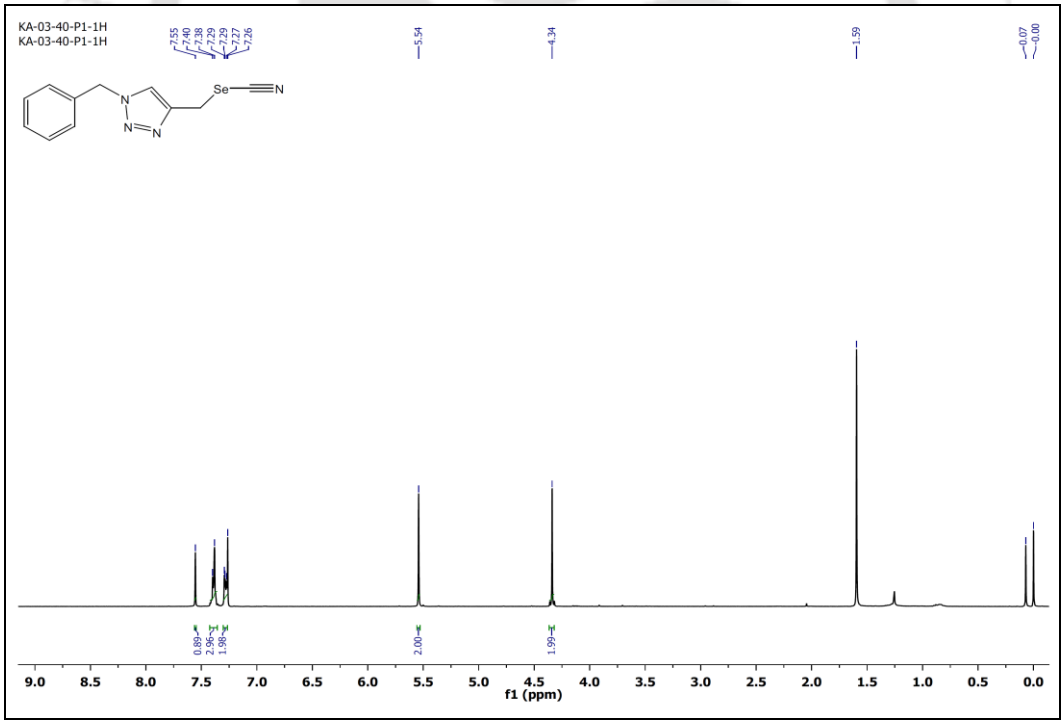

Figure A4.10. ^{1}H NMR spectrum ($CDCl_3$, 400 MHz) of compound **3.9**.

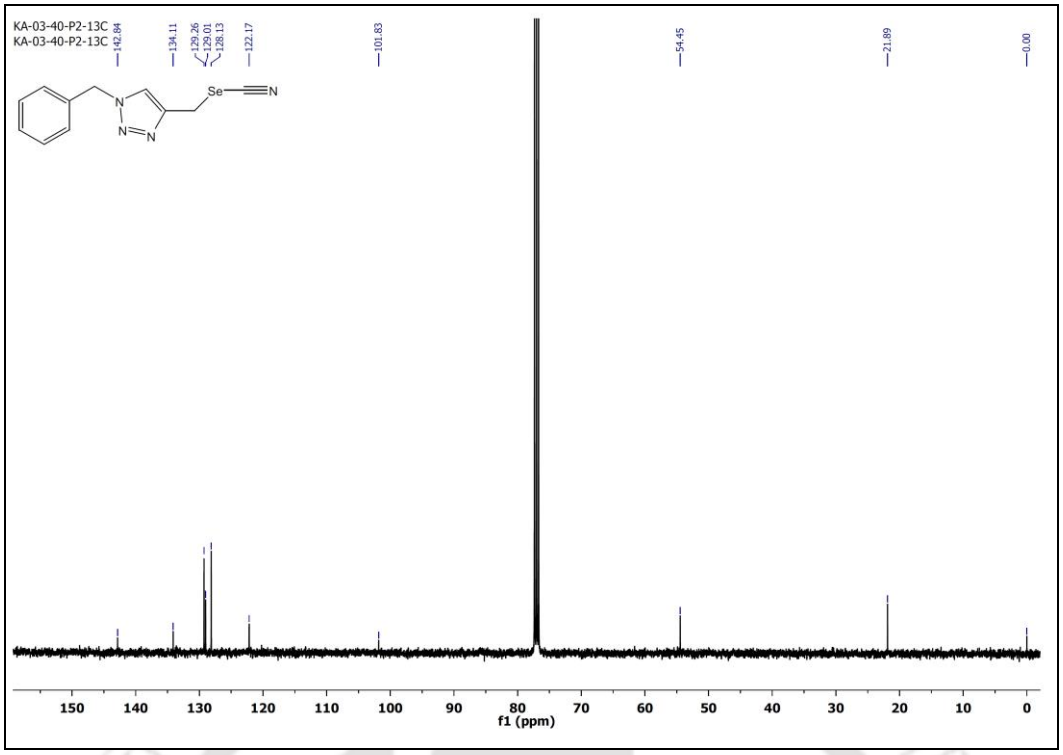

Figure A4.11. ^{13}C NMR spectrum ($CDCl_3$, 100 MHz) of compound **3.9**.

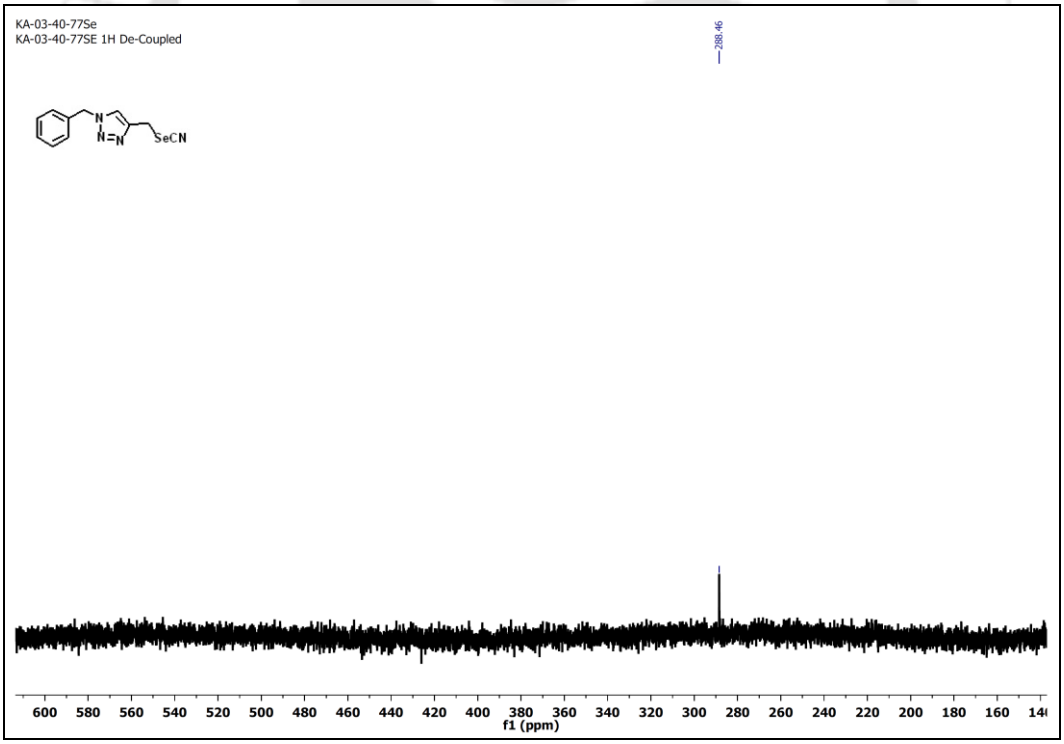

Figure A4.12. ^{77}Se NMR spectrum ($CDCl_3$, 76 MHz) of compound **3.9**.

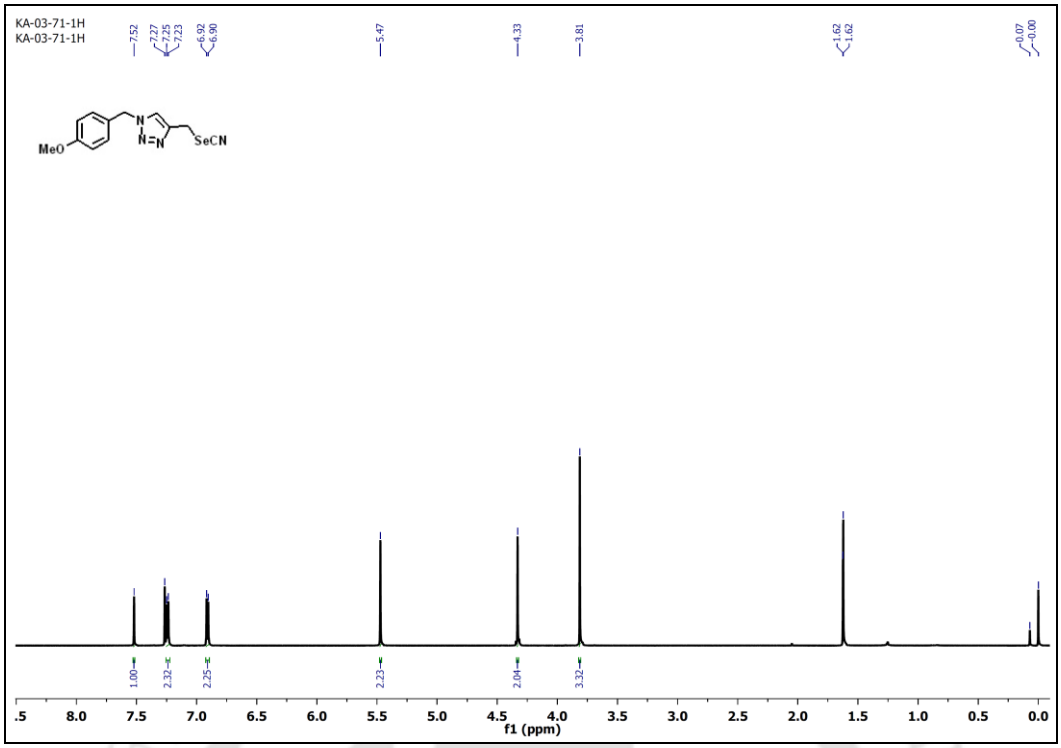

Figure A4.13. ^{1}H NMR spectrum ($CDCl_3$, 600 MHz) of compound **3.10**.

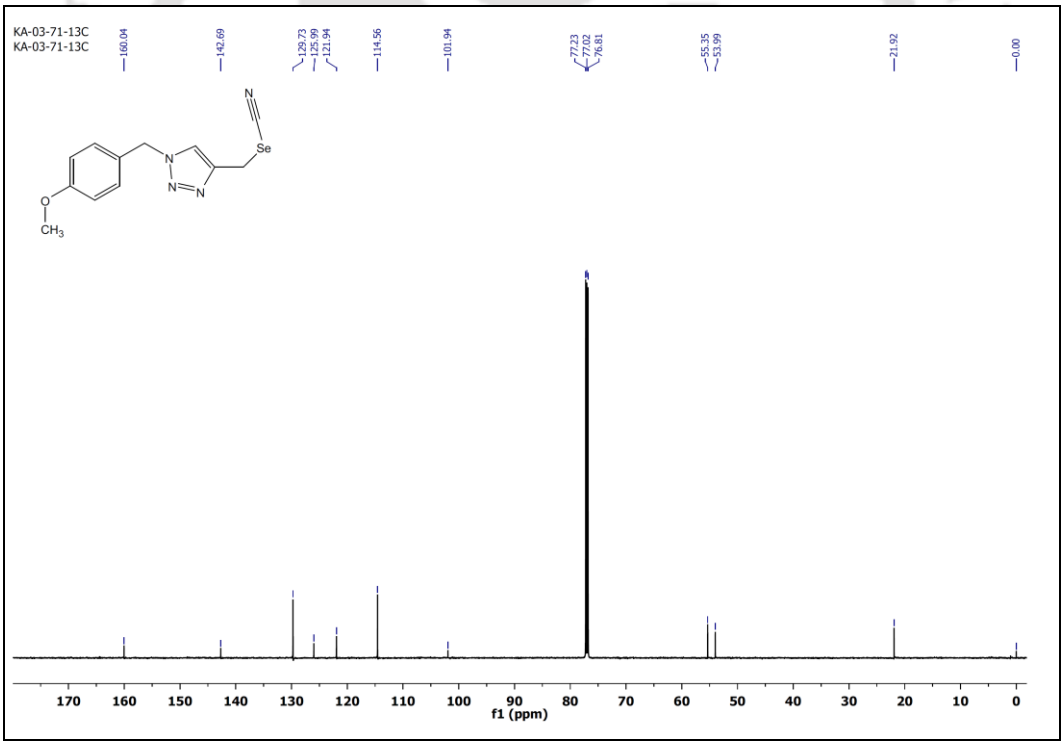

Figure A4.14. ^{13}C NMR spectrum ($CDCl_3$, 150 MHz) of compound **3.10**.

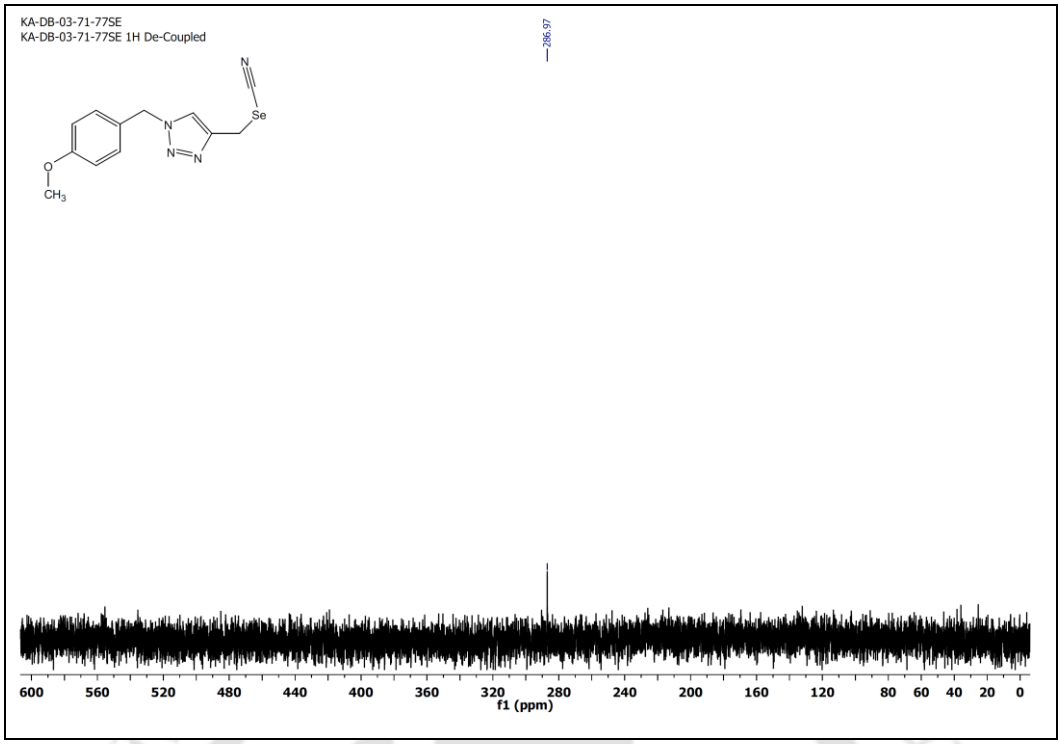

Figure A4.15. ^{77}Se NMR spectrum ($CDCl_3$, 76 MHz) of compound **3.10**.

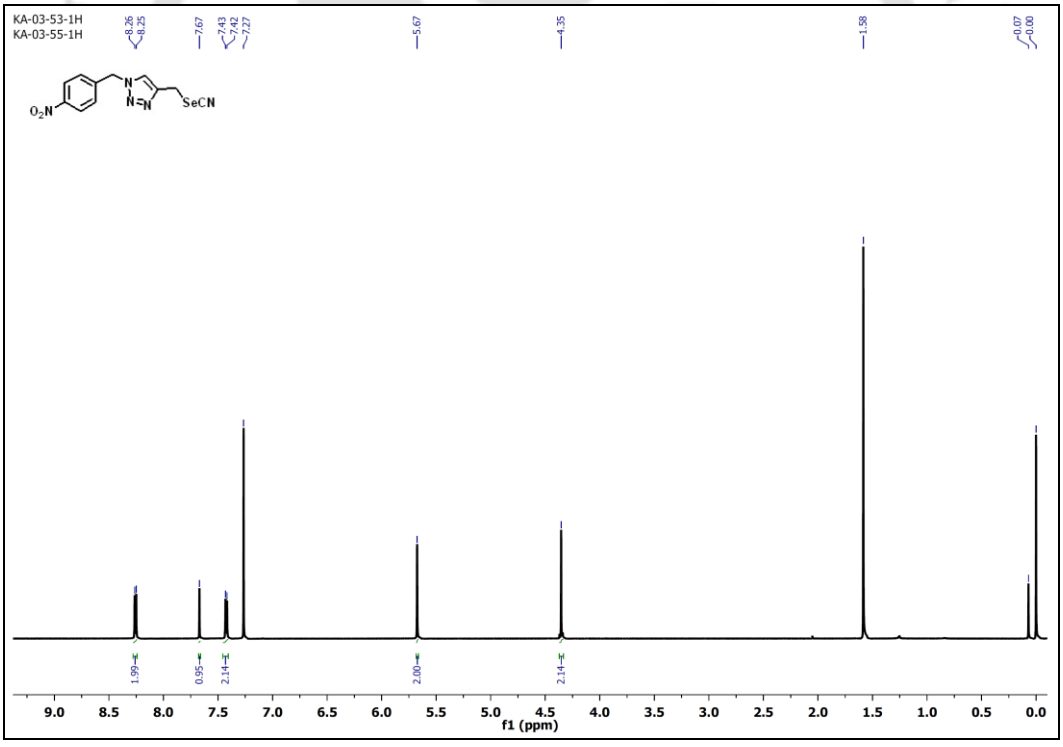

Figure A4.16. ^{1}H NMR spectrum ($CDCl_3$, 600 MHz) of compound **3.11**.

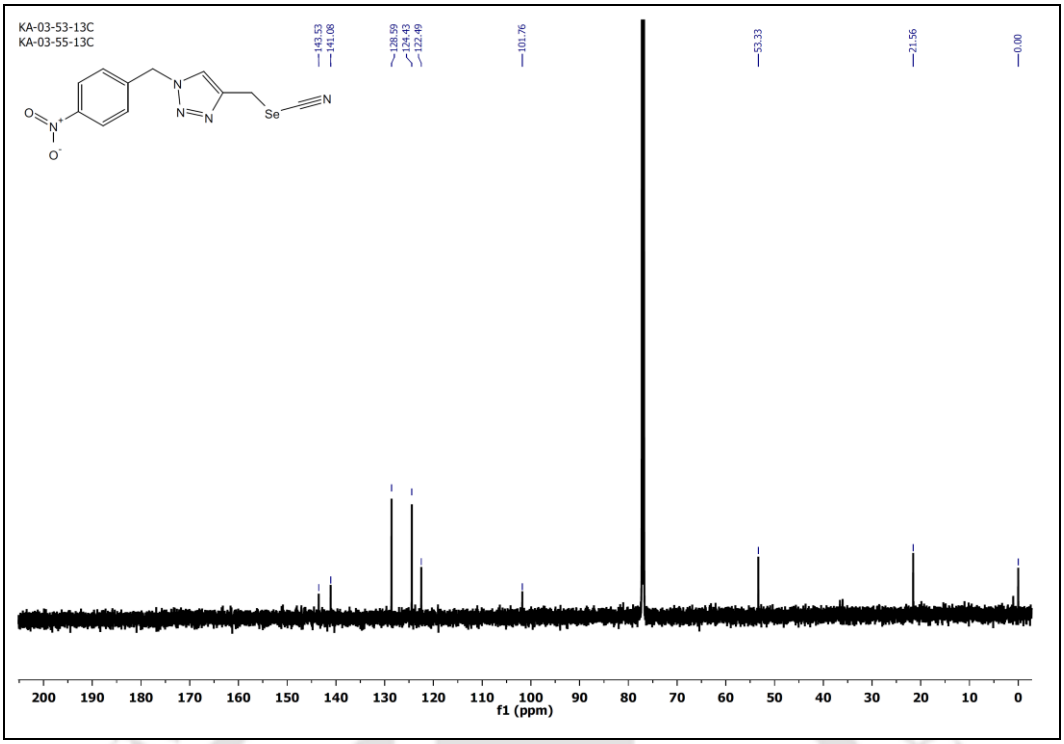

Figure A4.17. ^{13}C NMR spectrum ($CDCl_3$, 150 MHz) of compound **3.11**.

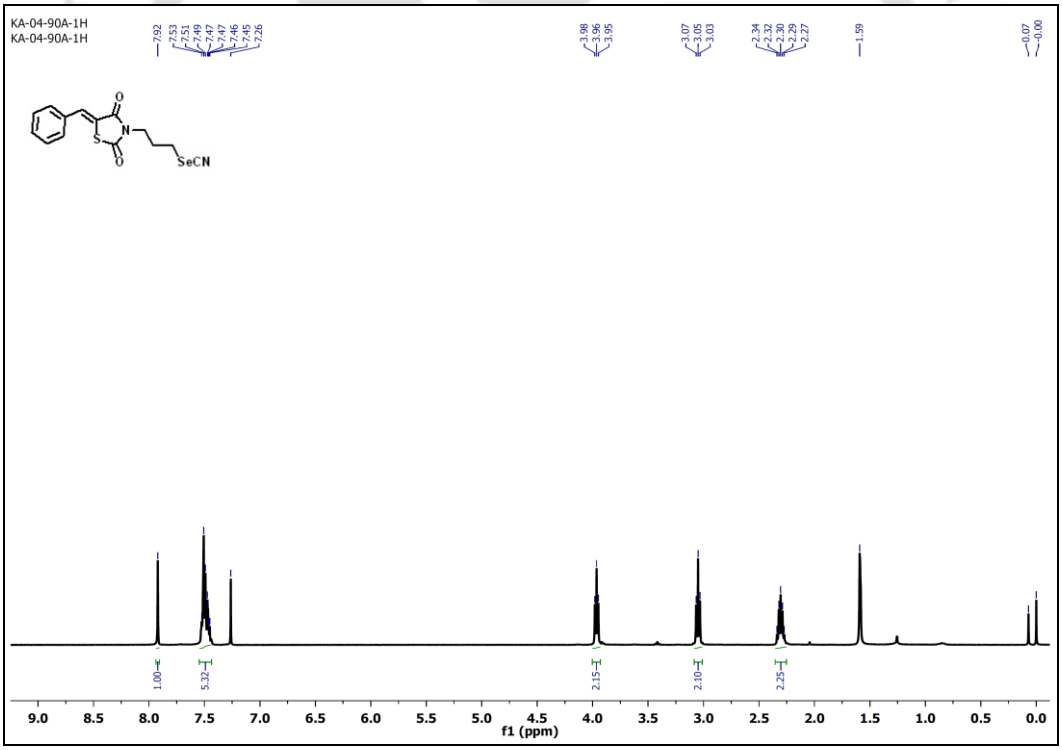

Figure A4.18. ^{1}H NMR spectrum ($CDCl_3$, 400 MHz) of compound **3.12**.

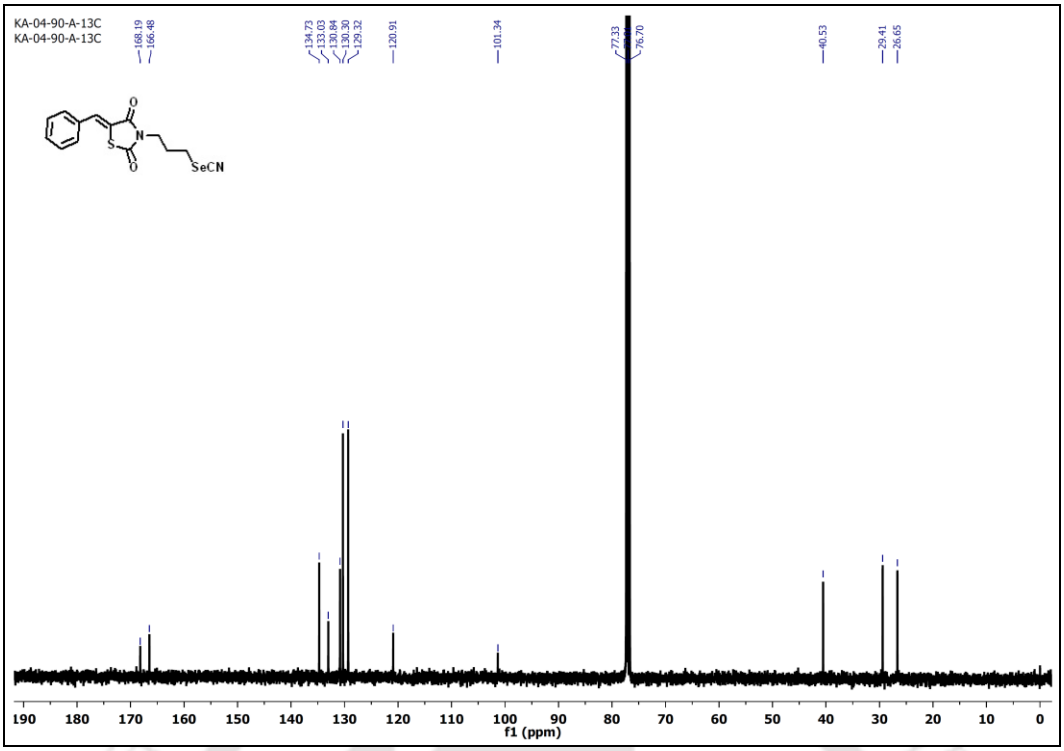

Figure A4.19. ^{13}C NMR spectrum ($CDCl_3$, 100 MHz) of compound **3.12**.

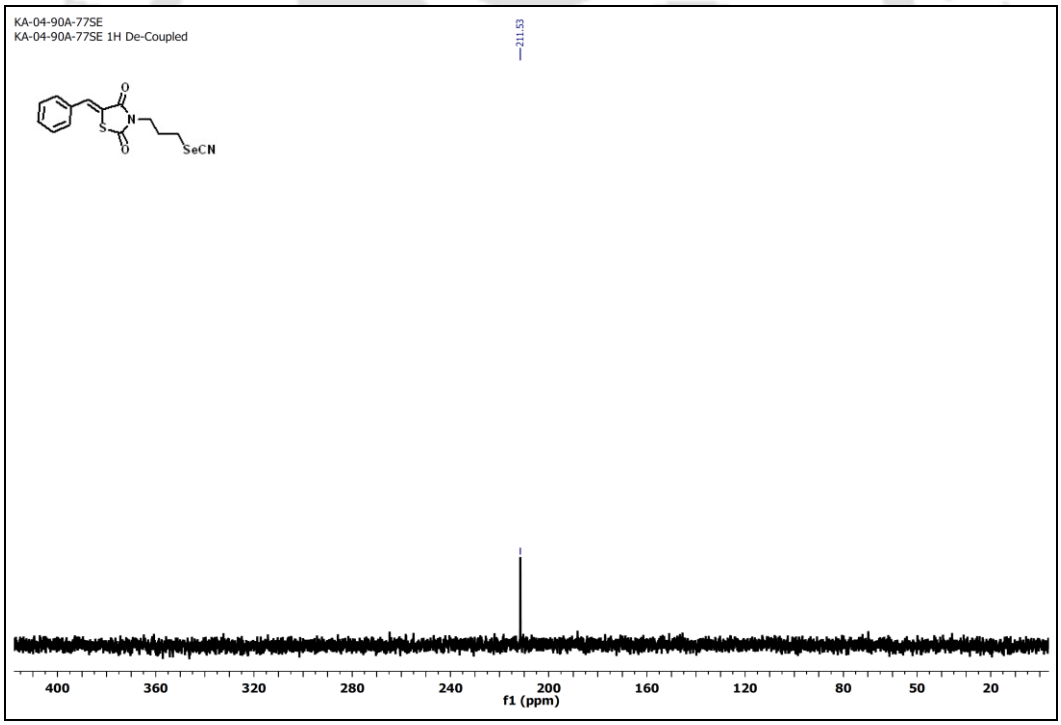

Figure A4.20. ^{77}Se NMR spectrum ($CDCl_3$, 76 MHz) of compound **3.12**.

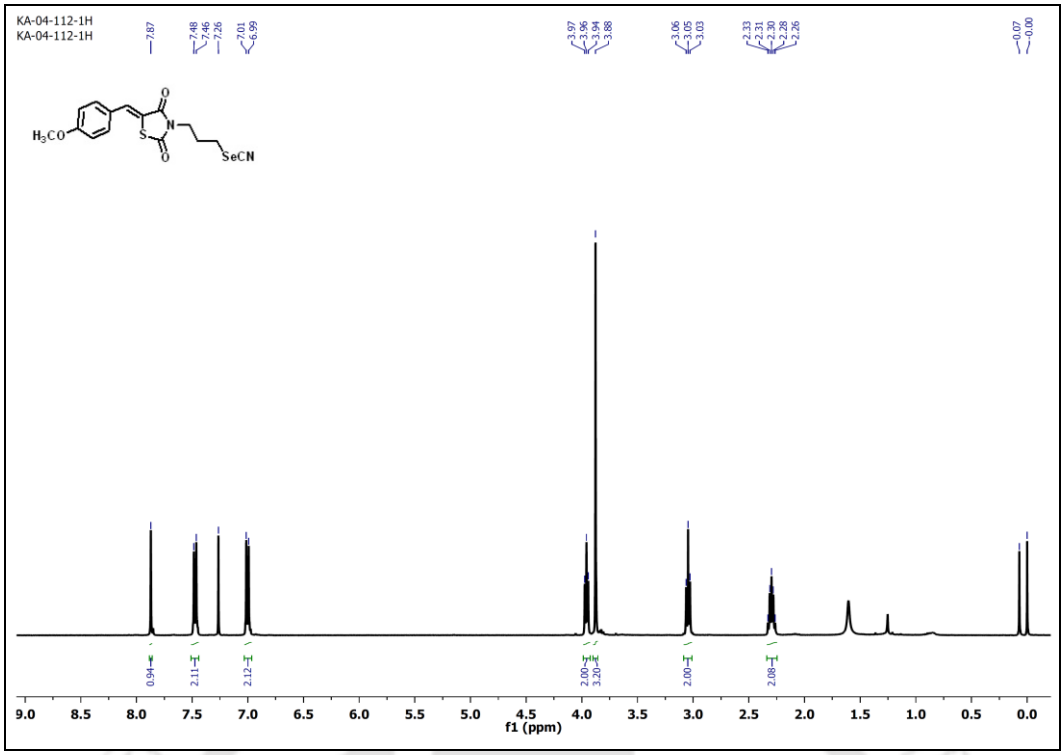

Figure A4.21. ^{1}H NMR spectrum ($CDCl_3$, 400 MHz) of compound **3.13**.

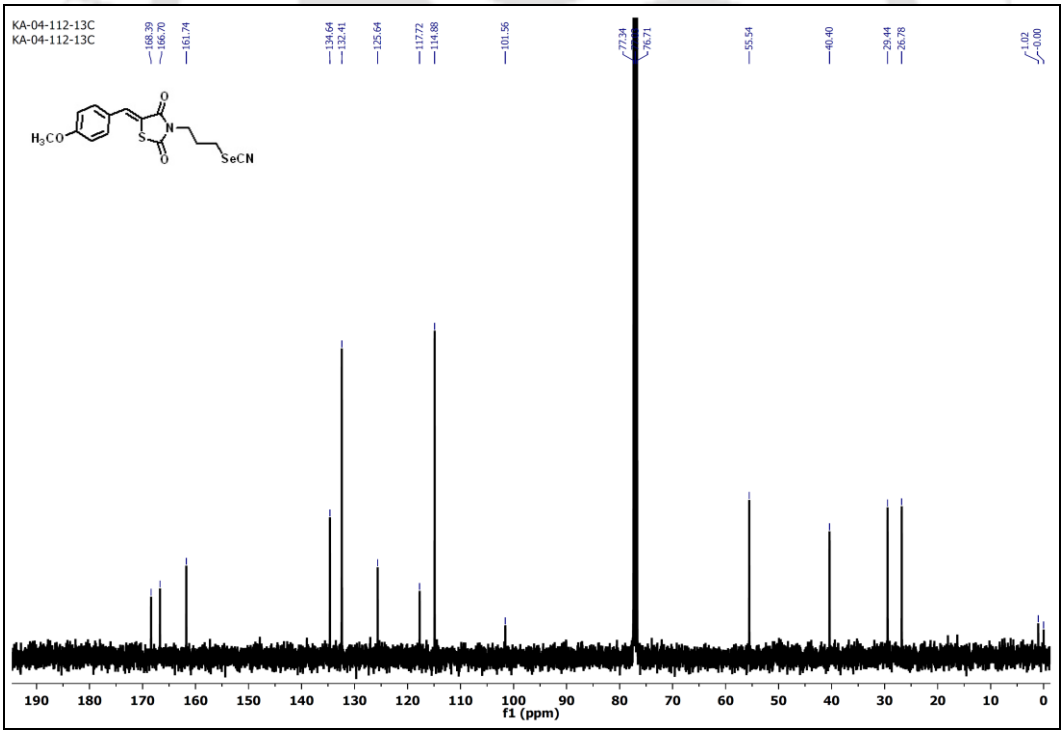

Figure A4.22. ^{13}C NMR spectrum ($CDCl_3$, 100 MHz) of compound **3.13**.

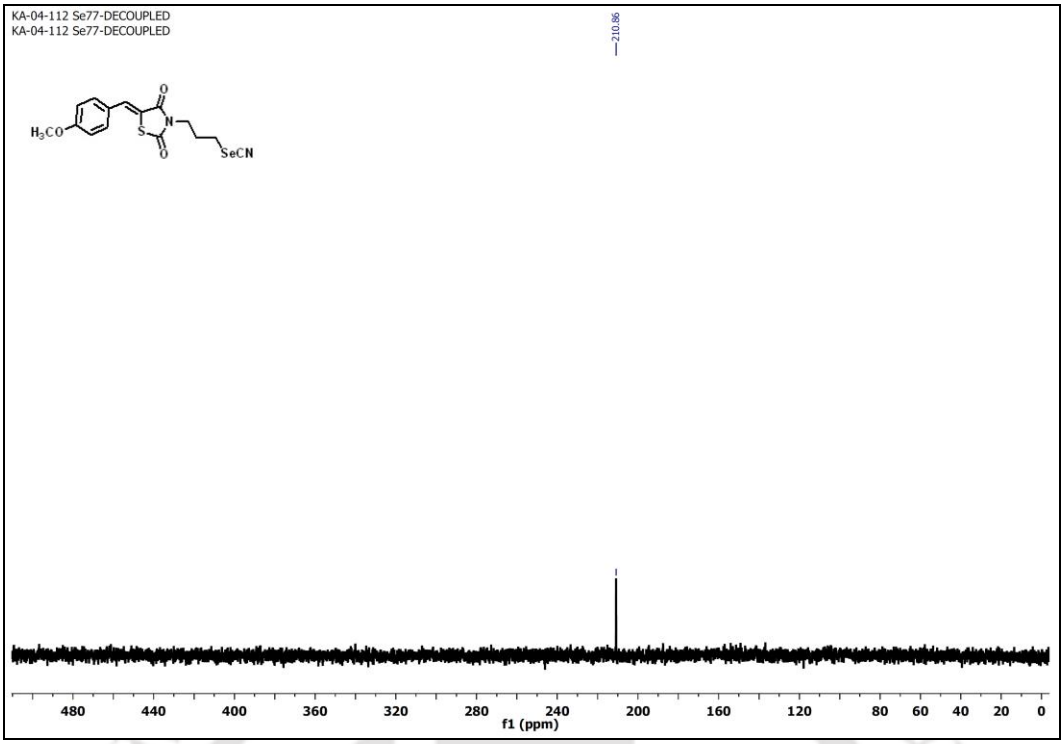

Figure A4.23. ^{77}Se NMR spectrum ($CDCl_3$, 76 MHz) of compound **3.13**.

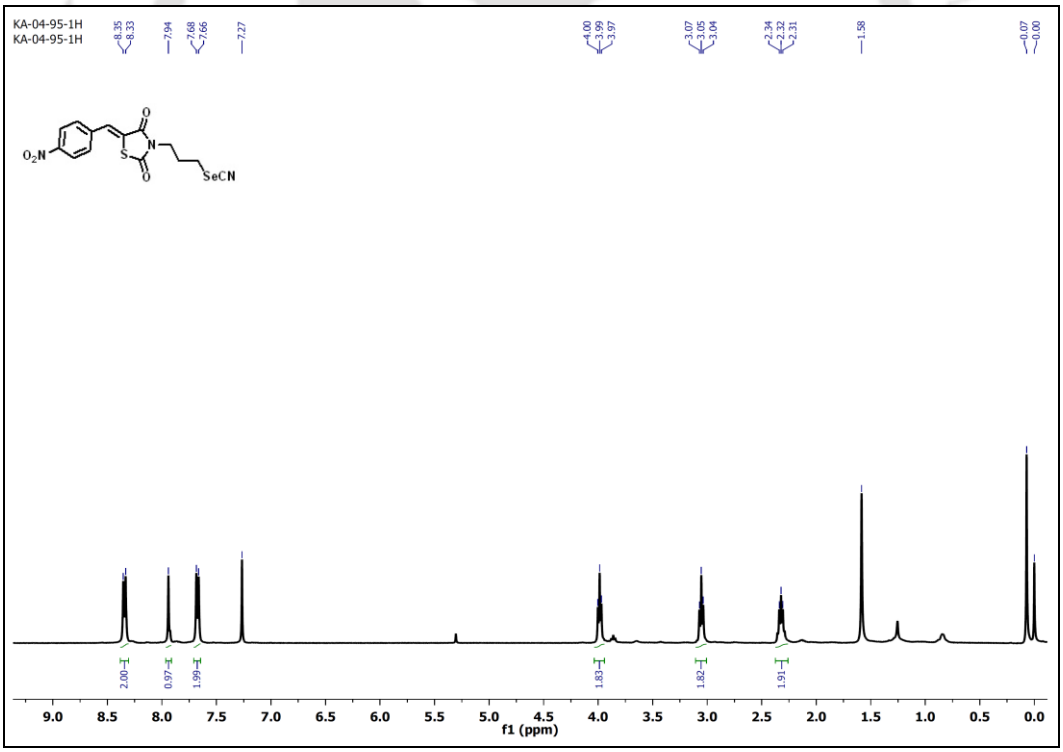

Figure A4.24. ^{1}H NMR spectrum ($CDCl_3$, 400 MHz) of compound **3.14**.

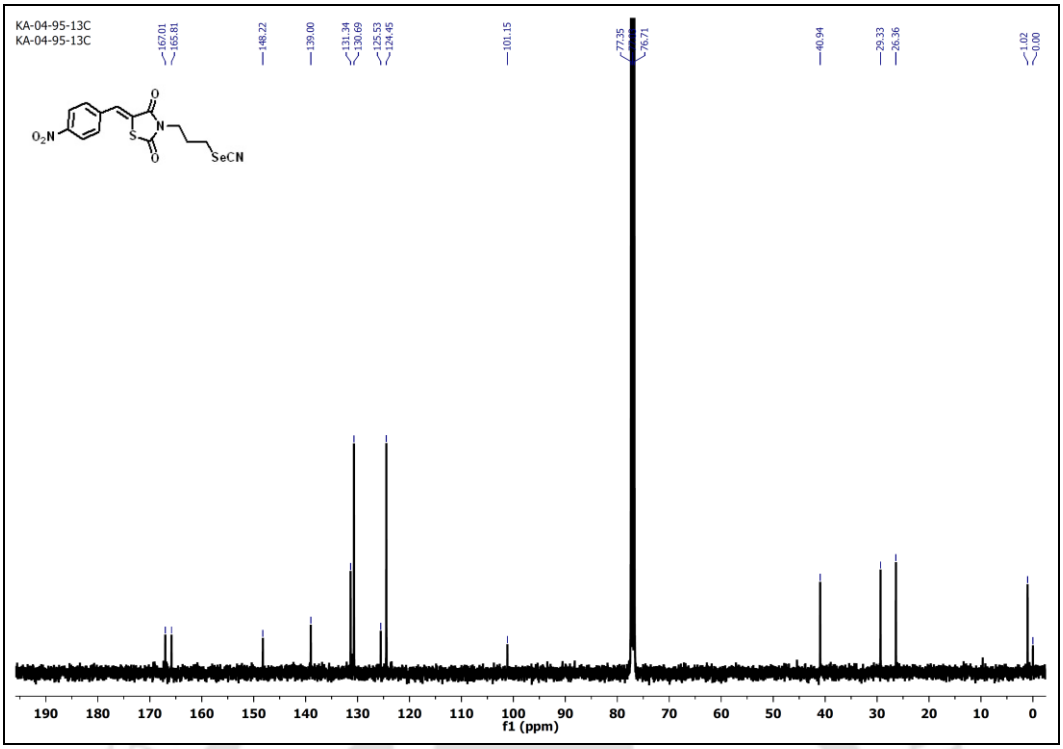

Figure A4.25. ^{13}C NMR spectrum ($CDCl_3$, 100 MHz) of compound **3.14**.

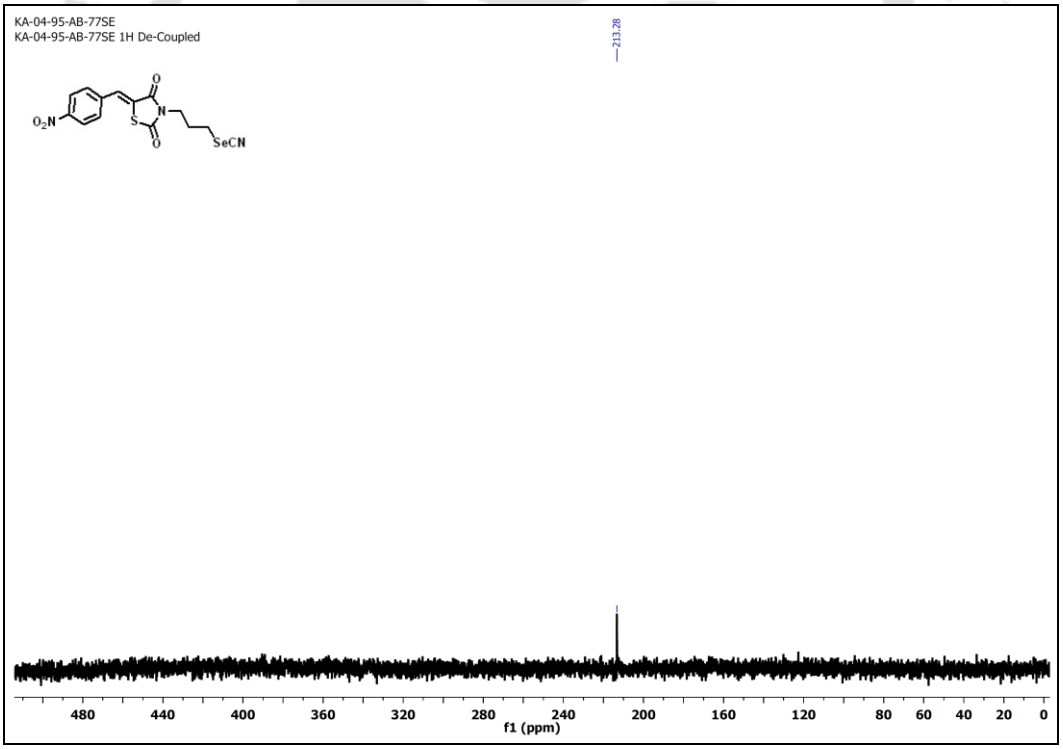

Figure A4.26. ^{77}Se NMR spectrum ($CDCl_3$, 76 MHz) of compound **3.14**.

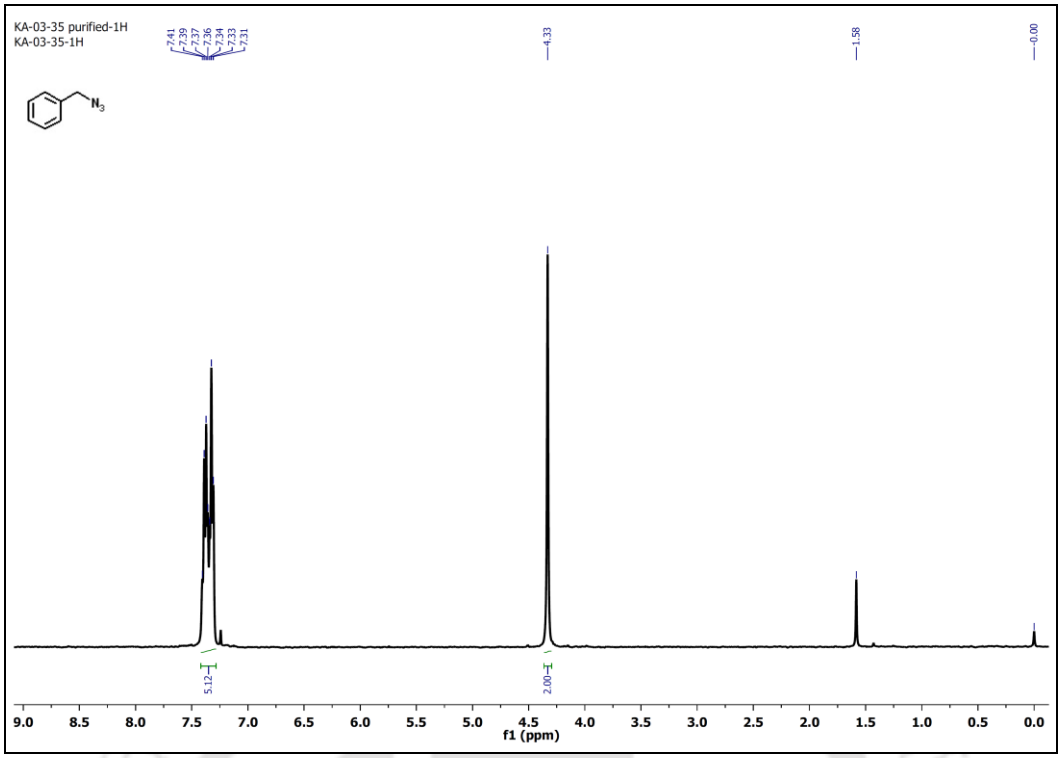

Figure A4.27. ^{1}H NMR spectrum ($CDCl_3$, 400 MHz) of compound **3.18**.

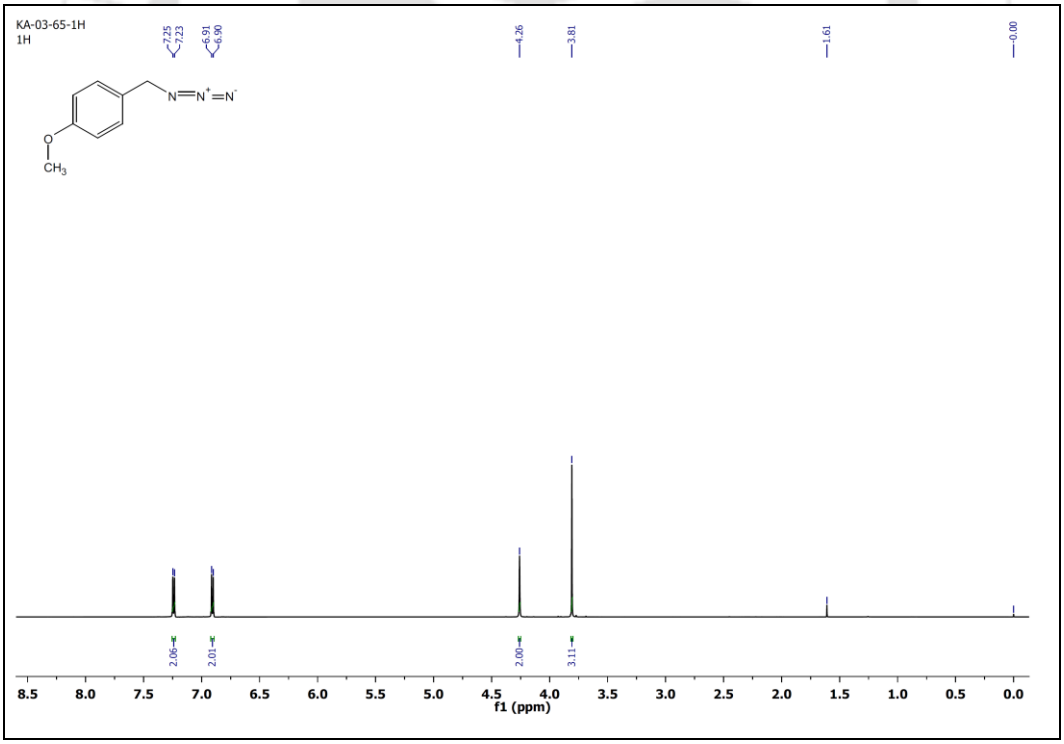

Figure A4.28. ^{1}H NMR spectrum ($CDCl_3$, 600 MHz) of compound **3.19**.

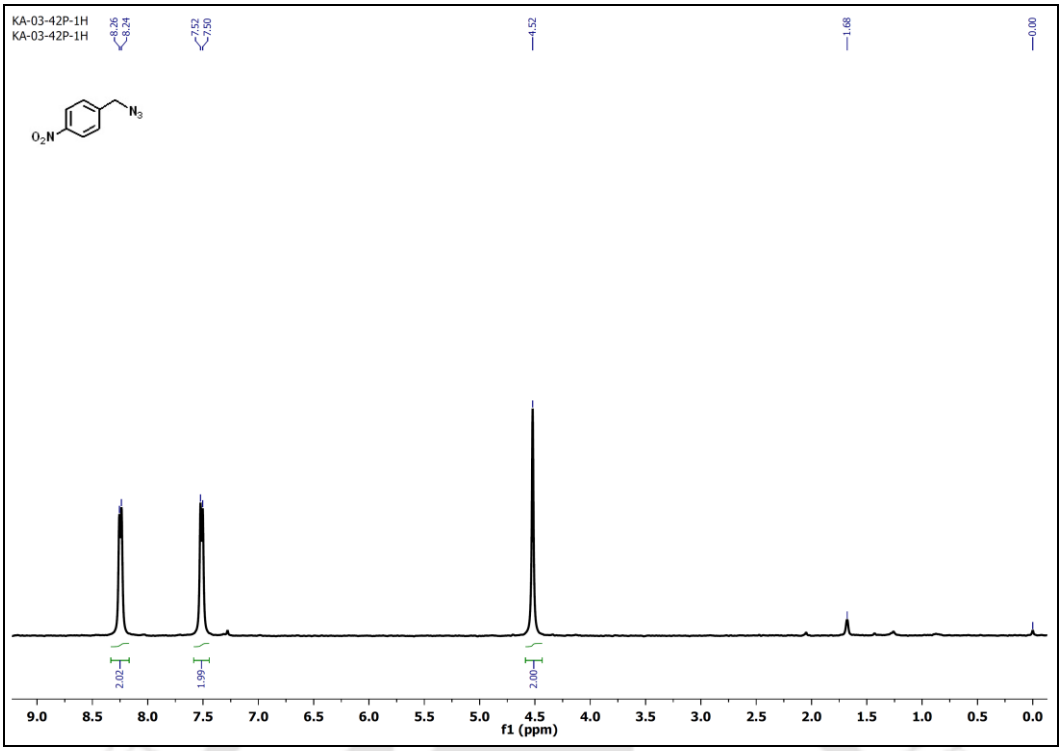

Figure A4.29. ^{1}H NMR spectrum ($CDCl_3$, 400 MHz) of compound **3.20**.

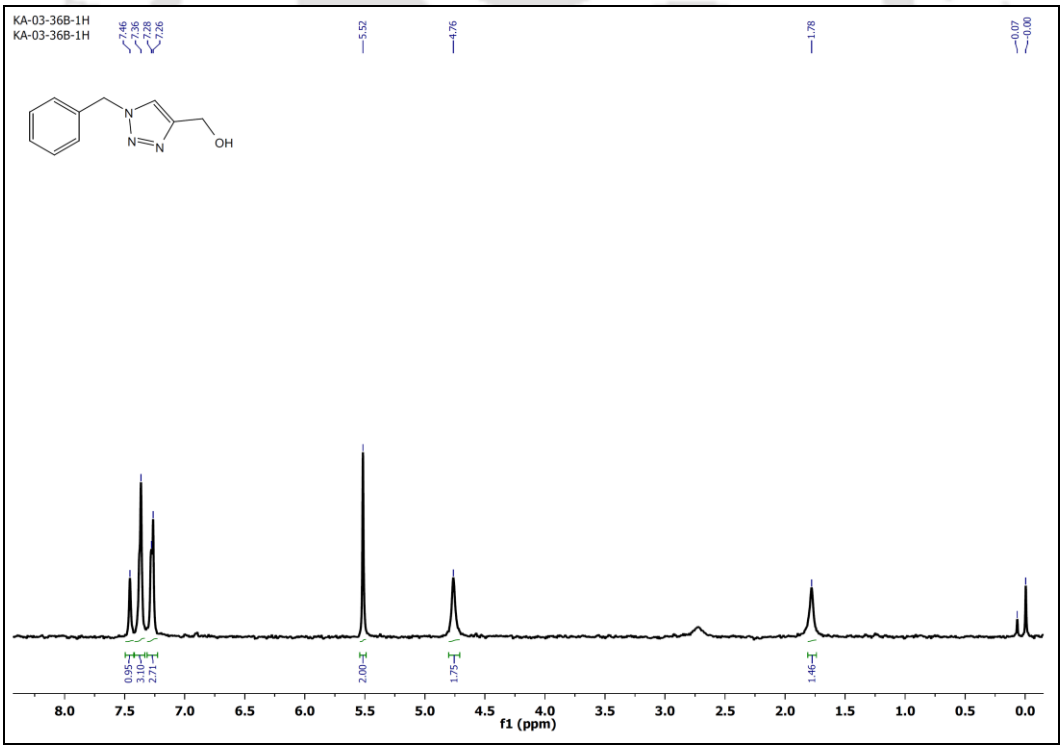

Figure A4.30. ^{1}H NMR spectrum ($CDCl_3$, 400 MHz) of compound **3.21**.

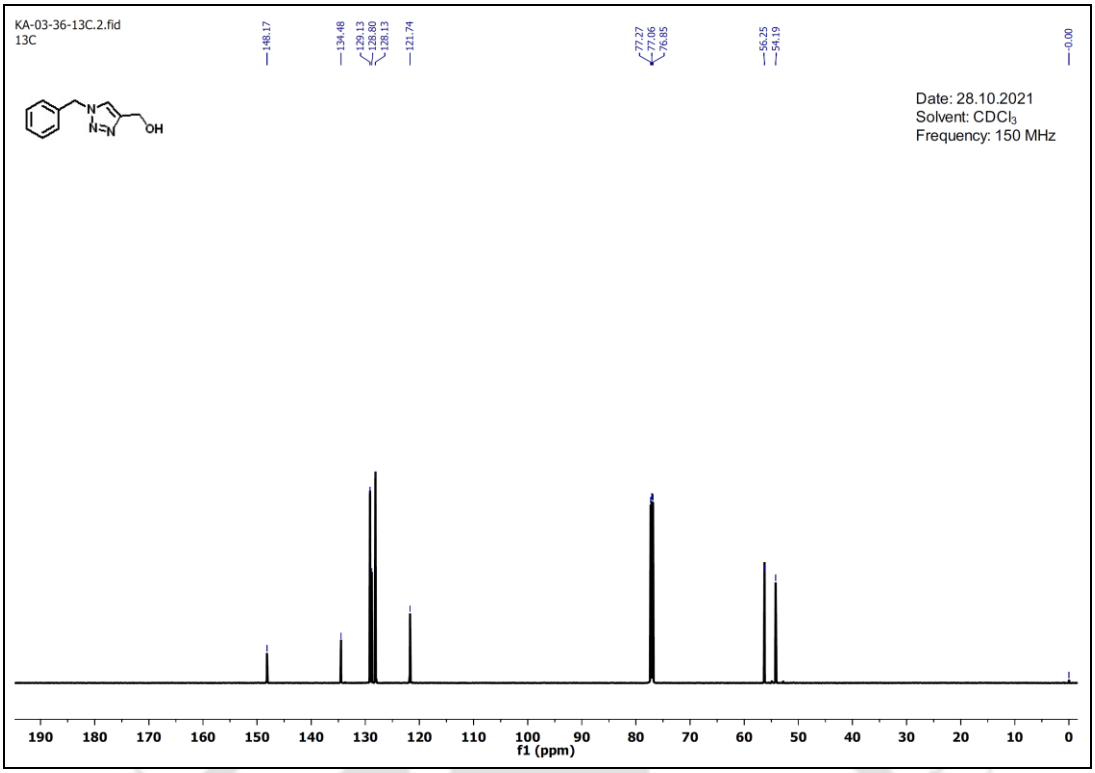

Figure A4.31. ^{13}C NMR spectrum ($CDCl_3$, 150 MHz) of compound **3.21**.

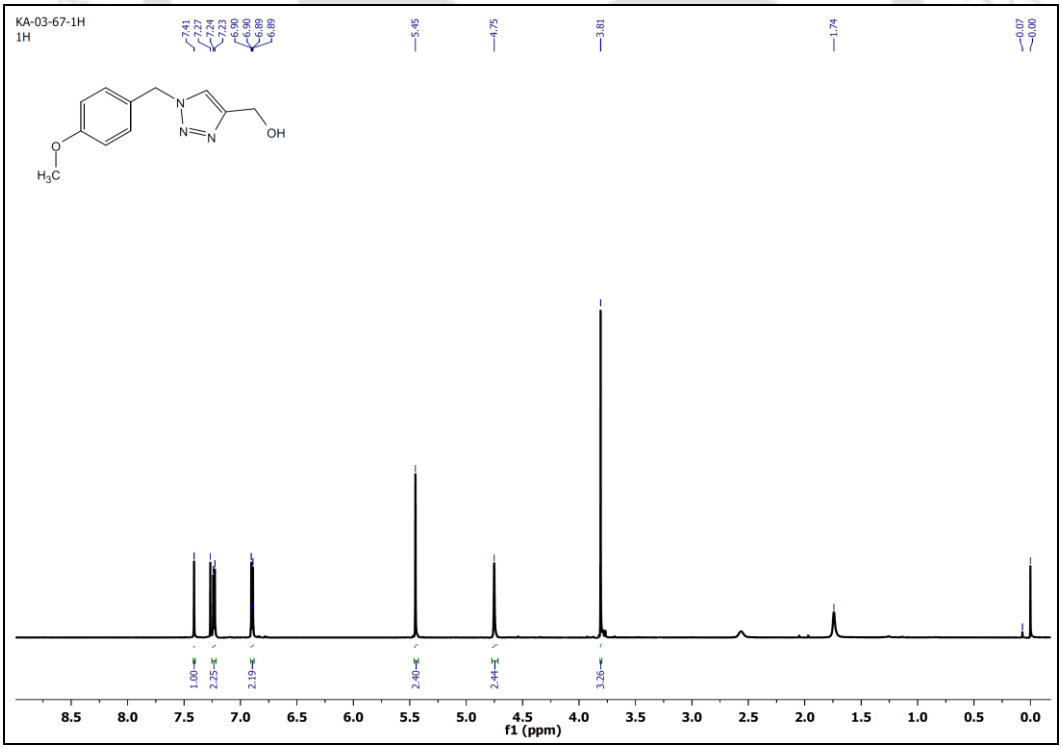

Figure A4.32. ^{1}H NMR spectrum ($CDCl_3$, 600 MHz) of compound **3.22**.

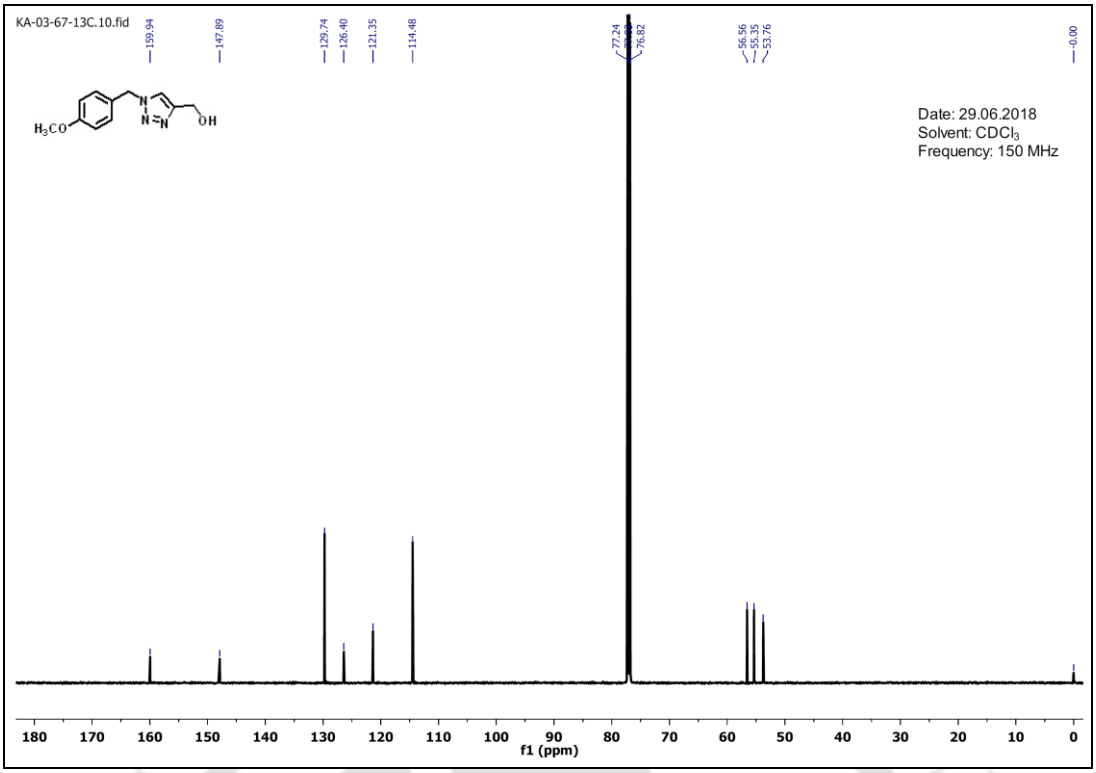

Figure A4.33. ^{13}C NMR spectrum ($CDCl_3$, 150 MHz) of compound **3.22**.

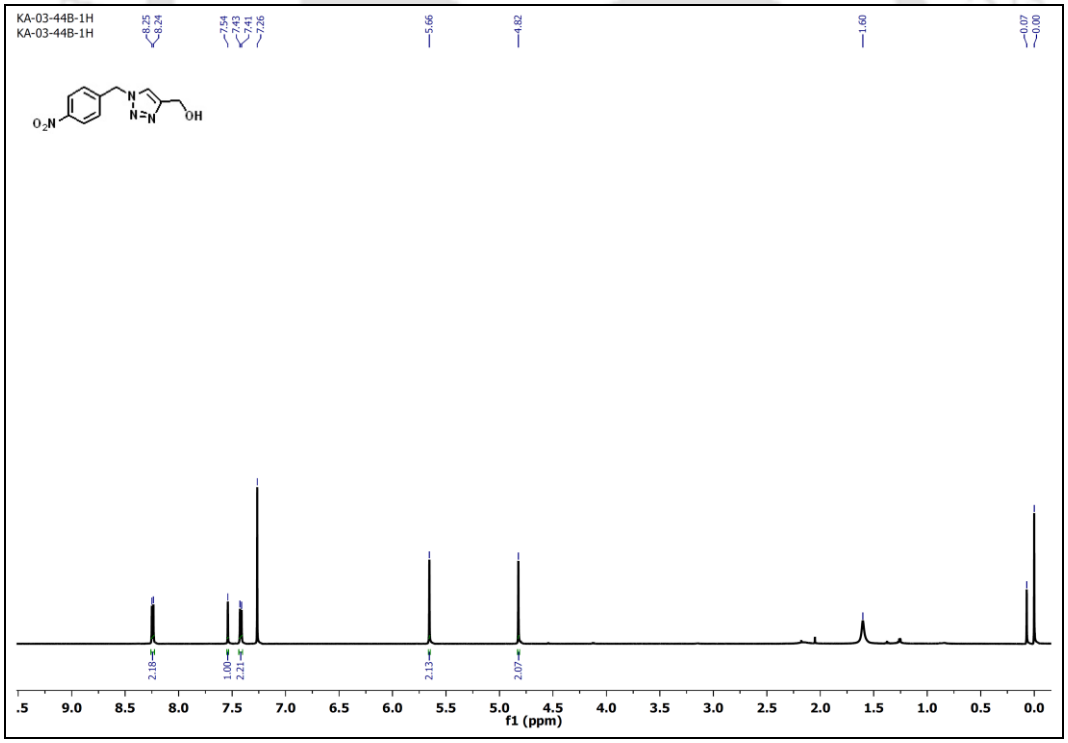

Figure A4.34. ^{1}H NMR spectrum ($CDCl_3$, 600 MHz) of compound **3.23**.

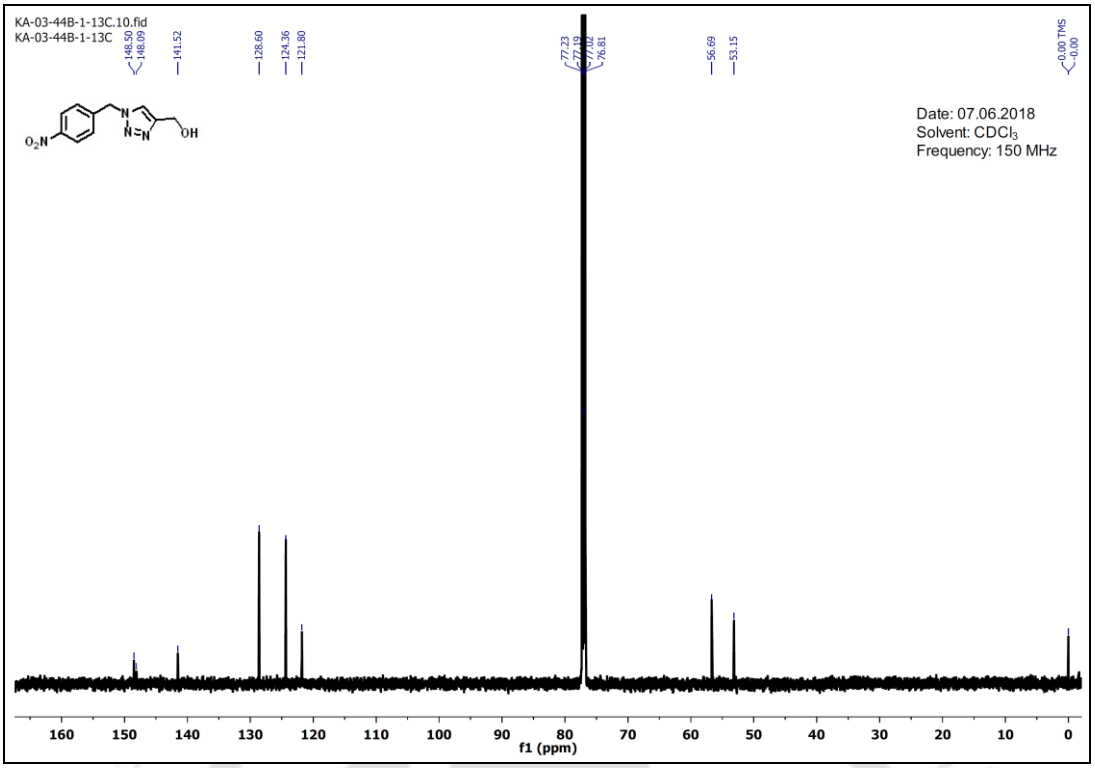

Figure A4.35. ^{13}C NMR spectrum ($CDCl_3$, 150 MHz) of compound **3.23**.

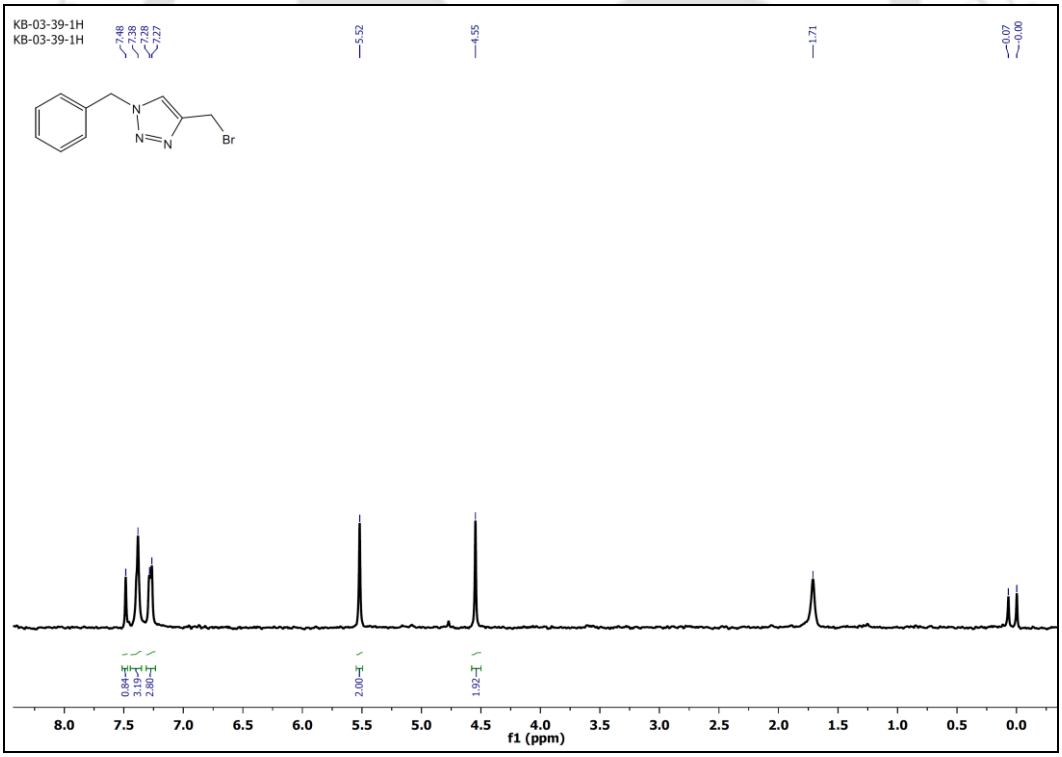

Figure A4.36. ^{1}H NMR spectrum ($CDCl_3$, 400 MHz) of compound **3.24**.

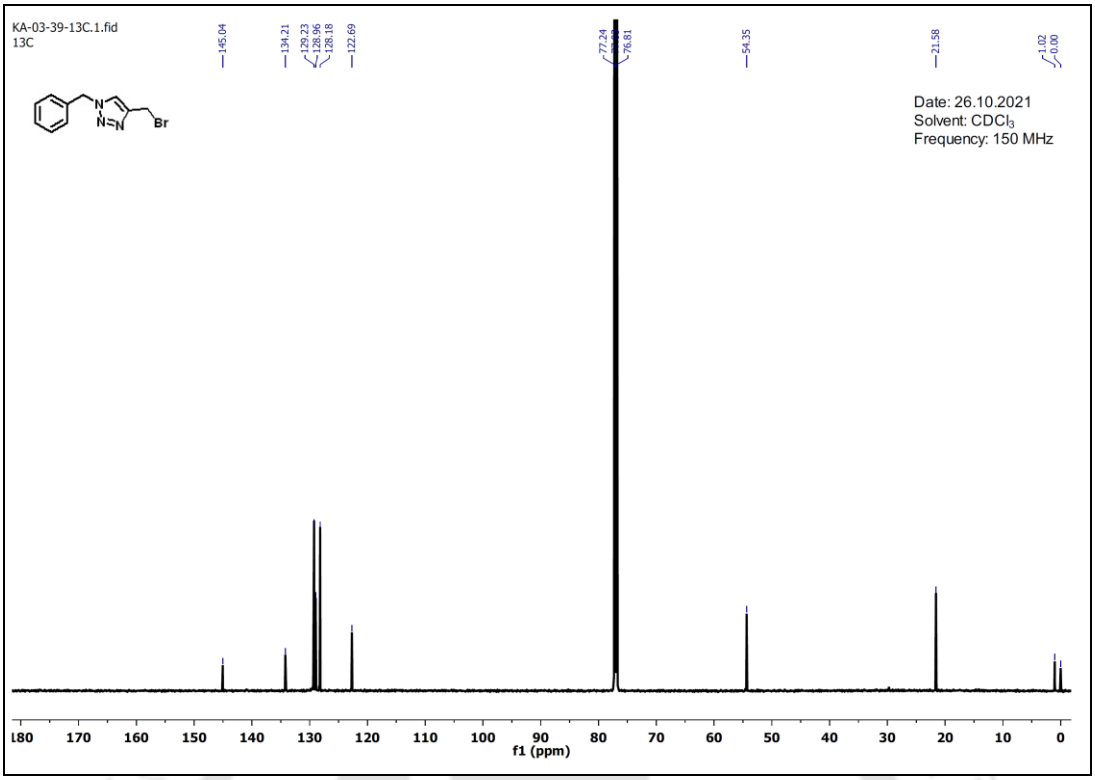

Figure A4.37. ^{13}C NMR spectrum ($CDCl_3$, 150 MHz) of compound **3.24**.

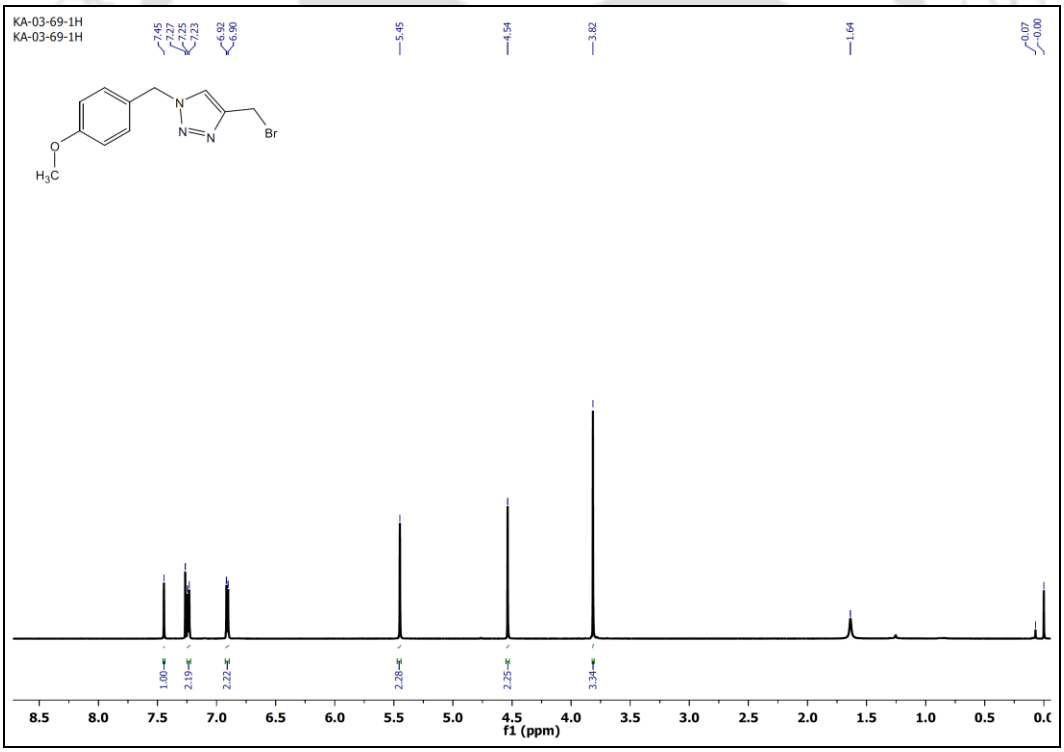

Figure A4.38. ^{1}H NMR spectrum ($CDCl_3$, 600 MHz) of compound **3.25**.

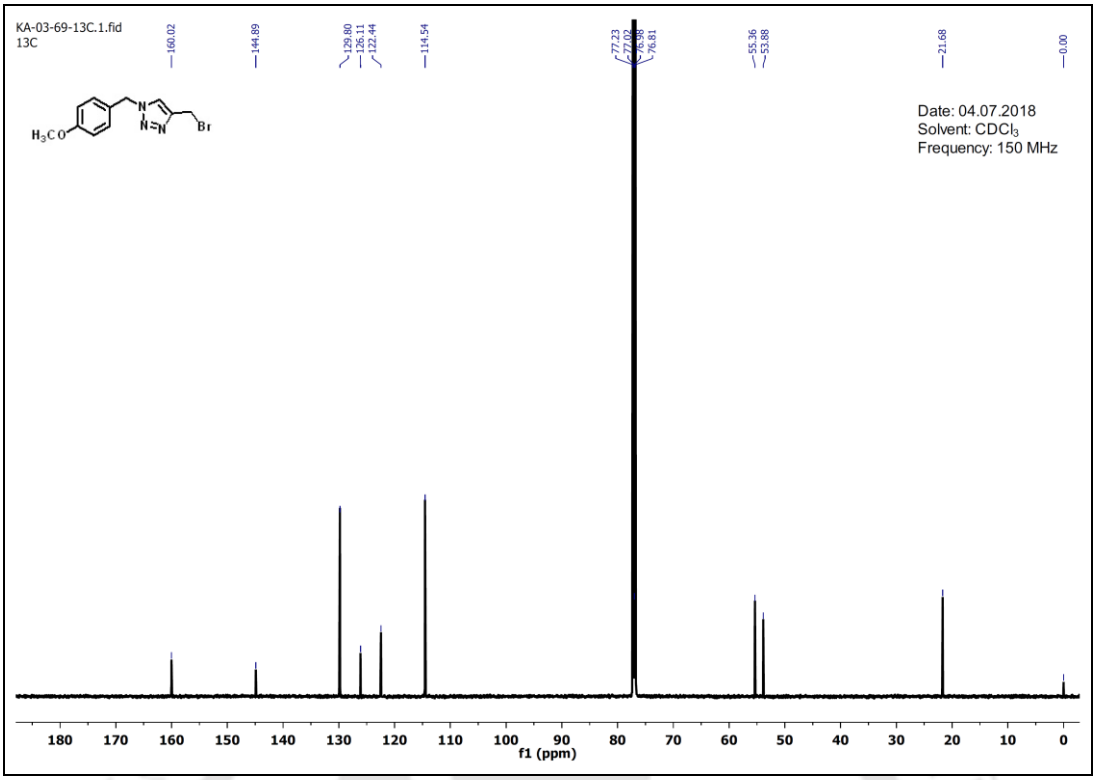

Figure A4.39. ^{13}C NMR spectrum ($CDCl_3$, 150 MHz) of compound **3.25**.

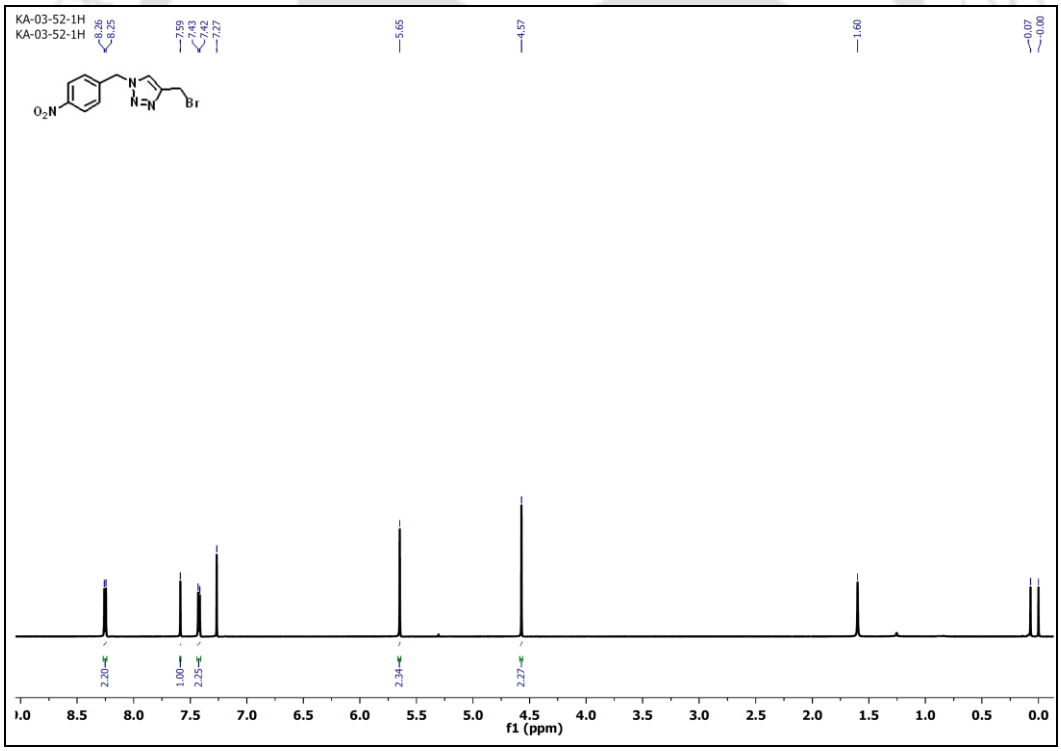

Figure A4.40. ^{1}H NMR spectrum ($CDCl_3$, 600 MHz) of compound **3.26**.

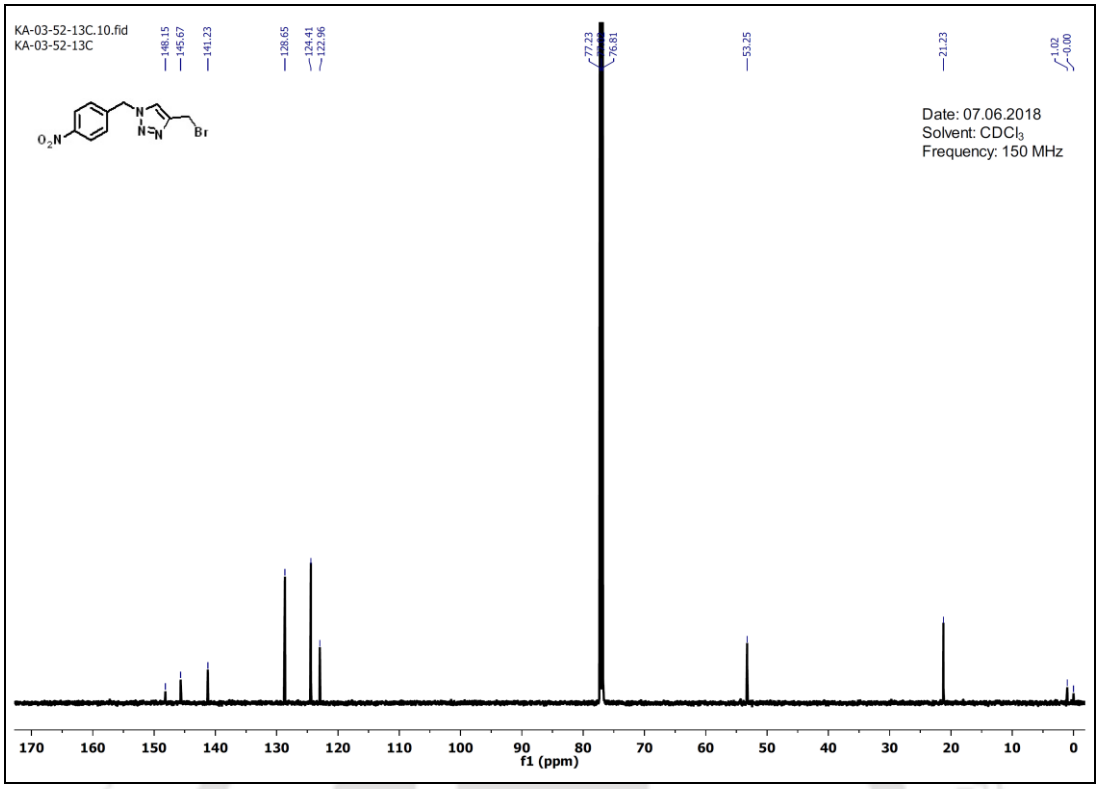

Figure A4.41. ^{13}C NMR spectrum ($CDCl_3$, 150 MHz) of compound **3.26**.

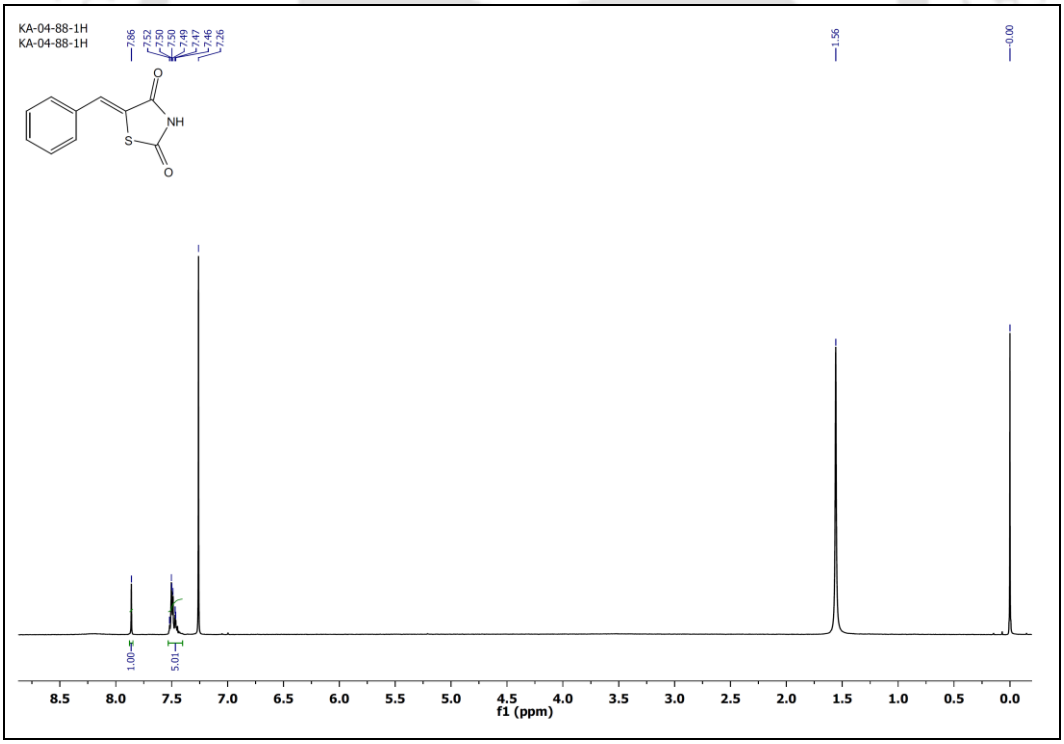

Figure A4.42. ^{1}H NMR spectrum ($CDCl_3$, 400 MHz) of compound **3.30**.

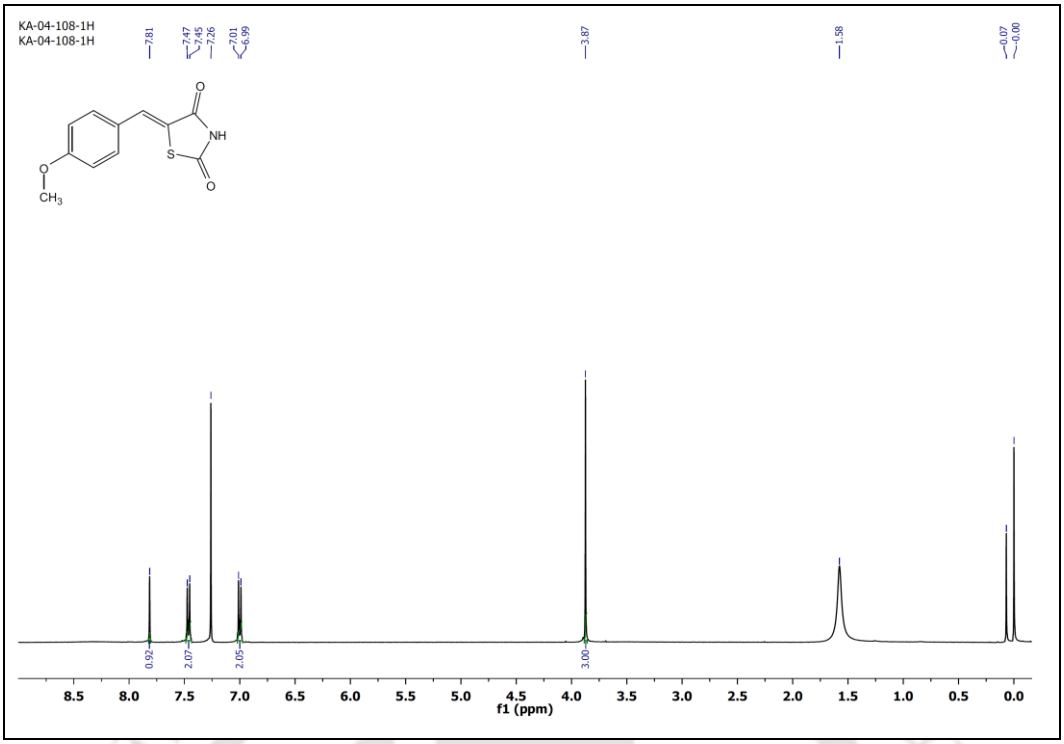

Figure A4.43. ^{1}H NMR spectrum ($CDCl_3$, 400 MHz) of compound **3.31**.

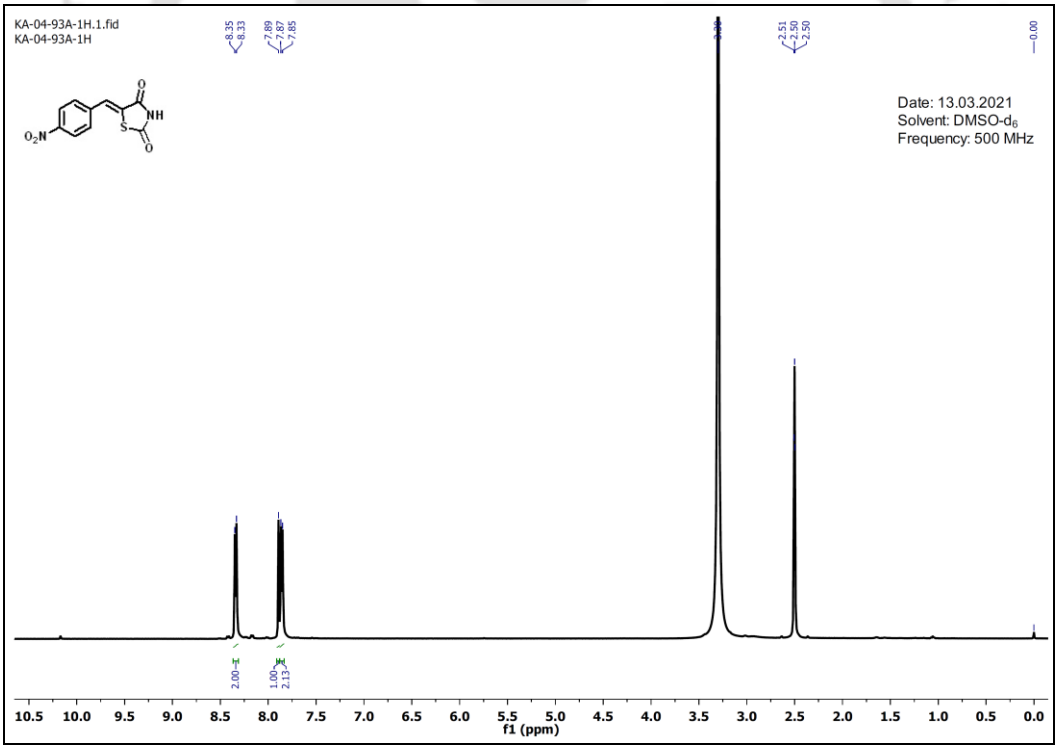

Figure A4.44. ^{1}H NMR spectrum (DMSO-d_6, 500 MHz) of compound **3.32**.

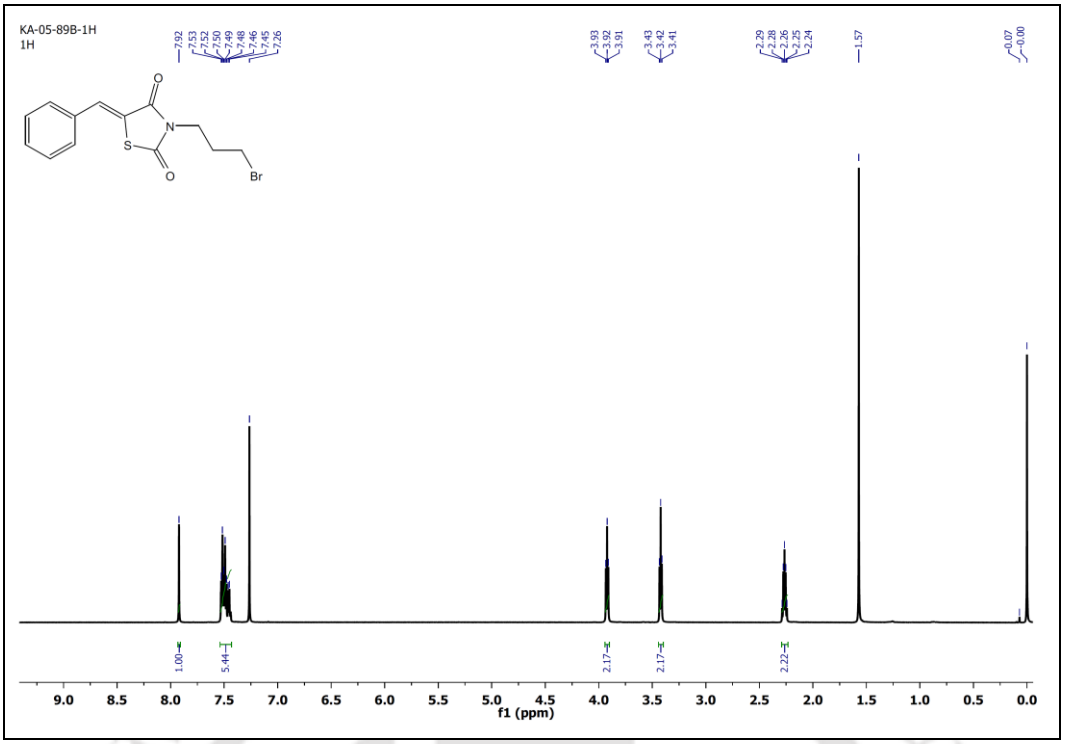

Figure A4.45. ^{1}H NMR spectrum ($CDCl_3$, 600 MHz) of compound **3.33**.

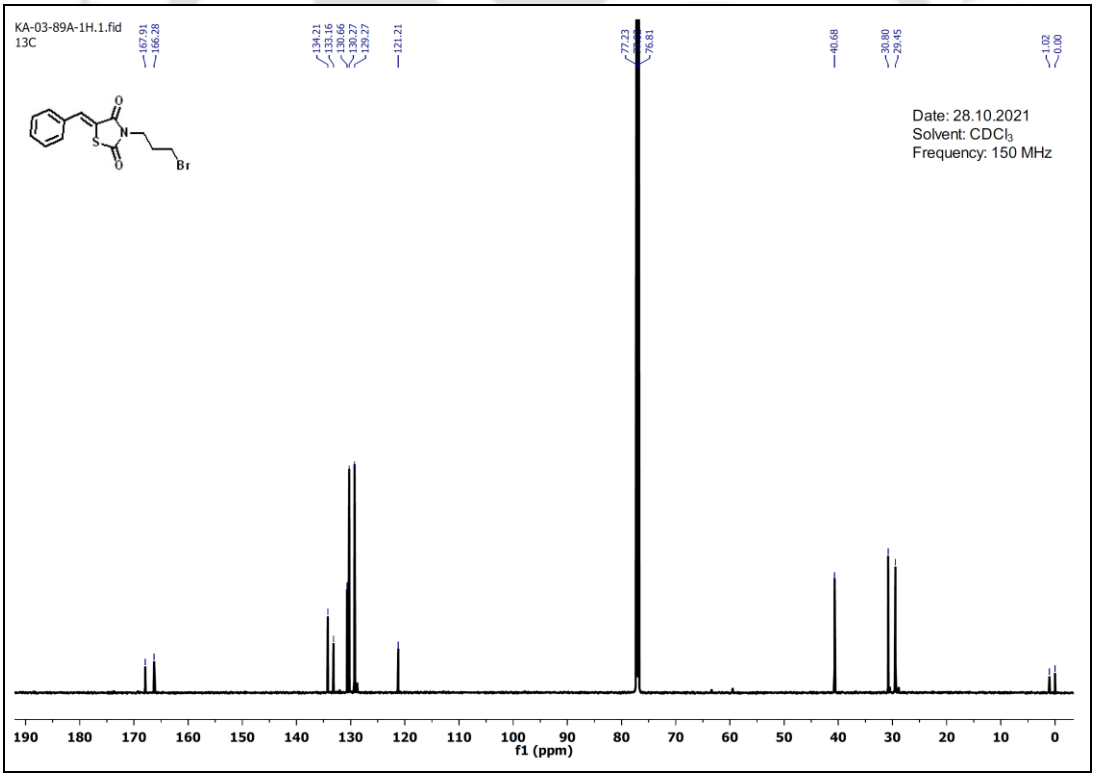

Figure A4.46. ^{13}C NMR spectrum ($CDCl_3$, 150 MHz) of compound **3.33**.

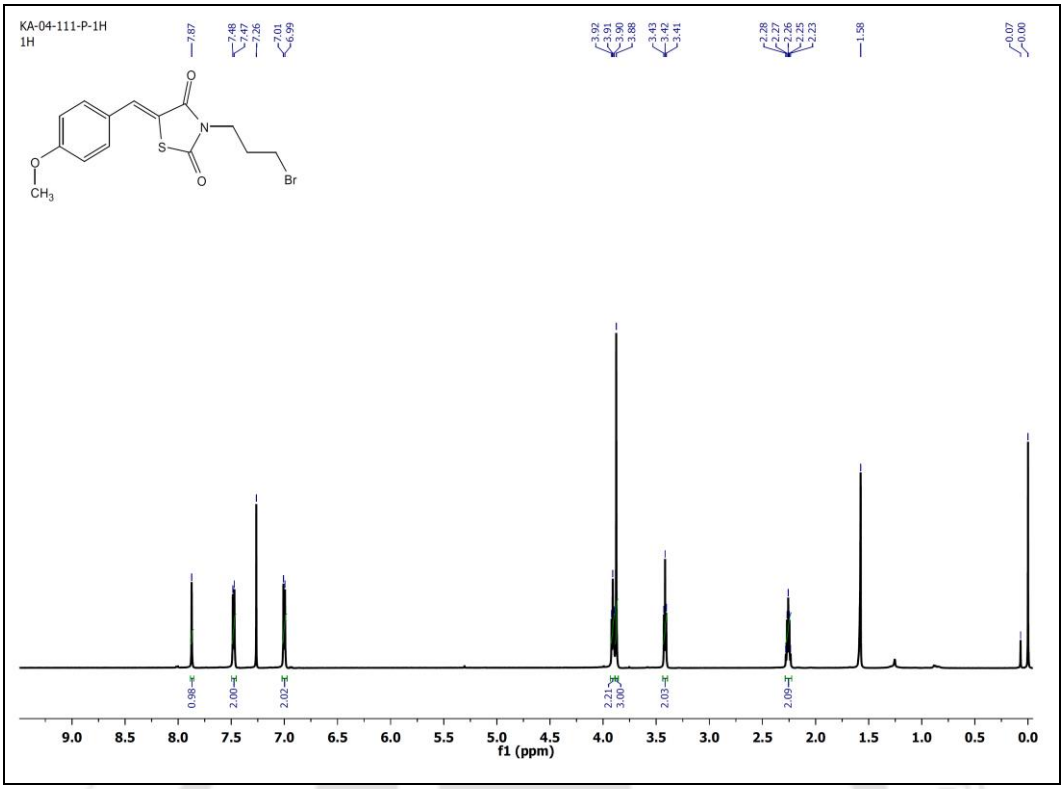

Figure A4.47. ^{1}H NMR spectrum ($CDCl_3$, 600 MHz) of compound **3.34**.

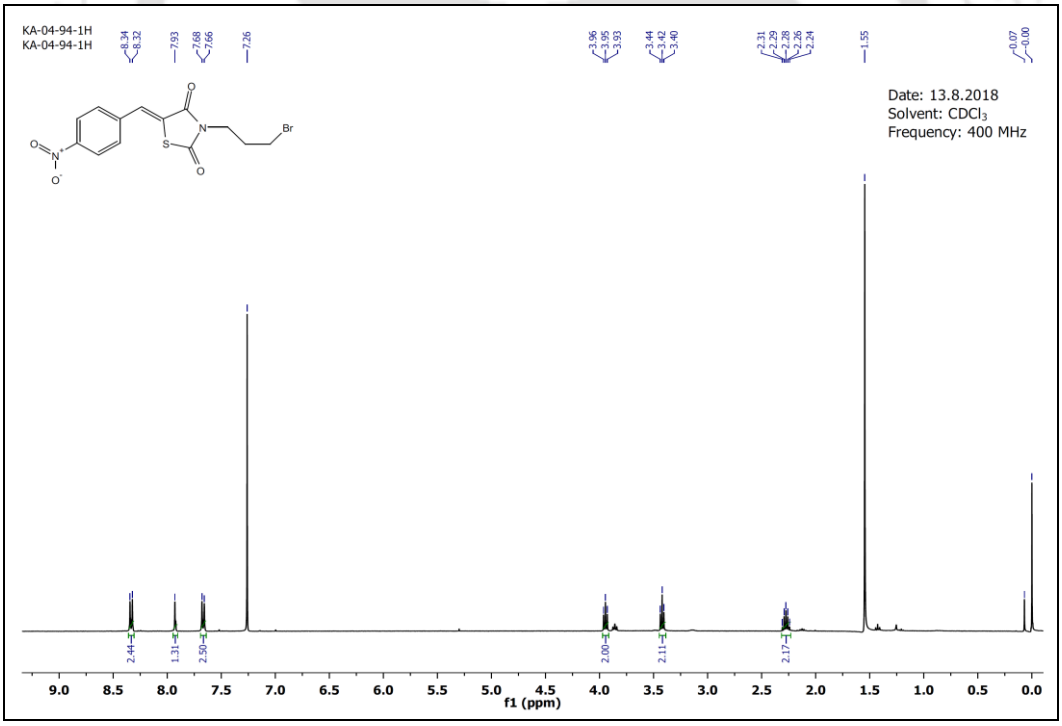

Figure A4.48. ^{1}H NMR spectrum ($CDCl_3$, 400 MHz) of compound **3.35**.

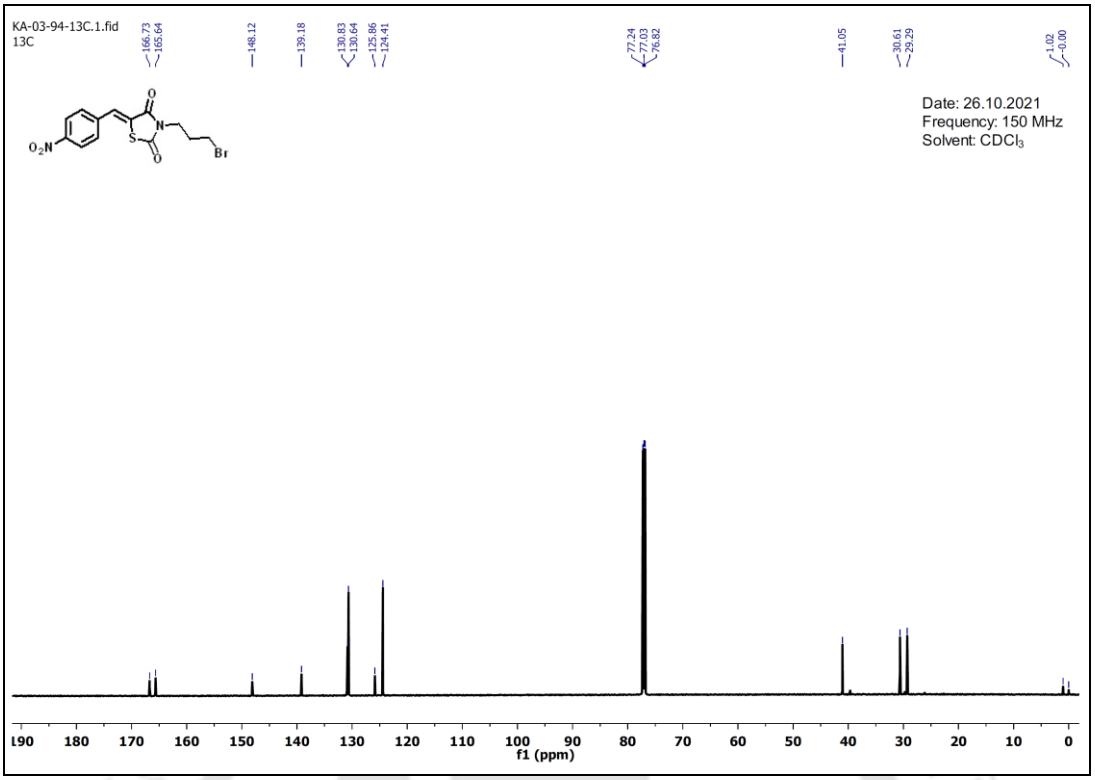

Figure A4.49. ^{13}C NMR spectrum ($CDCl_3$, 150 MHz) of compound **3.35**.

Annexure V

NMR spectral data of compounds discussed in Chapter 4

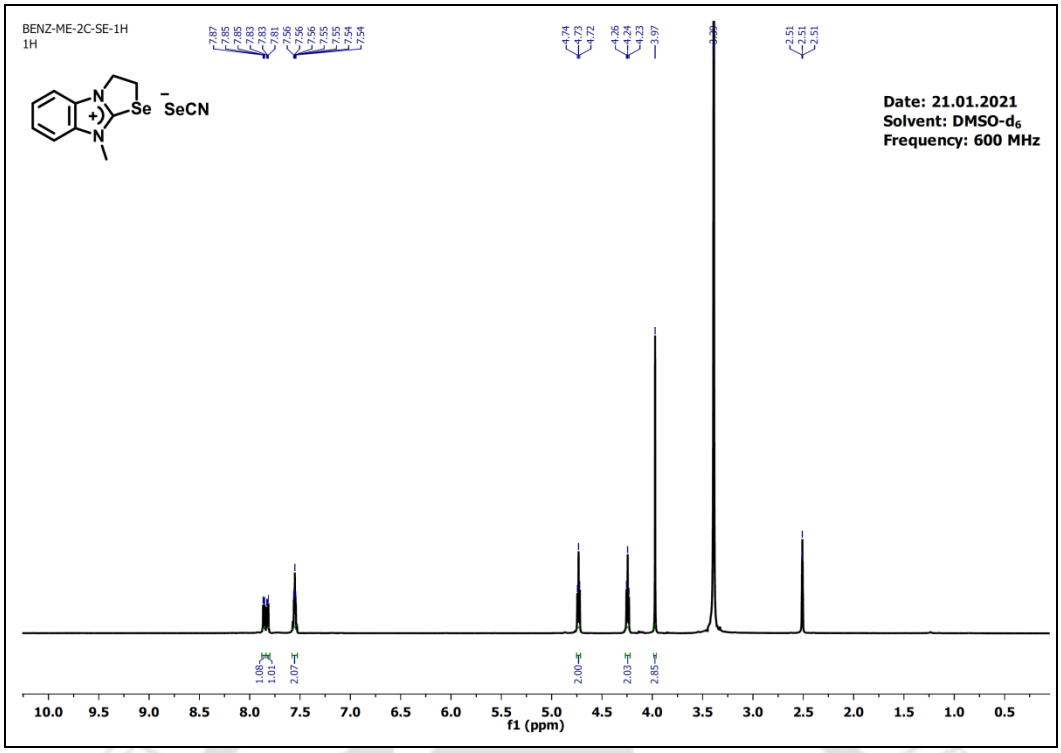

Figure A5.1. ^{1}H NMR spectrum (DMSO-d_6, 600 MHz) of compound **4.11a**.

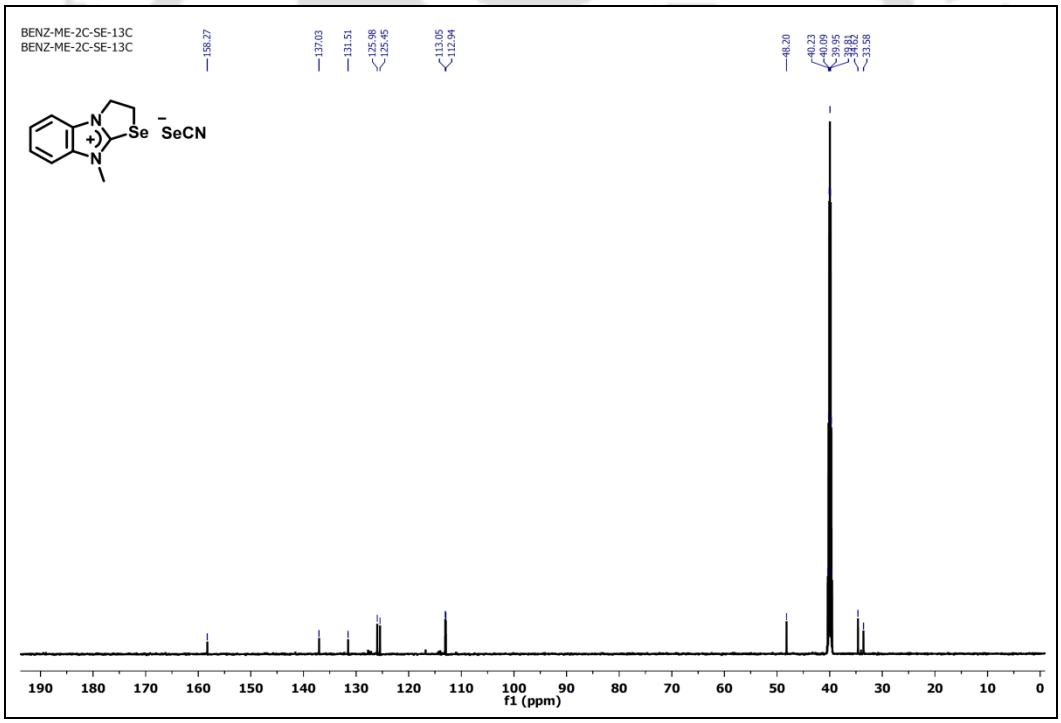

Figure A5.2.^{13}C NMR spectrum (DMSO-d_6, 150 MHz) of compound **4.11a**.

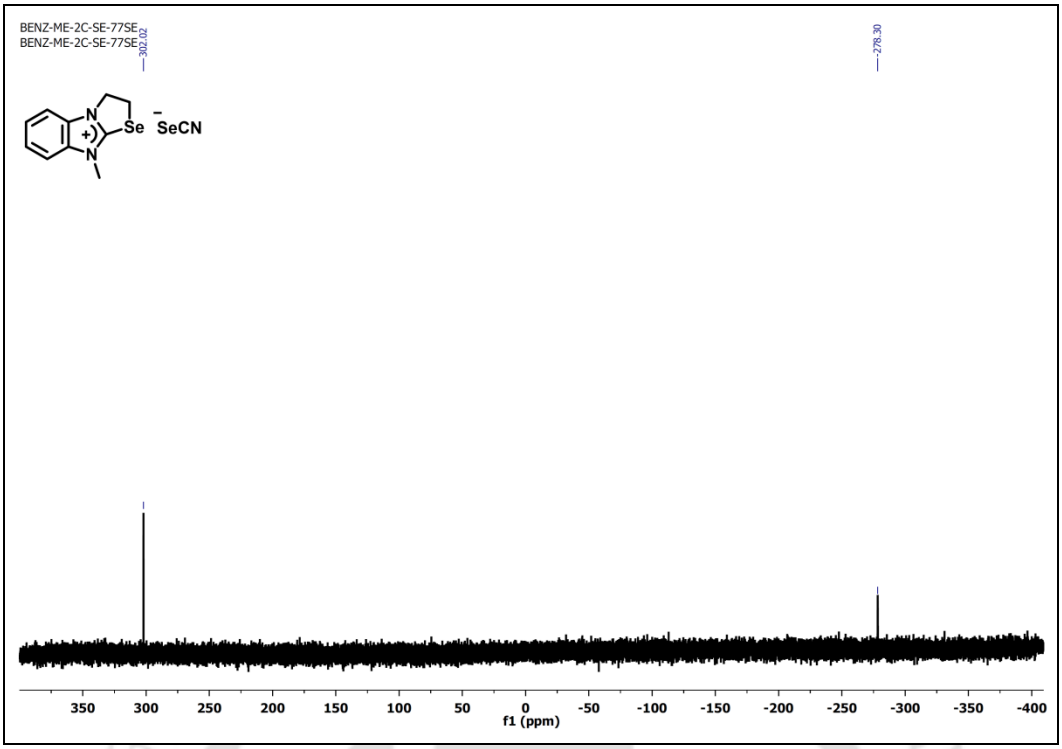

Figure A5.3. ^{77}Se NMR spectrum (DMSO-d_6, 114 MHz) of compound **4.11a**.

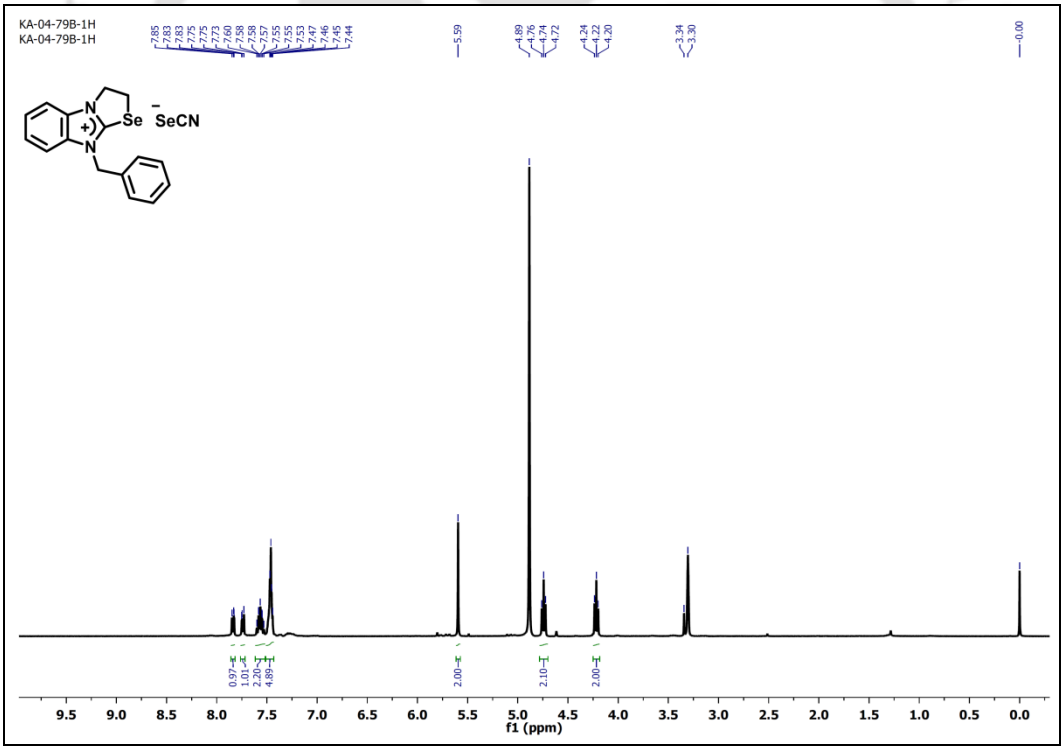

Figure A5.4. ^{1}H NMR spectrum (methanol-d_4, 400 MHz) of compound **4.11b**.

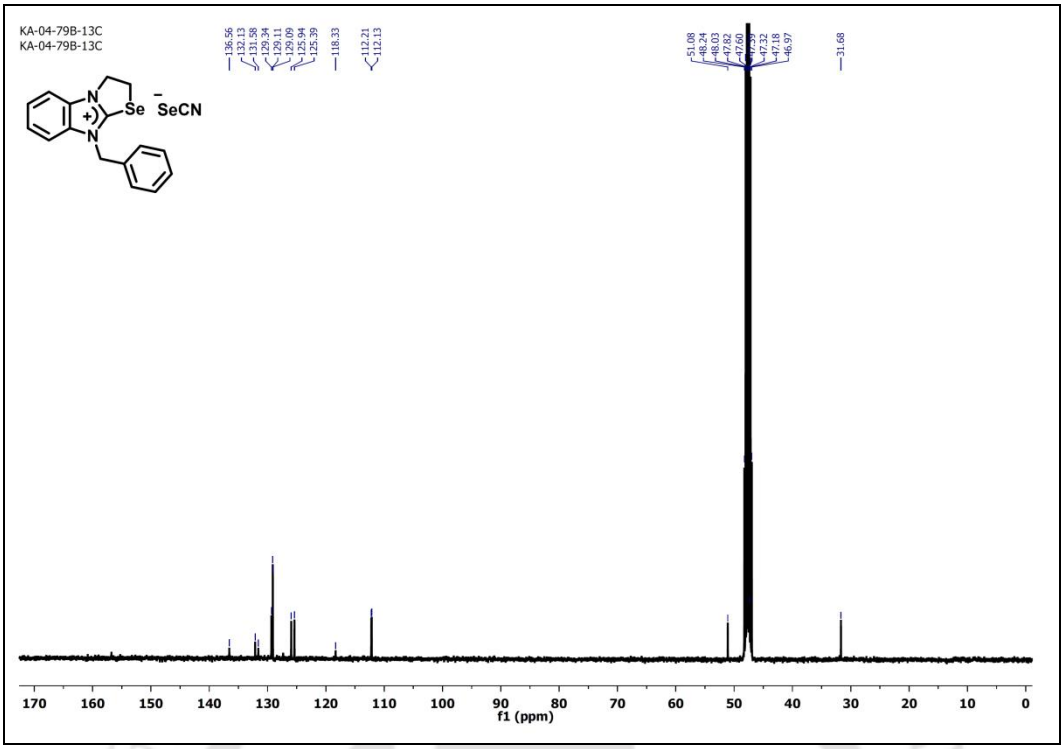

Figure A5.5. ^{13}C NMR spectrum (DMSO-d_6, 150 MHz) of compound **4.11b**.

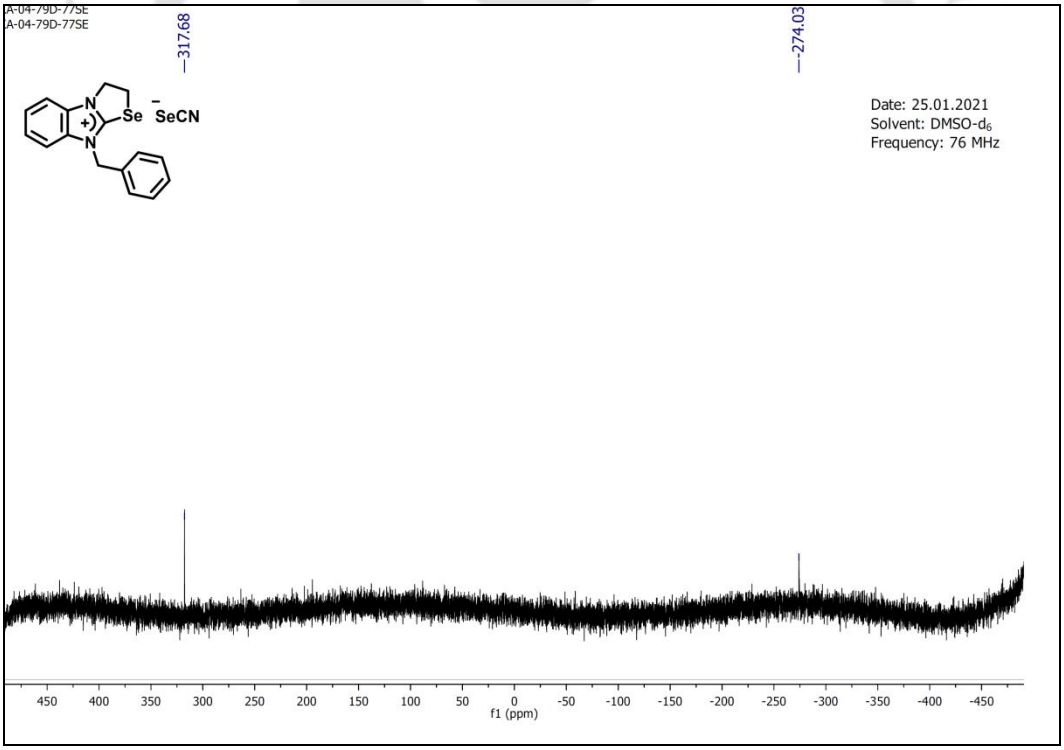

Figure A5.6. ^{77}Se NMR spectrum (DMSO-d_6, 76 MHz) of compound **4.11b**.

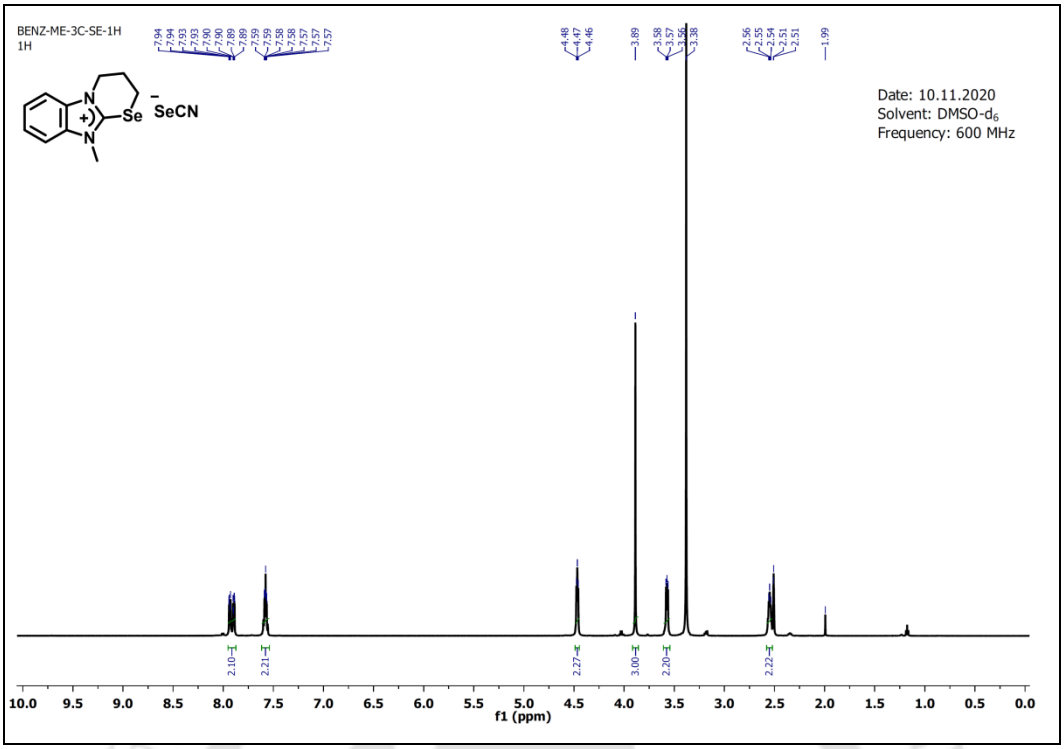

Figure A5.7. ^{1}H NMR spectrum (DMSO-d_6, 600 MHz) of compound **4.11c**.

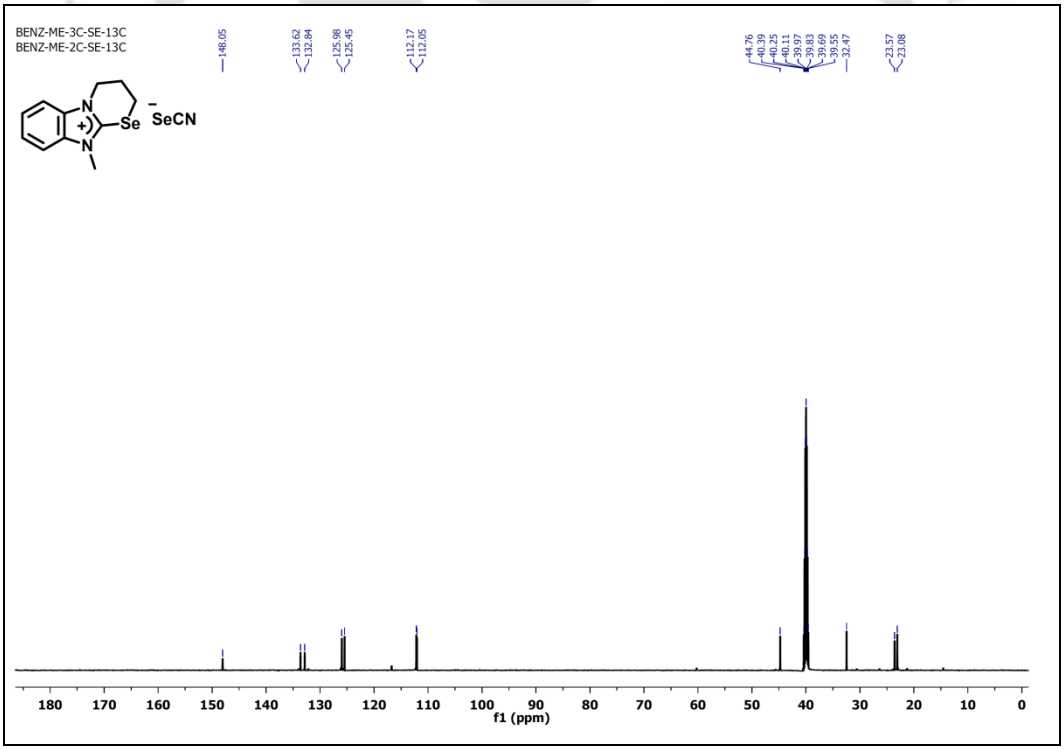

Figure A5.8. ^{13}C NMR spectrum (DMSO-d_6, 150 MHz) of compound **4.11c**.

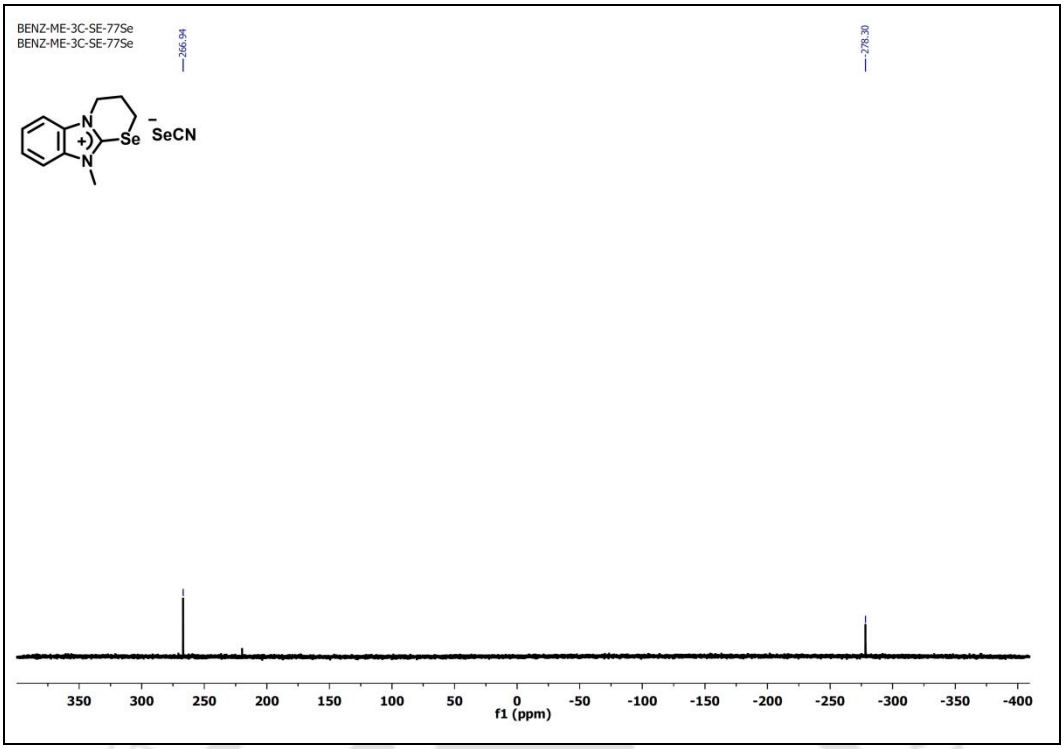

Figure A5.9. ^{77}Se NMR spectrum (DMSO-d_6, 114 MHz) of compound **4.11c**.

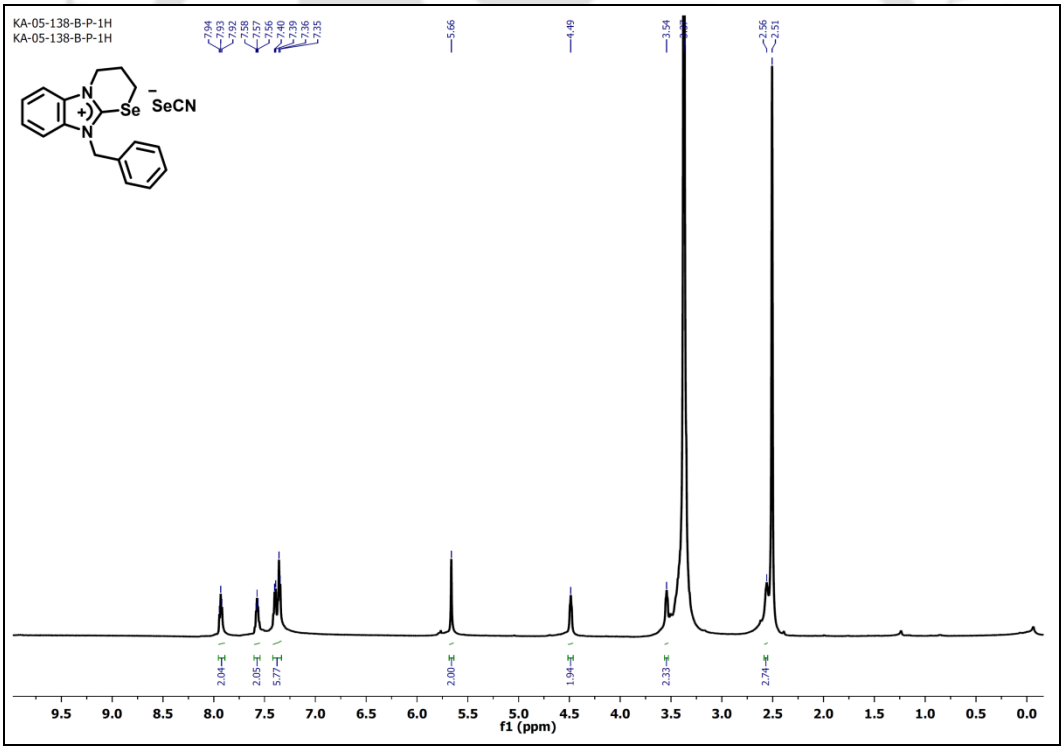

Figure A5.10. ^{1}H NMR spectrum (DMSO-d_6, 600 MHz) of compound **4.11d**.

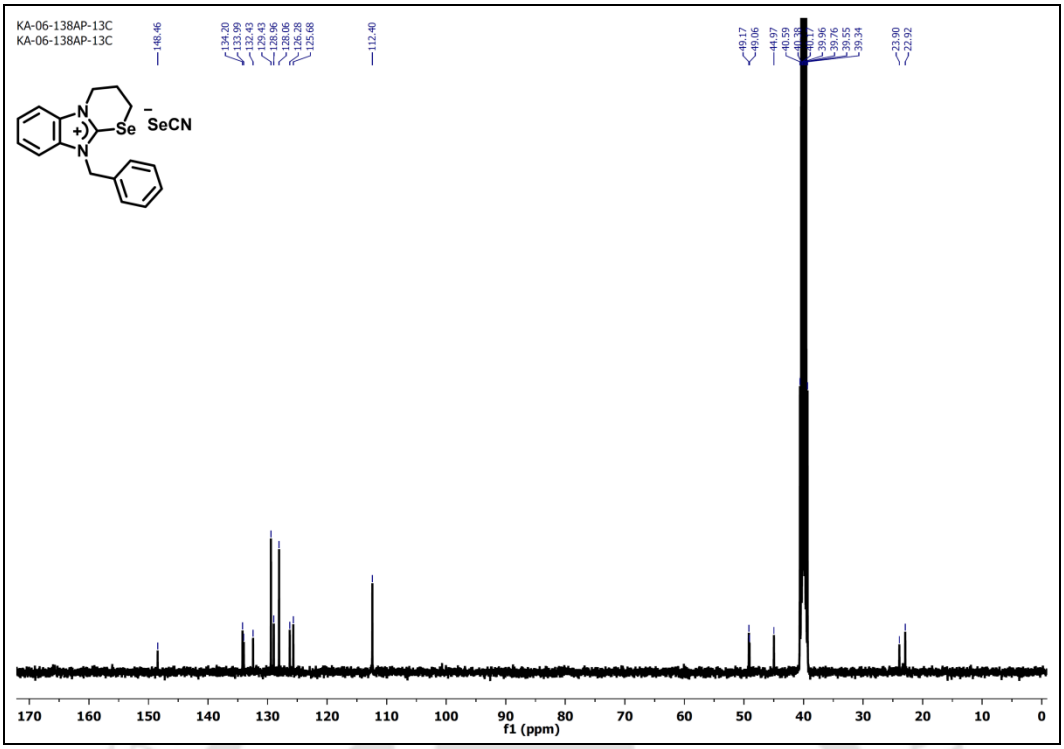

Figure A5.11. ^{13}C NMR spectrum (DMSO-d_6, 100 MHz) of compound **4.11d**.

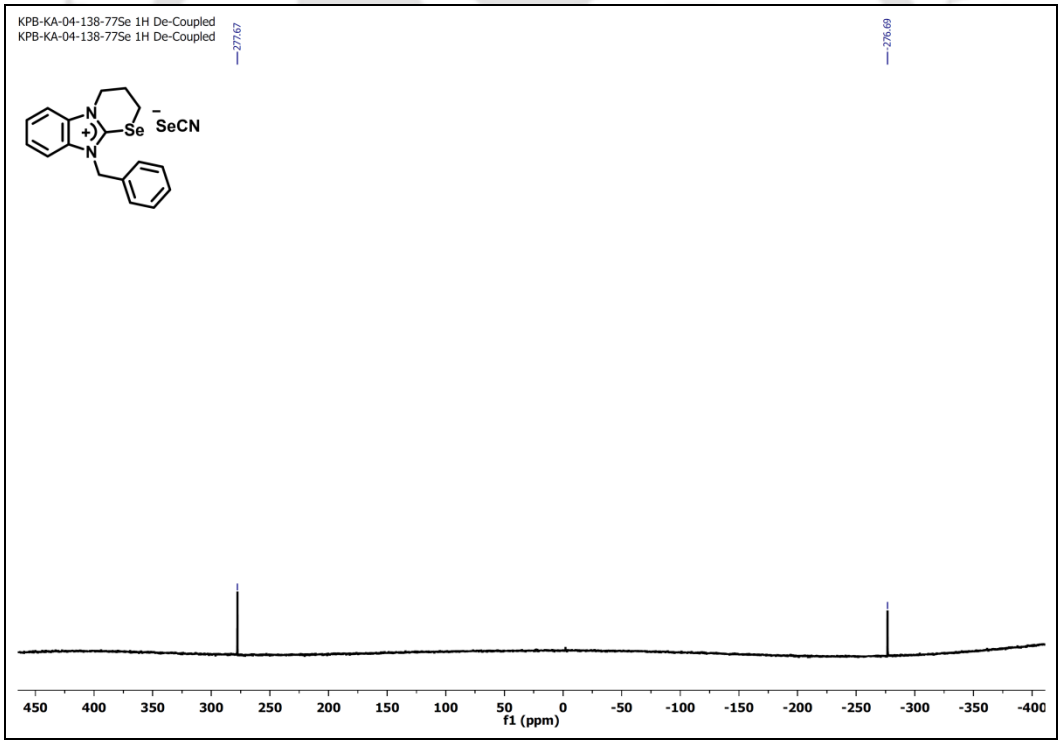

Figure A5.12. ^{77}Se NMR spectrum (DMSO-d_6, 76 MHz) of compound **4.11d**.

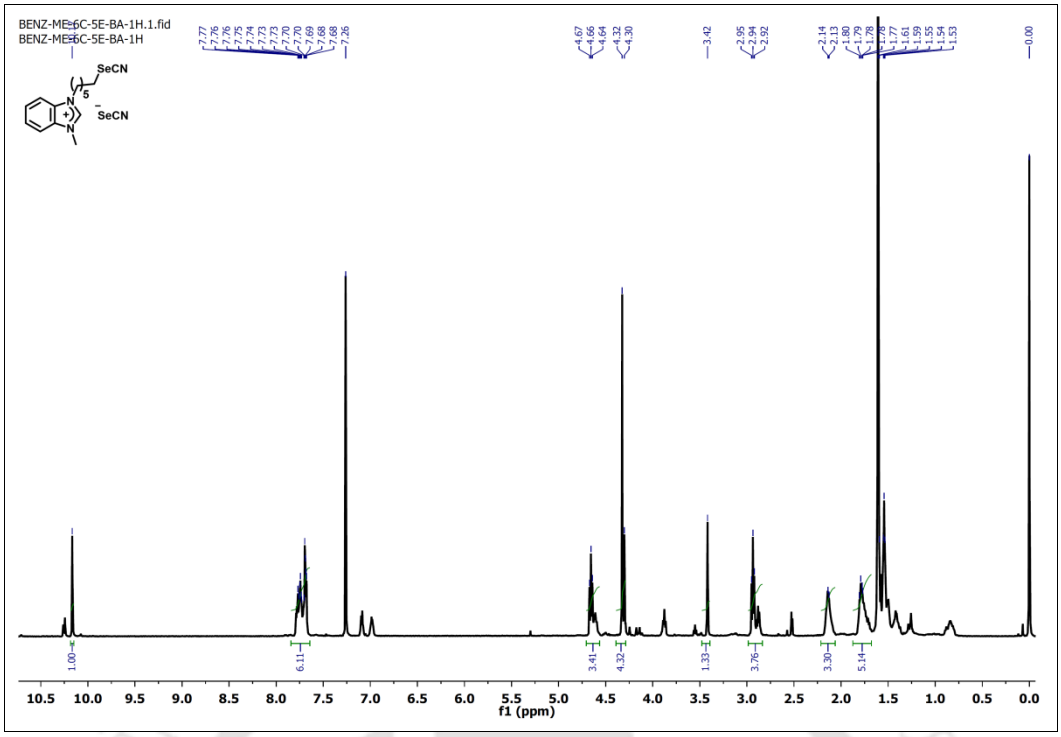

Figure A5.13. ^{1}H NMR spectrum ($CDCl_3$, 500 MHz) of compound **4.11e**.

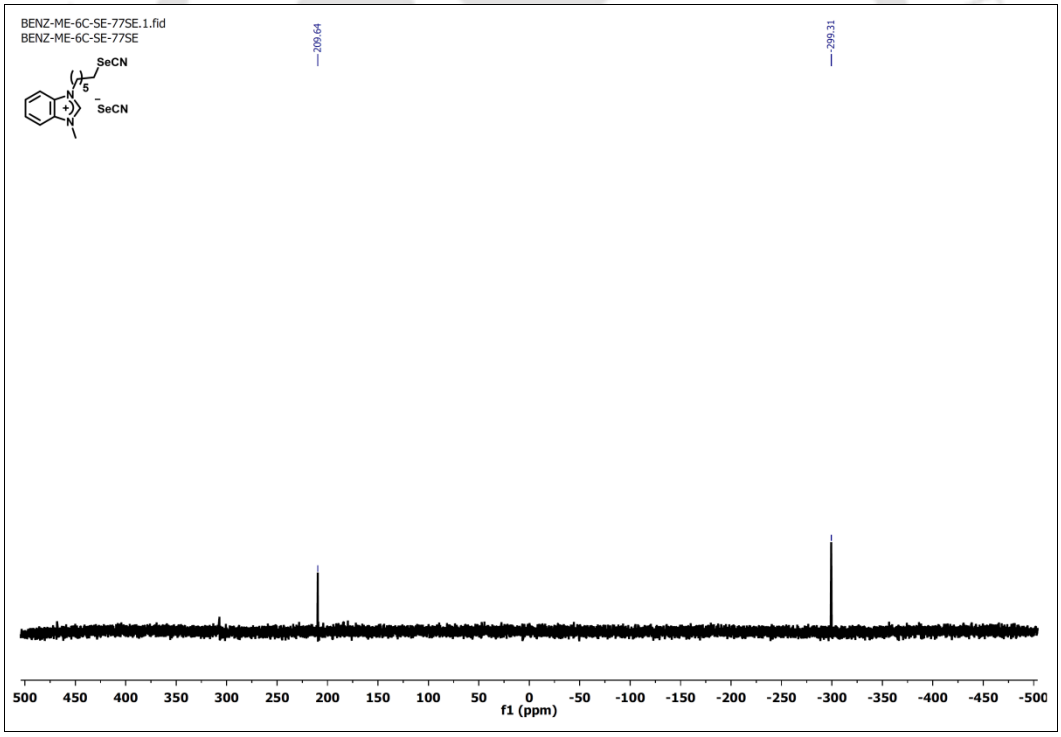

Figure A5.14. ^{77}Se NMR spectrum ($CDCl_3$, 95 MHz) of compound **4.11e**.

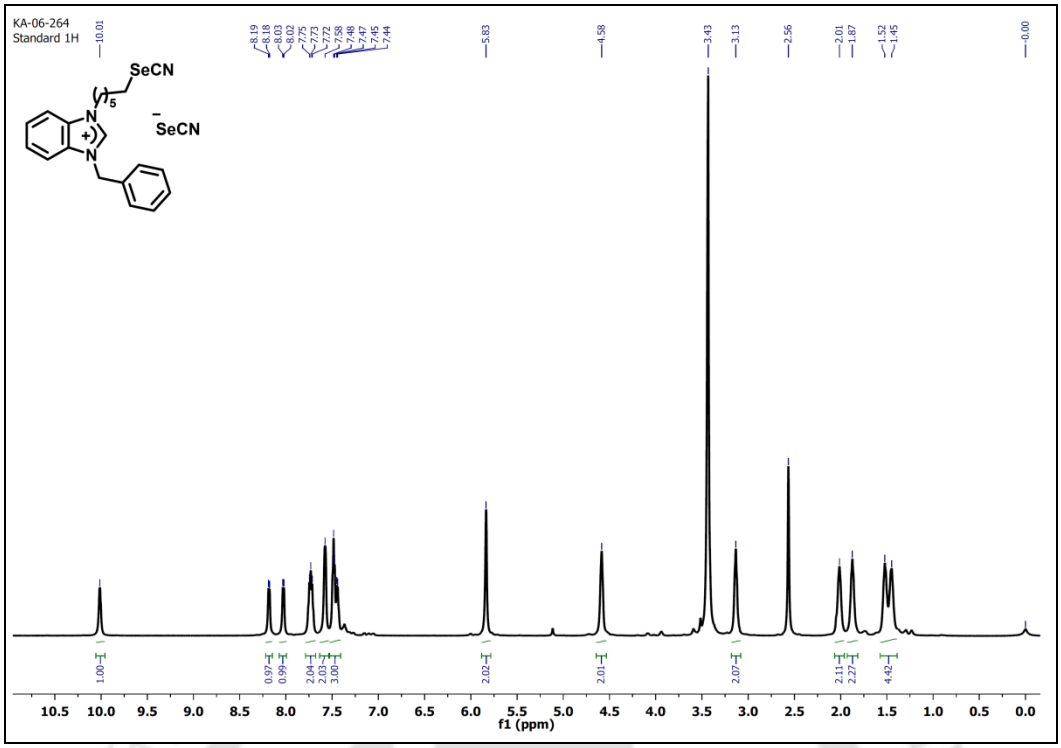

Figure A5.15. ^{1}H NMR spectrum (DMSO-d_6, 600 MHz) of compound **4.11f**.

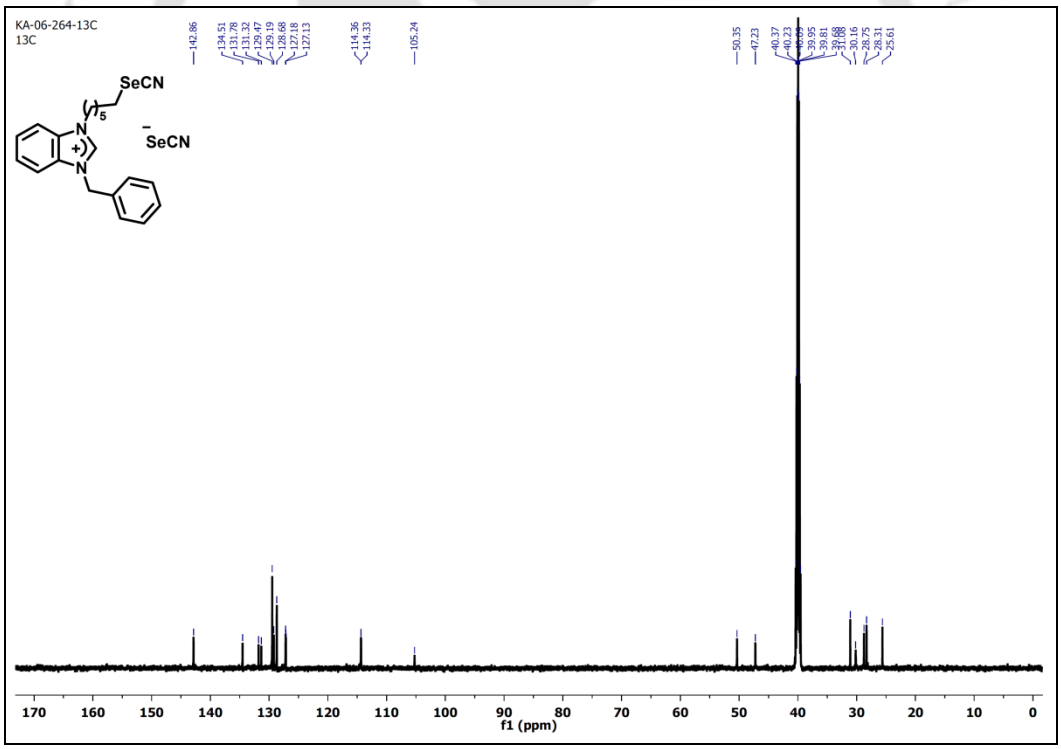

Figure A5.16. ^{13}C NMR spectrum (DMSO-d_6, 150 MHz) of compound **4.11f**.

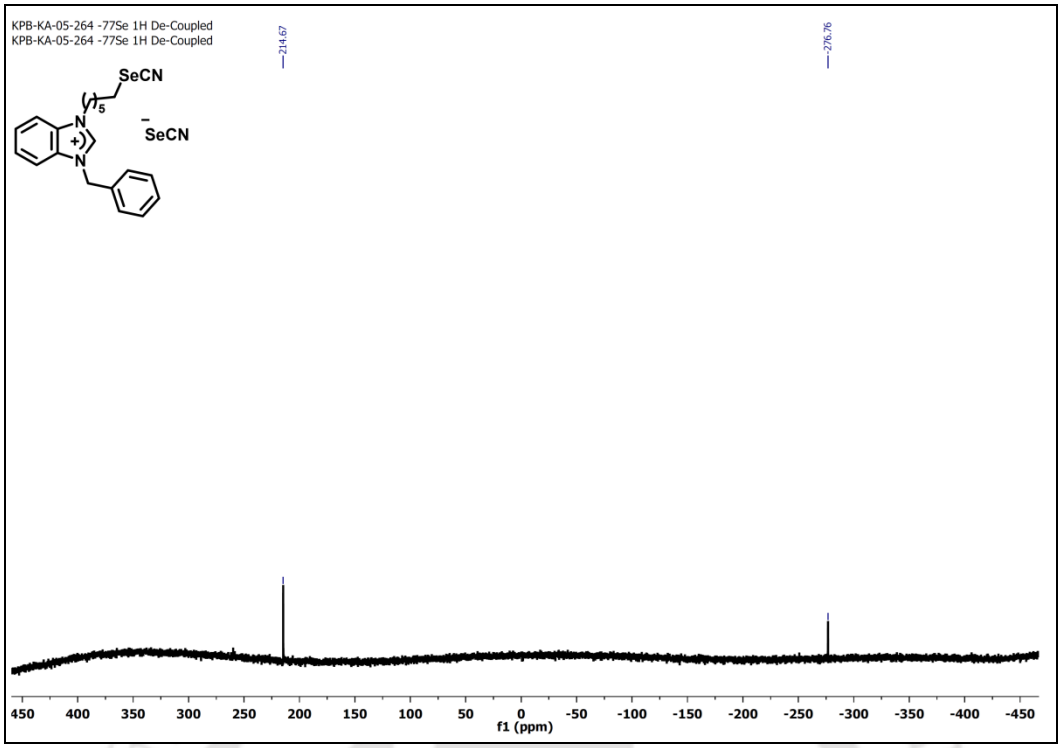

Figure A5.17. ^{77}Se NMR spectrum (DMSO-d_6, 76 MHz) of compound **4.11f**.

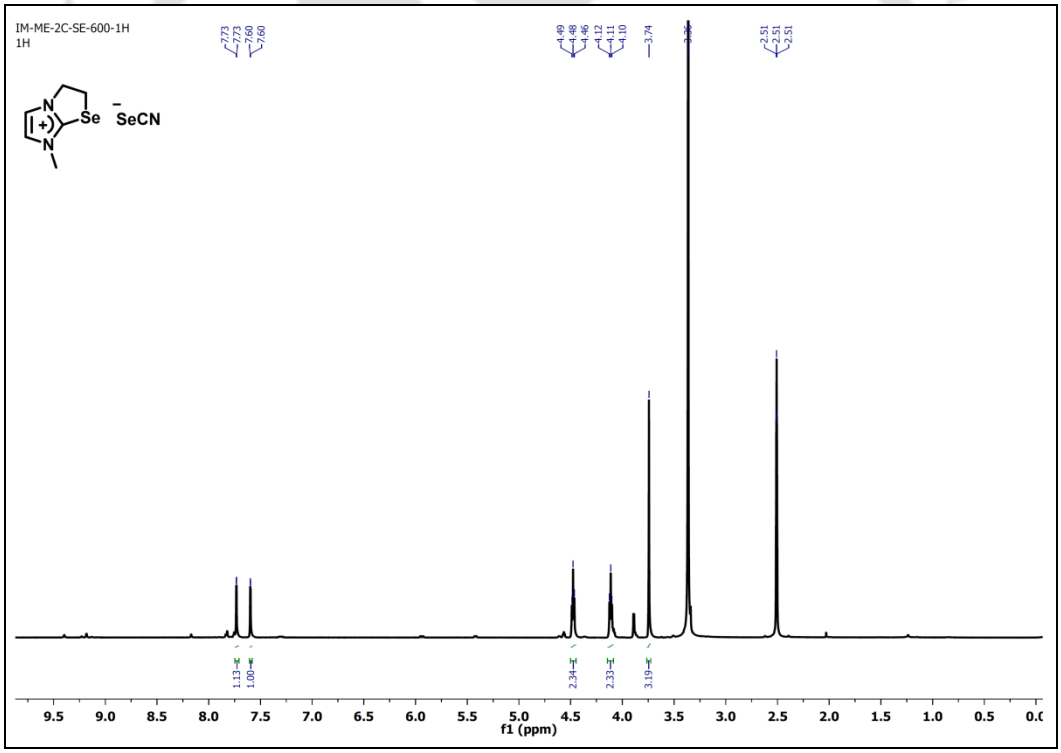

Figure A5.18. ^{1}H NMR spectrum (DMSO-d_6, 600 MHz) of compound **4.12a**.

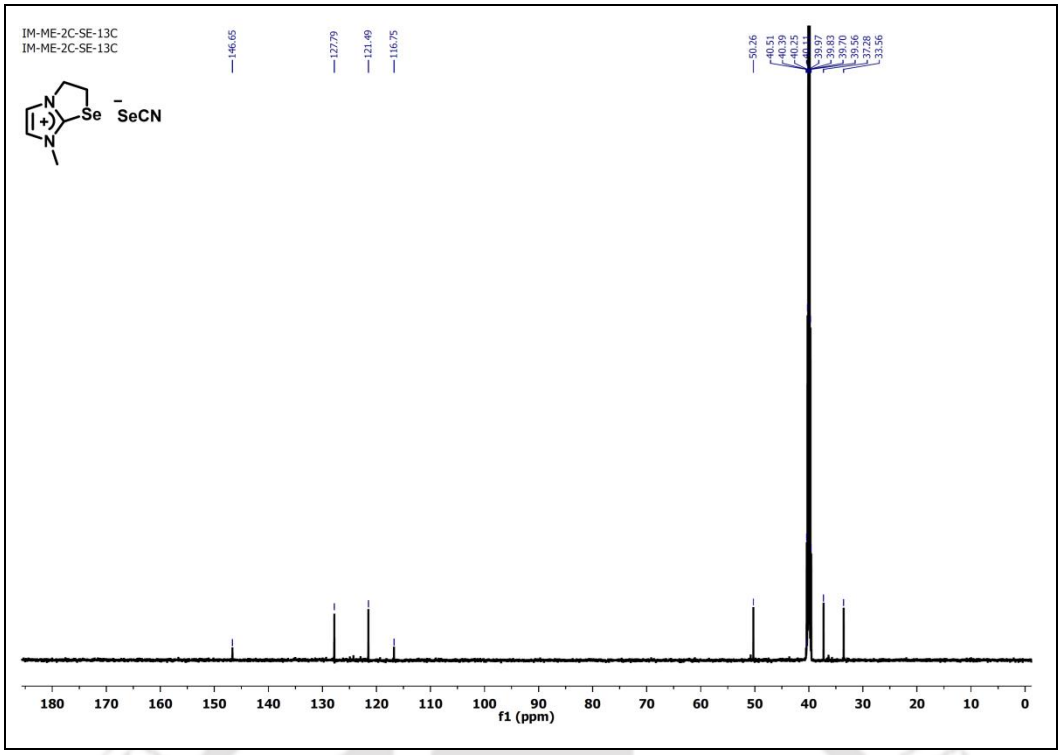

Figure A5.19. ^{13}C NMR spectrum (DMSO-d_6, 150 MHz) of compound **4.12a**.

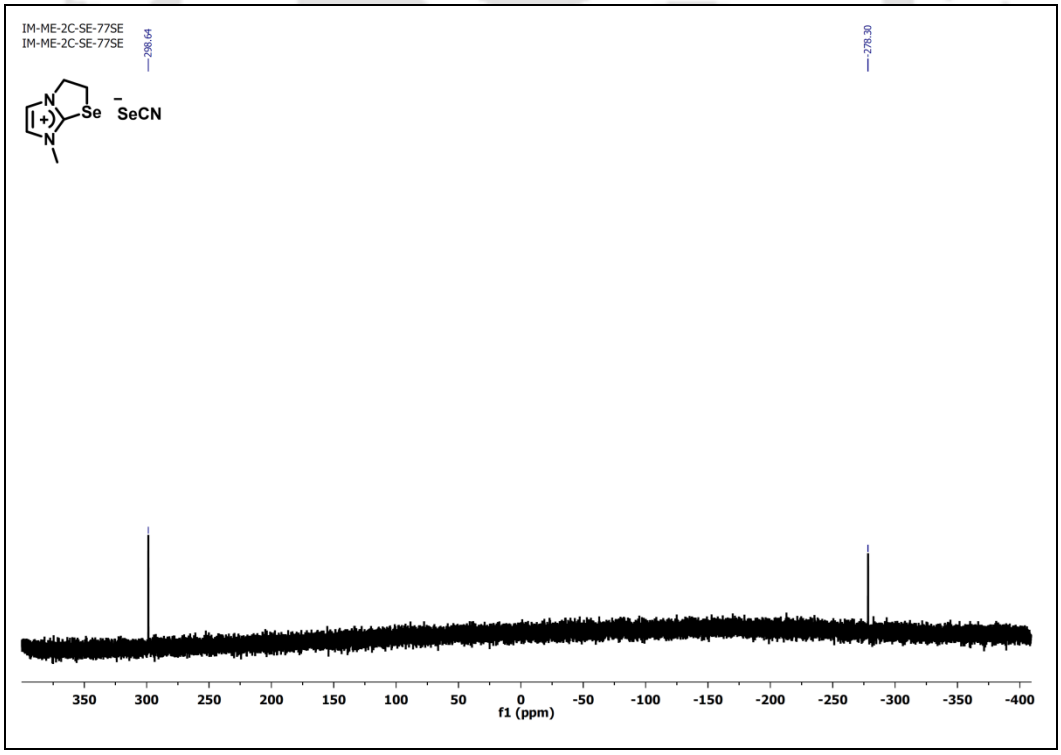

Figure A5.20. ^{77}Se NMR spectrum (DMSO-d_6, 114 MHz) of compound **4.12a**.

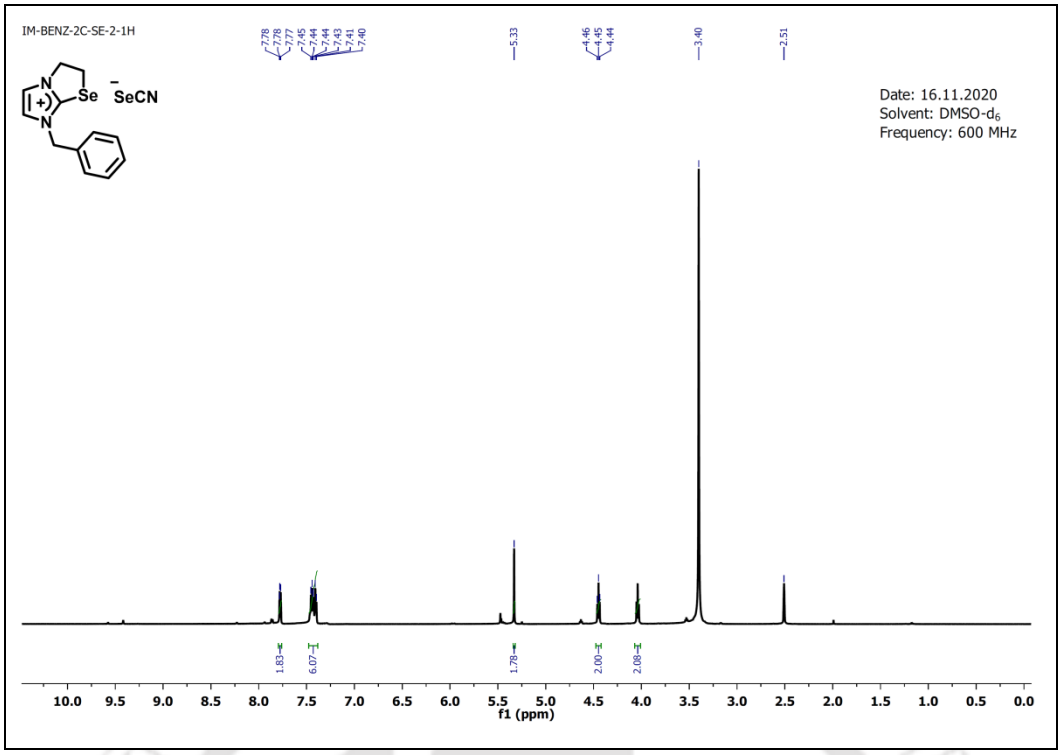

Figure A5.21. ^{1}H NMR spectrum (DMSO-d_6, 600 MHz) of compound **4.12b**.

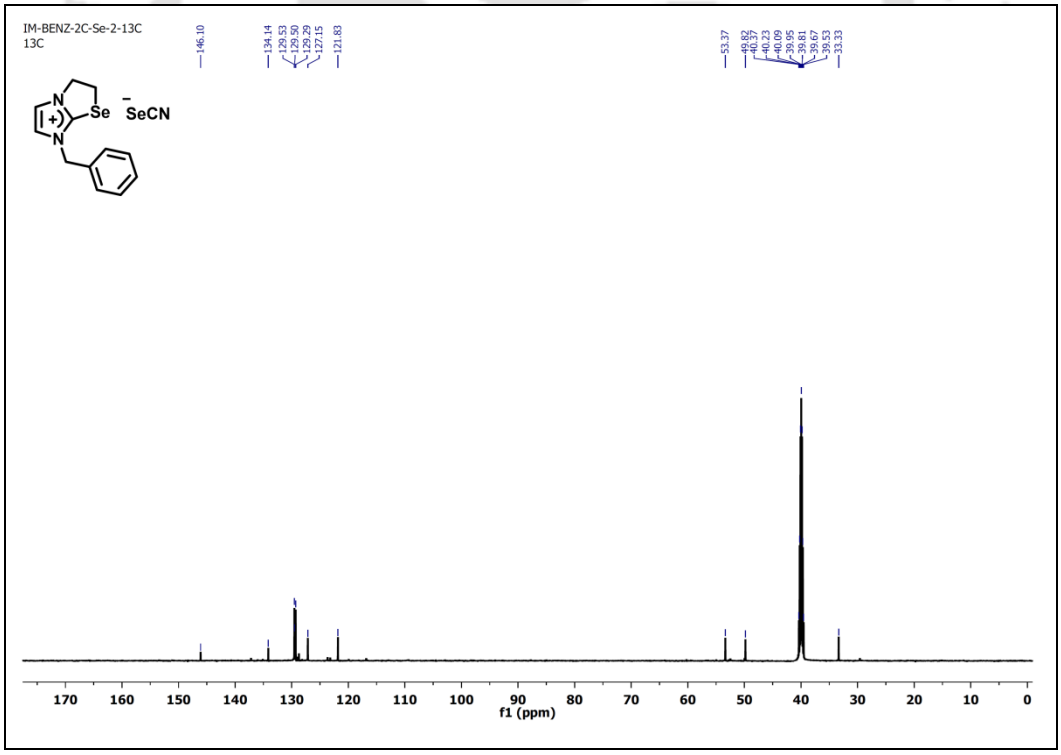

Figure A5.22. ^{13}C NMR spectrum (DMSO-d_6, 150 MHz) of compound **4.12b**.

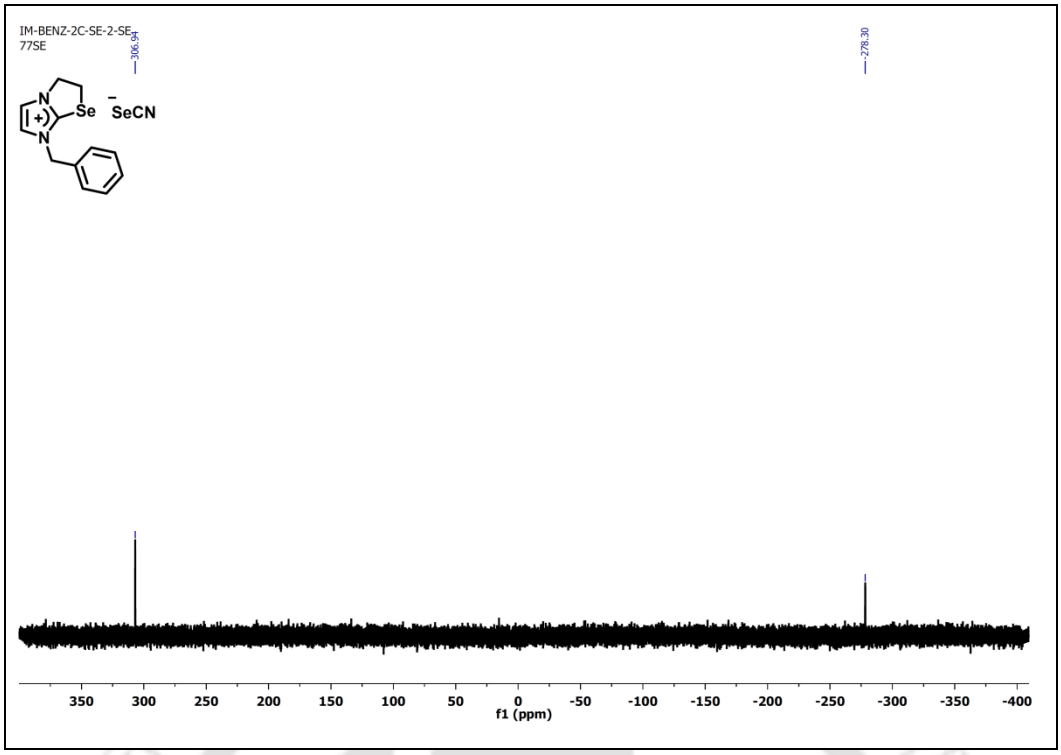

Figure A5.23. ^{77}Se NMR spectrum (DMSO-d_6, 114 MHz) of compound **4.12b**.

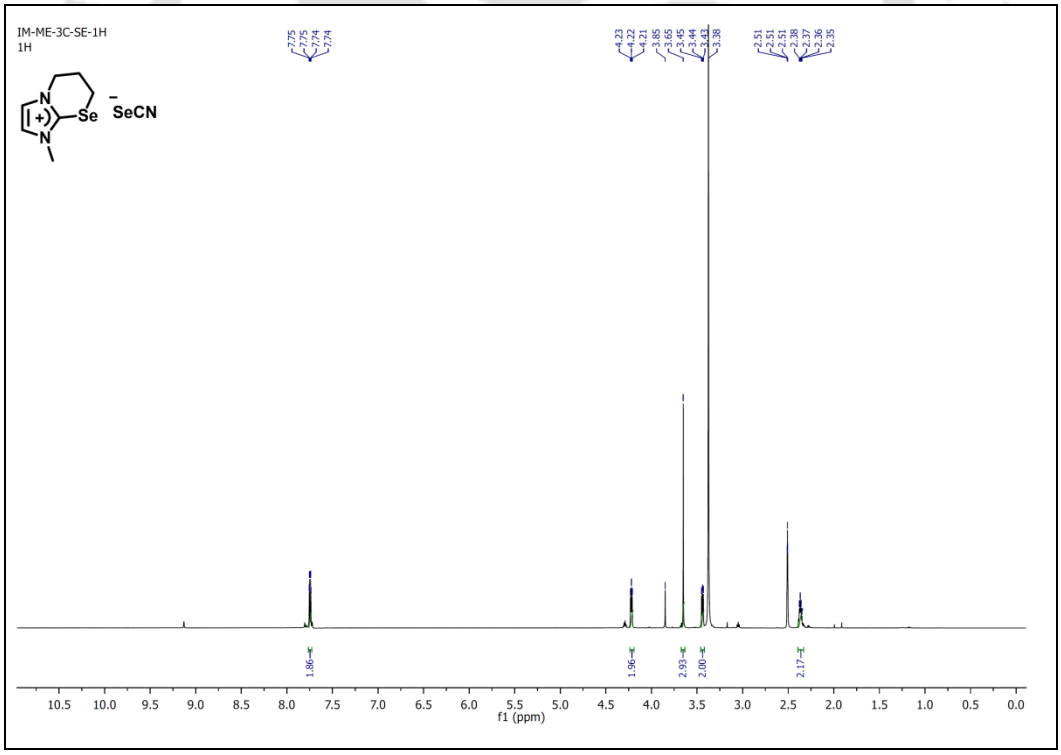

Figure A5.24. ^{1}H NMR spectrum (DMSO-d_6, 600 MHz) of compound **4.12c**.

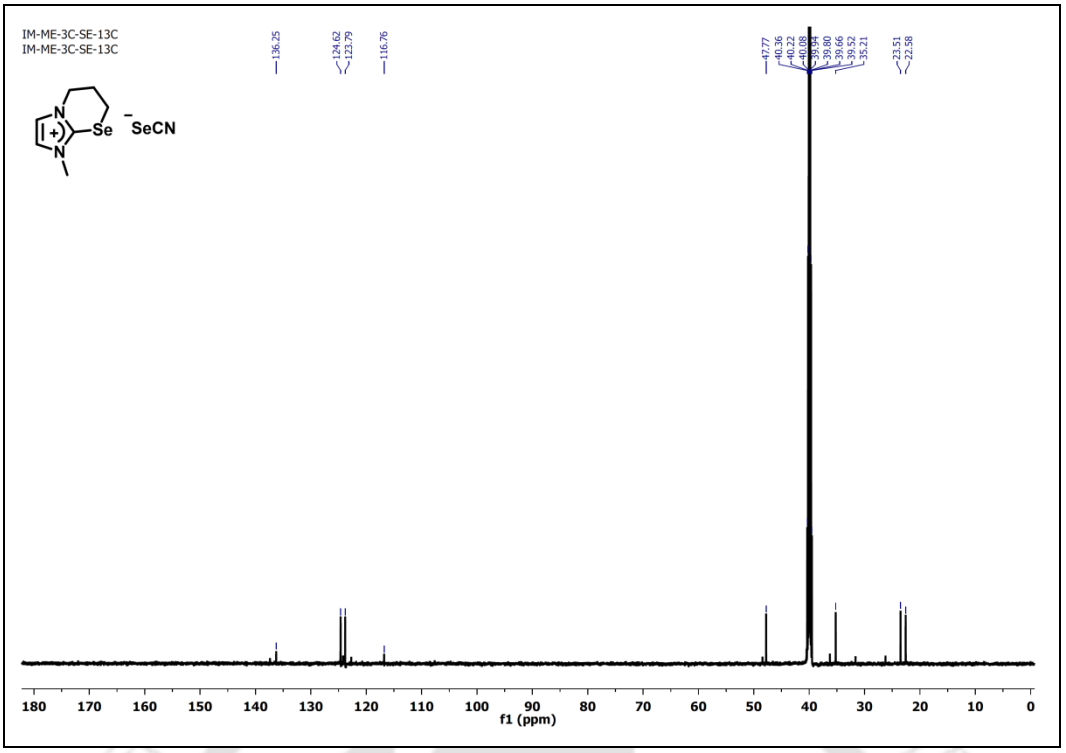

Figure A5.25. ^{13}C NMR spectrum (DMSO-d_6, 150 MHz) of compound **4.12c**.

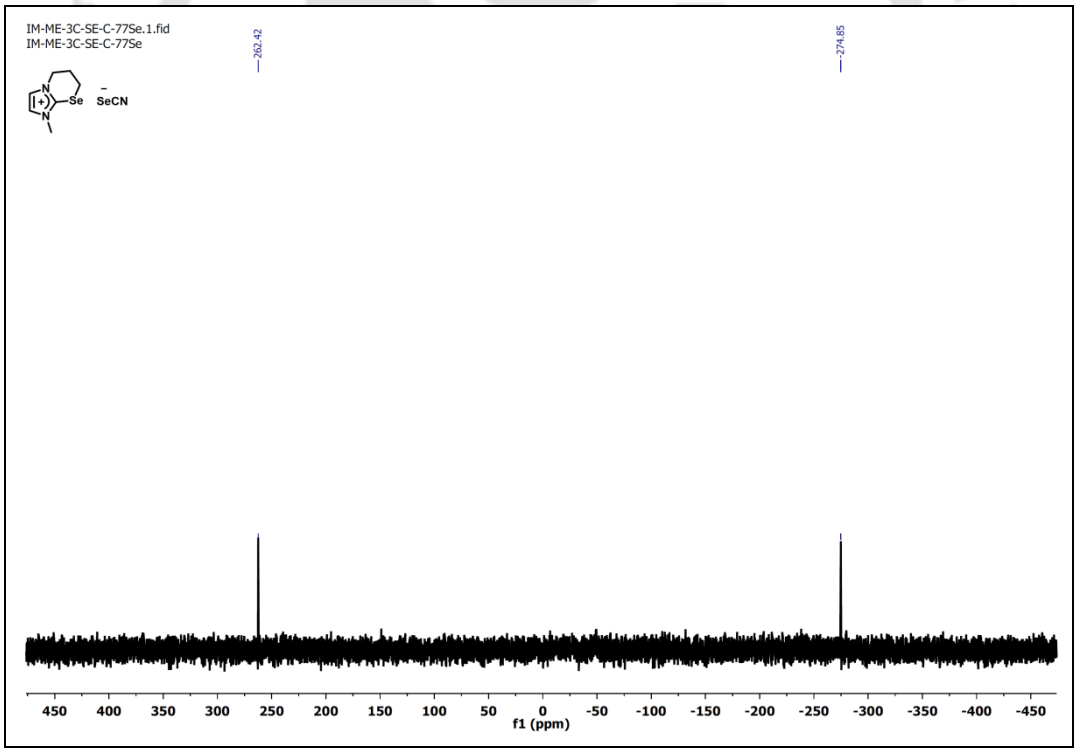

Figure A5.26. ^{77}Se NMR spectrum (DMSO-d_6, 95 MHz) of compound **4.12c**.

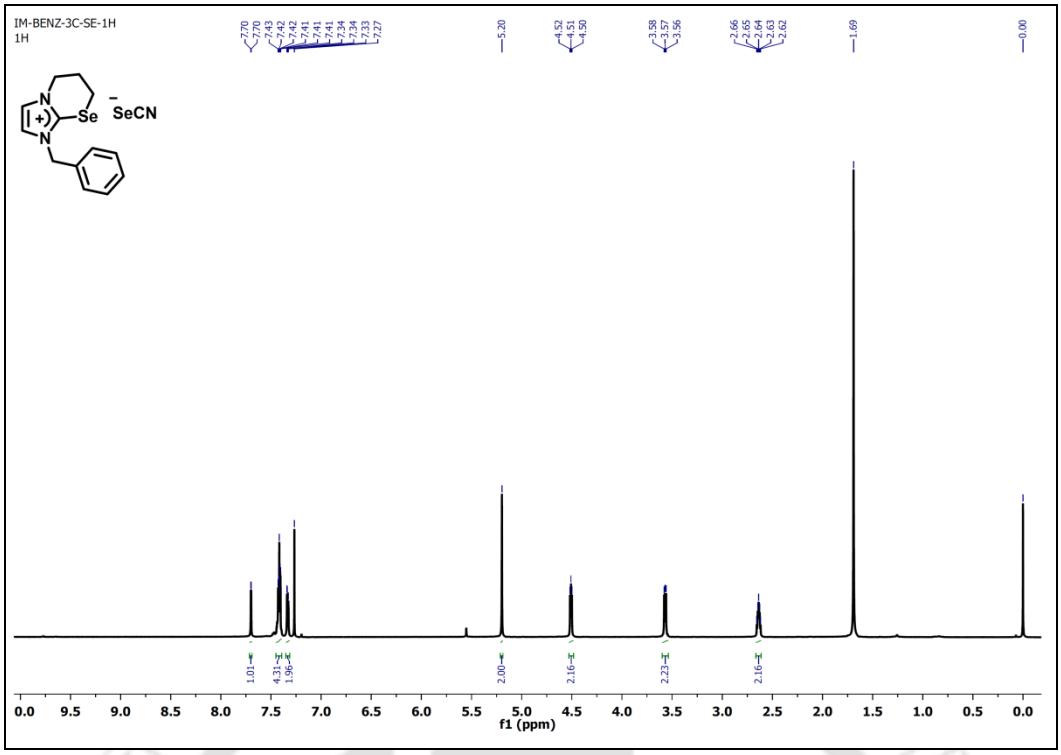

Figure A5.27. ^{1}H NMR spectrum ($CDCl_3$, 600 MHz) of compound **4.12d**.

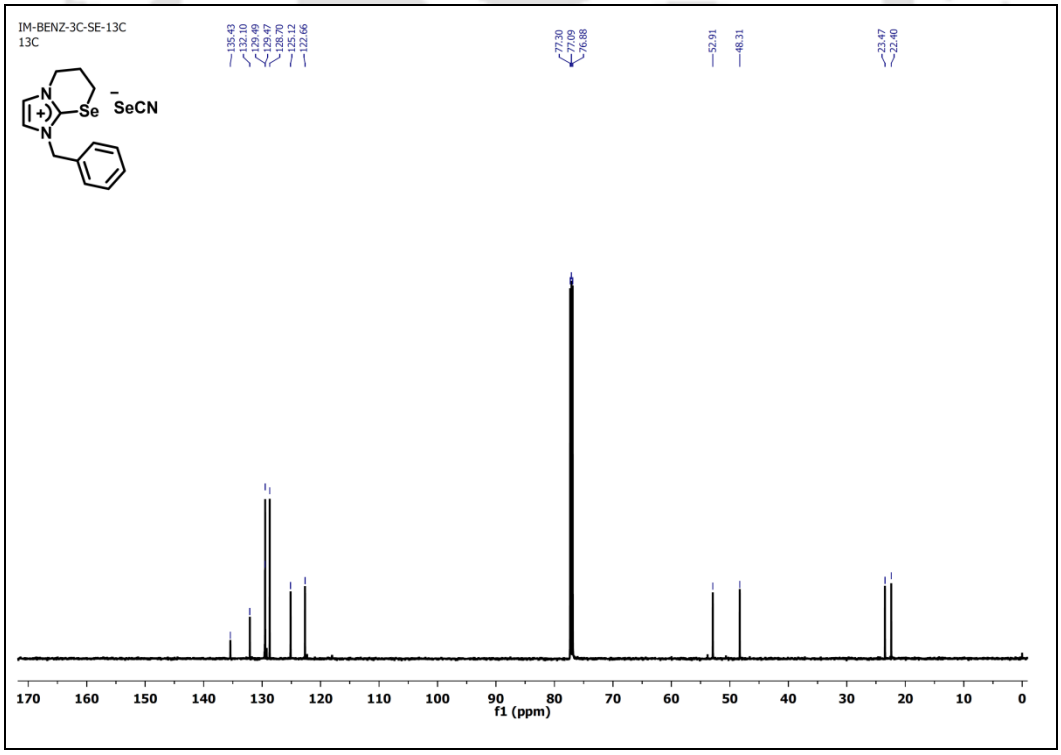

Figure A5.28. ^{1}H NMR spectrum ($CDCl_3$, 150 MHz) of compound **4.12d**.

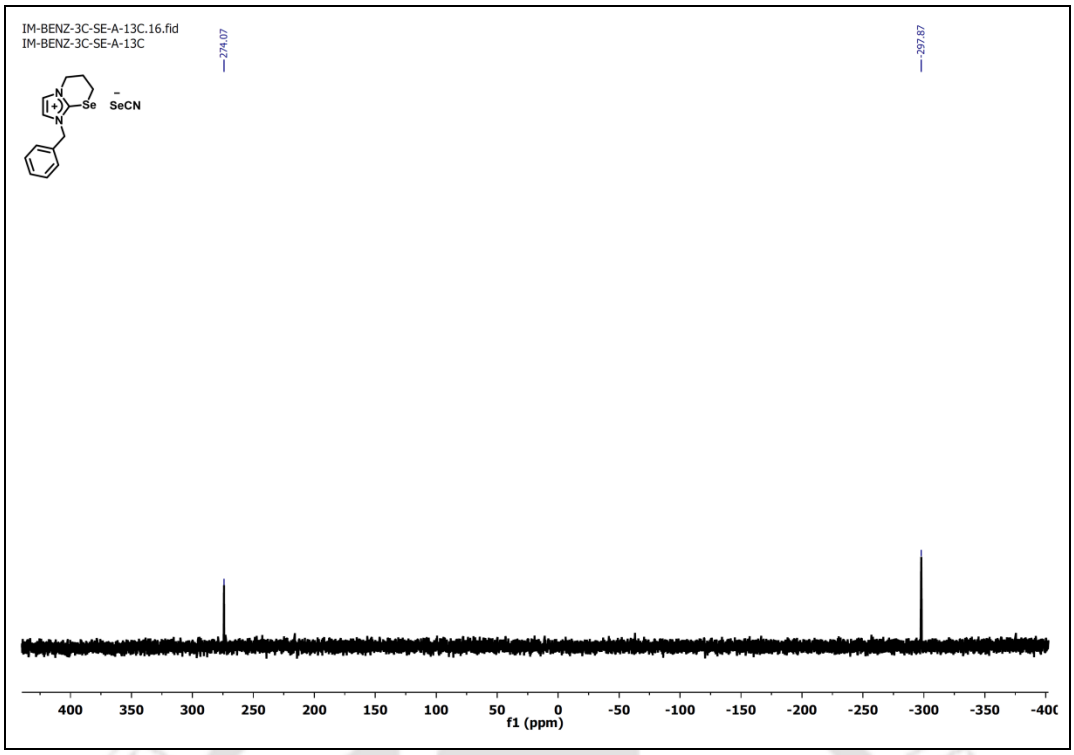

Figure A5.29. ^{77}Se NMR spectrum ($CDCl_3$, 95 MHz) of compound **4.12d**.

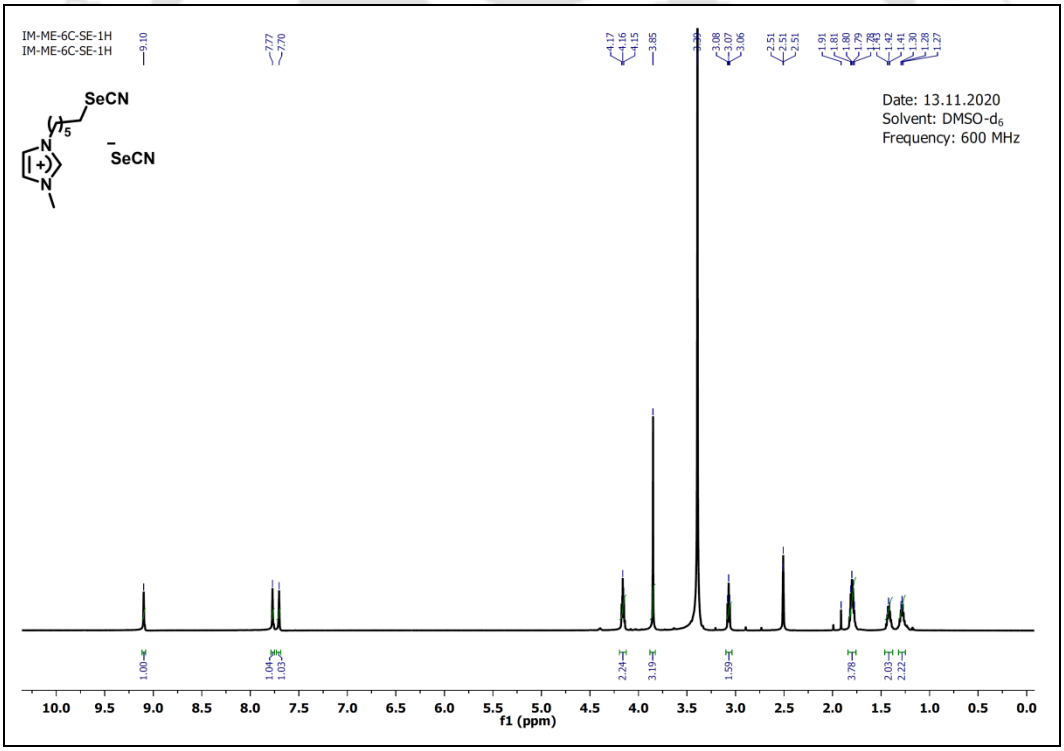

Figure A5.30. ^{1}H NMR spectrum (DMSO-d_6, 600 MHz) of compound **4.12e**.

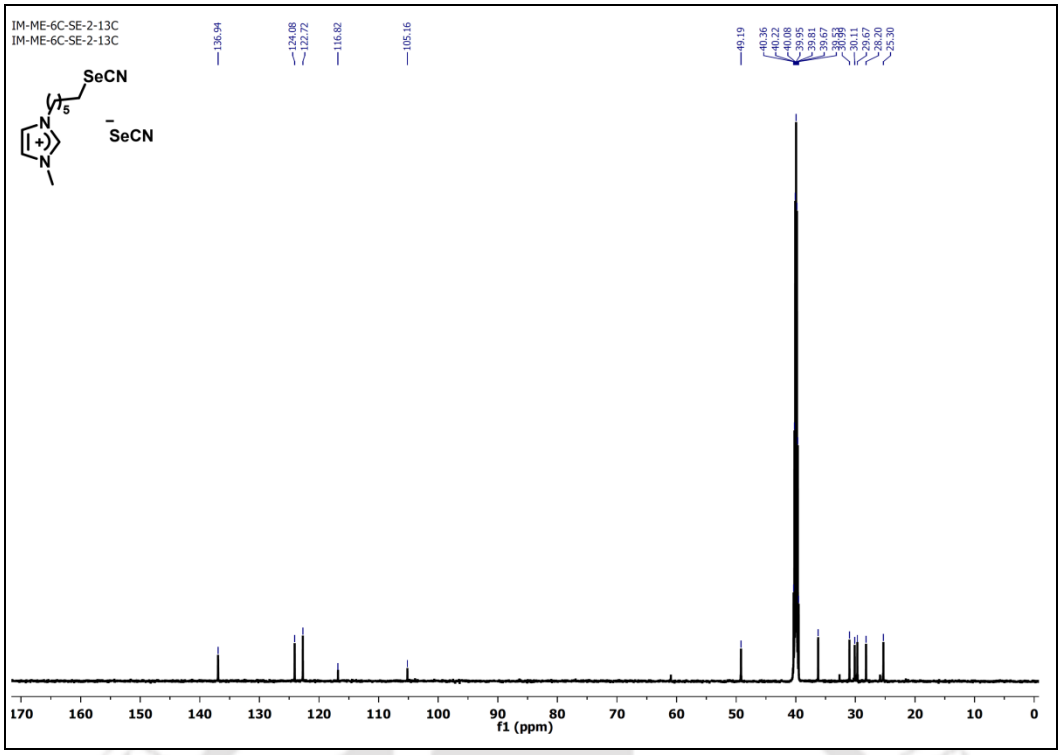

Figure A5.31. ^{13}C NMR spectrum (DMSO-d_6, 150 MHz) of compound **4.12e**.

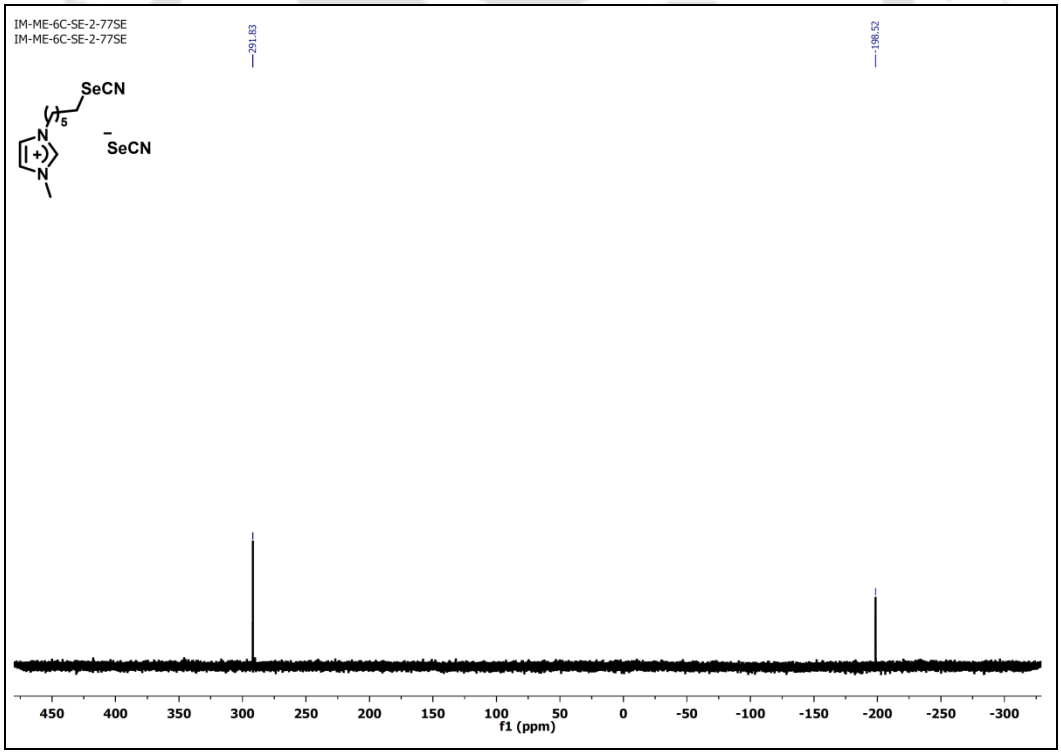

Figure A5.32. ^{77}Se NMR spectrum (DMSO-d_6, 114 MHz) of compound **4.12e**.

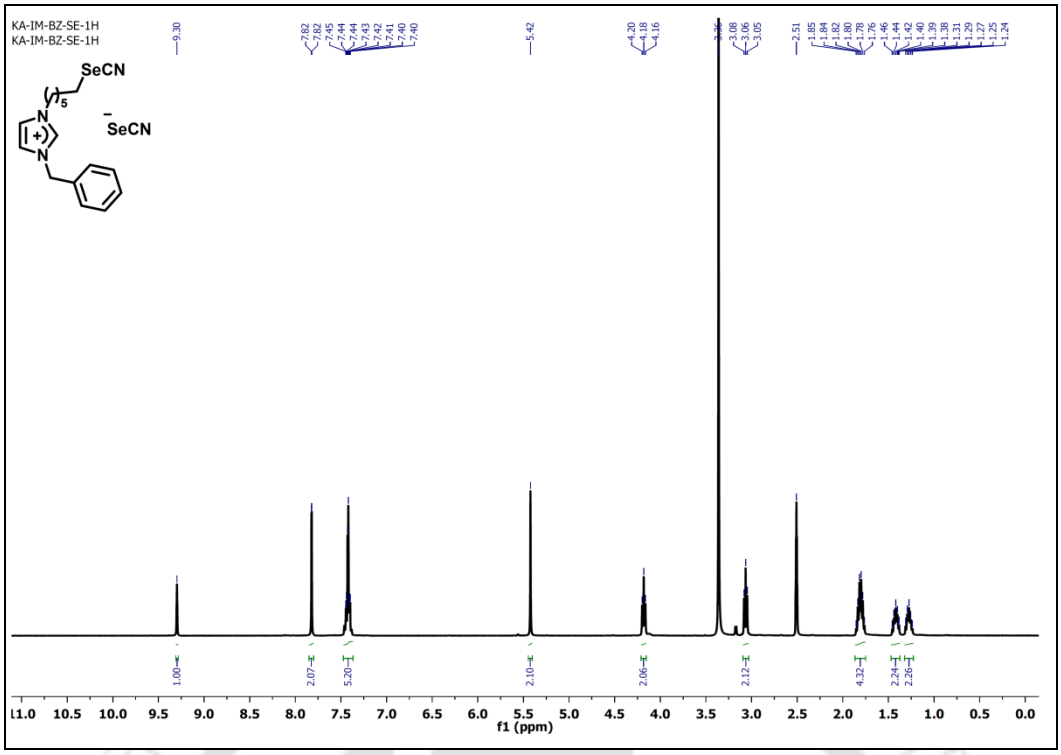

Figure A5.33. ^{1}H NMR spectrum (DMSO-d_6, 400 MHz) of compound **4.12f**.

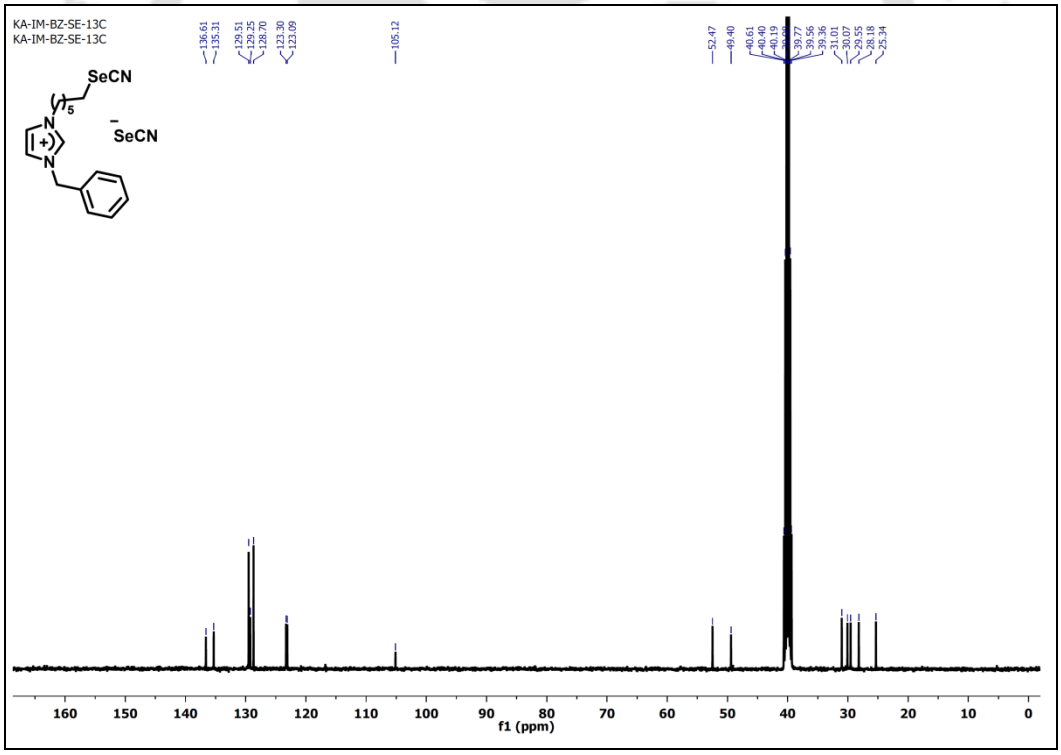

Figure A5.34. ^{13}C NMR spectrum (DMSO-d_6, 100 MHz) of compound **4.12f**.

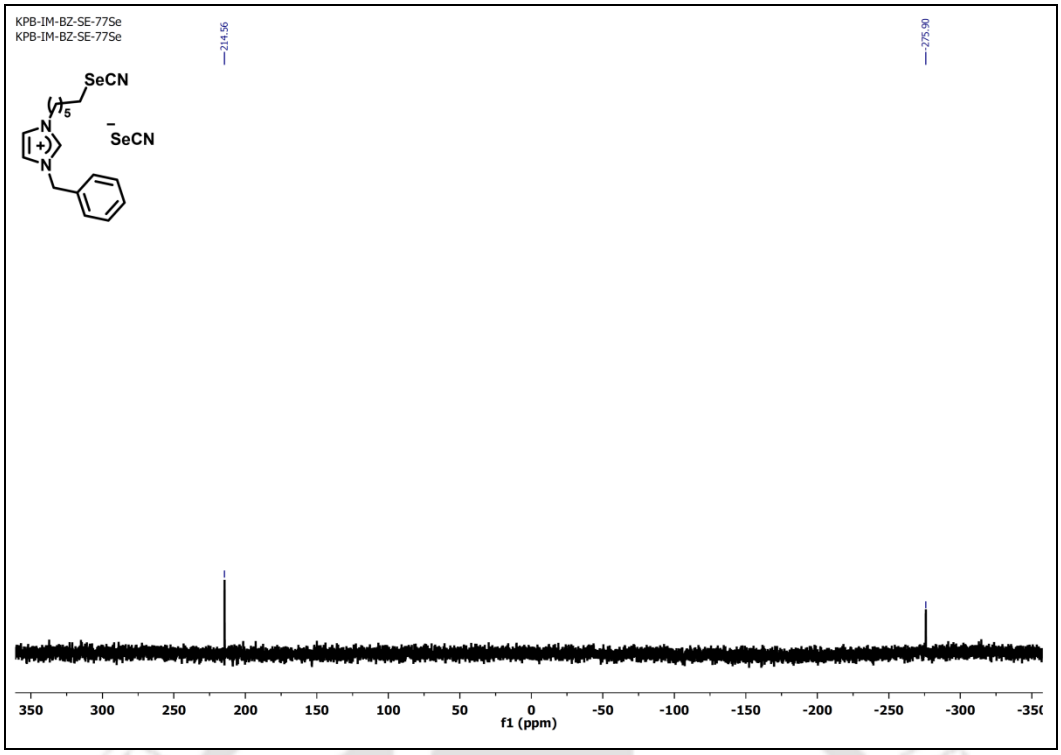

Figure A5.35. ^{77}Se NMR spectrum (DMSO-d_6, 76 MHz) of compound **4.12f**.

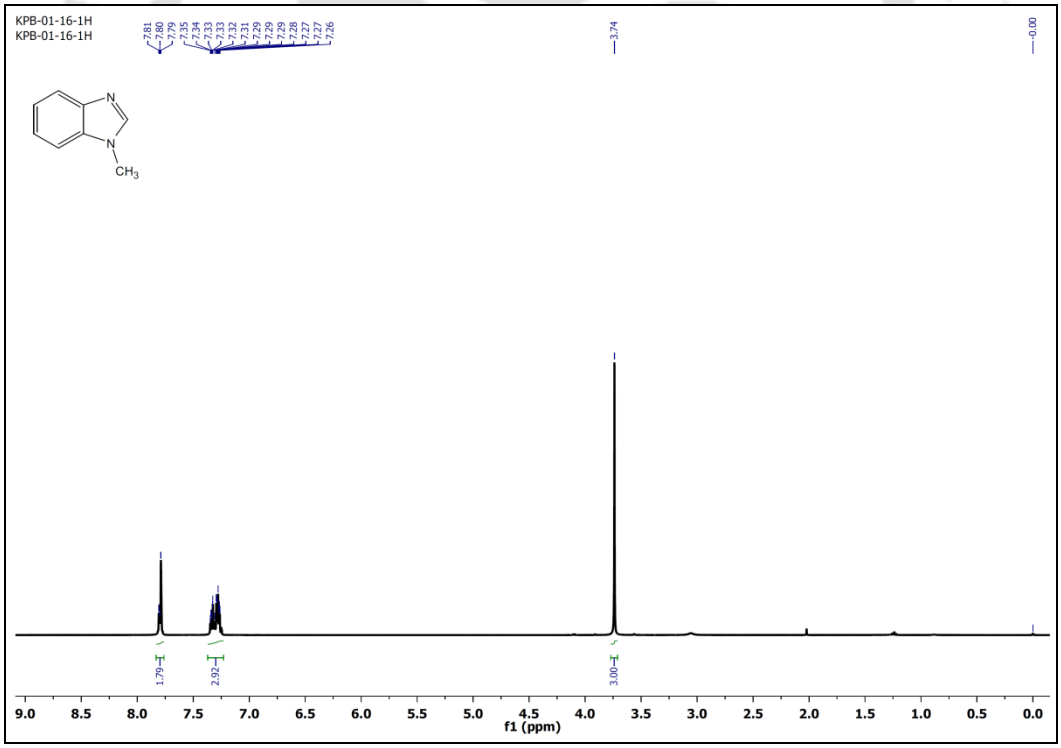

Figure A5.36. ^{1}H NMR spectrum ($CDCl_3$, 400 MHz) of compound **4.9a**.

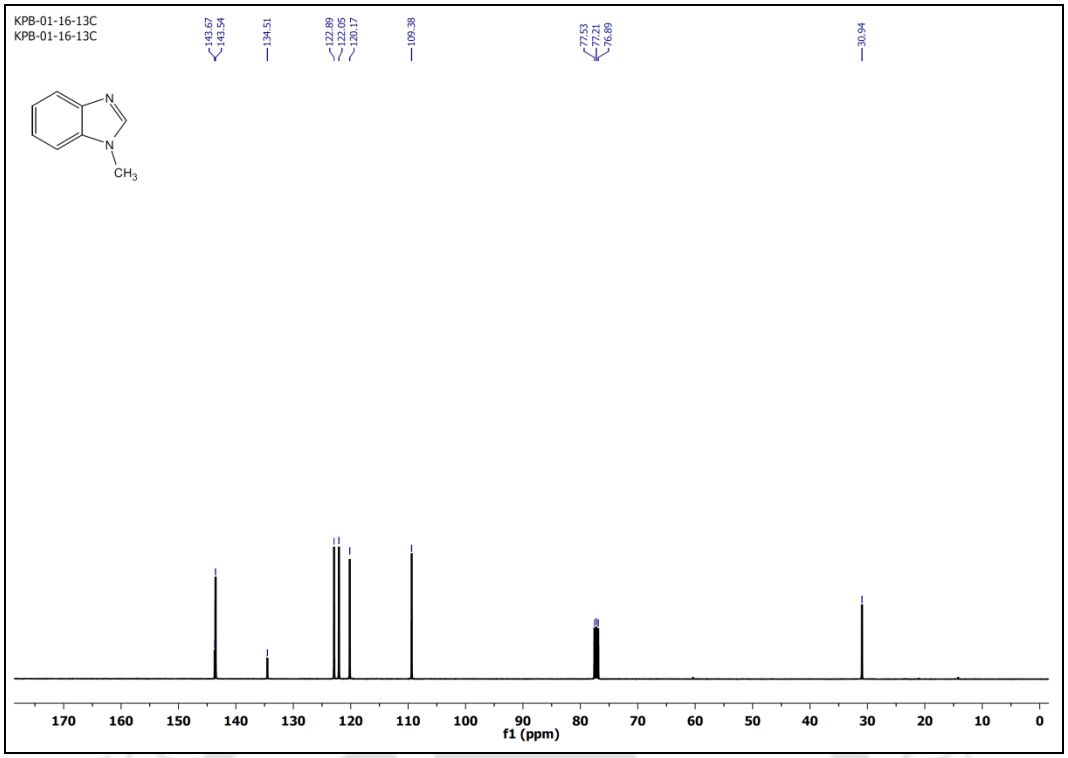

Figure A5.37. ^{13}C NMR spectrum ($CDCl_3$, 100 MHz) of compound **4.9a**.

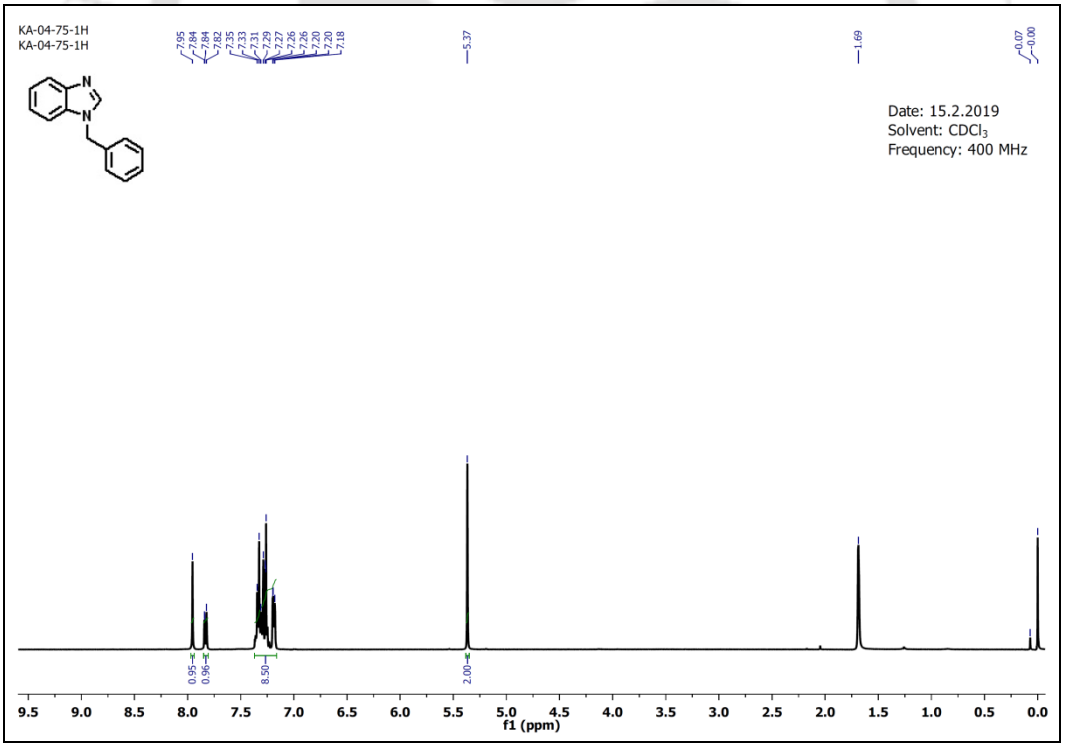

Figure A5.38. ^{1}H NMR spectrum ($CDCl_3$, 400 MHz) of compound **4.9b**.

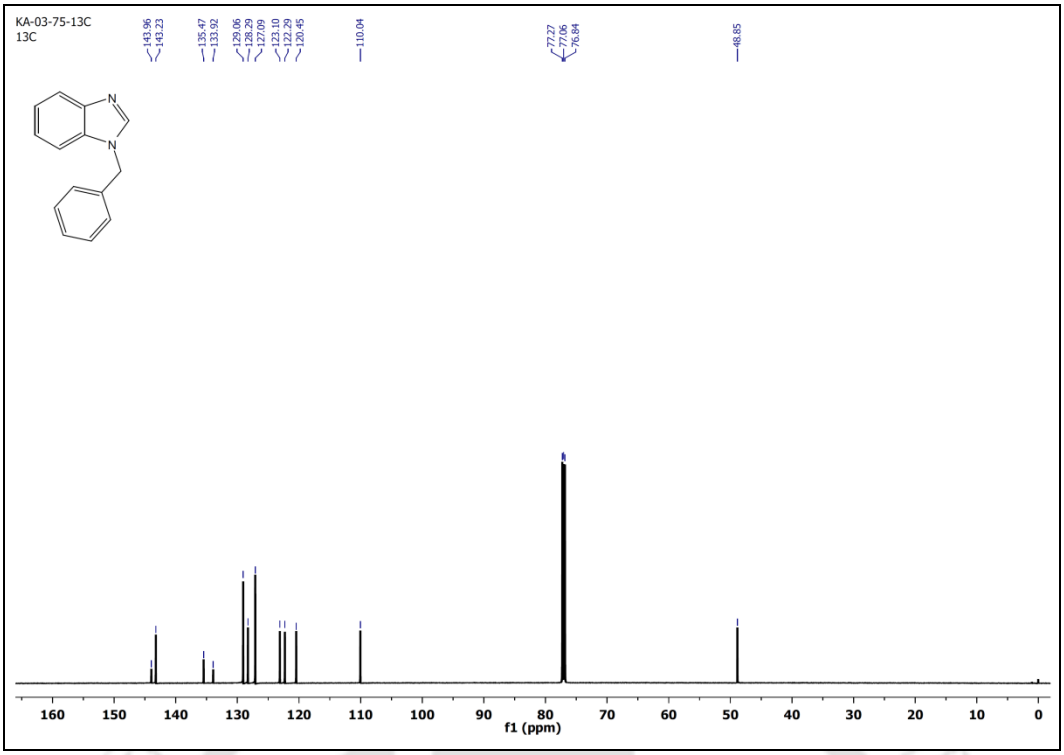

Figure A5.39. ^{13}C NMR spectrum ($CDCl_3$, 150 MHz) of compound **4.9b**.

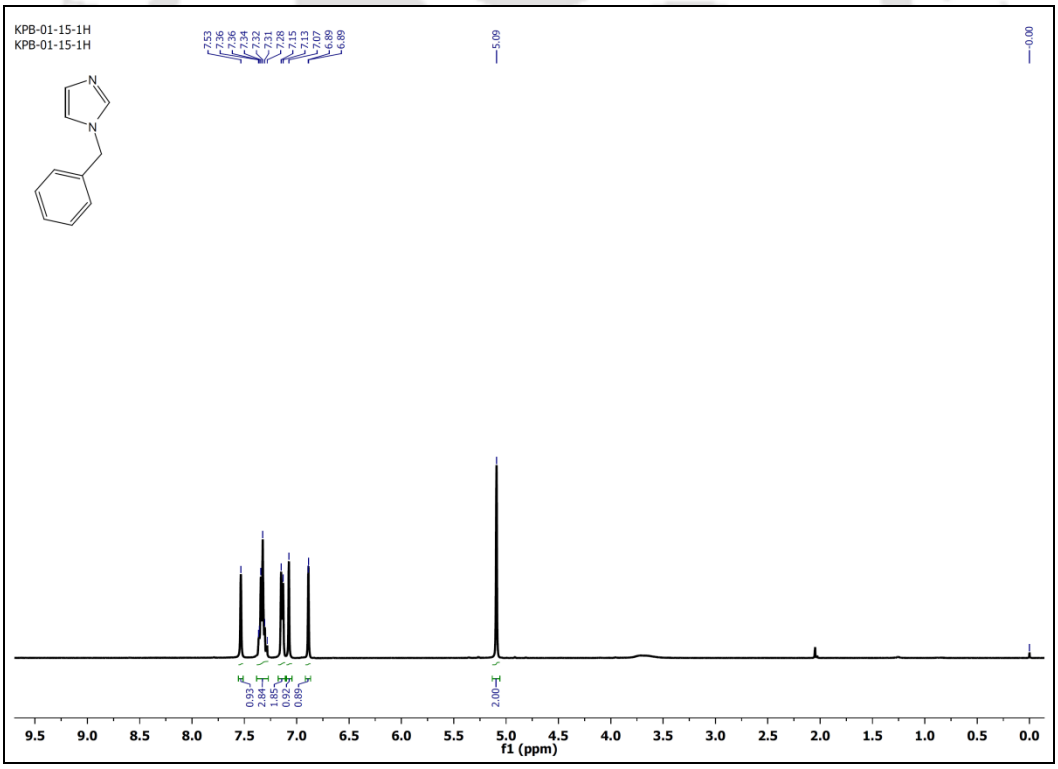

Figure A5.40. ^{1}H NMR spectrum ($CDCl_3$, 400 MHz) of compound **4.10b**.

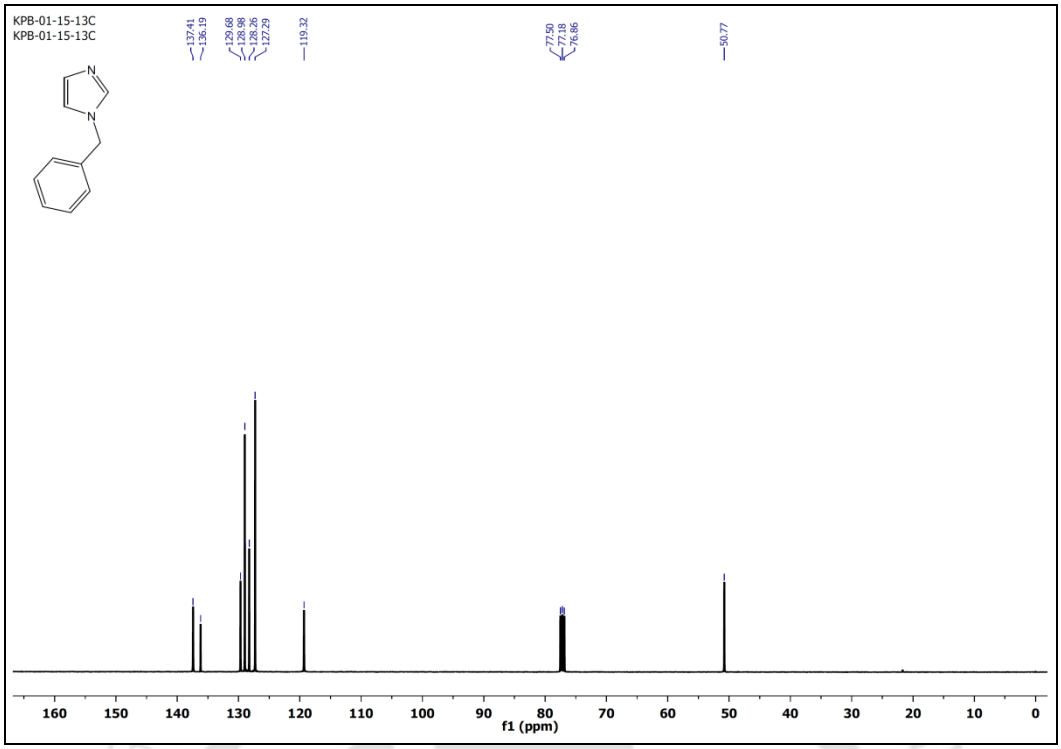

Figure A5.41. ^{13}C NMR spectrum ($CDCl_3$, 100 MHz) of compound **4.10b**.

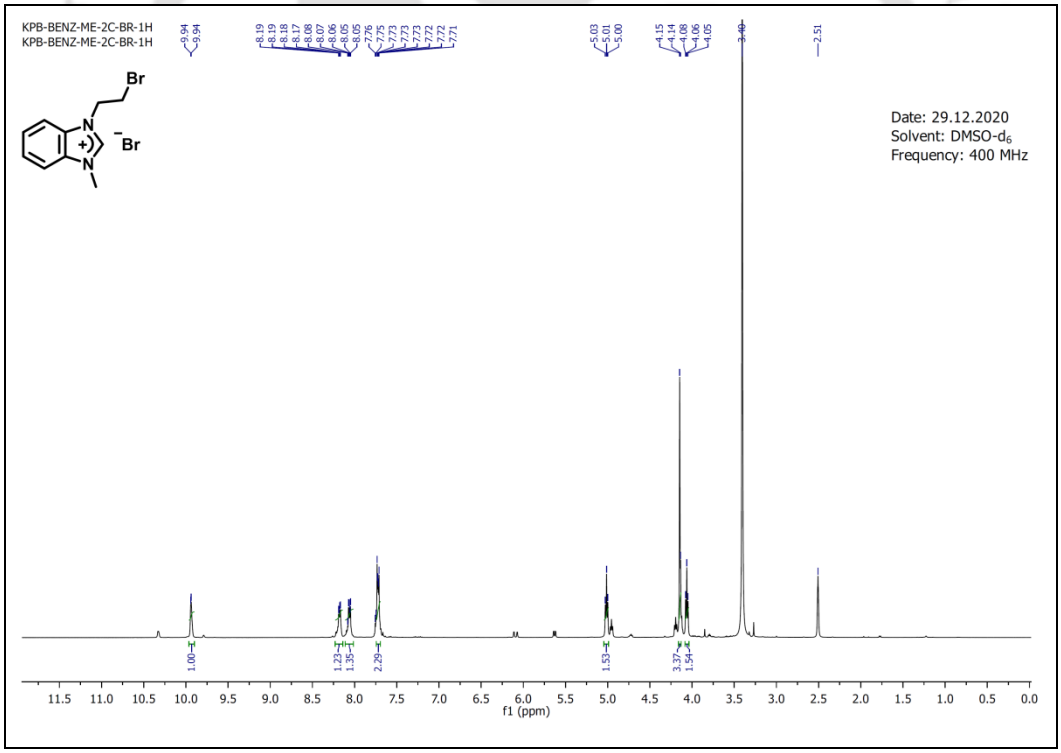

Figure A5.42. ^{1}H NMR spectrum (DMSO-d_6, 400 MHz) of compound **4.9a-1**.

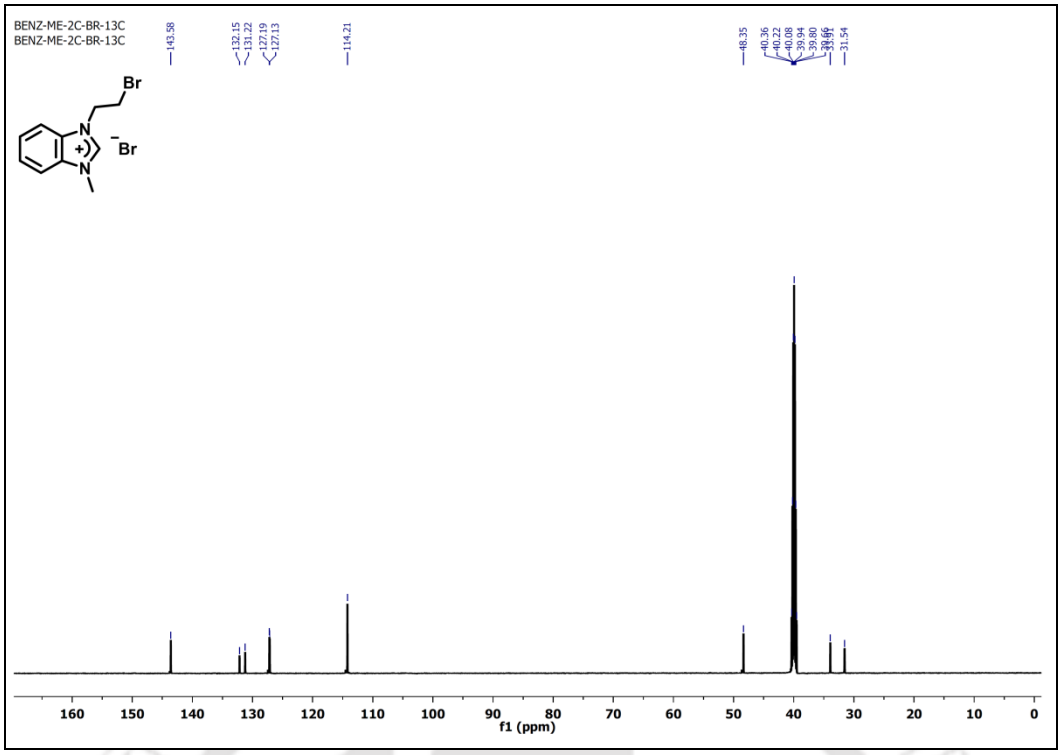

Figure A5.43. ^{13}C NMR spectrum (DMSO-d_6, 150 MHz) of compound **4.9a-1**.

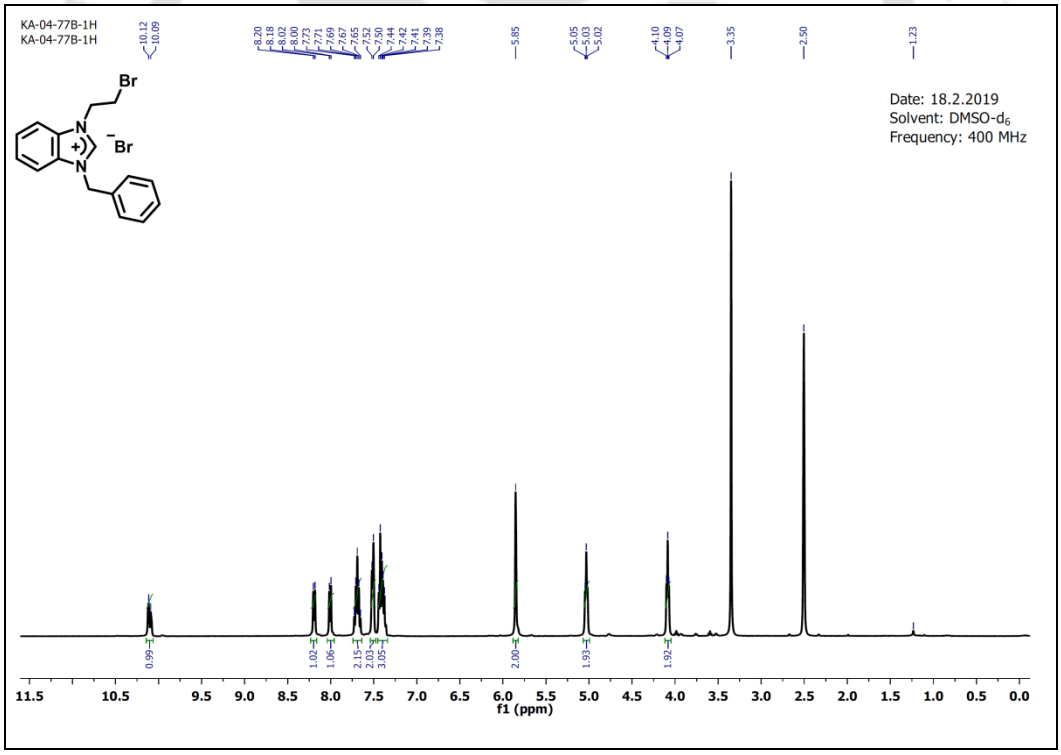

Figure A5.44. ^{1}H NMR spectrum (DMSO-d_6, 400 MHz) of compound **4.9b-1**.

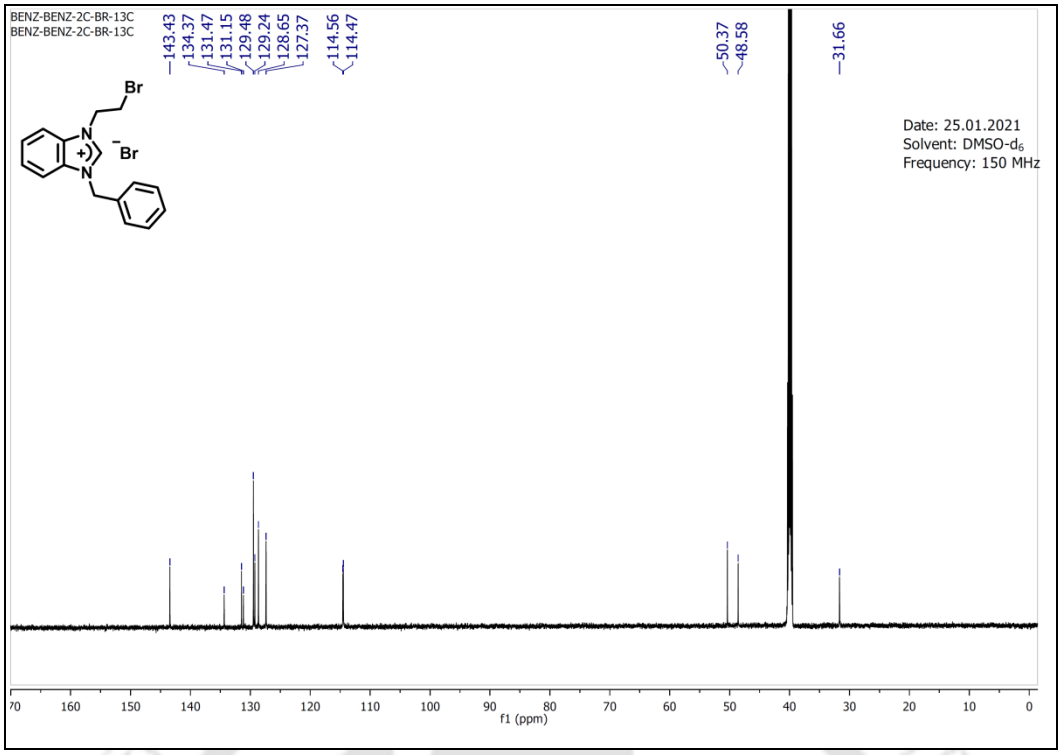

Figure A5.45. ^{13}C NMR spectrum (DMSO-d_6, 150 MHz) of compound **4.9b-1**.

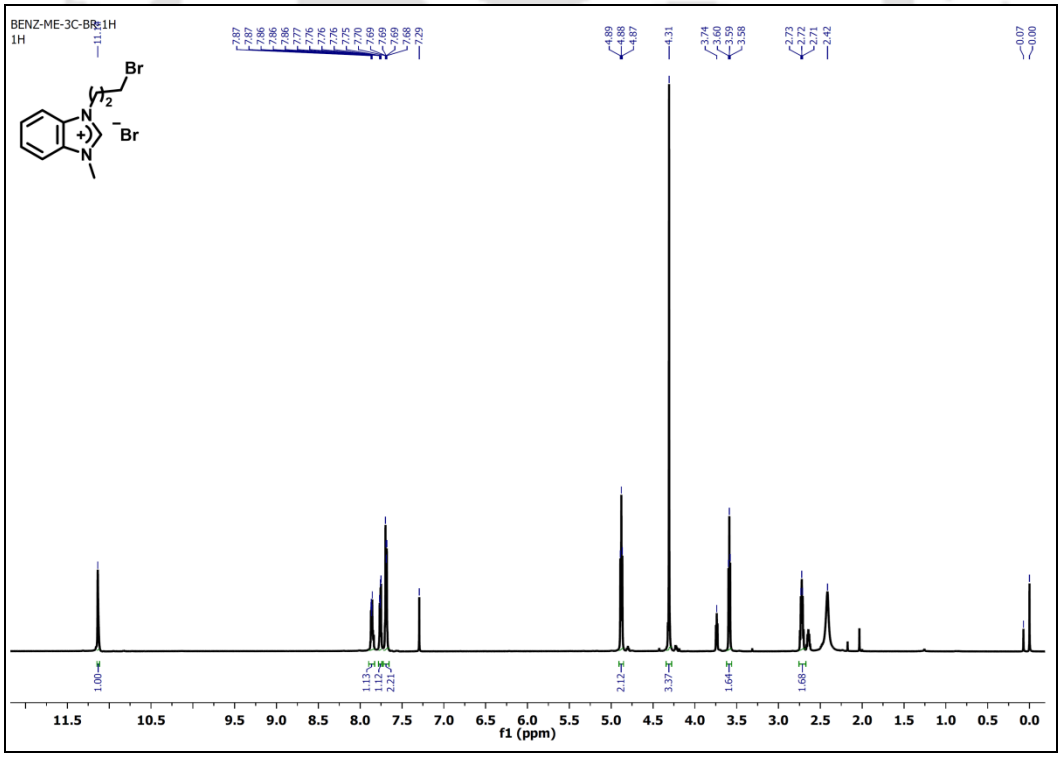

Figure A5.46. ^{1}H NMR spectrum ($CDCl_3$, 600 MHz) of compound **4.9a-2**.

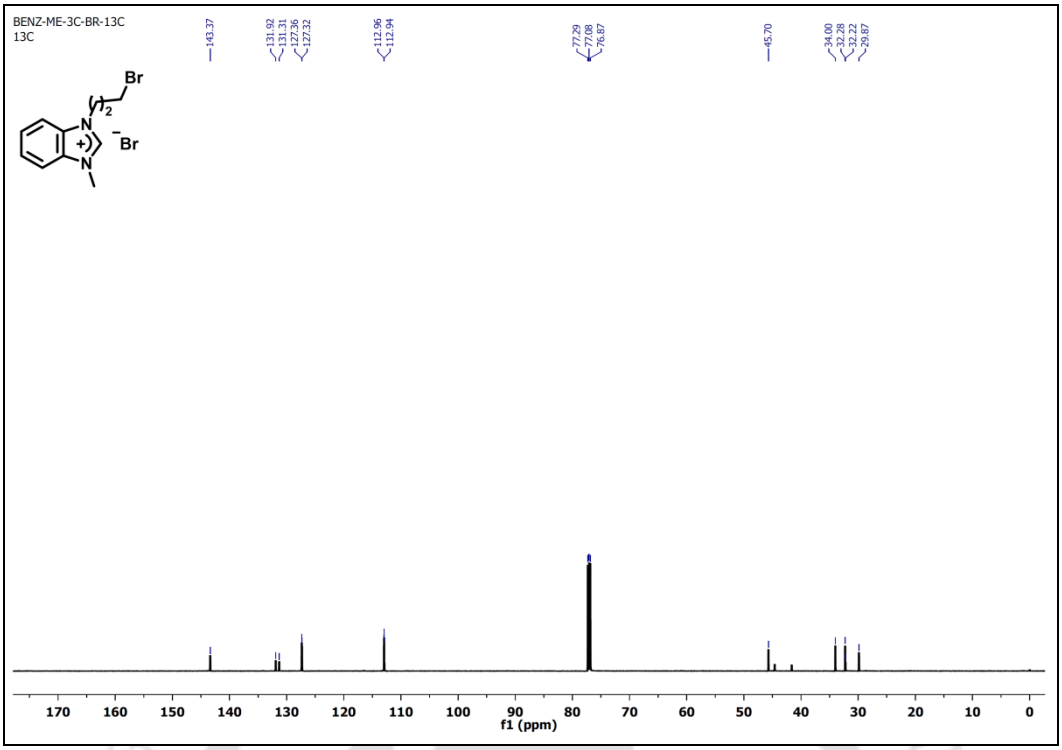

Figure A5.47. ^{13}C NMR spectrum ($CDCl_3$, 150 MHz) of compound **4.9a-2**.

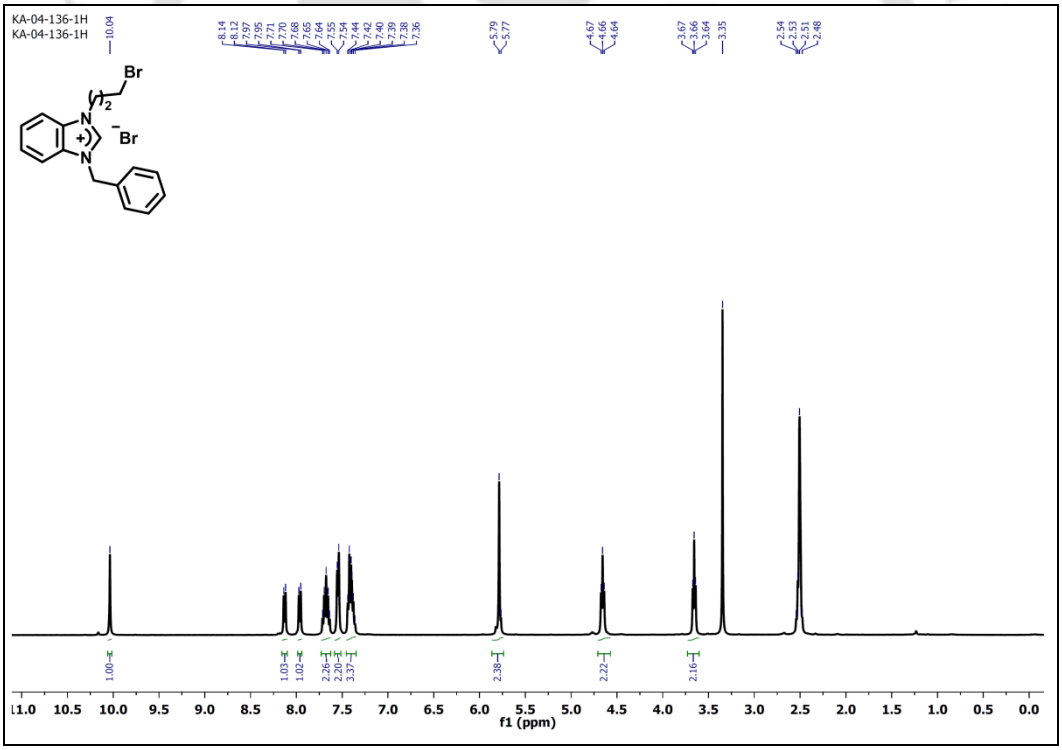

Figure A5.48. ^{1}H NMR spectrum (DMSO-d_6, 400 MHz) of compound **4.9b-2**.

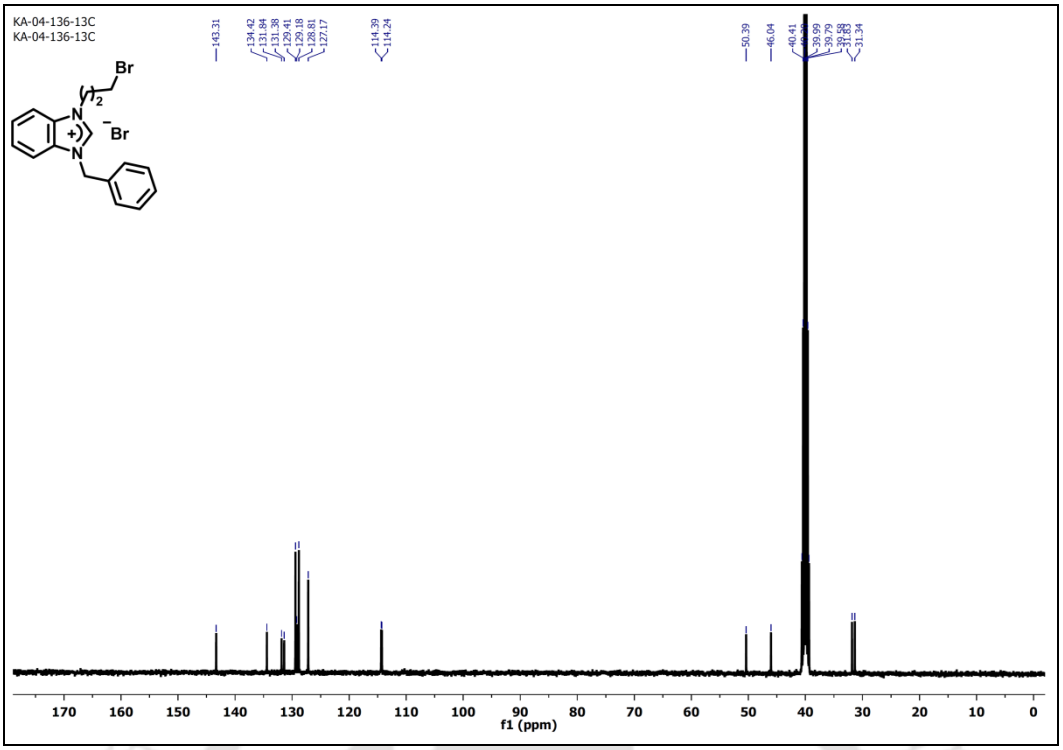

Figure A5.49. ^{13}C NMR spectrum (DMSO-d_6, 100 MHz) of compound **4.9b-2**.

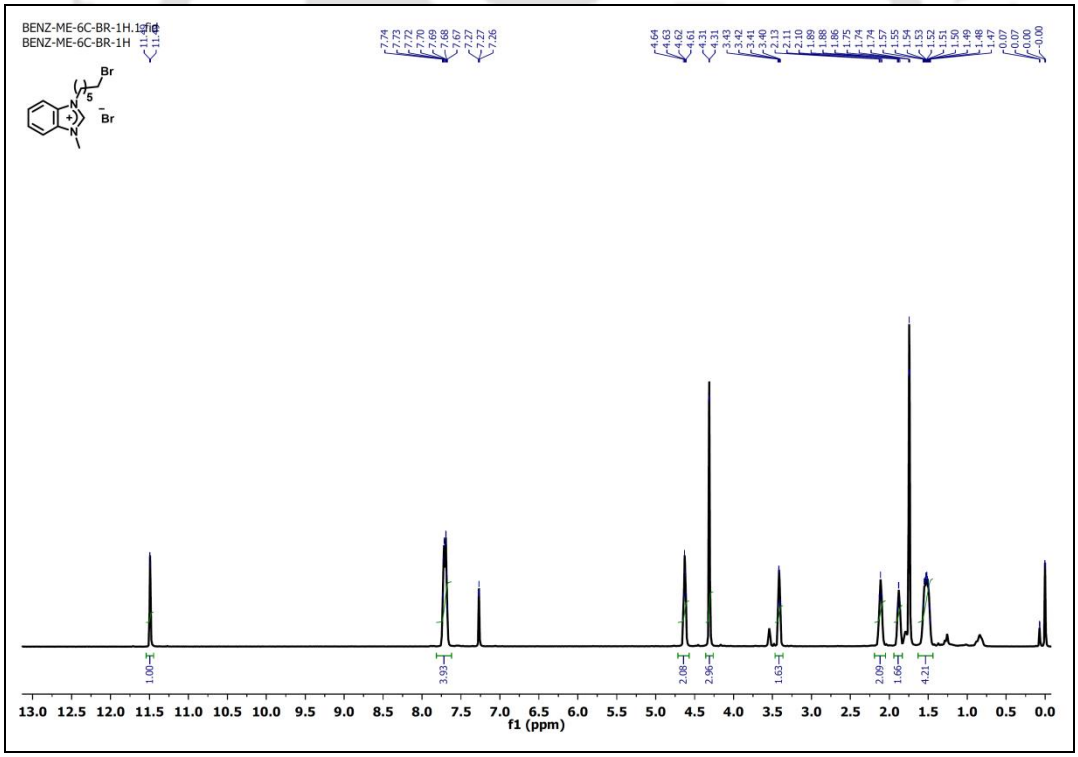

Figure A5.50. ^{1}H NMR spectrum ($CDCl_3$, 500 MHz) of compound **4.9a-5**.

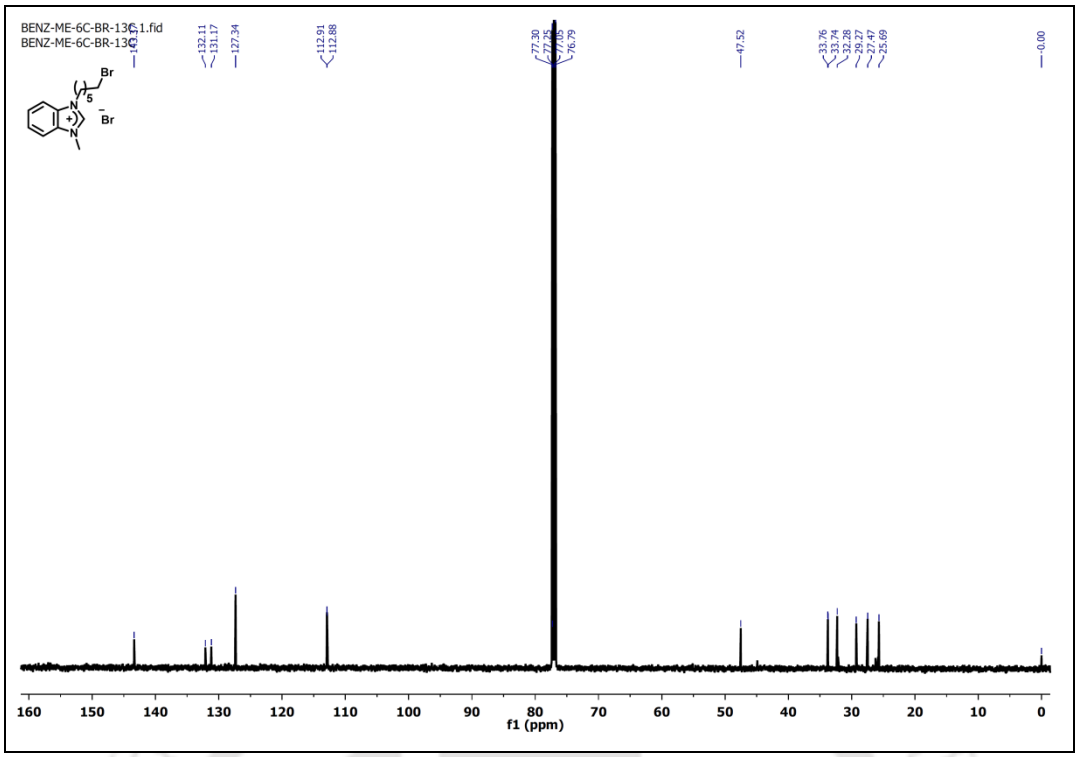

Figure A5.51. ^{13}C NMR spectrum ($CDCl_3$, 125 MHz) of compound **4.9a-5**.

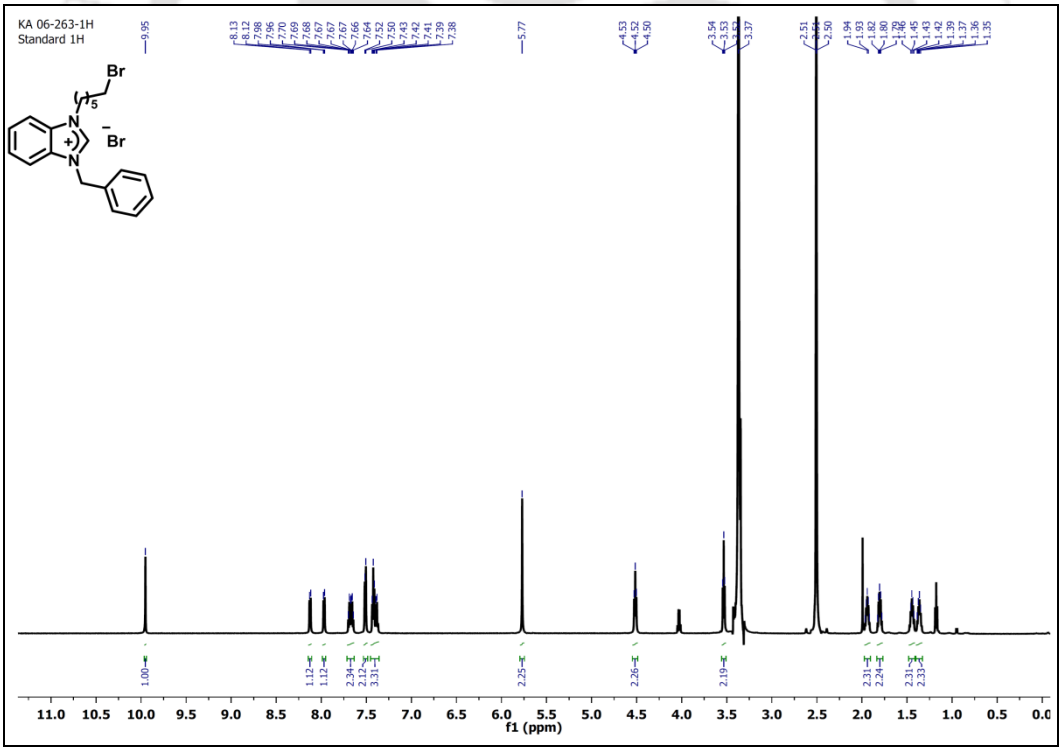

Figure A5.52. ^{1}H NMR spectrum (DMSO-d_6, 600 MHz) of compound **4.9b-5**.

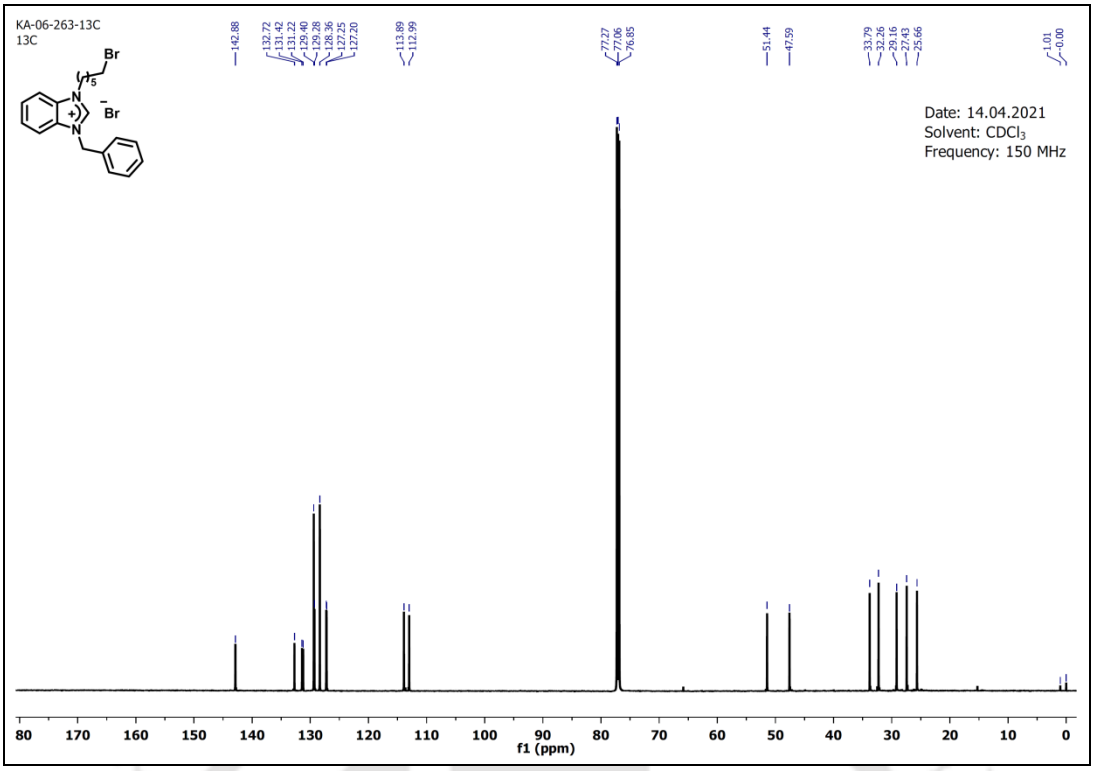

Figure A5.53. ^{13}C NMR spectrum ($CDCl_3$, 150 MHz) of compound **4.9b-5**.

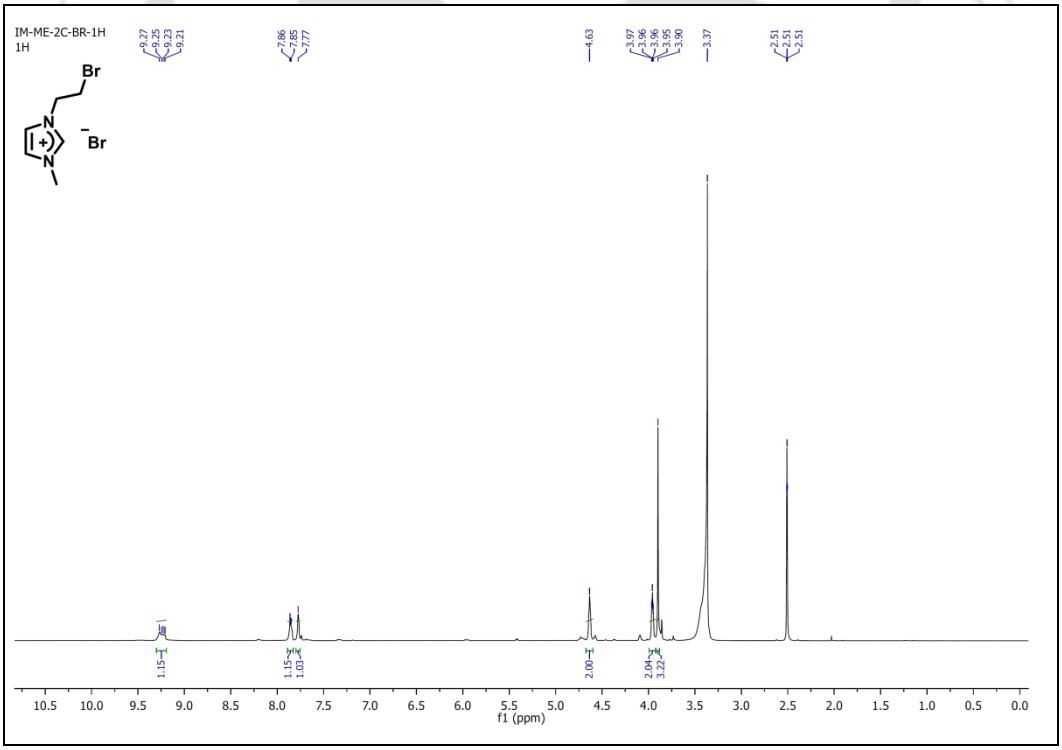

Figure A5.54. ^{1}H NMR spectrum (DMSO-d_6, 400 MHz) of compound **4.10a-1**.

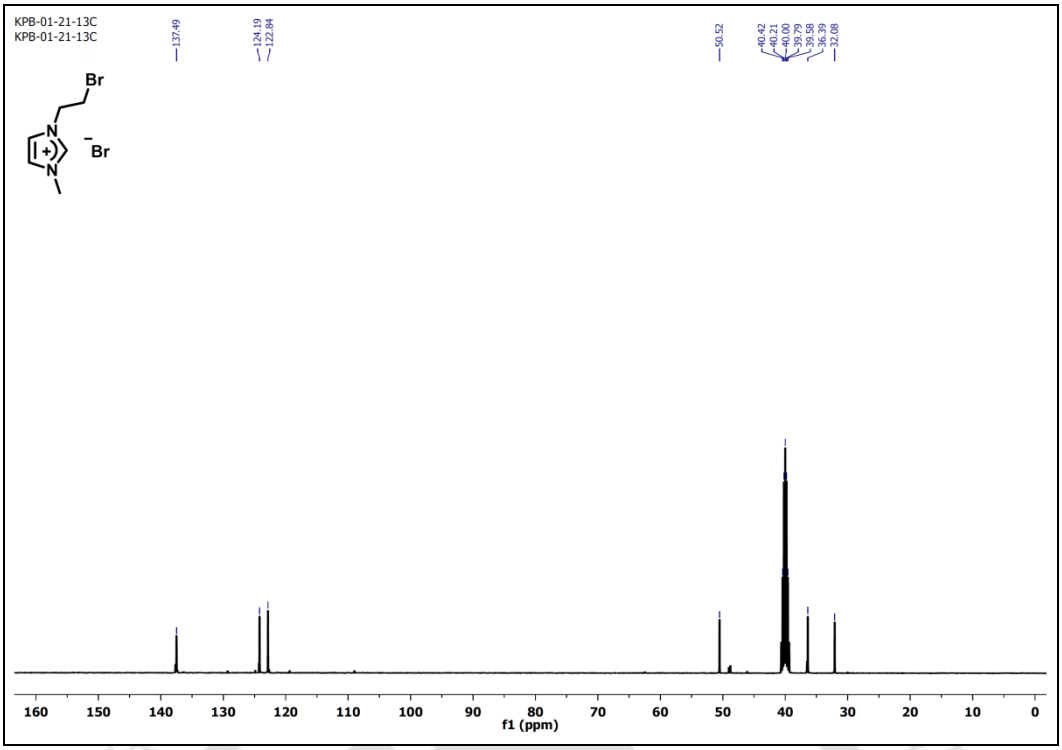

Figure A5.55. ^{13}C NMR spectrum (DMSO-d_6, 100 MHz) of compound **4.10a-1**.

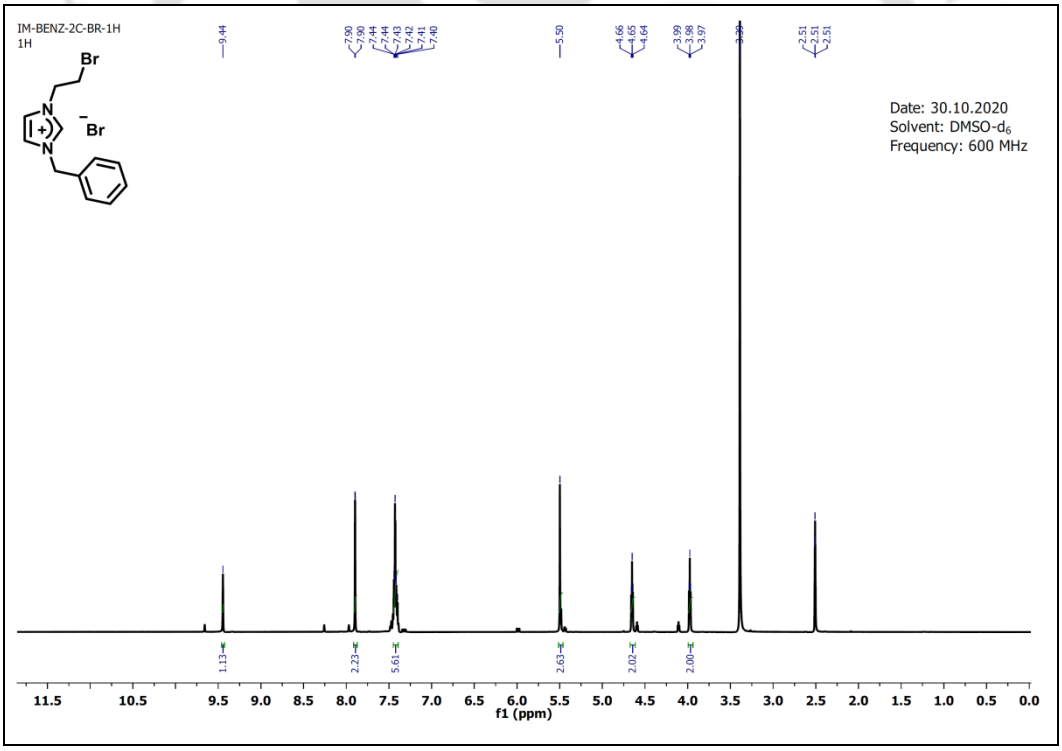

Figure A5.56. ^{1}H NMR spectrum (DMSO-d_6, 600 MHz) of compound **4.10b-1**.

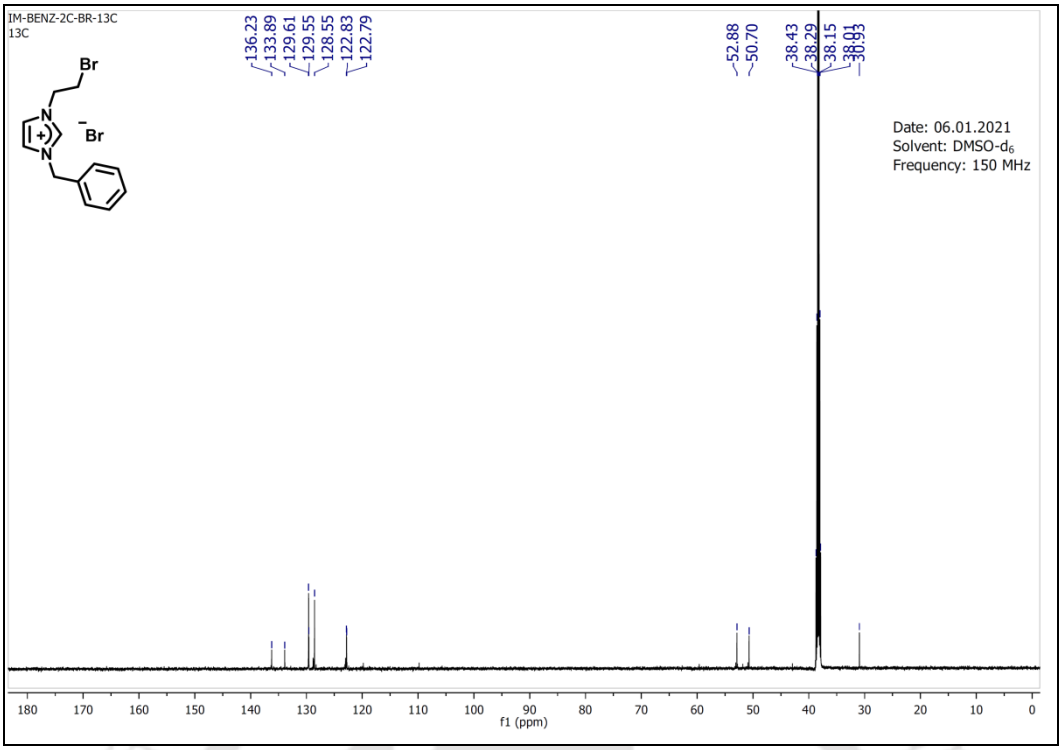

Figure A5.57. ^{13}C NMR spectrum (DMSO-d_6, 150 MHz) of compound **4.10b-1**.

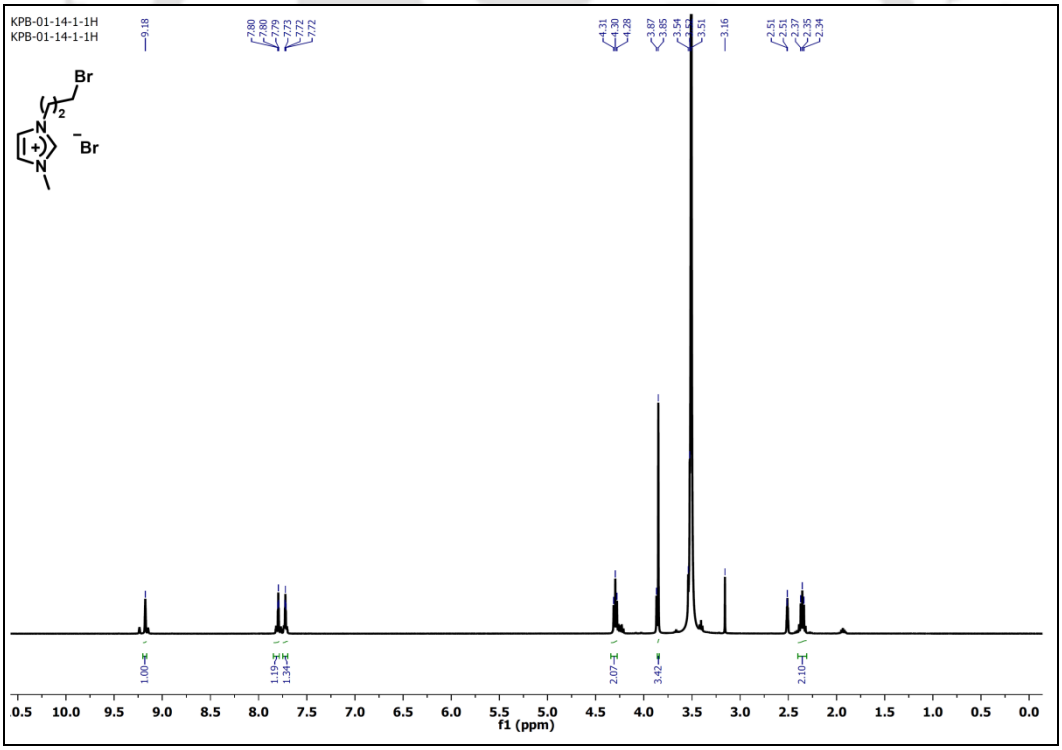

Figure A5.58. ^{1}H NMR spectrum (DMSO-d_6, 400 MHz) of compound **4.10a-2**.

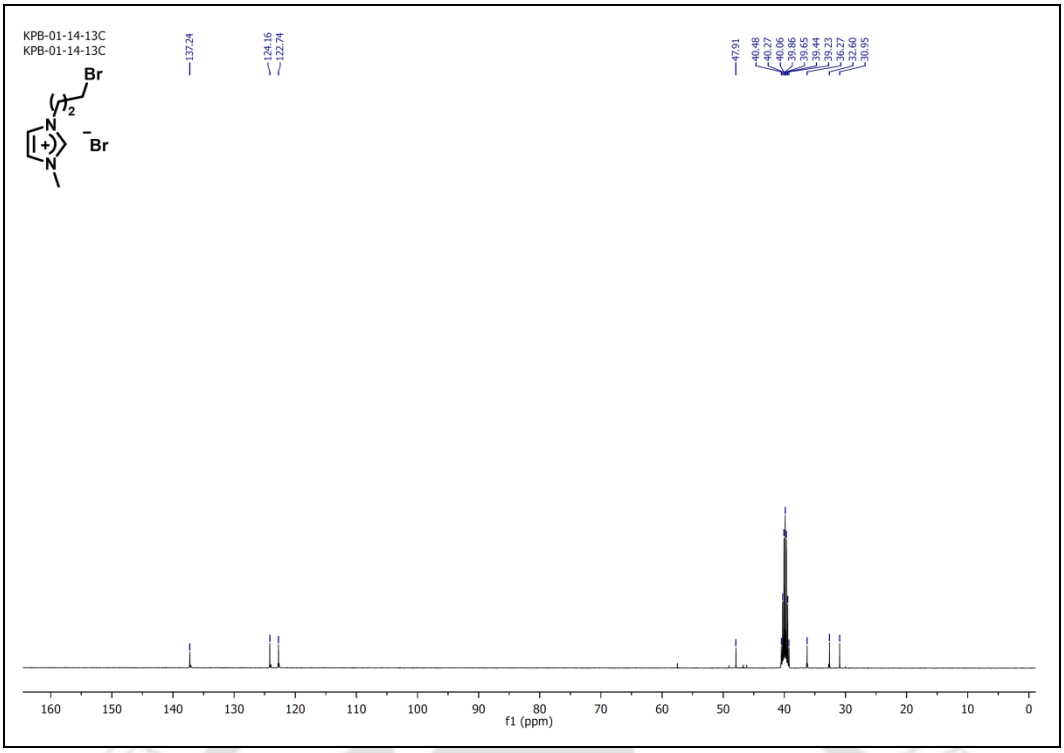

Figure A5.59. ^{13}C NMR spectrum (DMSO-d_6, 100 MHz) of compound **4.10a-2**.

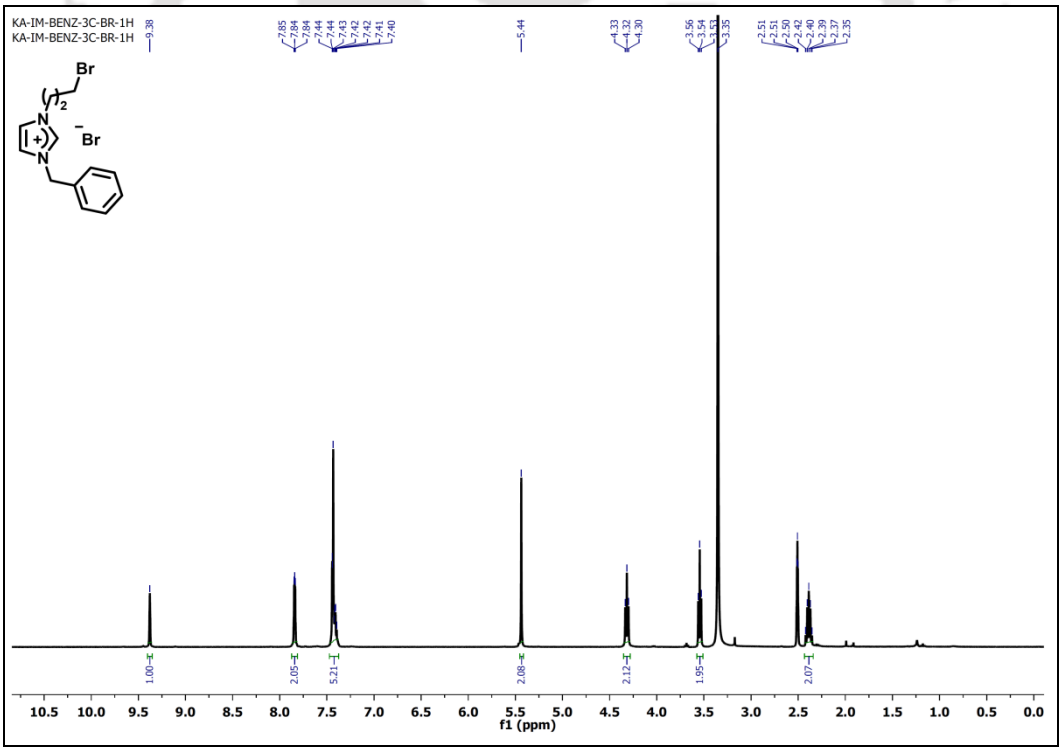

Figure A5.60. ^{1}H NMR spectrum (DMSO-d_6, 400 MHz) of compound **4.10b-2**.

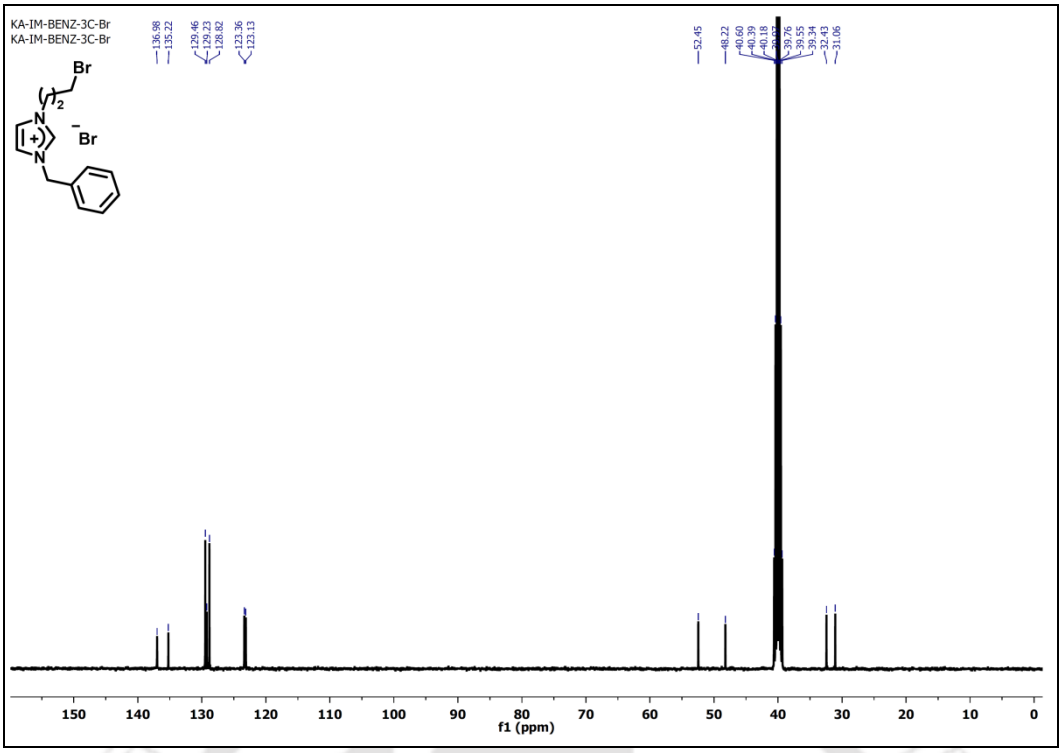

Figure A5.61. ^{13}C NMR spectrum (DMSO-d_6, 150 MHz) of compound **4.10b-2**.

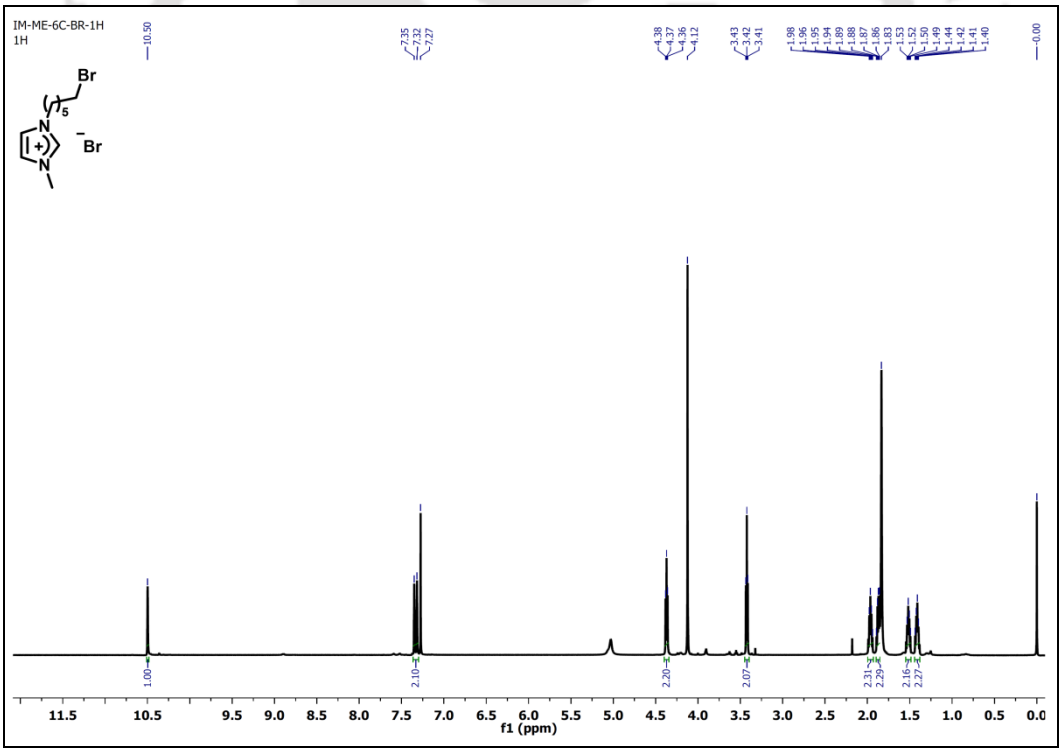

Figure A5.62. ^{1}H NMR spectrum ($CDCl_3$, 600 MHz) of compound **4.10a-5**.

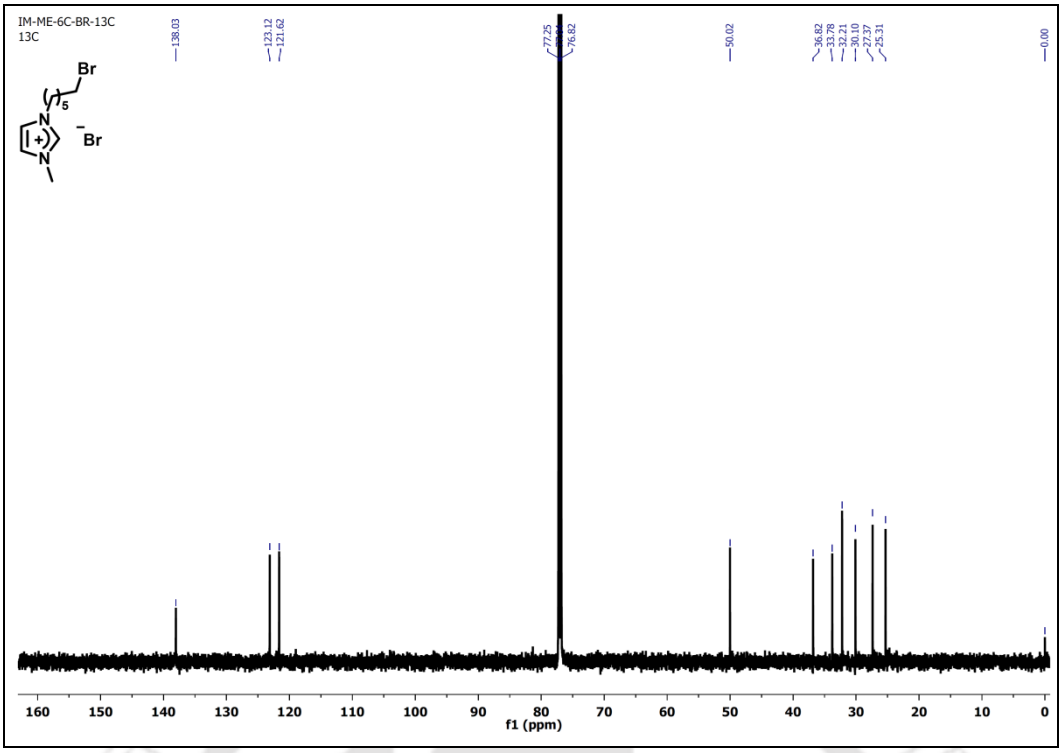

Figure A5.63. ^{13}C NMR spectrum ($CDCl_3$, 150 MHz) of compound **4.10a-5**.

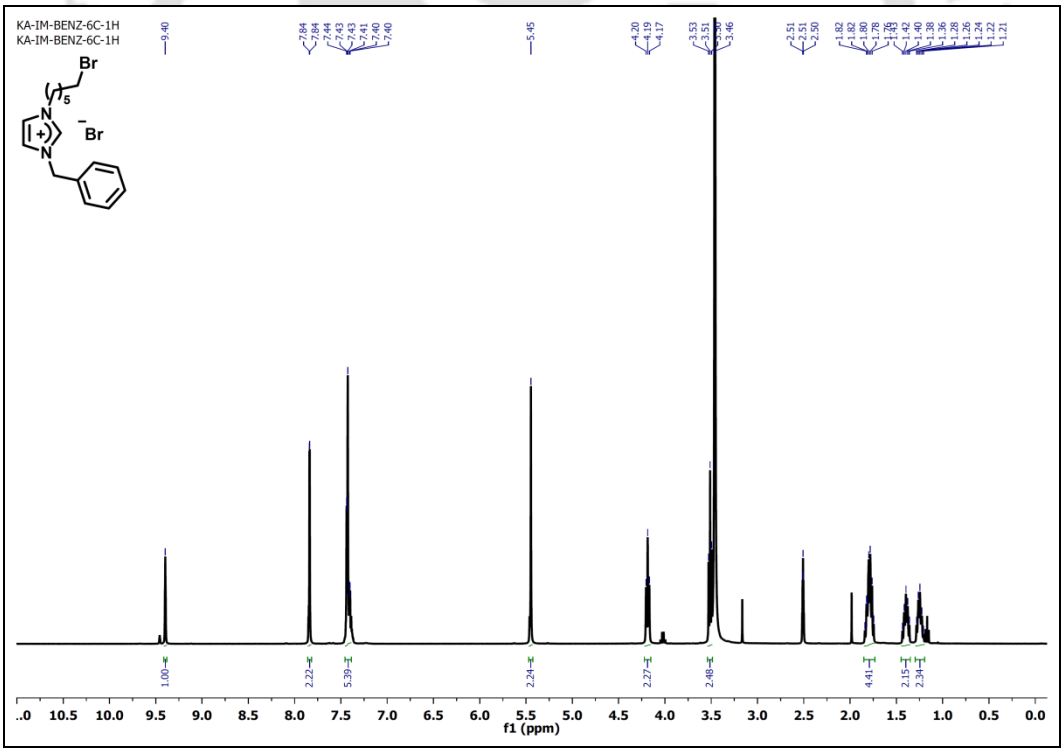

Figure A5.64. ^{1}H NMR spectrum (DMSO-d_6, 400 MHz) of compound **4.10b-5**.

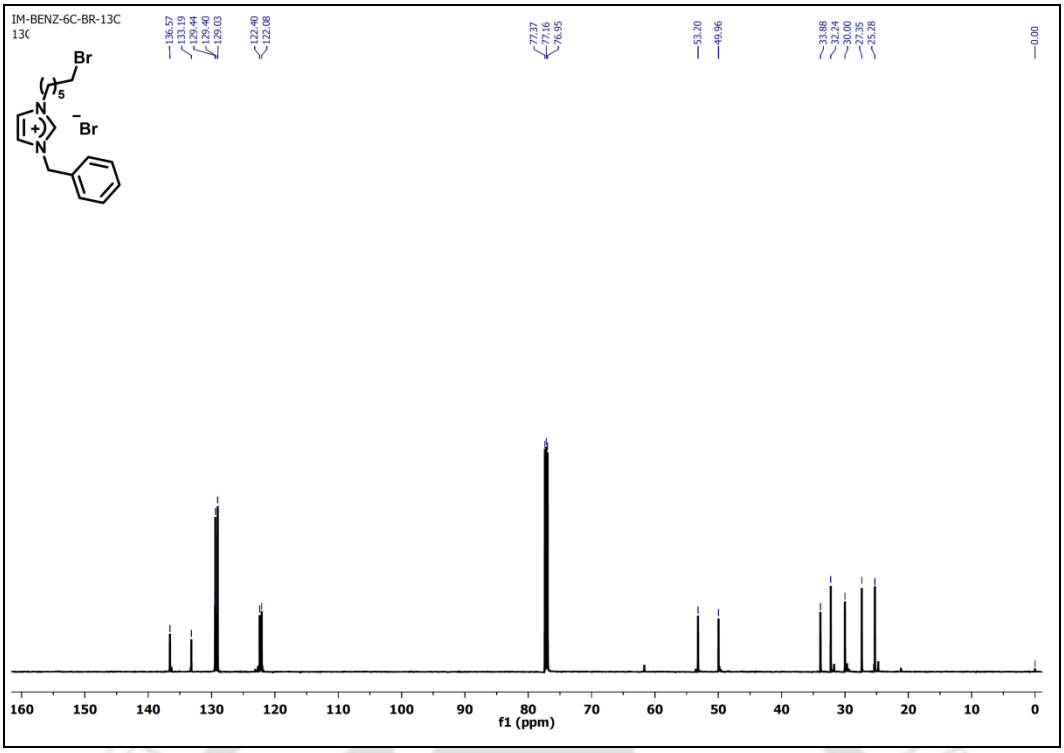

Figure A5.65. ^{13}C NMR spectrum ($CDCl_3$, 150 MHz) of compound **4.10b-5**.

Annexure VI

NMR spectral data of compounds discussed in Chapter 5

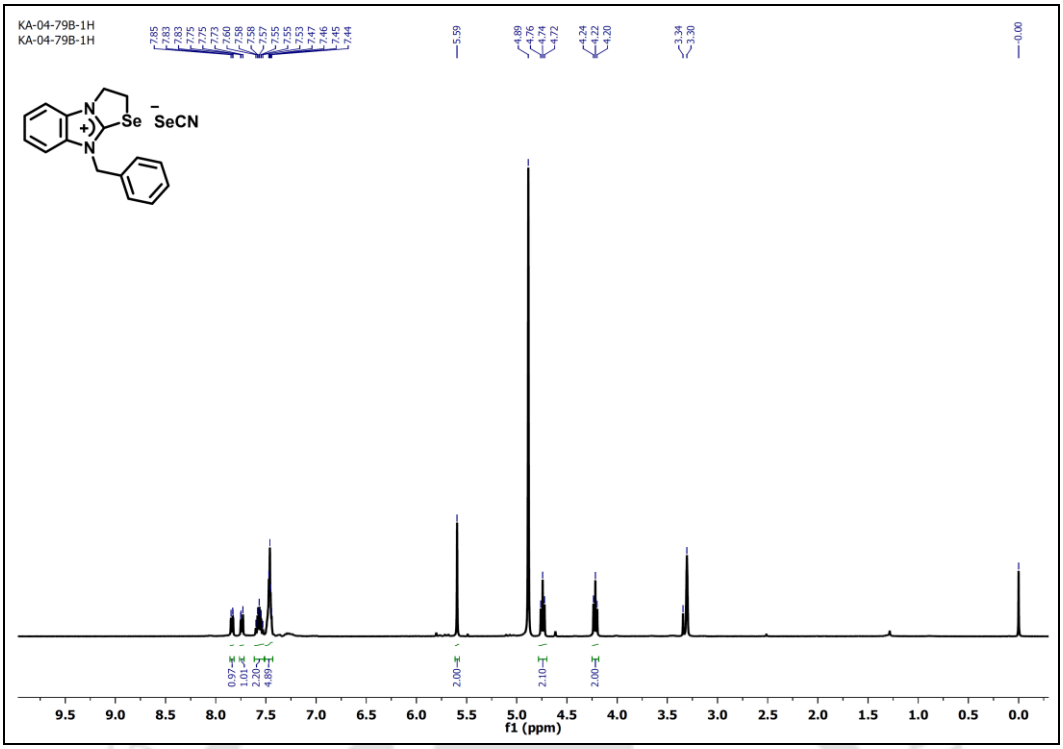

Figure A6.1. ^{1}H NMR spectrum (methanol-d_4, 400 MHz) of compound **4.11d**.

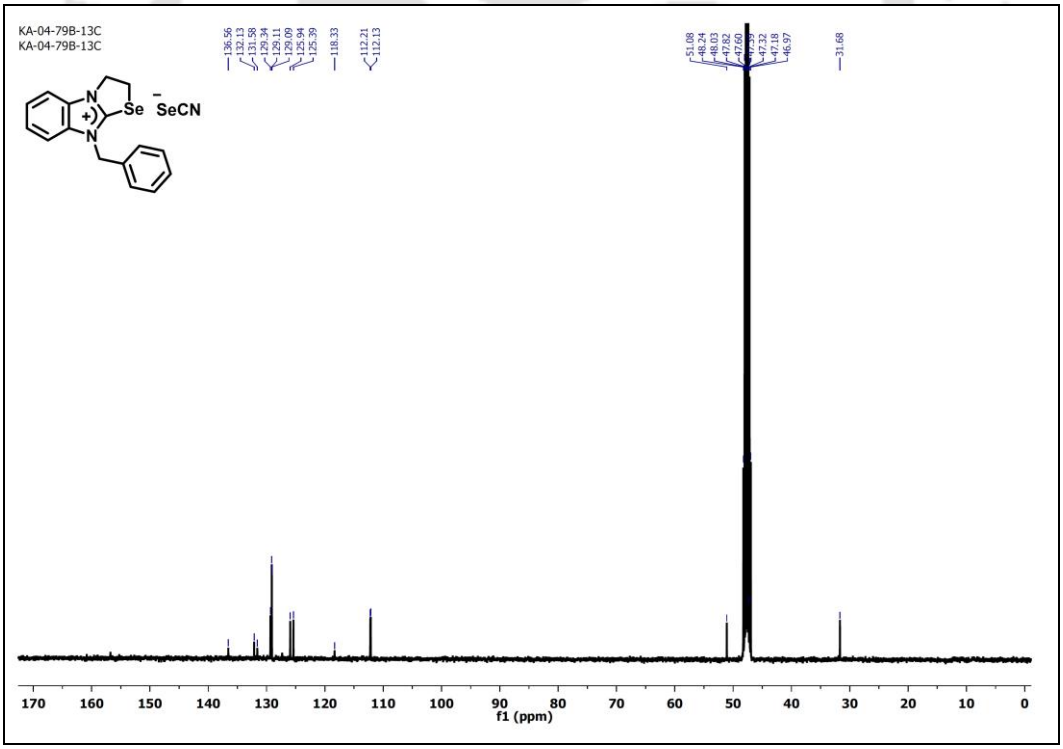

Figure A6.2. ^{13}C NMR spectrum (methanol-d_4, 100 MHz) of compound **4.11d**.

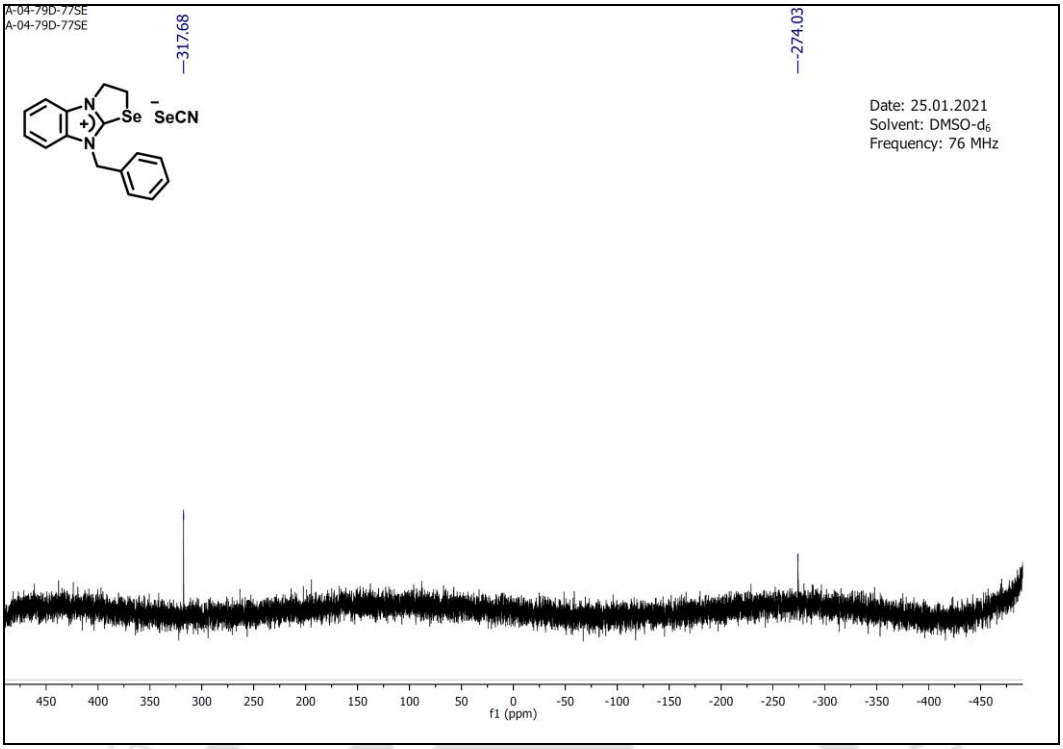

Figure A6.3. ^{77}Se NMR spectrum (DMSO-d_6, 76 MHz) of compound **4.11d**.

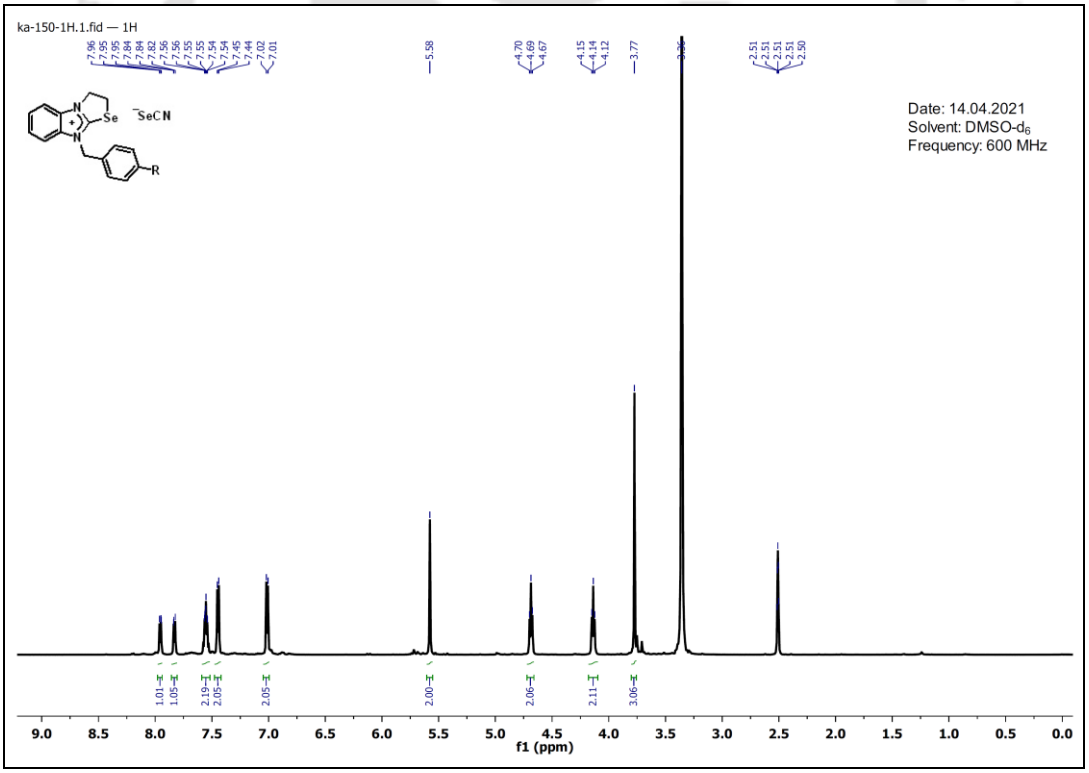

Figure A6.4. ^{1}H NMR spectrum (DMSO-d_6, 600 MHz) of compound **5.7**.

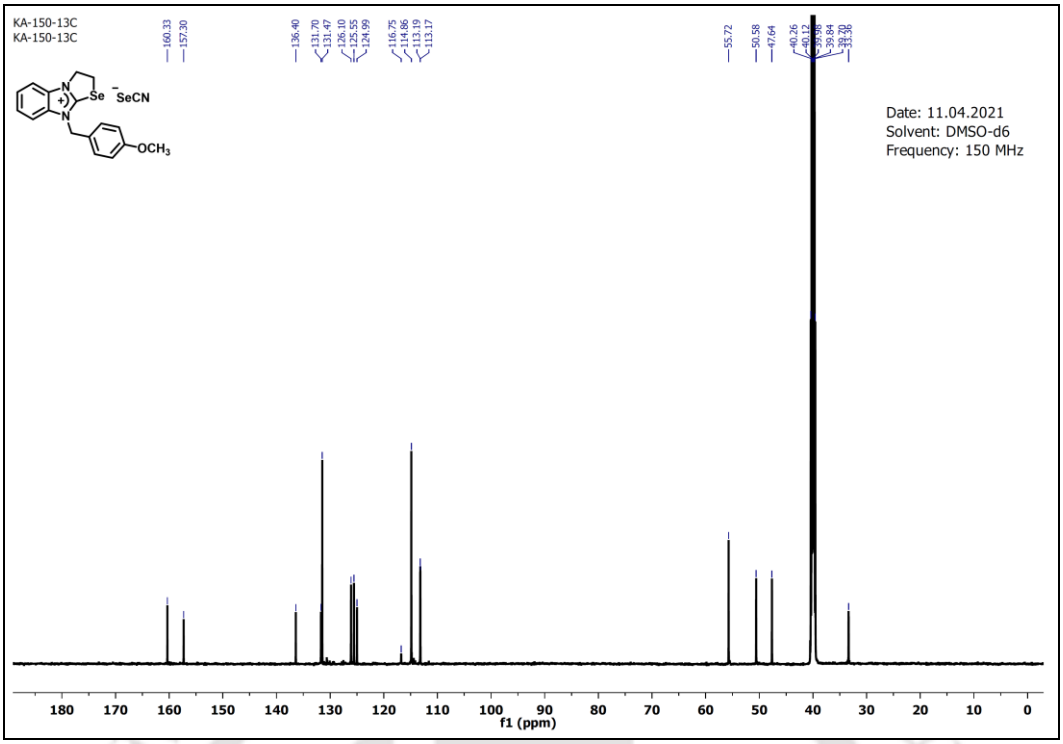

Figure A6.5. ^{13}C NMR spectrum (DMSO-d_6, 150 MHz) of compound **5.7**.

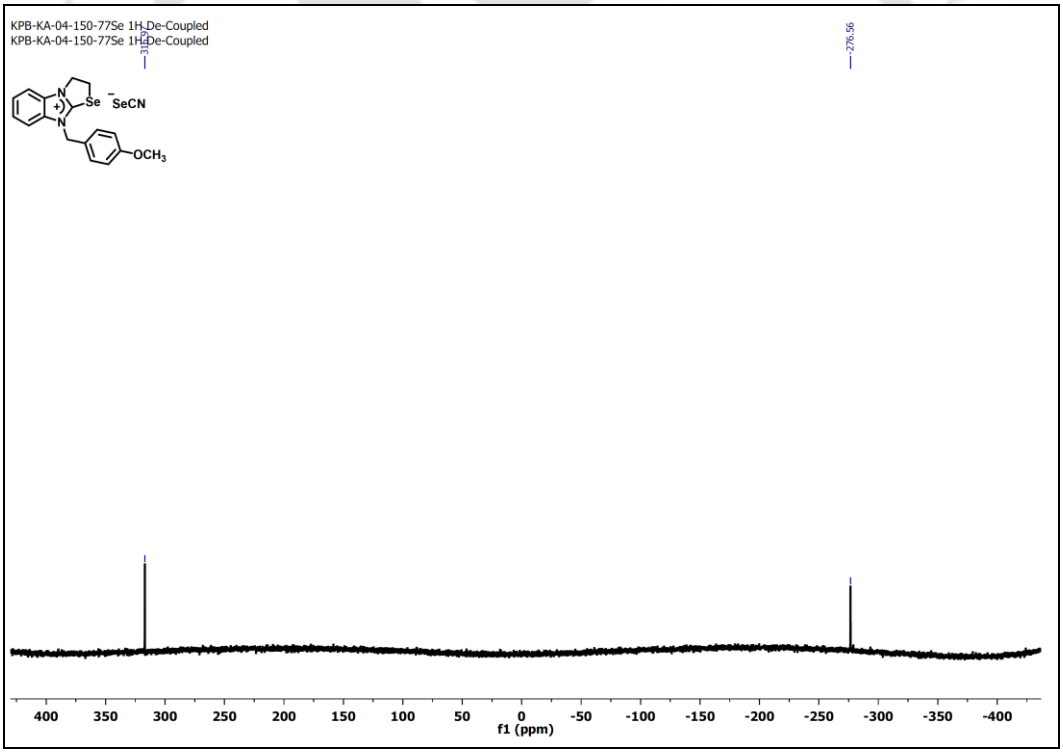

Figure A6.6. ^{77}Se NMR spectrum (DMSO-d_6, 76 MHz) of compound **5.7**.

(Compound **5.8** could not be purified and characterized)

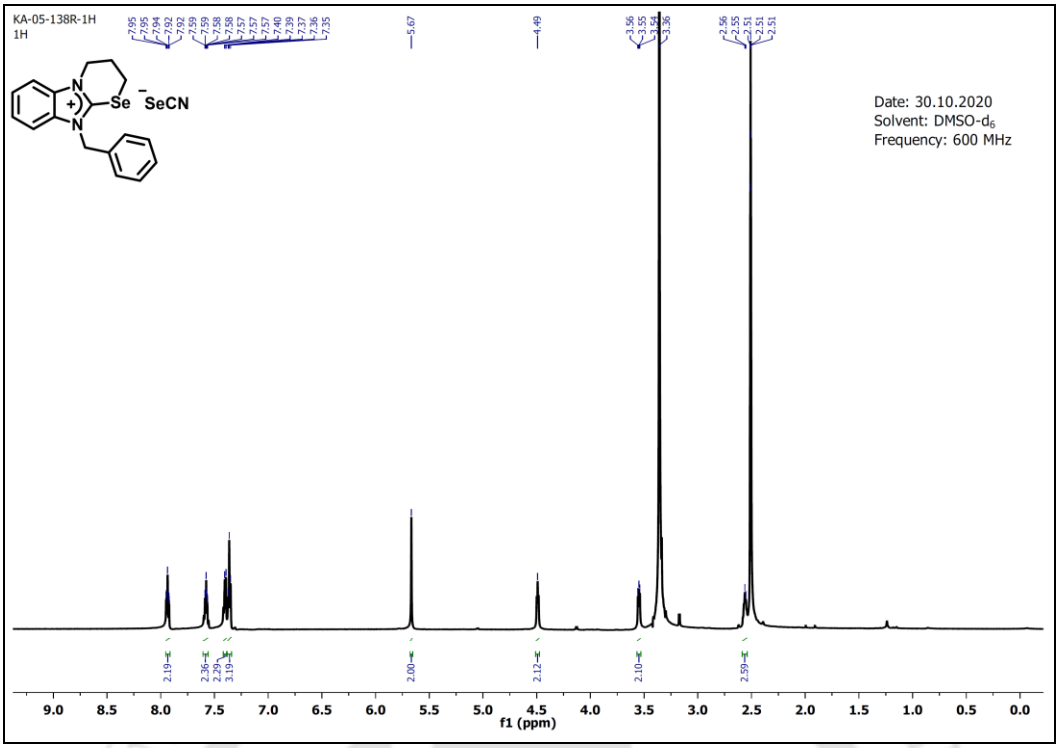

Figure A6.7. ^{1}H NMR spectrum (DMSO-d_6, 600 MHz) of compound **4.9b-2**.

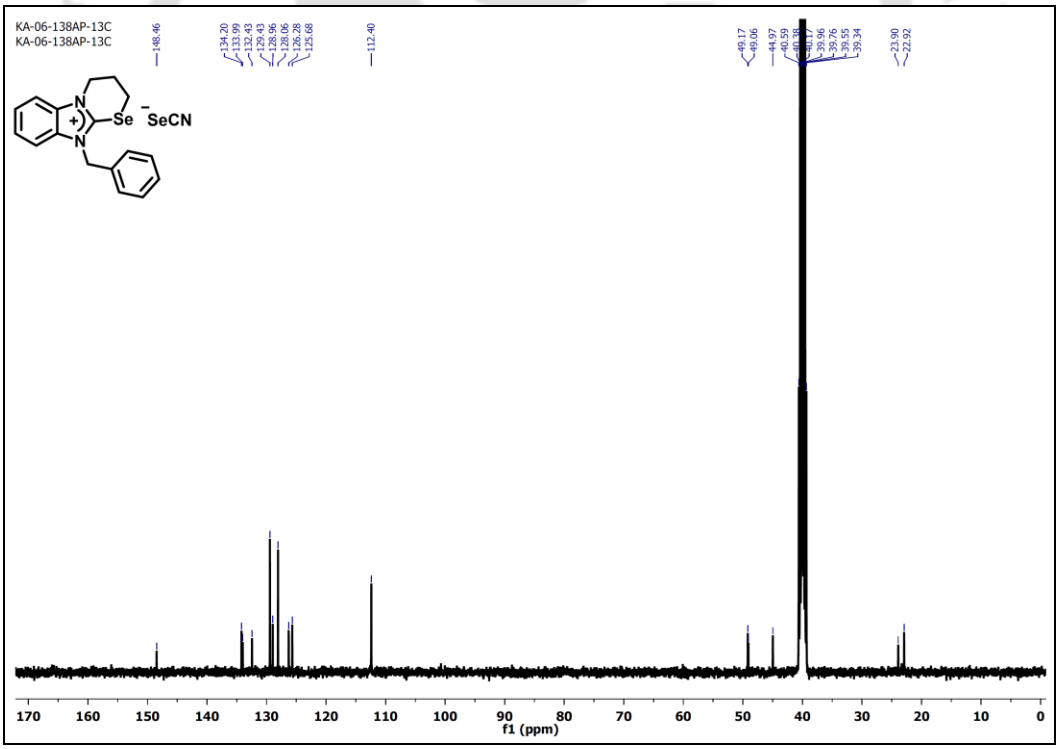

Figure A6.8. ^{13}C NMR spectrum (DMSO-d_6, 150 MHz) of compound **4.9b-2**.

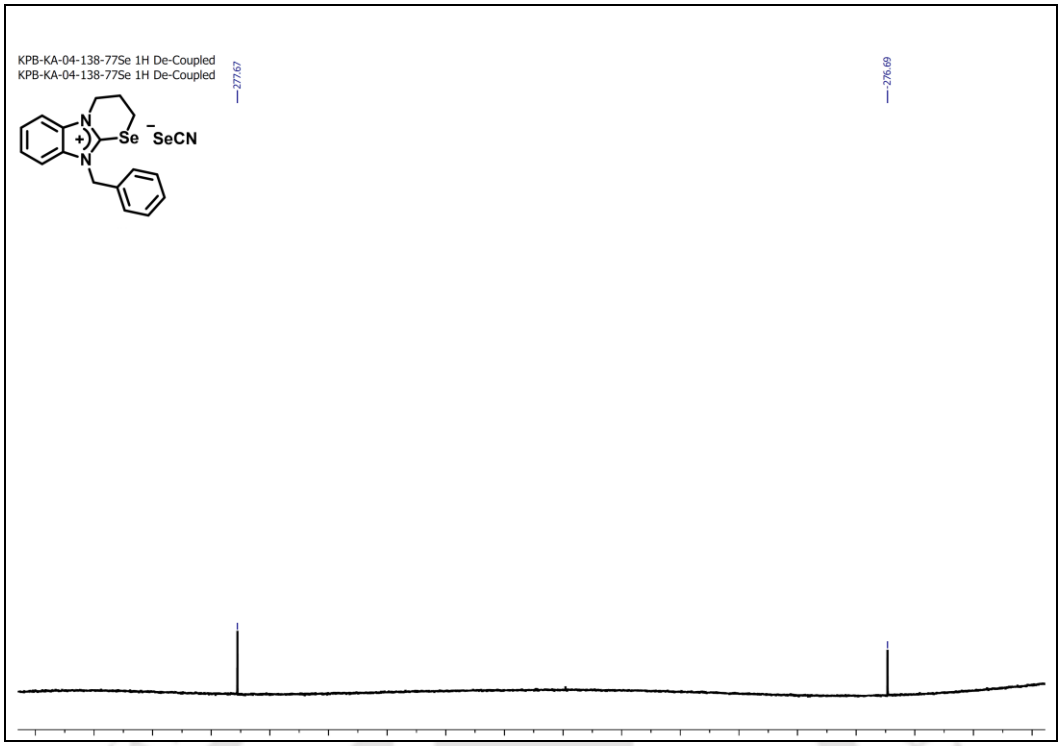

Figure A6.9. ^{77}Se NMR spectrum (DMSO-d_6, 114 MHz) of compound **4.9b-2**.

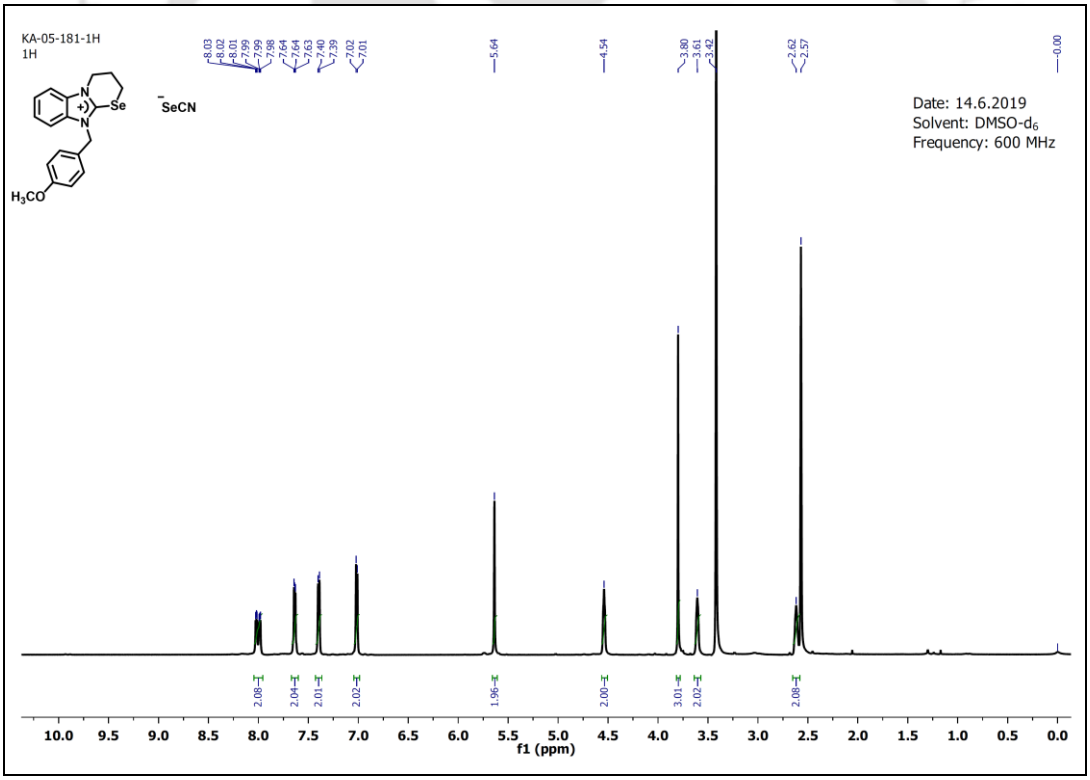

Figure A6.10. ^{1}H NMR spectrum (DMSO-d_6, 600 MHz) of compound **5.9**.

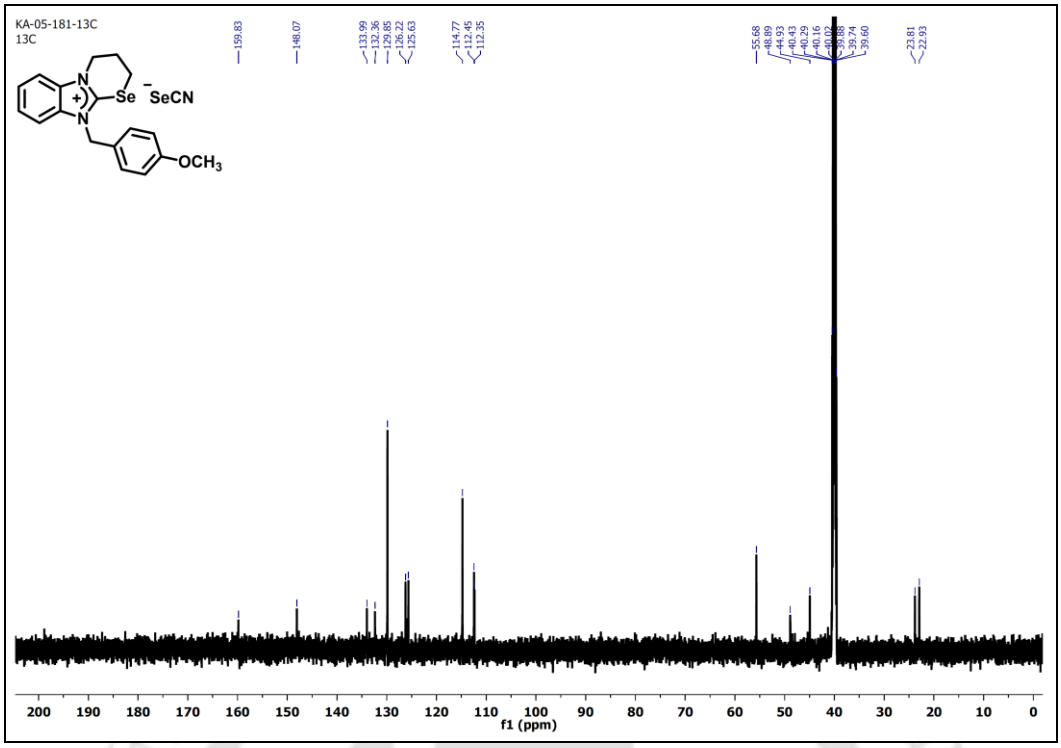

Figure A6.11. ^{13}C NMR spectrum (DMSO-d_6, 150 MHz) of compound **5.9**.

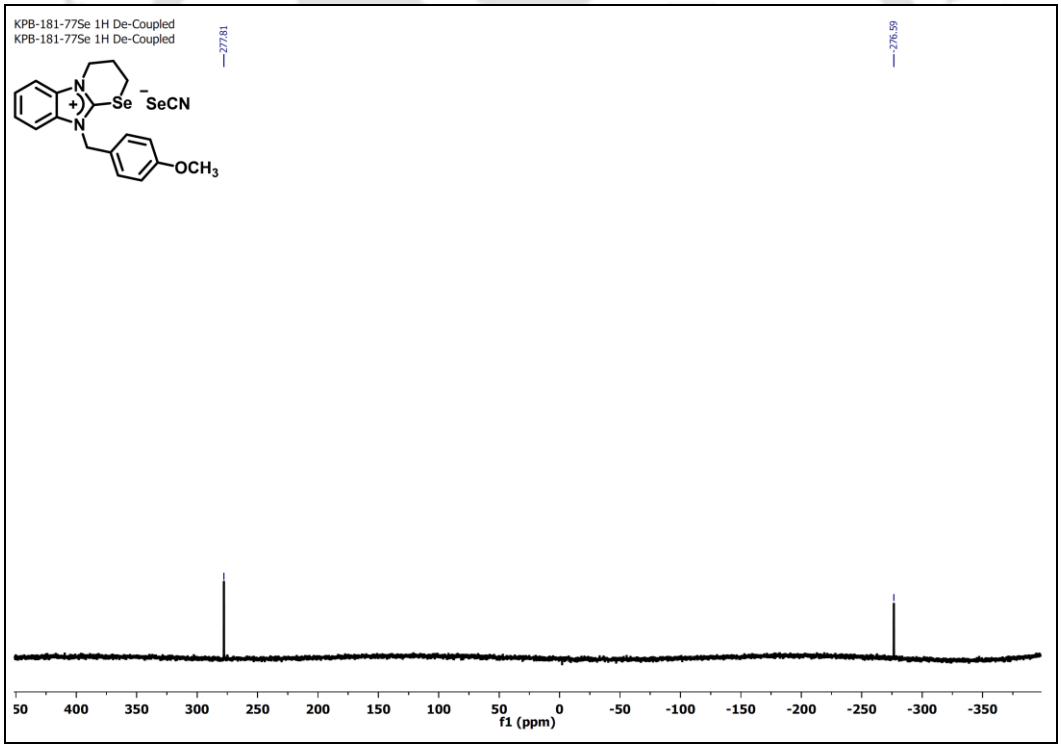

Figure A6.12. ^{77}Se NMR spectrum (DMSO-d_6, 76 MHz) of compound **5.9**.

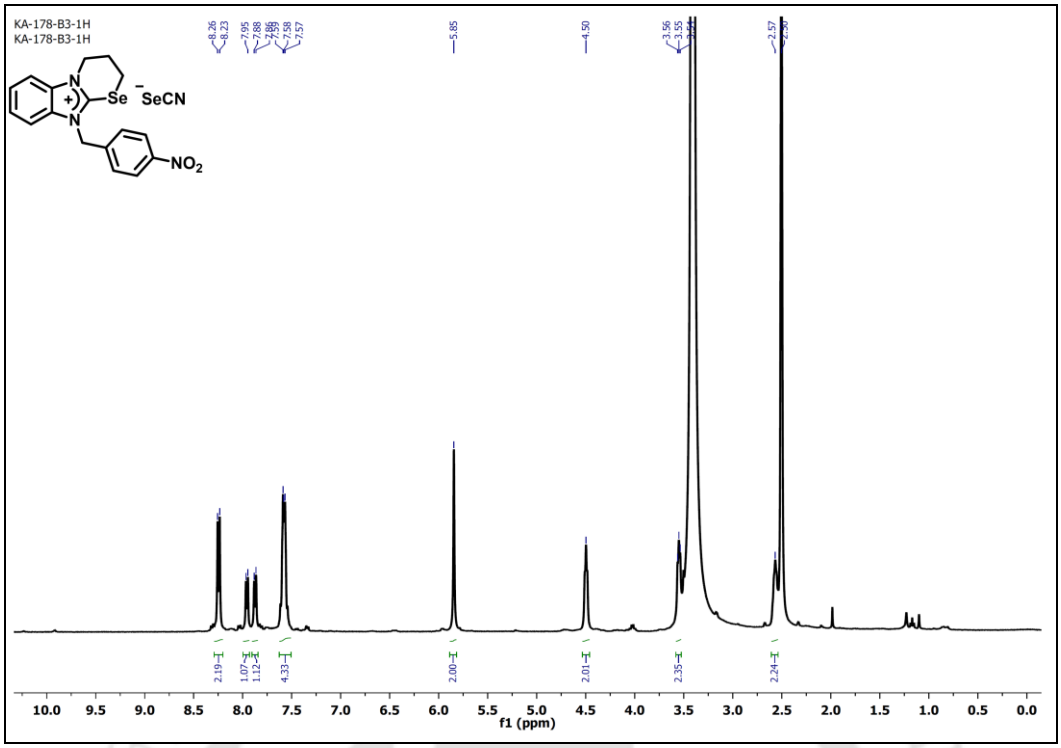

Figure A6.13. ^{1}H NMR spectrum (DMSO-d_6, 400 MHz) of compound **5.10**.

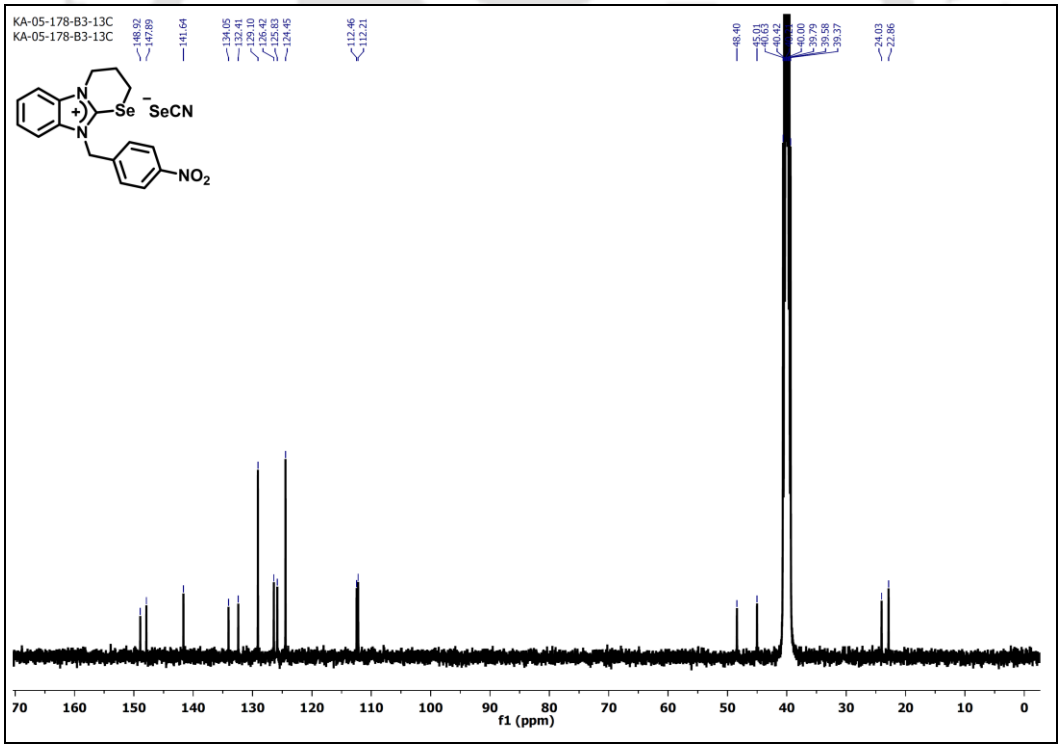

Figure A6.14. ^{13}C NMR spectrum (DMSO-d_6, 100 MHz) of compound **5.10**.

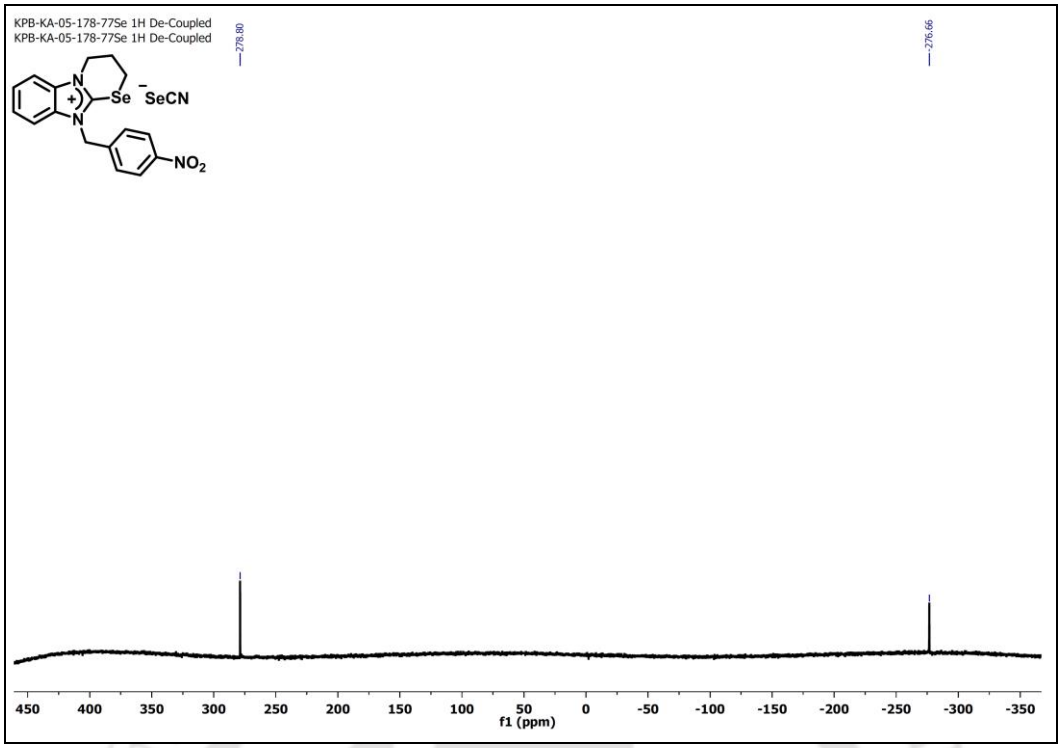

Figure A6.15. ^{77}Se NMR spectrum (DMSO-d_6, 76 MHz) of compound **5.10**.

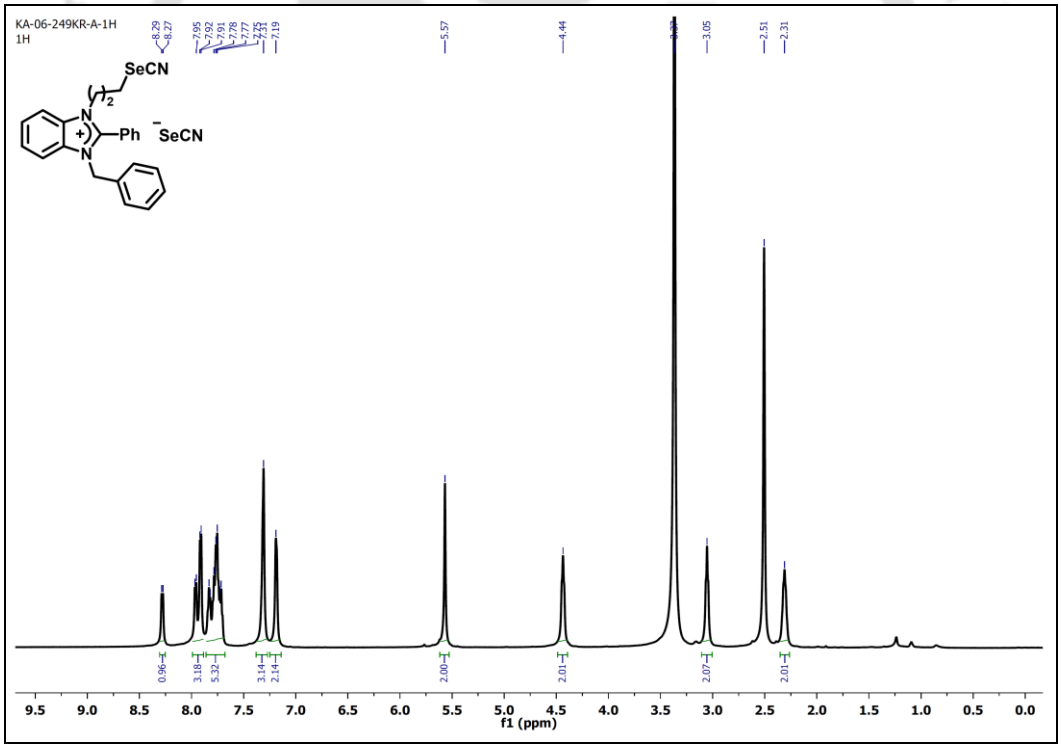

Figure A6.16. ^{1}H NMR spectrum (DMSO-d_6, 600 MHz) of compound **5.11**.

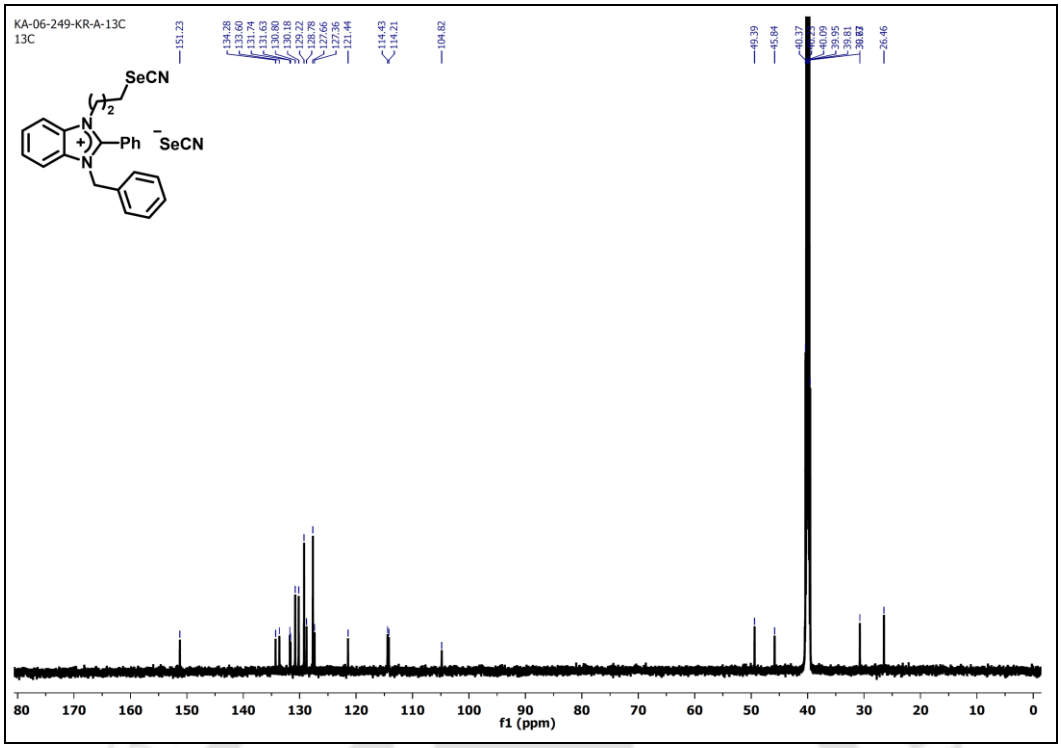

Figure A6.17. ^{13}C NMR spectrum (DMSO-d_6, 150 MHz) of compound **5.11**.

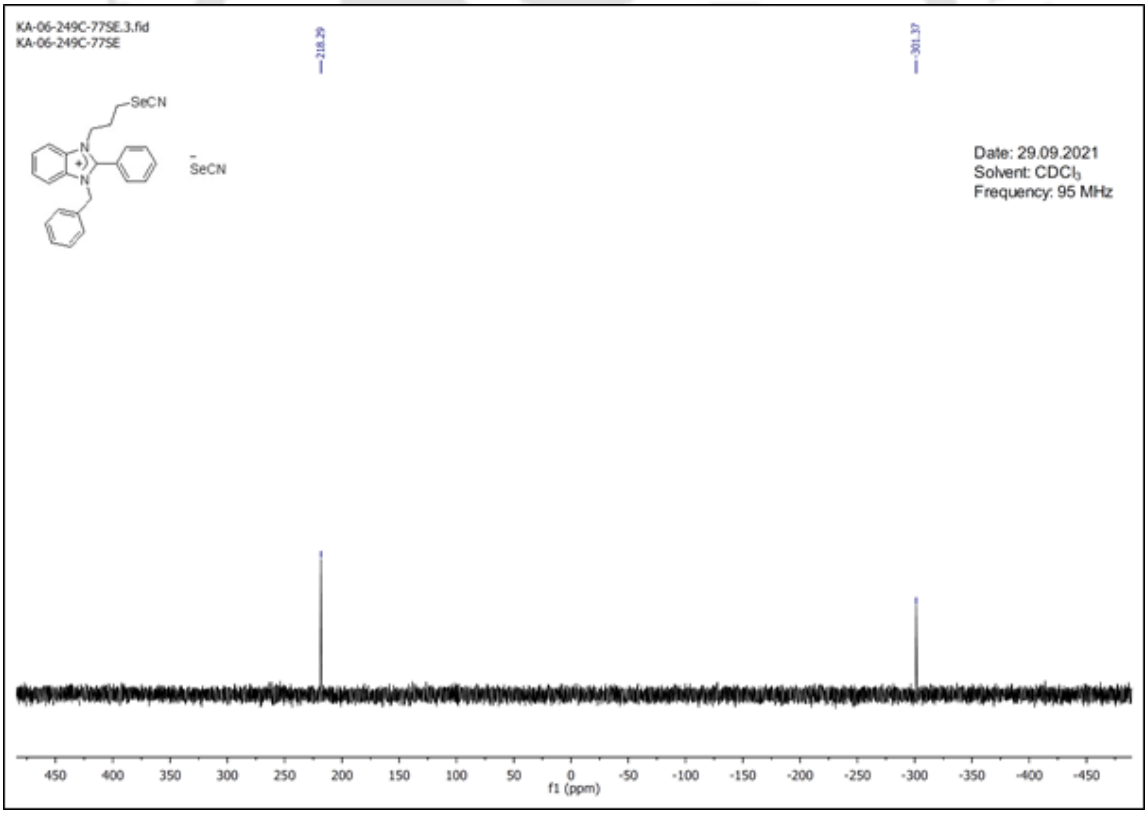

Figure A6.18. ^{77}Se NMR spectrum (DMSO-d_6, 150 MHz) of compound **5.11**.

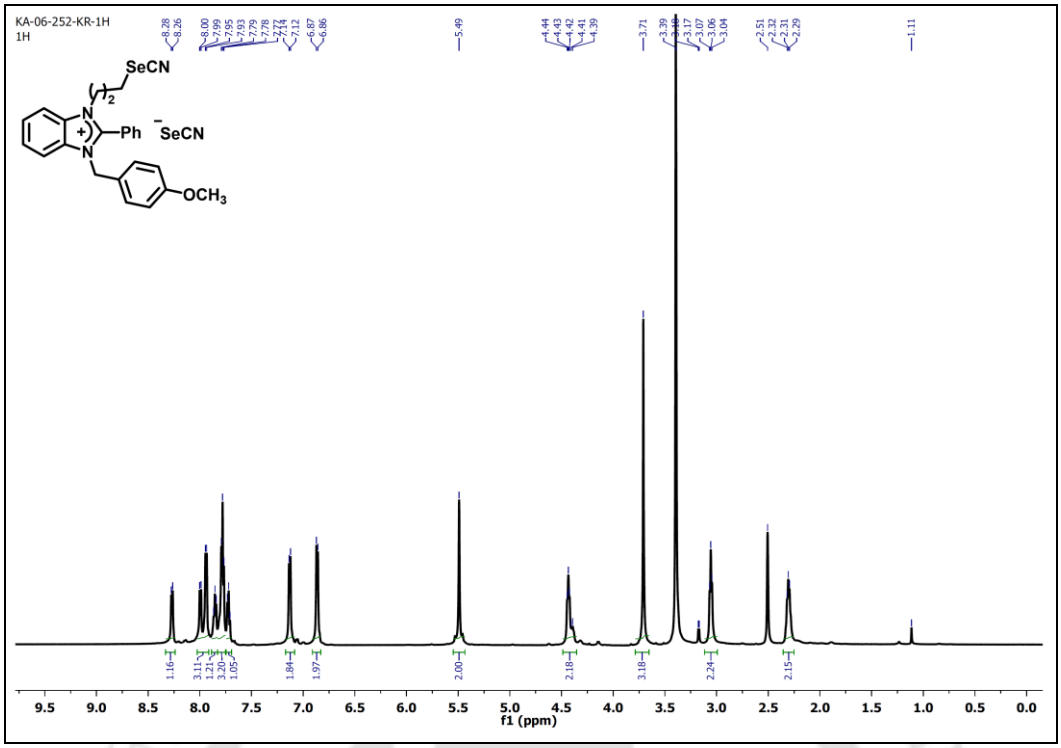

Figure A6.19. ^{1}H NMR spectrum (DMSO-d_6, 600 MHz) of compound **5.12**.

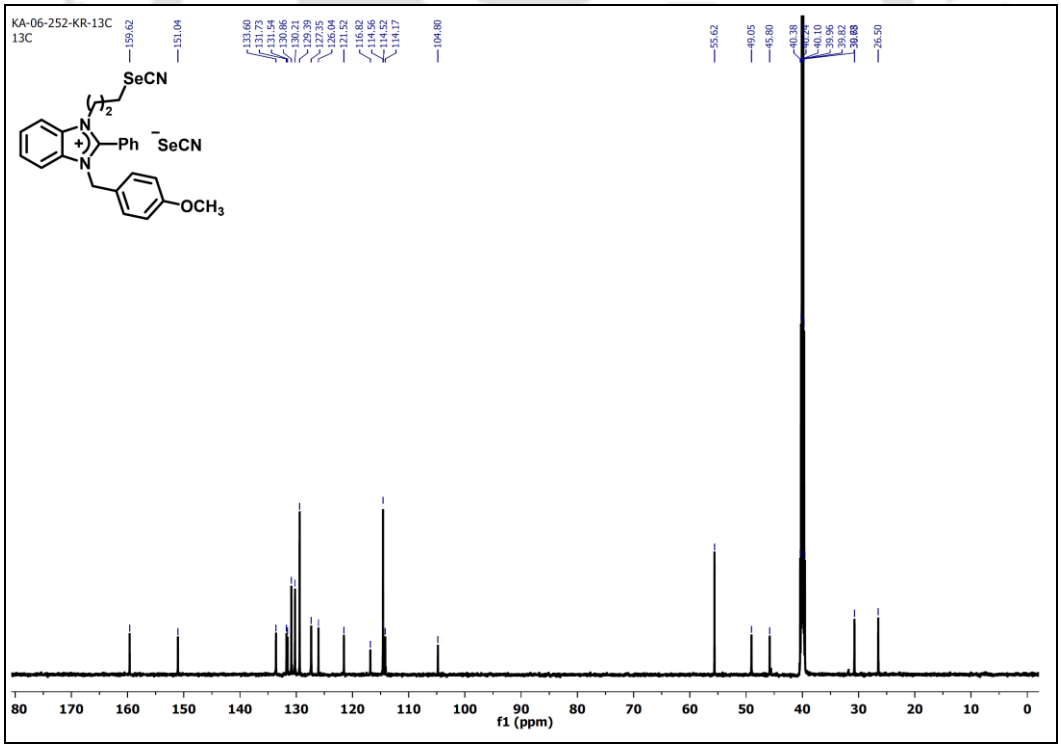

Figure A6.20. ^{13}C NMR spectrum (DMSO-d_6, 150 MHz) of compound **5.12**.

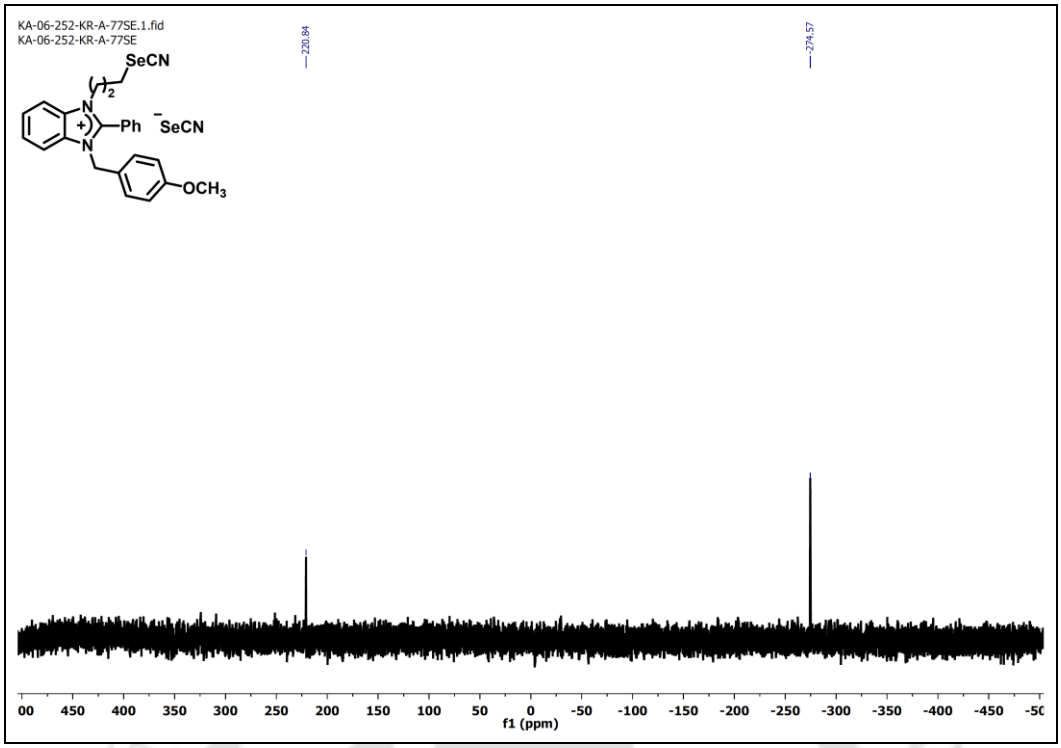

Figure A6.21. ^{77}Se NMR spectrum (DMSO-d_6, 95 MHz) of compound **5.12**.

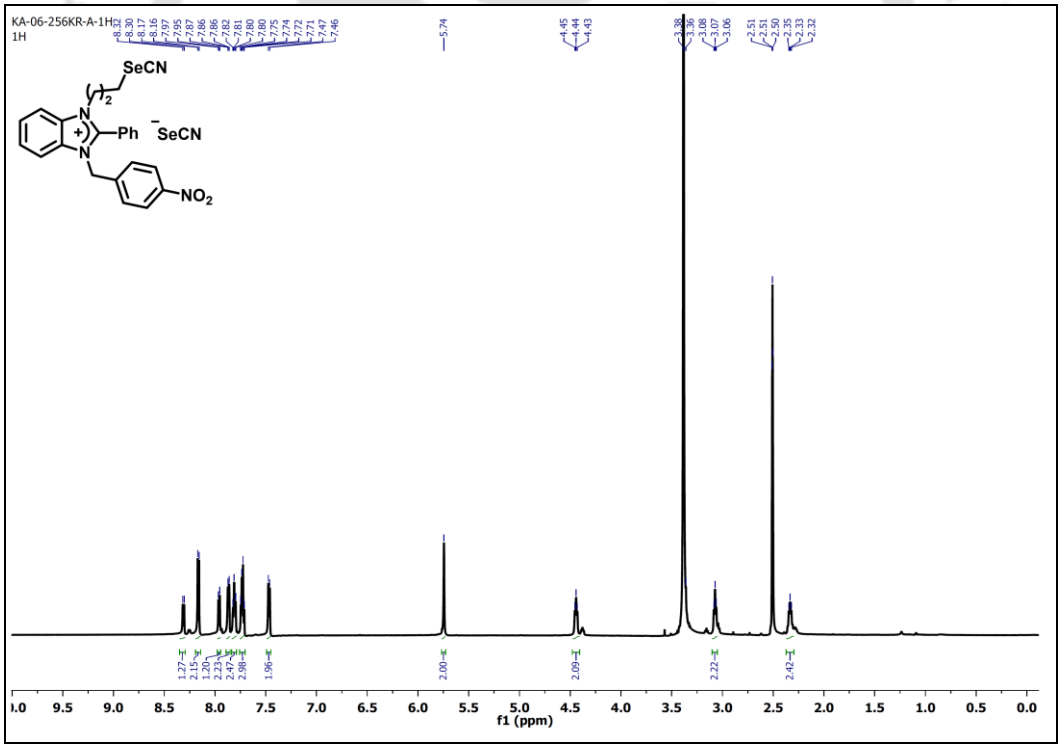

Figure A6.22. ^{1}H NMR spectrum (DMSO-d_6, 600 MHz) of compound **5.13**.

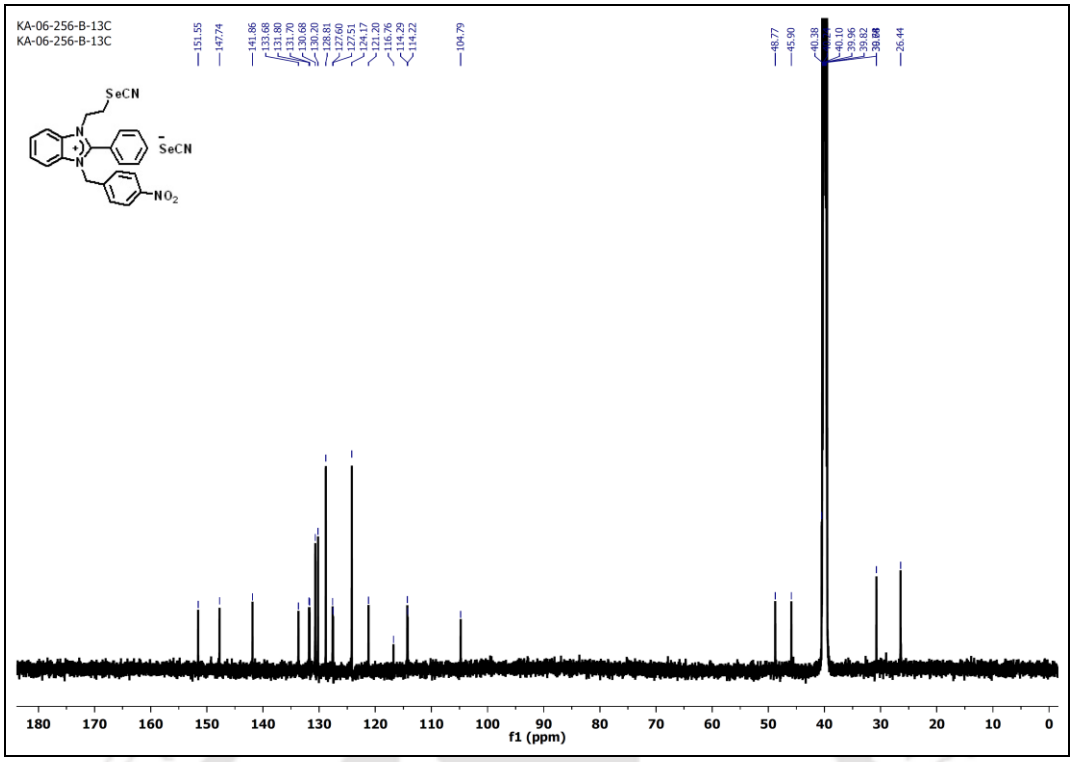

Figure A6.23. ^{13}C NMR spectrum (DMSO-d_6, 150 MHz) of compound **5.13**.

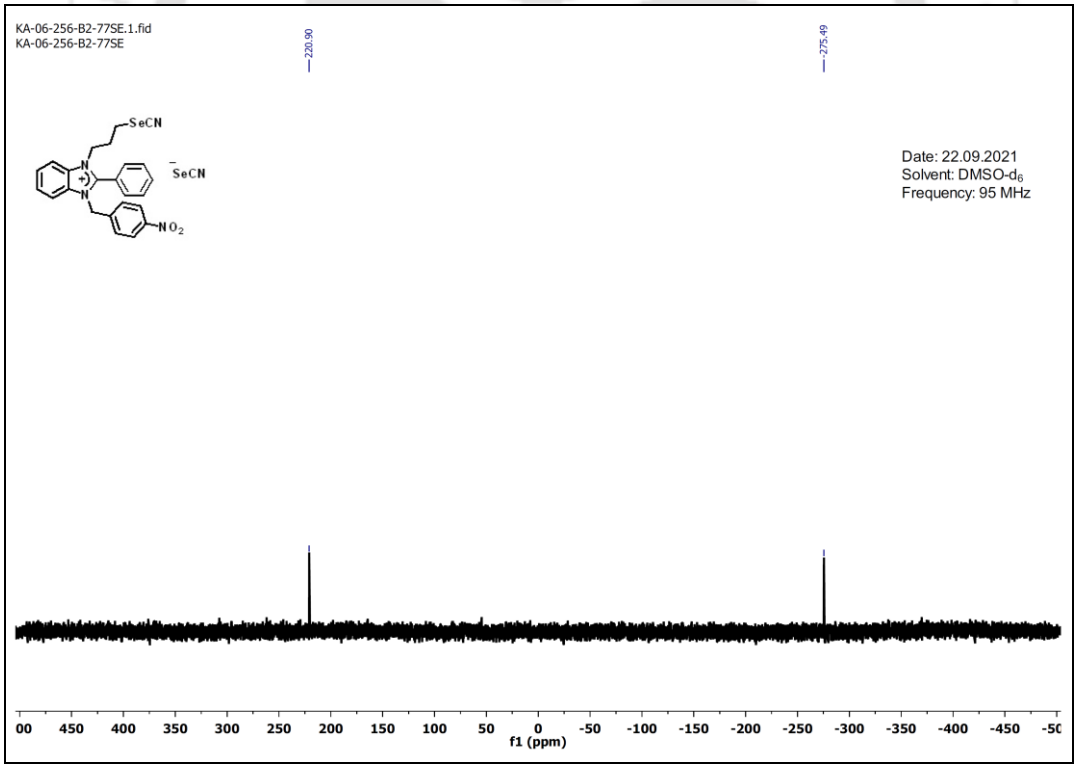

Figure A6.24. ^{77}Se NMR spectrum (DMSO-d_6, 95 MHz) of compound **5.13**.

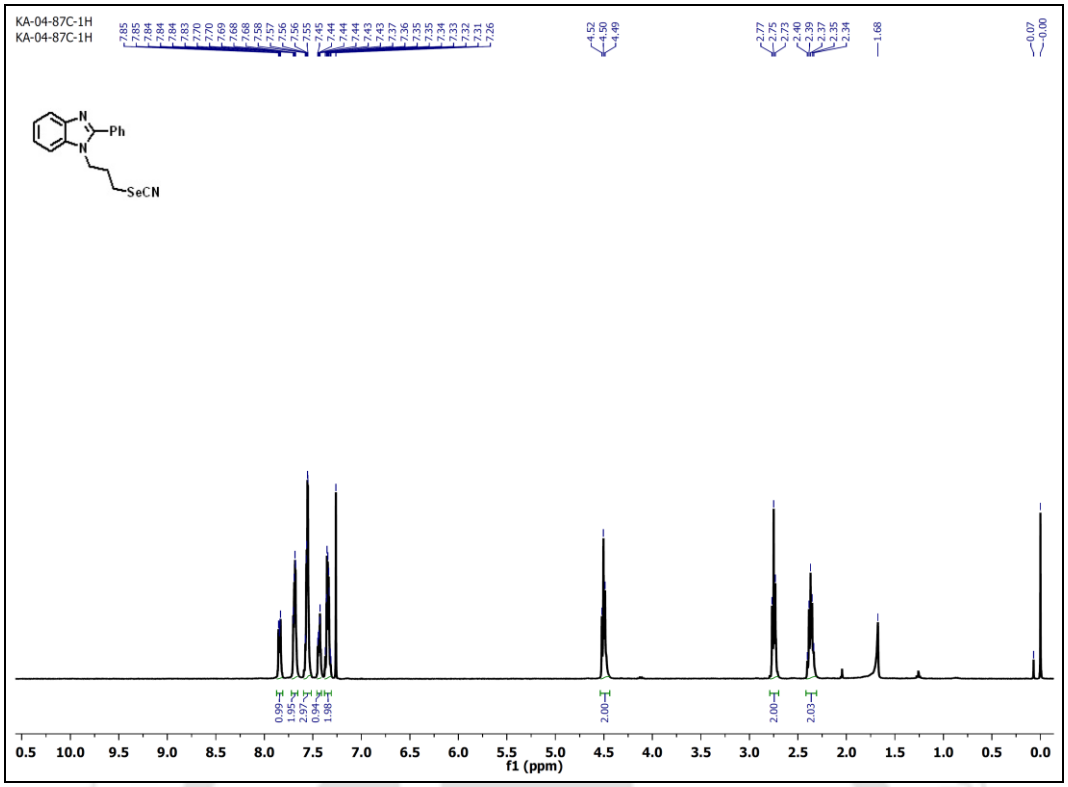

Figure A6.25. ^{1}H NMR spectrum ($CDCl_3$, 400 MHz) of compound **5.14**.

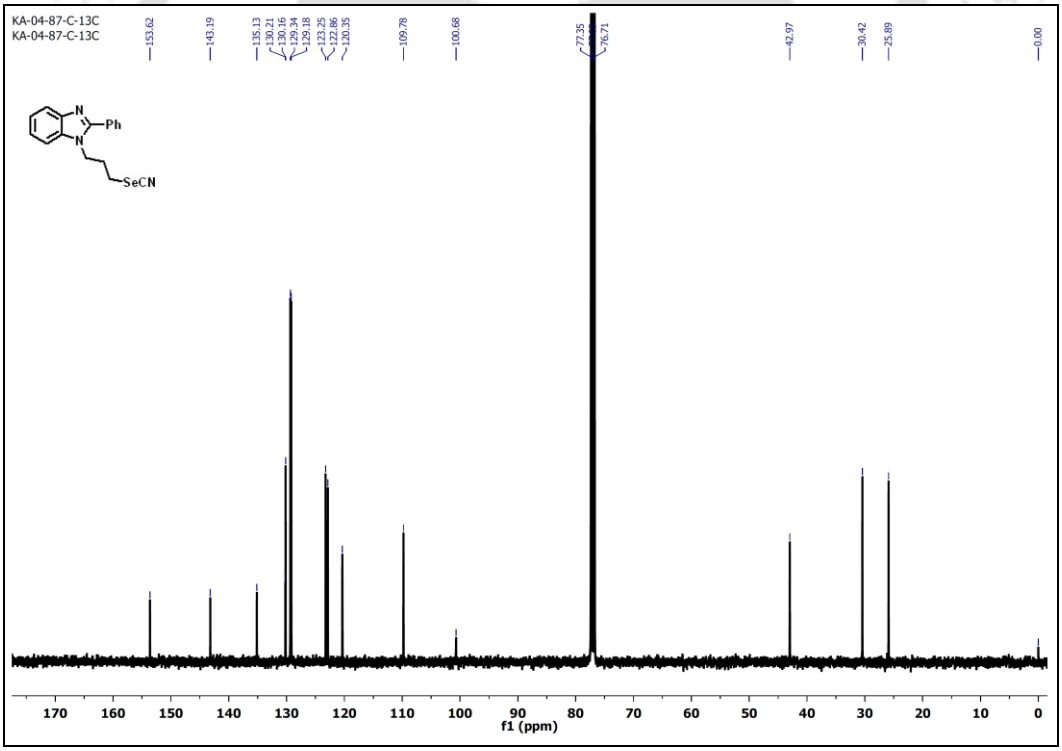

Figure A6.26. ^{13}C NMR spectrum ($CDCl_3$, 100 MHz) of compound **5.14**.

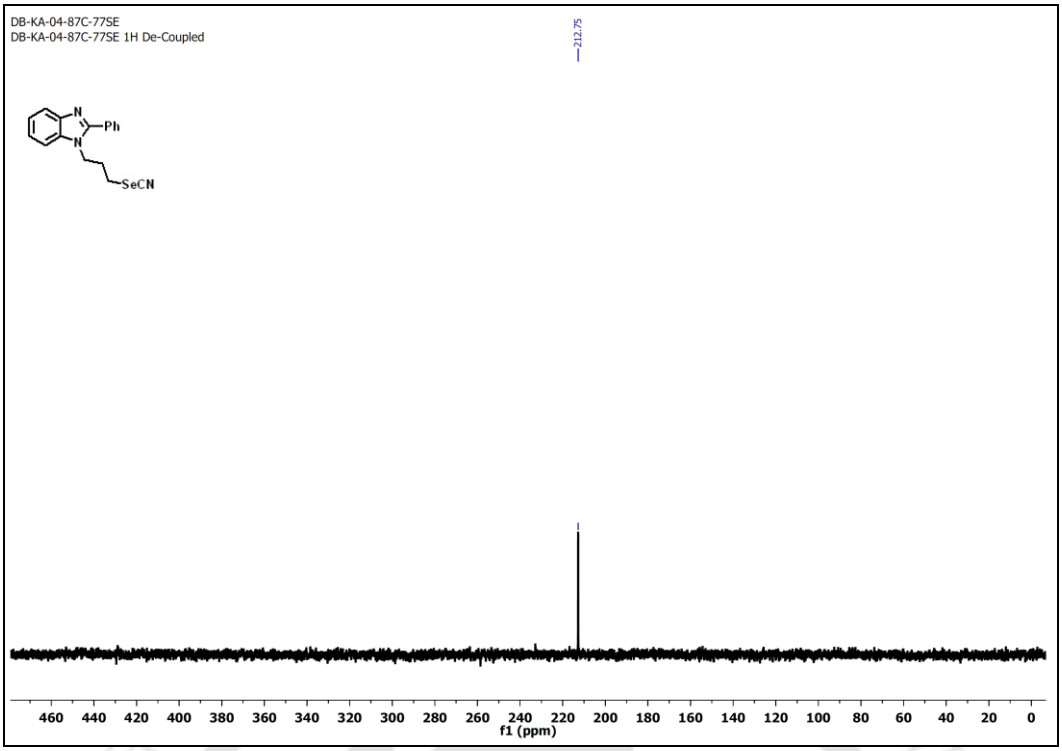

Figure A6.27. ^{77}Se NMR spectrum ($CDCl_3$, 76 MHz) of compound **5.14**.

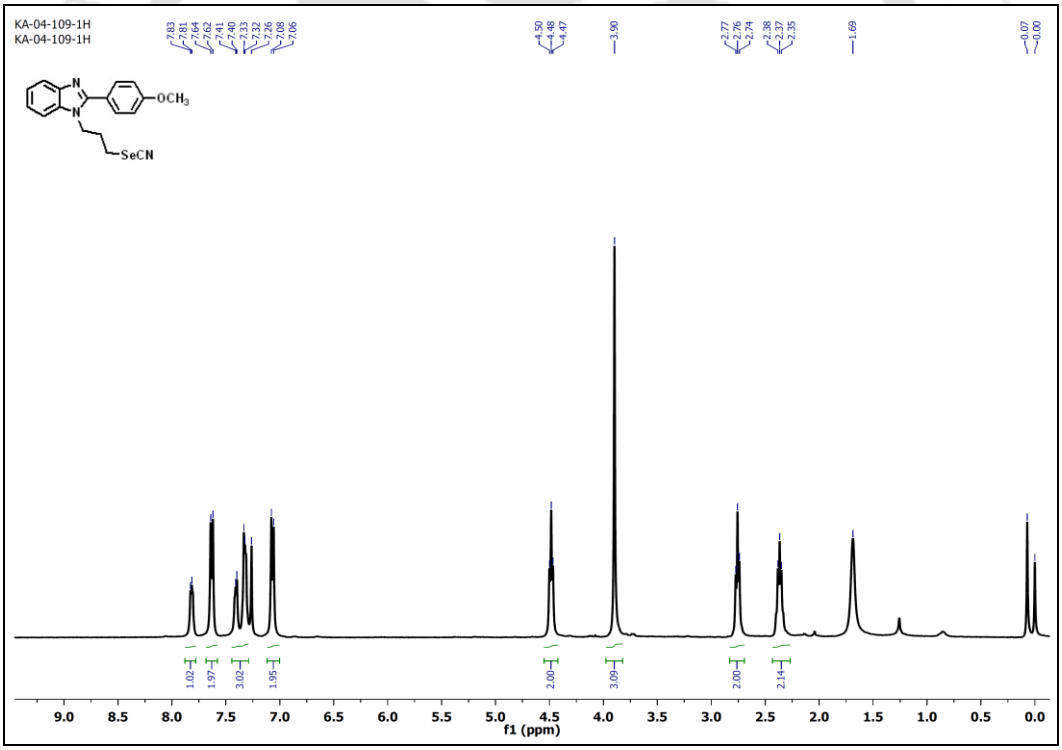

Figure A6.28. ^{1}H NMR spectrum ($CDCl_3$, 400 MHz) of compound **5.15**.

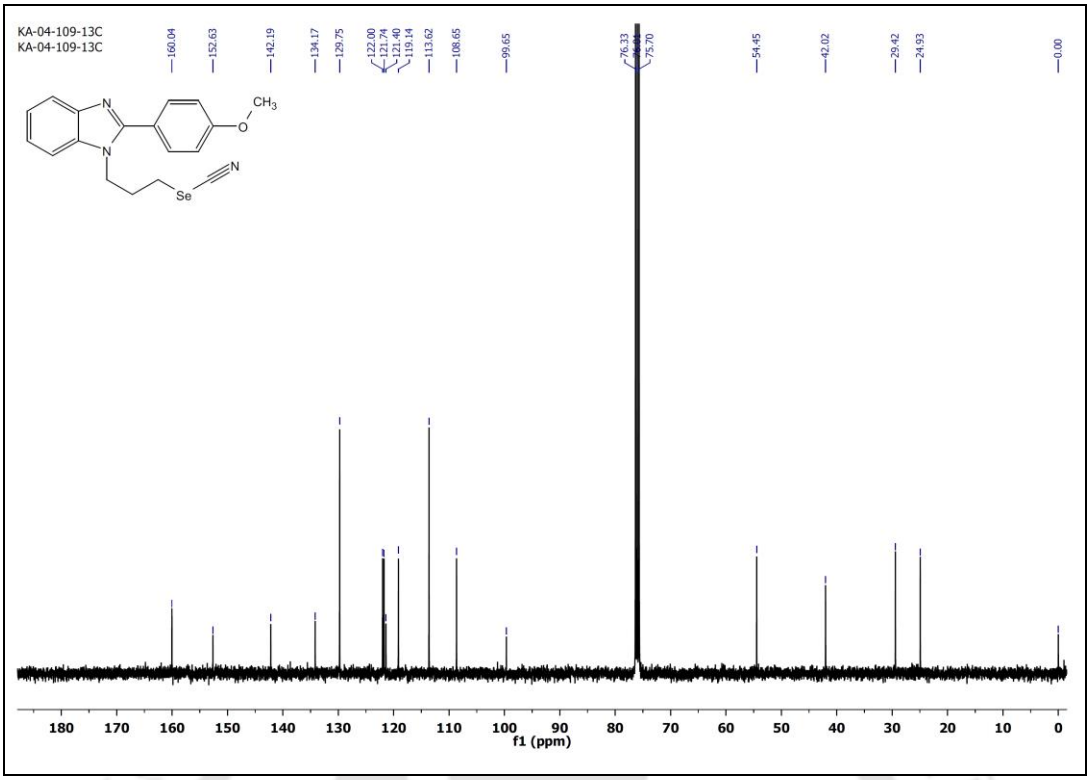

Figure A6.29. ^{13}C NMR spectrum ($CDCl_3$, 100 MHz) of compound **5.15**.

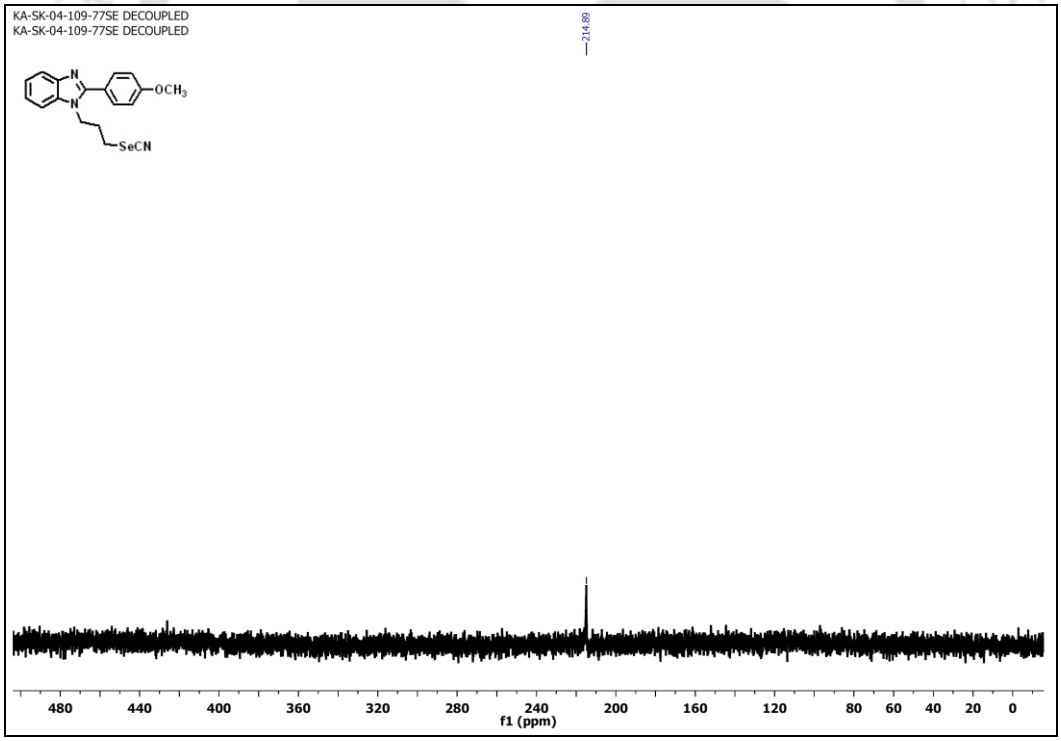

Figure A6.30. ^{77}Se NMR spectrum ($CDCl_3$, 76 MHz) of compound **5.15**.

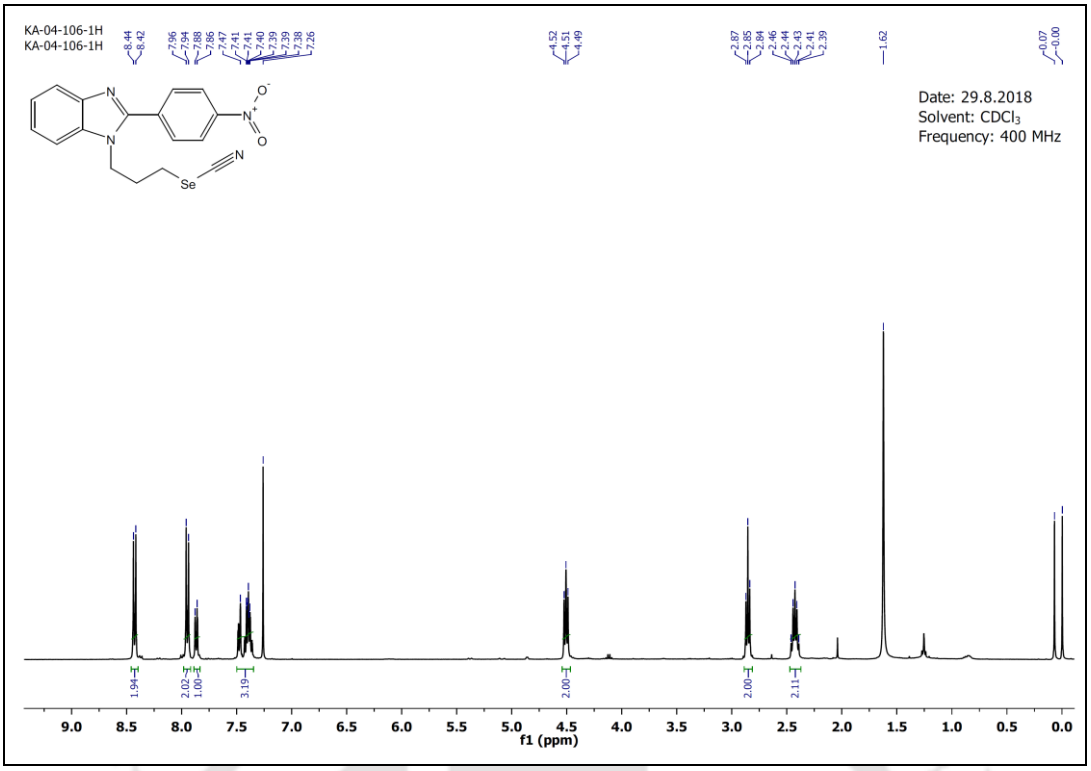

Figure A6.31. ^{1}H NMR spectrum ($CDCl_3$, 400 MHz) of compound **5.16**.

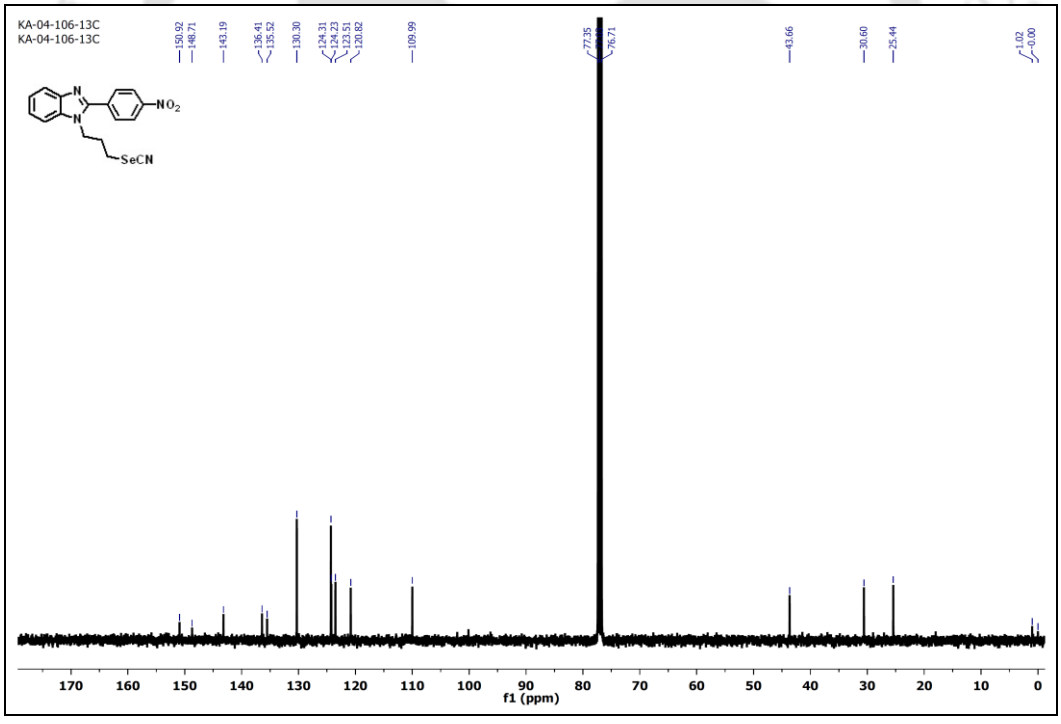

Figure A6.32. ^{13}C NMR spectrum ($CDCl_3$, 100 MHz) of compound **5.16**.

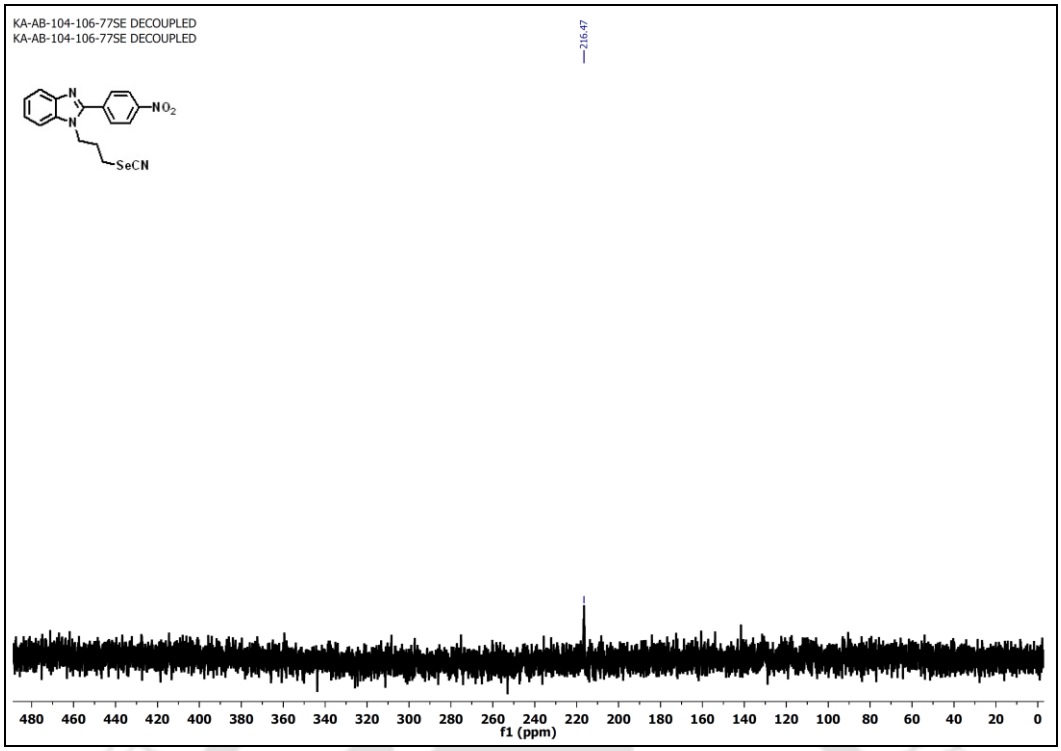

Figure A6.33. ^{77}Se NMR spectrum ($CDCl_3$, 76 MHz) of compound **5.16**.

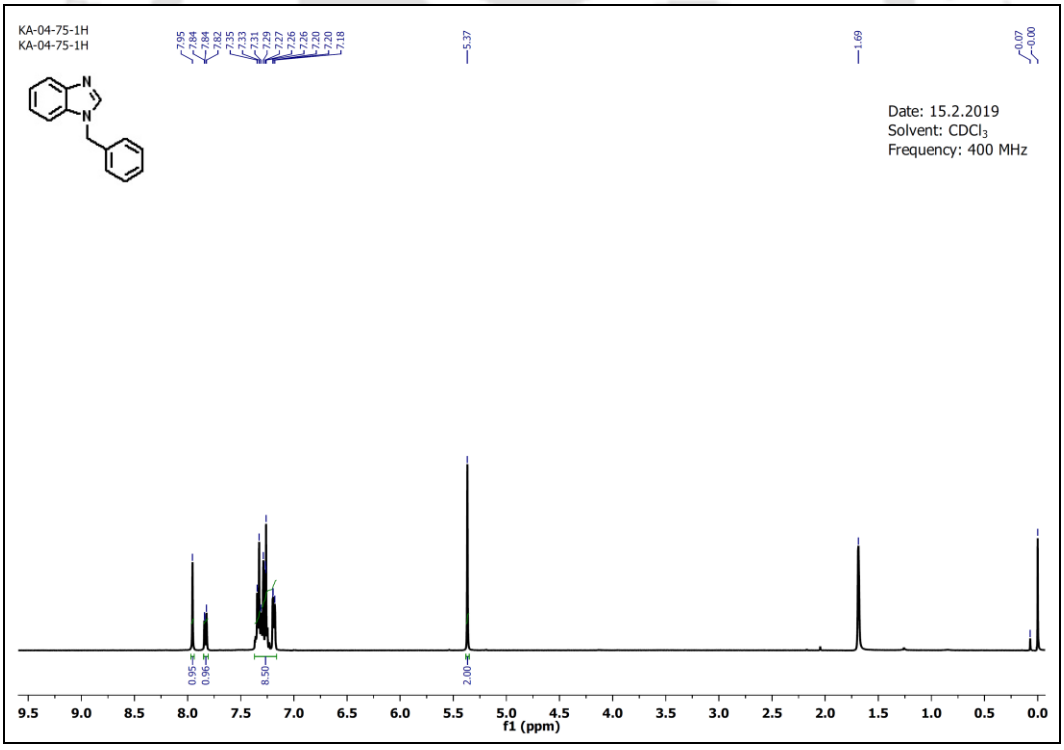

Figure A6.34. ^{1}H NMR spectrum ($CDCl_3$, 400 MHz) of compound **4.9b**.

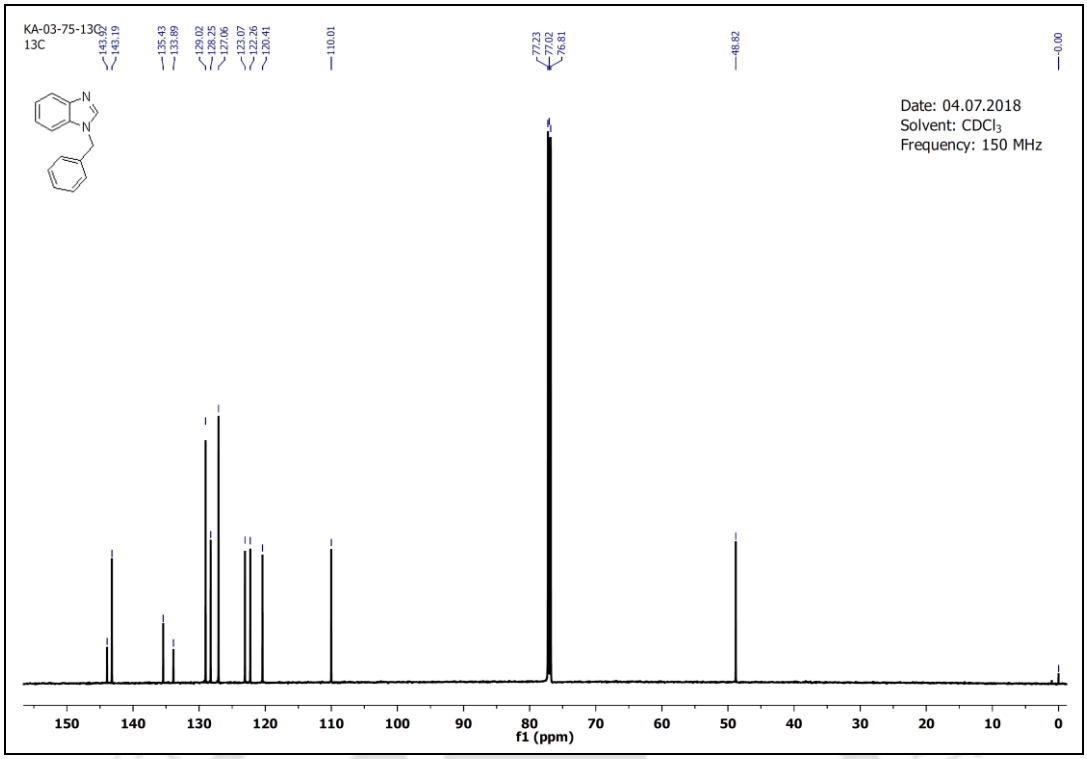

Figure A6.35. ^{13}C NMR spectrum ($CDCl_3$, 150 MHz) of compound **4.9b**.

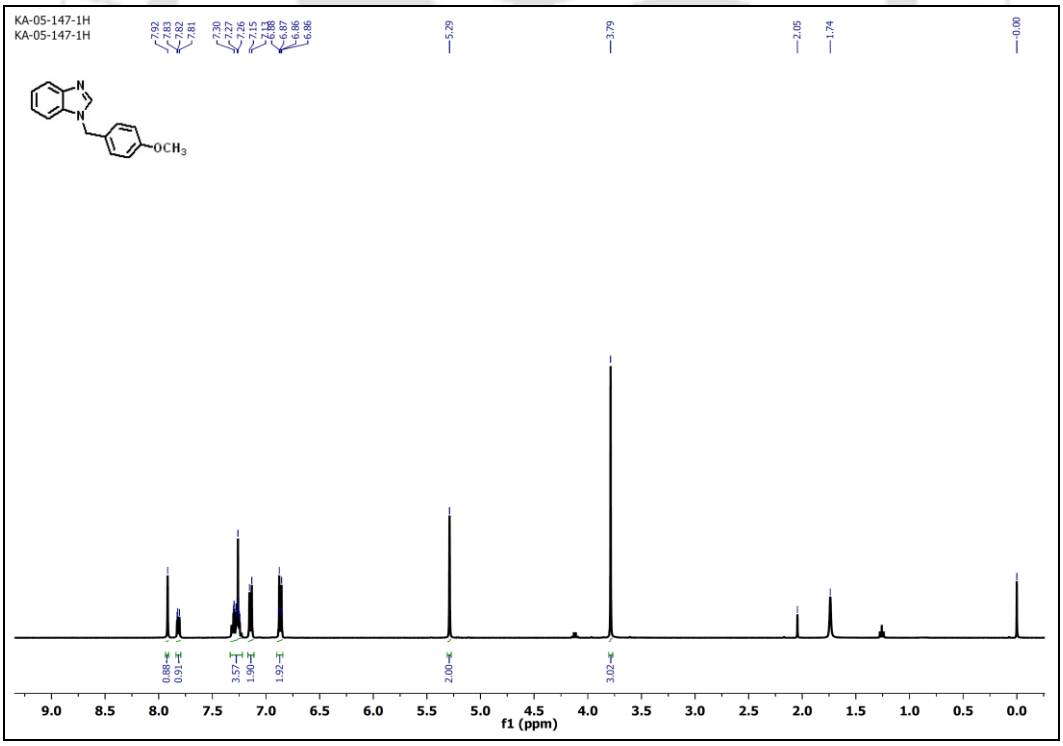

Figure A6.36. ^{1}H NMR spectrum ($CDCl_3$, 400 MHz) of compound **5.17**.

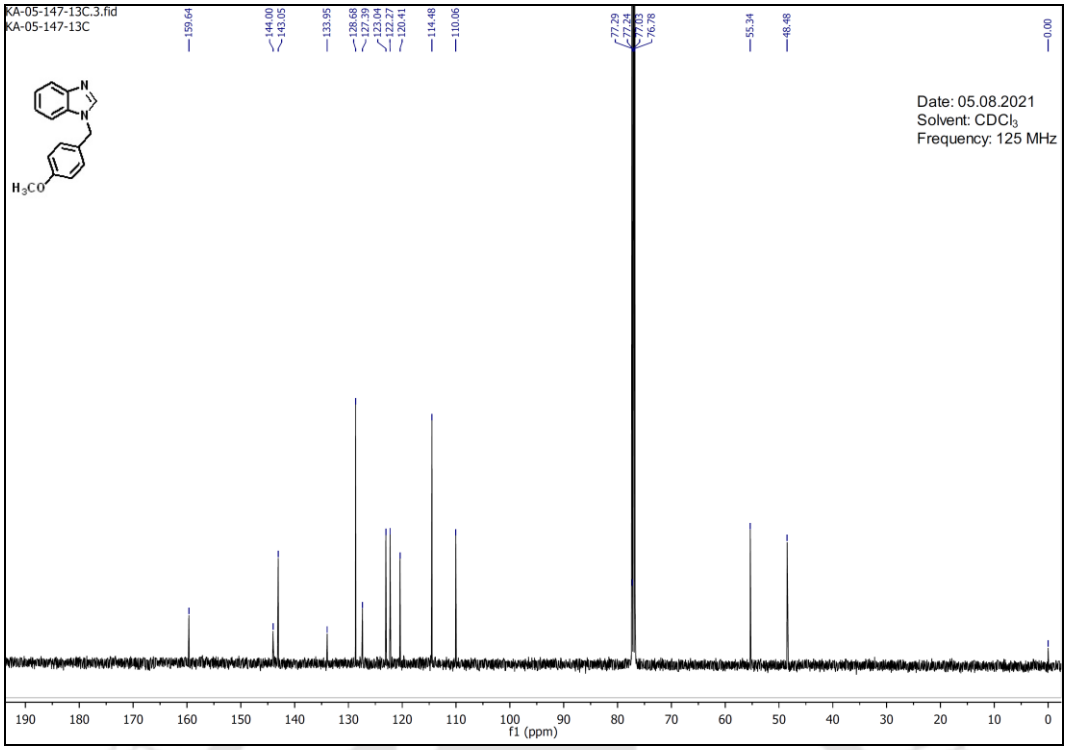

Figure A6.37. ^{13}C NMR ($CDCl_3$, 125 MHz) of compound **5.17**.

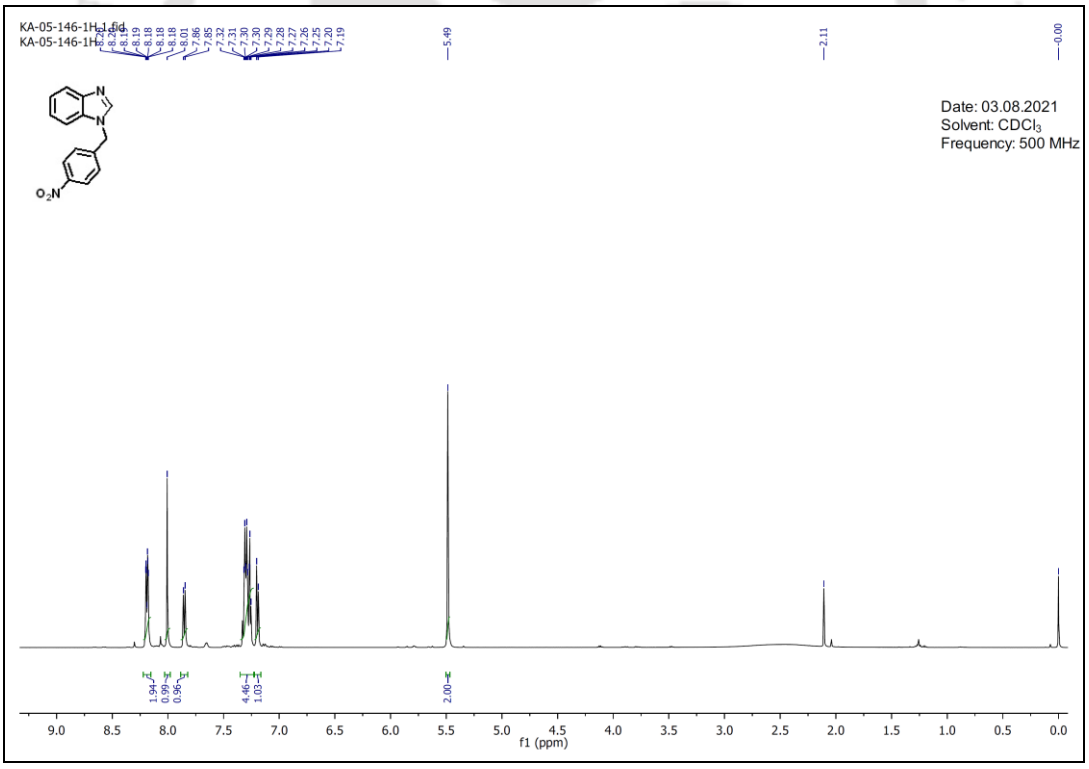

Figure A6.38. ^{1}H NMR spectrum ($CDCl_3$, 400 MHz) of compound **5.18**.

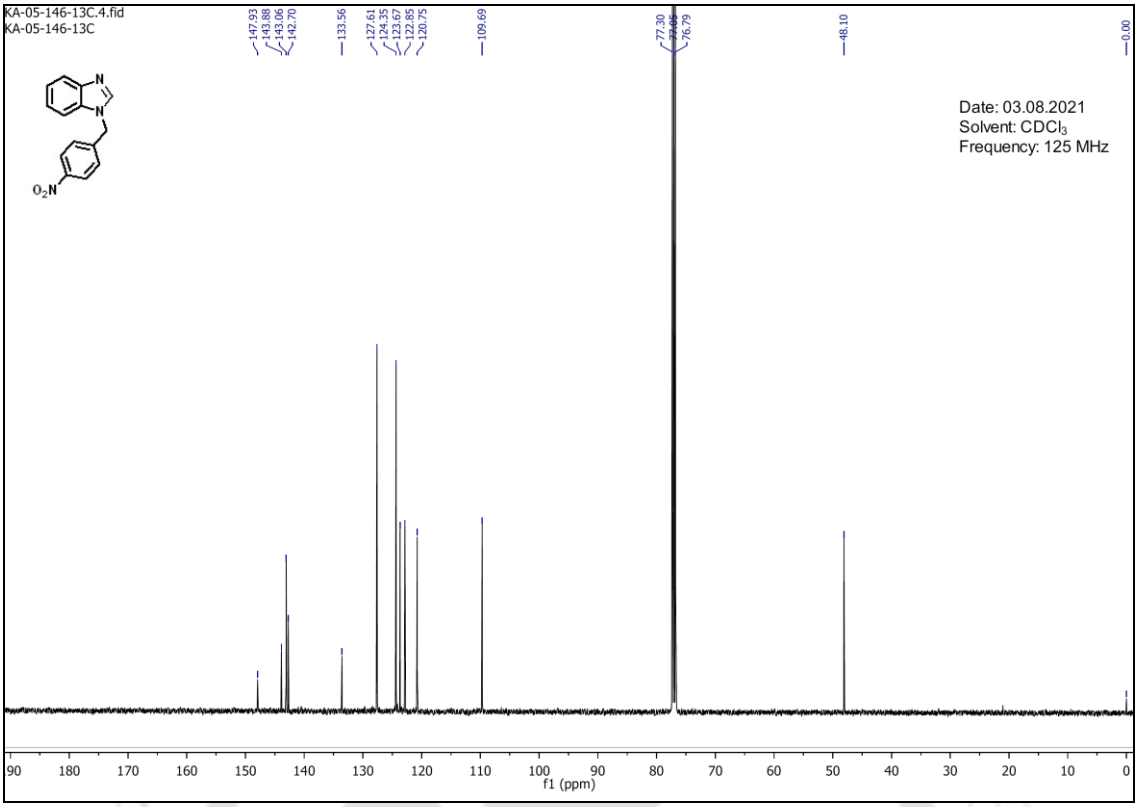

Figure A6.39. ^{13}C NMR ($CDCl_3$, 125 MHz) of compound **5.18**.

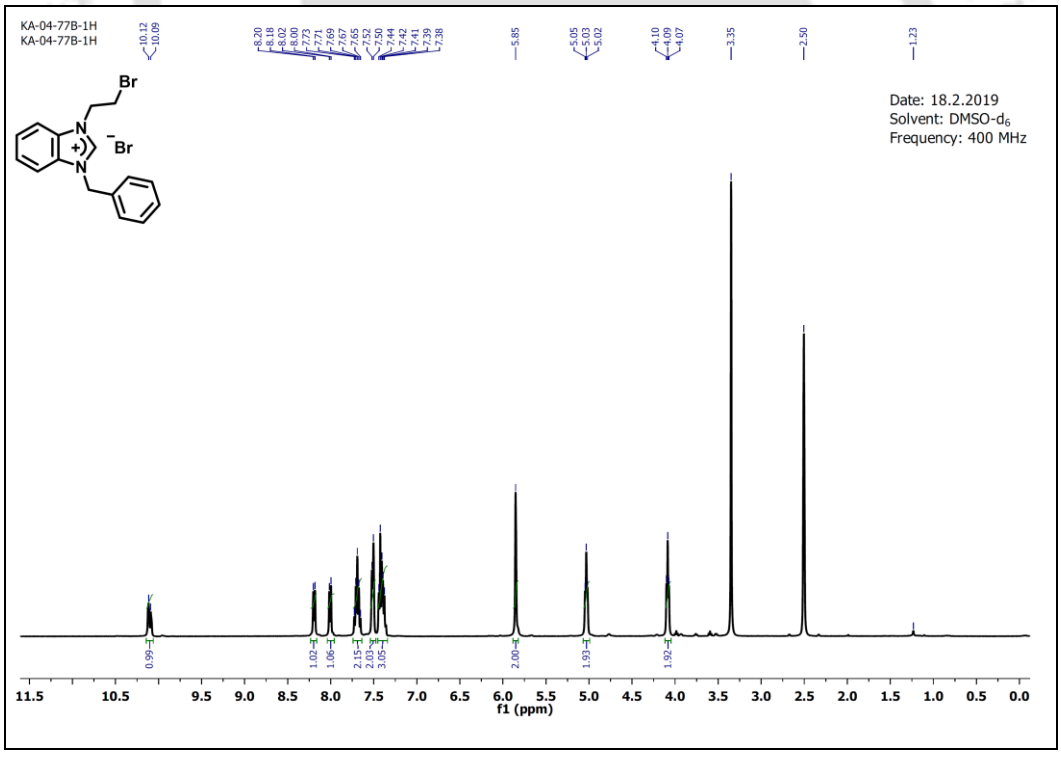

Figure A6.40. ^{1}H NMR spectrum (DMSO-d_6, 400 MHz) of compound **4.9b-1**.

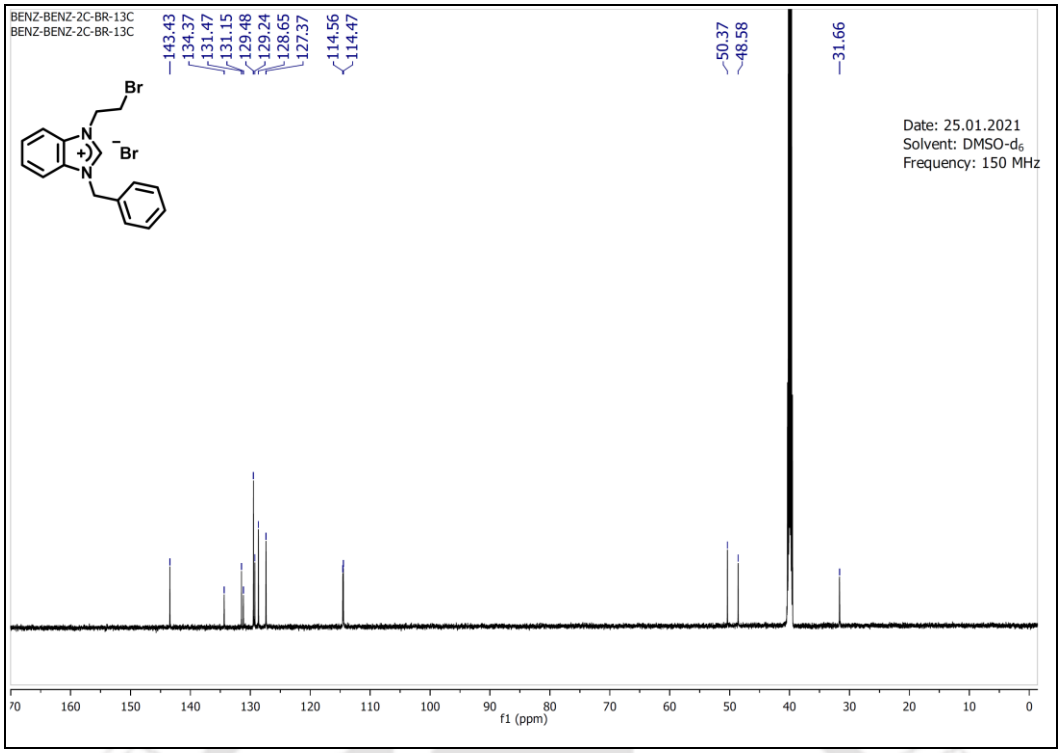

Figure A6.41. ^{13}C NMR spectrum (DMSO-d_6, 150 MHz) of compound **4.9b-1**.

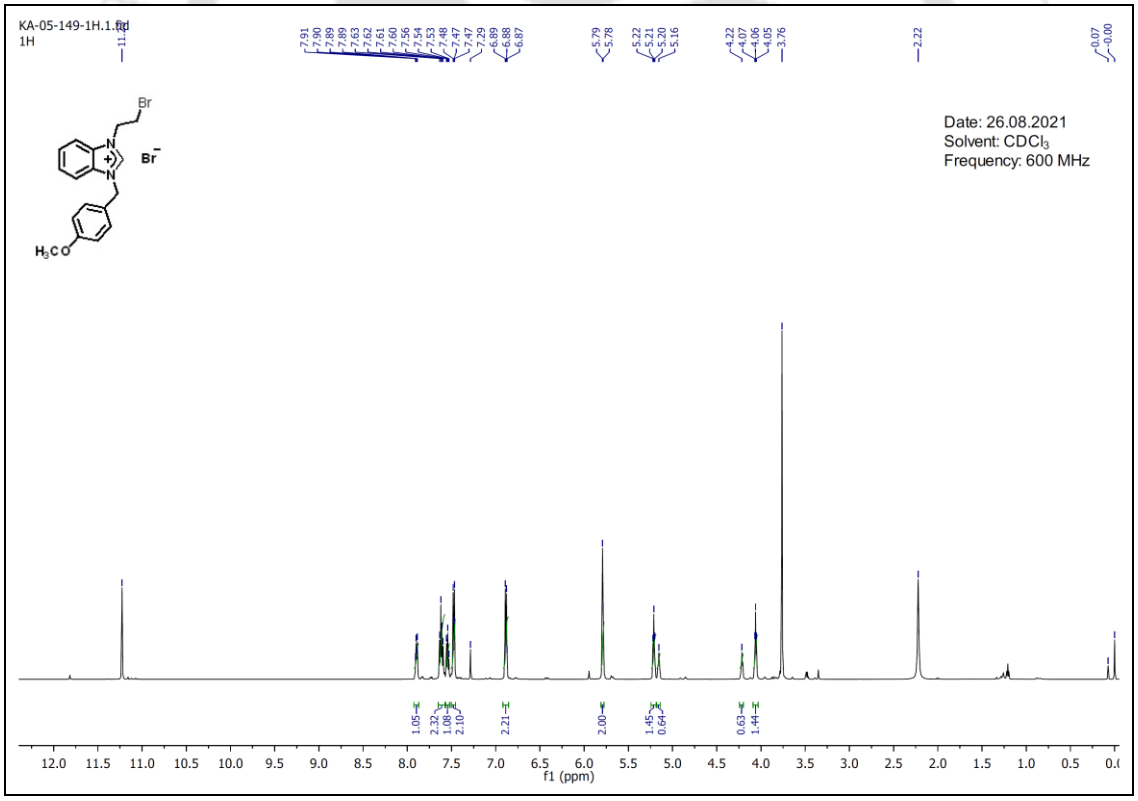

Figure A6.42. ^{1}H NMR spectrum ($CDCl_3$, 600 MHz) of compound **5.19**.

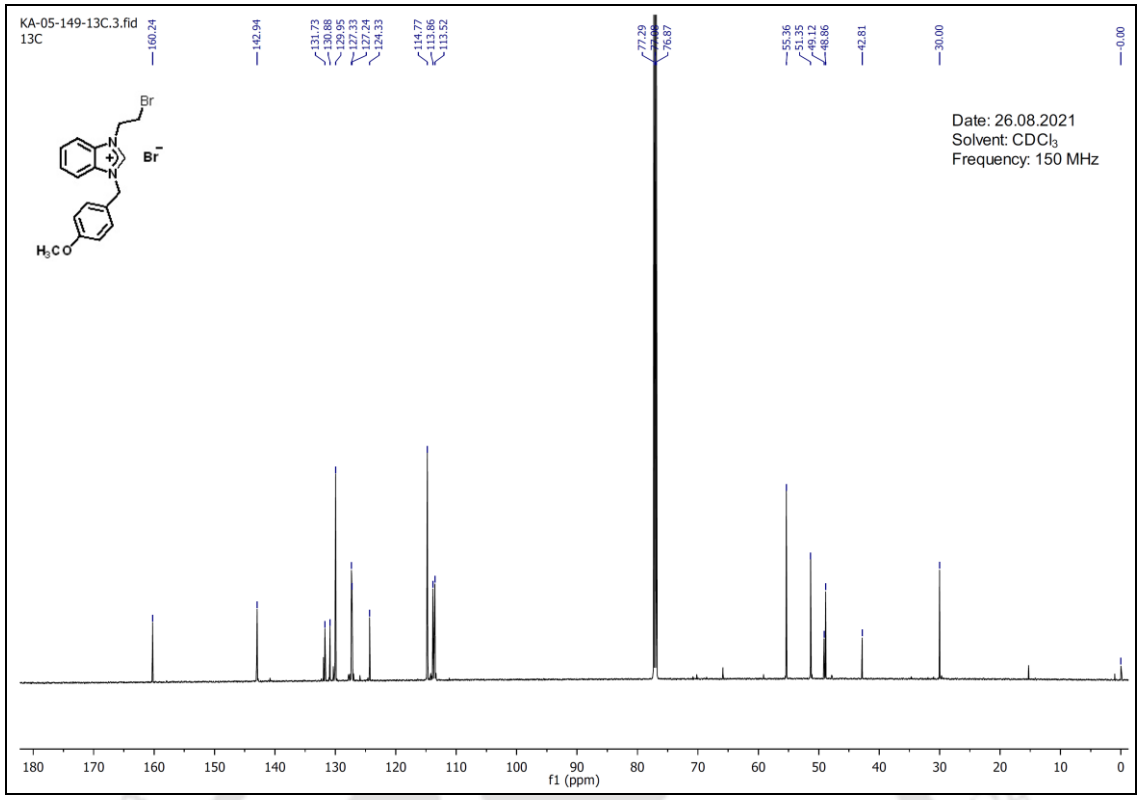

Figure A6.43. ^{13}C NMR ($CDCl_3$, 150 MHz) of compound **5.19**.

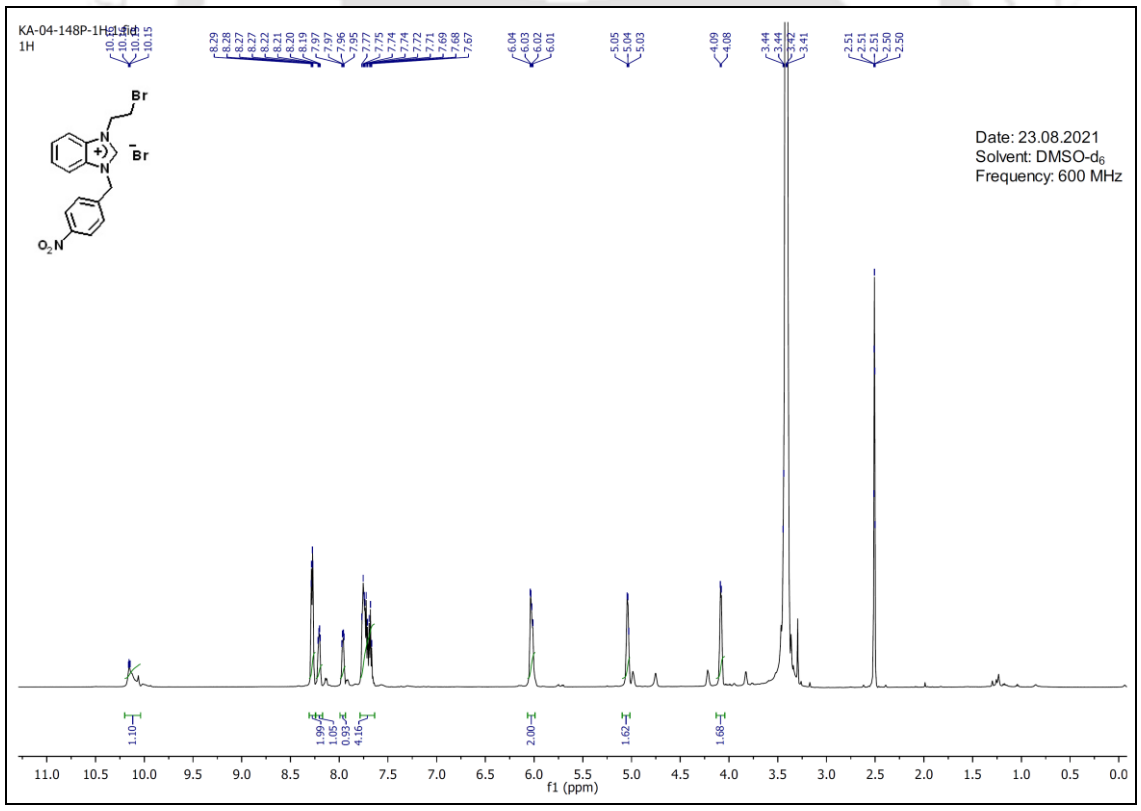

Figure A6.44. ^{1}H NMR spectrum (DMSO-d_6, 600 MHz) of compound **5.20**.

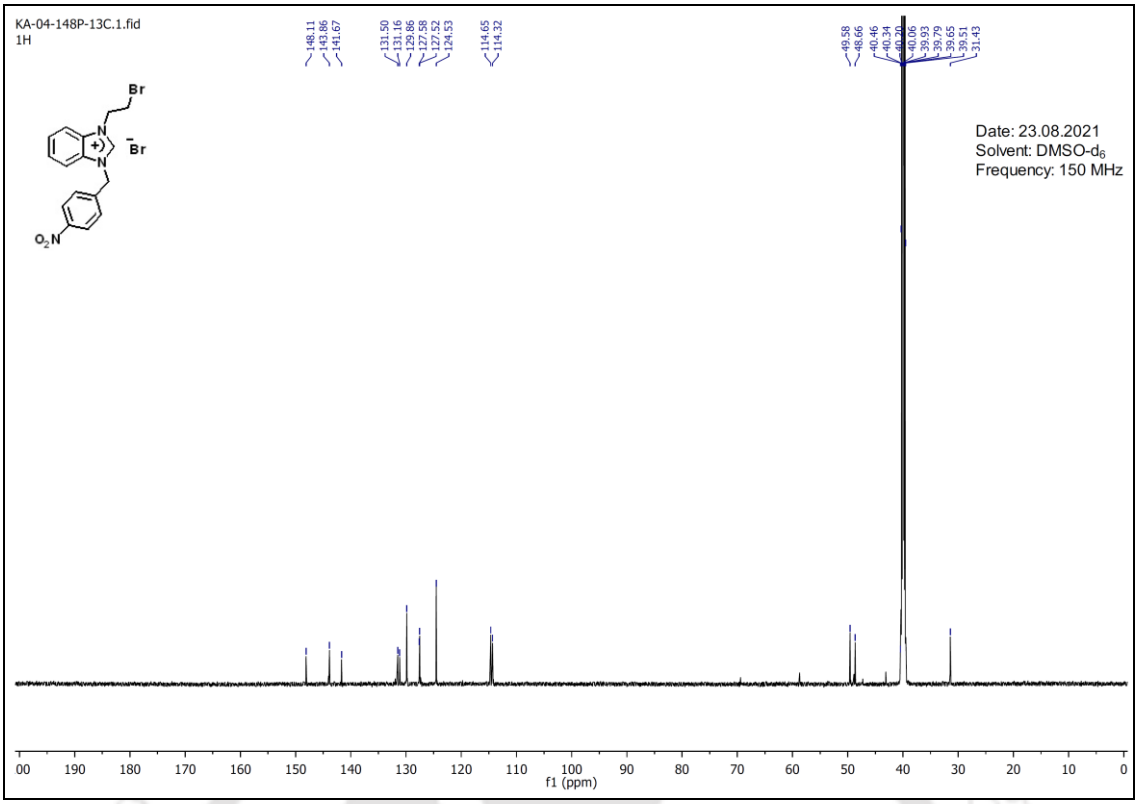

Figure A6.45. ^{13}C NMR (DMSO-d_6, 150 MHz) of compound **5.20**.

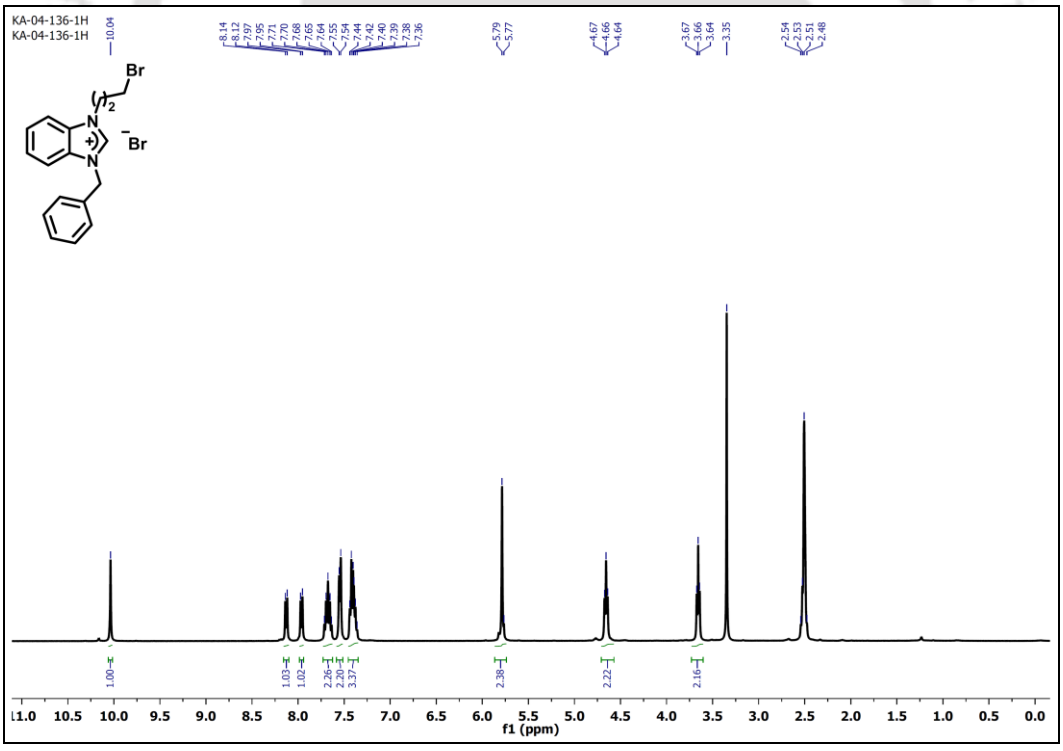

Figure A6.46. ^{1}H NMR spectrum (DMSO-d_6, 400 MHz) of compound **4.9b-2**.

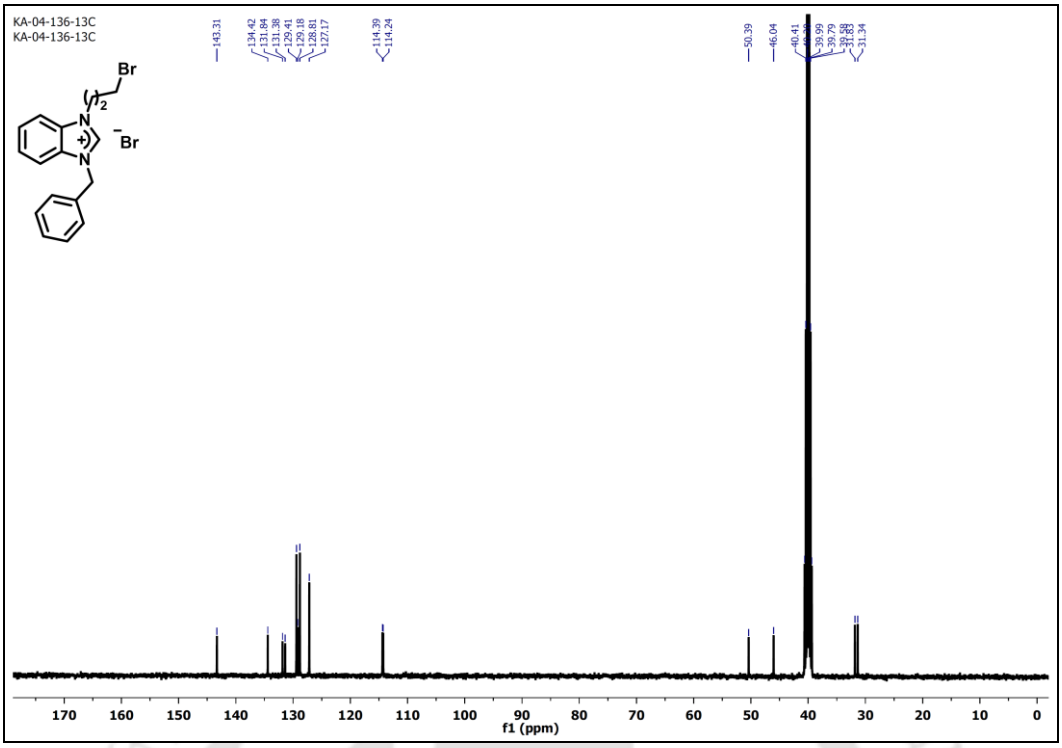

Figure A6.47. ^{13}C NMR spectrum (DMSO-d_6, 100 MHz) of compound **4.9b-2**.

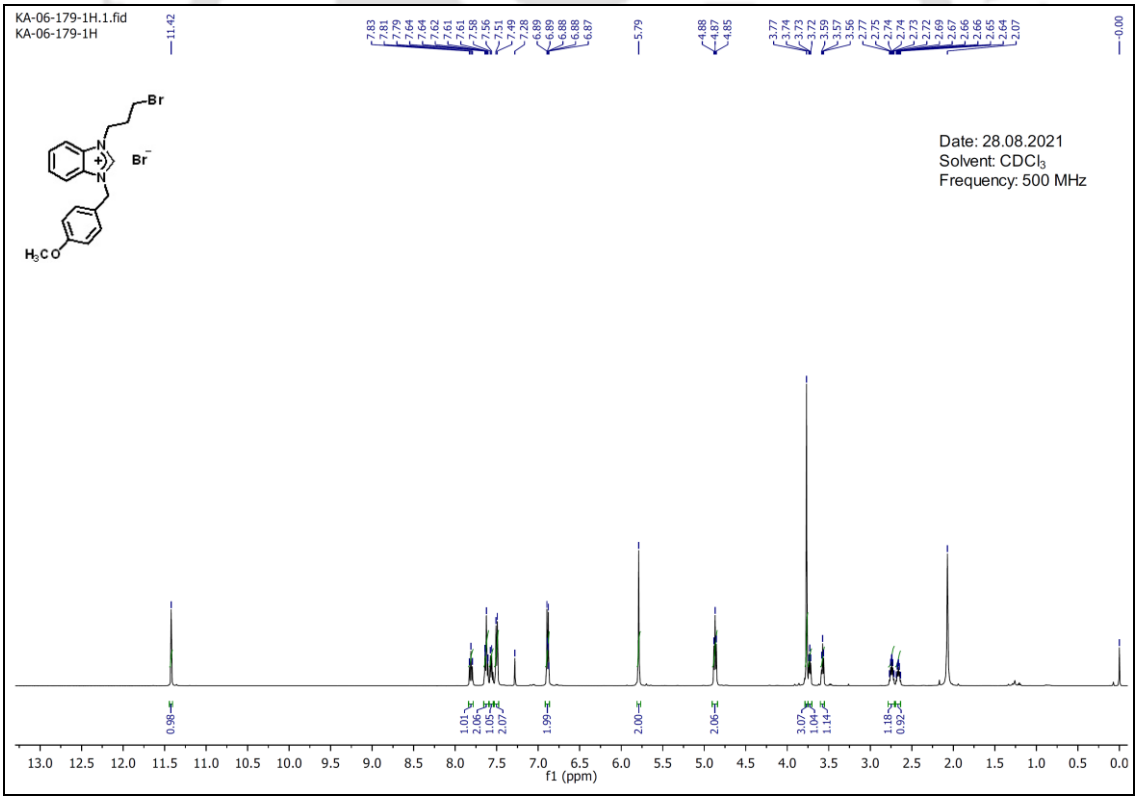

Figure A6.48. ^{1}H NMR ($CDCl_3$, 500 MHz) of compound **5.21**.

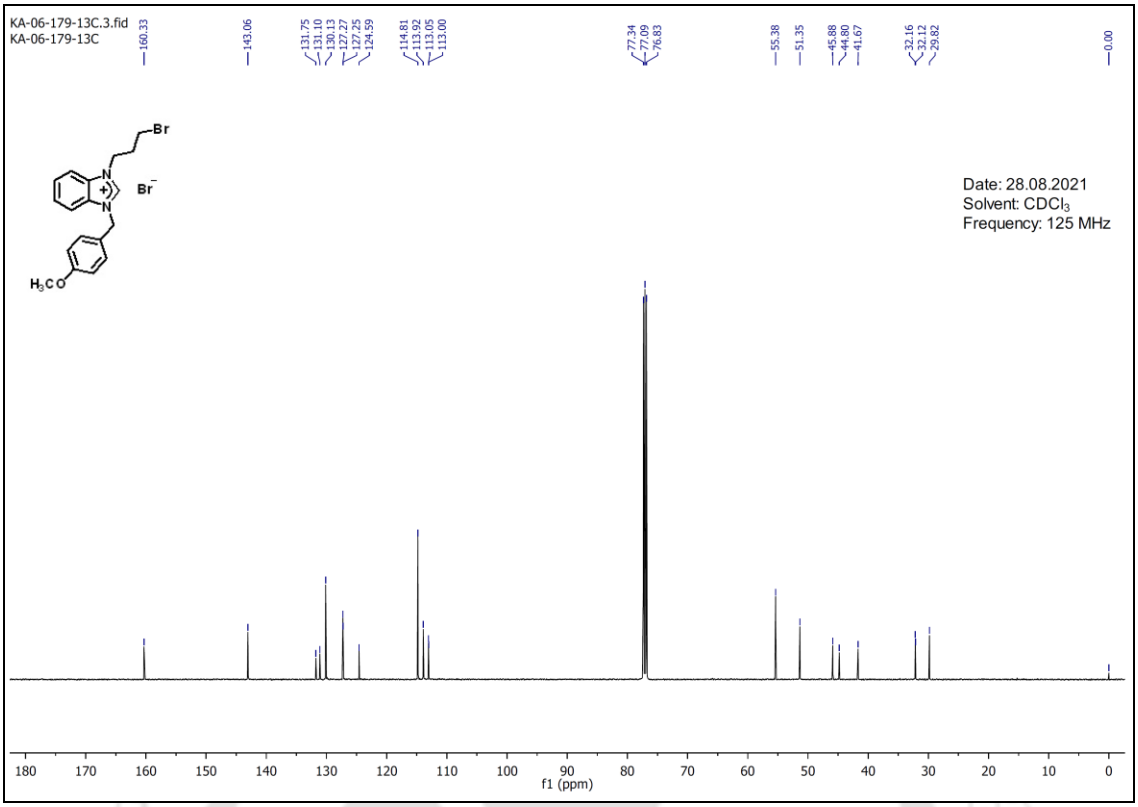

Figure A6.49. ^{13}C NMR ($CDCl_3$, 125 MHz) of compound **5.21**.

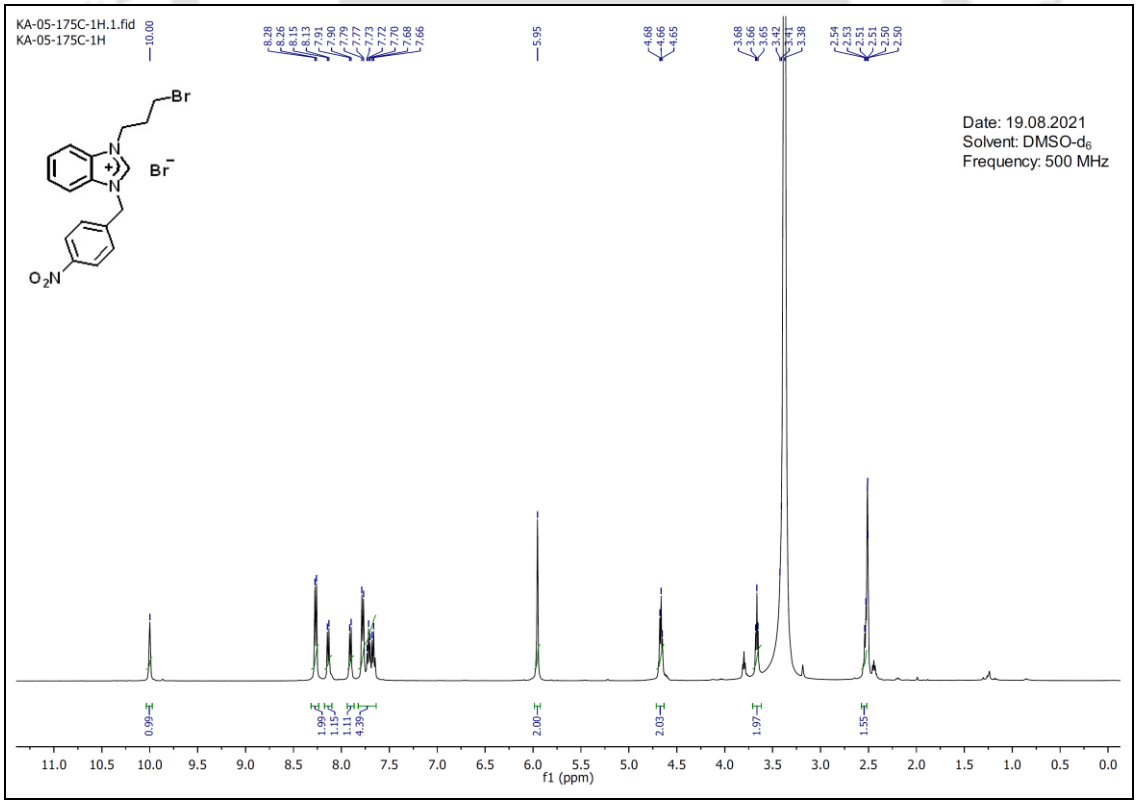

Figure A6.50. ^{1}H NMR spectrum (DMSO-d_6, 500 MHz) of compound **5.22**.

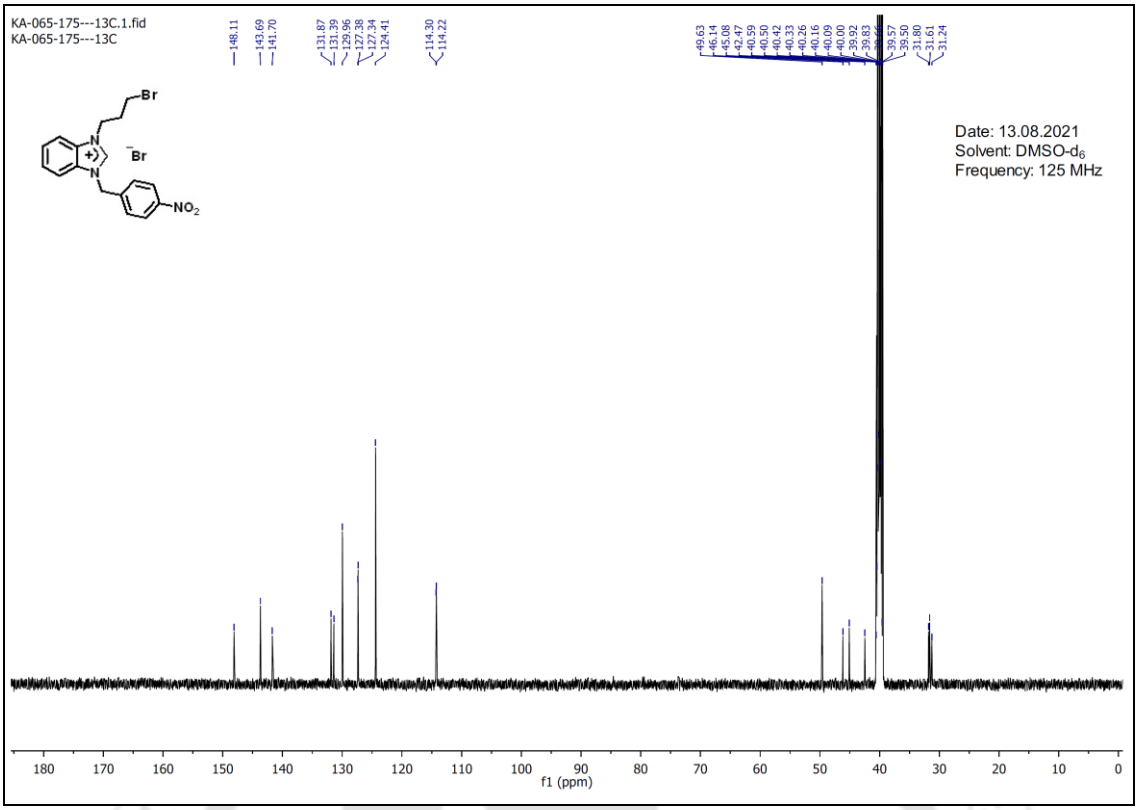

Figure S5.51. ^{13}C NMR (DMSO-d_6, 125 MHz) of compound **5.22**.

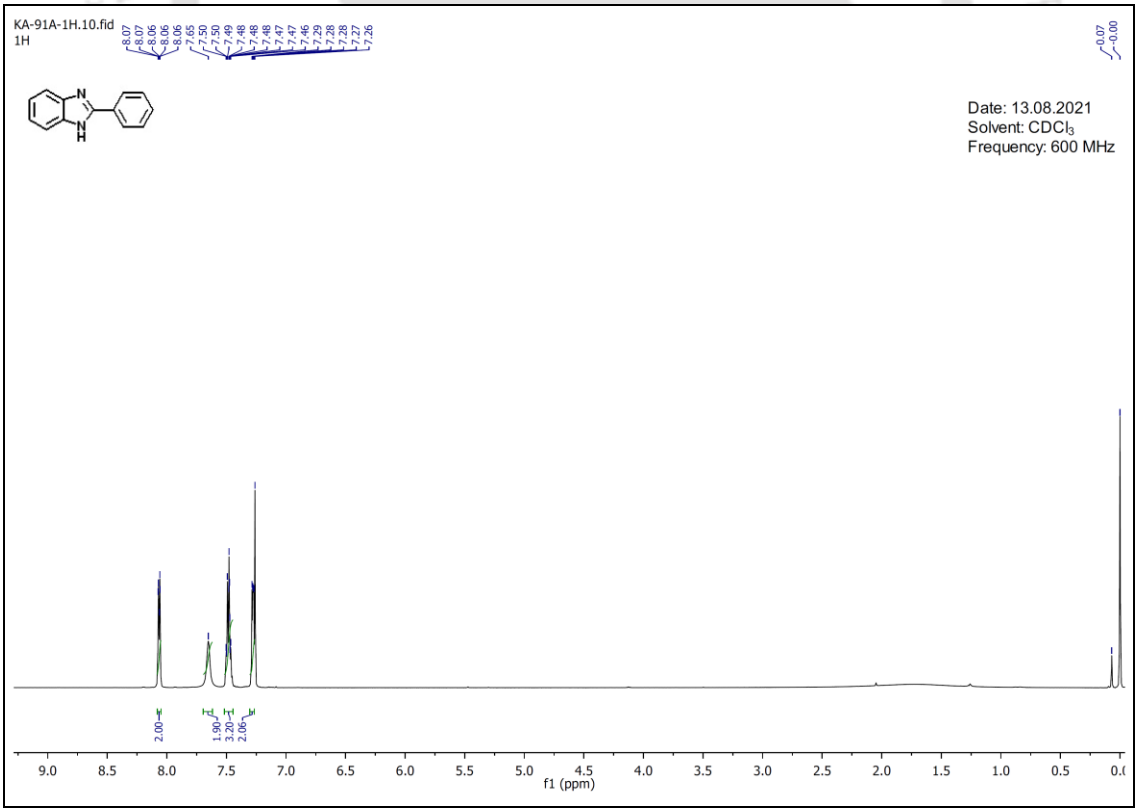

Figure S5.52. ^{1}H NMR spectrum ($CDCl_3$, 600 MHz) of compound **5.24**.

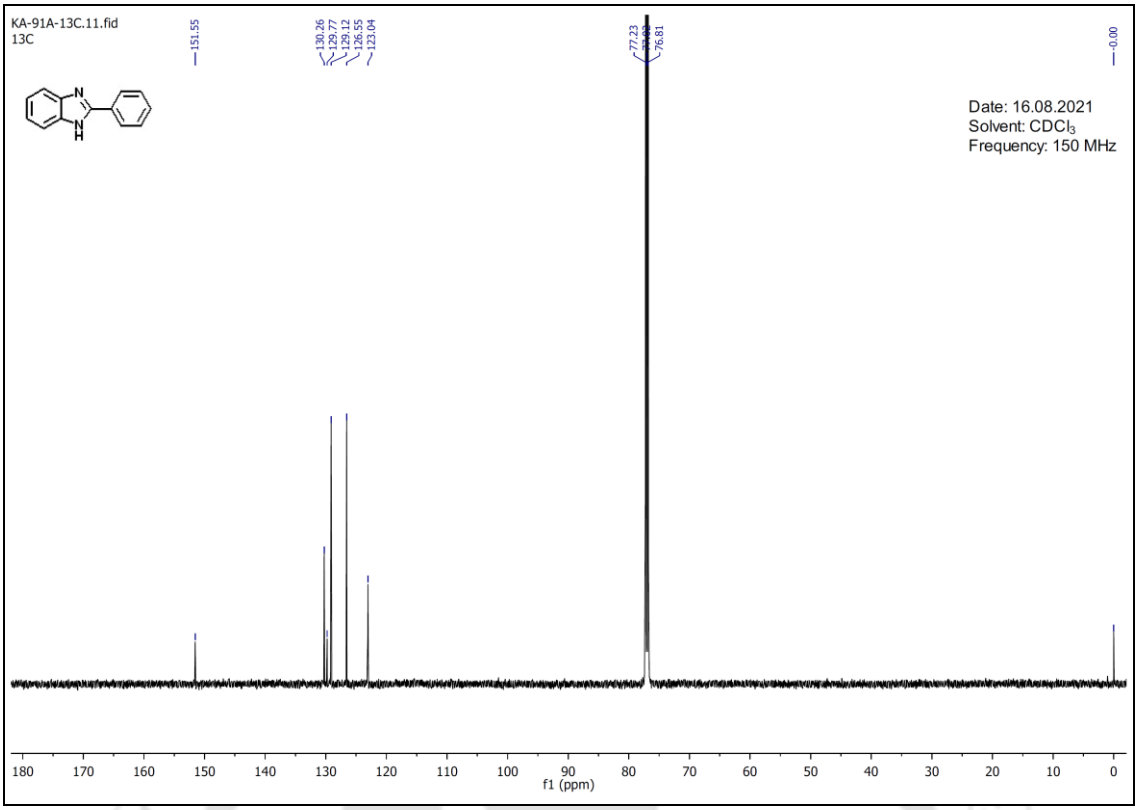

Figure S5.53. ^{13}C NMR ($CDCl_3$, 150 MHz) of compound **5.24**.

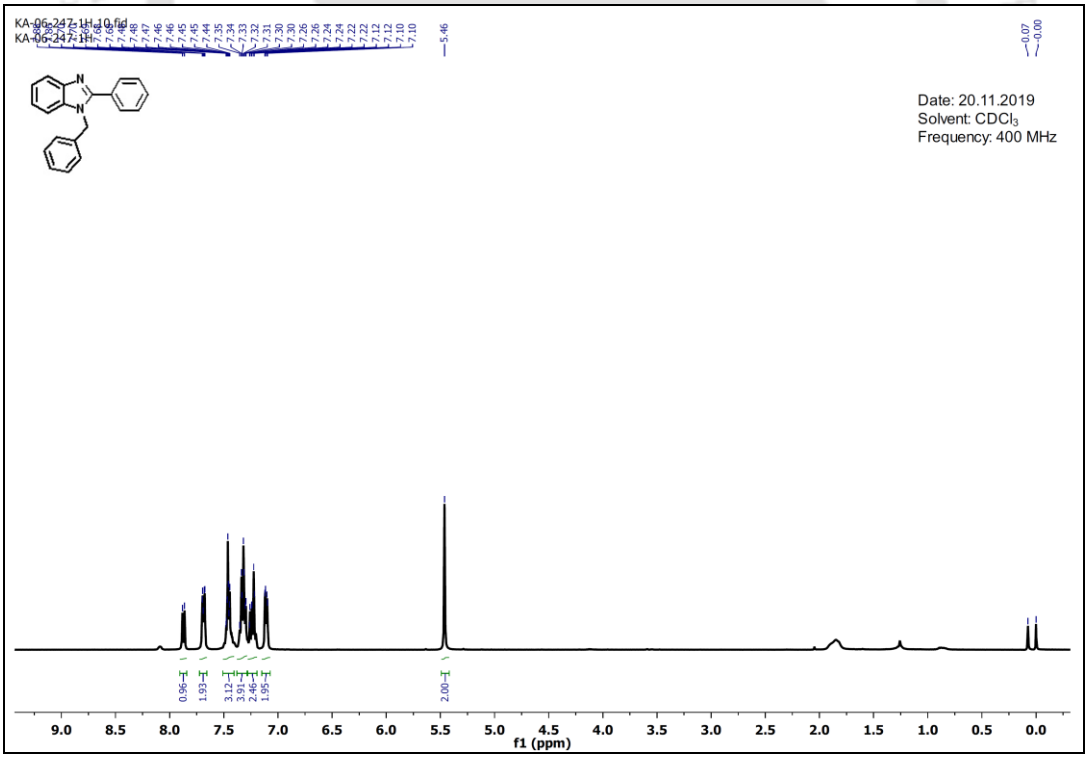

Figure S5.54. ^{1}H NMR spectrum ($CDCl_3$, 400 MHz) of compound **5.25**.

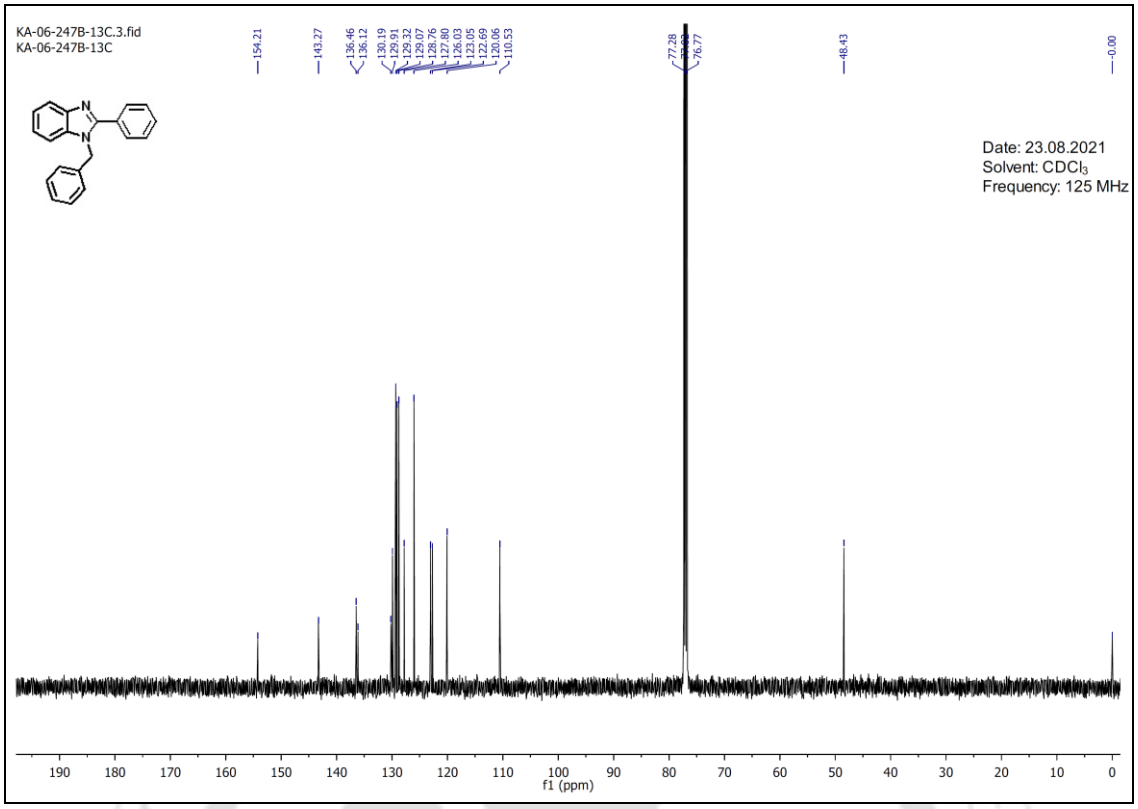

Figure S5.55. ^{13}C NMR ($CDCl_3$, 125 MHz) of compound **5.25**.

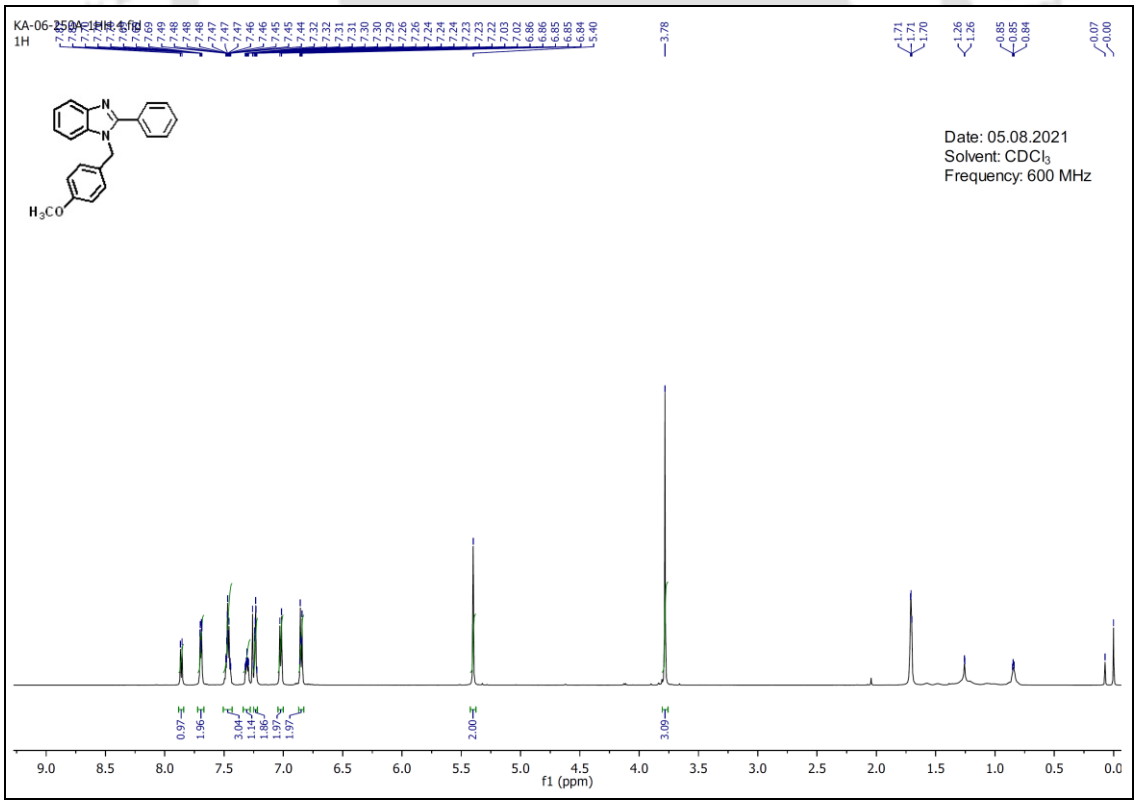

Figure S5.56. ^{1}H NMR spectrum ($CDCl_3$, 600 MHz) of compound **5.26**.

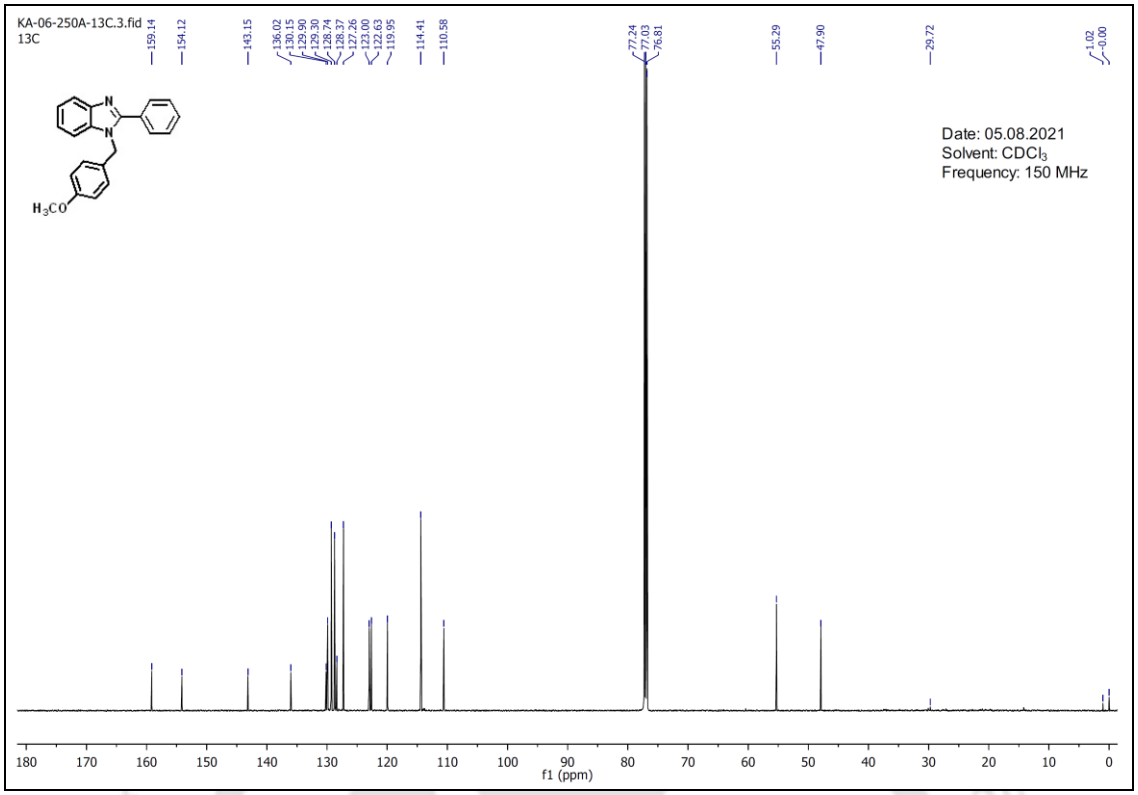

Figure S5.57. ^{13}C NMR ($CDCl_3$, 150 MHz) of compound **5.26**.

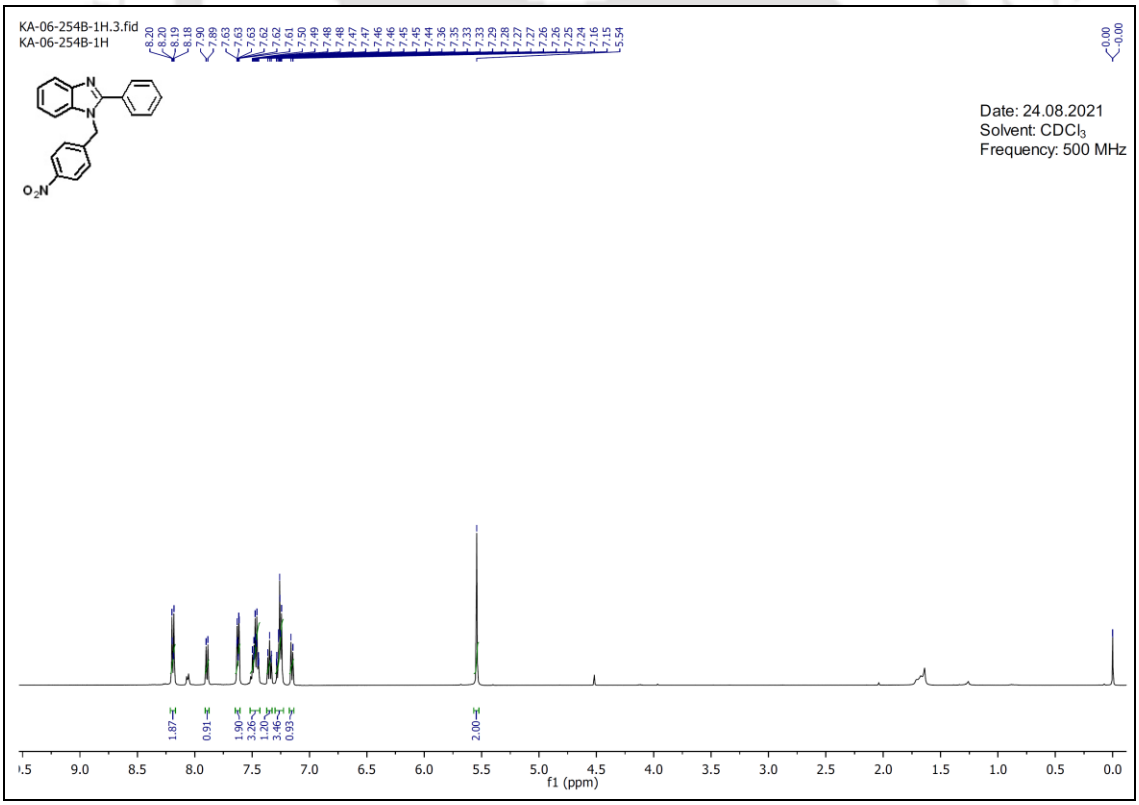

Figure S5.58. ^{1}H NMR spectrum ($CDCl_3$, 500 MHz) of compound **5.27**.

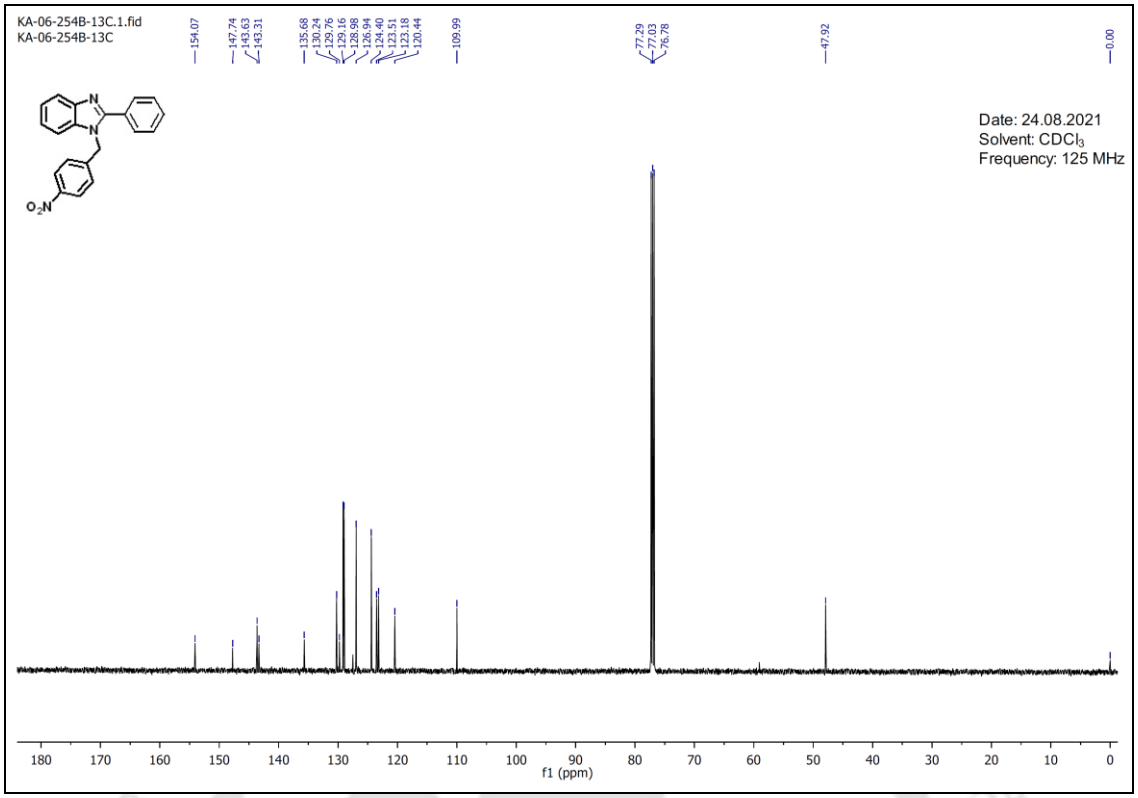

Figure S5.59. ^{13}C NMR ($CDCl_3$, 125 MHz) of compound **5.27**.

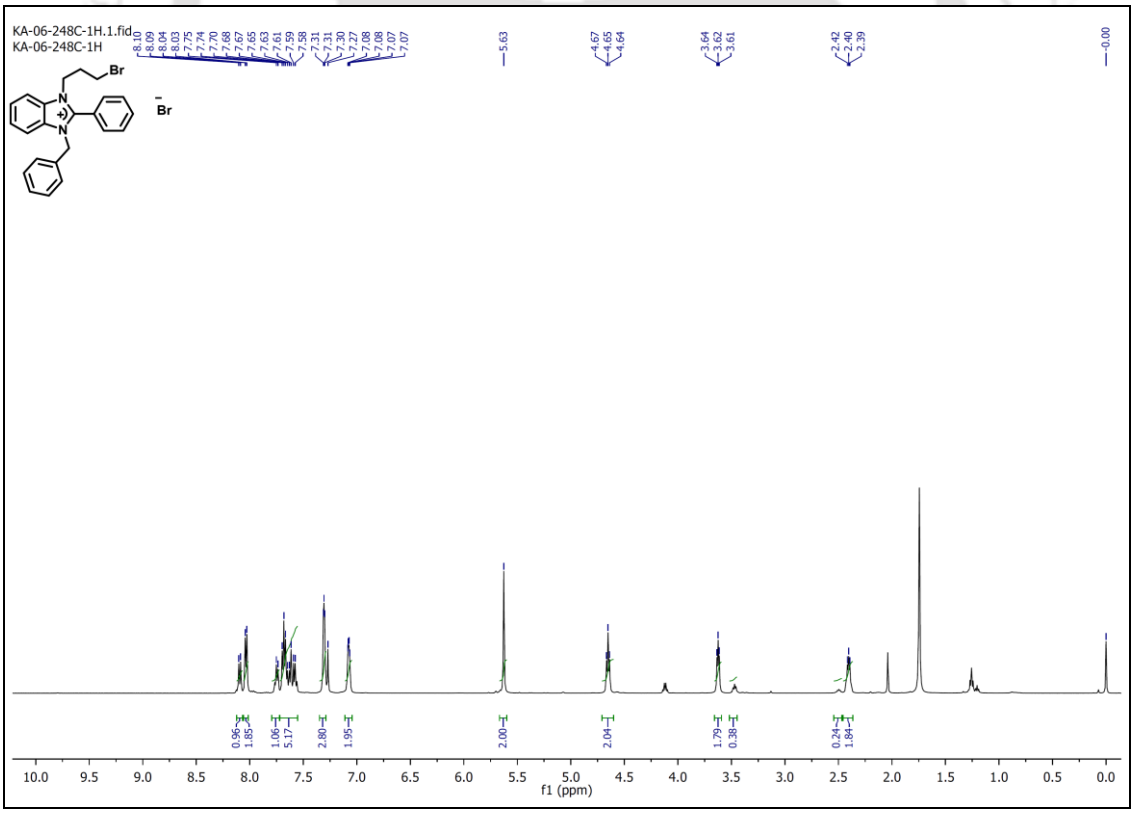

Figure S5.60. ^{1}H NMR spectrum ($CDCl_3$, 500 MHz) of compound **5.28**.

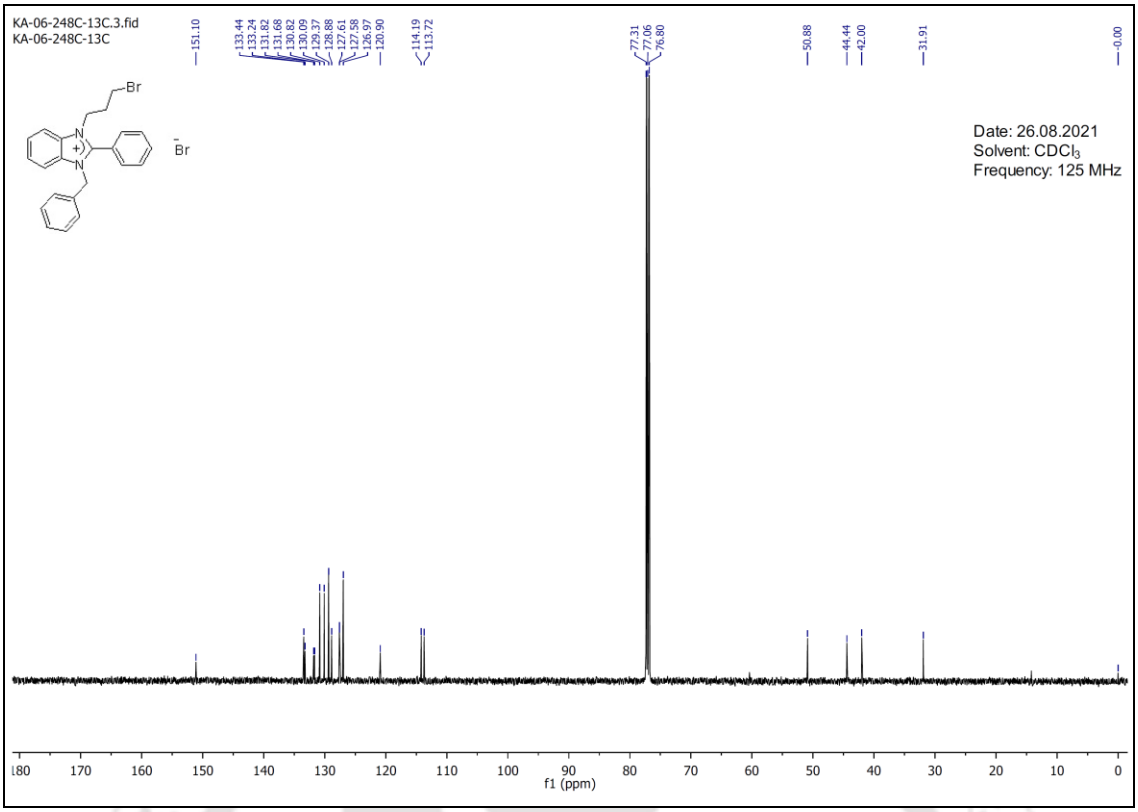

Figure S5.61. ^{13}C NMR ($CDCl_3$, 125 MHz) of compound **5.28**.

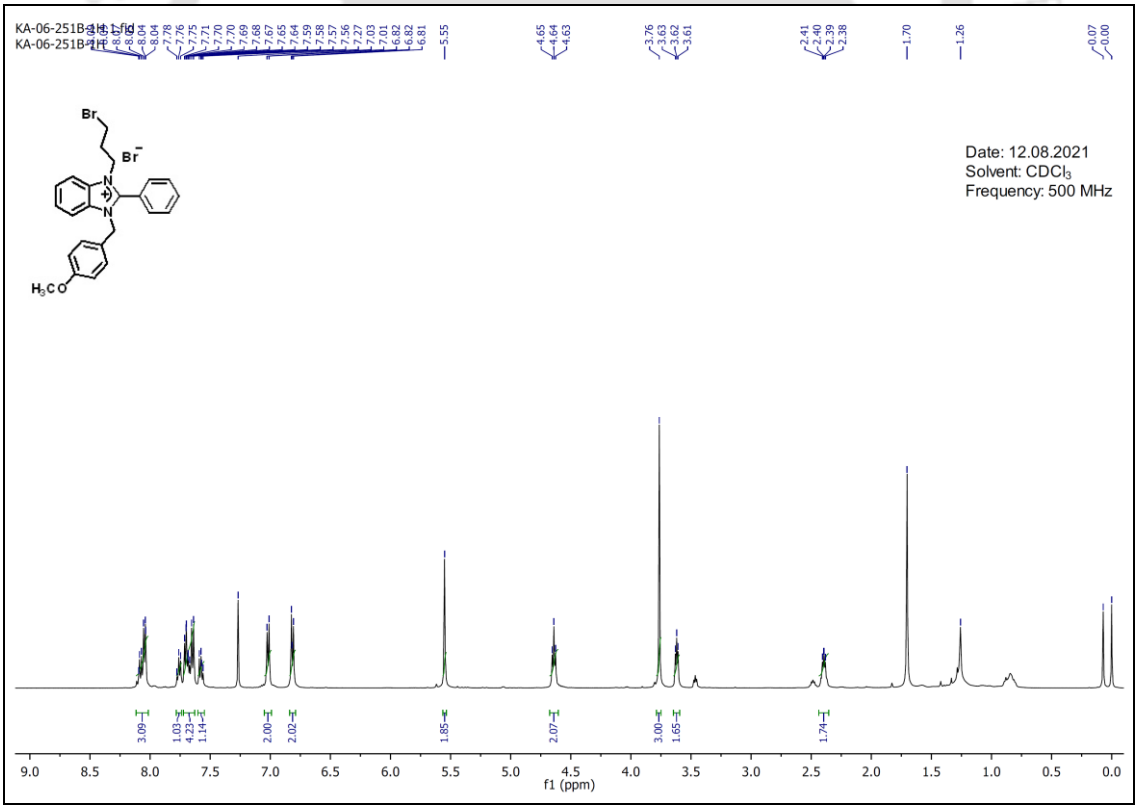

Figure S5.62. ^{1}H NMR ($CDCl_3$, 500 MHz) of compound **5.29**.

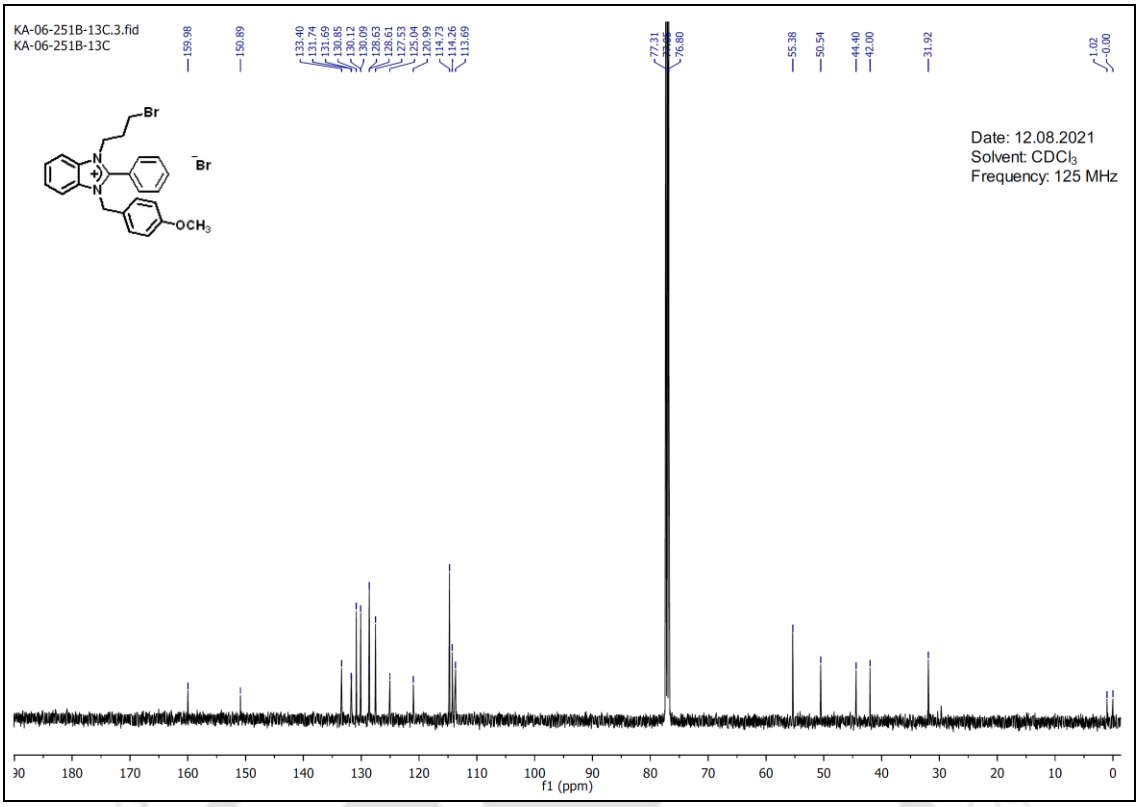

Figure S5.63. ^{13}C NMR ($CDCl_3$, 125 MHz) of compound **5.29**.

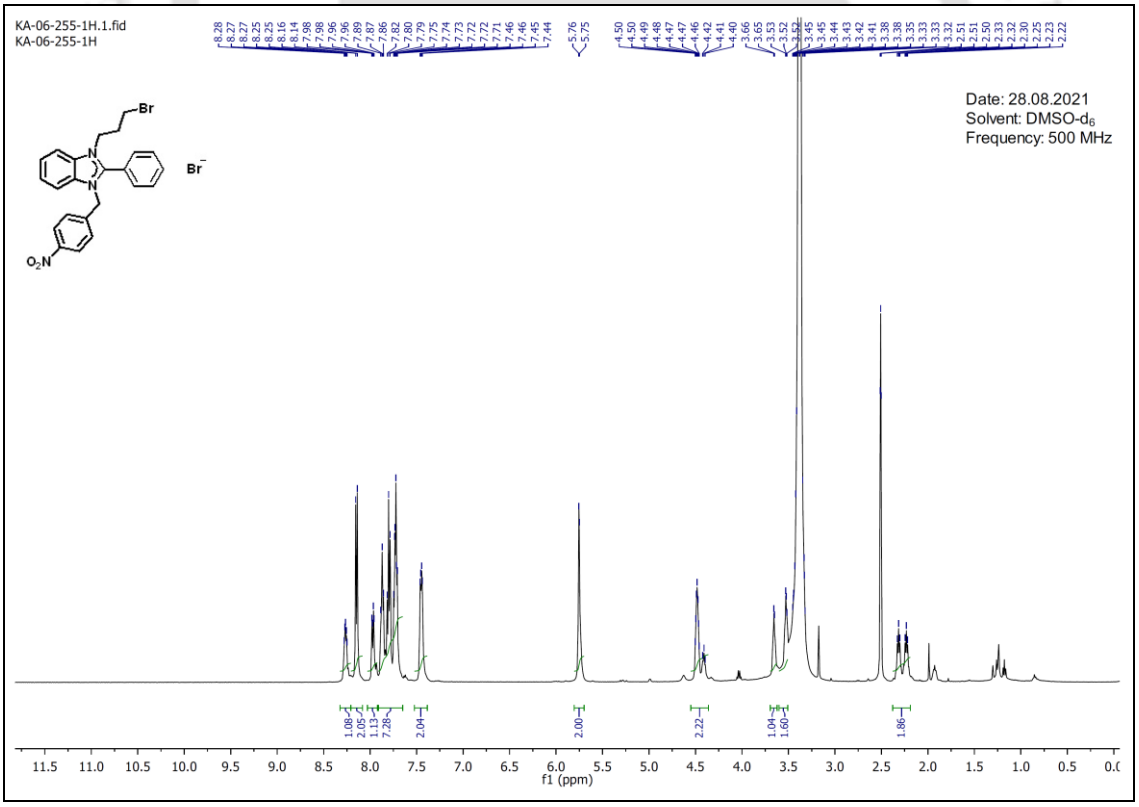

Figure S5.64. ^{1}H NMR spectrum (DMSO-d_6, 500 MHz) of compound **5.30**.

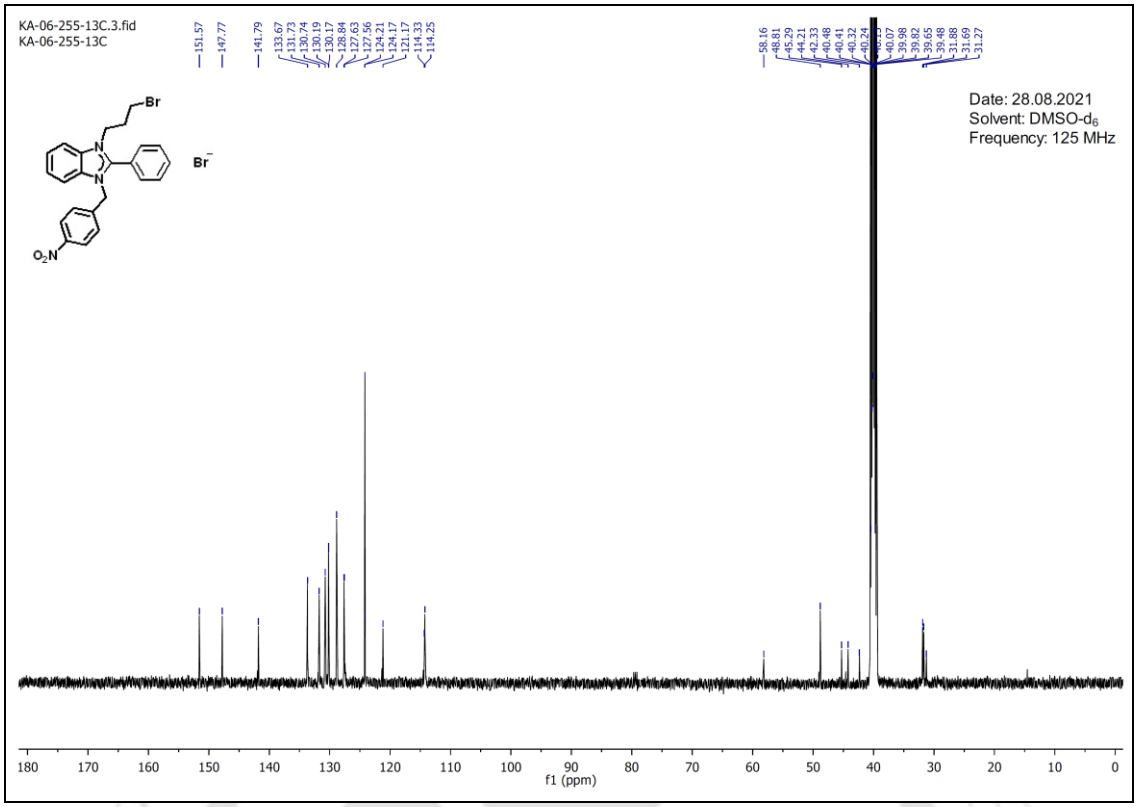

Figure S5.65. ^{13}C NMR (DMSO-d_6, 125 MHz) of compound **5.30**.

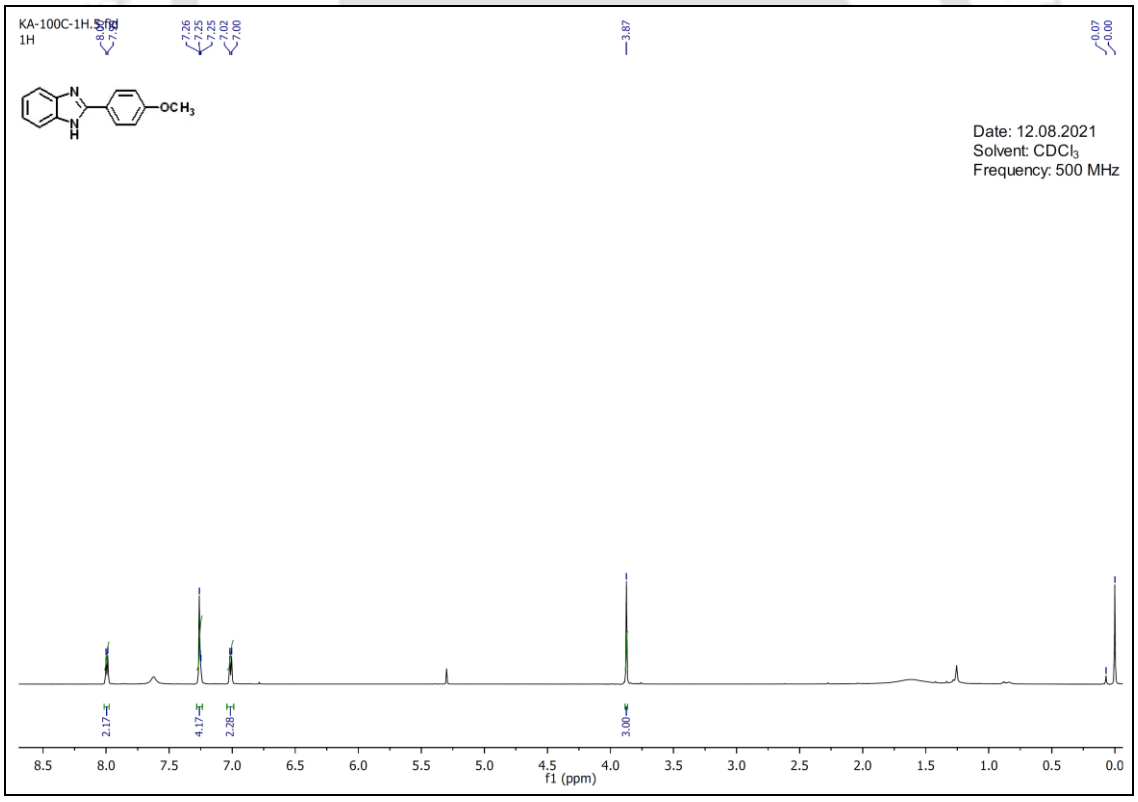

Figure S5.66. ^{1}H NMR spectrum ($CDCl_3$, 500 MHz) of compound **5.31**.

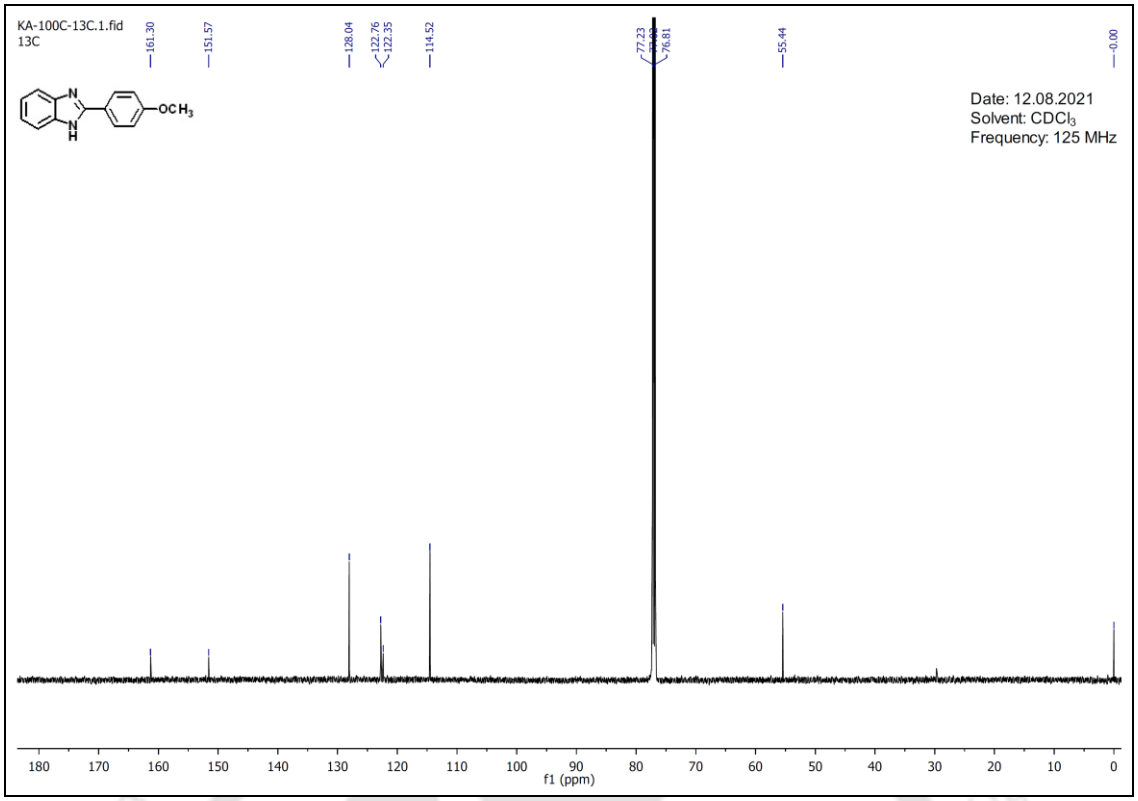

Figure S5.67. ^{13}C NMR ($CDCl_3$, 125 MHz) of compound **5.31**.

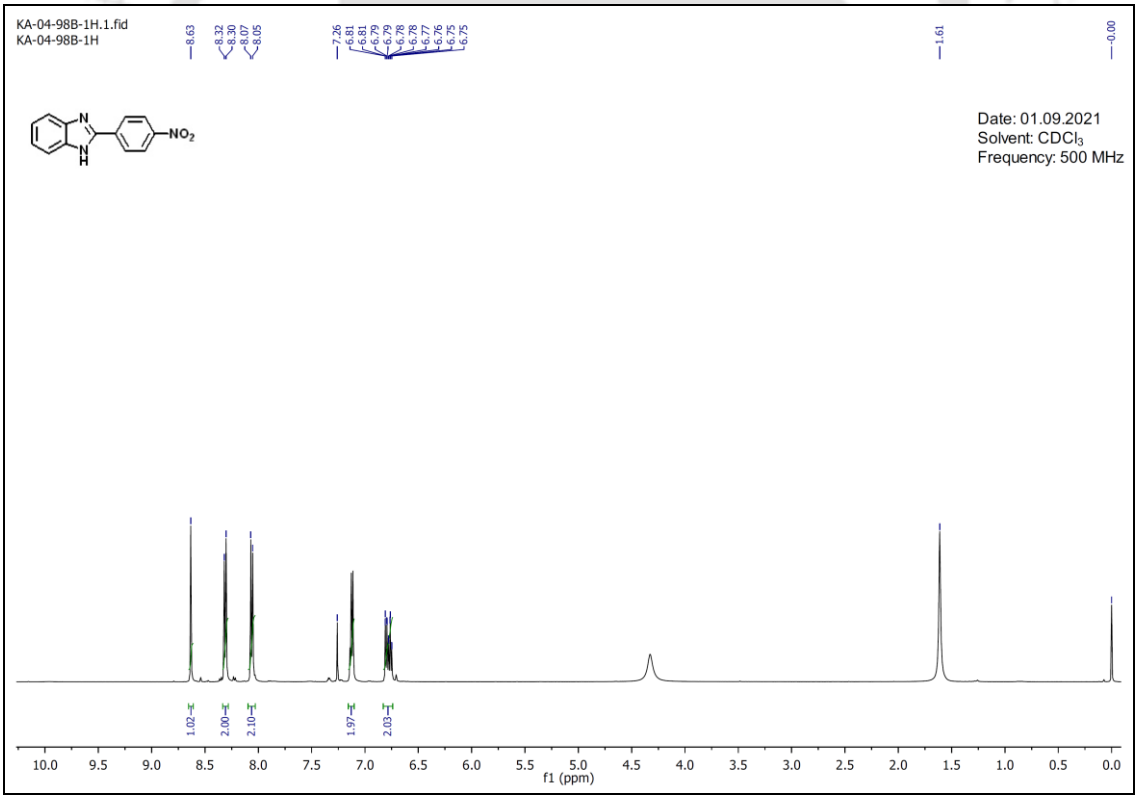

Figure S5.68. ^{1}H NMR ($CDCl_3$, 500 MHz) of compound **5.32**.

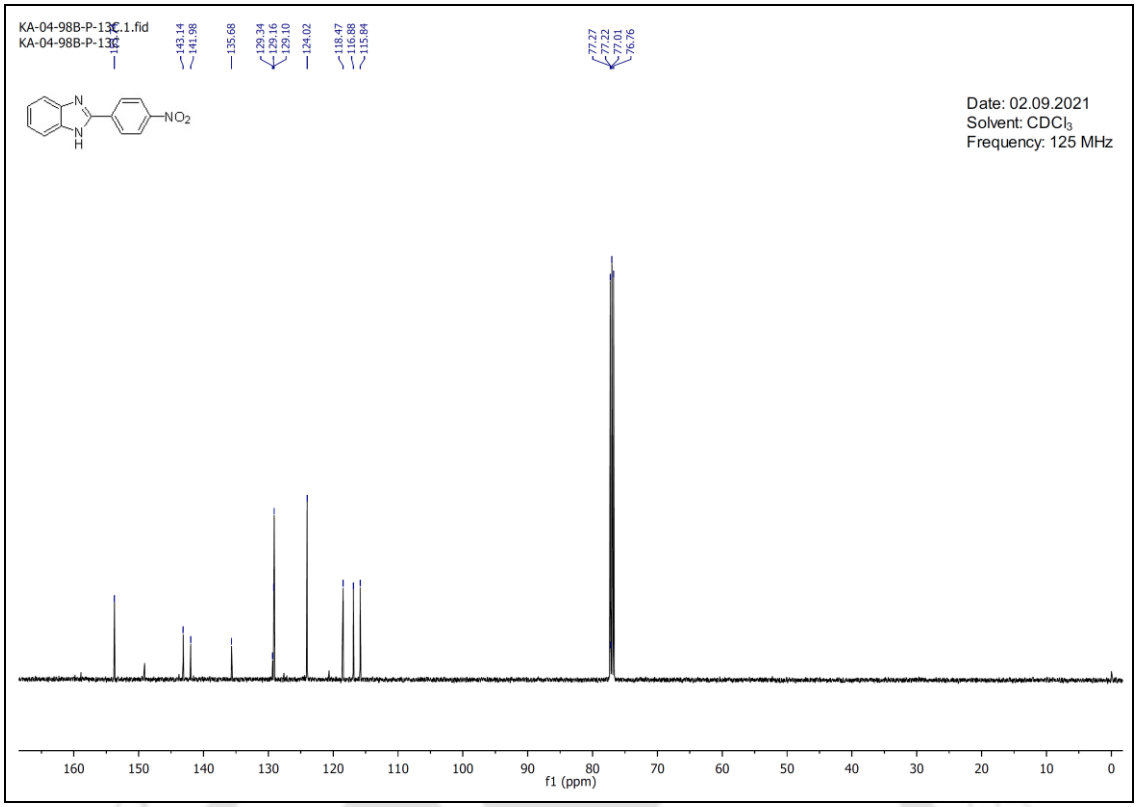

Figure S5.69. ^{13}C NMR ($CDCl_3$, 125 MHz) of compound **5.32**.

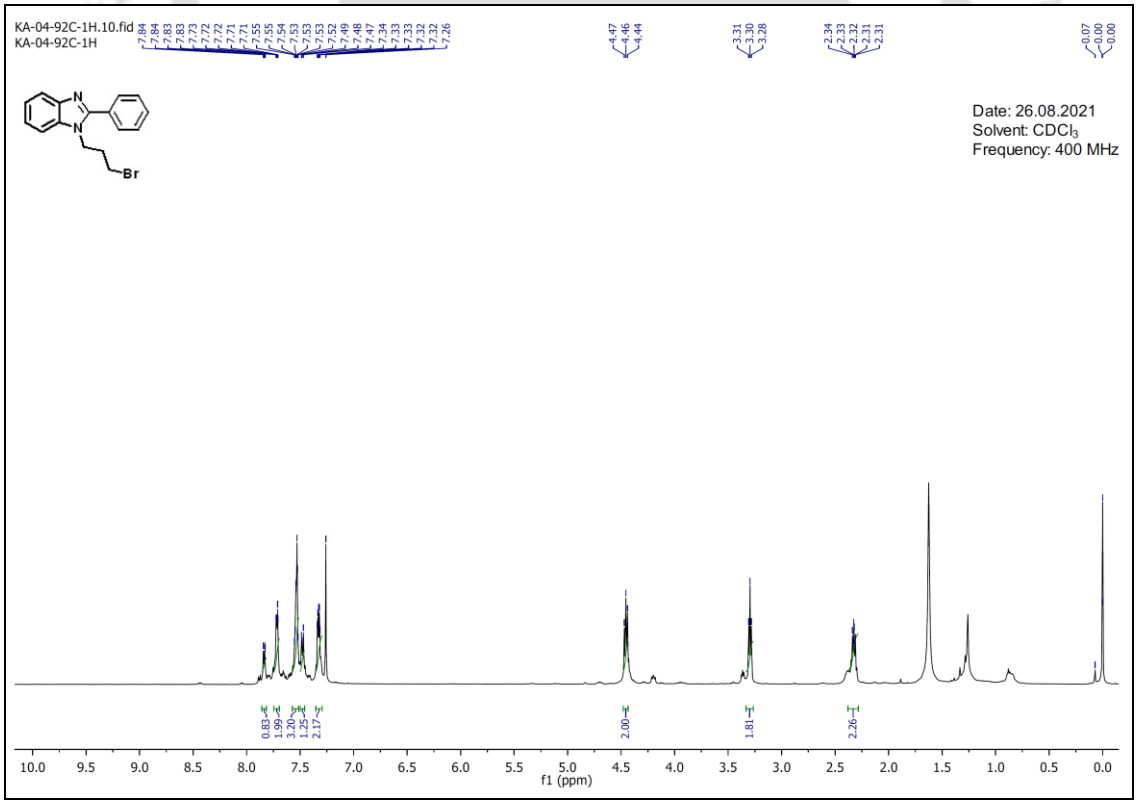

Figure S5.70. ^{1}H NMR ($CDCl_3$, 400 MHz) of compound **5.33**.

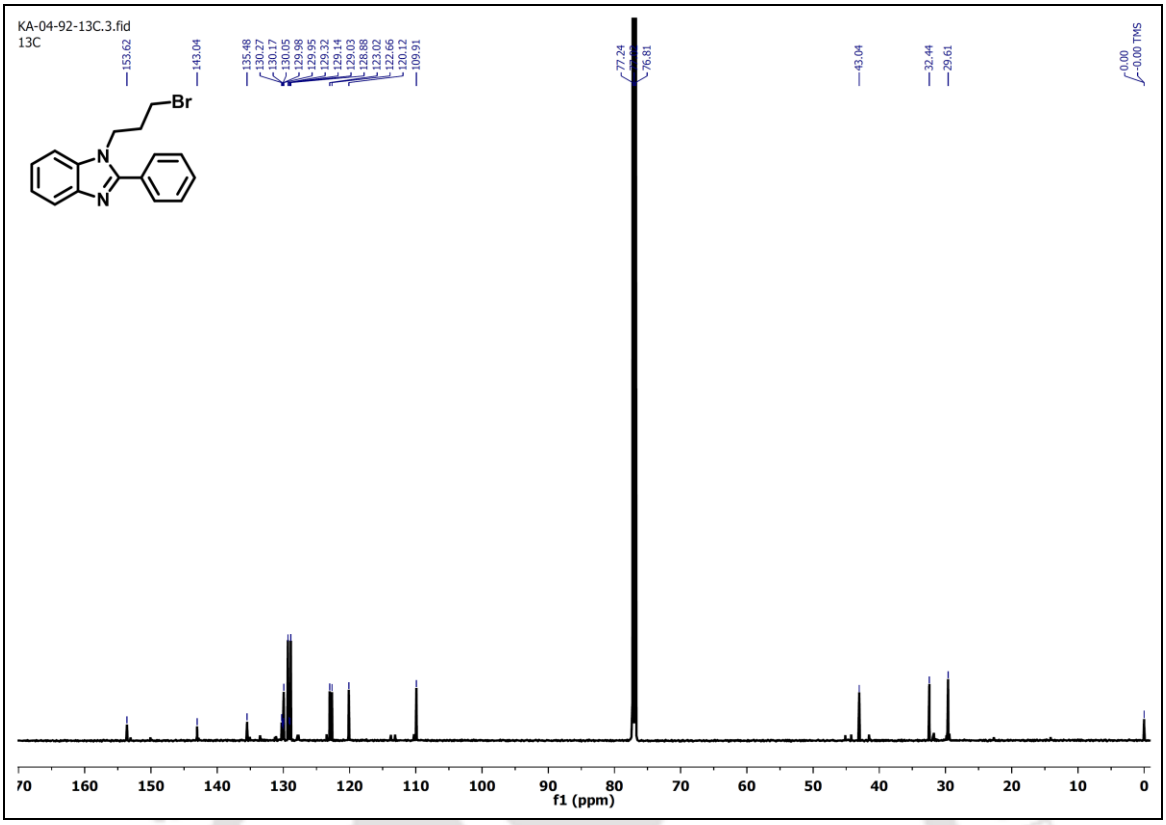

Figure S5.71. ^{13}C NMR ($CDCl_3$, 150 MHz) of compound **5.33**.

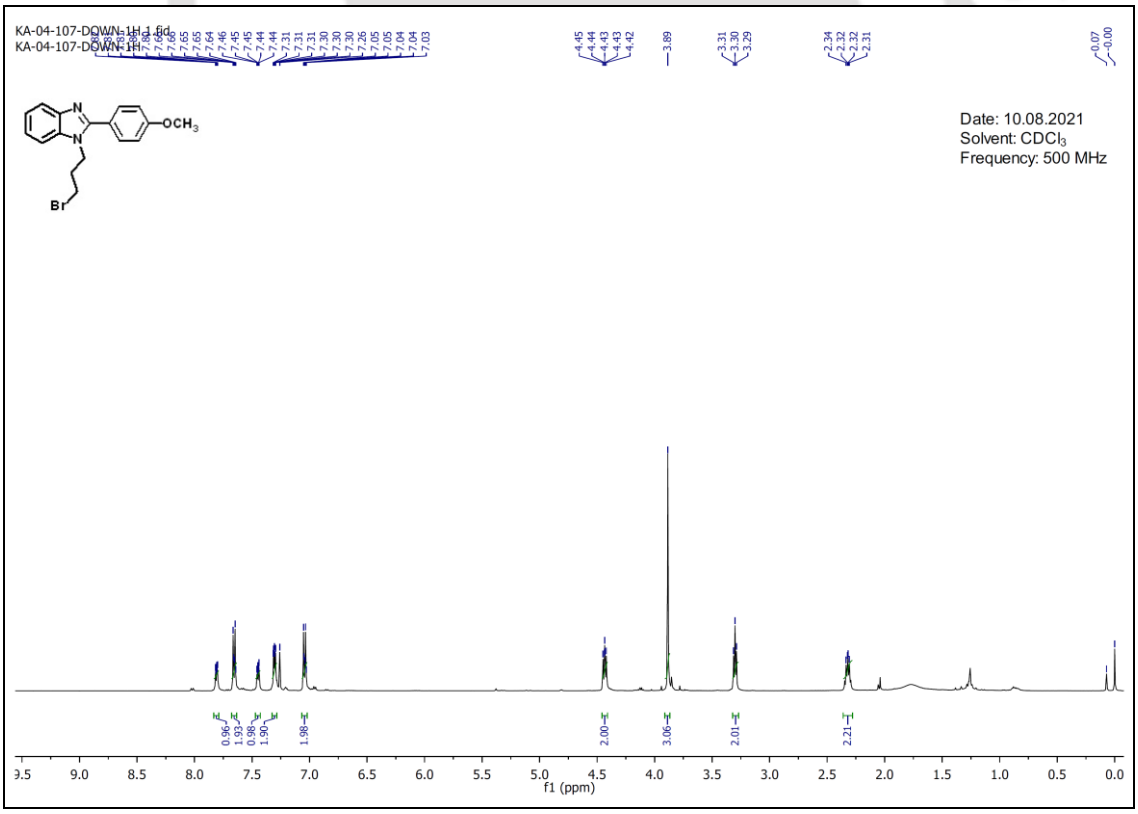

Figure S5.72. ^{1}H NMR ($CDCl_3$, 500 MHz) of compound **5.34**.

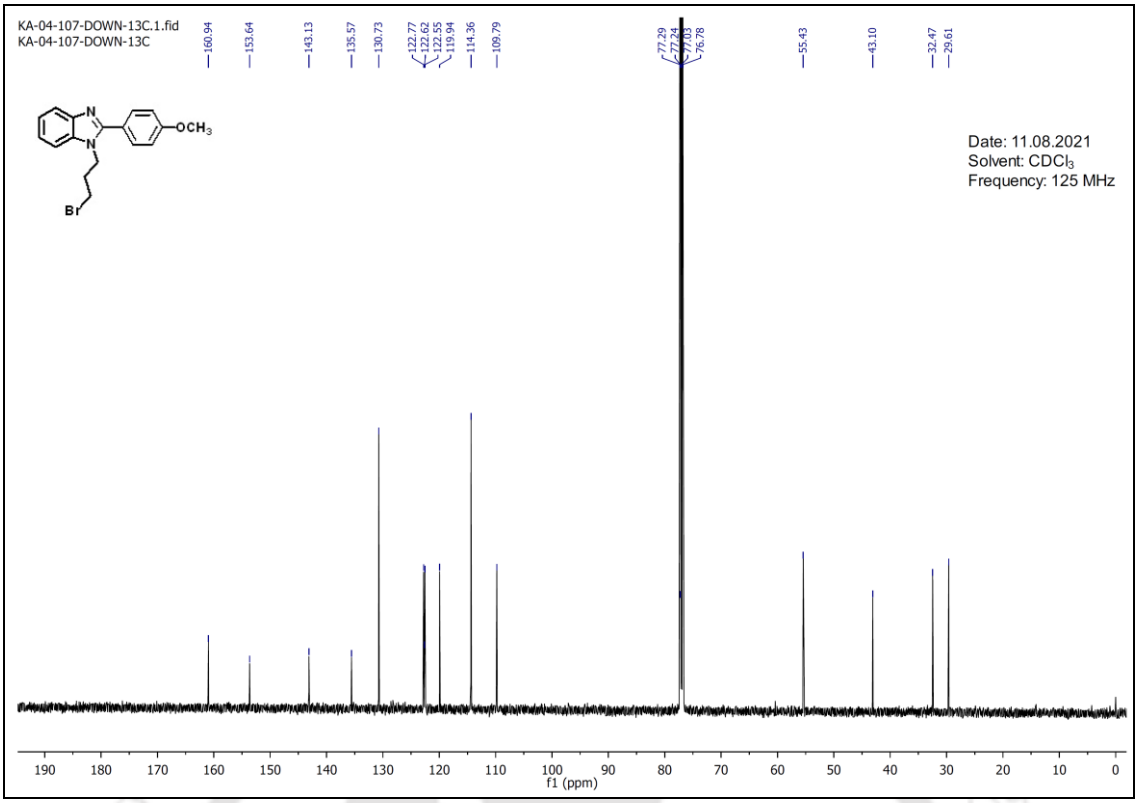

Figure S5.73. ^{13}C NMR ($CDCl_3$, 125 MHz) of compound **5.34**.

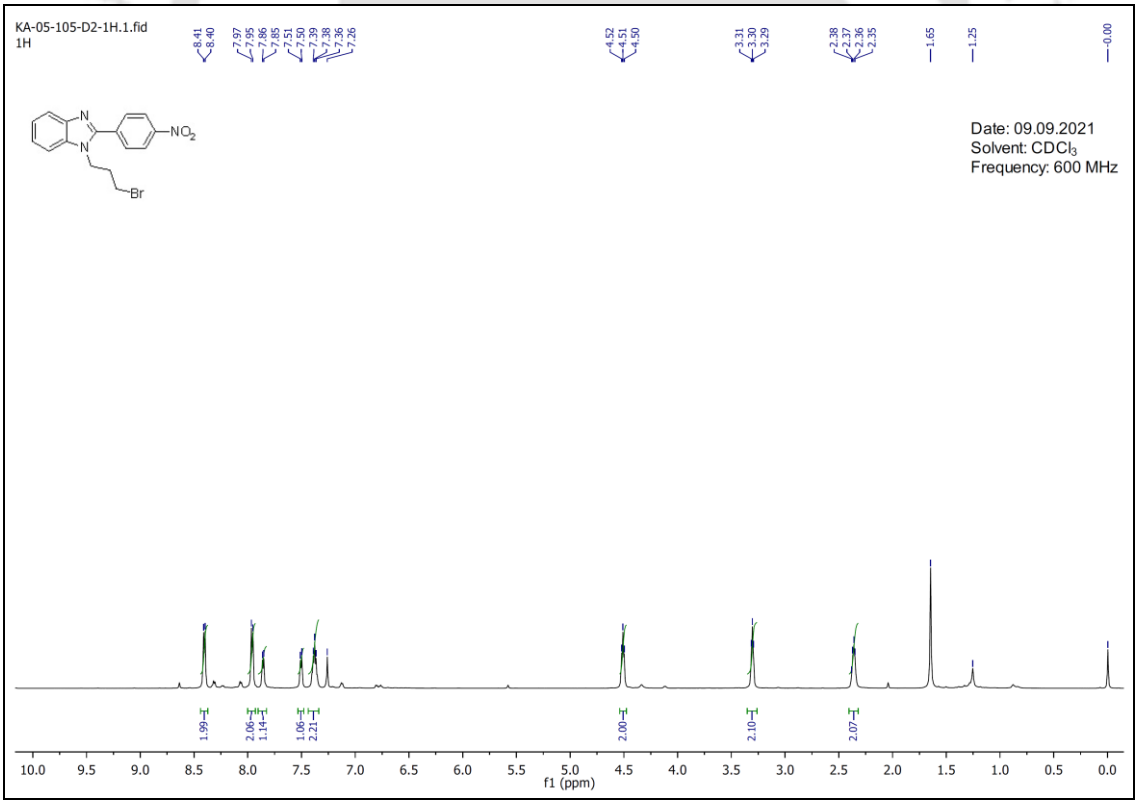

Figure S5.74. ^{1}H NMR ($CDCl_3$, 600 MHz) of compound **5.35**.

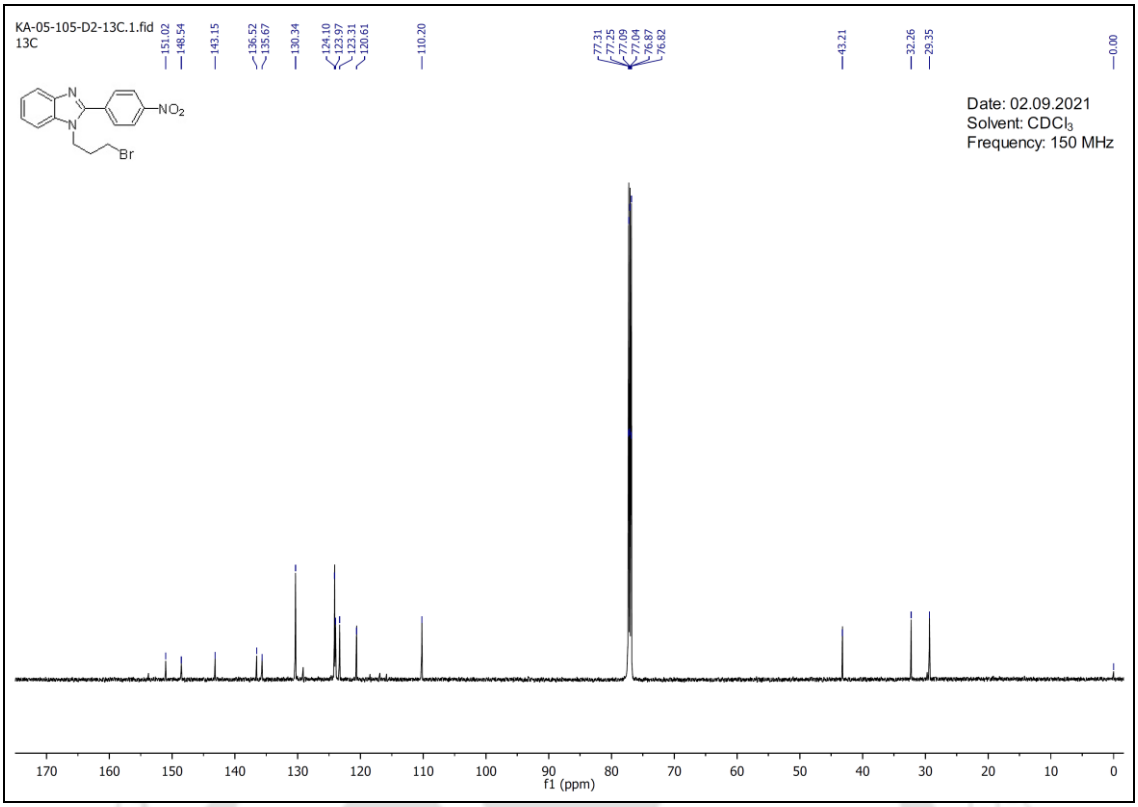

Figure S5.75. ^{13}C NMR ($CDCl_3$, 150 MHz) of compound **5.35**.